

Recent Advances in Disinfection By-Products

ACS SYMPOSIUM SERIES **1190**

Recent Advances in Disinfection By-Products

Tanju Karanfil, Editor

*Clemson University
Anderson, South Carolina*

Bill Mitch, Editor

*Stanford University
Stanford, California*

Paul Westerhoff, Editor

*Arizona State University
Tempe, Arizona*

Yuefeng Xie, Editor

*The Pennsylvania State University
Middletown, Pennsylvania*

Sponsored by the
ACS Division of Environmental Chemistry, Inc.



American Chemical Society, Washington, DC

Distributed in print by Oxford University Press



Library of Congress Cataloging-in-Publication Data

Recent advances in disinfection by-products / Tanju Karanfil, editor, Clemson University, Anderson, South Carolina [and three others] ; sponsored by the ACS Division of Environmental Chemistry, Inc.

pages cm. -- (ACS symposium series ; 1190)

Includes bibliographical references and index.

ISBN 978-0-8412-3076-7 -- ISBN 978-0-8412-3077-4 1. Disinfection and disinfectants.

I. Karanfil, Tanju. II. American Chemical Society. Division of Environmental Chemistry.

RA765.R43 2015

614.4'8--dc23

The paper used in this publication meets the minimum requirements of American National Standard for Information Sciences—Permanence of Paper for Printed Library Materials, ANSI Z39.48n1984.

Copyright © 2015 American Chemical Society

Distributed in print by Oxford University Press

All Rights Reserved. Reprographic copying beyond that permitted by Sections 107 or 108 of the U.S. Copyright Act is allowed for internal use only, provided that a per-chapter fee of \$40.25 plus \$0.75 per page is paid to the Copyright Clearance Center, Inc., 222 Rosewood Drive, Danvers, MA 01923, USA. Republication or reproduction for sale of pages in this book is permitted only under license from ACS. Direct these and other permission requests to ACS Copyright Office, Publications Division, 1155 16th Street, N.W., Washington, DC 20036.

The citation of trade names and/or names of manufacturers in this publication is not to be construed as an endorsement or as approval by ACS of the commercial products or services referenced herein; nor should the mere reference herein to any drawing, specification, chemical process, or other data be regarded as a license or as a conveyance of any right or permission to the holder, reader, or any other person or corporation, to manufacture, reproduce, use, or sell any patented invention or copyrighted work that may in any way be related thereto. Registered names, trademarks, etc., used in this publication, even without specific indication thereof, are not to be considered unprotected by law.

PRINTED IN THE UNITED STATES OF AMERICA

Foreword

The ACS Symposium Series was first published in 1974 to provide a mechanism for publishing symposia quickly in book form. The purpose of the series is to publish timely, comprehensive books developed from the ACS sponsored symposia based on current scientific research. Occasionally, books are developed from symposia sponsored by other organizations when the topic is of keen interest to the chemistry audience.

Before agreeing to publish a book, the proposed table of contents is reviewed for appropriate and comprehensive coverage and for interest to the audience. Some papers may be excluded to better focus the book; others may be added to provide comprehensiveness. When appropriate, overview or introductory chapters are added. Drafts of chapters are peer-reviewed prior to final acceptance or rejection, and manuscripts are prepared in camera-ready format.

As a rule, only original research papers and original review papers are included in the volumes. Verbatim reproductions of previous published papers are not accepted.

ACS Books Department

Preface

This book is part of a continuing series of books based on the chlorination conferences of the 1970s and 1980s and the more recent American Chemical Society (ACS) symposia on natural organic matter (NOM) and disinfection by-products (DBPs). These books have reflected the state-of-the-art in disinfection by-products (DBP) research around the world. The current book is based on a symposium entitled *Occurrence, Formation, Health Effects and Control of Disinfection By-Products in Drinking Water*, held at the 248th National Meeting of the ACS Division of Environmental Chemistry, in San Francisco, California, on August 10-14, 2014.

The formation, control, and health effects of DBPs in drinking water are issues of international concern because of the health effects (e.g., bladder cancer and potential adverse reproductive-development impacts) associated with exposure to certain DBPs. As a result, many countries, as well as the World Health Organization, have regulations and/or guidelines on acceptable concentrations of DBPs in water.

In recent years, DBP research worldwide has focused on determining the possible adverse health effects of emerging, yet unregulated, DBPs, specifically halogenated (e.g., iodinated) and non-halogenated nitrogenous (e.g., nitrosamines) DBPs. The breadth of DBP research is very broad from source waters (e.g., wastewater, wildfire, seawater intrusion influences) to treatment strategies and technologies, followed by distribution system and point of entry issues (e.g., biofilms, heating, swimming pools), as well as health effects and analytical method developments. Recent research is helping to understand factors controlling formation and to develop a cost-effective control of a wide range of regulated and emerging DBPs. Furthermore, the pace of research on emerging DBP toxicity has increased and generated diverse findings, with comparative toxicity and the molecular mechanisms leading to improved understanding of their toxicity pathways and potential adverse biological effects.

This book represents the latest research efforts to understanding these important DBP-related issues. The authors of the chapters in this book are a multidisciplinary group of scientists and engineers, who are conducting studies in many parts of the world. The chapters in this book address both regulated and emerging DBPs and are organized under the sections on DBP toxicology and health effects, modeling of DBP formation, precursors and reactions involving nitrosamines, and formation of halogenated DBPs. This book will be of interest to researchers, drinking water utility scientists and engineers, toxicologists, epidemiologists, and regulators interested in the formation and control of and exposure to DBPs.

We wish to thank all individuals who served as peer reviewers of our chapter manuscripts. We also wish to gratefully acknowledge the Water Research Foundation for their financial assistance in support of the symposium, and the Association of Environmental Engineering and Science Professors for their assistance in disseminating information on the symposium.

Tanju Karanfil

Department of Environmental Engineering and Earth Sciences
Clemson University
Anderson, South Carolina 29625

Bill Mitch

Department of Civil and Environmental Engineering
Stanford University
Stanford, California 94305

Paul Westerhoff

School of Sustainable Engineering and The Built Environment
Arizona State University
Tempe, Arizona 85287-3005

Yuefeng Xie

Civil and Environmental Engineering Programs
Capital College
The Pennsylvania State University
Middletown, Pennsylvania 17057

Chapter 1

Charting a New Path To Resolve the Adverse Health Effects of DBPs

Michael J. Plewa* and Elizabeth D. Wagner

Department of Crop Sciences and the Center of Advanced Materials for the Purification of Water with Systems, Safe Global Water Institute, University of Illinois at Urbana-Champaign, Urbana, Illinois 61801

*E-mail: mplewa@illinois.edu.

The disinfection of drinking water was an outstanding public health achievement of the 20th century. Disinfection by-products (DBPs) are the unintended consequence of reactions between disinfectants with organic and halide precursors in the source water. Exposure to DBPs is associated with unfavorable health effects from cancer induction to adverse pregnancy outcomes, yet the forcing agents responsible are largely unknown. Of over 600 DBPs identified, only 11 are regulated by the U.S. EPA and in many studies these are not the most toxic DBPs. Identified DBPs represent less than half of the total organic halogen in drinking water and only ~80 DBPs have been evaluated by systematic quantitative toxicological analyses. Epidemiological studies are hampered by problems with exposure metrics and the suite of DBPs present in drinking water. Although the last decade experienced increased interdisciplinary collaborations amongst chemists, biologists, epidemiologists and engineers, resolving the risks of DBPs follows a dated paradigm. A new integrated approach is required to determine the contaminants in source and drinking waters that increase health risks and to provide the foundation for novel disinfection practices. We suggest the following areas in resolving adverse health effects of DBPs: 1) identification and occurrence of emerging DBPs especially iodinated-DBPs and nitrogenous-DBPs, 2) quantitative, comparative *in vitro*

toxicology of DBPs and DBP classes, 3) a nationwide analysis on the toxicity of drinking waters, 4) determining the impact of DBP precursors and mixture effects on water toxicity, 5) understanding the molecular mechanisms of DBP toxicity, 6) identification of sensitive subpopulations to DBP toxicity, 7) employment of analytical chemistry and toxicity information as an essential part of epidemiological studies, and 8) engineering research on disinfection based on toxic outcomes.

Introduction

The disinfection of drinking water to reduce waterborne disease was arguably the greatest public health achievement of the 20th century (1). Chemical disinfectants inactivate pathogens in source waters; however, an unintended consequence is their reaction with natural organic matter (NOM), anthropogenic contaminants and bromide/iodide to form disinfection by-products (DBPs) (2). Factors including the concentration and type of organic matter, pH, temperature, disinfectant type and concentration, and contact time affect the formation of DBPs (3, 4). The most widely employed disinfectants include chlorine, chloramines, chlorine dioxide, and ozone; each disinfectant generates DBPs with a different spectra of chemical classes (5, 6). Since their discovery (7, 8) over 600 DBPs have been chemically characterized (9). This number of DBPs represents only a fraction of the total organic halogen (TOX) generated in disinfected water. Of this number, approximately 80 have undergone systematic, quantitative, comparative toxicological analyses (10–12). By extrapolation from TOX, the total number of DBPs may reach over 2,000. This may be an analytical chemist's dream in the search to identify all possible DBPs. However, it becomes an analytical biologist's dilemma to choose a DBP class or individual compound for comprehensive toxicological analyses. Unfortunately, DBPs represent a regulatory nightmare; of the hundreds of possibly highly toxic DBPs, the U.S. EPA currently regulates only 11 agents (10, 13). A large number of DBPs are cytotoxic, neurotoxic, mutagenic, genotoxic, carcinogenic and teratogenic (10). Epidemiological research demonstrated low but significant associations between disinfected drinking water and adverse health effects (10) including cancer of the bladder (14–16), colon (17, 18) and rectum (19). Some studies report a weak association with adverse pregnancy outcomes and DBPs; yet, the evidence is inconclusive (20–23).

Research into the formation, occurrence, toxicity, epidemiology and engineering processes have resulted in enhanced interest in the adverse impact of DBPs on the environment and the public health (12, 24–35). Although the last decade experienced increased interdisciplinary collaborations amongst chemists, biologists, epidemiologists and engineers, resolving the risks of DBPs follows a dated paradigm. A new integrated approach is required to determine the contaminants in source and drinking waters that increase health risks and to provide the foundation for novel disinfection practices.

Charting a New Pathway for Integrated DBP Research

Although there has been an increase in interdisciplinary studies, current DBP research is in many ways unintegrated. High quality work continues to be published on the formation and identification of emerging DBPs, comparative toxicology and the molecular mechanisms of DBP toxicity, exposure assessment, risk assessment and epidemiology as well as novel engineering processes to control DBPs in drinking water. Yet the future demands that we address complex questions regarding DBPs. Some of these questions include the following. What are the environmental and public health impacts of unidentified DBPs (~70% TOX)? What are the important DBP classes or individual agents that have epidemiological significance? Can we predict human health risks if we know the biological mechanisms of DBP toxicity? Can we integrate research in analytical chemistry, analytical biology and exposure assessment to enhance the resolution of epidemiological studies on the adverse health effects of DBPs? Can we use biological and chemical data to optimize engineering processes for wastewater reuse and desalination? These questions and indeed other crucial questions associated with DBPs may be addressed most efficiently by well planned, focused interdisciplinary science. In this paper we argue for a new pathway of integrated DBP research that includes the following.

- A nationwide drinking water *in vitro* toxicity survey.
- Analytical chemical analyses of the DBPs from the surveyed water samples expressing the highest levels of toxicity.
- Identification of the forcing agents associated with this toxicity.
- Definition of the molecular mechanisms of toxicity for the DBPs identified as forcing agents.
- Identification of selected human biomarkers associated with the molecular mechanisms of toxic DBP forcing agents.
- Identification of susceptible human subpopulations based on bio-markers.
- Definition of the modes of DBP exposure.
- Development of focused epidemiologic studies on exposed populations and integration of data with DBP exposure, toxicity, biomarkers and adverse health outcomes.

The information derived from this integrated interdisciplinary approach may form a cornerstone for optimizing engineering processes for water disinfection.

Nationwide Drinking Water *In Vitro* Toxicity Survey

In 2002 the U.S. EPA published a landmark study commonly referred to as the Nationwide Occurrence Study (36, 37). In this study, novel quantitative analytical methods were developed for measuring the priority DBPs; the occurrence of a wide variety of DBPs in drinking waters throughout the U.S. was determined; the effect of source water and treatment conditions on DBP formation was measured; the fate and transport of these DBPs in the distribution system were studied; and the identification of new DBPs was reported. This study clearly demonstrated

that hundreds of DBPs were differentially distributed in drinking waters within the U.S. However, the Nationwide Occurrence Study did not identify the toxicity of the water samples. In concert with the data generated by the Nationwide Occurrence Study, our laboratory developed mammalian cell microplate-based assays and generated *in vitro*, systematic, analytical, comparative databases on the chronic cytotoxicity and genotoxicity of individual DBPs. To date we have analyzed 87 DBPs (Table I). Their comparative cytotoxicity in Chinese hamster ovary (CHO) cells (LC_{50}) is presented in Figure 1 (carbon-based DBPs) and Figure 2 (nitrogen-containing DBPs). Their comparative genotoxicity is presented in Figure 3. These data provide a direct comparison of the cytotoxicity and genotoxicity of DBPs within a chemical class and among chemical classes and allow for detailed structure activity relationships to be studied by integrating analytical chemistry and analytical biology. The data for Figures 1-3 were published (12, 24–27, 29–31, 33, 38–43) and represent the largest toxicity database for DBPs. This work as well as recent bioanalytical research will provide a foundation to identify forcing agents that contribute to the toxicity of disinfected water.

Analytical Chemistry and the Identification of the Forcing Agents of Drinking Water Toxicity

To use these data most effectively, we propose that a nationwide *in vitro* toxicity survey of drinking waters be conducted. This study would employ bioanalytical assays (12, 44) to identify U.S. drinking waters that express enhanced *in vitro* toxicity. Source water characteristics such as pH, industrial pollutants, pharmaceutical contaminants, total organic carbon (TOC), dissolved organic carbon (DOC), specific UV absorbance, concentrations of I⁻ and Br⁻, disinfectant concentration, coagulants (polyDADMAC) and engineering practice all play a role in the toxicity of finished drinking water (2, 5, 6, 45–54).

Detailed analytical chemical studies for DBPs would be conducted with drinking waters that induce the highest adverse biological effects. The forcing agents (DBPs or classes of DBPs) that are associated with the toxicity would be identified and rank ordered (2).

Molecular Mechanisms of Action of the DBP Forcing Agents Associated with Enhanced Toxicity of Drinking Water

The regulated and unregulated DBPs that are identified as the forcing agents for drinking water toxicity would be the primary candidates for investigating their molecular modes of action. Currently few molecular mechanisms for specific DBP-induced toxicity have been reported. Although many of the adverse biological effects involved the induction of oxidative stress, the mechanisms that generate reactive oxygen species (ROS) follow different pathways and the DBPs may interact with different cellular targets to induce damage. ROS is the resulting insult that causes cellular dysfunction and is a phenomenon, not a mechanism *per se*. Cytotoxicity induced by bromate involves ROS-mediated mitogen activated protein kinases (MAPK) activation (55). The halobenzoquinones generate redox

reactions producing reactive metabolites that damage biological macromolecules (56). The primary cellular target molecule for the monohaloacetic acids (monoHAAs) is glyceraldehyde-3-phosphate dehydrogenase (GAPDH) (57). Inhibition of GAPDH leads to pyruvate starvation and mitochondrial stress that generates ROS (58, 59). New research demonstrated that the monohalonitriles, at non-cytotoxic concentrations, impact the M-phase of the cell cycle and induce hyperploidy in mammalian cells (35). These examples indicate that the molecular mechanisms of DBP toxicity involve a diversity of cellular targets and affect a host of different biological pathways.

Identification of Human Biomarkers Associated with Molecular Mechanisms of Toxic DBPs

In the context of this paper, a biomarker refers to a measurable indicator of an adverse biological state or condition induced or influenced by exposure to a toxic DBP. Biomarkers associated with a cellular mode of toxic action may provide a vehicle to identify adverse effects in an exposed human population. One promising approach is toxicogenomic analyses. With the combination of toxicology and genomics, toxicogenomics represents a powerful interdisciplinary tool to analyze the modulation of gene expression after exposure to a toxic agent. Metabolic pathways involved in the cellular responses to toxins can be identified and provide insight on the underlying biological mechanisms. Toxicogenomic research has identified a number of genes that demonstrate altered expression related to DBP exposure. *In vitro* toxicogenomic analyses of DBPs identified as forcing agents in drinking water toxicity would have high resolving power to identify human biomarkers that may be useful in selecting sensitive populations for epidemiological studies. To provide high resolving power for toxicological metrics, *in vitro* quantitative comparative toxicogenomic analyses must be conducted rather than screening studies (60). These experimental designs will demand that the genomic studies are conducted at non-cytotoxic levels. If DBP concentrations induce cell death, the RNA extracted for microarray analysis would be from dead or dying cells and may not reflect its molecular mechanism of toxicity. Also many toxicogenomic studies employ human tumor cell lines because they are easy to grow and yield large amounts of RNA (61). However, such studies may be difficult to interpret due to the genetic instability of tumor cell lines and their inherent aberrant gene expression. Because of these concerns we encourage the use of nontransformed human cells and treatment conditions with no or low cytotoxicity at equivalent biological effects. In order to generate quantitative comparative toxicogenomic analyses among a series of DBPs it is important to generate transcriptome profiles from cells that were exposed to agents at concentrations normalized to generate equivalent biological responses. As illustrated in Figure 4, the concentrations of IAA, BAA and CAA that induced equivalent genomic DNA damage (50%Tail DNA) were 22 μM , 57 μM and 3.4 mM, respectively (62). Employing concentrations that induce equivalent biological effects allow for the normalization of adverse biological effects and transcriptome profiles within a comparative experimental design and leads to more meaningful toxicogenomic information.

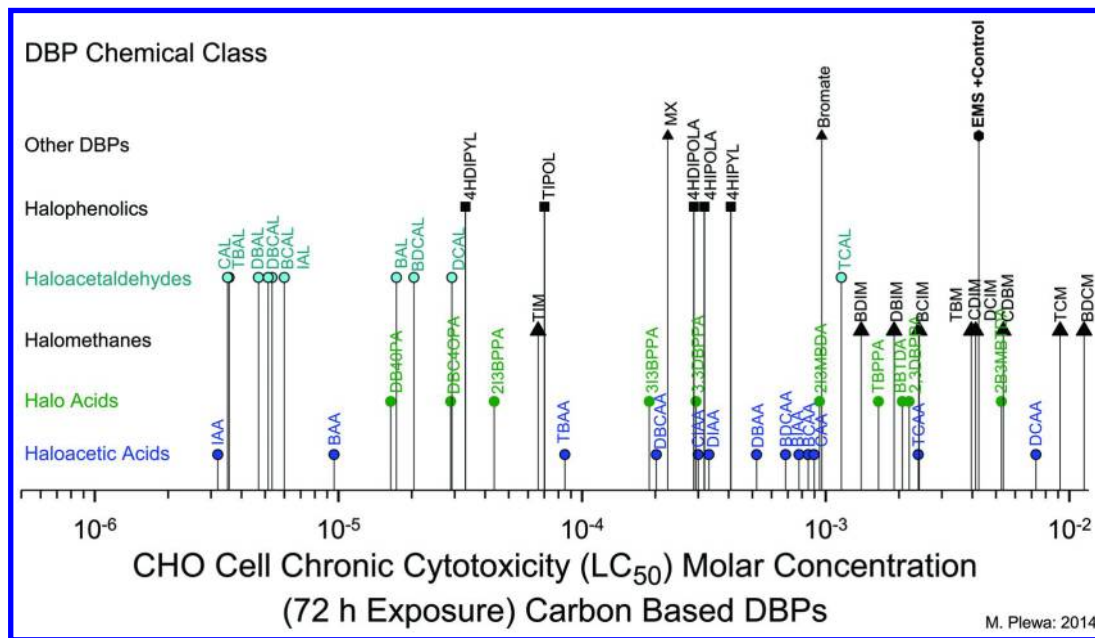


Figure 1. CHO cell chronic cytotoxicity analyses of carbon based DBPs. The abbreviations for the DBPs are listed in Table I. Each DBP is re-presented as its LC₅₀ concentration (50% cell density as compared to the negative control).

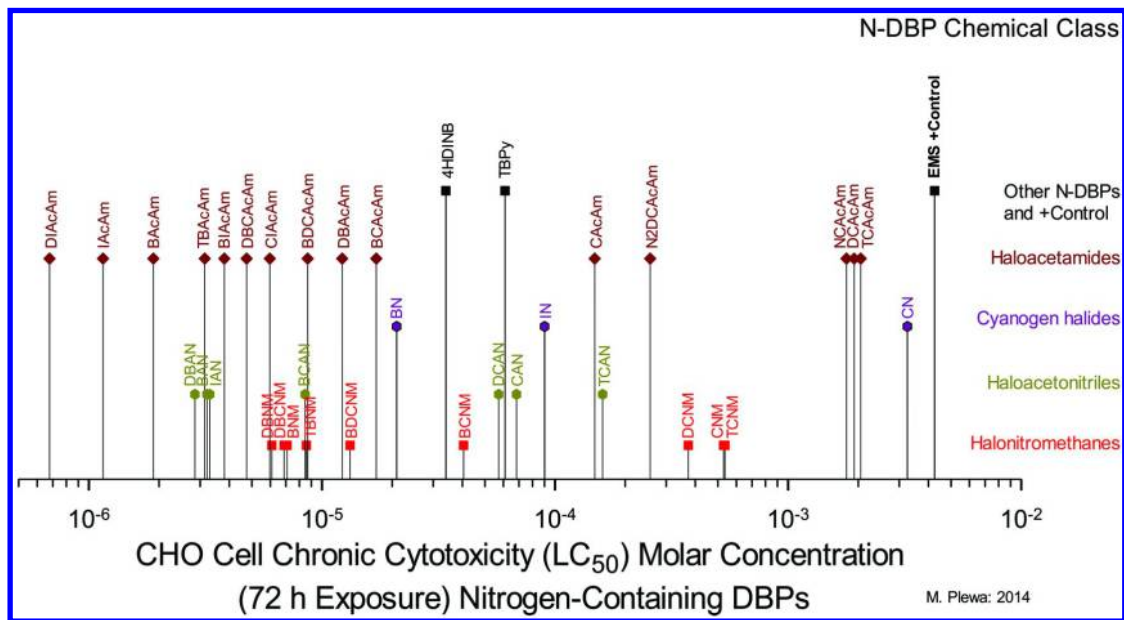


Figure 2. CHO cell chronic cytotoxicity analyses of N-DBPs. The abbreviations for the DBPs are listed in Table I. Each DBP is represented as its LC₅₀ concentration (50% cell density as compared to the negative control).

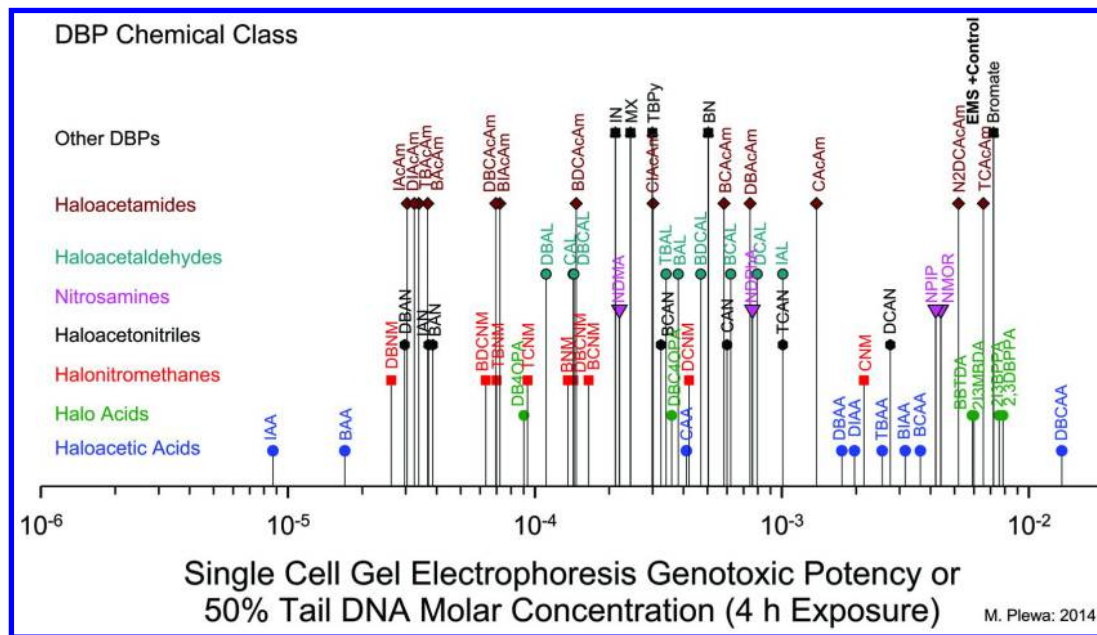


Figure 3. CHO cell genotoxicity analyses of DBPs. The abbreviations for the DBPs are listed in Table I. Each DBP is represented as its midpoint of the SCGE genotoxicity concentration-response curve or its 50%Tail DNA metric.

Table I. DBPs Analyzed for CHO Cell Cytotoxicity and Genotoxicity and Abbreviations

<i>Abbreviation</i>	<i>DBP</i>	<i>Abbreviation</i>	<i>DBP</i>
HAA	Haloacetic Acids	THM	Halomethanes
BAA	Bromoacetic acid	TIM	Triiodomethane
CAA	Chloroacetic acid	DBIM	Dibromiodomethane
IAA	Iodoacetic acid	BCIM	Bromochloriodomethane
DBAA	Dibromoacetic acid	TBM	Tribromomethane
DCAA	Dichloroacetic acid	CDBM	Chlorodibromomethane
DIAA	Diiodoacetic acid	TCM	Trichloromethane
BCAA	Bromochloroacetic acid	BDCM	Bromodichloromethane
BIAA	Bromiodoacetic acid	DCIM	Dichloriodomethane
CIAA	Chloriodoacetic acid	BDIM	Bromodiiodomethane
TBAA	Tribromoacetic acid	CDIM	Chlorodiiodomethane
TCAA	Trichloroacetic acid		
DBCAA	Dibromochloroacetic acid	HAL	Haloacetaldehydes
BDCAA	Bromodichloroacetic acid	BAL	Bromoacetaldehyde
		CAL	Chloroacetaldehyde
HA	Halo Acids	IAL	Iodoacetaldehyde
DB4OPA	3,3-Dibromo-4-oxopentanoic acid	DBAL	Dibromoacetaldehyde
DBC4OPA	3,3-Dibromochloro-4-oxopentanoic acid	DCAL	Dichloroacetaldehyde
2I3BPPA	2-Iodo-3-bromopropenoic acid	BCAL	Bromochloroacetaldehyde
3I3BPPA	3-Iodo-3-bromopropenoic acid	TBAL	Tribromoacetaldehyde
3,3DBPPA	3,3-Dibromopropenoic acid	TCAL	Trichloroacetaldehyde
2I3MBDA	2-Iodo-3-methylbutenedioic acid	DBCAL	Dibromochloroacetaldehyde
TBPPA	Tribromopropenoic acid	BDCAL	Bromodichloroacetaldehyde
BBTDA	2-Bromobutenedioic acid		
2,3DBPPA	2,3-Dibromopropenoic acid	HNM	Halonitromethanes

Continued on next page.

Table I. (Continued). DBPs Analyzed for CHO Cell Cytotoxicity and Genotoxicity and Abbreviations

<i>Abbreviation</i>	<i>DBP</i>	<i>Abbreviation</i>	<i>DBP</i>
2B3MBTDA	2-Bromo-3-methylbutenedioic acid	BNM	Bromonitromethane
		CNM	Chloronitromethane
		DBNM	Dibromonitromethane
HPYL	Halophenolics	DCNM	Dichloronitromethane
		BCNM	Bromochloronitromethane
4HIPOLA	4-Hydroxy-3-iodo-1-phenolic acid	TBNM	Tribromonitromethane
TIPOL	2,4,6-Triiodo-1-phenol	TCNM	Trichloronitromethane
		BDCNM	Bromodichloronitromethane
		DBCNM	Dibromochloronitromethane
HAN	Haloacetonitriles		
BAN	Bromoacetonitrile		
CAN	Chloroacetonitrile	HAcAm	Haloacetamides
IAN	Iodoacetonitrile	BAcAm	Bromoacetamide
DBAN	Dibromoacetonitrile	CACAm	Chloroacetamide
DCAN	Dichloroacetonitrile	IACAm	Iodoacetamide
BCAN	Bromochloroacetonitrile	DBAcAm	Dibromoacetamide
TCAN	Trichloroacetonitrile	DCAcAm	Dichloroacetamide
		DIACAm	Diiodoacetamide
CN	Cyanogen Halides	BIACAm	Bromoiodoacetamide
BN	Cyanogen Bromide	CIACAm	Chloroiodoacetamide
CN	Cyanogen Chloride	BCAcAm	Bromochloroacetamide
IN	Cyanogen Iodide	TBAcAm	Tribromoacetamide
		TCAcAm	Trichloroacetamide
NA	Nitrosamines	DBCACAm	Dibromochloroacetamide
NDMA	<i>N</i> -nitrosodimethylamine	BDCACAm	Bromodichloroacetamide
NDPhA	<i>N</i> -nitrosodiphenylamine	N2DCAcAm	<i>N,N</i> -Dichloroacetamide
NPIP	<i>N</i> -nitrosopiperidine	NCAcAm	<i>N</i> -Chloroacetamide
NMOR	<i>N</i> -nitrosomorpholine		

Continued on next page.

Table I. (Continued). DBPs Analyzed for CHO Cell Cytotoxicity and Genotoxicity and Abbreviations

Abbreviation	DBP	Abbreviation	DBP
		Other DBPs	
		Bromate	Bromate
		MX	3-chloro-4-(dichloromethyl)-5-hydroxy-2[5H]-furanone
		4HDINB	4-Hydroxy-3,5-diiodo-1-nitrobenzene
		TBPy	Tribromopyrrole

We conducted a series of quantitative gene array studies on the monoHAAs using quantitative real-time PCR (qRT-PCR) focused on pathways involving DNA damage and repair as well as pathways involved in responses to oxidative stress. Examples of pathways uncovered by transcriptome profiles of nontransformed human small intestine epithelial cells, line FHs 74 Int, after exposure to non-cytotoxic concentrations of the monoHAAs is presented in Table II (59, 62). Expression in DNA repair genes were modulated especially those involved in double strand DNA (dsDNA) damage repair (62, 63). These data are especially important because there is a strong association between p53, ATM, Brca1 and Brca2 proteins and dsDNA break repair pathways and tumorigenesis (64). Recently IAA was reported to induce malignant transformation and tumor induction (65).

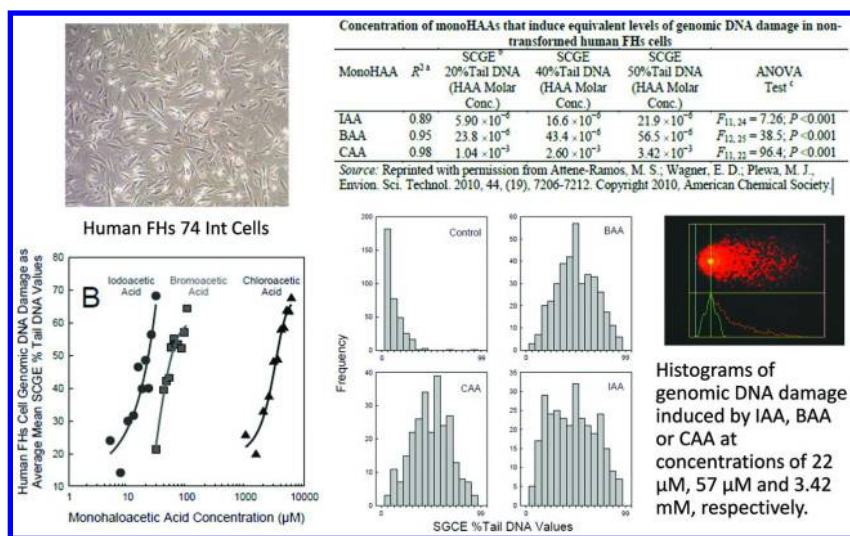


Figure 4. The selection of concentrations of the monoHAAs that generated equivalent biological effects (genomic DNA damage) in nontransformed human FHs74 Int cells for use in toxicogenomic studies.

Table II. MonoHAA-Induced Transcriptome Profile Pathways

<i>Cell Pathway</i>	<i>Monohaloacetic Acids</i>		
	<i>BAA</i>	<i>CAA</i>	<i>IAA</i>
ATM Signaling Pathway	•	•	•
Cell Cycle Control	•	•	
Cyclins and Cell Cycle Regulation		•	
FC Epsilon RI Signaling Pathway			•
MAPK Signaling Pathway	•		•
p53 Signaling Pathway	•		•
BRCA1, BRCA2 and ATR Mediated Cancer Susceptibility and dsDNA Repair Pathways	•	•	•
Nrf2/ARE-Dependent ROS Pathways	•	•	•
PTGS2 (COX2)-Mediated Pathways	•	•	•
MPO, LPO and NOX5 ROS Pathways	•	•	•
GRS/GSR Pathway	•	•	•
Peroxiredoxin Oxidative Stress Pathway	•	•	

Toxicogenomic profiles combined with enzyme inhibition studies and ATP quantification demonstrated the impact of the monoHAAs on energy metabolism (Table II) (58, 59). These studies uncovered other relevant pathways and potential human biomarkers for DBP-mediated health effects. These pathways include the hypohalous acid generating peroxidase enzymes lactoperoxidase (LPO) and myeloperoxidase (MPO), nicotinamide adenine dinucleotide phosphate (NADPH)-dependent oxidase 5 (NOX5), and PTGS2 (COX-2) mediated arachidonic acid metabolism. Many pathways of DBP toxic action involve the generation of ROS; the up-regulation of the Antioxidant Response Element (ARE) is an exceedingly sensitive and useful bioanalytical marker (44, 59, 66).

Identification of Susceptible Subpopulations Based on Human Biomarkers Associated with the Molecular Mechanisms of DBP Toxicity

From the gene array studies and from gene reporter studies suitable human molecular biomarkers are emerging that may be useful in identifying subpopulations that may have enhanced sensitivity to DBPs. These biomarker indicators include GAPDH polymorphisms (67), BRCA1 and BRCA2 polymorphisms (64), p53 polymorphisms (64), elevated COX2 expression (59) and cyclooxygenase-2 mediated production of PGE₂ (prostaglandin E₂) and COX2 polymorphisms (68), enhanced ARE expression (69), glutathione-S-transferase polymorphisms (70, 71), and DNA repair gene polymorphisms (72). These traits

within a subpopulation may make individuals more susceptible to the toxic action of DBPs and lead to adverse health outcomes. In concert with characterizing the number and concentrations of toxic DBPs as well as the toxicity of the drinking water, individuals expressing one or more of these polymorphisms may have heightened sensitivity and greater risk of adverse health effects. The use of these and other polymorphisms that interface the molecular pathways of toxicity of DBPs may provide greater resolution to epidemiological studies on DBPs and health issues.

Definition of DBP Exposure in Selected Waters with High Toxicity

In most epidemiological studies, the DBP metric is the concentration of trihalomethanes (THMs) in drinking water (73). Few studies have compared the number or concentrations of other DBPs or DBP classes with the overall toxicity of water samples. In the Health Impacts of Long-Term Exposure to Disinfection By-Products in Drinking Water (HIWATE) program, 95 DBPs were identified among 11 water samples from several cities in Europe. We found a correlation between the number of DBPs in the water samples and the induction of cytotoxicity in mammalian cells (74). Both cytotoxicity (Figure 5A) and genomic DNA damage (Figure 5B) demonstrated a positive association with the relative DBP concentration for each HIWATE water sample. The concentration of THMs alone may not be the best or most appropriate metric to quantify DBP exposure for drinking waters and other more comprehensive metrics are needed (73).

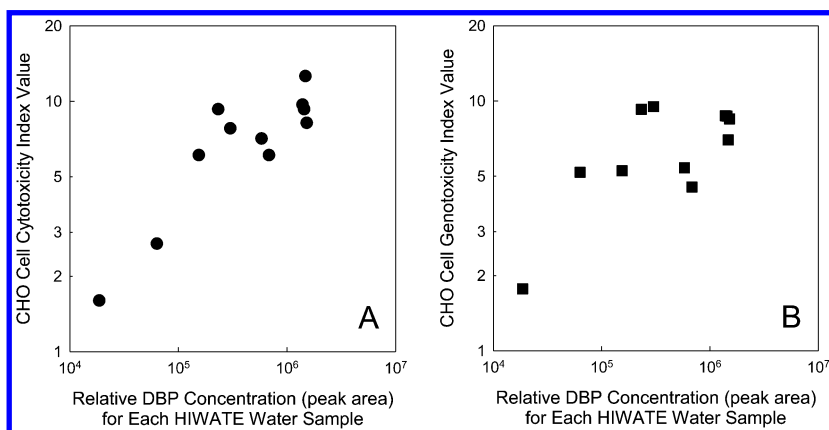


Figure 5. Mammalian cell cytotoxicity (A) and genotoxicity (B) responses as a function of the relative concentrations of DBPs in 11 drinking water samples.

Quantifying human exposure to DBPs is essential for precise risk assessment in epidemiological studies. Future studies would be aided by the development of metrics of exposure that would link the impact of DBPs in individuals with a

toxic response. An example of this was a study that reported genotoxic effects of swimmers in chlorinated pools (75). Enhanced bladder cancer rates were observed in swimmers exposed to disinfected pool water (76). Other biomarkers for DBP exposure include urinary trichloroacetic acid measurements in individuals exposed to DBPs (77–79). In a commentary, Kogevinas stated, “Future studies should be large, combine ecological and individual information on exposure, evaluate multiple chemicals and not only THMs, and evaluate multiple routes. In a situation of relatively low risks, even relatively small improvements in exposure assessment may make significant differences in the studies. The use of new evidence on mechanisms of these compounds including use of genotyping to evaluate effect modification should be promoted (73).”

Integration of Epidemiological Studies with DBP Exposure, Toxicity, Biomarkers, and Adverse Health Outcomes

Epidemiology is essential to our understanding of the role of DBP exposure in human disease. These environmental micropollutants pose a vexing problem. DBPs express a wide diversity of toxic response; however, this toxicity is spread across many hundreds of individual agents within a complex mixture. Most of the DBPs that comprise TOX are unknown. Of those that are known, only a relatively small group has been systematically analyzed for their capacity to induce adverse biological effects. Epidemiological advances leading to an understanding of health risks posed by DBPs will only occur with concomitant advances in exposure science, biomarkers of internal dose, biomarkers of affected pathways and biomarkers of population variability in susceptibility (80).

Creative approaches to the epidemiology of DBPs demand the development of studies that identify the forcing agents leading to the toxicity of drinking water as well as the identification of population segments of increased risk. These susceptible populations may be identified as susceptible because of demographics, genetics and lifestyles (1). In general, using a focused epidemiological approach will improve the quality of evidence. Achieving these improvements will require systematic, long-term interdisciplinary studies (Figure 6).

Conclusion

DBP exposure is a constant in modern life. Every time you take a drink of water, every time you prepare food, take a shower or swim in a swimming pool you are exposed to DBPs. The level of concern of the adverse health effects of these toxic agents is increasing with the increased level of compromised source waters used in the generation of drinking water. With the advent of climate change-mediated drought, increased reliance upon direct or indirect wastewater recycling or disinfected desalinated water, new emerging DBP classes are entering the drinking water stream.

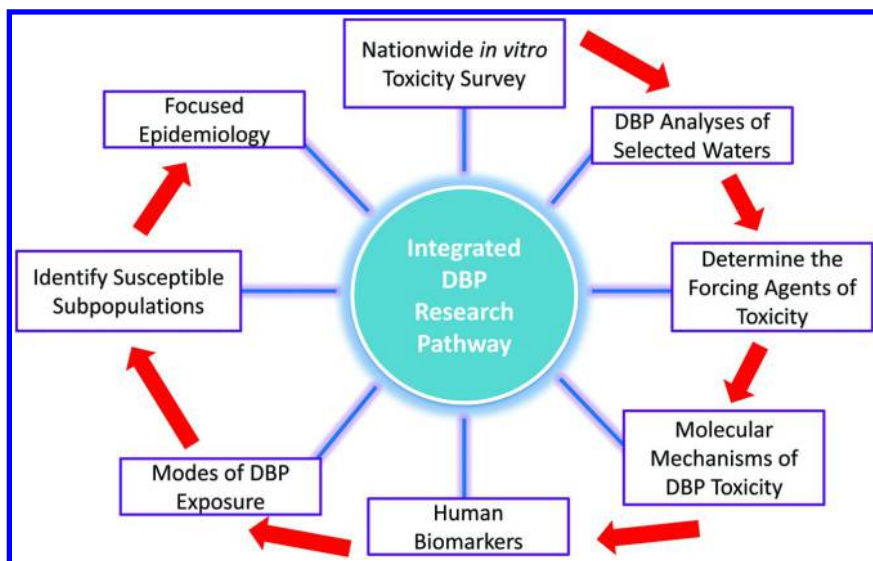


Figure 6. A new pathway for integrated DBP research.

Biologists, chemists and engineers must form teams to address problems posed by hazardous DBPs and other micropollutants in water. Systematic, comparative *in vitro* toxicology must be integrated as a feed-back information loop into innovative engineering processes to remove and degrade micropollutants and disinfect water. The biological mechanisms of DBP toxicity must be included in epidemiological studies. We must develop systems to prevent unintended toxic consequences as we move forward in the implementation of new methods to desalinate, decontaminate, reuse and disinfect water.

References

1. Calderon, R. L. The epidemiology of chemical contaminants of drinking water. *Food Chem. Toxicol.* **2000**, *38*, S13–20.
2. Richardson, S. D.; Postigo, C. Drinking water disinfection by-products. In *Emerging Organic Contaminants and Human Health*; Springer: Berlin, 2012; pp 93–137.
3. Singer, P. C. Control of disinfection by-products in drinking water. *J. Environ. Eng.* **1994**, *120*, 727–744.
4. Hong, H.; Xiong, Y.; Ruan, M.; Liao, F.; Lin, H.; Liang, Y. Factors affecting THMs, HAAs and HNMs formation of Jin Lan Reservoir water exposed to chlorine and monochloramine. *Sci. Total Environ.* **2013**, *444*, 196–204.
5. Zhang, X.; Echigo, S.; Minear, R. A.; Plewa, M. J., Characterization and comparison of disinfection by-products of four major disinfectants. In *Natural Organic Matter and Disinfection By-Products: Characterization and Control in Drinking Water*; Barrett, S. E., Krasner, S. W., Amy, G. L., Eds.; American Chemical Society: Washington, DC, 2000; pp 299–314.

6. Hua, G. H.; Reckhow, D. A. Comparison of disinfection byproduct formation from chlorine and alternative disinfectants. *Water Res.* **2007**, *41*, 1667–1678.
7. Rook, J. J. Formation of haloforms during chlorination of natural waters. *Water Treat. Exam.* **1974**, *23*, 234–243.
8. Bellar, T. A.; Lichtenbert, J. J.; Kroner, R. C. The occurrence of organohalides in chlorinated drinking waters. *J. Am. Water Works Assoc.* **1974**, *66*, 703–706.
9. Richardson, S. D., Disinfection by-products: formation and occurrence in drinking water. In *Encyclopedia of Environmental Health*; Nriagu, J. O., Ed.; Elsevier: Burlington, 2011; Vol. 1, pp 110–136.
10. Richardson, S. D.; Plewa, M. J.; Wagner, E. D.; Schoeny, R.; DeMarini, D. M. Occurrence, genotoxicity, and carcinogenicity of regulated and emerging disinfection by-products in drinking water: A review and roadmap for research. *Mutat. Res.* **2007**, *636*, 178–242.
11. Plewa, M. J.; Wagner, E. D. Drinking water disinfection by-products: comparative mammalian cell cytotoxicity and genotoxicity. In *Encyclopedia of Environmental Health*; Nriagu, J. O., Ed.; Elsevier: Burlington, 2011; Vol. 1, pp 806–812.
12. Plewa, M. J.; Wagner, E. D. *Mammalian Cell Cytotoxicity and Genotoxicity of Disinfection By-Products*; Water Research Foundation: Denver, CO, 2009; p 134.
13. U. S. Environmental Protection Agency, National primary drinking water regulations: Stage 2 disinfectants and disinfection byproducts rule. *Fed. Regist.* **2006**, *71*, 387–493.
14. Costet, N.; Villanueva, C. M.; Jaakkola, J. J.; Kogevinas, M.; Cantor, K. P.; King, W. D.; Lynch, C. F.; Nieuwenhuijsen, M. J.; Cordier, S. Water disinfection by-products and bladder cancer: is there a European specificity? A pooled and meta-analysis of European case-control studies. *Occup. Environ. Med.* **2011**, *68*, 379–385.
15. Villanueva, C. M.; Cantor, K. P.; Cordier, S.; Jaakkola, J. J.; King, W. D.; Lynch, C. F.; Porru, S.; Kogevinas, M. Disinfection byproducts and bladder cancer: a pooled analysis. *Epidemiology* **2004**, *15*, 357–367.
16. Bove, G. E.; Rogerson, P. A.; Vena, J. E. Case-control study of the effects of trihalomethanes on urinary bladder cancer risk. *Arch. Environ. Occup. Health* **2007**, *62*, 39–47.
17. King, W. D.; Marrett, L. D.; Woolcott, C. G. Case-control study of colon and rectal cancers and chlorination by-products in treated water. *Cancer Epidemiol., Biomarkers Prev.* **2000**, *9*, 813–818.
18. Rahman, M. B.; Driscoll, T.; Cowie, C.; Armstrong, B. K. Disinfection by-products in drinking water and colorectal cancer: a meta-analysis. *Int. J. Epidemiol.* **2010**, *39*, 733–745.
19. Bove, G. E., Jr.; Rogerson, P. A.; Vena, J. E. Case control study of the geographic variability of exposure to disinfectant byproducts and risk for rectal cancer. *Int. J. Health Geogr.* **2007**, *6*, 18.
20. Bove, F.; Shim, Y.; Zeitz, P. Drinking water contaminants and adverse pregnancy outcomes: a review. *Environ. Health Perspect.* **2002**, *110* (Suppl 1), 61–74.

21. Grellier, J.; Bennett, J.; Patelarou, E.; Smith, R. B.; Toledano, M. B.; Rushton, L.; Briggs, D. J.; Nieuwenhuijsen, M. J. Exposure to disinfection by-products, fetal growth, and prematurity: a systematic review and meta-analysis. *Epidemiology* **2010**, *21*, 300–313.
22. Colman, J.; Rice, G. E.; Wright, J. M.; Hunter, E. S., III; Teuschler, L. K.; Lipscomb, J. C.; Hertzberg, R. C.; Simmons, J. E.; Fransen, M.; Osier, M.; Narotsky, M. G. Identification of developmentally toxic drinking water disinfection byproducts and evaluation of data relevant to mode of action. *Toxicol. Appl. Pharmacol.* **2011**, *254*, 100–126.
23. Rivera-Nunez, Z.; Wright, J. M. Association of brominated trihalomethane and haloacetic acid exposure with fetal growth and preterm delivery in Massachusetts. *J. Occup. Environ. Med.* **2013**, *55*, 1125–1134.
24. Plewa, M. J.; Wagner, E. D.; Jazwierska, P.; Richardson, S. D.; Chen, P. H.; McKague, A. B. Halonitromethane drinking water disinfection byproducts: chemical characterization and mammalian cell cytotoxicity and genotoxicity. *Environ. Sci. Technol.* **2004**, *38*, 62–68.
25. Plewa, M. J.; Wagner, E. D.; Richardson, S. D.; Thruston, A. D., Jr.; Woo, Y. T.; McKague, A. B. Chemical and biological characterization of newly discovered iodoacid drinking water disinfection byproducts. *Environ. Sci. Technol.* **2004**, *38*, 4713–4722.
26. Muellner, M. G.; Wagner, E. D.; McCalla, K.; Richardson, S. D.; Woo, Y. T.; Plewa, M. J. Haloacetonitriles vs. regulated haloacetic acids: Are nitrogen containing DBPs more toxic? *Environ. Sci. Technol.* **2007**, *41*, 645–651.
27. Plewa, M. J.; Muellner, M. G.; Richardson, S. D.; Fasano, F.; Buettner, K. M.; Woo, Y. T.; McKague, A. B.; Wagner, E. D. Occurrence, synthesis and mammalian cell cytotoxicity and genotoxicity of haloacetamides: an emerging class of nitrogenous drinking water disinfection by-products. *Environ. Sci. Technol.* **2008**, *42*, 955–961.
28. Pals, J.; Clay, J.; Komaki, Y.; Marinas, B. J.; Wagner, E. D.; Plewa, M. J. Cyanogen halide drinking water disinfection byproducts. *Environ. Mol. Mutagen.* **2009**, *50*, 578.
29. Plewa, M. J.; Simmons, J. E.; Richardson, S. D.; Wagner, E. D. Mammalian cell cytotoxicity and genotoxicity of the haloacetic acids, a major class of drinking water disinfection by-products. *Environ. Mol. Mutagen.* **2010**, *51*, 871–878.
30. Wagner, E. D.; Hsu, K. M.; Lagunas, A.; Mitch, W. A.; Plewa, M. J. Comparative genotoxicity of nitrosamine drinking water disinfection byproducts in Salmonella and mammalian cells. *Mutat. Res.* **2012**, *741*, 109–115.
31. Kimura, S. Y.; Komaki, Y.; Plewa, M. J.; Mariñas, B. J. Chloroacetonitrile and N,2-dichloroacetamide formation from the reaction of chloroacetaldehyde and monochloramine in water. *Environ. Sci. Technol.* **2013**, *47*, 12382–12390.
32. Escobar-Hoyos, L. F.; Hoyos-Giraldo, L. S.; Londono-Velasco, E.; Reyes-Carvajal, I.; Saavedra-Trujillo, D.; Carvajal-Varona, S.; Sanchez-Gomez, A.; Wagner, E. D.; Plewa, M. J. Genotoxic and clastogenic effects

of monohaloacetic acid drinking water disinfection by-products in primary human lymphocytes. *Water Res.* **2013**, *47*, 3282–3290.

33. Wagner, E. D.; Osiol, J.; Mitch, W. A.; Plewa, M. J. Comparative in vitro toxicity of nitrosamines and nitramines associated with amine-based carbon capture and storage. *Environ. Sci. Technol.* **2014**, *48*, 8203–8211.
34. Ali, A.; Kurzawa-Zegota, M.; Najafzadeh, M.; Gopalan, R. C.; Plewa, M. J.; Anderson, D. Effect of drinking water disinfection by-products in human peripheral blood lymphocytes and sperm. *Mutat. Res.* **2014**, *770*, 136–143.
35. Komaki, Y.; Marinas, B. J.; Plewa, M. J. Toxicity of drinking water disinfection by-products: cell cycle alterations induced by monohaloacetoneitriles. *Environ. Sci. Technol.* **2014**, *48*, 11662–11669.
36. Weinberg, H. S.; Krasner, S. W.; Richardson, S. D.; Thruston, A. D., Jr. *The Occurrence of Disinfection By-Products (DBPs) of Health Concern in Drinking Water: Results of a Nationwide DBP Occurrence Study*; EPA/600/R02/068; U.S. Environmental Protection Agency National Exposure Research Laboratory: Athens, GA, 2002; pp 1–460.
37. Krasner, S. W.; Weinberg, H. S.; Richardson, S. D.; Pastor, S. J.; Chinn, R.; Scilimenti, M. J.; Onstad, G. D.; Thruston, A. D., Jr. The occurrence of a new generation of disinfection by-products. *Environ. Sci. Technol.* **2006**, *40*, 7175–7185.
38. Kargalioglu, Y.; McMillan, B. J.; Minear, R. A.; Plewa, M. J., A new assessment of the cytotoxicity and genotoxicity of drinking water disinfection by-products. In *Natural Organic Matter and Disinfection By-Products: Characterization and Control in Drinking Water*; Barrett, S. E., Krasner, S. W., Amy, G. L., Eds.; American Chemical Society: Washington, D.C., 2000; pp 16–27.
39. Plewa, M. J.; Kargalioglu, Y.; Vanker, D.; Minear, R. A.; Wagner, E. D. Mammalian cell cytotoxicity and genotoxicity analysis of drinking water disinfection by-products. *Environ. Mol. Mutagen.* **2002**, *40*, 134–142.
40. Richardson, S. D.; Thruston, A. D., Jr.; Rav-Acha, C.; Groisman, L.; Popilevsky, I.; Juraev, O.; Glezer, V.; McKague, A. B.; Plewa, M. J.; Wagner, E. D. Tribromopyrrole, brominated acids, and other disinfection byproducts produced by disinfection of drinking water rich in bromide. *Environ. Sci. Technol.* **2003**, *37*, 3782–3793.
41. Plewa, M. J.; Wagner, E. D.; Muellner, M. G.; Hsu, K. M.; Richardson, S. D., Comparative mammalian cell toxicity of N-DBPs and C-DBPs. In *Occurrence, Formation, Health Effects and Control of Disinfection By-Products in Drinking Water*; Karanfil, T., Krasner, S. W., Westerhoff, P., Xie, Y., Eds. American Chemical Society: Washington, D.C., 2008; Vol. 995, pp 36–50.
42. Richardson, S. D.; Fasano, F.; Ellington, J. J.; Crumley, F. G.; Buettner, K. M.; Evans, J. J.; Blount, B. C.; Silva, L. K.; Waite, T. J.; Luther, G. W.; McKague, A. B.; Miltner, R. J.; Wagner, E. D.; Plewa, M. J. Occurrence and mammalian cell toxicity of iodinated disinfection byproducts in drinking water. *Environ. Sci. Technol.* **2008**, *42*, 8330–8338.

43. Kimura, S. Y. *Formation of (Halo)Acetamides and (Halo)Acetonitriles from the Reaction of Monochloramine and (Halo)Acetaldehydes in Water*. University of Illinois at Urbana-Champaign, Urbana, IL, 2013.
44. Escher, B. I.; van Daele, C.; Dutt, M.; Tang, J. Y.; Altenburger, R. Most oxidative stress response in water samples comes from unknown chemicals: the need for effect-based water quality trigger values. *Environ. Sci. Technol.* **2013**, *47*, 7002–7011.
45. Yang, Y.; Komaki, Y.; Kimura, S.; Hu, H. Y.; Wagner, E. D.; Marinas, B. J.; Plewa, M. J. Toxic impact of bromide and iodide on drinking water disinfected with chlorine or chloramines. *Environ. Sci. Technol.* **2014**, *48*, 12362–12369.
46. World Health Organization. *Guidelines for Drinking Water Quality*, 4th ed.; United Nations: Geneva, Switzerland, 2011; Vol. 1, p 541.
47. Duirk, S. E.; Lindell, C.; Cornelison, C.; Kormos, J. L.; Ternes, T. A.; Attene-Ramos, M. S.; Osiol, J.; Wagner, E. D.; Plewa, M. J.; Richardson, S. D. Formation of toxic iodinated disinfection by-products from compounds used in medical imaging. *Environ. Sci. Technol.* **2011**, *45*, 6845–6854.
48. Postigo, C.; Richardson, S. D. Transformation of pharmaceuticals during oxidation/disinfection processes in drinking water treatment. *J. Hazard. Mater.* **2014**, *279*, 461–475.
49. Shen, R.; Andrews, S. A. Demonstration of 20 pharmaceuticals and personal care products (PPCPs) as nitrosamine precursors during chloramine disinfection. *Water Res.* **2011**, *45*, 944–952.
50. Schmidt, C. K.; Brauch, H. J. N,N-dimethylsulfamide as precursor for N-nitrosodimethylamine (NDMA) formation upon ozonation and its fate during drinking water treatment. *Environ. Sci. Technol.* **2008**, *42*, 6340–6346.
51. Wilczak, A.; Assadi-Rad, A.; Lai, H. H.; Hoover, L. L.; Smith, J. F.; Berger, R.; Rodigari, F.; Beland, J. W.; Lazzelle, L. J.; Kinicannon, E. G.; Baker, H.; Heaney, C. T. Formation of NDMA in chloraminated water coagulated with DADMAC cationic polymer. *J. Am. Water Work Assoc.* **2003**, *95*, 94–106.
52. Padhye, L.; Luzinova, Y.; Cho, M.; Mizaikoff, B.; Kim, J. H.; Huang, C. H. PolyDADMAC and dimethylamine as precursors of N-nitrosodimethylamine during ozonation: reaction kinetics and mechanisms. *Environ. Sci. Technol.* **2011**, *45*, 4353–4359.
53. Kemper, J. M.; Walse, S. S.; Mitch, W. A. Quaternary amines as nitrosamine precursors: a role for consumer products? *Environ. Sci. Technol.* **2010**, *44*, 1224–1231.
54. Park, S.-H.; Piyachaturawat, P.; Taylor, A. E.; Huang, C.-H. Potential N-nitrosodimethylamine (NDMA) formation from amine-based water treatment polymers in the reactions with chlorine-based oxidants and nitrosifying agents. *Water Sci. Technol.: Water Supply* **2009**, *9*, 279–288.
55. Zhang, X.; De Silva, D.; Sun, B.; Fisher, J.; Bull, R. J.; Cotruvo, J. A.; Cummings, B. S. Cellular and molecular mechanisms of bromate-induced cytotoxicity in human and rat kidney cells. *Toxicology* **2010**, *269*, 13–23.
56. Du, H.; Li, J.; Moe, B.; McGuigan, C. F.; Shen, S.; Li, X. F. Cytotoxicity and oxidative damage induced by halobenzoquinones to T24 bladder cancer cells. *Environ. Sci. Technol.* **2013**, *47*, 2823–2830.

57. Pals, J.; Ang, J.; Wagner, E. D.; Plewa, M. J. Biological mechanism for the toxicity of haloacetic acid drinking water disinfection byproducts. *Environ. Sci. Technol.* **2011**, *45*, 5791–5797.
58. Dad, A.; Jeong, C. H.; Pals, J.; Wagner, E. D.; Plewa, M. J. Pyruvate remediation of cell stress and genotoxicity induced by haloacetic acid drinking water disinfection byproducts. *Environ. Mol. Mutagen.* **2013**, *54*, 629–637.
59. Pals, J.; Attene-Ramos, M. S.; Xia, M.; Wagner, E. D.; Plewa, M. J. Human cell toxicogenomic analysis linking reactive oxygen species to the toxicity of monohaloacetic acid drinking water disinfection byproducts. *Environ. Sci. Technol.* **2013**, *47*, 12514–12523.
60. Collins, F. S.; Gray, G. M.; Bucher, J. R. Toxicology. Transforming environmental health protection. *Science* **2008**, *319*, 906–907.
61. Le Fevre, A. C.; Boitier, E.; Marchandau, J. P.; Sarasin, A.; Thybaud, V. Characterization of DNA reactive and non-DNA reactive anticancer drugs by gene expression profiling. *Mutat. Res.* **2007**, *619*, 16–29.
62. Attene-Ramos, M. S.; Wagner, E. D.; Plewa, M. J. Comparative human cell toxicogenomic analysis of monohaloacetic acid drinking water disinfection byproducts. *Environ. Sci. Technol.* **2010**, *44*, 7206–7212.
63. Muellner, M. G.; Attene-Ramos, M. S.; Hudson, M. E.; Wagner, E. D.; Plewa, M. J. Human cell toxicogenomic analysis of bromoacetic acid: a regulated drinking water disinfection by-product. *Environ. Mol. Mutagen.* **2010**, *51*, 205–214.
64. Khanna, K. K.; Jackson, S. P. DNA double-strand breaks: signaling, repair and the cancer connection. *Nat. Genet.* **2001**, *27*, 247–254.
65. Wei, X.; Wang, S.; Zheng, W.; Wang, X.; Liu, X.; Jiang, S.; Pi, J.; Zheng, Y.; He, G.; Qu, W. Drinking water disinfection byproduct iodoacetic acid induces tumorigenic transformation of NIH3T3 cells. *Environ. Sci. Technol.* **2013**, *47*, 5913–5920.
66. Neale, P. A.; Antony, A.; Bartkow, M. E.; Farre, M. J.; Heitz, A.; Kristiana, I.; Tang, J. Y.; Escher, B. I. Bioanalytical assessment of the formation of disinfection byproducts in a drinking water treatment plant. *Environ. Sci. Technol.* **2012**, *46*, 10317–10325.
67. Butterfield, D. A.; Hardas, S. S.; Lange, M. L. B. Oxidatively modified glyceraldehyde-3-phosphate dehydrogenase (GAPDH) and Alzheimer's disease: many pathways to neurodegeneration. *J. Alzheimers Dis.* **2010**, *20*, 369–393.
68. Pereira, C.; Pimentel-Nunes, P.; Brandao, C.; Moreira-Dias, L.; Medeiros, R.; Dinis-Ribeiro, M. COX-2 polymorphisms and colorectal cancer risk: a strategy for chemoprevention. *Eur. J. Gastroenterol. Hepatol.* **2010**, *22*, 607–613.
69. Wang, X.; Tomso, D. J.; Chorley, B. N.; Cho, H. Y.; Cheung, V. G.; Kleeberger, S. R.; Bell, D. A. Identification of polymorphic antioxidant response elements in the human genome. *Hum. Mol. Genet.* **2007**, *16*, 1188–1200.
70. Hayes, J. D.; Strange, R. C. Glutathione S-transferase polymorphisms and their biological consequences. *Pharmacology* **2000**, *61*, 154–166.

71. Cantor, K. P.; Villanueva, C. M.; Silverman, D. T.; Figueroa, J. D.; Real, F. X.; Garcia-Closas, M.; Malats, N.; Chanock, S.; Yeager, M.; Tardon, A.; Garcia-Closas, R.; Serra, C.; Carrato, A.; Castano-Vinyals, G.; Samanic, C.; Rothman, N.; Kogevinas, M. Polymorphisms in GSTT1, GSTZ1, and CYP2E1, disinfection by-products, and risk of bladder cancer in Spain. *Environ. Health Perspect.* **2010**, *118*, 1545–1550.
72. Andrew, A. S.; Karagas, M. R.; Nelson, H. H.; Guarrera, S.; Polidoro, S.; Gamberini, S.; Sacerdote, C.; Moore, J. H.; Kelsey, K. T.; Demidenko, E.; Vineis, P.; Matullo, G. DNA repair polymorphisms modify bladder cancer risk: a multi-factor analytic strategy. *Hum. Hered.* **2008**, *65*, 105–118.
73. Kogevinas, M. Epidemiological approaches in the investigation of environmental causes of cancer: the case of dioxins and water disinfection by-products. *Environ. Health* **2011**, *10* (Suppl 1), S3.
74. Jeong, C. H.; Wagner, E. D.; Siebert, V. R.; Anduri, S.; Richardson, S. D.; Daiber, E. J.; McKague, A. B.; Kogevinas, M.; Villanueva, C. M.; Goslan, E. H.; Luo, W.; Isabelle, L. M.; Pankow, J. F.; Grazuleviciene, R.; Cordier, S.; Edwards, S. C.; Righi, E.; Nieuwenhuijsen, M. J.; Plewa, M. J. The occurrence and toxicity of disinfection byproducts in European drinking waters in relation with the HIWATE epidemiology study. *Environ. Sci. Technol.* **2012**, *46*, 12120–12128.
75. Kogevinas, M.; Villanueva, C. M.; Font-Ribera, L.; Liviac, D.; Bustamante, M.; Espinoza, F.; Nieuwenhuijsen, M. J.; Espinosa, A.; Fernandez, P.; DeMarini, D. M.; Grimalt, J. O.; Grummt, T.; Marcos, R. Genotoxic effects in swimmers exposed to disinfection by-products in indoor swimming pools. *Environ. Health Perspect.* **2010**, *118*, 1531–1537.
76. Villanueva, C. M.; Cantor, K. P.; Grimalt, J. O.; Malats, N.; Silverman, D.; Tardon, A.; Garcia-Closas, R.; Serra, C.; Carrato, A.; Castano-Vinyals, G.; Marcos, R.; Rothman, N.; Real, F. X.; Dosemeci, M.; Kogevinas, M. Bladder cancer and exposure to water disinfection by-products through ingestion, bathing, showering, and swimming in pools. *Am. J. Epidemiol.* **2007**, *165*, 148–156.
77. Nieuwenhuijsen, M. J.; Toledano, M. B.; Elliott, P. Uptake of chlorination disinfection by-products; a review and a discussion of its implications for exposure assessment in epidemiological studies. *J. Exposure Anal. Environ. Epidemiol.* **2000**, *10*, 586–599.
78. Froese, K. L.; Sinclair, M. I.; Hrudey, S. E. Trichloroacetic acid as a biomarker of exposure to disinfection by-products in drinking water: a human exposure trial in Adelaide, Australia. *Environ. Health Perspect.* **2002**, *110*, 679–687.
79. Savitz, D. A. Invited commentary: biomarkers of exposure to drinking water disinfection by-products--are we ready yet? *Am. J. Epidemiol.* **2012**, *175*, 276–278.
80. Nachman, K. E.; Fox, M. A.; Sheehnan, M. C.; Burke, T. A.; Rodricks, J. V.; Woodruff, T. J. Leveraging epidemiology to improve risk assessment. *Open Epidemiol. J.* **2011**, *4*, 3–29.

Chapter 2

Analysis, Occurrence, and Toxicity of Haloacetaldehydes in Drinking Waters: Iodoacetaldehyde as an Emerging Disinfection By-Product

Cristina Postigo,^{*,1} Clara H. Jeong,² Susan D. Richardson,³ Elizabeth D. Wagner,² Michael J. Plewa,² Jane Ellen Simmons,⁴ and Damià Barceló^{1,5}

¹Department of Environmental Chemistry, Institute for Environmental Assessment and Water Research, (IDAEA-CSIC), Carrer Jordi Girona 18-26, 08034, Barcelona, Spain

²Department of Crop Sciences and the Center of Advanced Materials for the Purification of Water with Systems, Safe Global Water Institute, University of Illinois at Urbana-Champaign, Urbana, Illinois 61801, United States

³Department of Chemistry and Biochemistry, University of South Carolina, JM Palms Centre for GSR, 631 Sumter Street, Columbia, South Carolina 29208, United States

⁴National Health and Environmental Effects Research Laboratory, (NHEERL-U.S. EPA), 109 T.W. Alexander Drive, Research Triangle Park, North Carolina 27709, United States

⁵Catalan Institute for Water Research (ICRA), Parc Científic i Tecnològic de la Universitat de Girona, Edifici H2O, Carrer d'Emili Grahit, 101, 17003 Girona, Spain

*E-mail: cprqam@cid.csic.es.

Chlorinated and brominated haloacetaldehydes (HALs) are considered the 3rd largest class of disinfection by-products (DBPs) by weight. The iodinated HAL, iodoacetaldehyde, has been recently reported as an emerging DBP in finished drinking waters. Overall, iodinated DBPs, e.g., iodoacetic acids, iodoacetamides, and idonitriles, are among the most genotoxic of all DBPs identified. In this context, this chapter reviews the analytical methods available to date to determine HALs in water, and the concentrations at which they are present

in finished drinking waters. Since systematic toxicological effects have been only investigated for selected chloro- and bromo- HALs, a comparative study of the genotoxicity and cytotoxicity of this DBP class to mammalian cells is also presented.

Keywords: disinfection by-products; genotoxicity; cytotoxicity; occurrence; drinking waters; halogenated aldehydes; chloral hydrate; mammalian cells

Introduction

The nature and quantity of the disinfection by-products (DBPs) formed during water disinfection treatments is determined by the type of disinfectant agent used, the dose applied and the constituents present in the water among other factors (1–4). DBP formation, occurrence and health effects have been matters of scientific concern over the last three decades. More than 600 DBPs are known to date; however, less than 100 have been studied in depth, in terms of their occurrence, formation mechanisms, and toxicity. Moreover, 50% of the halogenated material formed during drinking water disinfection treatments (e.g., chlorination, chloramination, and ozonation) is still unknown, and so is the toxicological risk that it may pose to human health (5–7).

Studies on the toxicity of individual DBPs have been directed to investigate their potential carcinogenicity, genotoxicity, mutagenicity, and cytotoxicity. Such studies have aided health authorities of different countries in establishing regulations and guidelines to control the levels of specific DBPs in drinking waters, e.g., bromate, and trihalomethanes (THMs) in Europe (8) and the USA (9), and chlorite and haloacetic acids (HAAs) in the USA (9). However, there is still a good number of DBPs for which some toxicity data are available that are not regulated (6). This is the case for some halogenated acetaldehydes (HALs), which were also reported to be the third most abundant and widespread class of DBPs in drinking water behind THMs and HAAs in a U.S. Nationwide Occurrence Study (5, 10, 11). In this regard, chloral hydrate (CH), the hydrated form of trichloroacetaldehyde (TCAL), has been shown to be genotoxic in numerous prokaryotic and eukaryotic assay systems including mammalian cells, and mutagenic *in vivo* and *in vitro* (12–15). Similar to CH, dichloroacetaldehyde (DCAL) and chloroacetaldehyde (CAL) were reported to induce mitotic aneuploidy (16, 17). Regarding the bromine containing HALs, tribromoacetaldehyde (TBAL) was shown to be more effective than CH in inducing DNA breaks (18), and bromoacetaldehyde (BAL) was reported to irreversibly bind to DNA and proteins in rat liver microsomes (19).

Whereas the presence of CH in drinking waters as a DBP has been investigated since the late 1980s, most of the HALs were not quantitatively determined until 2006 for the first time, as standard solutions for these compounds were not commercially available (20). Moreover, data on the occurrence of iodo-containing HALs, e.g., iodoacetaldehyde (IAL), has been missing until now.

Note that iodinated DBPs like iodoacetic acids, iodoacetamides, and idonitriles, have been reported to be more toxic than their respective chlorinated and brominated analogues, and are among the most genotoxic of all DBPs identified (10, 21, 22).

In this context, the present manuscript reviews the actual analytical methods available to evaluate the occurrence of chloro-, bromo- and iodo-HALs in water, and the levels of this DBP class in source and treated waters. Since systematic toxicological effects have been only investigated for selected chloro- and bromo-HALs, a comparative study of the chronic genotoxicity and acute cytotoxicity of the complete set of HALs in mammalian cells is also presented.

Haloacetaldehyde Determination in Water

The chemical structures and main physical-chemical properties of the HALs investigated in water so far are shown in Figure 1. TCAL is converted to CH in water, thus, the latter is actually the one monitored in water samples. As it can be observed, HALs present very different physical chemical properties, and therefore, they cannot be analyzed at once using only one analytical procedure.

Analyte		Tri-HALs	
Abbreviation (CAS RN)		Trichloroacetaldehyde ⁽¹⁾	Chloral hydrate ⁽¹⁾
Molecular weight		TCAL (75-87-06)	(302-17-0) CH
Log Kow (KOWIN)		147.39	165.40
Solubility		0.99*	0.99*
Vapor pressure		30,000 mg/L*	793,000 mg/L*
		50.0 mm Hg*	14.99 mm Hg*
Mono-HALS		Di-HALS	
Chloroacetaldehyde ⁽¹⁾		Dichloroacetaldehyde ⁽¹⁾	
CAL (107-20-00) 78.50 0.09 110,700 mg/L 64.3 mm Hg*		DCAL (79-02-7) 112.94 0.27 140,000 mg/L 55.4 mm Hg*	
Bromoacetaldehyde ⁽²⁾		Dibromoacetaldehyde ⁽²⁾	
BAL (17157-48-1) 122.95 0.18 69,020 mg/L 19.8 mm Hg		DBAL (3039-13-2) 201.85 0.45 17,760 mg/L 1.3 mm Hg	
Iodoacetaldehyde ⁽²⁾		Bromochloroacetaldehyde ⁽²⁾	
IAL (57782-51-62) 169.95 0.59 19,190 mg/L 4.4 mm Hg		BCAL (98136-99-3) 157.39 0.36 34,780 mg/L 4.1 mm Hg	
		Tribromoacetaldehyde ⁽¹⁾	
		TBAL (115-17-3) 280.74 1.46 902 mg/l 1.5 mm Hg*	
		Dichlorobromoacetaldehyde ⁽²⁾	
		BDCAL (34619-29-9) 191.84 1.28 3,890 mg/L 2.1 mm Hg	
		Dibromochloroacetaldehyde ⁽²⁾	
		DBCAL (64316-11-6) 236.29 1.37 1,907 mg/L 0.4 mm Hg	

Figure 1. Physical-chemical properties of HALs. (*) Experimental value. Source data: ⁽¹⁾ Physprop database using CAS RN (<http://goo.gl/ukAJno>). ⁽²⁾ EPI Suite software using SMILES (<http://goo.gl/sSPHpr>).

Table 1 summarizes the different approaches used to determine HAL concentrations in water. All of them, as discussed in detail in the next subsections, follow different analyte extraction protocols. However, in all cases HAL detection is based on gas chromatography (GC) coupled to either electron capture (ECD) or mass spectrometry (MS) detection. Special consideration in the present review has been given to those methodologies covering a large number of HALs (20, 23–27).

Sample Collection and Preservation

Samples were usually collected in pre-cleaned amber glass bottles with polytetrafluoroethylene (PTFE) screw caps (26, 28) or in PTFE bottles (24), filled with no headspace to avoid evaporation of the most volatile compounds. The analysis of these compounds is recommended upon sample reception in the laboratory because HALs, mainly the brominated species, are very unstable in disinfected waters, and may degrade to their corresponding trihalomethanes (20, 25, 26), even in the dark and under cool conditions (4°C). Due to sample transport logistics, the time between sample collection and analysis may exceed 24 h. Therefore, sample preservation requires the addition of a dechlorinating agent and acidification of the sample to a pH below 4.5 to prevent analyte hydrolysis (20). In this regard, Serrano et al. (26) reported that the acidification of the sample with sulfuric acid to a pH of 3-3.5 was sufficient to maintain chloro- and bromo-HAL concentrations constant for 14 days at 4°C (BAL and IAL were not included in this study). On the other hand, whereas ammonium chloride and sodium sulfite react at pH 7 and 8 with bromochloroacetaldehyde (BCAL), bromodichloroacetaldehyde (BDCAL), dibromochloroacetaldehyde (DBCAL), CH, and TBAL present in water; sodium arsenite, sodium borohydride, and ascorbic acid did not show any negative effect on the stability of these HALs (25). However, only ascorbic acid has been recommended as a dechlorinating agent, as its decomposition effect has been investigated for the whole spectra of HALs, and when not in a large excess, it seems to preserve HAL concentrations in water, even that of IAL, at acidic pH (24).

Sample Extraction

The determination of CH concentrations in water, which is indeed the most investigated HAL so far, was achieved in most peer-reviewed research with diverse liquid-liquid extraction (LLE) approaches derived from EPA Method 551.1 for the determination of chlorination DBPs, chlorinated solvents, and halogenated pesticides/herbicides in drinking water (29). In all reviewed methods, CH was extracted from the water sample (10-50 mL), occasionally acidified, with a small volume of methyl *tert*-butyl ether (MTBE) (2-3 mL).

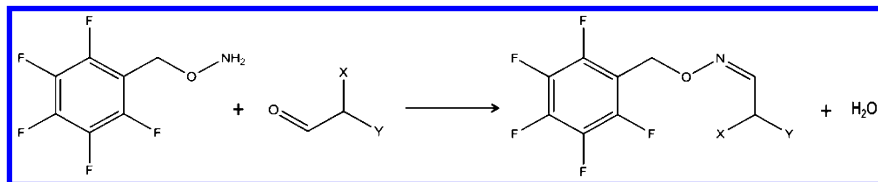
Table 1. Analytical Methodologies Used for HAL Analysis in Water

<i>HALs</i>	<i>Sample preservation</i>	<i>Analyte extraction (Sample volume)</i>	<i>Analyte detection (GC column)</i>	<i>LOD ($\mu\text{g/L}$)</i>	<i>Reference</i>
CH	Sodium sulfite (100 mg/L)	LLE with MTBE or pentane (50 mL)	GC-ECD DB-1 (30 m, 0.25 mm i.d, 1 μm) and Rtx-1301 (30 m, 0.25 mm i.d, 1 μm)	0.011**	(29)
DCAL, BCAL, DBAL, BDCAL, DBCAL, CH, TBAL	AscAc (35 mg/L) pH=3-4	SPE (Bond Elut PPL) (36 mL) LLE with MTBE (30 mL) *	GC-ECD / GC-MS DB-5 and DB-1 (30 m, 0.32 mm i.d, 1 μm) / Rtx 1 (30 m, 0.25 mm i.d, 1 μm)	1-2.5 (for SPE)**	(23)
DCAL, BCAL, DBAL, BDCAL, DBCAL, CH, TBAL	pH = 3-3.5	MLLE with ethyl acetate (9 mL)	LVI-PTV-GC-MS HP-5 MS (30 m, 0.25 mm i.d., 0.25 μm)	0.006 - 0.020	(26)
DCAL, BCAL, DBAL, BDCAL, DBCAL, CH, TBAL	AscAc (0.1 mL, 0.114 M) pH=4.5	LLE with MTBE (50 mL) *	GC-ECD / GC-MS DB-5 and DB-1 (30 m, 0.32 mm i.d, 1 μm)	0.03-0.05	(20)
CAL, BAL, DCAL, BCAL, DBAL	AscAc (12.5 mg/L) pH= 3.5	PFBHA derivatization + LLE with Hexane (100 mL)	GC-MS Zebtron ZB-5 (30 m, 0.25 mm i.d., 0.25 μm)	0.05-0.25	(24)
BDCAL, DBCAL, CH, TBAL	AscAc (12.5 mg/L) pH= 3.5	SPE (Oasis HLB) (100 mL)	GC-MS Zebtron ZB-5 (30 m, 0.25 mm i.d., 0.25 μm)	0.1-0.5	(24)

* LLE approach based on EPA 551.1.; ** RL: method reporting limit AscAc: ascorbic acid, ECD: electron capture detection, GC: gas chromatography, LLE: liquid-liquid extraction, LOD: method limit of detection, LVI-PTV-GC-MS: large volume injection - programmable temperature vaporizer, MLLE: micro liquid-liquid extraction, MS: mass spectrometry, MTBE: methyl *tert*-butyl ether, SPE: solid phase extraction.

Several grams of anhydrous Na_2SO_4 (2-14 g) or NaCl (4-15 g) were usually added to increase the ionic strength of the solution, and thus, to enhance the extraction of this polar compound (23, 27, 30–42). Liquid-liquid extraction with MTBE also proved to be suitable for the extraction of the remaining chloro and bromo containing tri-HALs, and the di-HALs, DCAL and BCAL (20, 25). A miniaturized approach of EPA Method 551.1 using 0.2 mL of ethyl acetate as the extracting solvent was recently developed by Serrano et al. (26) for the extraction of chloro and bromo containing di-HALs and tri-HALs from water. This fast and “green” method, e.g. minimal consumption of solvents and salts, provided slightly lower limits of detection (0.006-0.02 $\mu\text{g/L}$) than EPA Method 551.1 (0.02-0.03 $\mu\text{g/L}$) (26).

An approach based on EPA Method 556 (43) was applied for the extraction of very polar, low molecular weight, and high volatile aldehydes (and ketones), e.g., mono- and di-HALs (11, 24), which in their native form, are almost impossible to extract from water. This method consisted of the derivatization of these compounds with *O*-(2,3,4,5,6-pentafluorobenzyl)hydroxylamine (PFBHA) and subsequent LLE of the oximes formed with hexane. The derivatization reaction is shown in Scheme 1. This is also the analytical strategy selected for the extraction of the very polar IAL from water. Limits of detection achieved for mono- and di-HALs with this approach ranged between 0.05 $\mu\text{g/L}$ and 0.25 $\mu\text{g/L}$ (24).



Scheme 1. Derivatization reaction of PFBHA with mono- and di-HALs (mono-HALs: X= halogen and Y=H; di-HALs: X,Y = halogen)

Solid phase extraction (SPE) onto a modified styrene divinylbenzene polymer, i.e., Bond Elut PPL (Agilent) or a hydrophilic-lipophilic balanced polymer, i.e., Oasis HLB (Waters), was also applied to preconcentrate trihalo and dihalo species present in water (23, 24). Eluting solvents used were a mixture of hexane:dichloromethane (23) or MTBE (24). Contrary to the satisfactory recoveries obtained for TBAL, DCBAL, and BDCAL with both SPE sorbents, low recoveries were reported for di-HALs and the most polar tri-HAL, CH. Compared to the aforementioned extraction approaches, slightly higher limits of detection, always in the low $\mu\text{g/L}$ range, were obtained for the target HALs with SPE methods, i.e.: 1-2.5 $\mu\text{g/L}$ (23) or 0.1-0.5 $\mu\text{g/L}$ (24).

Analyte Detection

Regardless of the extraction method followed, HAL detection was always achieved by means of GC coupled to either ECD or MS. In most of the ECD based methods, due to the low specificity of this technique, a secondary column in addition to the primary analytical column was used for analyte confirmation (20, 23, 29, 33, 35, 44). GC/MS analysis was also used by Koudjonou and Lebel (20) for analyte confirmation. Electron ionization (EI) was used to acquire the analyte spectra, and chemical ionization (CI) was used to confirm the molecular weights of the compounds (20).

Although less sensitive than GC-ECD detection, selective GC/EI-MS detection was also commonly used in the selected ion monitoring (SIM) mode for HAL identification and quantification (23–27, 36, 37, 45). Serrano et al (26) showed that programmable temperature vaporizer (PTV)-based large volume injection (LVI) that allows injecting sample volumes between 20 and 50 μL is an effective tool for enhancing limits of detection of HAL analysis with GC/MS by one to two orders of magnitude over conventional splitless injection techniques (sample volume injected below 2 μL).

Quantification of individual HALs was usually performed with internal standard normalized response factors obtained from the analyses of multi-level fortified HAL-free waters (groundwater or Milli-Q purified water) extracted and analyzed under identical conditions as the real water samples (20, 23, 24, 26).

Haloacetaldehyde Occurrence in Water

The occurrence of HALs in treated waters (drinking water plant effluent, disinfected water at different locations of distribution systems, and swimming pool water) as reported in the peer-reviewed literature has been summarized in Table 2.

As mentioned previously and as it can be observed in Table 2, CH (the hydrated form of trichloroacetaldehyde, TCAL) is the most investigated halogenated aldehyde in water. Not only has its occurrence in drinking waters been a matter of study, but also its removal through different technologies (27, 33, 39, 46) and its formation mechanisms (30, 34, 47–51). The highest CH concentration was determined in swimming pool water (340 $\mu\text{g/L}$) (26), whereas maximum levels reported in drinking water surpassed in most cases 10 $\mu\text{g/L}$, but did not exceed 40 $\mu\text{g/L}$. The World Health Organization (WHO) has not considered it necessary to derive a drinking water guideline value for this compound, as it occurs at concentrations well below the calculated health-based tolerable daily intake (TDI) value of 100 $\mu\text{g/L}$ (52). The remaining halogenated aldehydes were usually found in drinking water at maximum levels below 10 $\mu\text{g/L}$.

The whole spectrum of HALs was recently investigated in seven drinking water treatment plants (DWTPs) in the USA (24). To date, this is the only study including BAL and IAL as target analytes (see Table 2). Figure 2 summarizes the frequency of detection and the concentration range measured for individual HALs in this study. All investigated HALs (10 total) were detected in all treated waters,

except IAL and TBAL, which were present in only 57% and 43% of the samples, respectively. IAL formation was exclusively observed during chloramination processes, and its contribution to total HAL concentrations ranged between 6 to 28% (24). Contrary to IAL, the other investigated mono-HALs presented the lowest overall concentrations of all target analytes.

Table 2. Occurrence of HALs in Disinfected Water

<i>HALs</i>	<i>Concentration (µg/L)**</i>	<i>Country</i>	<i>Reference</i>
CAL	0.2-0.3 ^{ef}	U.S.	(24)
	n.d. -2.4 ^{ef} / n.d.-2.1 ^{ds}	U.S.	(11)
BAL	<0.5-1.3 ^{ef}	U.S.	(24)
IAL	n.d.-4.6 ^{ef}	U.S.	(24)
DCAL	0.3-2.0 ^{ef} n.d.-14 ^{ef} / n.d.-16 ^{ds}	U.S.	(24) (5, 11)
	1.3-3.5 ^{ef} / 1.9 ^{ds} 1-3.3 ^{ef} / 1.1-3.6 ^{ds}	Canada	(20) (28)
	<0.01-4 ^{ds} / 1.8-23 ^p	Spain	(26)
DBAL	<0.3-3.1 ^{ef}	U.S.	(24)
	n.d.-1.7 ^{ef} / n.d. ^{ds} n.d.-1.1 ^{ef} / n.d.-1.0 ^{ds}	Canada	(20) (28)
	n.d. ^{ds} / n.d. ^p	Spain	(26)
BCAL	<0.3-2.2 ^{ef} n.d.-4 ^{ef} / n.d.-7 ^{ds}	U.S. U.S.	(24) (11)
	0.1-2.7 ^{ef} / 0.4-0.8 ^{ds} 0.6-2.7 ^{ef} / 0.4-3.1 ^{ds}	Canada	(20) (28)
	n.d. ^{ds} / n.d. ^p	Spain	(26)
CH (TCAL)	<0.3-4.1 ^{ef} n.d.-16 ^{ef} / n.d.-62 ^{ds}	U.S.	(24) (11)
	<0.1-15.1 ^{ef} / <0.1-22.5 ^{ds} 1.1-12 ^{ef} / 2.4-5.8 ^{ds} 1.3-6.9 ^{ef} / 1.4-8.9 ^{ds} 0.2-12.2 ^{ef+ds}	Canada	(57) (20) (28) (58)
	<1-12.1 ^{ds} 1.2-38 ^{ds} / 53-340 ^p	Spain	(40) (26)
	0.3-11 ^{ef} / 1-12.5 ^{ds}	Greece	(35)
	n.d.-5.4 ^{ef}	Japan	(59)
	n.d.-34.9 ^p n.d.-33.2 ^{ef}	Korea	(37) (60)

Continued on next page.

Table 2. (Continued). Occurrence of HALs in Disinfected Water

<i>HALs</i>	<i>Concentration (µg/L)**</i>	<i>Country</i>	<i>Reference</i>
	2.1* -12.2 ^{ds} n.d.-10.4 ^{ef+ds}	China	(42) (41)
	0.2-19 ^{ds}	Australia	(61)
	n.d.-8.6 ^{ds}	Poland	(45)
	0.4-8.9 ^{ds}	Poland	(55)
TBAL	n.d.-12.6 ^{ef} n.d.-3 ^{ef} / n.d.-2 ^{ds}	U.S.	(24) (11)
	n.d.-1.5 ^{ef} / n.d. ^{ds} n.d.-2 ^{ef} / n.d.-1.6 ^{ds}	Canada	(20) (28)
	n.d. ^{ds} / n.d. ^p	Spain	(26)
BDCAL	1.1-2.2 ^{ef}	U.S.	(24)
	0.3-7.2 ^{ef} / 1.5-2.4 ^{ds} 0.8-6.2 ^{ef} / 1-8.3 ^{ds}	Canada	(20) (28)
	n.d. ^{ds} / n.d. ^p	Spain	(26)
DBCAL	<1-2.9 ^{ef}	U.S.	(24)
	n.d.-11.5 ^{ef} / 0.7-0.9 ^{ds} 0.6-9 ^{ef} / 0.7-11.6 ^{ds}	Canada	(20) (28)
	n.d. ^{ds} / n.d. ^p	Spain	(26)

* median value, ** ef: plant effluent, ds: distribution system, p: swimming pool.

According to different studies, carbonyl compounds such as aldehydes, which are precursors of halogenated aldehydes, are the most common ozonation by-products (53, 54). Therefore the application of ozone before chlorination may increase the HAL formation potential. This was confirmed for CH in several studies (55, 56). Krasner et al. (56) also observed that tri-HAL concentrations were lower than di-HAL concentrations in chloramine-based systems, and that the formation of chloro and bromo containing di-HALs was also enhanced in those plants using ozone before chloramination. Contrary to what might be expected from these results, overall HAL levels formed in preozonation based systems investigated by Jeong et al. (24) were not higher than those generated in DWTPs that did not apply ozone. Moreover, the highest tri-HAL concentrations were found in chloraminated water, with TBAL the main contributing HAL species (44%) to total HAL levels (28.8 µg/L). However, these findings could be biased by the extraordinarily high concentrations of bromide (0.54 µg/L) present in the source water that had the highest HAL generation potential (24). If this sample is excluded in this analysis, the highest HAL concentration was observed for CH in chlorinated water, whereas the formation potential of CH during chloramination processes was very low (24). Bromine incorporation in HALs in the samples investigated by Jeong et al. (24) increased with bromide concentration of the

source water, as previously reported by Koudjonou et al. (28). In this regard, the lowest concentrations, and thus, contributions to total HAL levels, of the chlorine-based HAL species, CAL, DCAL, TCAL, and BDCAL, were measured in disinfected waters that originated from the highest bromide content source waters (24).

Besides haloacetaldehydes, additional halogenated aldehydes, i.e., iodobutanal, dichloropropenal, and 4-chloro-2-butenal, were identified in the U.S. Nationwide DBP Occurrence Study (5, 11). However, their concentrations and formation mechanisms have not been investigated yet.

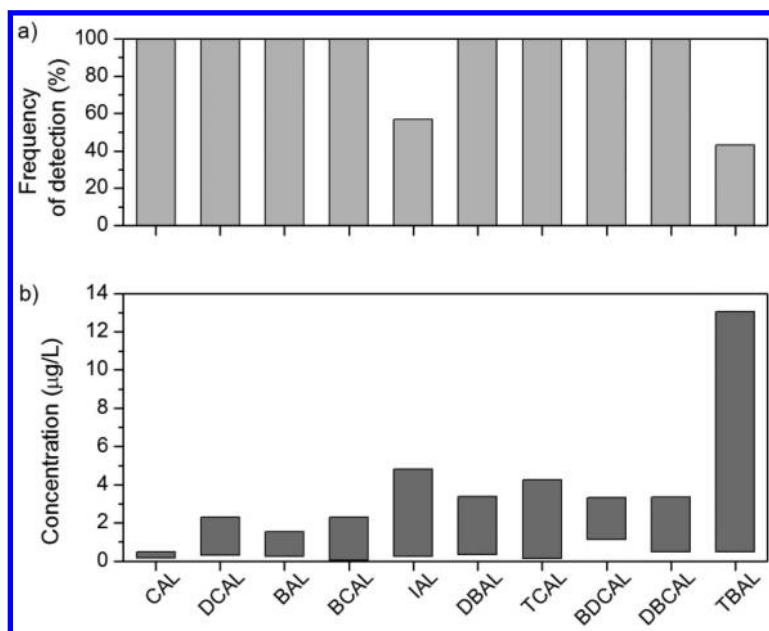


Figure 2. a) Frequency of detection and b) concentration range of individual HALs in finished drinking waters collected in US drinking water treatment plants (24).

Haloacetaldehyde Toxicity

As reviewed in the Introduction, toxicological studies were previously only conducted on CAL, BAL, DCAL, CH and TBAL. A recent study examined the genotoxicity and cytotoxicity of the complete set of the ten HALs, including IAL (24). These toxicity assays were performed in mammalian cells as described in the next subsections. Results obtained allowed comparison of the toxic potencies of individual HALs and of this DBP class with other DBP classes.

Toxicity Assays

Chinese Hamster Ovary Cells

Chinese hamster ovary (CHO) cell line AS52, clone 11-4-8 was used for the toxicity studies (62–64) and was maintained in modified Ham's F12 medium (Mediatech, Inc., Manassas, VA) supplemented with 5% heat-inactivated fetal bovine serum (FBS), 1% L-glutamine and 1% antibiotic-antimycotic solution (Invitrogen, Carlsbad, CA) at 37°C in a humidified atmosphere of 5% CO₂. The cells exhibit normal morphology, express cell contact inhibition, and grow as a monolayer without expressing neoplastic foci.

CHO Cell Chronic Cytotoxicity Assay

This bioanalytical assay measures the survivorship of the cells as the reduction in cell density as a function of the HAL concentration over a period of 72 h. (22, 65). The procedure was previously published (22, 65). In general, for each HAL concentration, 8 replicates were analyzed and the experiments were repeated 2-4 times. A concentration-response curve was generated for each HAL, and a regression analysis was generated for each curve. The LC₅₀ values were calculated, where the LC₅₀ represents the HAL concentration that induced a 50% reduction in cell density as compared to the concurrent negative controls.

Single Cell Gel Electrophoresis Assay

The single cell gel electrophoresis (SCGE) or “comet assay” quantitatively measures genomic DNA damage in individual nuclei (66–68). The detailed procedure of the microplate methodology used in this study was published elsewhere (68). The SCGE metric for genomic DNA damage induced by the HALs was the %Tail DNA value, which is the amount of DNA that migrated from the nucleus into the microgel (69). For each HAL concentration range where the cell viability was >70%, a concentration-response curve was generated. A regression analysis was used to fit the curve, and the concentration inducing a 50% Tail DNA value was calculated.

Comparative Haloacetaldehyde Toxicity

The CHO cell chronic cytotoxicity analyses (72 h exposures) of each HAL are summarized in Table 3. The mean bootstrap cytotoxicity index (CTI) (LC₅₀⁻¹)(10³) (±SE) values are presented in Figure 3a. An all pairwise ANOVA test of the CTI values generated a descending rank order of chronic cytotoxicity as TBAL ≈ CAL > DBAL ≈ BCAL ≈ DBCAL > IAL > BAL ≈ BDCAL > DCAL > TCAL, as it is shown in Figure 3a.

CHO cell acute genotoxicity analyses (4 h exposures) of each HAL are summarized in Table 3. An all pairwise ANOVA test of the GTI values generated a descending rank order of genotoxicity of the ten HALs as DBAL > CAL ≈ DBCAL > TBAL ≈ BAL > BDCAL > BCAL ≈ DCAL > IAL, as shown in Figure 3b. TCAL was not genotoxic.

Table 3. Mammalian Cell Cytotoxicity and Genotoxicity of HALs (24)

	<i>HALs</i>	<i>Lowest Cytotoxic Conc. (μM)^a</i>	<i>LC₅₀ (μM)^b</i>	<i>Lowest Genotoxic Conc. (μM)^c</i>	<i>50% Tail DNA (μM)^d</i>
Mono-HALs and Di-HALs	CAL	0.5	3.5	100	142.8
	BAL	8	17.3	200	381.2
	IAL	5	6.0	900	1009
	DCAL	8	29.3	800	795
	DBAL	2	4.7	50	111.3
	BCAL	2.5	5.3	500	621.4
	CH (TCAL)	375	116	NS	NS
Tri-HALs	TBAL	2	3.6	100	340.3
	BDCAL	10	20.4	300	470.4
	DBCAL	4	5.2	100	143.7

^a Lowest cytotoxic concentration was the lowest concentration of the HAL in the concentration-response curve that induced a statistically significant reduction in cell density as compared to the concurrent negative controls. ^b The LC₅₀ value is the concentration of the HAL, determined from a regression analysis of the data, that induced a cell density of 50% as compared to the concurrent negative controls. ^c The lowest genotoxic concentration was the lowest concentration of the HAL in the concentration-response curve that induced a statistically significant amount of genomic DNA damage as compared to the negative control. ^d The SCGE 50% Tail DNA value is the HAL concentration determined from a regression analyses of the data that was calculated to induce a 50% SCGE Tail DNA value.

We compared the CHO cell toxic potencies of the HALs to other DBP chemical classes with their calculated cytotoxicity and genotoxicity indices. The cytotoxicity index was determined by calculating the mean LC₅₀ value of all of the individual compounds of a single class of DBPs. The genotoxicity index was determined by calculating the mean SCGE genotoxic potency value, which is defined by the midpoint of the SCGE tail moment or the 50% Tail DNA values from the individual compounds within a single class of DBPs (22). Six DBP chemical classes were compared, including the THMs, HAAs, HALs, halonitromethanes, haloacetonitriles, and haloacetamides. As summarized in

Table 4, HALs constitute the second most cytotoxic DBP class, whereas they rank as the second least genotoxic DBP class.

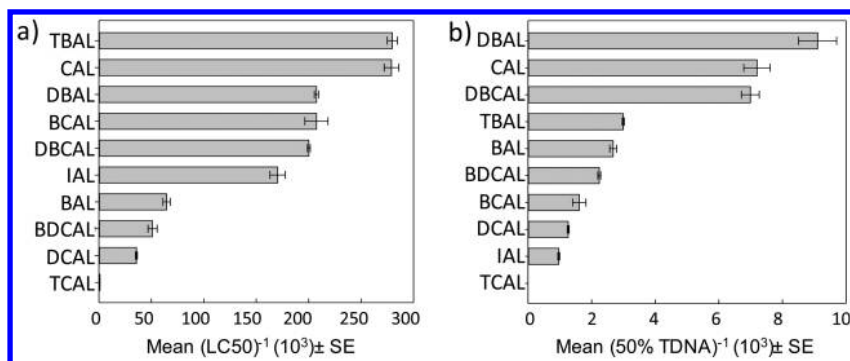


Figure 3. The mean bootstrap a) CHO cell cytotoxic index values (\pm SE) and b) CHO cell genotoxic index values (\pm SE) of the HALs (24).

Table 4. Mammalian Cell Cytotoxicity Index Values (CTI) and Genotoxicity Index Values (GTI) of DBP Chemical Classes (24)

DBP Class	CTI Values	GTI Values
Trihalomethanes	2.39	0
Haloacetic acids	39.3	14.8
Haloacetaldehydes	144	2.80
Halonitromethanes	75.0	11.4
Haloacetonitriles	16.0	11.5
Haloacetamides	302	12.3

Conclusions

Different analytical methods have been used to determine HALs in disinfected waters. Due to their very different physical-chemical properties, the complete set of nine chloro and bromo HALs and IAL cannot be analyzed by a unique approach. Regardless of the extraction approach followed, analyte detection is carried out by GC coupled to ECD or MS detection. The evaluation of the occurrence of HALs in drinking waters allowed this DBP class to be identified as the third largest group by weight of DBPs reported. Besides CH (TCAL), which is currently the most abundant HAL in drinking water, bromo containing acetaldehydes and IAL may be relevant in chloraminated waters that contain

high levels of bromide and iodide. Despite the fact that HAL concentrations may increase in preozonation-based systems, individual HAL concentrations in disinfected water strongly depend on the source water quality and the type of disinfection treatment applied. A systematic quantitative comparative study of their acute cytotoxicity and chronic genotoxicity to mammalian cells revealed HALs as the second most cytotoxic class of DBPs after haloacetamides. Taking all this into account, it is important to determine their potential health risks and to investigate their formation mechanisms to control their presence in drinking waters.

Acknowledgments

We would like to thank the drinking water treatment plants for generously providing us with samples. This work was supported by the EPA STAR Grant R834867. We appreciate support by the Center of Advanced Materials for the Purification of Water with Systems (WaterCAMPWS), a National Science Foundation Science and Technology Center, under Award CTS-0120978. C.J. was supported by a NIEHS Pre-doctoral Fellowship under Grant No. T32 ES007326. C.P. acknowledges support from the European Union Seventh Framework Programme (FP7/2007-2013) under grant agreement n° 274379 (Marie Curie IOF). This work has been financially supported by the Generalitat de Catalunya (Consolidated Research Groups “2014 SGR 418 - Water and Soil Quality Unit” and 2014 SGR 291 - ICRA). This work reflects only the author’s views. The EU is not liable for any use that may be made of the information contained therein. This work does not reflect EPA policy.

References

1. Liang, L.; Singer, P. C. Factors influencing the formation and relative distribution of haloacetic acids and trihalomethanes in drinking water. *Environ. Sci. Technol.* **2003**, *37*, 2920–2928.
2. Hua, G.; Reckhow, D. A. Comparison of disinfection byproduct formation from chlorine and alternative disinfectants. *Water Res.* **2007**, *41*, 1667–1678.
3. Shah, A. D.; Mitch, W. A. Halonitroalkanes, halonitriles, haloamides, and N-nitrosamines: A critical review of nitrogenous disinfection byproduct formation pathways. *Environ. Sci. Technol.* **2012**, *46*, 119–131.
4. Zhang, Z.; Echigo, S.; Minear, R. A.; Plewa, M. J., Characterization and comparison of disinfection by-products of four major disinfectants. In *Natural Organic Matter and Disinfection By-Products: Characterization and Control in Drinking Water*; Barrett, S. E., Krasner, S. W., Amy, G. L., Eds. American Chemical Society: Washington, DC, 2000; pp 299–314.
5. Krasner, S. W.; Weinberg, H. S.; Richardson, S. D.; Pastor, S. J.; Chinn, R.; Scilimenti, M. J.; Onstad, G. D.; Thruston, A. D., Jr. Occurrence of a new generation of disinfection byproducts. *Environ. Sci. Technol.* **2006**, *40*, 7175–7185.

6. Richardson, S. D.; Postigo, C., Drinking water disinfection by-products. In *Emerging Organic Contaminants and Human Health*; Barcelo, D., Ed.; The Handbook of Environmental Chemistry; Springer-Verlag: Berlin Heidelberg, 2012; Vol. 20, pp 93–138.
7. Plewa, M. J.; Wagner, E. D. Drinking water disinfection by-products: comparative mammalian cell cytotoxicity and genotoxicity. In *Encyclopedia of Environmental Health*; Nriagu, J. O., Ed.; Elsevier: Burlington, 2011; Vol. 1, pp 806-812.
8. Council Directive 98/83/EC of 3 November 1998 on the quality of water intended for human consumption. Official Journal of the European Communities L 330/32; <http://goo.gl/REht5N> (accessed November, 2014).
9. U.S. EPA. *Basic information about disinfection byproducts in drinking water: total trihalomethanes, haloacetic acids, bromate and chlorite*; <http://goo.gl/EEVHZ3> (accessed November, 2014).
10. Richardson, S. D.; Plewa, M. J.; Wagner, E. D.; Schoeny, R.; DeMarini, D. M. Occurrence, genotoxicity, and carcinogenicity of regulated and emerging disinfection by-products in drinking water: A review and roadmap for research. *Mutat. Res., Rev. Mutat. Res.* **2007**, *636*, 178–242.
11. Weinberg, H. S.; Krasner, S. W.; Richardson, S. D.; Thruston, A. D. J. *The Occurrence of Disinfection By-Products (DBPs) of Health Concern in Drinking Water: Results of a Nationwide DBP Occurrence Study*; National Exposure Research Laboratory, Office of Research and Development, U.S. Environmental Protection Agency: Athens, GA, 2002.
12. Beland, F. A. National Toxicology Program technical report on the toxicity and metabolism studies of chloral hydrate (CAS No. 302-17-0). Administered by Gavage to F344/N rats and B6C3F1 mice. *Natl. Toxicol. Program Toxic. Rep. Ser.* **1999**, *59*, A1–A7.
13. Furnus, C. C.; Ulrich, M. A.; Terreros, M. C.; Douhout, F. N. The induction of aneuploidy in cultured Chinese hamster cells by propionaldehyde and chloral hydrate. *Mutagenesis* **1990**, *5*, 323–326.
14. Allen, J. W.; Collins, B. W.; Evansky, P. A. Spermatid micronucleus analyses of trichloroethylene and chloral hydrate effects in mice. *Mutat. Res.* **1994**, *323*, 81–88.
15. Migliore, L.; Nieri, M. Evaluation of twelve potential aneuploidogenic chemicals by the in vitro human lymphocyte micronucleus assay. *Toxicol. In Vitro* **1991**, *5*, 325–336.
16. Crebelli, R.; Conti, G.; Conti, L.; Carere, A. Induction of Somatic Segregation by Halogenated Aliphatic-Hydrocarbons in *Aspergillus-Nidulans*. *Mutat. Res.* **1984**, *138*, 33–38.
17. Crebelli, R.; Conti, G.; Conti, G.; Carere, A. Chloroacetaldehyde is a powerful inducer of mitotic aneuploidy in *Aspergillus-Nidulans*. *Mutagenesis* **1990**, *5*, 165–168.
18. Liviak, D.; Creus, A.; Marcos, R. DNA damage induction by two halogenated acetaldehydes, byproducts of water disinfection. *Water Res.* **2010**, *44*, 2638–2646.
19. Guengerich, F. P.; Mason, P. S.; Stott, W. T.; Fox, T. R.; Watanabe, P. G. Roles of 2-haloethylene oxides and 2-haloacetaldehydes derived from vinyl

bromide and vinyl chloride in irreversible binding to protein and DNA. *Cancer Res.* **1981**, *41*, 4391–4398.

20. Koudjonou, B. K.; LeBel, G. L. Halogenated acetaldehydes: Analysis, stability and fate in drinking water. *Chemosphere* **2006**, *64*, 795–802.
21. Richardson, S. D.; Fasano, F.; Ellington, J. J.; Crumley, F. G.; Buettner, K. M.; Evans, J. J.; Blount, B. C.; Silva, L. K.; Waite, T. J.; Luther, G. W.; McKague, A. B.; Miltner, R. J.; Wagner, E. D.; Plewa, M. J. Occurrence and Mammalian Cell Toxicity of Iodinated Disinfection Byproducts in Drinking Water. *Environ. Sci. Technol.* **2008**, *42*, 8330–8338.
22. Plewa, M. J.; Wagner, E. D. *Mammalian Cell Cytotoxicity and Genotoxicity of Disinfection By-products*. Water Research Foundation: Denver, CO, 2009; p 134.
23. Chinn, R.; Lee, T.; Krasner, S. W.; Dale, M.; Richardson, S. D.; Pressman, J. G.; Speth, T. F.; Miltner, R. J.; Simmons, J. E. Solid phase extraction of 35 DBPs with analysis by GC/ECD and GC/MS. In *Proceedings of the Water Quality Technology Conference*; American Water Works Association: Denver, CO, 2007; pp 1–20, <http://goo.gl/U3h3cd> (accessed November, 2014).
24. Jeong, C. H.; Postigo, C.; Richardson, S. D.; Simmons, J. E.; Kimura, S. Y.; Marinas, B. J.; Barcelo, D.; Wagner, E. D.; Plewa, M. The occurrence and comparative toxicity of haloacetaldehyde disinfection byproducts in drinking water. *Environ. Sci. Technol.* **2014** submitted for publication.
25. Kristiana, I.; Lethorn, A.; Joll, C.; Heitz, A. To add or not to add: The use of quenching agents for the analysis of disinfection by-products in water samples. *Water Res.* **2014**, *59*, 90–98.
26. Serrano, M.; Silva, M.; Gallego, M. Micro liquid–liquid extraction combined with large-volume injection gas chromatography–mass spectrometry for the determination of haloacetaldehydes in treated water. *J. Chromatogr. A* **2011**, *1218*, 8295–8302.
27. Linge, K. L.; Blythe, J. W.; Buseti, F.; Blair, P.; Rodriguez, C.; Heitz, A. Formation of halogenated disinfection by-products during microfiltration and reverse osmosis treatment: Implications for water recycling. *Sep. Purif. Technol.* **2013**, *104*, 221–228.
28. Koudjonou, B.; LeBel, G. L.; Dabeka, L. Formation of halogenated acetaldehydes, and occurrence in Canadian drinking water. *Chemosphere* **2008**, *72*, 875–881.
29. Much, D. J.; Hautman, D. P. U.S. EPA Method 551.1. Methods for the Determination of Organic Compounds in Drinking Water - Supplement III - EPA/600/R-95/131; 1995.
30. Bond, T.; Henriot, O.; Goslan, E. H.; Parsons, S. A.; Jefferson, B. Disinfection byproduct formation and fractionation behavior of natural organic matter surrogates. *Environ. Sci. Technol.* **2009**, *43*, 5982–5989.
31. Bougeard, C. M. M.; Goslan, E. H.; Jefferson, B.; Parsons, S. A. Comparison of the disinfection by-product formation potential of treated waters exposed to chlorine and monochloramine. *Water Res.* **2010**, *44*, 729–740.

32. Cimetiere, N.; De Laat, J. Effects of UV-dechloramination of swimming pool water on the formation of disinfection by-products: A lab-scale study. *Microchem. J.* **2014**, *112*, 34–41.
33. Doederer, K.; Farré, M. J.; Pidou, M.; Weinberg, H. S.; Gernjak, W. Rejection of disinfection by-products by RO and NF membranes: Influence of solute properties and operational parameters. *J. Membr. Sci.* **2014**, *467*, 195–205.
34. Fang, J. Y.; Ma, J.; Yang, X.; Shang, C. Formation of carbonaceous and nitrogenous disinfection by-products from the chlorination of *Microcystis aeruginosa*. *Water Res.* **2010**, *44*, 1934–1940.
35. Golfinoopoulos, S. K.; Nikolaou, A. D. Survey of disinfection by-products in drinking water in Athens, Greece. *Desalination* **2005**, *176*, 13–24.
36. Hansen, K. M. S.; Zortea, R.; Piketty, A.; Vega, S. R.; Andersen, H. R. Photolytic removal of DBPs by medium pressure UV in swimming pool water. *Sci. Total Environ.* **2013**, *443*, 850–856.
37. Lee, J.; Jun, M.-J.; Lee, M.-H.; Lee, M.-H.; Eom, S.-W.; Zoh, K.-D. Production of various disinfection byproducts in indoor swimming pool waters treated with different disinfection methods. *Int. J. Hyg. Environ. Health* **2010**, *213*, 465–474.
38. Nikolaou, A.; Golfinoopoulos, S.; Rizzo, L.; Lofrano, G.; Lekkas, T.; Belgiorno, V. Optimization of analytical methods for the determination of DBPs: Application to drinking waters from Greece and Italy. *Desalination* **2005**, *176*, 25–36.
39. Radjenovic, J.; Farre, M. J.; Mu, Y.; Gernjak, W.; Keller, J. Reductive electrochemical remediation of emerging and regulated disinfection byproducts. *Water Res.* **2012**, *46*, 1705–1714.
40. Villanueva, C. M.; Castaño-Vinyals, G.; Moreno, V.; Carrasco-Turigas, G.; Aragonés, N.; Boldo, E.; Ardanaz, E.; Toledo, E.; Altzibar, J. M.; Zaldúa, I.; Azpiroz, L.; Goñi, F.; Tardón, A.; Molina, A. J.; Martín, V.; López-Rojo, C.; Jiménez-Moleón, J. J.; Capelo, R.; Gómez-Acebo, I.; Peiró, R.; Ripoll, M.; Gracia-Lavedan, E.; Nieuwenhuysen, M. J.; Rantakokko, P.; Goslan, E. H.; Pollán, M.; Kogevinas, M. Concentrations and correlations of disinfection by-products in municipal drinking water from an exposure assessment perspective. *Environ. Res.* **2012**, *114*, 1–11.
41. Wei, J. R.; Ye, B. X.; Wang, W. Y.; Yang, L. S.; Tao, J.; Hang, Z. Y. Spatial and temporal evaluations of disinfection by-products in drinking water distribution systems in Beijing, China. *Sci. Total Environ.* **2010**, *408*, 4600–4606.
42. Gan, W.; Guo, W.; Mo, J.; He, Y.; Liu, Y.; Liu, W.; Liang, Y.; Yang, X. The occurrence of disinfection by-products in municipal drinking water in China's Pearl River Delta and multipathway cancer risk assessment. *Sci. Total Environ.* **2013**, *447*, 108–115.
43. Munch, J. W.; Munch, D. J.; Winslow, S. D. U.S. EPA Method 556 for the Determination of Carbonyl Compounds in Drinking Water by Pentafluorobenzylhydroxylamine Derivatization and Capillary Gas Chromatography with Electron Capture Detection; 1997; <http://goo.gl/QDCtd5> (accessed November 2014).

44. Dąbrowska, A.; Świetlik, J.; Nawrocki, J. Formation of aldehydes upon ClO₂ disinfection. *Water Res.* **2003**, *37*, 1161–1169.
45. Włodyka-Bergier, A.; Bergier, T.; Kot, M. Occurrence of volatile organic chlorination by-products in water distribution system in Krakow (Poland). *Desalin. Water Treat.* **2014**, *52*, 3898–3907.
46. Włodyka-Bergier, A.; Rajca, M.; Bergier, T. Removal of halogenated by-products precursors in photocatalysis process enhanced with membrane filtration. *Desalin. Water Treat.* **2014**, *52*, 3698–3707.
47. Doederer, K.; Gernjak, W.; Weinberg, H. S.; Farré, M. J. Factors affecting the formation of disinfection by-products during chlorination and chloramination of secondary effluent for the production of high quality recycled water. *Water Res.* **2014**, *48*, 218–228.
48. Lyon, B. A.; Dotson, A. D.; Linden, K. G.; Weinberg, H. S. The effect of inorganic precursors on disinfection byproduct formation during UVchlorine/chloramine drinking water treatment. *Water Res.* **2012**, *46*, 4653–4664.
49. Yang, X.; Guo, W.; Lee, W. Formation of disinfection byproducts upon chlorine dioxide preoxidation followed by chlorination or chloramination of natural organic matter. *Chemosphere* **2013**, *91*, 1477–1485.
50. Yang, X.; Guo, W.; Zhang, X.; Chen, F.; Ye, T.; Liu, W. Formation of disinfection by-products after pre-oxidation with chlorine dioxide or ferrate. *Water Res.* **2013**, *47*, 5856–5864.
51. Yang, X.; Peng, J.; Chen, B.; Guo, W.; Liang, Y.; Liu, W.; Liu, L. Effects of ozone and ozone/peroxide pretreatments on disinfection byproduct formation during subsequent chlorination and chloramination. *J. Hazard. Mater.* **2012**, *239-240*, 348–354.
52. WHO - World Health Organization. *Guidelines for Drinking-Water Quality*, 4th ed.; 2011; <http://goo.gl/fW7qJG> (accessed October 2014).
53. Weinberg, H. S.; Glaze, W. H.; Krasner, S. W.; Scilimenti, M. J. Formation and removal of aldehydes in plants that use ozonation. *J. - Am. Water Works Assoc.* **1993**, *85*, 72–85.
54. Dabrowska, A.; Kasprzyk-Hordern, B.; Nawrocki, J. Aldehydes formation during water disinfection by ozonation and chlorination process. *Global NEST J.* **2005**, *7*, 61–71.
55. Dabrowska, A.; Nawrocki, J. Controversies about the occurrence of chloral hydrate in drinking water. *Water Res.* **2009**, *43*, 2201–2208.
56. Krasner, S. W.; Mitch, W. A.; Westerhoff, P.; Dotson, A. Formation and control of emerging C- and N-DBPs in drinking water. *J. - Am. Water Works Assoc.* **2012**, *104*, E582–E595.
57. Williams, D. T.; Lebel, G. L.; Benoit, F. M. Disinfection by-products in canadian drinking waters. *Chemosphere* **1997**, *34*, 299–316.
58. Aranda-Rodriguez, R.; Koudjonou, B.; Jay, B.; Lebel, G. L.; Benoit, F. M. Disinfection by-products (DBPs) in drinking water from eight systems using chlorine dioxide. *Water Qual. Res. J. Can.* **2008**, *43*, 11–22.
59. Kawamoto, T.; Makihata, N. Distribution of bromine/chlorine-containing disinfection by-products in tap water from different water sources in the Hyogo Prefecture. *J. Health Sci.* **2004**, *50*, 235–247.

60. Lee, K. J.; Kim, B. H.; Hong, J. E.; Pyo, H. S.; Park, S. J.; Lee, D. W. A study on the distribution of chlorination by-products (CBPs) in treated water in Korea. *Water Res.* **2001**, *35*, 2861–2872.
61. Simpson, K. L.; Hayes, K. P. Drinking water disinfection by-products: An Australian perspective. *Water Res.* **1998**, *32*, 1522–1528.
62. Hsie, A. W.; Brimer, P. A.; Mitchell, T. J.; Gosslee, D. G. The dose-response relationship for ultraviolet-light-induced mutations at the hypoxanthine-guanine phosphoribosyltransferase locus in Chinese hamster ovary cells. *Somatic Cell Genet.* **1975**, *1*, 383–389.
63. Tindall, K. R.; Stankowski, L. F., Jr; Machanoff, R.; Hsie, A. W. Detection of deletion mutations in pSV2gpt-transformed cells. *Mol. Cell. Biol.* **1984**, *4*, 1411–1415.
64. Wagner, E. D.; Rayburn, A. L.; Anderson, D.; Plewa, M. J. Analysis of mutagens with single cell gel electrophoresis, flow cytometry, and forward mutation assays in an isolated clone of Chinese hamster ovary cells. *Environ. Mol. Mutagen.* **1998**, *32*, 360–368.
65. Plewa, M. J.; Kargalioglu, Y.; Vanker, D.; Minear, R. A.; Wagner, E. D. Mammalian cell cytotoxicity and genotoxicity analysis of drinking water disinfection by-products. *Environ. Mol. Mutagen.* **2002**, *40*, 134–142.
66. Rundell, M. S.; Wagner, E. D.; Plewa, M. J. The comet assay: Genotoxic damage or nuclear fragmentation? *Environ. Mol. Mutagen.* **2003**, *42*, 61–67.
67. Tice, R. R.; Agurell, E.; Anderson, D.; Burlinson, B.; Hartmann, A.; Kobayashi, H.; Miyamae, Y.; Rojas, E.; Ryu, J. C.; Sasaki, Y. F. Single cell gel/comet assay: Guidelines for in vitro and in vivo genetic toxicology testing. *Environ. Mol. Mutagen.* **2000**, *35*, 206–221.
68. Wagner, E. D.; Plewa, M. J. Microplate-based comet assay. In *The Comet Assay in Toxicology*, Dhawan, A., Anderson, D., Eds.; Royal Society of Chemistry: London, 2008; pp 79–97.
69. Kumaravel, T. S.; Jha, A. N. Reliable Comet assay measurements for detecting DNA damage induced by ionising radiation and chemicals. *Mutat. Res., Genet. Toxicol. Environ. Mutagen.* **2006**, *605*, 7–16.

Chapter 3

Effect of Boiling on Halogenated DBPs and Their Developmental Toxicity in Real Tap Waters

Jiaqi Liu, Xiangru Zhang,* and Yu Li

Department of Civil and Environmental Engineering,
The Hong Kong University of Science and Technology,
Clear Water Bay, Kowloon, Hong Kong, China

*E-mail: xiangru@ust.hk.

The use of chlorine for disinfection results in the formation of halogenated disinfection by-products (DBPs) in tap water. Evidence has shown that halogenated DBPs may cause chronic adverse effects on human health, and brominated DBPs are generally significantly more toxic than their chlorinated analogues. Previously, the authors' group found that boiling of a simulated tap water for 5 min significantly reduced the overall levels of brominated and chlorinated DBPs, thus reducing the cytotoxicity of the simulated tap water to mammalian cells. In this study, we further investigated the effect of boiling on the level and developmental toxicity of halogenated DBPs in two "real" tap water samples. With a novel precursor ion scan approach using electrospray ionization-triple quadrupole mass spectrometry, the whole pictures of polar brominated and chlorinated DBPs in both tap water samples without and with boiling were revealed. After 5 min boiling, the concentrations of total organic bromine (a collective parameter for all brominated DBPs) in the two tap water samples decreased by 43.6% and 37.5%, respectively; the concentrations of total organic chlorine (a collective parameter for all chlorinated DBPs) in the two tap water samples decreased by 39.0% and 57.1%, respectively; the developmental toxicity of the two tap water samples decreased by 53.0% and 57.1%, respectively. This study suggests a simple

way to reduce the adverse health effect of halogenated DBPs in humans through tap water ingestion.

Introduction

With the purpose of inactivating harmful microorganisms and eradicating waterborne diseases, disinfection has been applied in drinking water treatment. Chlorine is a widely used disinfectant for drinking water. Chlorine-disinfected drinking water is distributed to households via a public water distribution system, in which a certain level of chlorine residual should be maintained to prevent regrowth of microorganisms in the water, especially when breaks or cracks occur in the pipeline. However, chlorinated disinfection by-products (DBPs) unintentionally form (from the reaction between hypochlorous acid and natural organic matter in source water) during chlorination in a drinking water treatment plant and in a water distribution system. Besides, source waters contain bromide ions resulting from geologic dissolution, seawater intrusion and human activities (1). During chlorination, hypochlorous acid can oxidize bromide to hypobromous acid, which subsequently reacts with natural organic matter in source water to generate brominated DBPs. Brominated DBPs have been reported to exhibit significantly higher toxicity than their chlorinated analogues (2–6).

Humans are unavoidably exposed to DBPs via water ingestion. It has been reported that the total cancer risks from the commonly known haloacetic acids and trihalomethanes mainly result from tap water ingestion (7). In most Western nations, tap water is directly drunk, whereas in some Asian nations, people are used to boiling tap water before drinking. Boiling has its own advantages, including effectively removing chlorine or chloramine residual and thus eliminating chlorinous taste and odor of the water (8); inactivating chlorine-resistant pathogenic protozoa *Cryptosporidium* and *Giardia* (9); and reducing some major DBPs (including trihalomethanes, haloacetic acids, halo ketones, haloacetonitriles, haloaldehydes, and halonitromethanes) (10–12).

Recently, a powerful precursor ion scan (PIS) approach with electrospray ionization-triple quadrupole mass spectrometry coupled with ultra performance liquid chromatography (UPLC/ESI-tqMS) has been developed for selectively detecting polar halogenated DBPs (13–19). By using this approach, the authors' group has studied the effect of boiling on the halogenated DBPs in a simulated tap water, and found that boiling for 5 min significantly reduced the halogenated DBPs and cytotoxicity of the water (20). However, a real tap water may be different from the simulated tap water because a real tap water originates from a real source water, which may contain a variety of organic and inorganic components including (micro)pollutants. Accordingly, the purpose of this study was to determine the effect of boiling on the halogenated DBPs and toxicity in real tap waters.

Hutchinson's group developed an *in vivo* assay using the sensitive embryo-larval stages of a polychaete, *Platynereis dumerilii*, which is a cosmopolitan species, extending from the tropics to cold temperate latitudes in both hemispheres (21, 22). The authors' group modified Hutchinson et al.'s

method and significantly lowered the relative standard deviation to <5% (5). The improved bioassay becomes a sensitive metric and has been successfully applied in determining the comparative developmental toxicity of individual DBPs (5, 23). In this study, *P. dumerilii* was employed to evaluate the comparative developmental toxicity of real tap waters without and with boiling.

Experimental Methods

Water Sampling and Characterization

Two source water samples (source waters 1 and 2) were collected at the inlets of two drinking water treatment plants. Correspondingly, two tap water samples that originated from the two drinking water treatment plants were collected at two faucets on the same day. Tap waters 1 and 2 corresponded to source waters 1 and 2, respectively. The collected water samples were filtered through 0.45 μm membrane. Dissolved organic carbon (DOC), UV absorbance, pH, and bromide concentration of each source water sample were measured with a total organic carbon analyzer (Model TOC-Vcsh, Shimadzu), a UV/visible spectrophotometer (GE healthcare, Ultrospec 4300 pro), a pH meter, and an ion chromatograph (Dionex DX500), respectively. Alkalinity in each source water sample and chlorine residual in each tap water sample were determined according to the Standard Methods (24). The characteristics of the source water samples were summarized in Table 1. The chlorine residual levels in tap waters 1 and 2 were 0.75 and 0.63 mg/L as Cl_2 , respectively. For comparison, the characteristics of the simulated source water used in the previous study were also listed in Table 1. This simulated source water was disinfected with 5 mg/L NaOCl as Cl_2 in darkness at ~ 21 $^\circ\text{C}$ for 15 h to generate the simulated tap water. No chlorine residual was detectable in the simulated tap water (20).

Table 1. Characteristics of Two Real Source Waters and the Simulated Source Water

Source water	1	2	Simulated ^a
DOC (mg/L as C)	2.68	2.06	3.00
UV ₂₅₄ absorbance (1/cm)	0.032	0.027	0.16
SUVA ^b (L/mg-m)	1.20	1.31	5.17
pH	6.94	7.22	8.50
Alkalinity (mg/L as CaCO_3)	25.1	22.1	90.0
Bromide ($\mu\text{g/L}$)	26.5	16.7	2000

^a The simulated source water was prepared with ultrapure water containing 3 mg/L Suwannee River humic acid as C, 90 mg/L NaHCO_3 as CaCO_3 , and 2 mg/L KBr as Br^- (20). ^b Specific UV absorbance.

Chemicals and Seawater

All chemical solutions were prepared from chemicals of reagent grade or above. 3,5-Dibromo-4-hydroxybenzaldehyde was purchased from Alfa Aesar. Bromobutenedioic acid, bromoacetic acid, dibromoacetic acid, bromochloroacetic acid, dichloroacetic acid, dibromochloroacetic acid, bromodichloroacetic acid, trichloroacetic acid, methyl *tert*-butyl ether (MtBE), and acetonitrile (HPLC-grade) were purchased from Sigma-Aldrich. Seawater was collected locally. Prior to use, it was filtered through 0.45 μm membrane, autoclaved at 121 $^{\circ}\text{C}$ for 20 min. After cooled to ambient temperature, the seawater was aerated for 15 min.

Pretreatment of Tap Water Samples with/without Boiling

Our previous study showed that boiling for 5 min obviously reduced the halogenated DBPs and toxicity of the simulated tap water (20). Accordingly, for either tap water 1 or tap water 2, two parallel samples (3.4 L each) were heated to boiling (at 100 $^{\circ}\text{C}$) in open 5 L glass beakers, and kept boiling for 5 min. Afterwards, both boiled water samples were cooled to ambient temperature quickly in an ice bath (to minimize the variation of the sample components during cooling). Then, both samples were brought to 3.4 L by adding ultrapure water, and the chlorine residual in each sample was measured (24). After boiling, no chlorine residual was detectable, which was consistent with Zhang's results (8).

One of the parallel samples was divided into two aliquots (300 mL and 3000 mL). The 300 mL aliquot was subjected to total organic halogen (TOX) measurement, and the 3000 mL aliquot was pretreated per Zhang et al.'s procedure (25). In brief, it was further divided into three 1000 mL aliquots, and each aliquot was first acidified to pH 0.5 with 70% (v/v) aqueous sulfuric acid, followed by the addition of sodium sulfate to saturation. Then, the acidified sample was extracted with 100 mL MtBE, and 70 mL of the organic layer was transferred to a rotary evaporator and concentrated to 0.5 mL. The 0.5 mL MtBE solutions obtained from three aliquots were combined together (totally \sim 1.5 mL) and mixed with 20 mL acetonitrile. The mixture was concentrated to 1 mL, and stored at 4 $^{\circ}\text{C}$. Prior to UPLC/ESI-tqMS measurement, the acetonitrile solution was diluted to 2 mL with ultrapure water, and filtered with 0.45 μm membrane. For the other parallel sample, 3000 mL was pretreated following the procedure above, except that after evaporation, the 0.5 mL MtBE solutions obtained from three aliquots were combined together and dried with nitrogen sparging. The solid obtained was stored at 4 $^{\circ}\text{C}$ and dissolved in seawater 1 h prior to the toxicity test as a toxicity test stock solution. This stock solution was diluted by seawater to various concentration factors (in comparison with the original water sample).

For comparison, two 3.4 L parallel aliquots of each tap water sample without boiling were pretreated following the procedure above, except that the chlorine residual in the 300 mL aliquot for TOX measurement was quenched with NaAsO_2 at 105% of the stoichiometric amount of the chlorine residual (26).

TOX Measurement

TOX was measured according to Standard Method 5320B (24), except that an off-line ion chromatograph was used as a halide separator and detector for the measurement of total organic chlorine (TOCl) and total organic bromine (TOBr) (26–28). Total organic iodine (TOI) was not included in this study because the TOI levels in the two tap waters were very low (about 1.3 $\mu\text{g/L}$ as I) (29). Each 300 mL tap water sample without or with boiling was adjusted to pH 2 with nitric acid. A 3-channel adsorption module (Mitsubishi Chemical Analytech) was used for activated carbon adsorption. After adsorption, the activated carbon columns were rinsed with 10 mL of 5000 mg/L KNO_3 as NO_3^- to remove inorganic halides and were subsequently subjected to pyrolysis at 1000 $^\circ\text{C}$ with an AQF-100 automatic quick furnace (Mitsubishi Chemical Analytech). The hydrogen halide and halogen gases produced from pyrolysis were absorbed in a 5 mL 0.003% H_2O_2 solution, which contained 2 mg/L KH_2PO_4 as PO_4^{3-} serving as an internal standard to estimate the volume variations introduced by the GA-100 gas absorption unit (Mitsubishi Chemical Analytech). Thus, TOCl and TOBr in the original water sample were converted and transferred into the absorption solution in the form of Cl^- and Br^- , respectively. One mL of the absorption solution was analyzed by an ICS-3000 ion chromatograph (Dionex) with an IonPac analytical column (AS19, 4 \times 250 mm) and a guard column (AG19, 4 \times 50 mm). A KOH eluent was generated by the EGC KOH cartridge (Dionex) at a flow rate of 1 mL/min. Chloride and bromide were separated with an isocratic eluent of 10 mM KOH from 0 to 10 min followed by a linear gradient eluent of 10–45 mM KOH from 10 to 25 min. The concentrations of the halides were quantified with a conductivity detector. The practical quantitation limits for TOCl and TOBr were 0.002 mg/L as Cl and 0.002 mg/L as Br, respectively (26). Each sample was subjected to triplicate TOX analyses.

(UPLC)/ESI-tqMS Analyses

An ESI-tqMS (Waters Acquity) was employed to analyze the pretreated water samples. The operation parameters were set according to previous studies (14, 20): ESI negative mode; capillary voltage 2.8 kV; cone voltage 30 V for chlorinated DBPs, and 15 V for brominated DBPs; desolvation temperature 350 $^\circ\text{C}$; source temperature 120 $^\circ\text{C}$; cone gas flow 50 L/h; desolvation gas flow 650 L/h; collision energy 30 eV for chlorinated DBPs, and 20 eV for brominated DBPs; Argon collision gas flow 0.25 mL/min; mass resolution 15 (1-unit resolution). By setting PISs m/z 79/81 (or m/z 35/37), all electrospray-ionizable brominated (or chlorinated) DBPs can be detected. Multi-channel analysis mode was used for data collection for all PISs (with a scan time of 0.3 s, run durations of 5 min for PISs m/z 79/81 and 7 min for PISs m/z 35/37), by which precursor ion intensities were substantially enhanced by accumulating multiple scans (1000 scans for PISs m/z 79/81 and 1400 scans for PISs m/z 35/37), and intensity fluctuation in a single scan was effectively eliminated.

A UPLC (Waters) was coupled with the ESI-tqMS for pre-separation. Seven μL of a pretreated water sample was injected into the UPLC with an HSS T3

column (Waters, 100×2.1 mm, $1.8 \mu\text{m}$ particle size). The eluent was kept at 0.50 mL/min and composed of water and acetonitrile. The composition of water/acetonitrile (v/v) changed linearly from 90/10 to 10/90 in the first 8 min, and returned within 0.1 min to 90/10, which was maintained for 1.9 min for re-equilibration. In UPLC/ESI-tqMS analyses, the desolvation gas flow was 800 L/h; the desolvation temperature was 400 °C; and the other operation parameters of ESI-tqMS were set as aforementioned. For a halogenated DBP detected by PISs, its structure was proposed based on the retention time in UPLC/ESI-tqMS multiple reaction monitoring (MRM) scan, the intensity ratio of selected MRM mass transition, and the fragment ions in product ion scans at the corresponding retention time. For a tentatively proposed structure of a detected DBP, the corresponding standard compound was purchased to confirm the proposed structure.

Developmental Toxicity Bioassay with *P. dumerilii*

Stock cultural conditions of *P. dumerilii* were maintained per the procedure by Hutchinson's group (21, 22), and the bioassay was conducted according to previous studies (5, 23). Briefly, the polychaete was cultivated in the seawater at 19 °C, and fed on a diet composed of chopped spinach, fish flakes and algae. Breeding of the polychaete was controlled at a daily illumination regime of 16 h light (at approximately 300 lux) and 8 h absolute darkness. The developmental toxicity tests were conducted with the polychaete embryos. To collect the embryos, sexually mature males and females were transferred to culturing bottles and allowed to spawn naturally in 50 mL seawater. As fertilization was confirmed, the developing embryos were transferred to a culturing tank containing 500 mL seawater. After 12 h fertilization, embryos were transferred to a 1.6 cm tissue culture testplate that contained seawater (as control) or test sample (with a total volume of 2.0 mL). The embryos were allowed to develop for another 12 h. By 24 h post-fertilization, normally developed embryos were expected to achieve the first larval (trochophore) stage. The numbers of normally developed and total embryos in the seawater control or test sample were counted with the aid of an inverted microscope, and the normal development percentage was calculated.

For either tap water without/with boiling, a preliminary test was conducted to determine the critical concentrated range, in which the highest and lowest concentration factors induced 100% abnormal development and a significant amount of abnormal development (the normal development percentage at the concentration factor was 5% less than that of the seawater control sample), respectively (5, 23). Then, a series of test samples (with different concentration factors within the critical concentrated range) were prepared by diluting the toxicity test stock solution with seawater, and another bioassay was conducted. Afterwards, a concentration factor-response curve was obtained for the water sample, and the EC_{50} value (the concentration factor at which the normal development percentage was 50% of that in the seawater control) was calculated via regression analysis using the software SigmaPlot 12 (Systat Software Inc., San Jose, CA). For all the water samples, duplicate developmental toxicity tests were conducted.

Results and Discussion

Reduction of TOX during Boiling

As shown in Figure 1, the concentrations of TOCl and TOBr in the two tap waters tested substantially reduced after 5 min boiling. In tap water 1, TOCl and TOBr were reduced by 39.0% and 43.6%, respectively; in tap water 2, TOCl and TOBr were reduced by 51.7% and 37.5%, respectively. The previous study (20) demonstrated that the TOX lost during boiling was caused by volatilization to air and conversion to inorganic halides. The reduction percentages of TOCl and TOBr by 5 min boiling in the simulated tap water (61.1% and 62.8%, respectively) (20) were higher than those in the two real tap waters, mainly because there was no chlorine residual in the simulated tap water. In the two real tap water samples, the chlorine residual might keep reacting with organic matter and bromide ions to form chlorinated and brominated DBPs during heating. However, chlorine residual decreases quickly with the increase of temperature, and it almost completely decays at 100 °C (8). Besides, the formed DBPs might decompose during the subsequent 5 min boiling at 100 °C (20). Accordingly, the “apparent” reduction of TOX after boiling was the combined result of formation, volatilization and decomposition.

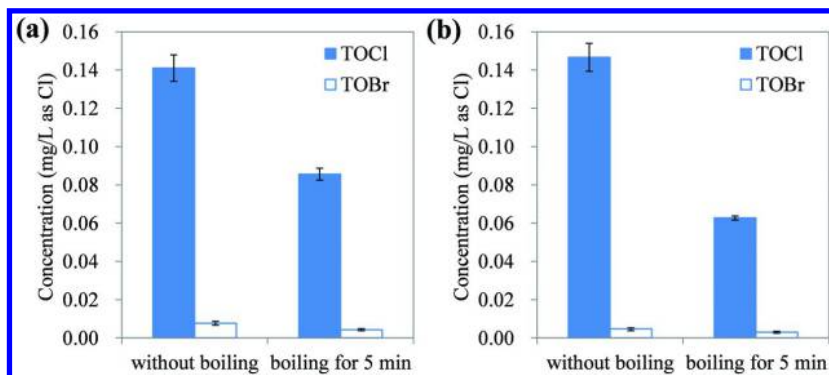


Figure 1. TOCl and TOBr concentrations in (a) tap water 1 and (b) tap water 2 without boiling and with 5 min boiling. Each datum presents the average and standard deviations of triplicate measurements.

Decomposition of Polar Brominated and Chlorinated DBPs during Boiling

Figure 2 summarizes the ESI-tqMS PIS spectra of m/z 79 of the two tap waters without and with 5 min boiling. For the brominated DBPs formed in the simulated tap water (20), nine of them (seven confirmed DBPs including bromoacetic acid, bromodichloroacetic acid, bromochloroacetic acid, bromobutenedioic acid, dibromochloroacetic acid, dibromoacetic acid and 3,5-dibromo-4-hydroxybenzaldehyde, and two proposed DBPs including bromopropenoic acid and dibromomethylbutenedioic acid) were also detected in the two real tap waters without boiling.

Figure 3 summarizes the ESI-tqMS PIS spectra of m/z 35 of two tap waters without and with 5 min boiling. The simulated source water contained 2 mg/L bromide, whereas the two real source waters contained significantly lower concentrations of bromide (Table 1). The decrease of bromide concentration in a source water could shift the DBPs (generated during chlorination) from fully brominated species to bromochloro-mixed species, and further to fully chlorinated species (14). Accordingly, the halogenated DBPs detected in the real tap waters were somewhat different from those in the simulated tap water. First, for dihaloacetic acids, dibromo- and bromochloro-acetic acids were detected in the simulated and real tap waters, but dibromoacetic acid showed a higher level in the simulated tap water than in real tap waters, and dichloroacetic acid was detected in both real tap waters. Second, for trihaloacetic acids, tribromo-, dibromochloro- and bromodichloro-acetic acids were detected in the simulated tap water, while tribromoacetic acid was not detected and trichloroacetic acid was detected in both real tap waters. Third, 2,4,6-tribromophenol, which has been confirmed in the simulated tap water, was not detected in either real tap water. However, ion clusters m/z 283/285/287 (with the isotopic abundance ratio of 1:2:1) and m/z 239/241/243 (with the isotopic abundance ratio of 3:4:1) were detected in PISs m/z 35 of both real tap waters, and they were proposed to be 2,4,6-dibromochlorophenol and 2,4,6-bromodichlorophenol, respectively. Fourth, ion cluster m/z 285/287 was detected in PIS m/z 79 of the simulated tap water, and it was proposed to be dibromomethylbutenedioic acid. This ion cluster was only detected in tap water 1, and ion clusters m/z 241/243 (with the isotopic abundance ratio of 3:1 in PIS m/z 79) and m/z 197/199 (with the isotopic abundance ratio of 3:1 in PIS m/z 35) were detected in both real tap waters. These two ion clusters were proposed to be bromochloromethylbutenedioic acid and dichloromethylbutenedioic acid. Additionally, some saturated aliphatic DBPs (which did not form in the simulated tap water) were detected in both real tap waters, including bromopropanoic acid, bromobutanedioic acid, bromochlorobutanedioic acid and dichlorobutanedioic acid.

Figure 4 shows the effect of boiling on the concentrations of the halogenated DBPs in the two real tap waters, based on the peak areas of the corresponding ion clusters in the UPLC/ESI-tqMS MRM chromatograms. More than half of the listed DBPs decomposed during boiling, including trihaloacetic acids (i.e., dibromochloro-, bromodichloro-, and trichloro-acetic acids), butenedioic acids (i.e., bromochloro-, dibromomethyl-, bromochloromethyl-, dichloromethyl-, trichloromethyl-butenedioic acids), butanedioic acids (i.e., bromochloro- and dichloro-butanedioic acids), and 2,4,6-trihalophenols (i.e., 2,4,6-dibromochlorophenol and 2,4,6-bromodichlorophenol). The decomposition mechanisms of trihaloacetic acids, dihalobutenedioic acids, dihalomethylbutenedioic acids, and trihalomethylbutenedioic acids included decarboxylation and hydrolysis (20).

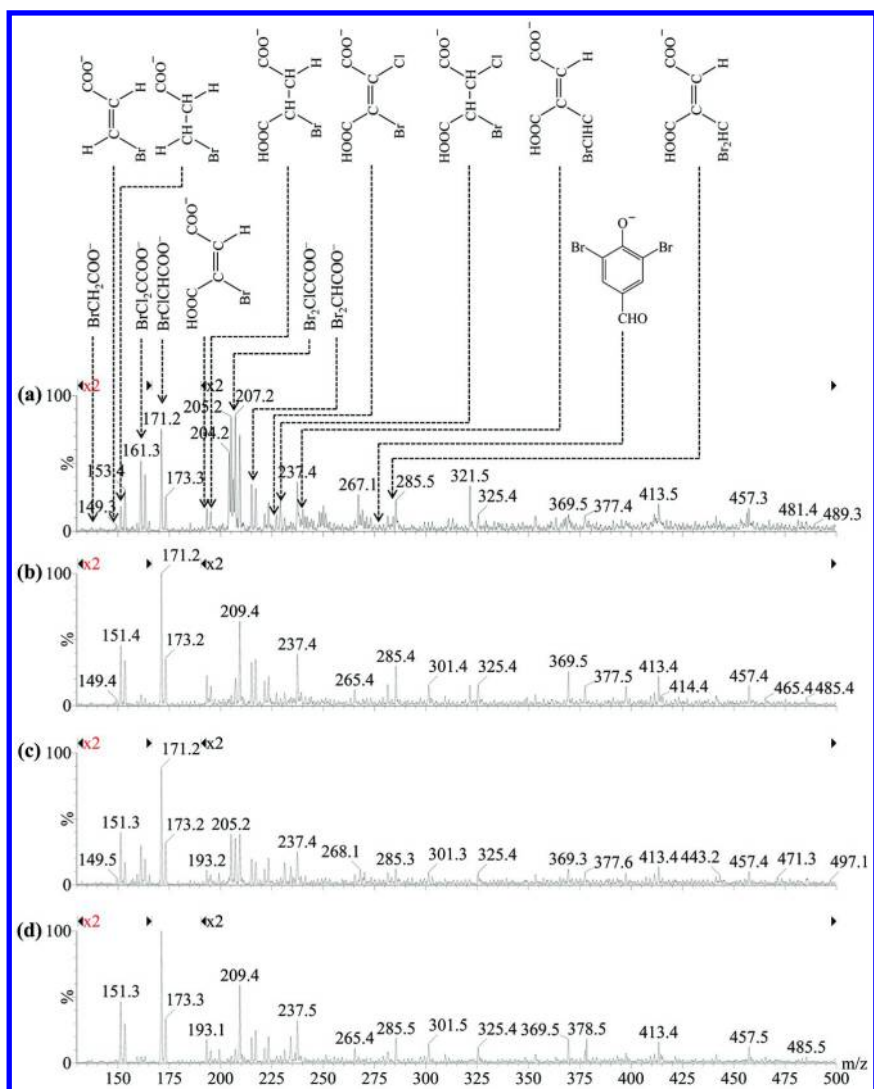


Figure 2. ESI-tqMS PIS spectra of m/z 79 of (a) tap water 1 without boiling, (b) tap water 1 with 5 min boiling, (c) tap water 2 without boiling, and (d) tap water 2 with 5 min boiling. The y-axes are on the same scale. Above the spectra shows the corresponding structures, of which bromoacetic acid, bromodichloroacetic acid, bromochloroacetic acid, bromobutenedioic acid, dibromochloroacetic acid, dibromoacetic acid and 3,5-dibromo-4-hydroxybenzaldehyde were confirmed with the standard compounds, while others were proposed structures.

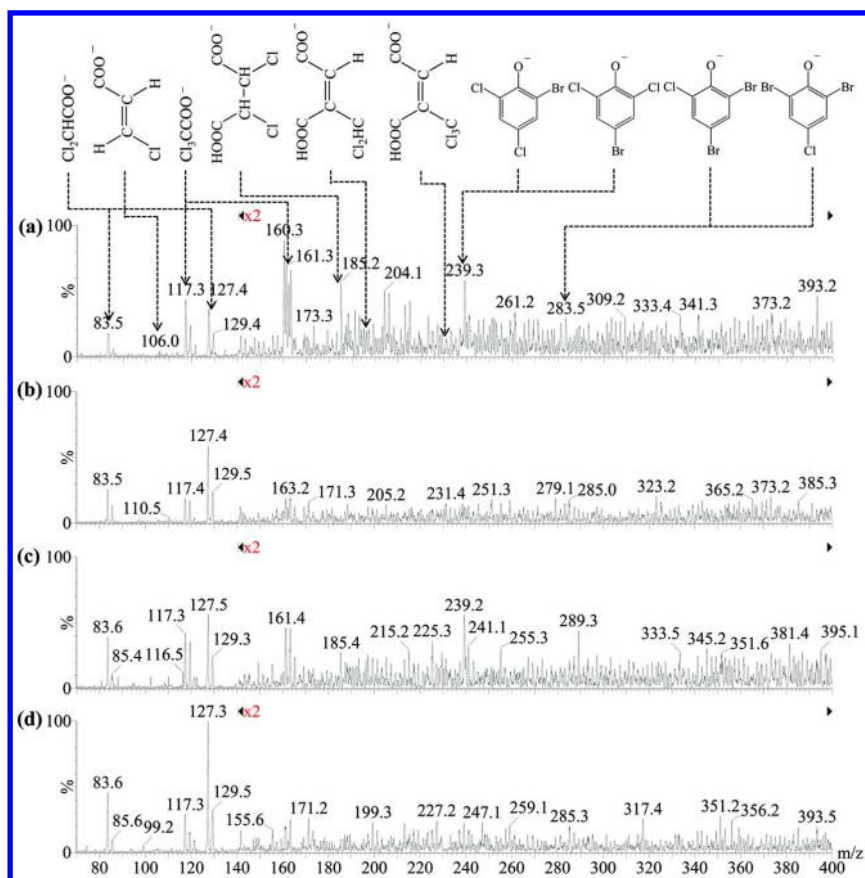


Figure 3. ESI-tqMS PIS spectra of m/z 35 of (a) tap water 1 without boiling, (b) tap water 1 with 5 min boiling, (c) tap water 2 without boiling, and (d) tap water 2 with 5 min boiling. The y-axes are on the same scale. Above the spectra shows the corresponding structures, of which dichloroacetic acid and trichloroacetic acid were confirmed with the standard compounds, while others were proposed structures.

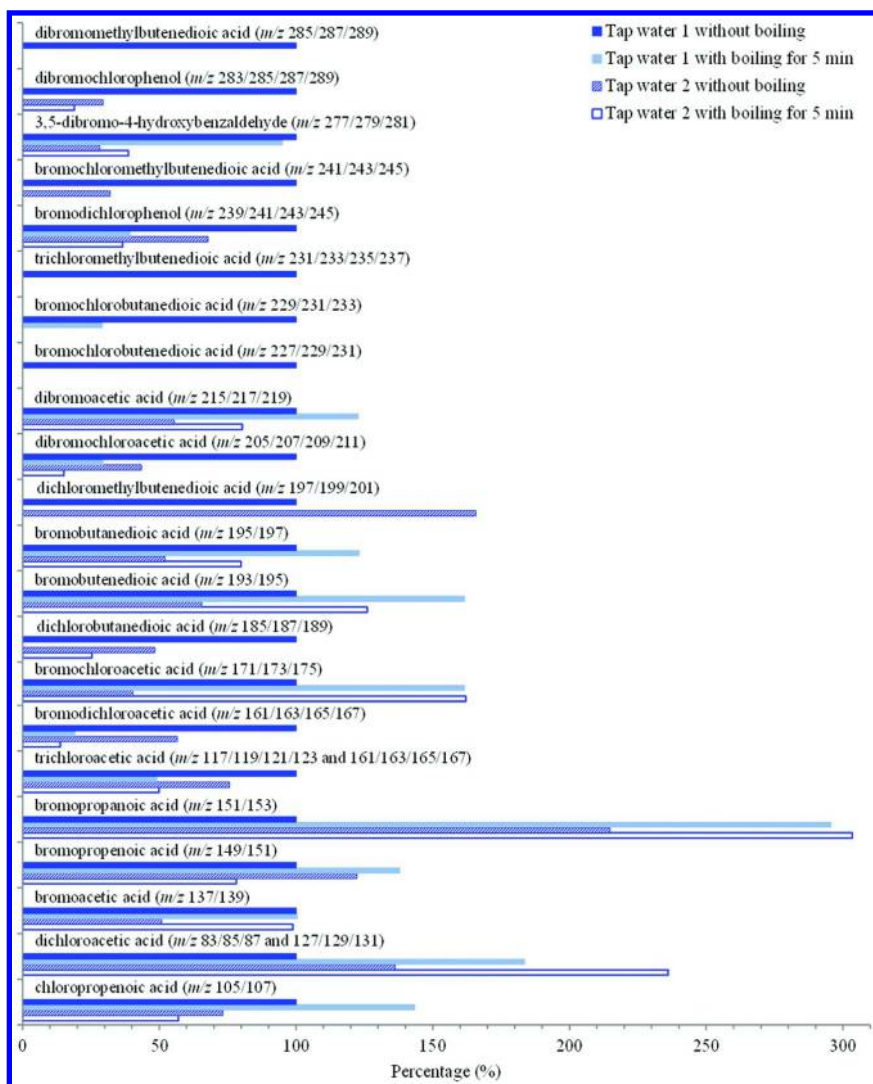


Figure 4. Effect of boiling on the concentrations of the confirmed or proposed halogenated DBPs in the tap waters. For each DBP, its peak area in the UPLC/ESI-tqMS MRM chromatogram of tap water 1 without boiling was defined as 100%, and its peak areas in the UPLC/ESI-tqMS MRM chromatograms of other samples were expressed as the percentages of the peak area of tap water 1 without boiling.

Boiling also resulted in accumulation of a few DBPs, including bromoacetic acid, dihaloacetic acids, bromobutenedioic acid, bromobutanedioic acid, and bromopropanoic acid. For some DBPs, boiling showed different impacts in the two real tap waters: The levels of bromo- and chloro-propenoic acids increased in tap water 1, but decreased in tap water 2; the level of 3,5-dibromo-4-hydroxybenzaldehyde decreased in tap water 1, but increased in tap water 2. Monohalopropenoic acids and monohalobutenedioic acids were found to decompose during boiling in the simulated tap water (20). However, in the real tap waters, their levels increased, possibly due to the continued reaction between chlorine residual and the organic matter and bromide ions during heating. It was also reported that some aromatic DBPs in the simulated tap water increased during boiling because of the degradation of their precursors (20). Tap water 2 might also contain the precursors of 3,5-dibromo-4-hydroxybenzaldehyde, leading to the increase of its level after boiling. Tap water 1 might not contain the precursors of 3,5-dibromo-4-hydroxybenzaldehyde, and both tap waters 1 and 2 might not contain the precursors of 2,4,6-dibromochlorophenol and 2,4,6-bromodichlorophenol. Besides, the decomposition of 2,4,6-dibromochlorophenol and 2,4,6-bromodichlorophenol caused the additional formation of dibromo-, bromochloro- and dichloro-acetic acids, following the mechanism proposed by Zhai and Zhang (13).

Total ion intensity (TII) in the ESI-tqMS PIS spectrum of m/z 79 (or m/z 35) can be approximately proportional to the total quantity of polar brominated (or chlorinated) DBPs in a water sample. It was defined as the sum of ion intensities from m/z 100 to 500 in the PIS spectrum of m/z 79 (or from m/z 50 to 400 in the PIS spectrum of m/z 35). After boiling, for tap water 1, the TII values in the PIS spectra of m/z 79 and m/z 35 decreased by 28.0% and 51.3%, respectively; for tap water 2, the TII values in the PIS spectra of m/z 79 and m/z 35 decreased by 17.4% and 36.4%, respectively.

Detoxification of Real Tap Water by Boiling

Since the levels of TOX and polar halogenated DBPs in the two tap waters were substantially reduced by 5 min boiling, the toxicity of the boiled tap waters was expected to be lower. Figure 5 shows the concentration factor-response curves of the developmental toxicity (against the polychaete *P. dumerilii*) of the two tap waters without and with boiling. A lower normal development percentage indicates a higher toxicity. Through regression analysis of the concentration factor-response curve, the EC_{50} value for each tap water without/with boiling was calculated (Table 2). A lower EC_{50} value represents a higher developmental toxicity potential (5, 23). Considering the EC_{50} values, the developmental toxicity of tap waters 1 and 2 was decreased by 53.0% and 57.1%, respectively, after boiling. These indicate that boiling is an effective “detoxification” method for real tap waters.

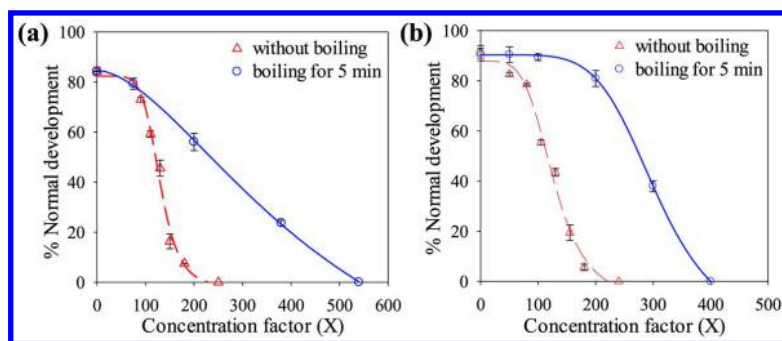


Figure 5. Concentration factor-response curves of the developmental toxicity against the polychaete *P. dumerilii* of (a) tap water 1 without boiling and with 5 min boiling, and (b) tap water 2 without boiling and with 5 min boiling. Each datum presents the mean of duplicate measurements and the difference between the mean and the measured value.

Table 2. Developmental Toxicity against the Polychaete *P. dumerilii* of Two Real Tap Waters without and with 5 min Boiling (n = 2)

Tap water	Concentration factor range (\times -fold)	EC_{50} (\times -fold)	R^2 ^a
1, without boiling	90-250	129	0.98
1, with boiling	75-540	274	0.99
2, without boiling	50-240	123	0.98
2, with boiling	50-400	286	0.99

^a The regression coefficient of the concentration factor-response curve for each water sample.

Conclusions

The results of TOX measurements and (UPLC)/ESI-tqMS analyses obtained in this study demonstrated that boiling for 5 min substantially reduced the brominated and chlorinated DBPs in real tap waters. Accordingly, boiling is an effective method for reducing human exposure to halogenated DBPs through tap water ingestion. From the data of developmental toxicity against the polychaete *P. dumerilii*, 5 min boiling significantly decreased the toxicity of tap waters. To further investigate the effect of boiling on “detoxification” of tap water, additional toxicity tests may be conducted with different bioassays, and relevant epidemiological studies may also be needed.

Acknowledgments

This research was supported by grants from the Research Grants Council of Hong Kong, China (projects 622412, 622913 and FSGRF12EG60). The authors thank Jingyi Jiang for her assistance in the DOC measurement, Dave Ho for his daily maintenance of the TOX analyzer, and Adriaan W. C. Dorresteyn (at the Johannes Gutenberg-Universität Mainz, Germany) for providing parental *P. dumerilii*.

References

1. Amy, G. L.; Siddiqui, M. S. *Strategies to Control Bromate and Bromide*; AWWA Research Foundation: Denver, CO, 1999; pp 7–8.
2. Richardson, S. D.; Plewa, M. J.; Wagner, E. D.; Schoeny, R.; DeMarini, D. M. Occurrence, genotoxicity, and carcinogenicity of regulated and emerging disinfection by-products in drinking water: a review and roadmap for research. *Mutat. Res., Rev. Mutat. Res.* **2007**, *636*, 178–242.
3. Pals, J. A.; Attene-Ramos, M. S.; Xia, M.; Wagner, E. D.; Plewa, M. J. Human cell toxicogenomic analysis linking reactive oxygen species to the toxicity of monohaloacetic acid drinking water disinfection byproducts. *Environ. Sci. Technol.* **2013**, *47*, 12514–12523.
4. Dad, A.; Jeong, C. H.; Pals, J. A.; Wagner, E. D.; Plewa, M. J. Pyruvate remediation of cell stress and genotoxicity induced by haloacetic acid drinking water disinfection by-products. *Environ. Mol. Mutagen.* **2013**, *54*, 629–637.
5. Yang, M.; Zhang, X. Comparative developmental toxicity of new aromatic halogenated DBPs in a chlorinated saline sewage effluent to the marine polychaete *Platynereis dumerilii*. *Environ. Sci. Technol.* **2013**, *47*, 10868–10876.
6. Liu, J.; Zhang, X. Comparative toxicity of new halophenolic DBPs in chlorinated saline wastewater effluents against a marine alga: Halophenolic DBPs are generally more toxic than haloaliphatic ones. *Water Res.* **2014**, *65*, 64–72.
7. Chowdhury, S.; Rodriguez, M. J.; Serodes, J. Model development for predicting changes in DBP exposure concentrations during indoor handling of tap water. *Sci. Total Environ.* **2010**, *408*, 4733–4743.
8. Zhang, A. L. Removal of chlorine residual in tap water by boiling or adding ascorbic acid. *Int. J. Eng. Res. Appl.* **2013**, *3*, 1647–1651.
9. Carey, C. M.; Lee, H.; Trevors, J. T. Biology, persistence and detection of *Cryptosporidium parvum* and *Cryptosporidium hominis* oocyst. *Water Res.* **2004**, *38*, 818–862.
10. Krasner, S. W.; Wright, J. M. The effect of boiling water on disinfection by-product exposure. *Water Res.* **2005**, *39*, 855–864.
11. Wu, W.; Benjamin, M. M.; Korshin, G. V. Effects of thermal treatment on halogenated disinfection by-products in drinking water. *Water Res.* **2001**, *35*, 3545–3550.

12. Zhang, X. L.; Yang, H. W.; Wang, X. M.; Fu, J.; Xie, Y. F. Formation of disinfection by-products: Effect of temperature and kinetic modeling. *Chemosphere* **2013**, *90*, 634–639.
13. Zhai, H.; Zhang, X. Formation and decomposition of new and unknown polar brominated disinfection byproducts during chlorination. *Environ. Sci. Technol.* **2011**, *45*, 2194–2201.
14. Pan, Y.; Zhang, X. Four groups of new aromatic halogenated disinfection byproducts: Effect of bromide concentration on their formation and speciation in chlorinated drinking water. *Environ. Sci. Technol.* **2013**, *47*, 1265–1273.
15. Zhai, H.; Zhang, X.; Zhu, X.; Liu, J.; Ji, M. Formation of brominated disinfection byproducts during chloramination of drinking water: New polar species and overall kinetics. *Environ. Sci. Technol.* **2014**, *48*, 2579–2588.
16. Zhai, H. Y.; Zhang, X. A new method for differentiating adducts of common drinking water DBPs from higher molecular weight DBPs in electrospray ionization-mass spectrometry analysis. *Water Res.* **2009**, *43*, 2093–2100.
17. Xiao, F.; Zhang, X.; Zhai, H.; Yang, M.; Lo, I. M. C. Effects of enhanced coagulation on polar halogenated disinfection byproducts in drinking water. *Sep. Purif. Technol.* **2010**, *76*, 26–32.
18. Xiao, F.; Zhang, X.; Zhai, H.; Lo, I. M. C.; Tipoe, G. L.; Yang, M.; Pan, Y.; Chen, G. H. New halogenated disinfection byproducts in swimming pool water and their permeability across skin. *Environ. Sci. Technol.* **2012**, *46*, 7112–7119.
19. Ding, G.; Zhang, X.; Yang, M.; Pan, Y. Formation of new brominated disinfection byproducts during chlorination of saline sewage effluents. *Water Res.* **2013**, *47*, 2710–2718.
20. Pan, Y.; Zhang, X.; Wagner, E. D.; Osiol, J.; Plewa, M. J. Boiling of simulated tap water: effect on polar brominated disinfection byproducts, halogen speciation, and cytotoxicity. *Environ. Sci. Technol.* **2014**, *48*, 149–156.
21. Hutchinson, T. H.; Jha, A. N.; Dixon, D. R. The polychaete, *Platynereis dumerilii* (Audouin and Milne-Edwards): A new species for assessing the hazardous potential of chemicals in the marine environment. *Ecotoxicol. Environ. Saf.* **1995**, *31*, 271–281.
22. Jha, A. N.; Hutchinson, T. H.; Mackay, J. M.; Elliott, B. M.; Dixon, D. R. Evaluation of the genotoxicity of municipal sewage effluent using the marine worm *Platynereis dumerilii* (Polychaeta: Nereidae). *Mutat Res., Genet. Toxicol. Environ. Mutagen.* **1997**, *391*, 179–188.
23. Yang, M.; Zhang, X. Halopyrroles: A new group of highly toxic DBPs formed in chlorinated saline wastewater. *Environ. Sci. Technol.* **2014**, *48*, 11846–11852.
24. APHA, AWWA, WEF. *Standard Methods for the Examination of Water and Wastewater*, 22th ed.; Washington, DC, 2012.
25. Zhang, X.; Talley, J. W.; Boggess, B.; Ding, G.; Birdsell, D. Fast selective detection of polar brominated disinfection byproducts in drinking water using precursor ion scans. *Environ. Sci. Technol.* **2008**, *42*, 6598–6603.

26. Liu, J.; Zhang, X. Effect of quenching time and quenching agent dose on total organic halogen measurement. *Int. J. Environ. Anal. Chem.* **2013**, *93*, 1146–1158.
27. Hua, G.; Reckhow, D. A. Determination of TOCl, TOBr and TOI in drinking water by pyrolysis and off-line ion chromatography. *Anal. Bioanal. Chem.* **2006**, *384*, 495–504.
28. Li, Y.; Zhang, X.; Shang, C. Effect of reductive property of activated carbon on total organic halogen analysis. *Environ. Sci. Technol.* **2010**, *44*, 2105–2111.
29. Gong, T.; Zhang, X. Determination of iodide, iodate and organo-iodine in waters with a new total organic iodine measurement approach. *Water Res.* **2013**, *47*, 6660–6669.

Chapter 4

Bromination and Chlorination of NOM: New Modeling Approaches and Mechanistic Insights

Paolo Roccaro,^{*,1} Federico G. A. Vagliasindi,¹ and Gregory V. Korshin²

¹Department of Civil Engineering and Architecture, University of Catania,
Viale A. Doria 6, 95125 Catania, Italy

²Department of Civil and Environmental Engineering,
University of Washington, Seattle, Washington 98195-2700

*E-mail: proccaro@dica.unict.it.

This study investigated formation of trihalomethanes (THMs), haloacetic acids (HAAs), haloacetonitriles (HANs) generated in two chlorinated surface waters. DBPs formation reactions and concurrent NOM transformations were examined based on the kinetic analysis of DBP concentrations and also via differential spectroscopy that quantifies the extent of NOM halogenation. The evolution of differential absorbance (ΔA) was correlated with both DBPs yields and speciation. The modeling of DBP formation using ΔA data showed the existence of compound-specific proportionality coefficients that change predictably as function of Br⁻ concentration but do not depend on chlorine concentration or reaction time. The presented approach was employed to develop a DBP formation model that is based on the kinetics of ΔA changes combined with the bromide-dependent DBP yield coefficients.

Background

Disinfection of drinking water by chlorine has dramatically reduced the transmission of potentially fatal waterborne diseases. The main issues that affect current chlorination practices include the limited efficiency of chlorine against some pathogens and formation of toxic disinfection by-products (DBPs) (*I*) formed as a result of reactions of chlorine and other halogen species with natural organic matter (NOM) to produce chlorinated, brominated and, in much

smaller levels, iodinated DBPs (2–4). Even though trihalomethanes (THMs) and haloacetic acids (HAAs) occur at the highest concentrations (up several hundred mg/L) in chlorinated water (5) and are the most regulated DBPs worldwide (6), more than 500 other individual DBPs have been identified (7).

DBP formation and speciation are affected by concentration and reactivity of NOM, levels of bromide, iodine and ammonia, chlorine dose, pH, temperature and reaction time (2, 4, 8–10). The formation of brominated DBPs is of particular concern because these compounds are much more toxic than their chlorinated analogues (5, 11, 12). The concentration of bromide in natural waters is usually considerably lower than 1 mg/L (10) but in some case Br⁻ concentrations up to 4 mg/L have been detected (13, 14).

Numerous alternative DBP formation models that use either statistical and mechanistic approaches have been presented in prior research (e.g., (15–17)). Due to the complexities of both NOM chemistry and halogenations processes *per se*, most efforts in DBP modelling have focused on the development of empirical/statistical models that predict DBP concentrations using numerous alternative expressions and a set of fitting parameters applied to represent a specific set of DBP data (18). While multi-parameter statistical fitting employed to develop these models can be very useful for a specific set of DBP generation conditions, they need to be recalibrated to be applicable to any water quality dissimilar from the dataset used to develop such models. Statistical fitting *per se* also does not provide any insights on DBP formation mechanisms whose inclusion in DBP modelling allows in principle for more concise and clear approaches.

Fundamentally, mechanistic approach to DBPs formation modelling incorporates clear assumptions that reflect the nature of NOM halogenation (e.g., formation of various intermediates, branching kinetic pathways), equilibria describing major aspects of the aquatic chemistry of halogen species, and a system of differential equations that represent the consumption of halogen species and reactive sites in NOM, generation and breakdown of halogenated intermediates and cleavage of individual DBP species from them. A number of such models employ the assumption that chlorine and bromine atoms are incorporated in the NOM substrate through several sequential steps of bromine and chlorine reactions with the reactive NOM sites (9, 19–21). In these models, relative yields of chlorinated and brominated products originating from the intermediates formed at each node of halogen incorporation are defined by the dimensionless ratios of the intrinsic kinetic rates of reaction of the corresponding intermediate with chlorine and bromine species (22, 23).

This approach can be combined with and enhanced by unambiguous measurements of the extent of engagement of the reactive sites in NOM by halogen species. This can be done using the principle of differential absorbance that quantifies the consumption of NOM reactive sites in halogenation reactions. Applications of this principle has allowed generating very strong relationships between concentrations of a wide range of individual or classes of DBPs and, on the other hands, intensities of differential absorbance measured at any desired wavelength (which frequently has been at 272 nm; the differential absorbance at this wavelength is accordingly denoted as ΔA_{272}) (24). These correlations have

been shown to be independent vs. chlorine doses, reaction times and temperature (25) but affected by pH or bromide concentration (26).

In this study we pursued the development of a combined approach that incorporates a kinetic model to represent changes of ΔA_{272} values as a function of time and bromide concentration while concentrations of individual DBPs are obtained in this approach by incorporating DBP vs. ΔA_{272} relationships. This approach was applied to the formation of three highly important classes of DBPs (THMs, HAAs and haloacetonitriles, HANs) generated for a highly varying reaction times and bromide levels.

Experimental

Chlorination experiments were conducted using Lake Washington (LW) water (Seattle, USA) and Ancipa water (Sicily, Italy). Main water quality parameters of LW and Ancipa waters are shown in Table 1.

All chemicals were ACS reagent grade or better. Solvents used in extractions were high-purity grade. Reagent water was obtained from a Millipore Super-Q Plus water system. Chlorine stock solution was prepared by dilution of a reagent grade sodium hypochlorite solution (5% available chlorine) with Milli-Q water.

Table 1. Main Water Quality Parameters of Lake Washington Water and Raw, Treated, and Fractionated Ancipa Water

<i>Water</i>	<i>DOC (mg/L)</i>	<i>SUVA₂₅₄ (L mg⁻¹ m⁻¹)</i>	<i>Br⁻ (mg/L)</i>
LW	3.0	2.20	0.02
Ancipa	2.9	2.89	0.05

Chlorination was carried out with free chlorine at pH 7.0 in the presence of 0.03 mol/L phosphate buffer in headspace-free 1.6 L PTFE sampling bags, which were used to prevent the loss of volatile DPBs when samples were taken at different reaction times (10 minutes to 7 days). Selected experiments were carried out at varying bromide concentrations (from its background levels to 2 mg/L) at chlorine dose of 1.5 mg Cl₂ per mg DOC. Chlorinated samples were analyzed for DBPs only if chlorine residual was found. Requisite amount of Na₂SO₃ or NH₄Cl were used to quench residual chlorine. Chlorine concentrations were determined using the DPD colorimetric method. Absorbance spectra were obtained with a Perkin-Elmer Lambda 18 spectrophotometer using 5 cm quartz cells. All reported spectra were normalized to the cell length of 1 cm. TOC was analyzed using an O.I. Analytical 1010 or a Shimadzu VCSH organic carbon analyzer. Concentrations of THMs, HANs and HAAs were determined using standard analytical procedures (EPA methods 551.1 and 552.2) and a Perkin-Elmer AutoSystem gas chromatograph equipped with an electron capture detector. Other aspects of these analyses are described in our previous publications (27, 28).

Results and Discussion

Kinetics of DBP Formation in Chlorinated Water

In agreement with the data of prior research (e.g., (2, 22, 25, 27)), concentrations of THMs, HAAs and dihaloacetonitriles (DHANs) increased gradually with time at given chlorine dose. Higher chlorine doses or temperatures caused higher levels of these DBPs species (25). For instance, Figure 1 shows the formation kinetics of CHCl_3 , CHCl_2Br and CHClBr_2 for chlorinated Ancipa water. Similar behaviour was observed for the other investigated individual DBPs formed in chlorinated Ancipa and LW water.

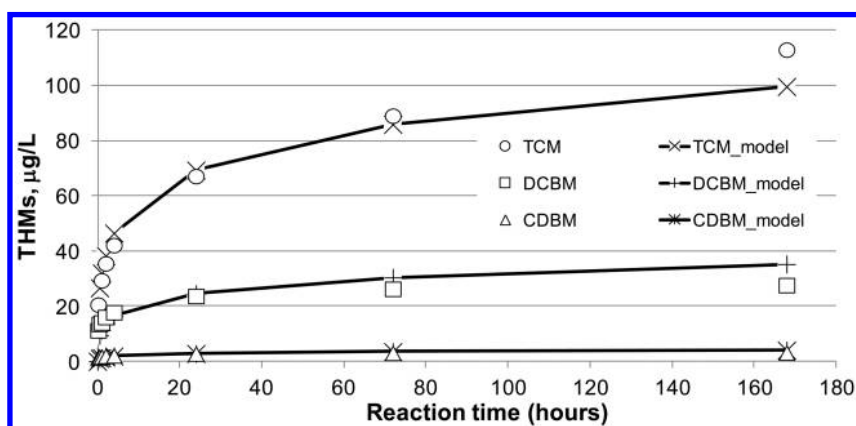


Figure 1. Kinetics of chloroform (TCM), dichlorobromomethane (DCM) and chlorodibromomethane formation for chlorinated Ancipa water.

Modelling the Kinetics of Changes of Differential Absorbance Using Dimensionless Ratios of Bromination/Chlorination Reaction Rates

In accord with the results of prior studies, bromide concentrations strongly affected the yields and speciation of THMs, HAAs and DHANs (9, 19, 20, 22, 23) favouring the formation of bromine-containing DBP and faster rates of their release at increased bromine levels.

While the presence of bromide did not appreciably affect the shape of the differential spectra, changes of the differential absorbance vs. time were faster at increasing bromide concentrations, especially for reaction times below four hours, as shown in Figure 2 for the kinetic profiles measured at a background bromide concentration (0.04 mg/L) and in the case of addition of 1 mg/L bromide. At higher reactions time, ΔA_{272} values tended to plateau and reach a level common for all examined conditions.

The formal description of the development of the differential absorbance vs. time and effects of bromine on it was pursued based on the three-site model similar to that used to model concentrations at varying bromine levels (22). Formally, the changes of differential absorbance at 272 nm vs. time were described by the following function:

$$\Delta A_{272}(t, Br) = \sum_{i=1}^3 \Delta A_{272,i}^{ult} \left[1 - \exp\left(-\left([HOCl] + \gamma_{S_i}^{A_{272}} [HOBr]\right) k_i^{A_{272}} t\right)\right] \quad (1)$$

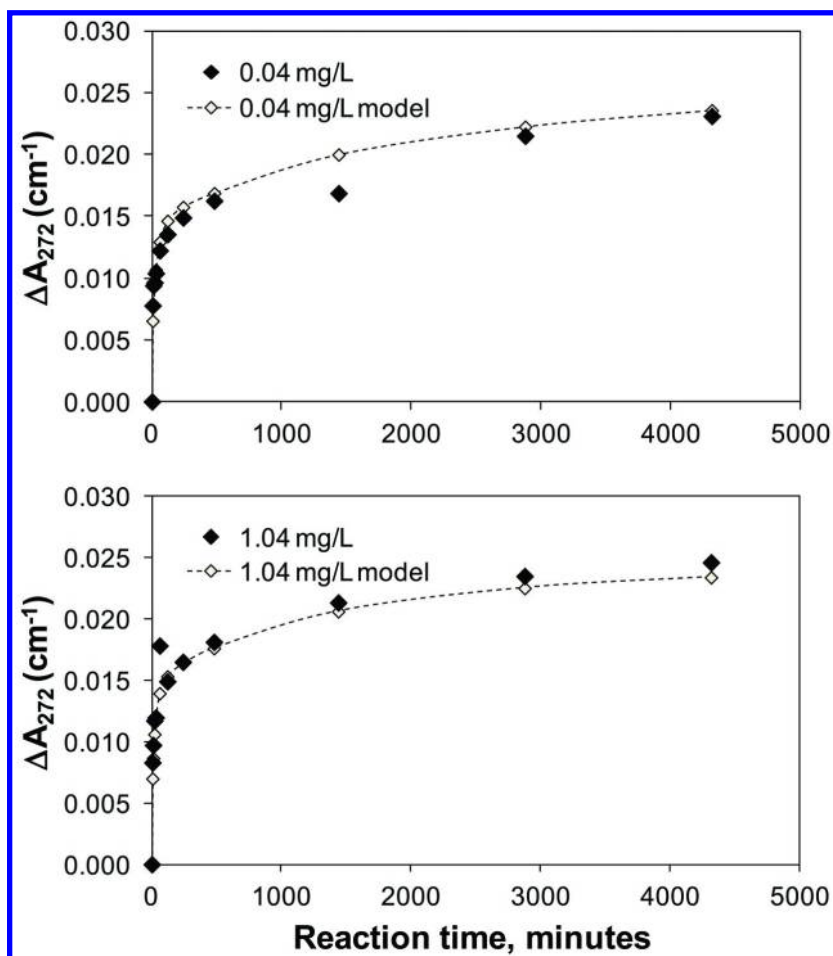


Figure 2. Kinetic profiles of the differential absorbance of chlorinated LK water in the presence of 0.04 and 1.0 mg/L bromide.

A more detailed analysis of this function was presented in our preceding publication (22). Suffice it to mention here that $\Delta A_{272,i}^{ult}$ values correspond to the changes of absorbance associated with the consumption of the operationally defined very fast, fast and slow NOM reactive sites while $k_i^{\Delta A_{272}}$ correspond to the reaction rates of each site with chlorine species. Dimensionless $\gamma_{S_i}^{\Delta A_{272}}$ values quantify the relative preference of bromination over chlorination for each site.

Fitting the experimental ΔA_{272} vs. time profiles using the above model showed that the very fast, fast and slow sites contribute to ca. 21%, 34% and 45%, respectively, of the overall change of absorbance observed at highest reaction times and bromide concentrations. The relative preferences of the sites to the bromination pathway were similar, with the $\gamma_{S_i}^{\Delta A_{272}}$ values of 5.1, 5.1 and 6.0 for the very fast, fast and slow sites, respectively. These values are comparable with those reported in prior research in formal descriptions of the speciation of THMs and HAAs (9, 19, 20, 22, 23).

The use of the above approach allowed achieving precise modelling of the changes of differential absorbance from the entire range of reactions (from 10 minutes to 3 days) and bromine concentrations (from 0.04 to 2.04 mg/L). This allowed using this model for predicting concentrations of individual DBPs species once ΔA_{272} values have been measured experimentally or calculated using the model. This aspect of our approach is discussed in the sections that follow.

Modelling DBPs Formation and Speciation via Differential Absorbance

As was mentioned above, prior studies have established the existence of very strong albeit non-linear correlations between differential absorbance (ΔA_{272}) and DBPs formation (24, 27). For individual DBP species, these correlations are independent of chlorine dose, reaction times, and temperature and they can be well represented by a power function (25). On the other hand, parameters of the fitting power function depend on the pH and bromide concentration.

Following these observation, the concentrations of DBPs were modelled in this study using ΔA_{272} as master parameter and the following expression:

$$DBP_i(t, Br, Cl_2, T, pH, NOM) = k_i(Br, pH, NOM) \Delta A_{272}^{x(Br, pH, NOM)} \quad (2)$$

In the above expression, DBP_i stands for the concentration of any target individual DBP compound, k_i is the proportionality coefficient specific to this species while x is the parameter of the fitting power function. As will be explained below, the parameters x was determined to have the same value for all examined DBPs.

Eq.2 can be useful for modelling concentrations of any target DBP (DBP_i) because it allows simplifying the number of water quality parameters that need to be taken into account. For a constant pH, Eq.2 can be simplified as:

$$DBP_i(t, Br, Cl_2, T, NOM) = k_i(Br, NOM) \Delta A_{272}^{x(Br, NOM)} \quad (3)$$

Fitting the experimental DBPs and ΔA_{272} values with Eq. 3 at varying bromide concentrations showed that a single value of $x=1.7$ can be used to fit the data for all the investigated DBPs and waters. This is demonstrated in Figure 3-6 for data sets showing these correlations for trichloroacetic acid (TCAA) and tribromoacetic acid (TBAA) formed in Lk. Washington water at bromide concentrations 0.1 and 1.0 mg/L. This result allows reducing Eq. 3 to the following simple form:

$$DBP_i(t, Br, Cl_2, T, NOM) = k_i(Br, NOM) \Delta A_{272}^{1.7} \quad (4)$$

Similarly to the results for Lk. Washington water, DBP concentrations found in chlorinated Ancipa water could be well fitted by using Eq. 4, as shown in Figure 1 for the formation kinetics of $CHCl_3$, $CHCl_2Br$ and $CHClBr_2$.

When represented vs. the concentration of bromide, values of the k_i proportionality coefficients obtained via the fitting of the experimental DBP and ΔA_{272} data exhibited a type of functional dependence similar to that of the dimensionless speciation coefficients for THMs, HAAs and HANs reported in prior studies (9, 19, 22, 23). This is demonstrated in Figure 7 and 8 that present the k_i coefficients for the trihalogenated (THAA) and dihalogenated HAAs (DHAA), respectively, formed in chlorinated LW water. As a result, the proportionality coefficients, k_i , are speciation coefficients which can be determined by the correlations between DBPs and differential absorbance, alternatively to the formal modeling, which employs dimensionless ratios of bromination/chlorination reaction rates.

The k_i coefficients have also been found to be strongly correlated with the logarithms of bromide concentrations (Figure 9-11). The fitting shown in these figures was achieved using second-order polynomial curves. In the case of DBPs containing only chlorine or bromine, the fitting predicted a gradual decrease or increases, respectively, of the k_i coefficients while for mixed compounds the behavior of these coefficients was non-monotonic (Figure 9-11).

The use of logarithms of bromide concentration and correlating them with the k_i coefficients appears to be a reasonably straightforward procedure that is expected to be applicable to any water quality. Further studies will demonstrate the extent of effects of NOM site-specificity on these correlations of NOM as well as on the absolute values of k_i coefficients.

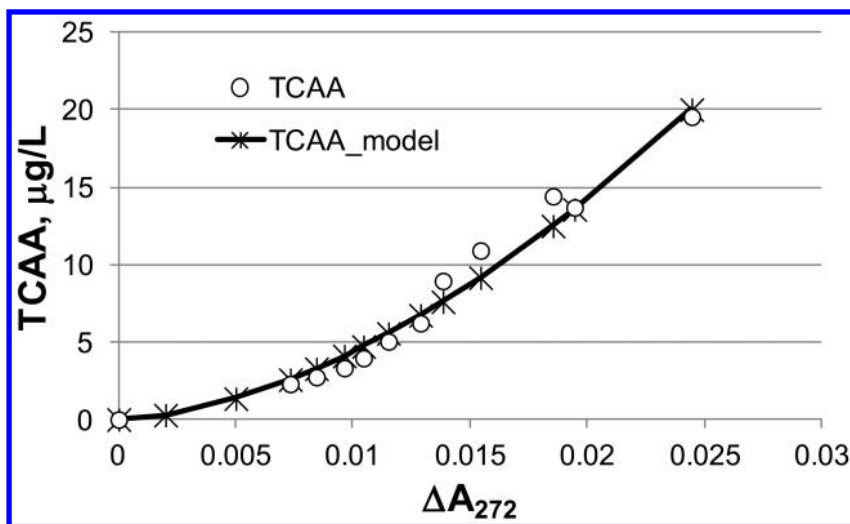


Figure 3. Correlations between concentration of trichloroacetic acid (TCAA) and differential absorbance at 272 nm for chlorinated LW water. Br=0.1 mg/L.

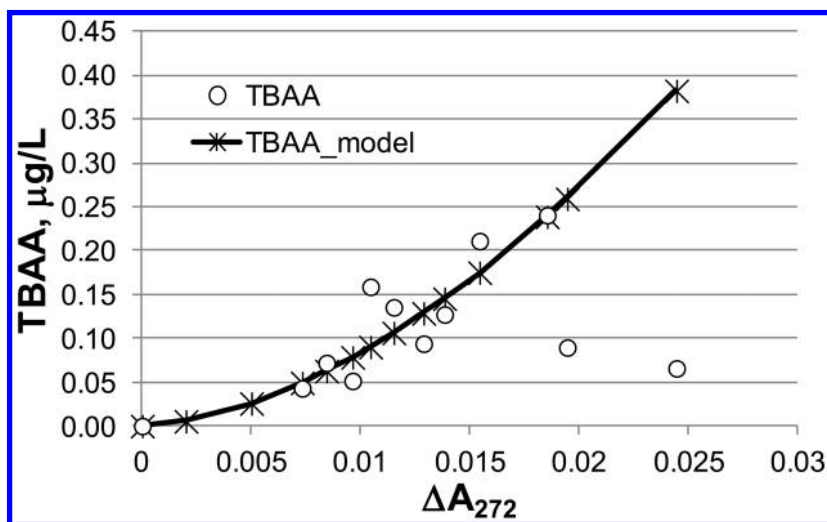


Figure 4. Correlations between concentrations of tribromoacetic acid (TBAA) and differential absorbance at 272 nm for chlorinated LW water. Br=0.1 mg/L.

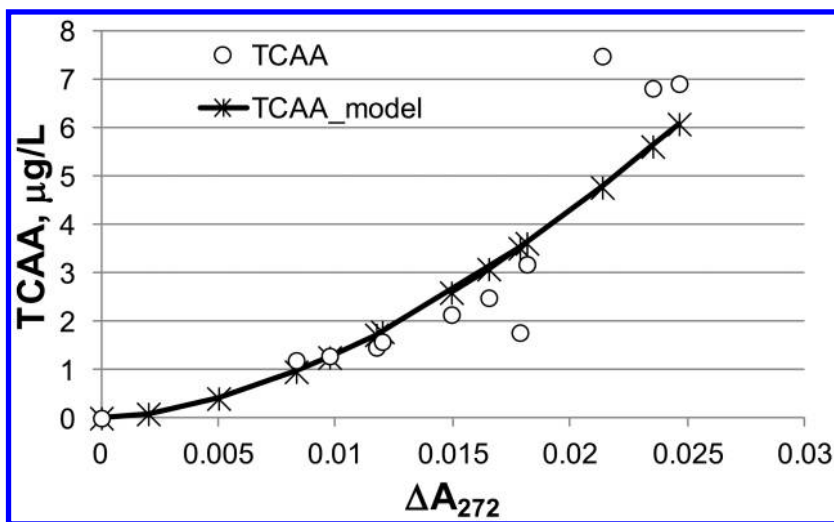


Figure 5. Correlations between trichloroacetic acid (TCAA) and differential absorbance at 272 nm for chlorinated LW water. Br=1.0 mg/L.

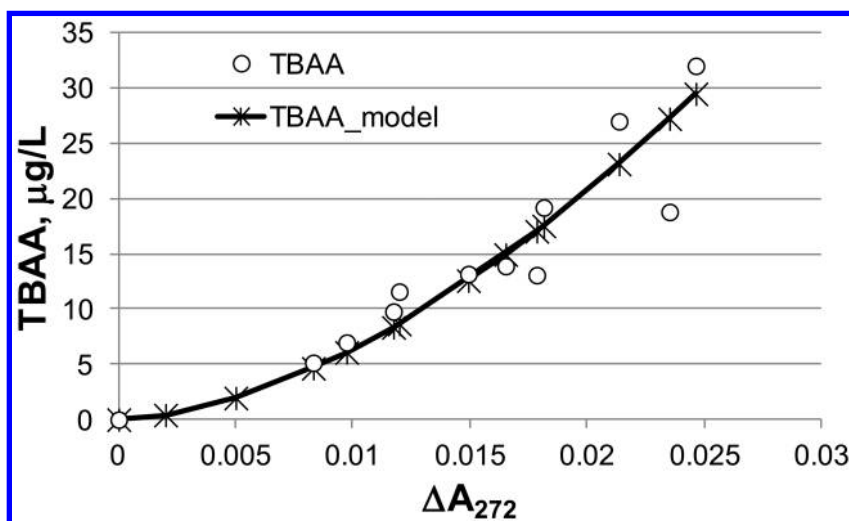


Figure 6. Correlations between concentrations of tribromoacetic acid (TBAA) and differential absorbance at 272 nm for chlorinated LW water. Br=1.0 mg/L.

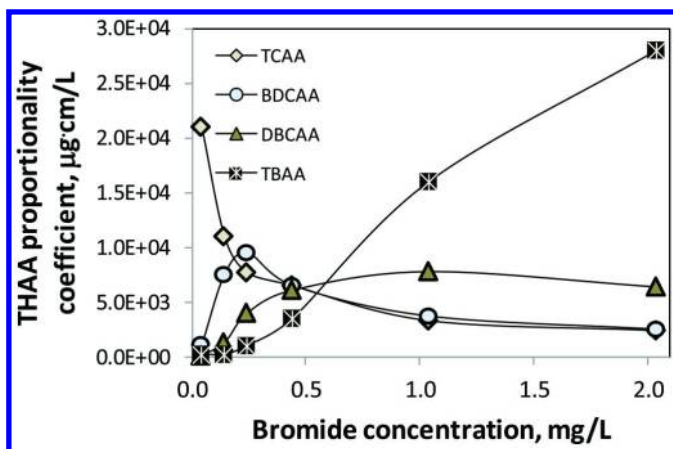


Figure 7. Effects of bromide concentration on the proportionality coefficients (k_i) for trichloroacetic (TCAA), bromodichloroacetic (BDCAA), dibromochloroacetic (DBCAA) and (TBAA) tribromoacetic acids formed in LW water.

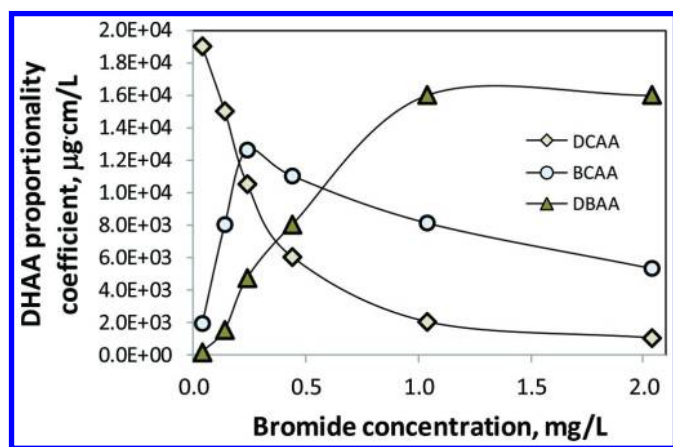


Figure 8. Effects of bromide concentration on the proportionality coefficients (k_i) for dichloroacetic acid (DCAA), bromochloroacetic acid (BCAA) and dibromoacetic acid (DBAA) formed in chlorinated LW water.

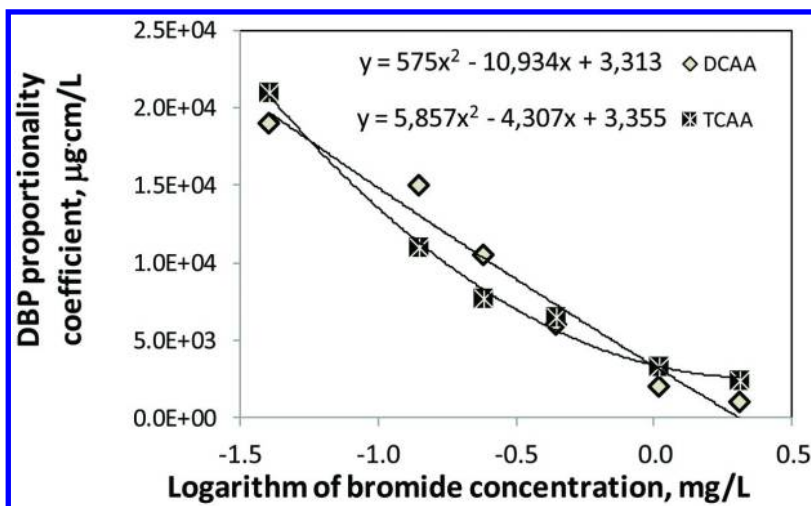


Figure 9. Correlations between proportionality coefficients (k_i) for dichloroacetic (DCAA) or trichloroacetic (TCAA) acids and logarithms of bromide concentrations. Data for chlorinated LW water.

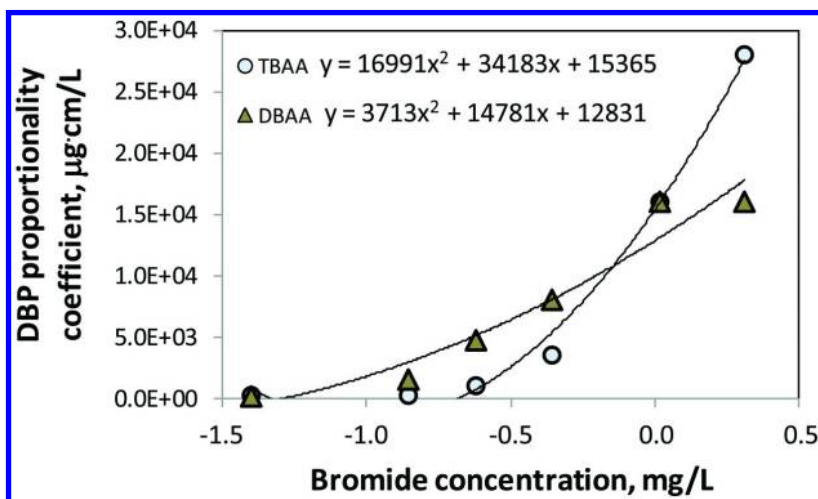


Figure 10. Correlations between proportionality coefficients (k_i) for dibromoacetic (DBAA) or tribromoacetic (TBAA) acids and logarithms of bromide concentration. Chlorinated LW water.

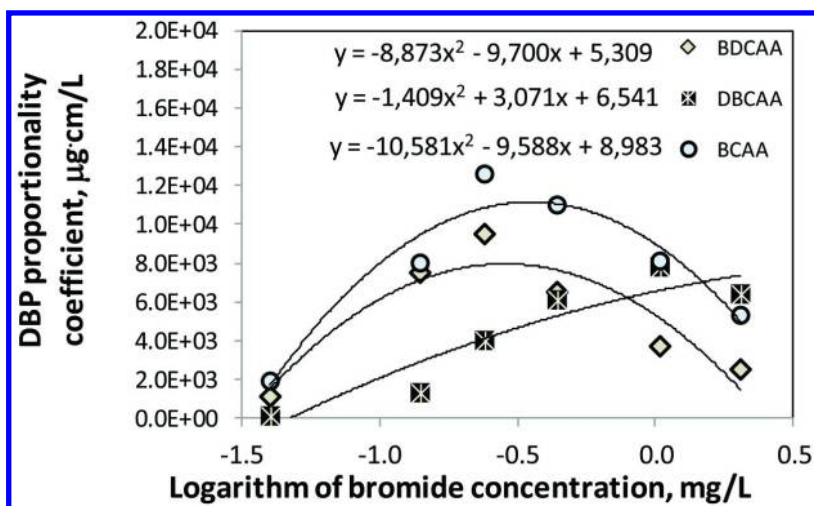


Figure 11. Correlations between proportionality coefficients (k_i) for bromodichloroacetic (BDCAA), dibromochloroacetic (DBCAA) and bromochloroacetic acids (BCAA) and logarithms of bromide concentrations. Chlorinated LW water.

Conclusions

This study examined the formation of THM, HAA and HAN species and concurrent NOM transformations reactions based on the kinetic analysis of DBPs data and also via differential spectroscopy. The approach treated the differential absorbance (ΔA_λ) as master parameter that can be used to predict concentrations of any selected individual DBP compounds. The kinetics of ΔA_λ changes was determined to be sensitive to the presence of bromide. It also reflected the fact of a faster bromination of NOM reactive sites, compared with the rates of chlorination. Comparison of ΔA_λ values and concurrently measured DBP concentrations showed that DBPs levels were correlated with ΔA_λ by a uniformly applicable power function having a 1.7 power coefficient but this function also contains a proportionality coefficient which is compound specific and varies with the bromide level. The proportionality coefficients were found to behave similarly to the formal speciation coefficients reported in prior research and are strongly correlated with logarithms of the bromide concentrations.

The joint interpretation of the kinetic DBP and differential absorbance data confirmed the applicability of the DBPs speciation model. The results indicate that both the absolute levels and speciation of several classes or bromine-containing DBPs can be interpreted and modeled based on the presented approach. Further research is needed to expand the modeling of DBPs formation to a wider range of surface waters as well as to examine its performance for chloraminated waters containing bromide and/or iodide.

Acknowledgments

This study was partially supported by the Water Research Foundation (Project #2597), the United States EPA/Cadmus (grant 069-UW-1), and the Italian Ministry of Instruction, University, and Research (MIUR), through the Research Projects of National Interest - PRIN 2009 (grant 20092MES7A_002). Paolo Roccaro and Gregory Korshin acknowledge the U.S.-Italy Fulbright Commission for supporting their research in the U.S. and in Italy, respectively. Views expressed in this paper do not necessarily reflect those of the funding agencies.

References

1. Sedlak, D. L.; von Gunten, U. The Chlorine Dilemma. *Science* **2011**, *331*, 42–43.
2. Reckhow, D. A.; Singer, P. C.; Malcolm, R. L.; Reckhow, D. A.; Singer, P. C.; Malcolm, R. L. 1990. Chlorination of humic materials: byproduct formation and chemical interpretations. *Environ. Sci. Technol.* **1990**, *24*, 1655–1664.
3. Richardson, S. D.; Thruston, A. D., Jr.; Rav-Acha, C.; Groisman, L.; Popilevsky, I.; Juraev, O.; Glezer, V.; McKague, A. B.; Plewa, M. J.; Wagner, E. D. Tribromopyrrole, brominated acids, and other disinfection byproducts produced by disinfection of drinking water rich in bromide. *Environ. Sci. Technol.* **2003**, *37*, 3782–3793.
4. Hua, G.; Reckhow, D. A.; Kim, J. Effect of bromide and iodide ions on the formation and speciation of disinfection byproducts during chlorination. *Environ. Sci. Technol.* **2006**, *40*, 3050–3056.
5. Richardson, S. D.; Plewa, M. J.; Wagner, E. D.; Schoeny, R.; DeMarini, D. M. Occurrence, genotoxicity, and carcinogenicity of regulated and emerging disinfection byproducts in drinking water: a review and roadmap for research. *Mutation Res.* **2007**, *636*, 178–242.
6. Roccaro, P.; Mancini, G.; Vagliasindi, F. G. A. Water intended for human consumption – part I: compliance with European water quality standards. *Desalination* **2005**, *176*, 1–11.
7. Krasner, S. W.; Weinberg, H. S.; Richardson, S. D.; Pastor, S. J.; Chinn, R.; Scilimenti, M. J.; Onstad, G. D.; Thruston, A. D. Occurrence of a new generation of disinfection byproducts. *Environ. Sci. Technol.* **2006**, *40*, 7175–7185.
8. Leenheer, J. A.; Crouè, J.-P. Characterizing dissolved aquatic organic matter, comprehensive approach to preparative isolation and fractionation of dissolved organic carbon from natural waters and waste waters. *Environ. Sci. Technol.* **2003**, *37*, 18A–26A.
9. Cowman, G. A.; Singer, P. C. Effect of bromide ion on haloacetic acid speciation resulting from chlorination and chloramination of aquatic humic substances. *Environ. Sci. Technol.* **1996**, *30*, 16–24.
10. Obolensky, A.; Singer, P. C. Halogen substitution patterns among disinfection byproducts in the information collection rule database. *Environ. Sci. Technol.* **2005**, *39*, 2719–2730.

11. Zhang, L.; Xu, L.; Zeng, Q.; Zhang, S.-H.; Xie, H.; Liu, A.-L.; Lu, W.-Q. Comparison of DNA damage in human-derived hepatoma line (HepG2) exposed to the fifteen drinking water disinfection byproducts using the single cell gel electrophoresis assay. *Mutat. Res.* **2012**, *741*, 89–94.
12. Yang, M.; Zhang, X. Comparative developmental toxicity of new aromatic halogenated dbps in a chlorinated saline sewage effluent to the marine polychaete *Platynereis dumerilii*. *Environ. Sci. Technol.* **2013**, *47*, 10868–10876.
13. Heller-Grossman, L.; Idin, A.; Relis, B. L.; Rebhun, M. Formation of cyanogen bromide and other volatile DBPs in the disinfection of bromide-rich lake water. *Environ. Sci. Technol.* **1999**, *33*, 932–937.
14. Magazinovic, R. S.; Nicholson, B. C.; Mulcahy, D. E.; Davey, D. E. Bromide levels in natural waters: its relationship to levels of both chloride and total dissolved solids and the implications for water treatment. *Chemosphere* **2004**, *57*, 329–335.
15. Francis, R. A.; Vanbriesen, J. M.; Small, M. J. Bayesian statistical modeling of disinfection byproduct (DBP) bromine incorporation in the ICR database. *Environ. Sci. Technol.* **2010**, *44*, 1232–1239.
16. Chowdhury, S.; Champagne, P.; McLellan, P. J. Models for predicting disinfection byproduct (DBP) formation in drinking waters: a chronological review. *Sci. Total Environ.* **2009**, *407*, 4189–206.
17. Heeb, M. B.; Criquet, J.; Zimmermann-Steffens, S. G.; von Gunten, U. Oxidative treatment of bromide-containing waters: formation of bromine and its reactions with inorganic and organic compounds - a critical review. *Water Res.* **2014**, *48*, 15–42.
18. Sadiq, R.; Rodriguez, M. Disinfection byproducts (DBPs) in drinking water and predictive models for their occurrences: a review. *Sci. Total Environ.* **2004**, *321*, 21–46.
19. Nokes, C. J.; Fenton, E.; Randall, C. J. Modeling the formation of brominated trihalomethanes in chlorinated drinking waters. *Water Res.* **1999**, *33*, 3557–3568.
20. Chang, E. E.; Lin, Y. P.; Chiang, P. C. Effects of bromide on the formation of THMs and HAAs. *Chemosphere* **2001**, *43*, 1029–1034.
21. Pan, Y.; Zhang, X. Four groups of new aromatic halogenated disinfection byproducts: effect of bromide concentration on their formation and speciation in chlorinated drinking water. *Environ. Sci. Technol.* **2013**, *47*, 1265–1273.
22. Roccaro, P.; Chang, H.-S.; Vagliasindi, F. G. A.; Korshin, G. V. Modeling bromide effects on yields and speciation of dihaloacetonitriles formed in chlorinated drinking water. *Water Res.* **2013**, *47*, 5995–6006.
23. Roccaro, P.; Korshin, G. V.; Cook, D.; Chow, C. W. K.; Drikas, M. Effects of pH on the speciation coefficients in models of bromide influence on the formation of trihalomethanes and haloacetic acids. *Water Res.* **2014**, *62*, 117–126.
24. Korshin, G. V.; Li, C.-W.; Benjamin, M. M. The decrease of UV absorbance as an indicator of TOX formation. *Water Res.* **1997**, *31*, 946–949.

25. Roccaro, P.; Chang, H.-S.; Vagliasindi, F. G. A.; Korshin, G. V. Differential absorbance study of effects of temperature on chlorine consumption and formation of disinfection byproducts in chlorinated water. *Water Res.* **2008**, *42*, 1879–1888.
26. Roccaro, P.; Vagliasindi, F. G. A. Differential versus absolute UV absorbance approaches in studying NOM reactivity in DBPs formation: comparison and applicability. *Water Res.* **2009**, *43*, 744–750.
27. Korshin, G. V.; Wu, W. W.; Benjamin, M. M.; Hemingway, O. Correlations between differential absorbance and the formation of individual DBP species. *Water Res.* **2002**, *36*, 3273–3282.
28. Roccaro, P.; Vagliasindi, F. G. A.; Korshin, G. V. Quantifying the formation of nitrogen-containing disinfection by-products in chlorinated water using absorbance and fluorescence indexes. *Water Sci. Technol.* **2011**, *63*, 40–44.

Chapter 5

Modeling NDMA Formation Kinetics During Chloramination of Model Compounds and Surface Waters Impacted by Wastewater Discharges

Jinwei Zhang,¹ David Hanigan,² Ruqiao Shen,³ Susan Andrews,³ Pierre Herckes,¹ and Paul Westerhoff^{*,2}

¹Department of Chemistry and Biochemistry, Arizona State University, Tempe, Arizona 85287-1604, United States

²School of Sustainable Engineering and the Built Environment, Arizona State University, Tempe, Arizona 85287-3005, United States

³Department of Civil Engineering, University of Toronto, Toronto, Ontario M5S 1A4, Canada

*E-mail: P.WESTERHOFF@asu.edu. Telephone: 1-480-965-2885.

N-nitrosodimethylamine (NDMA) is a chloramination disinfection by-product (DBP). Despite extensive research on NDMA occurrence and evaluation of formation potential from select precursors and in different matrices, less information exists on the kinetics of NDMA formation. A kinetic model is developed and parameterized using the limited amount of previously published kinetic data involving addition of model compounds to pH buffered ultrapure water and/or surface waters containing organic matter. A simple second-order kinetic model was developed using a NDMA precursor concentration, based upon a measured maximum NDMA concentration as the initial precursor concentration, and measured monochloramine concentrations. The second order model was able to fit NDMA formation kinetics well by determining the best-fit apparent rate constant (k_{app}), suggesting the model represents a common rate limiting step and/or an intermediate product. An associated reaction may exist during the transformation of a wide variety of precursors into NDMA. Values for k_{app} ranged by approximately one-order of magnitude and were lower in the presence of

natural organic matter (NOM), which may suggest that more reactive chloramine species or NDMA intermediate products are scavenged by NOM. Overall, the modeling suggests lines of future research to help elucidate and predict NDMA formation mechanisms such that strategies to control its formation could be applied during drinking water treatment.

Introduction

Over the past decades, N-nitrosamines (NAs), which form as disinfection by-products during chlorination, in particular chloramination, have emerged as a great concern because of an increasing use of chloramines by water utilities for residual disinfection to meet trihalomethane (THM) and haloacetic acid (HAA) regulations (1). NAs were included in the Unregulated Contaminant Monitoring Rule 2 (UCMR2) and then listed on the third Contaminant Candidate List (CCL3) (2). The USEPA classifies NAs as probable human carcinogens in drinking water at low ng/L levels associated with a 10^{-6} lifetime cancer risk. California's Office of Environmental Health Hazard Assessment (OEHHA) set a notification level of 10ng/L for NDMA (3). Because of their high carcinogenic potential, the USEPA may soon make a regulatory determination for NAs.

N-nitrosodimethylamine (NDMA) is the most commonly investigated nitrosamine. Most studies have found that NDMA is rather associated with chloramination than with chlorination (4–6). Systems with high plant effluent NDMA (i.e., >50 ng/L) typically use chloramines as the primary rather than secondary disinfectant (6), reflecting the potential for precursor deactivation by strong pre-oxidants such as chlorine. Due to the long time-scale for nitrosamine formation, plants with long in-plant chloramine contact times (e.g., 12–18 hr) tend to have higher NDMA concentrations in the plant effluent than those with short (e.g., 0.5–2 hr) contact times (7). NDMA concentrations tend to increase throughout chloraminated distribution systems (7–11).

Primary amines can be nitrosated to yield primary NAs, however the latter are unstable and decay nearly instantaneously (12). Secondary amines can be transformed to their stable NA analogues and most research focused on NDMA formation from dimethylamine (DMA) (13–17). However, some studies indicated that the presence of DMA was not sufficient to explain the NDMA formed in surface water and wastewaters (18, 19). Tertiary amines may also serve as nitrosamine precursors. For example, trimethylamine (TMA) would decay instantly upon chlorination or chloramination to release DMA and then quantitatively form NDMA (20). Mechanistic studies indicate that yields of NDMA from chloramination of most secondary and tertiary amines are very low (~0–3%) but recently a subset of tertiary amines were found to have substantially higher NDMA yields (up to 90%) compared to previously studied precursors (21–23). In particular, ranitidine, a widely found amine-based pharmaceutical, forms NDMA at yields higher than 80% (21, 23). It was suggested that the electron donating group (furan ring) in ranitidine favors the reaction with chloramine

leading to higher NDMA yields. The differences of NDMA formation yields among tertiary amines revealed the importance of tertiary amine structures (N bond leaving group) on the NDMA formation. The higher yields also suggest that tertiary amines can form nitrosamines without proceeding through a secondary amine intermediate (24).

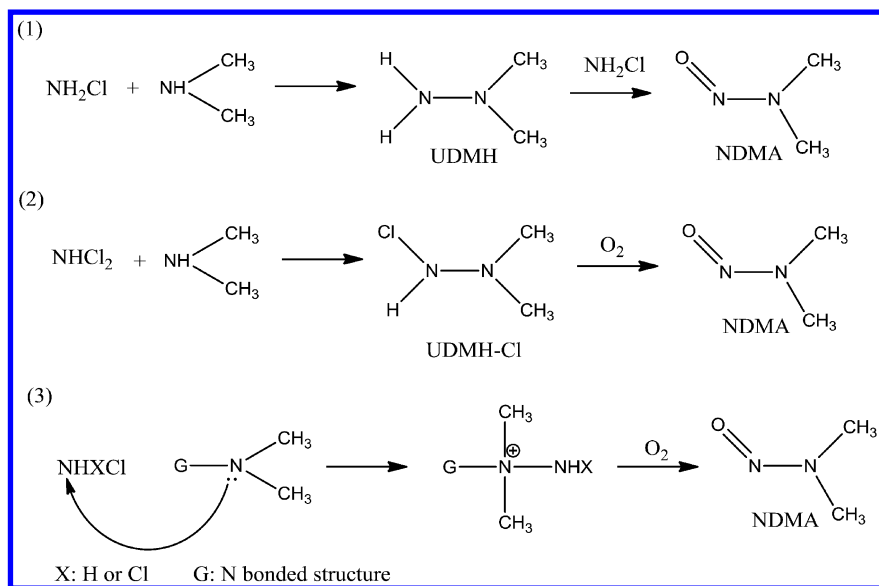


Figure 1. NDMA formation pathways as proposed in the literature: (1) Choi and Valentine, 2002; Mitch and Sedlak, 2002. (2) Schreiber and Mitch, 2006. (3) Selbes et al. 2013.

Several NDMA formation mechanisms during chloramination had been proposed (Figure 1). Mechanistic studies using DMA as the model precursor found that unprotonated DMA undergoes nucleophilic substitution with monochloramine, yielding the unsymmetrical dimethylhydrazine (UDMH) intermediate. This UDMH is then oxidized by monochloramine to NDMA (13, 25). The importance of chloramine speciation and presence of dissolved oxygen was later discovered and a second mechanism proposed ((2) in Figure 1). Here, dichloramine reacts to yield NDMA via the formation of the chlorinated UDMH intermediate (UDMH-Cl) and this UDMH-Cl is then oxidized by oxygen to produce NDMA (15). Based upon competition reaction kinetics, it has been suggested that the monochloramine mechanism (1) is negligible compared to dichloramine (2) pathway. As the molar yield of NDMA from DMA is low (i.e., <5%) compared to that from other compounds (e.g., ranitidine), it was suspected that a third pathway, other than through DMA, exists. Compounds such

as ranitidine may follow a different series of reactions involving nucleophilic attack of the amine group on chloramines ((3) in figure 1) (26). Through this pathway, NDMA formed from ranitidine was more sensitive to monochloramine (21). Suspected NDMA precursors with electron withdrawing groups may preferentially react with monochloramine while compounds with electron donating groups react preferentially with dichloramine (24, 27). Many suspected precursors could react with both monochloramine and dichloramine. Therefore, NDMA formation is likely a combination of reactions between NDMA precursors and both chloramine species.

Despite extensive research on yields of NDMA from model compounds and in surface water or wastewater (19, 20, 23), less information exists related to NDMA formation kinetics in the latter water sources. NDMA formation from DMA has been initially modeled through UDMH and Cl-UDMH pathways ((1) and (2) in figure 1) and the latter successfully predicted NDMA formation over a range of conditions (15). A statistical model was proposed to predict NDMA formation kinetics from pharmaceutical compounds such as ranitidine in various water matrices (23). In addition, natural organic matter (NOM) was also investigated as a source of precursors in a NDMA formation model (28). No attempt has been ever made to model NDMA formation in wastewater or wastewater-impacted waters. The challenge for a model development lies in the multitude of precursors and precursor types present and hence the possibility of having various mechanisms, with distinct kinetics occurring simultaneously.

The aim of this work is to formulate and evaluate a NDMA formation kinetics model that is applicable to different water sources and model compounds. A simple second-order kinetic reaction model was developed for NDMA formation. In this model, the precursor concentration, quantified as the maximum NDMA concentration formed during chloramination under specific water conditions, and chloramine decay were used to predict transformation of precursors to NDMA. The model was parameterized using NDMA formation data from literature data on NOM and model precursor compounds (i.e. ranitidine). The optimization of the kinetic model parameters and the resulting model performance are discussed.

Model Description

NDMA Formation Model

As detailed in the introduction, three different pathways for NDMA formation have been proposed (Figure 1). The original concept of the model was that different types of precursors may proceed along different mechanistic pathways with different chloramine species and the reactions may potentially involve oxygen to produce NDMA. Such a model would classify NDMA precursors (nM quantities) as having either higher or lower yields and presumably different reaction rates with different chloramine species. In a first step, using data obtained from our research of NDMA formation in wastewater, we developed a simple second-order model for the reaction of NDMA precursors (P) in the presence of monochloramine (NH_2Cl):

$\frac{dP}{dt} = -k_{mono}[P][NH_2Cl] - k_{di}[P]\alpha[NH_2Cl]$	Equation 1a
$= -(k_{mono} + k_{di}\alpha)[P][NH_2Cl]$	Equation 1b
$= -k_{app}[P][NH_2Cl]$	Equation 1c

where $[NH_2Cl]$, $[NHCl_2]$ = monochloramine or dichloramine concentration at time t

$[P]$ = NDMA precursor concentration at time t

k_{mono} , k_{di} = rate constant of NDMA formation from monochloramine or dichloramine

k_{app} = second order rate constant of NDMA formation in our model

α = ratio of dichloramine and monochloramine

Table 1 shows the decomposition reactions for chloramines in water (29). The relationship between monochloramine and dichloramine derives from reactions 3, 4 and 5. Dichloramine forms via an acid catalyzed reaction from two monochloramines, then dichloramine reacts instantaneously with monochloramine, producing nitrogen gas. In this assumption, dichloramine occurs at a low concentration and at steady state. Thus, the dichloramine concentrations can be represented as a proportion (α) of monochloramine. Equation 1 shows the formation kinetics of NDMA as a combination of both chloramines reactions. k_{mono} and k_{di} were the rate constants for mono- and di-chloramine reactions respectively. A new apparent rate constant k_{app} was then used in Equation 1c as the best fit second-order rate constant ($M^{-1}s^{-1}$) in terms of monochloramine and NDMA precursor. Measured monochloramine was used in the model to represent all chloramines since it is the dominant source of chloramines in neutral and basic conditions, and is easier to measure compared to dichloramine.

Equation 1c simplifies NDMA formation kinetics in different water matrices despite there being various reactions pathways of chloramines and probably multiple groups of precursor species with highly variable yields (0.017% for TMA, 90% for ranitidine) and influences of various water quality parameters on chloramine decay in water. Currently there is no method to predict NDMA formation kinetics, and most research has relied upon simulated distributed system (SDS) tests ($NH_2Cl < 2.5mg/L$) or formation potential (FP) tests ($NH_2Cl > 100mg/L$). Even model compounds such as DMA showed variable NDMA yields (21, 30). Organic compound concentrations were thought to be associated with NDMA formation from NOM. However, there was no correlation between NDMA formation (or precursor concentration) and UV_{254} or DOC in natural waters or in wastewaters (31). P_0 is the maximum NDMA formation which is measurable in NDMA kinetic tests. Together with the measurement of monochloramine, the model is designed to simulate the NDMA formation processes. The concentration of NDMA at any time ($[NDMA(t)]$) would be

related to the maximum amount of NDMA precursors available for reaction in an experiment ($[P]_0 = [NDMA_{max}]$) as follows:

$$[NDMA(t)] = [P]_0 - [P] \quad \text{Equation 2}$$

where $[P]$ NDMA precursor concentration at time t

The measured concentration of NH_2Cl or an estimated simulated monochloramine decomposition is used in the model (28, 32). NDMA formation data at different time points were fitted to the model using Kintecus (33) and the rate constant, k_{app} , was optimized with the highest correlation coefficient between experimental values and model fitting.

Table 1. Chloramine Decomposition Kinetics and Associated Rate Constants (29)

	<i>Reaction</i>	<i>Rate Constant</i>
1	$HOCl + NH_3 \rightarrow NH_2Cl + H_2O$	$k_1 = 1.0 \times 10^{10} M^{-1}h^{-1}$
2	$NH_2Cl + H_2O \rightarrow HOCl + NH_3$	$k_2 = 0.1 h^{-1}$
3	$HOCl + NH_2Cl \rightarrow NHCl_2 + H_2O$	$k_3 = 1.26 \times 10^6 M^{-1}h^{-1}$
4	$NHCl_2 + H_2O \rightarrow HOCl + NH_2Cl$	$k_4 = 2.3 \times 10^{-3} h^{-1}$
5	$NH_2Cl + NH_2Cl \rightarrow NHCl_2 + NH_3$	k_d^*
6	$NHCl_2 + NH_3 \rightarrow NH_2Cl + NH_2Cl$	$k_6 = 2.0 \times 10^8 M^{-1}h^{-1}$
7	$NH_2Cl + NHCl_2 \rightarrow N_2 + 3H^+ + 3Cl^-$	$k_7 = 55.0 M^{-1}h^{-1}$
8	$NHCl_2 + H_2O \rightarrow NOH + 2HCl$	$k_8 = 6.0 \times 10^5 M^{-1}h^{-1}$
9	$NOH + NHCl_2 \rightarrow N_2 + H_2O + HCl$	$k_9 = 1.0 \times 10^8 M^{-1}h^{-1}$
10	$NOH + NH_2Cl \rightarrow N_2 + H_2O + HCl$	$k_{10} = 3.0 \times 10^7 M^{-1}h^{-1}$
11	$NH_4^+ \rightarrow NH_3 + H^+$	$pK_a = 9.3$
12	$H_2CO_3 \rightarrow HCO_3^- + H^+$	$pK_a = 6.3$
13	$HCO_3^- \rightarrow CO_3^{2-} + H^+$	$pK_a = 10.3$

* $k_d = k_H[H^+] + k_{H_2CO_3}[H_2CO_3] + k_{HCO_3}[HCO_3^-]$; $k_H = 2.5 \times 10^7 M^{-2}h^{-1}$; $k_{HCO_3} = 800 M^{-2}h^{-1}$; $k_{H_2CO_3} = 40000 M^{-2}h^{-1}$.

Monochloramine Degradation

Monochloramine decays over time due to hydrolysis and reaction with organic and inorganic species (Table 1). Autodecomposition or hydrolysis forms other oxidants such as free chlorine or dichloramine, which would react with DOC. Another pathway is, in the presence of NOM, monochloramine reacting directly with organic matter. The rate of monochloramine loss in both

pathways was found to be dependent on experimental conditions such as initial monochloramine concentration, DOC or pH (34). It was difficult to accurately simulate monochloramine decomposition with detailed models published in previous research because various parameters (i.e. fast and slow reactive fractions of NOM) need to be reoptimized since they are specific to reaction conditions. A simple first order degradation model with respect to monochloramine is used to simulate the decay of monochloramine in the presence of NDMA precursors (Equation 3). The rate constant is specific to experiment conditions and representative for similar water qualities in general.

$$\frac{d[NH_2Cl]}{dt} = -k_{decay}[NH_2Cl] \quad \text{Equation 3}$$

Results and Discussion

Modeling of NDMA Formation in NOM

Chen et al. modeled NDMA formation from reactions between NOM and monochloramine (28). They suggested that NOM in surface waters could be oxidized involving two types of reactive sites of monochloramine loss. A portion of the dissolved organic carbon (DOC) could react with monochloramine rapidly within hours and the other part had a much slower reaction with free chlorine (over days). However, their model had five parameters (i.e. fast and slow reactive fractions of NOM) to be optimized which would vary between water sources. Here we fitted their experimental data with our model. The monochloramine decay was modeled as a first order reaction in Equation 2 and the monochloramine decay rate constants are shown in Table 2. The decay rate of monochloramine increased when pH was reduced from 9 to 7 since at low pH monochloramine would decay to dichloramine more easily (Reaction 5, Table 1).

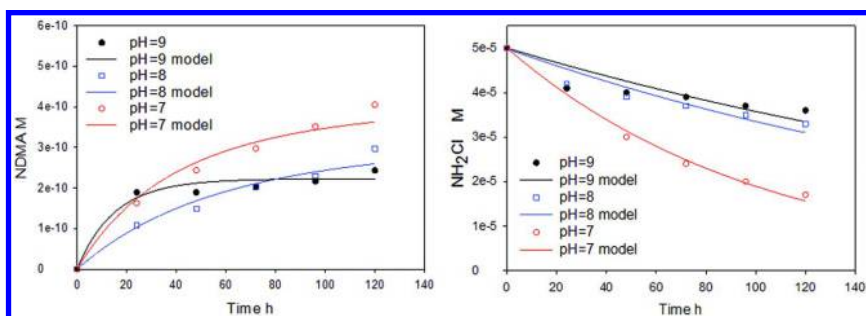


Figure 2. Model prediction of NDMA formation and monochloramine decay at various pH in surface water. (Symbols: observation data, lines: model predictions. Data from Chen et al. 2006 (28))

Then the NDMA formation data was fitted with our second order model (Figure 2). NDMA concentration at 120 h was used as $NDMA_{max}$ (P_0) although NDMA formation had not reached its maximum at this time. The model fits NDMA formation over time well at pH 7, 8 or 9. However, at pH 6 when dichloramine is more prevalent chloramine species, the model was not able to simulate the NDMA formation because our assumption that dichloramine is proportional to monochloramine is not valid at pH 6. NDMA formation yields appear to increase with decreasing pH from 9 to 7 due to presence of more dichloramine at lower pH. The optimized rate constant k_{app} varied within a factor of three for different pH conditions, however, no obvious correlation was found between pH values and k_{app} .

Table 2. Optimized NDMA Formation Rate Constant and Monochloramine Decomposition Rate Constants in NOM under Various Reaction Conditions. (Data from Chen et al. 2006 (28)). R^2 Is Correlation Coefficient between Model and Observation. Notes: Experiments Were Conducted at pH 7 with Variable Cl/N ratios (and Ammonia Concentrations): ^a 0.7 (0.07 mM NH_3); ^b 0.3 (0.17 mM NH_3); ^c 0.10 (0.5 mM NH_3)

<i>pH</i>	$k_{app} M^{-1}s^{-1} (R^2)$	$k_{decay} (h^{-1})$
9	0.25 (0.96)	3.4E-03
8	0.09 (0.96)	4.0E-03
7	0.15 ^a (0.95) 0.12 ^b (0.95) 0.10 ^c (0.84)	9.7E-03 4.1E-03 2.5E-03

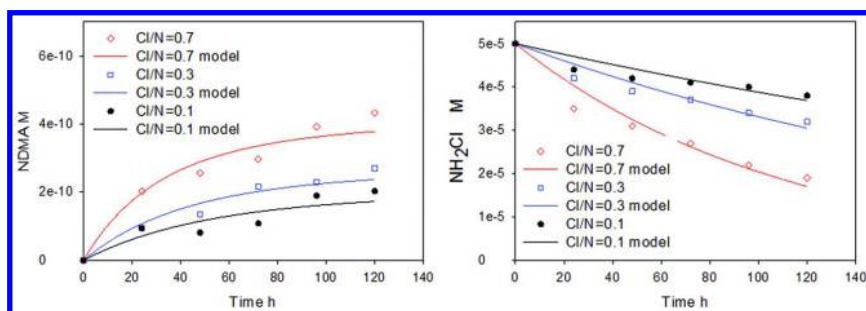


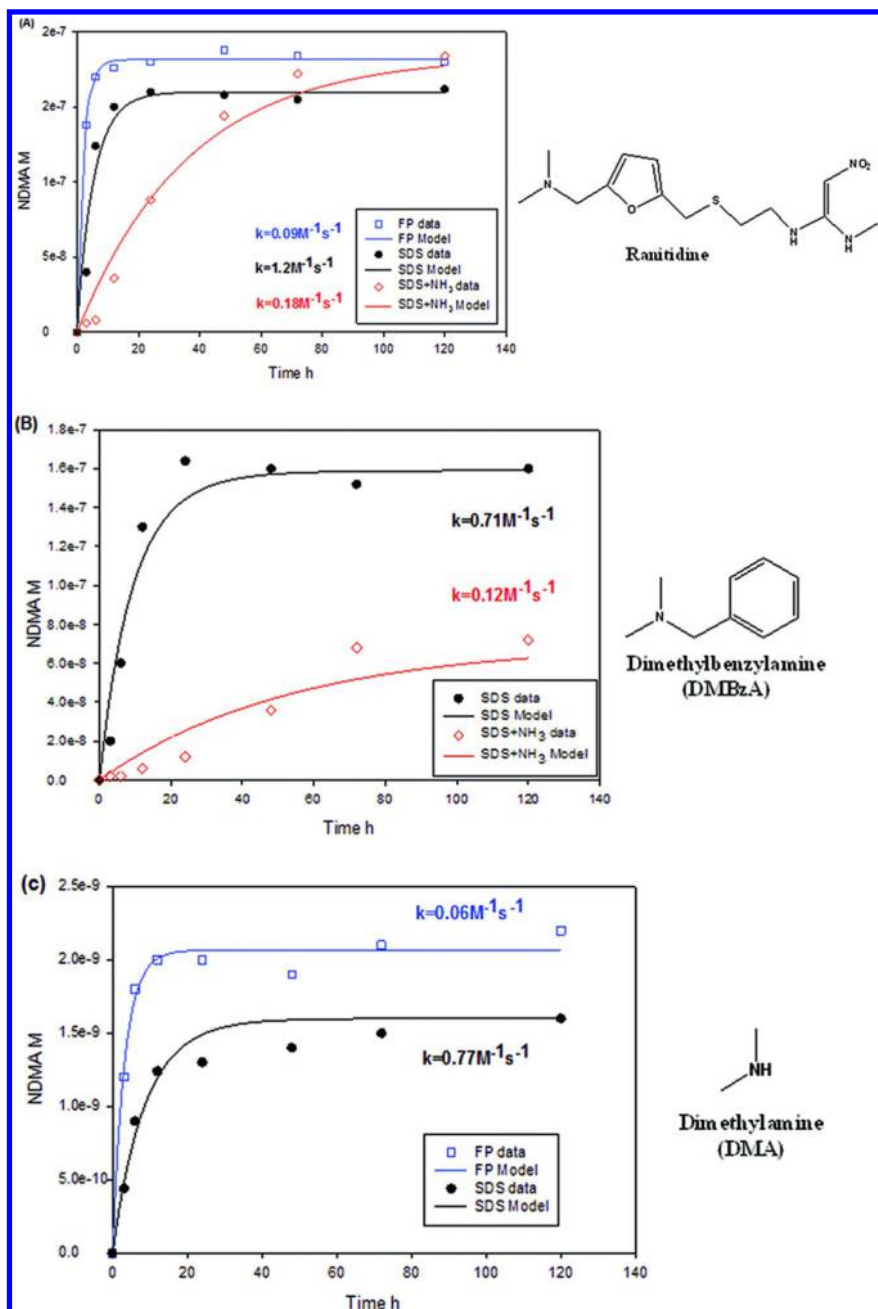
Figure 3. Model prediction of NDMA formation and monochloramine decay at various ammonia concentrations (Cl/N ratio) in surface water: (Symbols: observation data, lines: model predictions, pH=7. Data from Chen et al. 2006 (28))

The NDMA formation data in surface waters with various Cl/N ratios in Chen's work was also fitted with our model. Both monochloramine decay and NDMA formation were well predicted (Figure 3). Results showed that a decreasing Cl/N ratio reduced monochloramine decay rates, NDMA formation rates and NDMA yields. This was the result of dichloramine formation being favored at high Cl/N ratios (low ammonia concentrations) according to reaction 3 in Table 1. With the monochloramine degradation measurements shown in Chen's work (28), the model successfully predicted NDMA formation over time in surface waters from pH 7 to 9 and in conditions of Cl/N ratio from 0.1 to 0.7.

Modeling of NDMA Formation from Model Compounds

In addition to NOM, model compounds such as DMA and ranitidine were also studied in NDMA formation kinetics experiments. Selbes reported NDMA formation from various amine precursors (35). However, NDMA formation kinetics were not discussed. Here we apply our model to the NDMA kinetics data of five precursor compounds from Selbes' work (35). DMA and four tertiary amines (trimethylamine (TMA), dimethylisopropylamine (DMiPA), dimethylbenzylamine (DMBzA) and ranitidine) were selected. These five precursors were chloraminated by Selbes in three reaction conditions: in distilled deionized water at pH 7.5, a formation potential (FP) test condition with 1.4mM monochloramine, and simulated distribution system (SDS) with 0.04mM monochloramine, and SDS condition with 100 mg/L ammonia to minimize dichloramine formation according to Reaction 3 in Table 1.

Monochloramine decay data was not published in Selbes' work. The monochloramine model simulation in NOM in Chen's work showed that pH has a more significant effect on monochloramine decay than DOC concentrations or Cl/N ratio. A monochloramine decay rate of 0.007 h⁻¹, between the rate constants at pH 7 (0.01 h⁻¹) and pH 8 (0.004 h⁻¹) in Chen's work, was used to predict monochloramine decomposition in the deionized water. Figure 4 shows NDMA formation data obtained from Selbes' work and model fitting for precursors under various conditions and the resulting rate constants are shown in the figure and listed in Table 3. The model successfully fitted the NDMA formation kinetics for all five chemicals in most tests. However, in SDS condition with excess ammonia, our model overestimates NDMA formation in the first half reaction time and underestimates NDMA in the second half period for ranitidine and DMBzA. It was the same with DMiPA in the SDS condition test. In previous studies it was found that ranitidine and DMBzA were more sensitive to monochloramine and DMiPA was only sensitive to dichloramine (27). In NDMA formation from tertiary amines such as ranitidine, an intermediate could form by nucleophilic substitution between ranitidine and monochloramine (26, 27). A possible explanation could be, in conditions with high monochloramine concentrations in FP tests, this intermediate degrades quickly to form NDMA. Therefore, the presence of intermediates could 'delay' the NDMA formation and make our model overestimate NDMA formation.



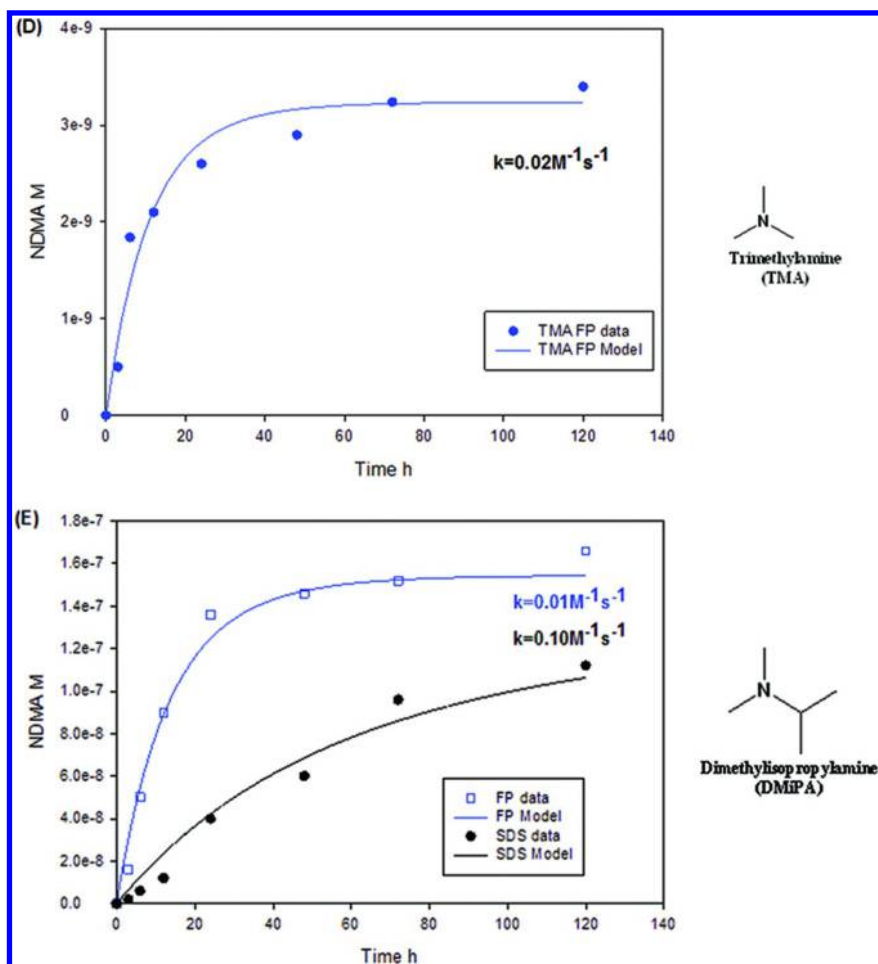


Figure 4. NDMA formation from model precursor compound data (Symbols), model fitting (Lines) in FP tests (NH_2Cl 1.4mM, pH=7.5), SDS conditions (NH_2Cl 0.04mM, pH=7.5) and SDS conditions with excess ammonia. (NDMA data from Selbes, 2014 (35))

Although $k_{\text{app}} \times [\text{NH}_2\text{Cl}]$ was greater in the FP tests, indicating a faster NDMA formation in FP conditions than in SDS conditions, the optimized rate constants (k_{app}) in the FP tests were less than under SDS conditions, by an order of magnitude for model compounds. Compared to amine precursor concentrations (200nM) in Selbes' work, the monochloramine concentrations (1.4mM) were more than 5000 times the precursor concentrations in the FP test. Thus, in the FP test, there is a substantial excess of monochloramine present that reduced the rate constant. Rate constants k_{app} of ranitidine, DMBzA and DMA are similar and that of DMiPA is much smaller. The similar k_{app} between ranitidine and DMA was unexpected

since DMA and ranitidine have very different yields (<3% and 80% respectively) and different proposed NDMA formation mechanisms. In SDS conditions with excess ammonia, optimized k_{app} for both ranitidine and DMBzA are less than those under SDS conditions, suggesting dichloramine reactions may be important. The dichloramine reaction rate constant, which is the difference between k_{app} between two conditions, was found to be greater than the monochloramine rate constant.

Table 3. Optimized Rate Constant k_{app} for Model Compounds under Various Reaction Conditions. (NDMA data from Selbes, 2014 (35))

Compounds	NDMA Yields in FP test %	k_{app} $M^{-1}s^{-1}$ (R^2)		
		FP test	SDS	SDS+ excess ammonia
Ranitidine	~80	0.09 (0.99)	1.2 (0.92)	0.18 (0.97)
DMBzA	~80	-	0.71 (0.92)	0.12 (0.87)
DMA	1.1	0.06 (0.98)	0.77 (0.96)	-
TMA	1.7	0.02 (0.97)	-	-
DMiPA	83	0.01 (0.98)	0.1 (0.96)	-

Modeling of NDMA Formation of Pharmaceutical Compounds in the Presence of NOM

Our model was also applied to NDMA formation by amine precursors in the presence of NOM in natural waters. Shen et al. investigated the NDMA formation kinetics of pharmaceutical compounds in three water matrices (MQ water: TOC=0mg/L, Lake: TOC=2mg/L, River: TOC=6mg/L) under simulated distribution system condition (SDS, $NH_2Cl=0.035mM$ or $0.07mM$) (23). Four pharmaceutical compounds, sumatriptan, chlorphenamine, doxylamine and ranitidine were used in the kinetic experiments. Measured monochloramine decay concentrations over time in Shen's work were used to model monochloramine decomposition. Model fitting and optimized rate constants are shown in Figure 5 and Table 4. The model in equation 1c simulates NDMA formation from ranitidine in MQ water with a high correlation coefficient ($R^2>0.93$) and yields an optimized rate constant of $1.3 M^{-1}s^{-1}$. This is similar to the rate constant ($1.2 M^{-1}s^{-1}$) in Selbes' work under similar reaction conditions (DDW water, SDS, $NH_2Cl=0.04mM$) and demonstrates that our model is applicable to predict NDMA formation from ranitidine and monochloramine under similar reaction conditions.

However, for all four pharmaceutical precursors, the model overestimates the NDMA formation in the first half experiment time and underestimated NDMA in the second half. This is possibly due to the formation of an intermediate that delays the NDMA formation, as suggested previously.

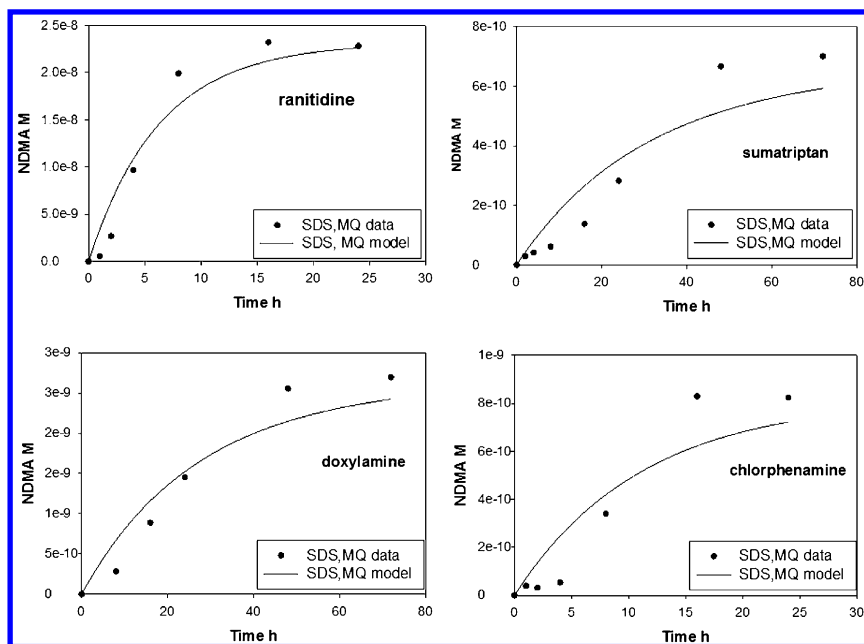


Figure 5. NDMA formation from pharmaceutical compounds under SDS condition (MQ water; $NH_2Cl=0.035mM$, $pH=7$), data (symbols) and model fitting (lines). (NDMA data from Shen et al., 2011 (23))

Table 4. Optimized Rate Constant k_{app} for Model Compounds in Different Water Matrices with Varied TOC. (NDMA Data from Shen et al. 2011 (23))

Compounds	NDMA Yields in SDS MQ %	$k_{app} M^{-1}s^{-1} (R^2)$		
		SDS	2mg/L TOC	6mg/L TOC
ranitidine	~90	1.3 (0.93)	0.82	0.25
sumatriptan	~2	0.28 (0.86)	0.24	0.08
chlorphenamine	3	0.73 (0.90)	-	0.22
doxylamine	10	0.28 (0.84)	-	0.13

In Shen’s work on NDMA formation from pharmaceutical compounds in natural waters, there was an initial lag-time when NDMA formation did not increase for all four pharmaceutical compounds in lake and river waters. The lag-time was longer at higher TOC concentrations. However, the lag-time could not be simulated with our proposed model. In Shen’s work it was suggested that there was NOM-pharmaceutical binding that inhibited the initial NDMA

formation (23). In addition, dichloramine has a lower electron density on nitrogen due to two chlorine atoms so it would be a more preferable species to interact with negatively charged NOM. Thus in the presence of NOM, dichloramine could more easily react with NOM compared to monochloramine and hence NDMA formation from dichloramine would be suppressed by NOM.

To better understand how NOM affects NDMA formation rates, our proposed model was adjusted to fit the kinetics data. As there is no NDMA formed during the lag-time, we start the model simulation at the end of the NDMA formation lag. The lag time was removed and the kinetics data was refitted with our model. The model fits the experimental data better for all four pharmaceutical compounds (Figure 6) and the optimized rate constants were listed in Table 3. The optimized second-order rate constants k_{app} were found to decrease with increasing TOC concentrations. This can be explained by a competition between NOM and model compounds to react with mono- and/or di-chloramine. In the river water samples (TOC=6mg/L), the optimized rate constants k_{app} for the pharmaceutical model compounds were in the range of 0.08 to 0.25M⁻¹s⁻¹ (Table 4) and were comparable to the rate constants (0.02 to 0.09 M⁻¹s⁻¹) of NDMA formation from NOM in surface waters with similar TOC concentration (TOC=3.4mg/L) in Chen's work we discussed previously. By using the lag model, we were able to compare the rate constant of NDMA formation at different DOC concentrations and reveal how the DOC impacted the NDMA formation kinetics.

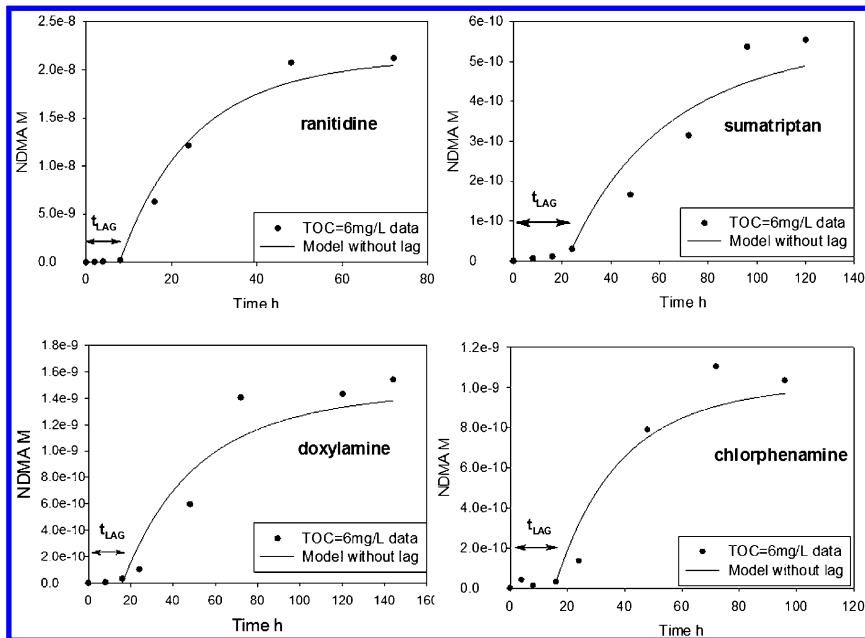


Figure 6. NDMA formation of amine precursors in river water (SDS, pH=7, TOC=6mg/L) and modeling of NDMA formation without lag-time, data (symbols) and model fitting (lines). (NDMA data from Shen et al., 2011 (23))

Summary and Conclusions

A model was developed and parameterized based on NDMA formation trends observed in the literature. Results show that a second-order kinetic rate model simulates NDMA formation from NOM and model precursors over a range of reaction conditions. A narrow range of rate constants were obtained and appear to indicate a similar rate-limiting reaction step among different precursors and water sources. Though the model was not intended to reveal the relative importance of mono- or di- chloramine reactions in NDMA formation kinetics, it is applicable to describe how water conditions such as DOC and pH affect NDMA formation kinetics. In real water utilities, the model could be used to predict NDMA formation by measuring the NDMA_{max} and monochloramine.

The proposed model needs to be further evaluated using a wider range of reaction conditions. For example, the importance of dissolved oxygen needs be investigated since it was found to be an important factor in NDMA formation from different amines such as DMA and ranitidine. NDMA kinetics test could be performed in other water matrices such as wastewater effluents. In addition, further detailed characterization of more precursors and their kinetics studies could help better understand NDMA formation in different water sources and a more precise model could be developed.

Acknowledgments

This research was supported by the Water Research Foundation (Project 4499, managed by Djanette Khiari), American Water Works Association Abel Wolman Fellowship, Water Environment Federation Canham Scholarship, and the Arizona State University Fulton School of Engineering Dean's Fellowship.

References

1. Krasner, S. W.; Mitch, W.; McCurry, D. L.; Westerhoff, P.; Hanigan, D. Formation, Precursors, Control, and Occurrence of Nitrosamines in Drinking Water: A Review. *Water Res.* **2013**, *47*, 4433–4450.
2. EPA, U. *Contaminant Candidate List 3 (CCL3)*; 2009, <http://water.epa.gov/scitech/drinkingwater/dws/ccl/ccl3.cfm> (accessed September 26th, 2014).
3. OEHHA. *Public Health Goal for Chemicals in Drinking Water: N-Nitrosodimethylamine*; California Environmental Protection Agency: Sacramento, CA, 2006.
4. Mitch, W.; Kraner, S.; Westerhoff, P.; Dotson, A. Occurrence and Formation of Nitrogenous Disinfection By-products. *Water Research Foundation Report*; Water Research Foundation: Denver, CO, 2009.
5. Boyd, J. M.; Hruday, S. E.; Richardson, S. D.; Li, X. F. Solid-phase extraction and high-performance liquid chromatography mass spectrometry analysis of nitrosamines in treated drinking water and wastewater. *Trends Anal. Chem.* **2011**, *30* (9), 1410–1421.

6. Russell, C. G.; Blute, N. K.; Via, S.; Wu, X.; Chowdhury, Z.; More, R. Nationwide assessment of nitrosamine occurrence and trends. *J. AWWA* **2012**, *104* (3), 57–58.
7. Krasner, S. W.; Westerhoff, P.; Mitch, W. A.; Skadsen, J. Case Studies on Nitrosamine Formation and Control at Full-Scale Drinking Water Treatment Plants. Presented at 2012 AWWA Wat. Qual. Technol. Conf., Toronto, Ontario, 2012.
8. Valentine, R. L.; Choi, J.; Chen, Z.; Barrett, S. E.; Hwang, C. J.; Guo, Y.; Wehner, M.; Fitzsimmons, S.; Andrews, S. A.; Werker, A. G.; Brubacher, C.; Kohut, K. D., Factors affecting the formation of NDMA in water and occurrence. AWWA Research Foundation: Denver, CO, 2005.
9. Krasner, S. W.; Westerhoff, P.; Chen, B.; Rittmann, B. E.; Amy, G. Occurrence of disinfection byproducts in united states wastewater treatment plant effluents. *Environ. Sci. Technol.* **2009**, *43* (21), 8320–8325.
10. Liew, D.; Linge, K. L.; Joll, C.; Heitz, A.; Trolio, R.; Breckler, L.; Henderson, R.; Charrois, J. W. A.; Formation of Nitrogenous Disinfection By-Products (N-DBPs) in Raw and Treated Drinking Water. In *Ozwater '11*, May 9–11 2011, Australian Water Association: Adelaide, 2011.
11. Krasner, S. W.; Scilimenti, M. J.; Lee, C. F. T. Occurrence and Formation of NDMA in Consecutive Systems in a Major Metropolitan Area. *Proc. 2012 AWWA Water Quality Technology Conference*; AWWA: Denver, CO, 2012.
12. Ridd, J. H. Nitrosation, Diazotisation, and Deamination. *Q. Rev. Chem. Soc.* **1961**, *15* (4), 418–441.
13. Mitch, W. A.; Sedlak, D. L. Formation of N-nitrosodimethylamine (NDMA) from dimethylamine during chlorination. *Environ. Sci. Technol.* **2002**, *36* (4), 588–595.
14. Choi, J.; Valentine, R. L. Formation of N-nitrosodimethylamine (NDMA) from reaction of monochloramine: a new disinfection by-product. *Water Res.* **2002**, *36* (4), 817–824.
15. Schreiber, I. M.; Mitch, W. A. Nitrosamine formation pathway revisited: The importance of chloramine speciation and dissolved oxygen. *Environ. Sci. Technol.* **2006**, *40* (19), 6007–6014.
16. Shah, A.; Mitch, W. A. Halonitroalkanes, halonitriles, haloamides and N-nitrosamines: A critical review of nitrogenous disinfection byproduct (N-DBP) formation pathways. *Environ. Sci. Technol.* **2012**, *46* (1), 119–131.
17. Schreiber, I. M.; Mitch, W. A. Occurrence and fate of nitrosamines and nitrosamine precursors in wastewater-impacted surface waters using boron as a conservative tracer. *Environ. Sci. Technol.* **2006**, *40* (10), 3203–3210.
18. Gerecke, A. C.; Sedlak, D. L. Precursors of N-nitrosodimethylamine in natural waters. *Environ. Sci. Technol.* **2003**, *37* (7), 1331–1336.
19. Mitch, W. A.; Sedlak, D. L. Characterization and fate of N-nitrosodimethylamine precursors in municipal wastewater treatment plants. *Environ. Sci. Technol.* **2004**, *38* (5), 1445–1454.
20. Mitch, W. A.; Schreiber, I. M. Degradation of tertiary alkylamines during chlorination/chloramination: Implications for formation of aldehydes, nitriles, halonitroalkanes, and nitrosamines. *Environ. Sci. Technol.* **2008**, *42* (13), 4811–4817.

21. Le Roux, J.; Gallard, H.; Croue, J. P. Chloramination of nitrogenous contaminants (pharmaceuticals and pesticides): NDMA and halogenated DBPs formation. *Water Res.* **2011**, *45* (10), 3164–3174.
22. Shen, R.; Andrews, S. A. Demonstration of 20 pharmaceuticals and personal care products (PPCPs) as nitrosamine precursors during chloramine disinfection. *Water Res.* **2011**, *45* (2), 944–952.
23. Shen, R. Q.; Andrews, S. A. NDMA formation kinetics from three pharmaceuticals in four water matrices. *Water Res.* **2011**, *45* (17), 5687–5694.
24. Selbes, M.; Kim, D.; Ates, N.; Karanfil, T. The Roles Of Tertiary Amine Structure, Background Organic Matter And Chloramine Species On NDMA Formation. *Water Res.* **2013**, *47* (2), 945–953.25.
25. Choi, J.; Valentine, R. L. Formation of N-nitrosodimethylamine (NDMA) from reaction of monochloramine: a new disinfection by-product. *Water Res.* **2002**, *36* (4), 817–824.
26. Le Roux, J.; Gallard, H.; Croue, J. P.; Papot, S.; Deborde, M. NDMA Formation by Chloramination of Ranitidine: Kinetics and Mechanism. *Environ. Sci. Technol.* **2012**, *46* (20), 11095–11103.
27. Liu, Y. D.; Selbes, M.; Zeng, C.; Zhong, R.; Karanfil, T. Formation Mechanism of NDMA from Ranitidine, Trimethylamine, and Other Tertiary Amines during Chloramination: A Computational Study. *Environ. Sci. Technol.* **2014**, *48* (15), 8653–8663.
28. Chen, Z.; Valentine, R. L. Modeling the formation of N-nitrosodimethylamine (NDMA) from the reaction of natural organic matter (NOM) with monochloramine. *Environ. Sci. Technol.* **2006**, *40* (23), 7290–7297.
29. Ozekin, K.; Valentine, R. L.; Vikesland, P. J. Modeling the decomposition of disinfecting residuals of chloramine. *Water Disinfection and Natural Organic Matter: Characterization and Control*; Minear, R. A., Amy, G. L., Eds.; American Chemical Society: Washington, DC, 1996; Vol. 649, pp 115–125.
30. Mitch, W.; Krasner, S. W.; Westerhoff, P.; Dotson, A. *Occurrence and Formation of Nitrogenous Disinfection By-Products (Final Report, Project #3014)*; AwwaRF/USEPA: Denver, CO, 2009; p 145.
31. Chen, B. Y.; Westerhoff, P. Predicting disinfection by-product formation potential in water. *Water Res.* **2010**, *44* (13), 3755–3762.
32. Vikesland, P. J.; Ozekin, K.; Valentine, R. L. Monochloramine decay in model and distribution system waters. *Water Res.* **2001**, *35* (7), 1766–1776.
33. Ianni, J. C., Kintecus. *Windows Version 2.80*, 2002, www.kintecus.com, (accessed September 10, 2014).
34. Duirk, S. E.; Gombert, B.; Croué, J.-P.; Valentine, R. L. Modeling monochloramine loss in the presence of natural organic matter. *Water Res.* **2005**, *39* (14), 3418–3431.
35. Selbes, M. The effects of amine structure, chloramine species and oxidation strategies on the formation of N-nitrosodimethylamine. Ph.D. Thesis, Clemson University, Clemson, South Carolina, 2014.

Chapter 6

Meta-Analysis of Trihalomethane Formation Models and Application to Bromide Intrusion

Treavor H. Boyer*

Department of Environmental Engineering Sciences, Engineering School of Sustainable Infrastructure & Environment (ESSIE), University of Florida, P.O. Box 116450, Gainesville, Florida 32611-6450

*E-mail: thboyer@ufl.edu.

This research evaluated previously published trihalomethane (THM) formation models for their statistical robustness to be applied outside of their original calibration data set, and be used as a predictive tool at the water utility scale. All models predicted THM4 (i.e., the sum of the four chlorine- and bromine-containing THM species) based on the chlorination of natural waters and were developed using different combinations of precursor types (i.e., organic carbon concentration, UV-absorbing substances, and bromide concentration) and chlorination conditions (i.e., chlorine dose, pH, temperature, and time) as explanatory variables. All models were log (base 10) transformed into a common format, and were evaluated using a nationally representative water quality and THM4 formation data set based on the statistical metrics standard error, mean absolute percentage error, R^2 , and adjusted R^2 . The most robust $\log_{10}(\text{THM4})$ formation models had standard error equal to 0.226–0.262 and adjusted R^2 equal to 0.696–0.783. The THM4 formation models that included bromide as an explanatory variable tended to under predict THM4 formation as a function of increasing bromide concentration. Overall, the results of this research show that several previously published THM4 formation models were developed with the appropriate explanatory variables and calibrated with a sufficiently broad data set such that the models may give a reasonable prediction of THM4 formation, depending on the level of accuracy desired, for chlorinated water conditions separate from the original

calibration data set. However, the majority of THM4 formation models were not sensitive to changing bromide concentration, and as such, under predicted THM4 formation at bromide concentrations greater than 500 $\mu\text{g/L}$.

1. Introduction

Numerous empirical models have been developed to predict the formation of disinfection by-products (DBPs) (1–5). The majority of the models are on the formation of THM4 (i.e., the sum of the four chlorine- and bromine-containing trihalomethanes) following chlorination of natural waters. The THM4 and other DBP formation models are typically developed using multiple regression techniques based on DBP formation considering key explanatory variables. The most relevant and frequently used explanatory variables include dissolved organic carbon (DOC) or total organic carbon (TOC) concentration, UV absorbance (typically at 254 nm; UV_{254}), bromide ion (Br^-) concentration, chlorine dose (Cl_2), reaction time (t), pH, and temperature (T) (6). For instance, many of the models are empirical multiple-parameter power function models of the form $\text{THM4} = a(\text{DOC})^b(\text{UV}_{254})^c(\text{Br}^-)^d(\text{Cl}_2)^e(t)^f(T)^g$ where a , b , c , d , e , f , and g are constants. THM4 and other DBP formation models take the form of multiple-parameter power function models because this type of model is able to empirically describe the DBP formation trends that have been experimentally observed based on changes in precursor concentration and chlorination conditions. The multiple-parameter power function model is linearized by log transformation to the form $\log(\text{THM4}) = \log(a) + b \cdot \log(\text{DOC}) + c \cdot \log(\text{UV}_{254}) + d \cdot \log(\text{Br}^-) + e \cdot \log(\text{Cl}_2) + f \cdot \log(t) + g \cdot \log(T)$. The linearized equation is solved using multiple regression techniques by which values for the independent variable and explanatory variables are input into the model, and the constants (i.e., regression coefficients) are estimated such that the error between model predictions and known values are minimized (4). The input values for multiple regression use a variety of water quality and chlorination data sets, some of which include a wide range of values for the explanatory variables while others are more limited. For example, although bromide is a key precursor in DBP formation, many chlorine-based THM and haloacetic acid formation models have been developed for low bromide waters and therefore lack bromide as an explanatory variable (7, 8).

The usefulness of previously published DBP formation models depends on the desired accuracy and the temporal and spatial scale of interest. For example, at the molecular level, DBP formation models can provide insight on DBP formation mechanisms (9), where the predictive accuracy of the model may be less important relative to understanding the reaction pathway. As another example, DBP formation models can be used at the utility scale to assess changes in water quality or treatment modifications, and the consequent implications of these changes on DBP formation (3, 10, 11). In this case, the predictive accuracy (or predictive capability) of the models is the important consideration. For instance, Lu et al. developed a site-specific THM4 formation model to evaluate water

utility compliance with the U.S. EPA Disinfectants/Disinfection By-Products Rule under different water quality and treatment conditions (3). Many water utilities, however, do not have the resources to develop DBP formation models that are specific to their water supply and treatment processes. As such, there is a need for previously published DBP formation models to be generally applicable at the water utility scale to aid in daily operation and long term planning. This is especially true for small water systems and water systems that are experiencing an increased frequency of extreme events or changes in water quality. The usefulness, however, of applying previously published DBP formation models at the water utility scale will depend on the robustness of the existing models. In particular, can DBP formation models developed and calibrated locally be applied globally?

Accordingly, the goal of the research described in this chapter was to evaluate previously published DBP formation models for their statistical robustness to be applied separately from their original calibration data set so as to be used at the water utility scale as a predictive tool. The specific objectives of the work were to (1) evaluate the predictive capability of previously published chlorine-based THM4 formation models using a nationally representative data set on THM4 formation, and (2) evaluate the sensitivity and application of the THM4 formation models for water sources that experience an increase in bromide concentration. This research focused on THM4 formation by chlorine because it constitutes that largest number of previously published DBP formation models, and because THM4 formation and speciation during chlorination is strongly influenced by bromide concentration.

2. Methods

Previously published chlorine-based THM4 formation models were collected from peer-reviewed journal articles and reports as described in detail elsewhere (6). The models evaluated in this research are listed in Table 1. The models follow the multiple-parameter power function format or log-transformed power function format. The model number is the same as used in previous work (6). For subsequent analysis, the THM4 formation models were divided into two categories; those that included bromide as an explanatory variable and those that did not include bromide as an explanatory variable. The predictive capability of the THM4 formation models was assessed by log (base 10) transformation of the power function models to a common format, i.e., $\log y = a + b_1 \log x_1 + b_p \log x_p$, where y is the predicted THM4 concentration (in $\mu\text{g/L}$), x_1 to x_p are explanatory variables, a and b_1 to b_p are regression coefficients, and p is the number of explanatory variables. The power function models were log transformed to linearize all models, which was the original form of the models used in the multiple regression analysis, and to allow for graphical display of all THM4 data, which ranged from 1 to 1000 $\mu\text{g/L}$. For each model, the predicted $\log_{10}(\text{THM4})$ was compared with the measured $\log_{10}(\text{THM4})$ using the following statistical metrics: linear coefficient of determination or R-squared (R^2), adjusted R-squared ($\text{adj-}R^2$), standard error (SE), and mean absolute percentage error (MAPE).

Table 1. Summary of THM4 Formation Models Evaluated in this Work

<i>No.</i> ^a	<i>Model</i> ^b	<i>Ref</i>
2	$\text{THM4} = 0.82(\text{pH} - 2.8)\text{TOC}(\text{Cl}_2)^{0.25}(\text{t})^{0.36}$	(15)
5c,d	$\text{THM4} = 7.21(\text{TOC})^{0.004}(\text{UV}_{254})^{0.534}(\text{Cl}_2 - 7.6\text{NH}_3)^{0.224}(\text{t})^{0.255}(\text{Br}^- + 1)^{2.01}(\text{T})^{0.480}(\text{pH} - 2.6)^{0.719}$	(16)
6	$\text{THM4} = 12.7254(\text{TOC})^{0.291}(\text{t})^{0.2706}(\text{Cl}_2)^{-0.0719}$	(17)
7	$\text{THM4} = 108.8(\text{TOC})^{0.2466}(\text{t})^{0.2956}(\text{UV}_{254})^{0.9919}(\text{Cl}_2)^{0.126}$	(17)
8	$\text{THM4} = 131.7492(\text{t})^{0.2931}(\text{UV}_{254})^{1.075}(\text{Cl}_2)^{0.1064}$	(17)
9	$\text{THM4} = 14.6(\text{pH} - 3.8)^{1.01}(\text{Cl}_2)^{0.206}(\text{UV}_{254})^{0.849}(\text{t})^{0.306}$	(18)
10	$\text{THM4} = 0.0412(\text{DOC})^{1.10}(\text{Cl}_2)^{0.152}(\text{Br}^-)^{0.068}(\text{T})^{0.61}(\text{pH})^{1.60}(\text{t})^{0.260}$	(5)
11	$\text{THM4} = 0.044(\text{DOC})^{1.030}(\text{t})^{0.262}(\text{pH})^{1.149}(\text{Cl}_2)^{0.277}(\text{T})^{0.968}$	(19)
12	$\text{THM4} = 1.392(\text{DOC})^{1.092}(\text{pH})^{0.531}(\text{T})^{0.255}$	(19)
15	$\text{THM4} = 10^{-1.385}(\text{DOC})^{1.098}(\text{Cl}_2)^{0.152}(\text{Br}^-)^{0.068}(\text{T})^{0.609}(\text{pH})^{1.601}(\text{t})^{0.263}$	(4)
16	$\text{THM4} = 0.42(\text{UV}_{254})^{0.482}(\text{Cl}_2)^{0.339}(\text{Br}^-)^{0.023}(\text{T})^{0.617}(\text{pH})^{1.609}(\text{t})^{0.261}$	(4)
17e	$\text{THM4} = 0.283(\text{DOC} \cdot \text{UV}_{254})^{0.421}(\text{Cl}_2)^{0.145}(\text{Br}^-)^{0.041}(\text{T})^{0.614}(\text{pH})^{1.606}(\text{t})^{0.261}$	(4)
18	$\text{THM4} = 0.00253(\text{DOC})^{1.22}(\text{Cl}_2)^{0.442}(\text{T})^{1.34}(\text{pH})^{1.75}(\text{t})^{0.34}$	(4)
19e	$\text{THM4} = 0.012(\text{DOC} \cdot \text{UV}_{254})^{0.47}(\text{Cl}_2)^{0.48}(\text{T})^{1.10}(\text{pH})^{2.38}(\text{t})^{0.35}$	(4)
20f	$\text{THM4} = 3.296(\text{DOC})^{0.801}(\text{Cl}_2)^{0.261}(\text{Br}^-)^{0.223}(\text{t})^{0.264}$	(4)
21 f	$\text{THM4} = 75.7(\text{UV}_{254})^{0.593}(\text{Cl}_2)^{0.332}(\text{Br}^-)^{0.0603}(\text{t})^{0.264}$	(4)
22 f	$\text{THM4} = 23.9(\text{DOC} \cdot \text{UV}_{254})^{0.403}(\text{Cl}_2)^{0.225}(\text{Br}^-)^{0.141}(\text{t})^{0.264}$	(4)
24	$\text{THM4} = 4.527(\text{t})^{0.127}(\text{Cl}_2)^{0.595}(\text{TOC})^{0.596}(\text{Br}^-)^{0.103}(\text{pH})^{0.66}$	(20)

<i>No.</i> ^a	<i>Model</i> ^b	<i>Ref</i>
28	$\text{THM4} = 0.0001(\text{Cl}_2)^{3.14}(\text{pH})^{1.56}(\text{TOC})^{0.69}(\text{t})^{0.175}$	(1)
29	$\text{THM4} = 0.0707(\text{TOC} + 3.2)^{1.314}(\text{pH} - 4.0)^{1.496}(\text{Cl}_2 - 2.5)^{-0.197}(\text{T} + 10)^{0.724}$	(11)
30	$\log_{10}(\text{THM4}) = 1.078 + 0.398\log_{10}(\text{TOC}) + 0.158\log_{10}(\text{T}) + 0.702\log_{10}(\text{Cl}_2)$	(21)
31 ^e	$\text{THM4} = 10^{-1.375(\text{t})^{0.258}(\text{Cl}_2/\text{DOC})^{0.194}(\text{pH})^{1.695}(\text{T})^{0.507}(\text{Br}^-)^{0.218}}$	(22)
32 ^e	$\text{THM4} = 10^{-0.038(\text{Cl}_2)^{0.654}(\text{pH})^{1.322}(\text{t})^{0.174}(\text{SUVA})^{0.712}}$	(8)
35 ^{d,g}	$\ln(\text{THM4}) = 6.11 + 0.211\ln(\text{t}) + 1.64\ln(\text{Br}^-) + 0.34\ln(\text{Cl}_2) - 0.80\ln(\text{T})$	(23)
38 ^d	$\text{THM4} = 1147(\text{DOC})^{0.00}(\text{UV}_{254})^{0.83}(\text{Br}^- + 1)^{0.27}$	(24)

^a Model numbers from Ged et al. (*6*) Models are shown in format as originally presented, i.e., power function model or log-transformed, linearized model. Statistical analysis was conducted on log transformed (base 10) models. ^b Units: THM4 (μg/L), Br⁻ (μg/L) unless noted otherwise, DOC (mg/L), TOC (mg/L), UV₂₅₄ (1/cm), pH (-), T (° C), t (h), Cl₂ (mg/L), SUVA (L/mg·m). ^c NH₃ term neglected. ^d Br⁻ (mg/L). ^e Combined terms separated following logarithm rules. ^f Not corrected for pH to maintain consistent format with other log transformed models. ^g All terms divided by ln(10) to convert model to log base 10.

The statistical metrics used in this work provide different goodness of fit measurements for the predicted $\log_{10}(\text{THM4})$ data from the different models with respect to the $y = x$ line. For instance, R^2 and adjusted R^2 measure how close the predicted data conform to a linear relationship with the measured data. In addition, the adjusted R^2 accounts for the number of explanatory variables in the model. The higher the value for R^2 and adjusted R^2 , the better the predicted data conforms to a linear relationship with the experimental data, with R^2 and adjusted R^2 having a maximum value of 1. R^2 was calculated using the RSQ function in Microsoft Excel as $\text{RSQ}(\log_{10}(\text{THM4}_i) \text{ predicted}, \log_{10}(\text{THM4}_i) \text{ measured})$. Adjusted R^2 was calculated from R^2 as $1 - (1 - R^2)((n - 1)/(n - p - 1))$ where n is the sample size and p is the number of explanatory variables in the model. The SE is the standard error of the estimate and measures the accuracy of the prediction, i.e., the average distance between the predicted value and the $y = x$ line. The SE has the same units as the response variable. The smaller the value of SE, the higher the accuracy of the prediction. SE was calculated in Microsoft Excel using the sum of squares of differences function as $\text{SQRT}(\text{SUMXMY2}(\log_{10}(\text{THM4}_i) \text{ measured}, \log_{10}(\text{THM4}_i) \text{ predicted})/n)$. The MAPE is a measure of the accuracy of the predictions, and has the formula $\sum \text{abs}[(\log_{10}(\text{THM4}_i) \text{ measured} - \log_{10}(\text{THM4}_i) \text{ predicted})/\log_{10}(\text{THM4}_i) \text{ measured}]/n$ where the summation is over all data and the final value is expressed as a percent. The MAPE formula was calculated in Microsoft Excel. The smaller the value of MAPE, the more accurate the prediction by the model.

The measured THM4 data and corresponding water quality and chlorination conditions came from a national study of bromide in U.S. drinking water supplies (12). The subset of THM4 formation models that included bromide as an explanatory variable were evaluated for their sensitivity to changing bromide concentration. The bromide-containing THM4 formation models were evaluated using a data set that measured THM4 formation for increasing bromide concentration with all other water quality and chlorination conditions constant (13). Finally, the bromide-containing THM4 formation models were used to simulate the change in THM4 concentration that would occur for different scenarios of seawater intrusion based on a bromide to total dissolved solids (TDS) mass ratio of 0.0019134 for standard seawater (14).

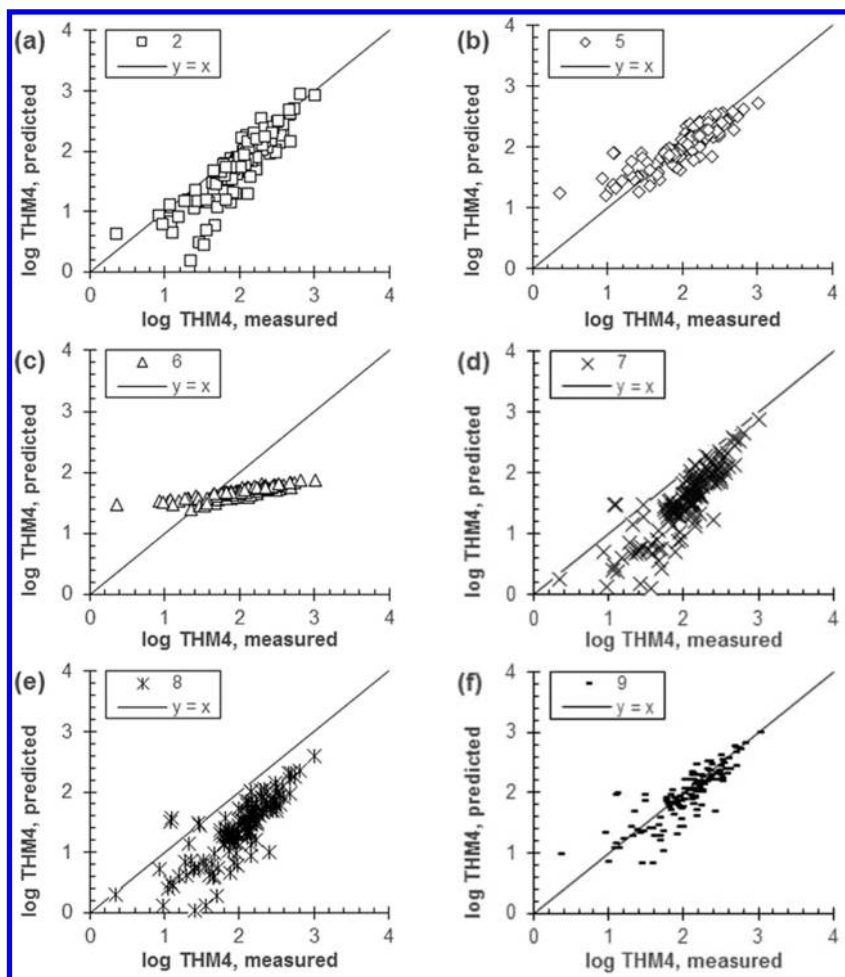
3. Results and Discussion

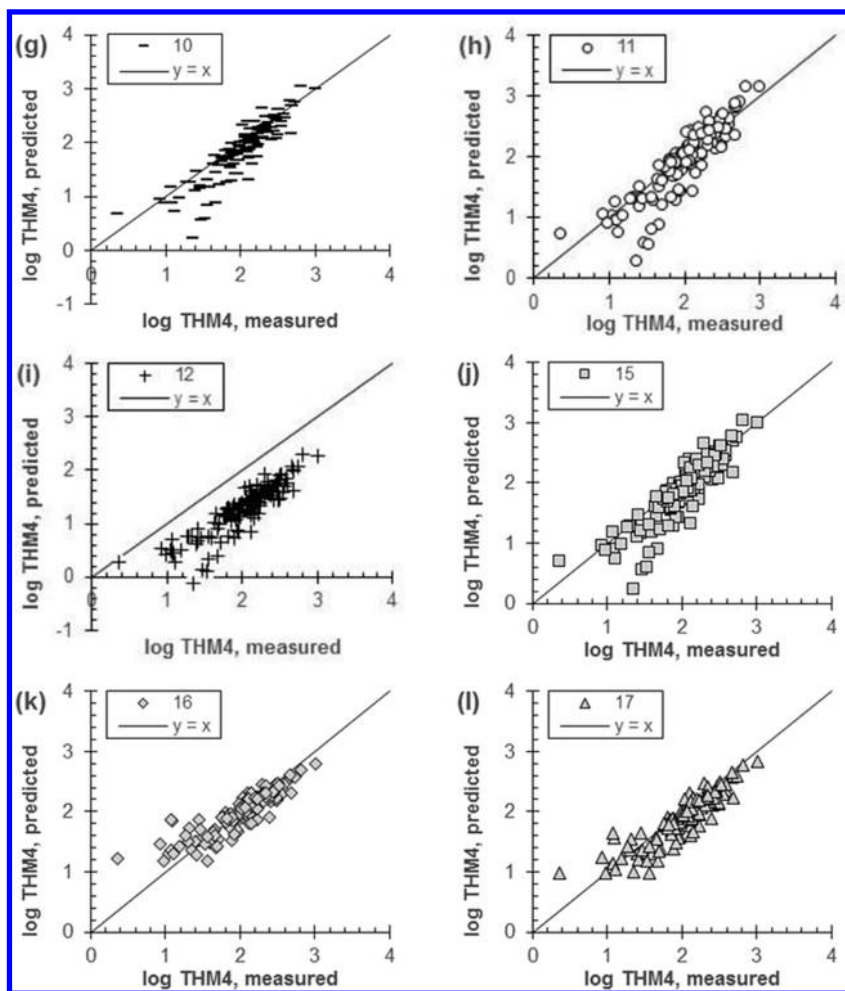
3.1. Predictive Capability of THM4 Formation Models

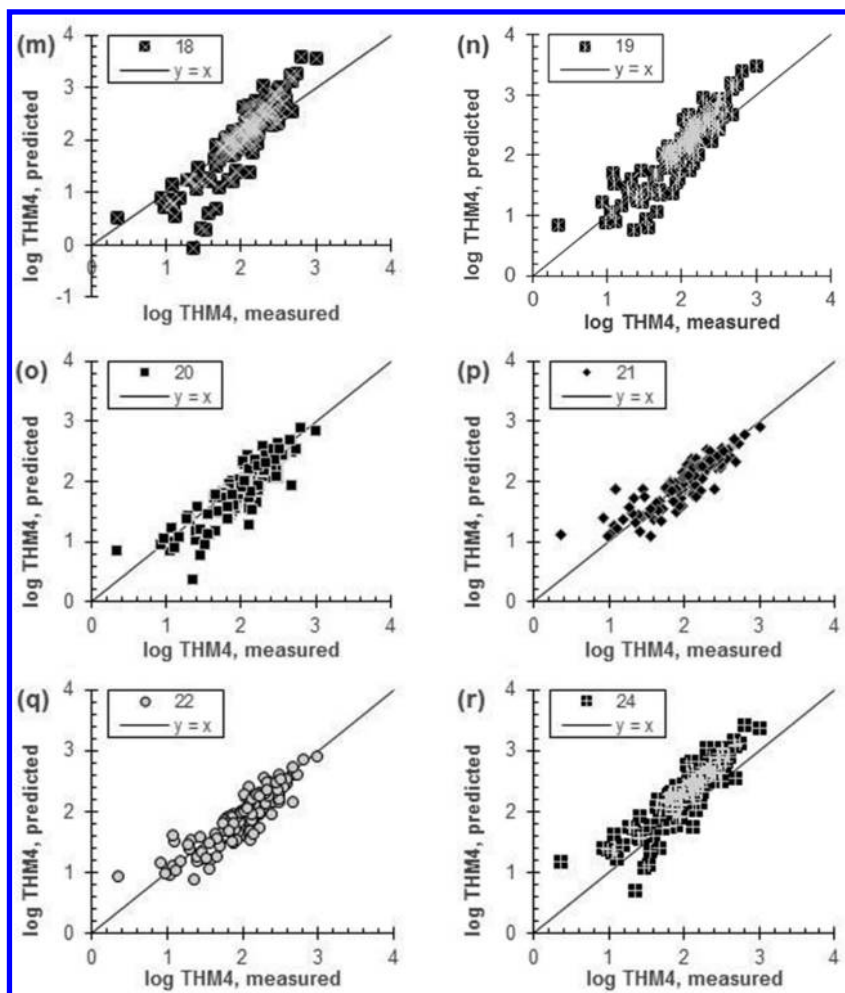
Figure 1 shows individual plots of each THM4 formation model in terms of $\log_{10}(\text{THM4})$ predicted versus $\log_{10}(\text{THM4})$ measured. The $y = x$ line is included in each plot to illustrate perfect agreement between model predictions and measured data, which would give $R^2 = 1$, $\text{SE} = 0$, and $\text{MAPE} = 0\%$. Many of the THM4 formation models evaluated in this work give predictions that are tightly scattered along the $y = x$ line, e.g., models 5, 9, 16, 17, 19, 21, and 22 have MAPE equal to 30 to 38% (see Table 2), thereby illustrating relatively accurate predictions. This is a somewhat surprising result considering that the

THM4 formation models were originally calibrated using their own unique data sets. This suggests that many of the models were developed to include the correct collection of explanatory variables (i.e., precursor types and concentrations, and chlorination conditions) and were calibrated using data sets in which the explanatory variables covered a range of reasonable values. For instance, the nationally representative data set that was used to evaluate the predictive capability of the THM4 formation models had minimum, maximum, and average values of the explanatory variables as follows: DOC (0.11, 18, 3.0 mg/L), UV_{254} (0.003, 0.533, 0.078 1/cm), Br^- (2.5, 446, 76.6 $\mu\text{g/L}$), Cl_2 (0.34, 54, 9.0 mg/L), pH (constant 7), T (constant 20°C), and t (constant 96 h) (12). The DOC range in the national data set covers almost the entire range of DOC that would be expected during water treatment (25). As discussed in the next section, however, the bromide range of < 500 $\mu\text{g/L}$ is limited to freshwater with very low saline water inputs (13). The predictive capability of several of the models, e.g., 8 and 12, could be improved by increasing the constant while keeping the same value for the regression coefficients for the explanatory variables. This represents a hybrid approach in which a water utility could slightly modify an existing THM4 formation model using historic water quality and THM4 formation data but not redo the multiple regression analysis to develop an entirely new model.

Table 2 provides a summary of the goodness of fit statistics that quantify the predictive capability of the log (base 10) transformed THM4 formation models. The models with the lowest SE were models 21 (SE = 0.226), 22 (SE = 0.230), 16 (SE = 0.232), 30 (SE = 0.234), 17 (SE = 0.235), 5 (SE = .241), and 9 (SE = 0.262). It is important to recognize that the SE values are for $\log_{10}(\text{THM4})$, i.e., log base 10 scale, such that a small value in SE can translate to a large variation in THM4 concentration depending on the magnitude of $\log_{10}(\text{THM4})$. Table 3 illustrates the accuracy of the model estimates for $\log_{10}(\text{THM4}) = 1.6$ (40 $\mu\text{g/L}$) and $\log_{10}(\text{THM4}) = 1.9$ (80 $\mu\text{g/L}$). For example, for a $\log_{10}(\text{THM4})$ model prediction of 1.6, the model prediction \pm one SE is 24 to 67 $\mu\text{g/L}$ after anti-log transformation. However, for a $\log_{10}(\text{THM4})$ model prediction of 1.9, the model prediction \pm one SE is 48 to 135 $\mu\text{g/L}$ after anti-log transformation, which is too wide of a range to be useful for regulatory compliance. Among the models with the lowest SE discussed above, model 9 had the lowest MAPE (30%) and model 22 had the highest adjusted R^2 . Models 5, 16, 17, 21, and 22 included Br^- , UV_{254} , Cl_2 , and t as common explanatory variables. These four explanatory variables represent the minimum set of explanatory variables needed to accurately predict THM4 formation. For instance, Br^- and UV_{254} represent both inorganic and organic precursor material in THM4 formation, and Cl_2 and t dictate the extent of the chlorination reaction.







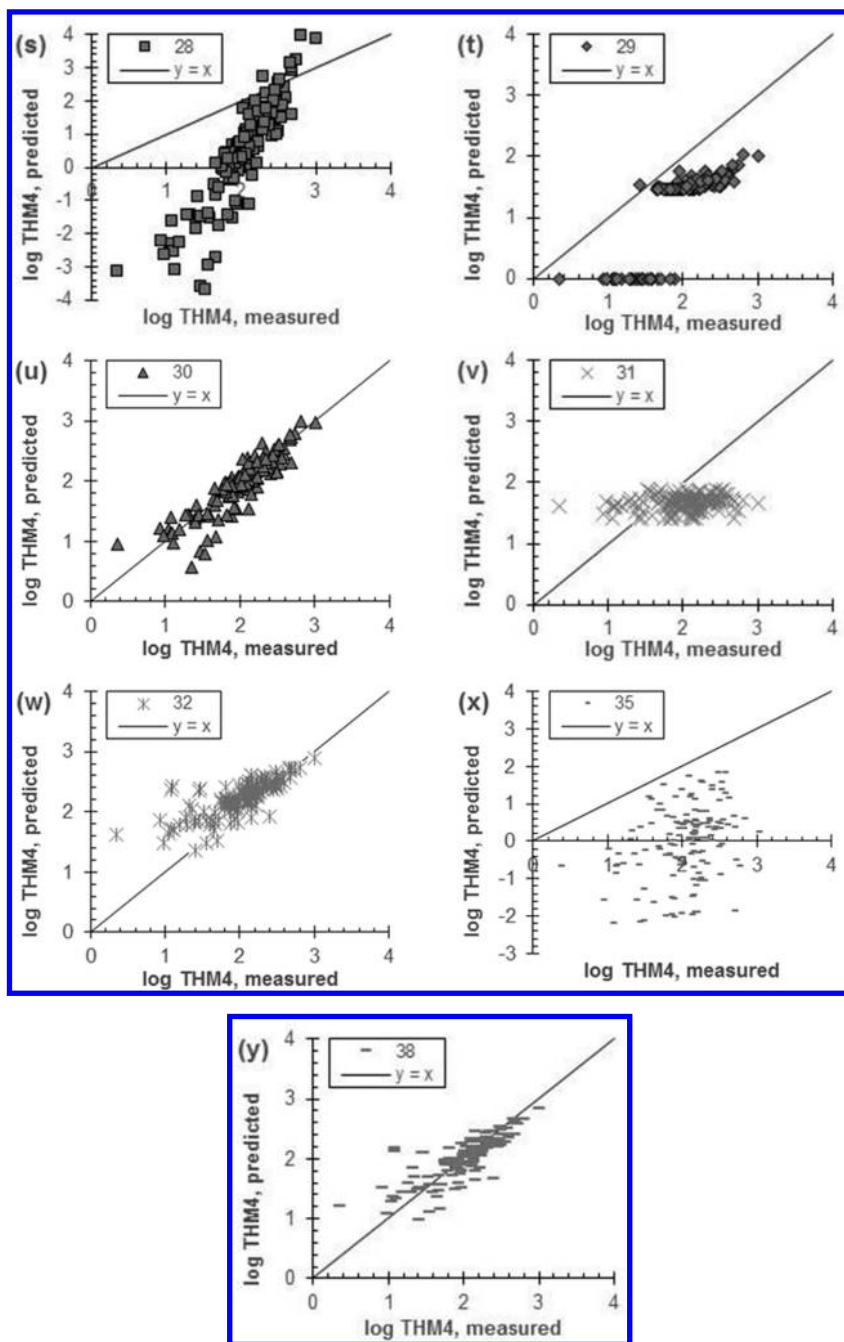


Figure 1. $\log_{10}(\text{THM4})$ measured versus $\log_{10}(\text{THM4})$ predicted. Model number given in legend. Measured THM4 is 145 unique samples.

Table 2. Summary of Goodness of Fit Statistics for Log (Base 10) Transformed THM4 Formation Models.

<i>Model^a</i>	<i>SE</i>	<i>MAPE</i>	<i>R²</i>	<i>adj-R²</i>	<i>p</i>	<i>Bromide</i>
2	0.346	36%	0.759	0.752	4	no
5	0.241	38%	0.749	0.736	7	yes
6	0.500	56%	0.759	0.754	3	no
7	0.563	31%	0.726	0.719	4	no
8	0.669	36%	0.671	0.664	3	no
9	0.262	30%	0.704	0.696	4	no
10	0.294	34%	0.766	0.756	6	yes
11	0.272	34%	0.759	0.750	5	no
12	0.767	51%	0.759	0.754	3	no
15	0.291	34%	0.766	0.756	6	yes
16	0.232	37%	0.765	0.755	6	yes
17	0.235	33%	0.790	0.779	7	yes
18	0.365	35%	0.759	0.750	5	no
19	0.299	35%	0.788	0.779	6	no
20	0.285	35%	0.747	0.739	4	yes
21	0.226	34%	0.759	0.752	4	yes
22	0.230	31%	0.791	0.783	5	yes
24	0.375	50%	0.767	0.758	5	yes
28	2.028	150%	0.759	0.752	4	no
29	0.646	28%	0.535	0.518	4	no
30	0.234	37%	0.759	0.754	3	no
31	0.559	59%	0.046	0.005	6	yes
32	0.370	50%	0.610	0.595	5	no
35	2.235	132%	0.113	0.087	4	yes
38	0.273	36%	0.646	0.641	2	yes

^a N = 145 for all models except model 29, N = 118.

Table 3. Illustration of Predictive Accuracy of Model 21 (SE = 0.226) and Model 9 (SE = 0.262).

<i>THM4</i> , $\mu\text{g/L}$	$\log_{10}(\text{THM4})$	<i>SE</i>	$\log_{10}(\text{THM4})$ – <i>SE</i>	<i>Anti-</i> $\log(\log_{10}(\text{THM4})$ – <i>SE</i>), $\mu\text{g/L}$	$\log_{10}(\text{THM4})$ + <i>SE</i>	<i>Anti-</i> $\log(\log_{10}(\text{THM4})$ + <i>SE</i>), $\mu\text{g/L}$
40	1.6	0.226	1.38	24	1.83	67
80	1.9	0.226	1.68	48	2.13	135
40	1.6	0.262	1.34	22	1.86	73
80	1.9	0.262	1.64	44	2.16	146

3.2. Application of THM4 Formation Models to Bromide Intrusion

The concentration of bromide in the aquatic environment can range from less than 25 $\mu\text{g/L}$ in freshwater to 67 mg/L in seawater (26). Brackish water, such as seawater-impacted groundwater and surface water, can have bromide concentrations on the order of 1 mg/L and higher (13, 27). The concern pertaining to THM4 formation is the increase in bromide that occurs with seawater intrusion into fresh groundwater and surface water, and the consequent increase in brominated THMs upon chlorination (13). Hence, THM4 formation models would be particularly useful if the models could accurately predict changes in THM4 concentration due to changing bromide concentration. Figure 2 evaluates the predictive capability of the THM4 formation models that included bromide as an explanatory variable. Figure 2a shows $\log_{10}(\text{THM4})$ predicted versus $\log_{10}(\text{THM4})$ measured. The measured THM4 data were from experiments in which seawater was added to fresh groundwater and then chlorinated under uniform formation conditions (13). The increase in bromide from seawater resulted in a dramatic increase in measured THM4, and a shift from predominantly chloroform in low bromide water ($< 100 \mu\text{g/L Br}^-$) to predominantly bromoform in high bromide water ($> 500 \mu\text{g/L Br}^-$) (13). The seawater represented 2% v/v or less of the freshwater–seawater mixture, which allowed for all other water quality characteristics to remain approximately constant. The predicted $\log_{10}(\text{THM4})$ was calculated by inputting the water quality characteristics and chlorination conditions of the freshwater–seawater mixture samples into the THM4 models. The results in Figure 2a show a linear relationship between $\log_{10}(\text{THM4})$ predicted and $\log_{10}(\text{THM4})$ measured with R^2 values equal to 0.918–0.984. However, most of the data do not conform to the $y = x$ line, which indicates poor agreement between the model predictions and experimental measurements. For example, SE values for all models (excluding model 5) ranged from 0.228 to 1.264. Predicted data using model 5 showed very good agreement with the experimental measurements based on SE, with SE equal to 0.092. The main difference between model 5 and the other models that included bromide as an explanatory variable was the higher value of the regression coefficient for Br^- in model 5 than the other models (see Table 1). This made model 5 more responsive to changes in bromide concentration.

Figure 2b shows the THM4 concentration, i.e., the anti-log of $\log_{10}(\text{THM4})$ predicted, as a function of increasing bromide concentration. The data in Figure 2b are anti-log transformed to better see the sensitivity of the predicted THM4 concentration as a function of bromide concentration. The THM4 formation models show several important trends with respect to increasing bromide concentration. Foremost, many of the models were not sensitive to changing bromide concentration, and as such, under predicted THM4 formation with increasing bromide concentration. The low sensitivity of the models to changing bromide concentration was anticipated based on the small value of the regression coefficient for Br^- in many of the models. Models 5 and 35 showed the greatest sensitivity in terms of increasing THM4 concentration with increasing bromide concentration, and these models also had the largest values for the bromide regression coefficient among the models that included bromide as an explanatory

variable (see Table 1). Model 5 was the only model that could relatively accurately predict THM4 formation at low and high bromide concentrations, which was indicated in Figure 2a and by the low SE of 0.092. However, despite model 5 being the most accurate model, the predicted data showed a different trend than the measured data in terms of increasing THM4 concentration with increasing bromide. Model 35 predicted increasing THM4 concentration with increasing bromide concentration; however, the predictions were not accurate as shown in Figure 2a and by the high SE of 1.264. In summary, at bromide concentration in the range of 50–100 $\mu\text{g/L}$, there were models that both under predicted and over predicted THM4 formation (see Figure 2b). This was because other factors are more important than bromide on THM4 formation at low bromide concentrations, such as the concentration and character of DOC. At bromide concentration greater than 500 $\mu\text{g/L}$, all models under predicted THM4 formation. Thus, there is a clear need for THM4 formation models that are calibrated using water quality data sets that contain bromide in the range of 500 $\mu\text{g/L}$ to greater than 1 mg/L .

Given that model 5, among the models considered, showed the best agreement between predicted THM4 concentration and measured THM4 concentration for the condition of increasing bromide concentration, it was used to predict THM4 formation under a more generalized scenario of seawater intrusion. In particular, Figure 3 shows THM4 formation as a function of increasing TDS where the bromide concentration was calculated from the bromide-to-TDS ratio for standard seawater (14). Model 5 includes TOC, UV_{254} , Br^- , Cl_2 , t, pH, and T as explanatory variables; the value used for each variable is given in the caption to Figure 3. The variables represent reasonable values for finished drinking water, e.g., 1 mg/L TOC and Cl_2 -to-TOC mass ratio of 2 (25). Figure 3 shows that THM4 increases steadily with increasing TDS, which is due to the increasing bromide concentration as shown in Figure 2b. An interesting data point in Figure 3 is 500 mg/L TDS, which is equivalent to THM4 formation of 144 $\mu\text{g/L}$. Thus, at the secondary standard for TDS, THM4 formation exceeds its primary maximum contaminant level. This is significant because secondary drinking water standards are not health-based, whereas primary drinking water standards are in place to protect public health (28). Hence, the model predictions in Figure 3 suggest that seawater intrusion, and in particular the co-transport of bromide with chloride, will be problematic in terms of increasing the formation of THM4 well before the water would become unpalatable due to high TDS. Furthermore, laboratory studies have shown that high chloride concentrations can catalyze the formation of highly reactive bromine species during chlorination, which further increases the formation of brominated DBPs (29). Overall, the results in Figure 3 illustrate a new and unique challenge for drinking water treatment because there are a limited number of processes that can effectively remove bromide and seawater intrusion is expected to increase in many coastal areas due over pumping, changes in recharge, and sea-level rise (30, 31).

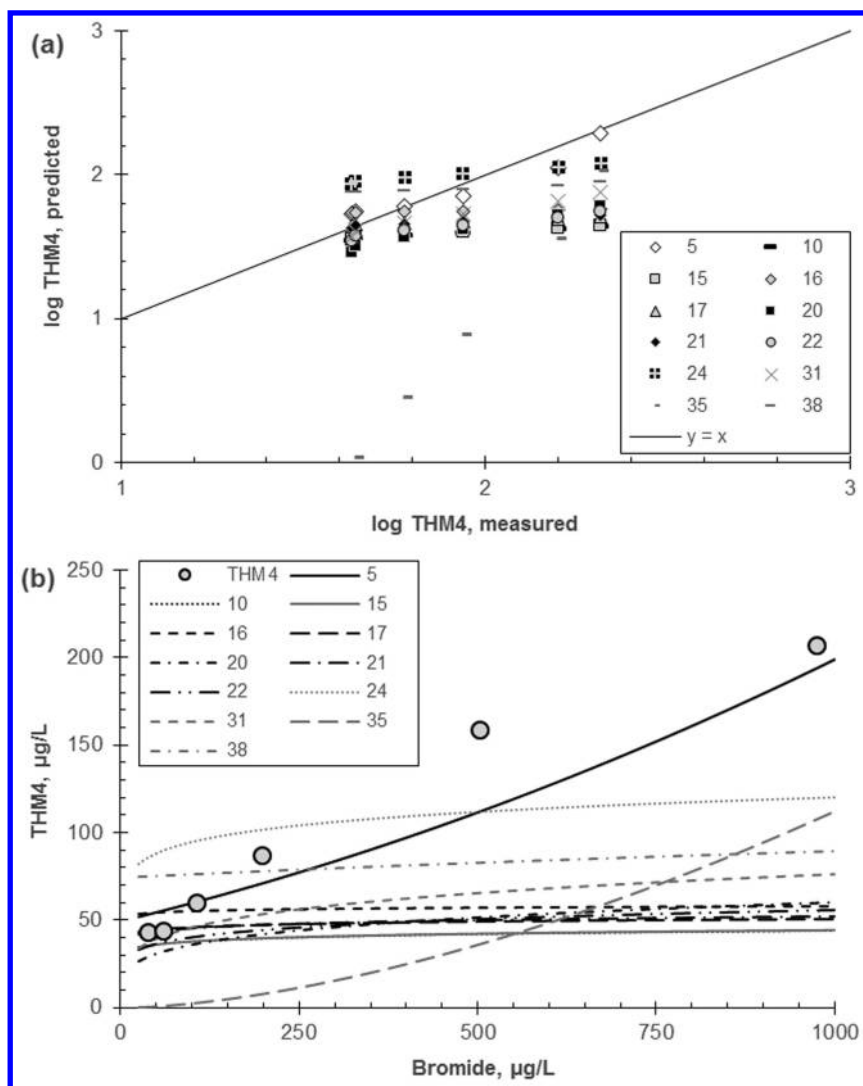


Figure 2. (a) $\log_{10}(\text{THM4})$ measured versus $\log_{10}(\text{THM4})$ predicted. Model number given in legend. Measured THM4 is 6 unique samples. (b) Measured and predicted THM4 as a function of increasing bromide concentration. Measured THM4 data from Ged et al. (13) Model number given in legend. Experimental conditions and model inputs: DOC = 1.4 mg/L, UV_{254} = 0.037 1/cm, pH 8, T = 20 °C, chlorine dose = 2.7 mg/L as Cl_2 , time = 24 h, bromide = variable.

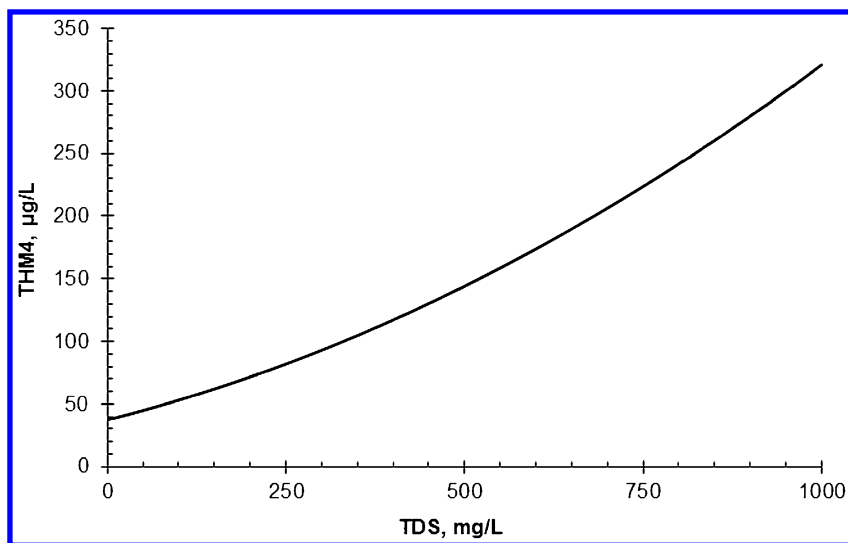


Figure 3. THM4 predicted by model 5 as a function of increasing TDS. Model inputs: DOC = 1.0 mg/L, $SUVA_{254} = 2.5$ L/mg·m, $UV_{254} = 0.025$ 1/cm, pH 8, $T = 20$ °C, chlorine dose = 2.0 mg/L as Cl_2 , time = 24 h, Br^- (mg/L) = $0.0019134 \times TDS$ (mg/L) from Millero et al. (14)

4. Conclusions

Several previously published THM4 formation models were determined to be moderately robust in their model development and calibration such that the models could be applied at the water utility scale using water quality and chlorination conditions separate from the original calibration data set. For example, the anti-log transformation of $\log_{10}(\text{THM4}) \pm \text{SE}$ for $\log_{10}(40) = 1.6 \pm 0.226$ gives an accuracy of 24 to 67 µg/L for a target THM4 concentration of 40 µg/L. This example used the highest level of accuracy that was obtained in this work, so there is the potential for some of these models to be used at the water utility scale. In particular, the more statistically robust THM4 formation models determined in this work are expected to be useful for small water systems and water systems experiencing frequent changes in water quality, such as variable TOC concentrations. With minimal to no modification, water utilities can use these models to predict THM4 and help inform short-term operation and long-term planning. One caveat to the THM4 formation models evaluated in this work was the low sensitivity of many of the models to increasing bromide concentration. Hence, previously published THM4 formation models should be used with caution if the application of the model is predicting THM4 concentration under conditions of variable bromide concentration, such as the case of seawater intrusion. An important side result of the bromide sensitivity analysis was the illustration that THM4 concentration could reach problematic

levels ($> 100 \mu\text{g/L}$) when the TDS was at or below its secondary standard of 500 mg/L . This highlights a new challenge for drinking water treatment whereby seawater intrusion, with its drivers in urbanization and global climate change, can alter the water matrix and dramatically increase the formation of DBPs, especially brominated DBPs.

Acknowledgments

This publication is based upon work supported by the University of Florida Research Opportunity Seed Fund award: Florida as a Laboratory for Global Urbanization, Sea Level Rise, and Future Health Risks of Drinking Water Sources.

References

1. Chowdhury, S.; Champagne, P.; McLellan, P. J. Models for predicting disinfection byproduct (DBP) formation in drinking waters: A chronological review. *Sci. Total Environ.* **2009**, *407*, 4189–4206.
2. Chowdhury, S.; Champagne, P.; McLellan, P. J. Investigating effects of bromide ions on trihalomethanes and developing model for predicting bromodichloromethane in drinking water. *Water Res.* **2010**, *44*, 2349–2359.
3. Lu, O.; Krasner, S. W.; Liang, S. Modeling approach to treatability analyses of an existing treatment plant. *J. Am. Water Work Assoc.* **2011**, *103*, 103–117.
4. Sohn, J.; Amy, G.; Cho, J.; Lee, Y.; Yoon, Y. Disinfectant decay and disinfection by-products formation model development: chlorination and ozonation by-products. *Water Res.* **2004**, *38*, 2461–2478.
5. Amy, G. L.; Siddiqui, M.; Ozekin, K.; Zhu, H. W.; Wang, C. *Empirical based models for predicting chlorination and ozonation byproducts: haloacetic acids, chloral hydrate, and bromate*. Report CX 819579.; U.S. Environmental Protection Agency: Washington, D.C., 1998.
6. Ged, E. C.; Chadik, P. A.; Boyer, T. H. Predictive capability of chlorination disinfection byproducts models. *J. Environ. Manage.* **2015**, *149*, 253–262.
7. Nikolaou, A. D.; Golfinopoulos, S. K.; Arhonditsis, G. B.; Kolovoyiannis, V.; Lekkas, T. D. Modeling the formation of chlorination by-products in river waters with different quality. *Chemosphere* **2004**, *55*, 409–420.
8. Uyak, V.; Ozdemir, K.; Toroz, I. Multiple linear regression modeling of disinfection by-products formation in Istanbul drinking water reservoirs. *Sci. Total Environ.* **2007**, *378*, 269–280.
9. Gallard, H.; von Gunten, U. Chlorination of natural organic matter: kinetics of chlorination and of THM formation. *Water Res.* **2002**, *36*, 65–74.
10. Black, B. D.; Harrington, G. W.; Singer, P. C. Reducing cancer risks by improving organic carbon removal. *J. Am. Water Work Assoc.* **1996**, *88*, 40–52.
11. Uyak, V.; Toroz, I.; Meric, S. Monitoring and modeling of trihalomethanes (THMs) for a water treatment plant in Istanbul. *Desalination* **2005**, *176*, 91–101.

12. Amy, G.; Siddiqui, M.; Zhai, W.; DeBroux, J.; Odem, W., *Survey of Bromide in Drinking Water and Impacts on DBP Formation*. AWWA Research Foundation: Denver, CO, 1993.
13. Ged, E. C.; Boyer, T. H. Effect of seawater intrusion on formation of bromine-containing trihalomethanes and haloacetic acids during chlorination. *Desalination* **2014**, *345*, 85–93.
14. Millero, F. J.; Feistel, R.; Wright, D. G.; McDougall, T. J. The composition of Standard Seawater and the definition of the Reference-Composition Salinity Scale. *Deep Sea Res., Part I* **2008**, *55*, 50–72.
15. Urano, K.; Wada, H.; Takemasa, T. Empirical rate equation for trihalomethane formation with chlorination of humic substances in water. *Water Res.* **1983**, *17*, 1797–1802.
16. Malcolm-Pirnie *Bay-Delta Water Quality Modeling. Report No. 15-041*; Prepared for the Metropolitan Water District of Southern California: White Plains, NY, December 1993.
17. Chang, E. E.; Chao, S. H.; Chiang, P. C.; Lee, J. F. Effects of chlorination on THMs formation in raw water. *Toxicol. Environ. Chem.* **1996**, *56*, 211–225.
18. Rathbun, R. E. Regression equations for disinfection by-products for the Mississippi, Ohio and Missouri rivers. *Sci. Total Environ.* **1996**, *191*, 235–244.
19. Rodriguez, M. J.; Serodes, J.; Morin, M. Estimation of water utility compliance with trihalomethane regulations using a modelling approach. *J. Water Supply: Res. Technol.--AQUA* **2000**, *49*, 57–73.
20. Al-Omari, A.; Fayyad, M.; Qader, A. Modeling trihalomethane formation for Jabal Amman water supply in Jordan. *Environ. Model Assess.* **2004**, *9*, 245–252.
21. Toroz, I.; Uyak, V. Seasonal variations of trihalomethanes (THMs) in water distribution networks of Istanbul City. *Desalination* **2005**, *176*, 127–141.
22. Hong, H. C.; Liang, Y.; Han, B. P.; Mazumder, A.; Wong, M. H. Modeling of trihalomethane (THM) formation via chlorination of the water from Dongjiang River (source water for Hong Kong's drinking water). *Sci. Total Environ.* **2007**, *385*, 48–54.
23. Semerjian, L.; Dennis, J.; Ayoub, G. Modeling the formation of trihalomethanes in drinking waters of Lebanon. *Environ. Monit. Assess.* **2009**, *149*, 429–436.
24. Chen, B. Y.; Westerhoff, P. Predicting disinfection by-product formation potential in water. *Water Res.* **2010**, *44*, 3755–3762.
25. Obolensky, A.; Singer, P. C.; Shukairy, H. M. Information collection rule data evaluation and analysis to support impacts on disinfection by-product formation. *J. Environ. Eng.-ASCE* **2007**, *133*, 53–63.
26. Hem, J. D., Study and interpretation of the chemical characteristics of natural water. *United State Geological Survey Water-Supply Paper 2254* 1985, *Alexandria, VA*.
27. Magazinovic, R. S.; Nicholson, B. C.; Mulcahy, D. E.; Davey, D. E. Bromide levels in natural waters: its relationship to levels of both chloride and total dissolved solids and the implications for water treatment. *Chemosphere* **2004**, *57*, 329–335.

28. USEPA, *Drinking Water Contaminants: National Primary Drinking Water Regulations [website]*. <http://water.epa.gov/drink/contaminants/index.cfm>; accessed 09/23/2013, 2013.
29. Sivey, J. D.; Arey, J. S.; Tentscher, P. R.; Roberts, A. L. Reactivity of BrCl, Br₂, BrOCl, Br₂O, and HOBr Toward Dimethenamid in Solutions of Bromide + Aqueous Free Chlorine. *Environ. Sci. Technol.* **2013**, *47*, 1330–1338.
30. Watson, K.; Farré, M. J.; Knight, N. Strategies for the removal of halides from drinking water sources, and their applicability in disinfection by-product minimisation: A critical review. *J. Environ. Manage.* **2012**, *110*, 276–298.
31. Werner, A. D.; Bakker, M.; Post, V. E. A.; Vandenbohede, A.; Lu, C.; Ataie-Ashtiani, B.; Simmons, C. T.; Barry, D. A. Seawater intrusion processes, investigation and management: Recent advances and future challenges. *Adv. Water Resour.* **2013**, *51*, 3–26.

Chapter 7

Nitrosamine Precursors and Wastewater Indicators in Discharges in the Sacramento-San Joaquin Delta

Chih-Fen Tiffany Lee,* Stuart W. Krasner, Michael J. Scimanti,
Matthew Prescott, and Yingbo C. Guo

Water Quality Section, Metropolitan Water District of Southern California,
700 Moreno Avenue, La Verne, California 91750-3303

*E-mail: Clee@mwdh2o.com.

Wastewater treatment plant (WWTP) discharges in the Sacramento-San Joaquin Delta were shown to be a source of N-nitrosodimethylamine (NDMA) and N-nitrosomorpholine (NMOR), as well as precursors for NDMA and N-nitrosopyrrolidine (NPYR). NDMA and NPYR were disinfection by-products, whereas NMOR was a wastewater contaminant. Nitrosamines were not found downstream of the WWTPs due to dilution with river water and/or sunlight photolysis, whereas NDMA precursor loadings in the river downstream of the WWTPs were at higher levels than at the upstream sites. The anticonvulsant primidone and the artificial sweetener sucralose were found to be good wastewater indicators and the percentage of treated wastewater in the Sacramento River (2-3%) and the San Joaquin River (2-14%) was determined by these. Moreover, the increase in NDMA precursor loadings in downstream sites was consistent with the wastewater volumetric contributions to river flow.

Introduction

The Sacramento-San Joaquin Delta (Delta) is at the nexus of a California statewide water system, which provides a critical water supply (State Project Water [SPW]) to 23 million people in California. The Delta is at the confluence of the Sacramento and San Joaquin Rivers (Figure 1). The Delta empties into the Pacific

Ocean via an estuary to the San Francisco Bay. Due to tidal activity, especially during droughts, there can be tidal actions in the San Joaquin River. There are nine wastewater treatment plants (WWTPs) discharging from 0.3 to 181 million gallons per day (MGD) into the Delta (1). The City of Stockton and Sacramento Regional operate the two largest WWTPs in the Delta. They discharge into the San Joaquin and Sacramento River, respectively (Figure 1).

Wastewater discharges (effluent organic matter [EfOM]) contain emerging chemical contaminants, such as nitrosamines and their precursors, and pharmaceuticals and personal care products (PPCPs). EfOM is known to be one of the major sources of N-nitrosodimethylamine (NDMA) precursors (2). NDMA is a disinfection by-product (DBP) preferentially formed by chloramines (3). N-Nitrosomorpholine (NMOR) is also commonly detected in wastewater discharges, where it appeared to be a wastewater contaminant and not a DBP *per se* (4).

Nitrosamines are known to be probable human carcinogens, and they have gained a lot of attention from health and regulatory agencies in the United States (U.S.) and internationally (5). Although there is no federal regulation for nitrosamines in drinking water, the California State Water Resources Control Board Division of Drinking Water (DDW) set a notification level of 10 ng/L each for NDMA and two other nitrosamines (6). The objective of this study was to evaluate the presence and fate of NDMA, other nitrosamines, their precursors, and selected PPCPs in the Delta, including seasonal and year-to-year variability.

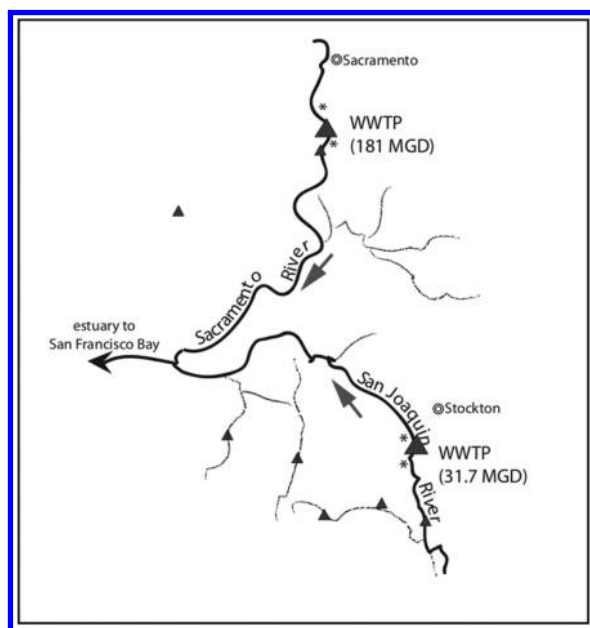


Figure 1. Map of Sacramento–San Joaquin Delta (triangles = WWTPs).

Experimental

Overview of Study

The sampling sites in this study included locations upstream and downstream of the Stockton and Sacramento Regional WWTPs, and WWTP effluent or river water immediately adjacent to the discharge. Table 1 lists the sampling locations. There were a total of eight sampling events: both watersheds were sampled in six of them, covering summer, fall, and winter seasons over a two-year period; only the San Joaquin River and the Stockton WWTP were sampled in two additional events. The samples were analyzed for eight nitrosamines, including NDMA, NMOR, and N-nitrosopyrrolidine (NPYR). Certain PPCPs found in wastewater can be used as conservative indicators of wastewater impacts in drinking water supplies. The indicators used in this project were primidone (an anticonvulsant drug) (7, 8) and sucralose (an artificial sweetener - Splenda®) (9). The percentage of treated wastewater in the rivers was calculated as the ratio of the concentrations of these indicators in the rivers against their concentrations in the WWTP effluents. In addition, modeling of volumetric contributions of the WWTP discharges to the river flow was estimated using a simulation model.

Table 1. Sampling Locations in the Study

<i>Sampling Location</i>	
<i>San Joaquin River Watershed</i>	<i>Sacramento River Watershed</i>
Upstream of Stockton WWTP	Upstream of Sacramento Regional WWTP
Stockton WWTP filter effluent	Sacramento Regional WWTP outfall (grab sample in Sacramento River by discharge)
Stockton WWTP plant effluent	
Downstream of Stockton WWTP	Downstream of Sacramento Regional WWTP

Study Sites

Stockton WWTP

The Stockton WWTP was a tertiary treatment plant. The advanced treatment units included oxidation ponds, wetlands, nitrifying biotowers, dissolved air floatation (DAF), and mix media filters. The effluent was chlorinated and ammonia was added (if needed; ammonia was present or not, depending on how well the biotowers nitrified the water to form chloramines). The tertiary processes provided additional treatment to clean up the wastewater, including removal of ammonia, algae, and a final filtering through sand, gravel, and anthracite coal to remove more organic material and fine suspended particles.

The Sacramento Regional WWTP was a secondary treatment plant. Secondary treatment included a conventional aerobic biological treatment process and secondary clarification. The effluent was poorly nitrified. Chlorine was added, which should have reacted with the ammonia to form chloramines.

Analytical Methods

Nitrosamines

Standard method 6450B was used to measure eight nitrosamines: NDMA, N-nitrosomethylethylamine (NMEA), N-nitrosodiethylamine (NDEA), N-nitrosodi-n-propylamine (NDPA), N-nitrosodi-butylamine (NDBA), NPYR, N-nitrosopiperidine (NPIP), and NMOR. Nitrosamines were extracted and concentrated using solid-phase extraction (SPE) with Amborsorb 572 resin and were analyzed using gas chromatography/mass spectrometry (GC/MS) with chemical ionization (10). Nitrosamine concentrations were determined by comparison of the area ratio of a unique product ion to one of the isotopically labeled internal standards (i.e., d₆-NDMA, d₁₄-NDPA, and ¹⁵N₂-NDEA) against calibration curves made from method (SPE) standards. The minimum reporting level (MRL) for each nitrosamine was 2 ng/L.

Nitrosamine Precursors

Nitrosamine precursors were determined using formation potential (FP) tests (11, 12). Nitrosamine FP tests were conducted in the presence of chloramines. Filtered (0.45- μ m) samples were chloraminated on a reactivity basis (based on the amount of organic carbon) and held for 3 days at pH 8 at 25°C. The chlorine dose was based on the level of total organic carbon (TOC) (i.e., Cl₂ = 3 x TOC, weight basis), and the amount of ammonia was calculated based on a chlorine-to-nitrogen (Cl₂/N) weight ratio of 3:1. In the tests, ammonia was added before chlorine in order to form chloramines with no free chlorine contact time. Note, if ammonia was present in the sample, this was factored into how much more was added in the FP test. For poorly nitrified wastewaters, no ammonia was added in the FP test, and the resultant Cl₂/N weight ratio was typically in the range of 1:1 to 2:1.

PPCPs

PPCPs were concentrated using a SPE workstation with HLB cartridges (Waters, Milford, MA) and were analyzed using liquid chromatography/tandem MS (LC/MS/MS) with a 2.0-mm C18 reversed-phase high pressure LC (HPLC) column (13). For primidone, the MS was operated under an electrospray positive ion mode. PPCPs were identified by matching both the retention time and the

MS/MS transition in the samples with those in authentic standards. An isotope dilution technique was used for quantitation (14). The MRL for primidone was 2 ng/L.

Sucralose

Filtered (0.45- μ m) water samples were injected directly onto the C18 HPLC column equipped with a 2.0-mm C18 guard column. The MS was operated under an electrospray negative ion mode. Sucralose was identified as were other PPCPs. An isotope dilution technique was used for quantitation with d₆-sucralose. The MRL was 0.2 μ g/L.

Hydraulic Flow Modeling

The California Department of Water Resources (DWR) used the Delta Simulation Model II (DSM2) to study the complex hydraulic system in the Delta (15). DSM2 was a mathematical model for dynamic simulation of one-dimensional hydrodynamics, water quality, and particle tracking in a network of riverine or estuarine channels.

Results and Discussion

N-Nitrosamines and Their Precursors in the Stockton WWTP

Studies have shown that WWTPs may remove N-nitrosamines present in the wastewater (16). Studies in the U.S. showed that chloramination of treated wastewater can form N-nitrosamines above the background level (4). Moreover, studies in the U.S. showed that N-nitrosamine precursors were present in secondary or tertiary treated wastewater (2). In the Stockton WWTP, NDMA, NPYR and NMOR were detected in FP samples. Figure 2 shows the impact of the tertiary treatment process on N-nitrosamine FP. NDMA FP was over 1000 ng/L after secondary treatment; however, the concentration dropped significantly after the tertiary treatment began and remained fairly constant throughout the whole process. Similar trends were observed for NPYR FP and NMOR FP.

In addition to measuring the N-nitrosamine FP, the amount of N-nitrosamines formed after chloramine addition at the WWTP was determined. Figure 3 shows there was no NDMA detected at or above the MRL in the WWTP filter effluent; however, the formation of NDMA spiked up at the WWTP effluent (interquartile range ~4-82ng/L, median ~18 ng/L) due to chloramine usage. Unlike NDMA, NMOR was present before chloramine addition, and its occurrence stayed the same after chloramine addition, as NMOR was a wastewater contaminant and not a DBP (4). Although NMOR was detected in some of the FP tests, its concentration in the FP test was often no different than that of the water before FP testing. Neither NDMA nor NMOR were detected downstream of the WWTP. This was likely due to dilution in the river water and/or sunlight photolysis (17).

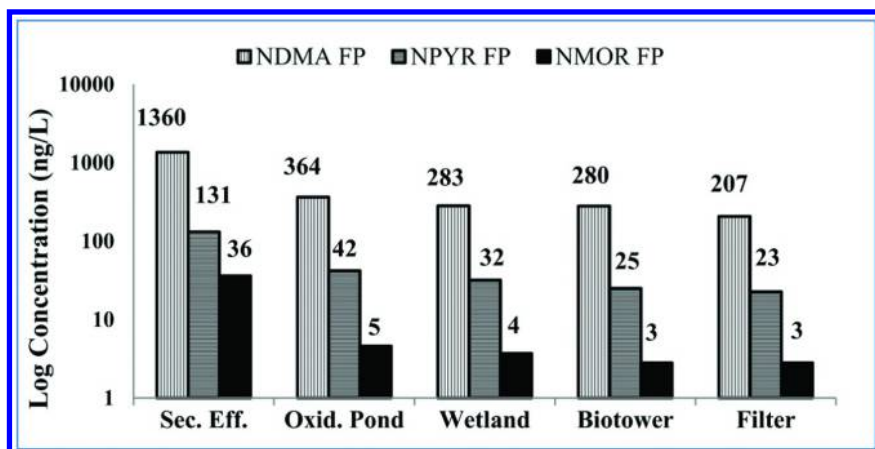


Figure 2. Impact of tertiary treatment on N-nitrosamine FP at the Stockton WWTP.

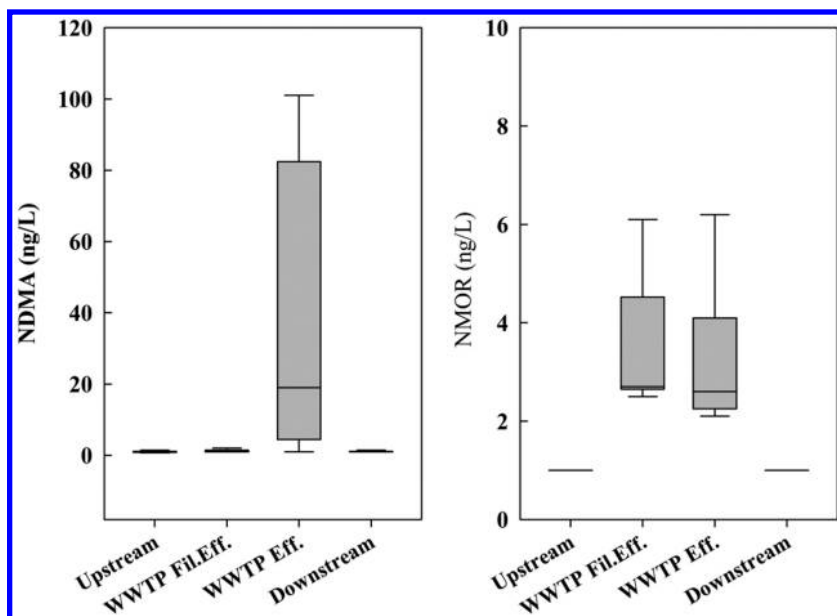


Figure 3. NDMA and NMOR in the San Joaquin River and at the Stockton WWTP (bottom and top of the box = 25th to 75th percentile, line through the box = median, bottom and top of the whiskers = 10th to 90th percentile).

Wastewater Indicators in WWTPs and Estimated Wastewater Effluent

Figure 4 shows the concentrations of the wastewater indicators in the effluent of the Stockton WWTP. The interquartile range (25th to 75th percentile) of sucralose concentrations was 24 to 31 $\mu\text{g/L}$, which compared well with the typical range detected in other U.S. WWTP effluents of 20-30 $\mu\text{g/L}$ (median = 27 $\mu\text{g/L}$) (9). The interquartile range of primidone concentrations, 109 to 136 ng/L , also fell within the typical range of other U.S. WWTPs of 100-200 ng/L (7).

An effluent sample site was not available from the Sacramento Regional WWTP, so the sampling location was a depth sample in the Sacramento River near the discharge pipe (outfall); all samples were grab samples. The effluent sample was diluted to varying extents by river flow. The percent effluent in the sample was estimated based on either the sucralose or primidone concentration, assuming a similar level at the Sacramento Regional WWTP as that detected at the Stockton WWTP (Figure 4). These percentages were similar to estimates based on the ammonia level in the sample and the ammonia concentration in discharge records. The N-nitrosamine FP data from the Sacramento Regional WWTP discharge sample were corrected for dilution to provide an estimate of the levels likely present in the WWTP effluent as part of the effort to follow the fate of the precursors in the Sacramento River (Figure 5).

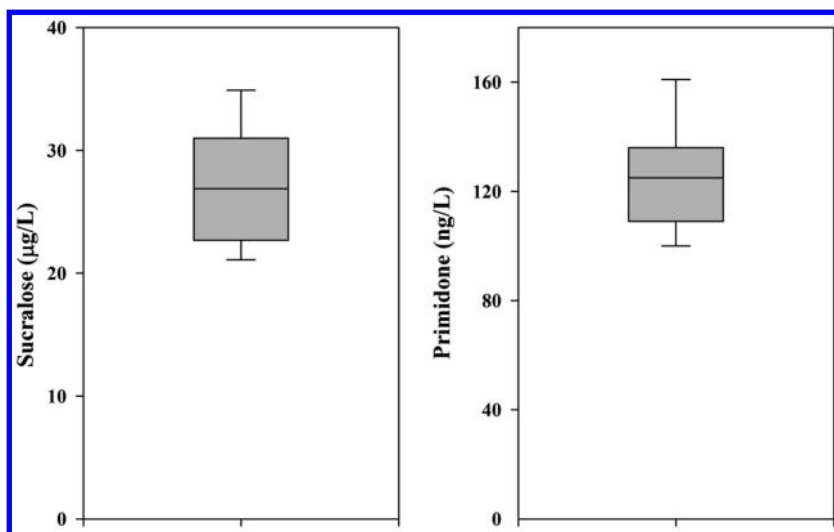


Figure 4. Concentrations of the wastewater indicators in the effluent of the Stockton WWTP.

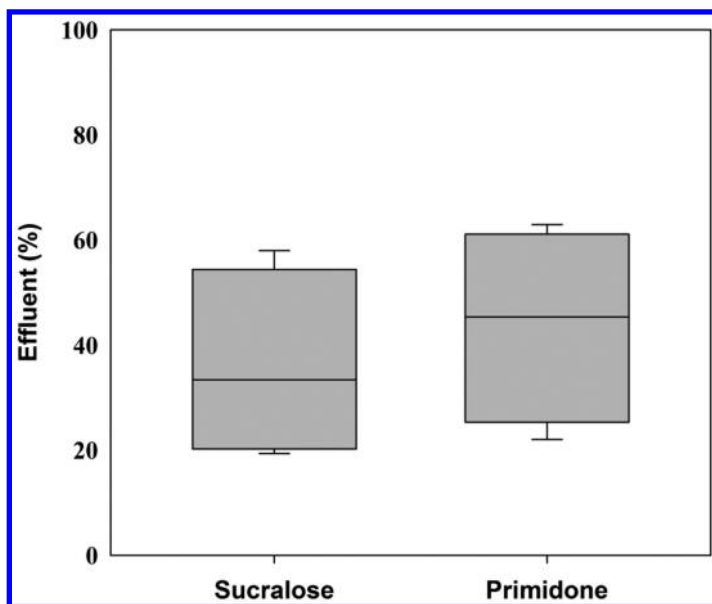


Figure 5. Estimated percent WWTP effluent in Sacramento Regional WWTP outfall samples based on sucralose and primidone.

Impact of WWTP Effluents in the Sacramento and San Joaquin Rivers

Figures 6 and 7 show the occurrence of NDMA precursors in the Sacramento and San Joaquin Rivers upstream and downstream of the WWTPs, and in the WWTP effluents during the six main sampling events. The percent effluent in the Sacramento Regional WWTP outfall sample was estimated based on primidone and then the NDMA FP in the WWTP effluent was back calculated. The San Joaquin WWTP effluent had 206-358 ng/L (median = 218 ng/L) and the Sacramento Regional WWTP effluent was estimated to have had 227-812 ng/L (median = 508 ng/L). In the Sacramento River, the NDMA precursor levels were higher downstream of the WWTP (9-22 ng/L [median = 17 ng/L]) than upstream (4-9 ng/L [median = 5 ng/L]), due to the wastewater discharge from the Sacramento Regional WWTP. In the San Joaquin River, in most cases, higher NDMA precursor levels were found downstream of the WWTP (e.g., 12-48 ng/L [median = 40 ng/L]) than upstream (e.g., 7-38 ng/L [median = 16 ng/L]). However, in some cases, the upstream location either had similar or higher levels of NDMA precursors than downstream. These events were due to “reverse river flow,” where the direction of the natural flow was reversed due to tidal action (the effect of the tidal flow into the Delta and the surrounding estuaries on the flow of the river). Sucralose and primidone had similar trends as the NDMA FP in the San Joaquin River during reverse river flow sampling events.

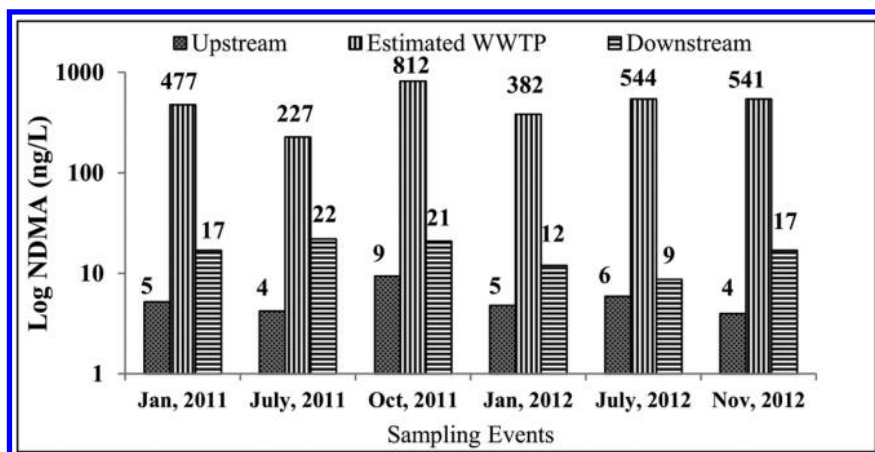


Figure 6. NDMA precursors in the Sacramento River and estimated in the Sacramento Regional WWTP effluent (based on primidone).

Table 2 shows an example of the impact of the Stockton WWTP discharge on the San Joaquin River. There was 35 $\mu\text{g/L}$ of sucralose and 132 ng/L of primidone in the WWTP effluent. Higher levels of primidone (9.1 ng/L increase) and sucralose (2.7 $\mu\text{g/L}$ increase) were observed at the downstream sample site due to the wastewater discharge from the Stockton WWTP. Based on these wastewater indicators, the downstream site was ~7-8% higher in EfOM than the upstream location (e.g., (5.3 $\mu\text{g/L}$ of sucralose downstream – 2.6 $\mu\text{g/L}$ of sucralose upstream)/35 $\mu\text{g/L}$ of sucralose in the WWTP effluent). In terms of the NDMA FP, there was a higher level downstream of the WWTP (20 ng/L increase).

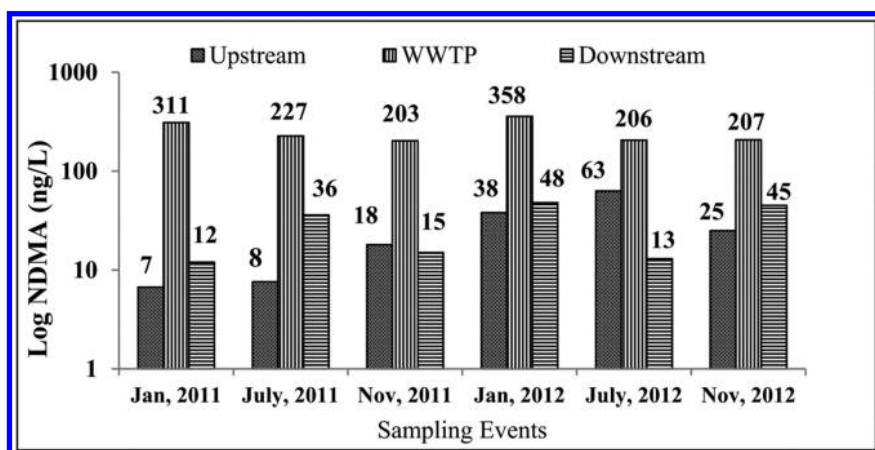


Figure 7. NDMA precursors in the San Joaquin River and in the Stockton WWTP effluent (reverse flows during the November 2011 and July 2012 sample events).

Table 2. Concentrations of the Wastewater Indicators and NDMA FP in the San Joaquin River and in the Stockton WWTP Effluent (November 2012)

	<i>NDMA FP</i>	<i>Primidone</i>	<i>Sucralose</i>
	ng/L	ng/L	µg/L
Upstream	25	9.5	2.6
WWTP	283	132	34.9
Downstream	45	18.6	5.3
Estimated % Effluent	10 %	7 %	8 %

Based on the wastewater indicators, it was predicted that the NDMA FP should have increased by ~20-23 ng/L, consistent with the observed increase. Note, there was a smaller WWTP upstream of the Stockton WWTP, which contributed to the presence of these contaminants in the upstream sample location. However, in this study, the focus was on the incremental contribution of the Stockton WWTP to the precursor loading in the river.

Figure 8 shows the relationship of the wastewater indicators to NDMA FP in both river/WWTP systems. On a central tendency basis, the slope of the trend line was steeper for the Sacramento River/WWTP system. For example, 10 µg/L of sucralose corresponded to ~90 ng/L of NDMA FP in the San Joaquin River, whereas the same amount of sucralose corresponded to a higher level of NDMA FP (>150 ng/L) in the Sacramento River. This was probably due (in part) to the different treatment processes at the Sacramento Regional and Stockton WWTPs; the Sacramento Regional WWTP only had secondary treatment, whereas the Stockton WWTP had tertiary treatment. Tertiary treatment can remove NDMA precursors; however, tertiary treatment should have little effect on removing these wastewater indicators.

Percentage of River Flow that Was Wastewater-Impacted

DSM2 can calculate stages, flows, velocities, transport of individual particles, and mass transport processes for conservative and non-conservative constituents, including salts, water temperature, dissolved oxygen, and dissolved organic carbon. DMS2 was used to determine the volumetric fraction of WWTP effluent at certain locations, downstream of the WWTPs.

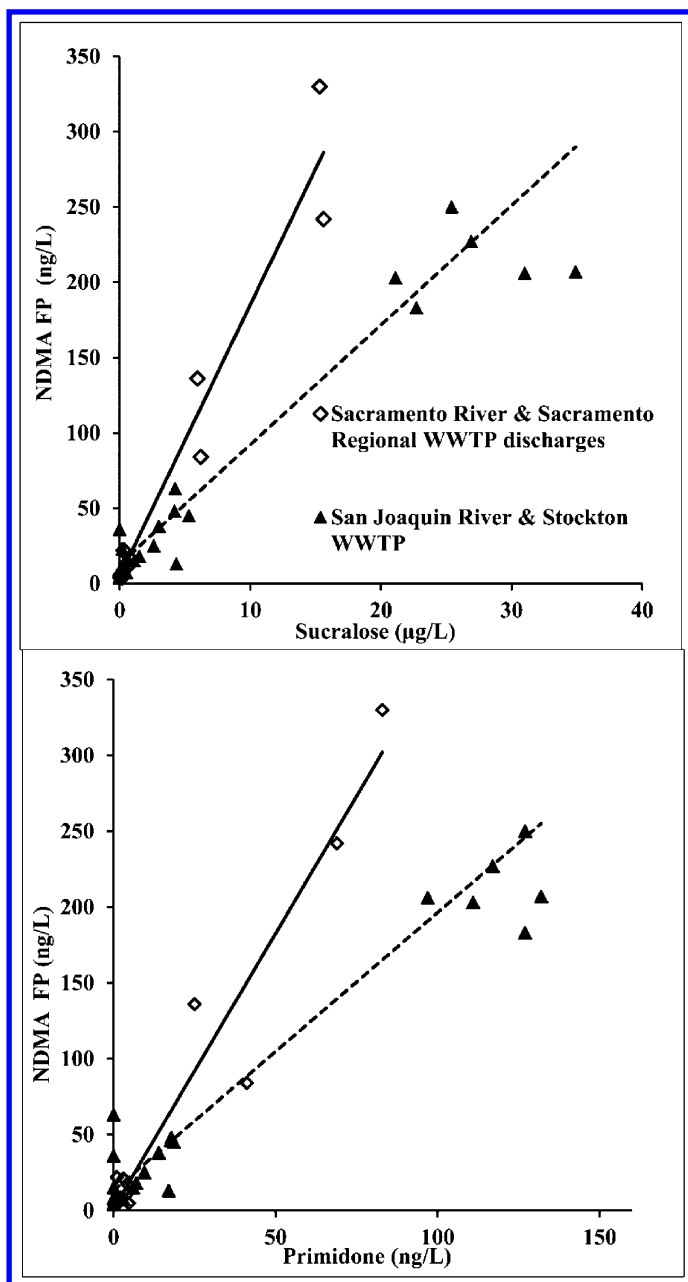


Figure 8. Relationship of the wastewater indicators to NDMA FP in the Sacramento and San Joaquin Rivers and at the corresponding WWTPs (Sacramento Regional WWTP outfall data plotted as measured, without correction for dilution of the WWTP effluent in the river).

Figure 9 shows the percent wastewater effluent in these two rivers as estimated by the model. The data from the model was a daily average of the river flow, whereas the data from our sampling events were based on grab samples. In the San Joaquin River, the percent WWTP effluent in the downstream location fluctuated from 2 to 14%, whereas the Sacramento River percentage remained steady at 2-4%. This was due to the higher river flow of the Sacramento River. The average annual river flow of Sacramento River was 23,469 cubic foot per second (cfs), whereas in the San Joaquin River it was 4,460 cfs.

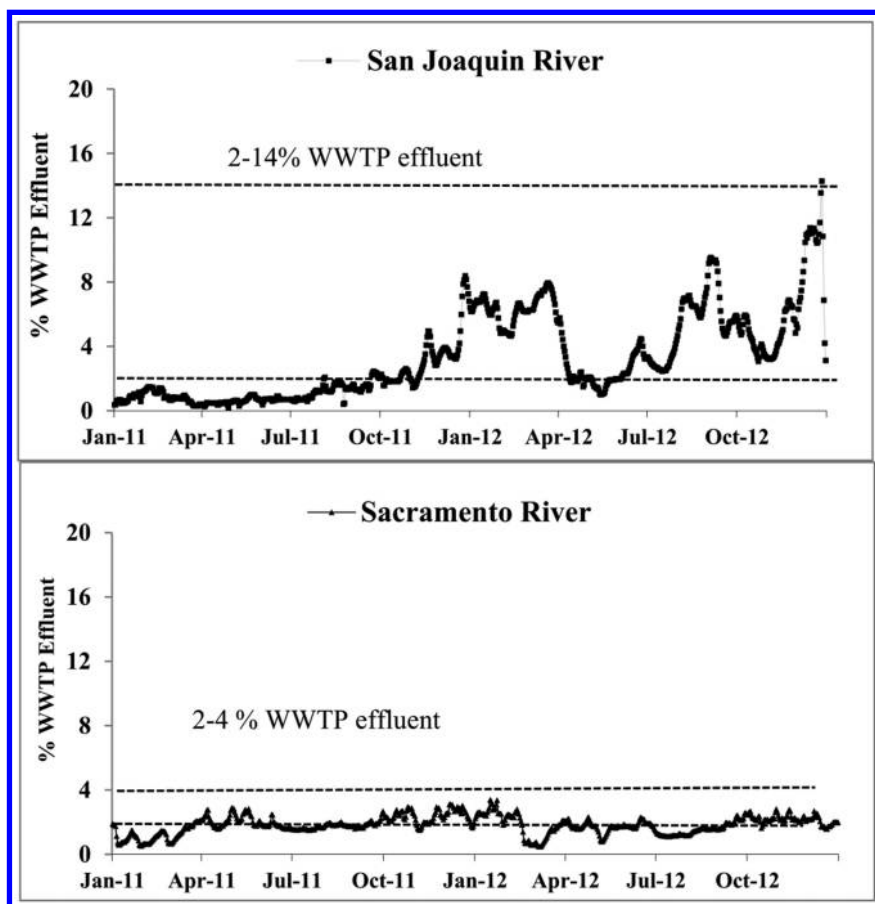


Figure 9. Estimated percentage of WWTP effluent in downstream San Joaquin and Sacramento River sample sites (volume basis) from hydraulic flow modeling.

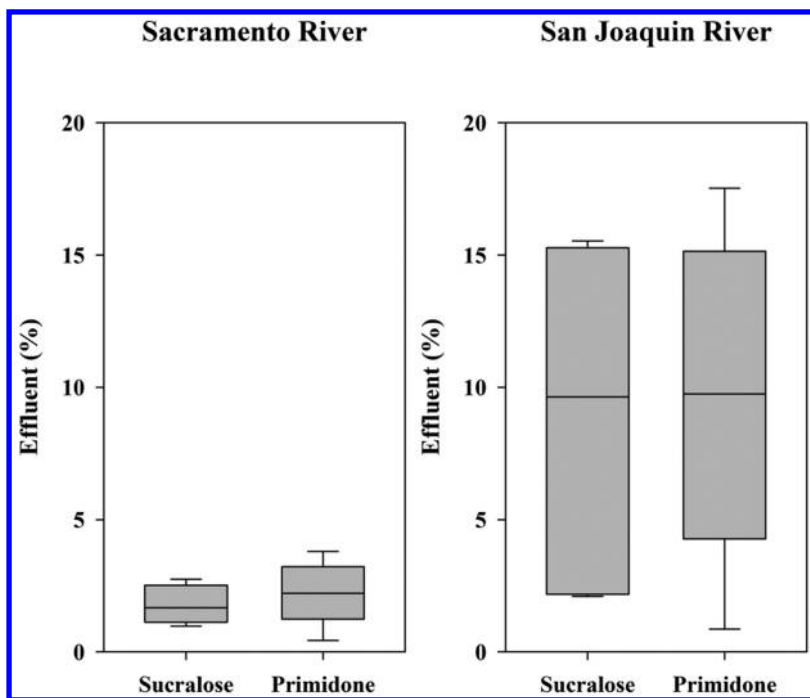


Figure 10. Estimated percent of WWTP effluent in downstream Sacramento River and San Joaquin River sample sites based on the wastewater indicators

Figure 10 shows that both wastewater indicators had good agreement in the estimation of percent WWTP effluent in the downstream locations in these two rivers. Moreover, the estimations based on wastewater indicators matched well with the hydraulic flow-calculated contributions.

Conclusions

Effluents from the two largest WWTPs in the Delta were shown to be an important source of NDMA precursors in a major source of drinking water for 23 million Californians. NDMA precursor loadings in the river were detected downstream of the WWTPs at higher levels than at the upstream sites, where the increase was consistent with the percent of river flow due to the WWTP discharge. However, due to river dilution and/or solar photolysis, the nitrosamines formed or present at the WWTP were not detected at or above the MRLs downstream of these WWTPs. The anticonvulsant primidone and the artificial sweetener sucralose were found to be good wastewater indicators, and the percentage of treated wastewater in the rivers was determined based on these indicators. In addition, the volumetric wastewater contribution to river flow was determined using a hydraulic simulation model, which matched the percent effluent estimations based on the wastewater

indicators. A good relationship was found between the level of NDMA precursors in the river/WWTP systems and the wastewater indicators, where the slope of the trend line was steeper for the river system with the WWTP with secondary treatment as compared to the system with the tertiary treatment process.

Acknowledgments

The authors gratefully acknowledge support from the staff of the California DWR and the City of Stockton, with special thanks going to Carol DiGiorgio (DWR) and Laura Lazzelle (City of Stockton).

References

1. Guo, Y. C.; Krasner, S. W.; Fitzsimons, S.; Woodside, G.; Yamachika, N. *Source, Fate, and Transport of Endocrine Disruptors, Pharmaceuticals, and Personal Care Products in Drinking Water Sources in California*; National Water Research Institute: Fountain Valley, Ca., May 2010, pp 14–21
2. Krasner, S. W.; Westerhoff, P.; Chen, B.; Rittmann, B. E.; Nam, S.-N.; Amy, G. Impact of Wastewater Treatment Processes on Organic Carbon, Organic Nitrogen, and DBP Precursors in Effluent Organic Matter. *Environ. Sci. Technol.* **2009**, *43* (8), 2911–2918.
3. Mitch, W. A.; Sharp, J. O.; Trussell, R. P.; Valentine, R. L.; Alvarez-Cohen, L.; Sedlak, D. L. N-Nitrosodimethylamine as a Drinking Water Contaminant: A review. *Environ. Eng. Sci.* **2003**, *20* (5), 389–404.
4. Krasner, S. W.; Westerhoff, P.; Chen, B.; Rittmann, B. E.; Amy, G. Occurrence of Disinfection Byproducts in United States Wastewater Treatment Plant Effluents. *Environ. Sci. Technol.* **2009**, *43* (21), 8320–8325.
5. Krasner, S. W.; Mitch, W. A.; McCurry, D. L.; Hanigan, D.; Westerhoff, P. Formation, Precursors, Control, and Occurrence of Nitrosamines in Drinking Water: A review. *Wat. Res.* **2013**, *47* (13), 4434–4446.
6. California Environmental Protection Agency State Water Resources Control Board. *NDMA and Other Nitrosamines - Drinking Water Issues*; http://www.waterboards.ca.gov/drinking_water/certlic/drinkingwater/NDMA.shtml [cited November 1, 2014].
7. Krasner, S. W.; Pastor, S. J.; Garcia, E. A. Measurement of the Pharmaceutical Primidone as a Conservative Tracer of Wastewater Influences in Drinking Water Supplies. In *Proceedings of 2006 American Water Works Association (AWWA) Water Quality Technology Conference (WQTC)*; AWWA: Denver, CO, 2006.
8. Guo, Y. C.; Krasner, S. W. Occurrence of Primidone, Carbamazepine, Caffeine, and Precursors for N-Nitrosodimethylamine in Drinking-Water Sources Impacted by Wastewater. *J. Am. Water Resour. Assoc.* **2009**, *45*, 58–67.
9. Oppenheimer, J.; Eaton, A.; Badruzzaman, M.; Haghani, A.; Jacangelo, J. Occurrence and Suitability of Sucralose as an Indicator Compound of

Wastewater Loading to Surface Waters in Urbanized Region. *Water Res.* **2011**, *45*, 4019–4027.

10. APHA, AWWA, and WEF. *Standard Methods for the Examination of Water and Wastewater*, Method 6450, Nitrosamines; Washington DC, 2008.
11. Krasner, S. W.; Scilimenti, M. J.; Guo, Y. C.; Hwang, C. J.; Westerhoff, P. Development of DBP and Nitrosamine Formation Potential Tests for Treated Wastewater, Reclaimed Water, and Drinking Water. In *Proceedings of 2004 American Water Works Association (AWWA) Water Quality Technology Conference (WQTC)*; AWWA: Denver, CO, 2004.
12. Krasner, S. W.; Scilimenti, M. J.; Mitch, W. A.; Westerhoff, P.; Dotson, A. Using Formation Potential tests to Elucidate the Reactivity of DBP precursors with Chlorine versus with Chloramines. *Proceedings of 2007 American Water Works Association (AWWA) Water Quality Technology Conference (WQTC)*; AWWA: Denver, CO, November 18–22, 2007.
13. Vanderford, B. J.; Pearson, R. A.; Rexing, D. J.; Snyder, S. A. Analysis of Endocrine Disruptors, Pharmaceuticals, and Personal Care Products in Water Using Liquid Chromatography/Tandem Mass Spectrometry. *Anal. Chem.* **2003**, *75*, 6265–6274.
14. Vanderford, B. J.; Snyder, S. A. Analysis of Pharmaceuticals in Water by Isotope Dilution Liquid Chromatography/Tandem Mass Spectrometry. *Environ. Sci. Technol.* **2006**, *40*, 7312–7320.
15. Department of Water Resources Bay-Delta. *Delta Simulation Model II -- DSM2*; <http://baydeltaoffice.water.ca.gov/modeling/deltamodeling/models/dsm2/dsm2.cfm> [cited November 1, 2014]
16. Krauss, M.; Longrée, P.; Dorusch, F.; Ort, C.; Hollender, J. Occurrence and Removal of N-nitrosamines in Wastewater Treatment Plant. *Water Res.* **2009**, *43* (17), 4381–4391.
17. Chen, B.; Lee, W.; Westerhoff, P.; Krasner, S. W.; Herckes, P. Solar Photolysis Kinetics of Disinfection Byproducts. *Water Res.* **2011**, *44* (11), 3401–3409.

Chapter 8

National Occurrence of *N*-Nitrosodimethylamine (NDMA)

An Investigation of 38 Australian Drinking Water Supplies

Deborah Liew,¹ Julie Culbert,^{2,3} Kathryn Linge,^{*,1} Maria José Farré,^{4,7}
Nicole Knight,⁵ Jim Morran,² David Halliwell,⁶ Gayle Newcombe,²
and Jeffrey W. A. Charrois¹

¹Curtin Water Quality Research Centre, Curtin University, GPO Box U1987
Perth, Western Australia 6845, Australia

²Australian Water Quality Centre, GPO Box 1751, Adelaide,
South Australia 5001, Australia

³School of Agriculture, Food and Wine, The University of Adelaide, PMB 1,
Glen Osmond, South Australia, 5064, Australia

⁴Advanced Water Management Centre, University of Queensland,
Brisbane, Queensland 4072, Australia

⁵Smart Water Research Centre, School of Environment, Griffith University,
Southport, Queensland 4222, Australia

⁶Water Research Australia Limited, Docklands, Victoria 3008 Australia

⁷Present address: Catalan Institute for Water Research, Scientific and
Technological Park of the University of Girona, Girona, Spain

*E-mail: k.linge@curtin.edu.au.

To date, limited exposure data have been published on *N*-nitrosodimethylamine (NDMA) occurrence in Australian drinking water. Here, we present a comprehensive analysis of data from the largest survey of NDMA in Australian drinking water, with a total of 211 samples, from 38 drinking water treatment plants across five states and one territory. Samples were collected at the treatment plants after disinfection as well as in the distribution systems. Only nine water treatment plants reported NDMA above 5 ng/L. NDMA was detected in more than half of the samples collected (57 of 87) from these plants, but all detections were below the Australian Drinking Water

Guideline (100 ng/L). In agreement with other studies, NDMA was more frequently detected in chloraminated waters than chlorinated waters. The dosing of certain coagulant aids, and addition of ammonia prior to chlorine during chloramination were key factors in the formation of NDMA. Overall the results show that the drivers for NDMA formation in Australia are similar to those found in other studies worldwide.

Introduction

The formation of *N*-nitrosodimethylamine (NDMA) in disinfected water supplies has attracted worldwide attention, given it has been classified as a potent carcinogen (1). Health guidelines for NDMA adopted by agencies around the world range from between 9 and 100 ng/L (2–6). NDMA has been detected in both chlorinated and chloraminated drinking waters, although higher concentrations have generally been associated with systems using chloramine as the disinfectant (7–9). While reported NDMA concentrations in drinking water supplies have tended to be lower than 10 ng/L (10), higher concentrations (>100 ng/L) have been observed with increasing residence time in the distribution system (11–13). Some studies have also reported the presence of NDMA in some raw waters (i.e. without disinfection) (12, 14). Factors that impact NDMA formation in drinking water include source water quality and the presence of precursors (15–17), choice of disinfectant (8, 12, 14), operational parameters such as pH or disinfectant dose (16), use of ion-exchange resins or certain nitrogen-containing coagulants (7, 18), and the residence time in distribution systems (11–13).

While some monitoring programs have been established by state water authorities or water utilities, there are limited published data on NDMA occurrences in Australian drinking water. This paper consolidates results of NDMA occurrence surveys collected across five states and one territory in Australia between 2007–2013, representing the most comprehensive analysis of NDMA concentrations in Australian drinking water supplies. Survey data were analysed to determine the impact of water treatment processes on NDMA formation, and to identify key factors in the formation of NDMA in Australian drinking water treatment plants (DWTPs).

Methods

Sample Sites

A total of 211 samples were collected from 38 DWTPs around Australia (five states and one territory) between 2007 and 2013, with the majority (85%) collected between 2009 and 2011. The samples were collected as part of individual studies or monitoring programs undertaken by research organisations across Australia, and data were subsequently combined for this study. The DWTPs studied included ten from Victoria, three from New South Wales, two from South Australia, all studied by the Australian Water Quality Centre (AWQC), ten from

Western Australia and three from the Northern Territory, studied by the Curtin Water Quality Research Centre (CWQRC), and ten from Queensland, studied by the Smart Water Research Centre (SWRC) at Griffith University, and the Advanced Water Management Centre (AWMC) at the University of Queensland. While some studies did test for other *N*-nitrosamines in addition to NDMA, there were significant variations in analytical method and limits of reporting. Therefore this paper discusses NDMA occurrence only as it was the only *N*-nitrosamine measured in all studies.

In terms of disinfection, 18 of the 38 DWTPs tested used chlorine and 14 DWTPs used chloramine. Six plants used mixed disinfection treatment trains; four plants used pre-ozonation followed by chlorination or chloramination (DWTPs 29, 31, 37 and 38) and two plants used UV disinfection in addition to chlorine or chloramine disinfection for additional microbial protection (DWTPs 14 and 24). Figure 1 shows the general classification of these DWTPs according to pre-treatment process before disinfection. Disinfection (chlorination or chloramination) was the sole treatment process for eight DWTPs (21%), while four plants (11%) utilised filtration (e.g., granulated activated carbon or membrane filtration) or sedimentation without coagulation before disinfection. One disinfection-only plant (DWTP 15) that utilised chloramine is unusual because the raw water reservoir includes pre-treated groundwater, surface water and desalinated water, and both chloramination and chlorination are used in the large distribution system to maintain residual. All other DWTPs (26, 68%) utilised coagulation for treatment, with 15 plants following a relatively conventional treatment process (coagulation, flocculation, sedimentation, filtration and disinfection, with pH adjustment and pre-chlorination as required). Four plants (DWTPs 2, 3, 23, and 30) utilised coagulation and direct filtration (e.g. membranes or dissolved air flotation and filtration) instead of clarification by sedimentation. Seven DWTPs had atypical aspects to their pre-treatment, including incorporation of desalinated water (DWTPs 5 and 36), use of ion exchange resins for NOM removal (DWTP 21), and ozonation throughout the treatment process (DWTPs 29, 31, 37 and 38). The target chlorine or chloramine residuals leaving each DWTP were generally between 1 and 3 mg/L, although three chloramination plants (DWTP 14, 15 and 26) servicing large distribution systems had treatment plant target residuals of between 3 and 4.5 mg/L.

In addition to sampling, operational data were collected for each plant, including description of the treatment regime, the use and dose of primary coagulants and coagulant aids, disinfection dose(s), pH, target disinfectant residual leaving the plant, and system detention time at the sampling point. In the case of chloramination, details of the order and time between chlorine and ammonia addition were also obtained. Where possible, operational parameters were obtained for the exact dates when samples were collected, although for some DWTPs or systems little or no data were available and collection of operational data were challenging for systems where the water authorities providing distribution system water samples were not responsible for initial water treatment. Physicochemical characteristics such as pH, total dissolved solids (TDS), temperature, dissolved organic carbon (DOC) and disinfectant residuals were also recorded for raw and treated water samples, where possible.

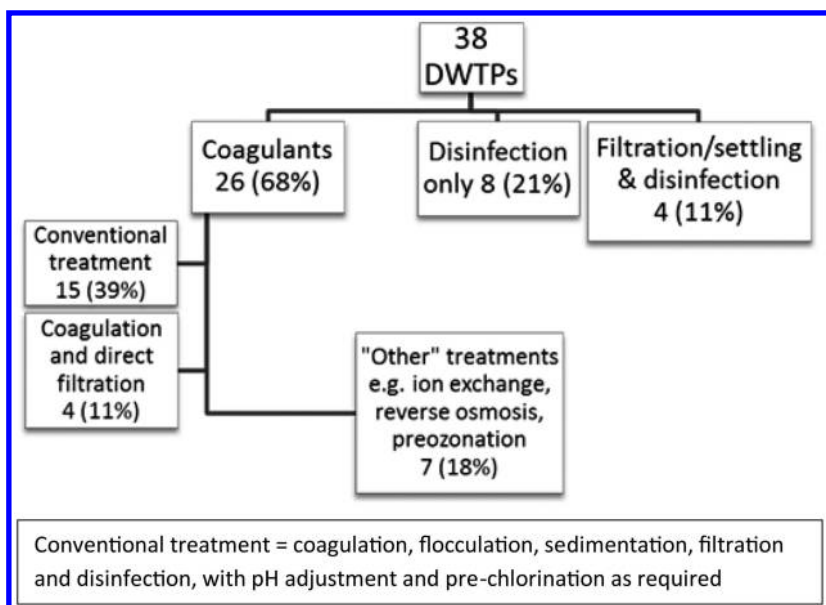


Figure 1. General classification of DWTPs surveyed in this study according to treatment type (percentages reported as percent of total number of drinking water treatment plants (DWTPs)).

Sampling and NDMA Analysis

Table 1. Details of Sampling and Analytical Methods for NDMA for Each Laboratory

<i>Laboratory</i>	<i>AWQC</i>	<i>CWQRC</i>	<i>QHFSS</i>
Preservation Agent	Sodium thiosulphate pentahydrate 120 mg/L	Ascorbic acid 20 mg/L	Sodium thiosulphate 80-100 mg/L
Sample volume	500 mL	1000 mL	1000 mL
Blanks	Tap water treated with UV light	Ultrapure water and quenching agent	Ultrapure water
SPE cartridge resin	35-50 mesh activated charcoal	LiChrolut® EN and Carboxen™ 572	Coconut charcoal
Ionisation mode (GC-MS)	Positive CI with isobutane	Positive CI with ammonia	Positive CI with ammonia

Samples were collected in glass amber bottles or aluminium foil-covered polyethylene bottles containing a quenching agent, kept cool and in the dark in an ice box during transport to the laboratory, and then refrigerated in the dark at 4°C until extraction. All laboratories used laboratory blank samples to quantify contamination introduced through the analytical process. In addition, CWQRC also included trip and field blanks in each sampling event to determine if there was any contamination through the sampling process, storage and transport. Trip blanks remained unopened until analysis, and field blanks were opened at each sampling location. Samples were then analysed for NDMA at one of three laboratories, AWQC, CWQRC or Queensland Health Forensic and Scientific Services (QHFSS). Analysis was carried out using solid-phase extraction (SPE) followed by gas chromatography-mass spectrometry (GC-MS), with minor variations between laboratories. Details of small variations between the sampling protocol and analytical method used by each laboratory are listed in Table 1. The concentration of NDMA was quantified against a deuterated internal standard (isotope dilution procedure) and the limits of reporting (LOR) ranged between 1 ng/L and 5 ng/L.

All three laboratories undertook two rounds of inter-laboratory comparison testing as part of the NDMA survey undertaken by the AWQC and funded by Water Quality Research Australia (WQRA, now known as Water Research Australia Ltd). During each round, duplicate samples containing between 10 and 130 ng/L NDMA were sent to each independent laboratory for analysis. Results obtained from CWQRC and QHFSS compared well with those of the AWQC. With the exception of one sample, all results were within 13% relative standard deviation (RSD) (19).

Data Analysis

All data, excluding blanks and replicates, were pooled into a common dataset. The normality of the dataset was tested by calculation of the Kolmogorov-Smirnov Statistic and the Shapiro-Wilk Statistic (SPSS Statistics v20) and the data were found to have a poor fit to the normal distribution curve. Therefore median was chosen for data analysis rather than average because it is less affected by outliers and because it is more suited for data that does not follow a normal distribution. As the LOR for NDMA analyses varied for each of the testing laboratories, the highest LOR was chosen as the limit for all samples. Therefore if a result was < 5 ng/L then it was allocated a value of < 5 ng/L (i.e. zero for calculations), and this will influence percentage detection calculations and other statistics.

Calculation of median concentrations incorporated all data points including samples reported to be below LOR, and these were assumed to be equal to the LOR for the purposes of that calculation. While this conservative approach will overestimate the actual median concentration of chemicals reported below LOR in more than 50% of samples, it was deemed appropriate given our primary goal of assessing the safety of treated drinking water. As most samples (>80%) did not contain NDMA above the LOR, average and median concentrations were also calculated solely based on samples in which NDMA \geq 5 ng/L.

Results and Discussion

Overview of Occurrence Data

A total of 211 post-disinfection samples were collected and analysed in this study. Of these, 95 samples were collected at, or within 2km of, the treatment plant and 116 were collected in the distribution system. The Australian Drinking Water Guidelines recommend maintaining a chlorine or chloramine residual greater than 0.5 mg/L for control of *Naegleria fowleri* (1) and therefore we expected disinfectant residual throughout the distribution system. Disinfectant residual data collected in 27 of the 38 DWTP confirmed this, although the residual was not always > 0.5 mg/L.

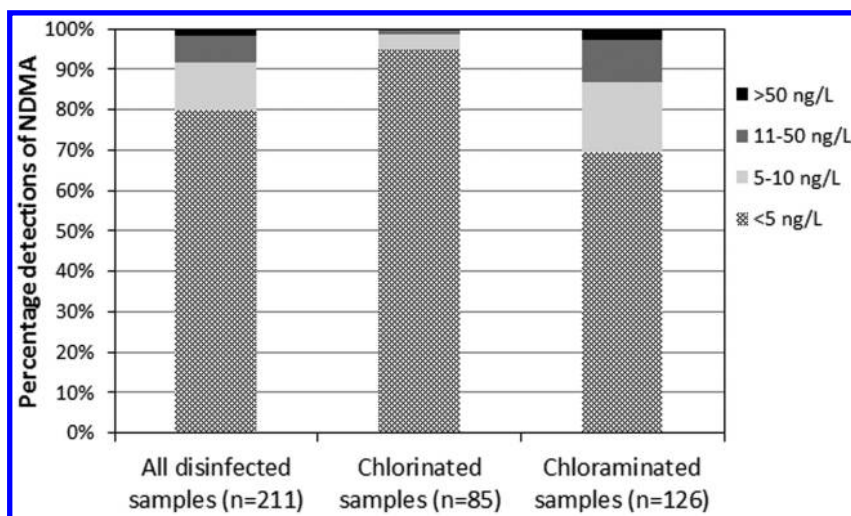


Figure 2. Distribution of NDMA concentrations in all water samples. There was a higher frequency of detection and higher concentrations in chloraminated samples than in chlorinated samples.

Figure 2 shows that the majority (80%, $n = 169$) of all samples contained NDMA concentrations below 5 ng/L, while 12% ($n = 25$) contained NDMA concentrations between 5 and 10 ng/L. As the majority of all disinfected samples measured NDMA below 5 ng/L, the median concentration of all disinfected samples was also < 5 ng/L. Of the 211 disinfected samples, 126 were from chloraminated systems while the remaining 85 were from chlorinated systems. Figure 2 shows that only 5% ($n = 4$) of samples from chlorinated systems contained NDMA above 5 ng/L. On the other hand, 30% ($n = 38$) of samples from chloraminated systems were measured with NDMA levels of 5 ng/L or higher. Chloraminated samples also recorded a much higher maximum NDMA concentration (74 ng/L) than the chlorinated samples (14 ng/L).

Further data analysis demonstrated that all NDMA detects ≥ 5 ng/L were from nine specific DWTPs, where 48% of all samples ($n = 88$) contained NDMA > 5 ng/L (Table 2). There was a wide variation in observed NDMA levels, with two DWTPs (4 and 14) exhibiting significantly higher levels of NDMA (up to 46 ng/L and 74 ng/L, respectively) than the other plants. The high NDMA concentrations measured in DWTP 4 and 14 have previously been studied, and were attributed to factors that include poor source water quality, the method of chloramination and DWTP management practices (20). Despite these results, all detections were below the Australian Drinking Water Guideline of 100 ng/L for NDMA.

As shown in Table 2, where NDMA was present at ≥ 5 ng/L, the median concentration for distribution system samples was generally higher than for treatment plant samples, with the exception of DWTP 4. In addition, a higher percentage of distribution system samples contained NDMA compared to the treatment plant samples (30% versus 8%). This is consistent with results of other surveys suggesting that NDMA can continue to form and increase with time in the distribution system (11–13).

Table 2. Summary of the Percentage Detections, Median and Maximum NDMA Concentrations Observed for Each of the Nine Dwtps That Detected NDMA in One or More Samples. TP = Treatment Plant; DS = Distribution System. Results Are Determined Using the Maximum LOR for These Nine DWTPs (3 ng/L).

<i>Plant No. and Disinfection type</i>	<i>% detect ≥ 3 ng/L (total no. samples)</i>	<i>Median (maximum) (ng/L)</i>	<i>Median of TP samples (ng/L)</i>	<i>Median of DS samples (ng/L)</i>
2 Chloramine	67% (9)	3 (12)	n.a.	3
3 Chloramine	67% (6)	4 (5)	4	4
4 Chloramine	100% (6)	53 (74)	74	39
5 Chloramine	75% (4)	7 (21)	<3	15
9 Chlorine	44% (9)	< 3 (9)	n.a.	< 3
10 Chlorine	33% (9)	< 3 (14)	n.a.	< 3
13 Chloramine	100% (9)	7 (10)	4	8
14 Chloramine	100% (9)	19 (46)	15	23
15 Chloramine	50% (26)	< 3 (10)	<3	4

n.a. = not available; no TP samples were analysed at these plants.

Influence of Operational Parameters on NDMA Formation in Chloraminated Systems

While there was insufficient data to investigate NDMA formation in chlorinated DWTPs due to the limited number of detections, the dataset was further evaluated to assess the factors influencing NDMA formation in the 16 chloraminated systems.

Table 3. NDMA Occurrence and Corresponding Factors (Y = Yes, N = No) in Chloramination Plants. Plants in Which NDMA Was Detected Are Bolded. n.d. = not detected, n.a. = data not available

<i>Plant No.</i>	<i>Median NDMA ng/L</i>	<i>Polymer used as coagulant aids</i>	<i>Addition of ammonia first</i>	<i>Raw Water DOC >10 mg/L</i>
2	3	Y	N	n.a.
3	4	Y	Y	N
4	53	N	Y	Y
5	7	Y	Y	Y
6	n.d.	N	n.a.	n.a.
7	n.d.	N	n.a.	n.a.
8	n.d.	N	n.a.	n.a.
12	n.d.	Y	N	N
13	7	Y	N	Y
14	19	Y	Y	Y
15	3	N	Y	N
25	n.d.	N	N	n.a.
26	n.d.	N	N	n.a.
27	n.d.	N	N	n.a.
36	n.d.	Y	N	n.a.
38	n.d.	N	N	n.a.

Relationships between operational parameters and NDMA concentrations in chloraminated waters were initially assessed by calculation of Spearman's correlation coefficients (SPSS Statistics v20). However, it was found that correlations were heavily skewed by the significantly higher NDMA concentrations reported in DWTP 4. Furthermore, the dataset was quite limited as only seven of the 16 chloraminating DWTPs had detections of NDMA in their waters. Instead, the dataset was qualitatively evaluated with focus on impact

of chloramination practice (order of reagent addition and contact time), use of nitrogen-containing coagulants and coagulant aids, as well as raw water chemistry on NDMA formation. Table 3 presents a summary of the key factors and NDMA concentrations in the 16 DWTPs using chloramination. The influence of these factors on formation of NDMA are discussed in detail below.

Chloramination Practice

The order of chlorine and ammonia addition during chloramination has previously been reported to have a significant effect on NDMA formation (18, 21–23). Contact with free chlorine prior to ammonia addition can reduce NDMA formation, because chlorinated NDMA precursors tend to be less reactive (22–24). In contrast, the addition of chlorine after ammonia has been shown to enhance NDMA formation from dimethylamine, a model NDMA precursor, by up to an order of magnitude (22). This increase was attributed to the localised formation of dichloramine at the point of chlorine addition, due to high localised Cl:N ratio. NDMA formation from dichloramine is higher than from monochloramine.

Table 4. Distribution of NDMA Concentrations in Chloraminated Samples Based on Order of Addition of Chlorine and Ammonia

<i>Order of addition</i>	<i>% detect \geq 5 ng/L (total no. of samples)</i>	<i>Median (ng/L)</i>	<i>Maximum (ng/L)</i>
Chlorine first	19% (54)	< 5	12
Ammonia first	55% (51)	6	74

The disinfection practice at eight of the 16 chloraminating DWTPs in this study was to chlorinate prior to adding ammonia, while five DWTPs added ammonia prior to chlorine. There was no chloramination information available for the remaining three plants (21 samples). Typically, the time between addition of ammonia and chlorine ranged from seconds to a few minutes but DWTPs that added chlorine first employed a longer contact time (2.5–30 hours). Table 4 compares NDMA concentrations for DWTPs that use the two different reagent addition scenarios. Only two of the eight DWTPs that practise chlorine addition first, had NDMA detected post-disinfection, while all five plants that practised ammonia addition first had NDMA detected in one or more of their samples. Higher NDMA concentrations were also found in waters that were treated with ammonia first compared to those that were treated with chlorine first. The two DWTPs with the highest average NDMA concentrations (DWTP 4 and 14) both added ammonia before chlorine.

Coagulation and Coagulation Aids

Most of the DWTPs in this study (25 out of 38) used coagulation as part of their water treatment process. Alum was the most commonly used coagulant, but other coagulants such as ferric chloride and Magnasol 489, a mixture of polyaluminium chlorohydrate and polydiallyldimethyl ammonium chloride (polyDADMAC), were also used. The primary coagulant dose varied greatly, ranging from 5 mg/L to 240 mg/L. There was no correlation observed between the primary coagulant dose and NDMA concentration in the treated water. In some instances where no coagulant was used, NDMA was still observed in the final product water suggesting the presence of precursors in the raw water.

Fifteen of the DWTPs also employed various coagulant aids, which varied in dose, ranging from 0.005 mg/L to 4.7 mg/L. Even though higher coagulant doses can potentially remove more NDMA precursors, the use of certain coagulant aids can potentially add NDMA precursors to the water. For example, polyDADMAC, a nitrogen-based polymeric coagulant has received attention for its reported propensity to form NDMA during chloramination (18, 25). PolyDADMAC was used in some water treatment plants in South Australia and Queensland, including some of the DWTPs presented here.

While there was no clear evidence to suggest that the generic use of coagulant aids resulted in higher level of NDMA in the disinfected water, when coagulant aids were utilised, NDMA was only observed when polyDADMAC and/or Magnafloc LT22 was used in chloraminating DWTPs. NDMA was not detected in DWTPs that used other coagulant aids (e.g. Flopam AN 910 PWG, Magnafloc LT20, Magnafloc LT21, Magnafloc LT25, Nalco 44560, Nalco 3482, Magnafloc LT425, SNF AN 905). Among the six DWTPs utilizing PolyDADMAC, NDMA was detected in two of the three chloraminating plants between 7-46 ng/L, but was not detected in any of the three plants using chlorine disinfection. PolyDADMAC consists of quaternary amines with dimethylamine-functional groups and it has been proposed that NDMA formation can occur from both the dimethylamine-moieties (25, 26) or the quaternary amines themselves (27), which act as NDMA precursors. In this study higher NDMA concentrations were observed in plants using polyDADMAC, when chloramination was the disinfection process and not chlorination. This suggests that polyDADMAC may have an influence in forming NDMA in DWTPs, but only when chloramine disinfection is used.

Only four DWTPs utilised Magnafloc LT22 as the exclusive coagulant aid, all of which practiced chloramination, and all of which detected NDMA at least once. Magnafloc LT22 is a polyacrylamide-based polymer and there have been no studies to-date relating NDMA formation to its use. However, certain polyacrylamides used in water treatment have been reported to form NDMA also through the dimethylamine-moieties in the polymer structure (25, 26). While the exact composition of Magnafloc LT22 was unknown, it is possible that its structure contains dimethylamine-moieties which can explain the NDMA formation observed in these plants.

In order to assess the contribution of these nitrogen-based polymers towards NDMA formation during water treatment, NDMA formation potentials (FP)

were determined from different commercially available coagulant aids used in Australia. Coagulant aids (10 mg/L) were dosed with a high concentration of monochloramine and analysed for NDMA after seven days of contact time, based on the procedure by Mitch *et al.* (28). Of the five coagulant aids tested, only polyDADMAC and Magnafloc LT22 formed > 10 ng/L NDMA (Table 5). PolyDADMAC showed an extremely high NDMA FP of 15,000 ng/L, several orders of magnitude higher than any of the other coagulant aids. While Magnafloc LT22 had a high NDMA FP (160 ng/L), formation was much lower than that from polyDADMAC. While both polymers may have the potential to form NDMA during chloramination, the extent of their impact will depend on specific water treatment conditions. Doses of chloramine and coagulant aids used in the DWTPs are much lower than the conditions of the FP procedure. Therefore the contribution of Magnafloc LT22 to NDMA formation may not be significant; on the other hand, the use of polyDADMAC could still have significant potential for NDMA formation under DWTP conditions due to its high FP.

Table 5. NDMA Formation Potentials of Various Coagulant Aids. Coagulant Aids (10 mg/L, Buffered to pH 7) were Dosed with 2mM Monochloramine (140 mg/L Cl₂) and Analysed for NDMA after Seven Days Contact Time, Based on the Procedure by Mitch *et al.* (28). Samples (50 mL) Were Analysed by Liquid-Liquid Extraction Followed by GC-MS with Ammonia PCI.

<i>Sample</i>	<i>NDMA FP (ng/L)</i>
Blank (Ultrapure water)	< 2
Flopam AN 910 PWG	6
Magnafloc LT25	6
Magnafloc 800 HP	6
Magnafloc LT22	160
PolyDADMAC	15,000

A previous study of NDMA formation from polyDADMAC compared the role of the bulk polymer with degraded components or impurities of the polymer solution, by performing NDMA FP experiments on polyDADMAC before and after dialysis (29). The dialysis retentate was found to have a much higher NDMA FP than the dialysis permeate, suggesting that most of the observed NDMA formation was due to interaction of monochloramine with the retained polymer, rather than with small degraded molecules or impurities. In another study, it was reported that polyDADMAC remains as a contaminant in treated water when it is used as a sole coagulant, but not when it is used in conjunction with alum (30). In the DWTPs surveyed here, polyDADMAC was typically used with alum, however, these findings suggest that even higher concentrations of NDMA can be expected if polyDADMAC is used as the primary coagulant.

Raw Water Chemistry

Raw water parameters, including pH, TDS, temperature, DOC and turbidity, were evaluated for relationships with NDMA concentrations, by calculation of Spearman's correlation coefficients (R). There were no correlations observed between NDMA concentrations and any raw water parameters, except for DOC. As shown in Table 3, it appears that higher NDMA concentrations (> 5 ng/L) were found in plants with higher raw water DOC (> 10 mg/L). Raw water DOC showed a significant positive correlation with average NDMA concentrations ($R = 0.9$, $p < 0.01$, data not shown) However, the relationship was heavily skewed by the significantly higher NDMA concentrations reported in DWTP 4, and there was no significant correlation observed when data from DWTP 4 was removed.

Furthermore, six of the eight DWTPs practised some form of conventional treatment and/or filtration before disinfection, and therefore some DOC removal is expected before disinfection. Raw water DOC therefore cannot be directly related to NDMA formation in these cases. Another limitation is that the concentrations of NDMA and its precursors are typically orders of magnitude lower than DOC (ng/L compared with mg/L), and may not be directly comparable.

DWTP 4, which did not use any form of coagulation, exhibited the highest NDMA concentrations. A previous study (20) has also identified that DWTP 4 had poor source water quality, and the treatment process (microfiltration) was not effective in removing DOC. However, laboratory tests using DWTP 4 source water demonstrated that, even with alum coagulation, NDMA precursors were not effectively removed compared with total DOC (20). This is consistent with previous findings that NDMA precursors are usually low molecular weight hydrophilic compounds (31), and are therefore unlikely to be effectively removed through conventional treatment processes.

There are clearly limitations in assessing NDMA formation according to bulk parameters such as DOC and organic nitrogen. Rather, the nature of natural organic matter in the source water is more important for determining NDMA and can vary for each water source. Measurements of NDMA precursors (i.e. NDMA-FP) may be a more useful indication of the potential of a source water to produce NDMA under certain water treatment conditions.

Conclusions

The concentration of NDMA in Australian drinking water was variable, but all detections were below the Australian Drinking Water Guideline of 100 ng/L. As expected, chloraminating plants were found to have higher concentrations, and more frequent detections of NDMA than chlorinating plants. The order of reagent addition during chloramination had a significant impact on NDMA formation, where the addition of ammonia before chlorine typically led to higher NDMA concentrations, as compared to addition of chlorine first. Under certain conditions, some nitrogen-containing coagulant aids may provide precursors for NDMA formation upon chloramination. Employing free chlorine contact time before ammonia addition can help to control NDMA formation in chloraminating systems. These findings are the first demonstration of the influence of operational

factors on NDMA formation in Australian DWTPs at the full-scale, and overall they are consistent with previously reported findings from both laboratory studies and other drinking water systems worldwide.

Acknowledgments

We acknowledge the following people for their technical assistance: Andrew Chan and Geoff Chidlow of CWQRC; Con Kapralos, Jules Leach and Najwa Slyman of AWQC; Neil Holling of QHFSS; Claire McInnes from Water Research Australia. We thank the following people for their sampling assistance: Liza Breckler, Ralph Henderson and Fern Burgess of Water Corporation (WA), Deb Gale of Seqwater and other Seqwater staff. Thanks also goes to Adam Holman for his study on water treatment polymers, and Glendon Shaw and Kalinda Watson for research support at SWRC. CWQRC research was funded by the Australian Research Council (LP110100548), Water Research Australia Ltd and the Water Corporation of Western Australia (WCWA). AWQC research was part of Water Research Australia Project 1018-09 and thanks the participating water authorities. SWRC research was funded by the Urban Water Security Research Alliance. AWMC acknowledges the tailored collaboration between Seqwater and Water Research Foundation, and would like to thank Djanette Khiari, manager of Water Research Foundation Project #4484, and the project advisory committee for their support. Dr Maria Jose Farre also acknowledges the European Commission for funding project 623711 under the FP7-PEOPLE-2013-IIF - Marie Curie Action: “International Incoming Fellowships”.

References

1. IARC, Some N-Nitroso compounds. *IARC Monographs on the Evaluation of Carcinogenic Risks to Humans*; International Agency for Research on Cancer, World Health Organisation: Lyon, France, 1978; Vol. 17, p 365.
2. Boyd, J. M.; Charrois, J. W. A.; Hofmann, R.; Hrudey, S. E. NDMA and other N-nitrosamines – health risk assessment and management. In *Disinfection By-Products – Relevance to Human Health*; Hrudey, S., Charrois, J. W. A., Eds.; IWA Publishing: London, 2012; pp 125–144.
3. *Ontario Regulation 169/03, Schedule 2, Chemical Standards, Ontario Safe Drinking Water Act*; Ontario Ministry of Environment: Toronto, 2002.
4. *Guidelines for Canadian Drinking Water Quality – Summary Table*; Water, Air and Climate Change Bureau, Healthy Environments and Consumer Safety Branch, Health Canada: Ottawa, Ontario, 2012.
5. *Guidance on the Water Supply (Water Quality) Regulations 2000 specific to N-nitrosodimethylamine (NDMA) concentrations in drinking water*; Drinking Water Inspectorate: London, U.K., 2008.
6. *Australian Drinking Water Guidelines 6*; National Health and Medical Research Council, National Resource Management Ministerial Council: Canberra, Australia, 2011.

7. Najm, I.; Trussell, R. R. NDMA Formation in Water and Wastewater. *J. Am. Water Works Assoc.* **2001**, *93*, 92–99.
8. Valentine, R. L.; Choi, J.; Chen, Z.; Barrett, E.; Hwang, C. *Factors Affecting the Formation of NDMA in Water and Occurrence*; AWWA Research Foundation: Denver, CO, 2005.
9. Liew, D.; Linge, K. L.; Heitz, A.; Joll, C. A. Nitrogenous DBPs in drinking water: toxicity, regulation, analysis, occurrence and control. In *Disinfection By-Products – Relevance to Human Health*; Hrudey, S., Charrois, J. W. A., Eds.; IWA Publishing: London, 2012; pp 83–124.
10. Mitch, W. A.; Sharp, J. O.; Trussell, R. R.; Valentine, R. L.; Alvarez-Cohen, L.; Sedlak, D. L. N-nitrosodimethylamine (NDMA) as a drinking water contaminant: a review. *Environ. Eng. Sci.* **2003**, *20*, 389–404.
11. Zhao, Y. Y.; Boyd, J.; Hrudey, S. E.; Li, X. F. Characterization of New Nitrosamines in Drinking Water Using Liquid Chromatography Tandem Mass Spectrometry. *Environ. Sci. Technol.* **2006**, *40*, 7636–7641.
12. Charrois, J. W. A.; Boyd, J. M.; Froese, K. L.; Hrudey, S. E. Occurrence of N-nitrosamines in Alberta public drinking-water distribution systems. *J. Environ. Eng. Sci.* **2007**, *6*, 103–114.
13. Charrois, J. W. A.; Arend, M. W.; Froese, K. L.; Hrudey, S. E. Detecting N-Nitrosamines in Drinking Water at Nanogram Per Liter Levels Using Ammonia Positive Chemical Ionization. *Environ. Sci. Technol.* **2004**, *38*, 4835–4841.
14. Zhao, Y. Y.; Boyd, J. M.; Woodbeck, M.; Andrews, R. C.; Qin, F.; Hrudey, S. E.; Li, X. F. Formation of N-nitrosamines from Eleven Disinfection Treatments of Seven Different Surface Waters. *Environ. Sci. Technol.* **2008**, *42*, 4857–4862.
15. Asami, M.; Oya, M.; Kosaka, K. A nationwide survey of NDMA in raw and drinking water in Japan. *Sci. Total. Environ.* **2009**, *407*, 3540–3545.
16. Brisson, I. J.; Levallois, P.; Tremblay, H.; Serodes, J.; Deblois, C.; Charrois, J.; Taguchi, V.; Boyd, J.; Li, X. F.; Rodriguez, M. J. Spatial and temporal occurrence of N-nitrosamines in seven drinking water supply systems. *Environ. Monit. Assess.* **2013**, *185*, 7693–7708.
17. Gerecke, A. C.; Sedlak, D. L. Precursors of N-Nitrosodimethylamine in Natural Waters. *Environ. Sci. Technol.* **2003**, *37*, 1331–1336.
18. Wilczak, A.; Assadi-Rad, A.; Lai, H. H.; Hoover, L. L.; Smith, J. F.; Berger, R.; Rodigari, F.; Beland, J. W.; Lazzelle, L. J.; Kinicannon, E. G.; Baker, H.; Heaney, C. T. Formation of NDMA in chloraminated water coagulated with DADMAC cationic polymer. *J. Am. Water Works Assoc.* **2003**, *95*, 94–106.
19. Newcombe, G.; Morran, J.; Culbert, J.; Slyman, N.; Leach, J.; Kapralos, C. *Occurrence and management of NDMA and other nitrogenous disinfection by-products in Australian drinking and recycled waters. WQRA Project 1018 Milestone Report No 5*. Water Quality Research Australia: Adelaide SA, 2012.
20. Culbert, J.; Morran, J.; Slyman, N.; Smith, B.; Newcombe, G. Occurrence and Management of Nitrosamines in Australian Drinking and Recycled

Water. OzWater'12 Conference Proceedings, Sydney, Australia, May 8–10, 2012.

21. Mitch, W. A.; Oelker, G. L.; Hawley, E. L.; Deeb, R. A.; Sedlak, D. L. Minimization of NDMA formation during chlorine disinfection of municipal wastewater by application of pre-formed chloramines. *Environ. Eng. Sci.* **2005**, *22*, 882–890.
22. Schreiber, I. M.; Mitch, W. A. Influence of the Order of Reagent Addition on NDMA Formation during Chloramination. *Environ. Sci. Technol.* **2005**, *39*, 3811–3818.
23. Charrois, J. W. A.; Hrudey, S. E. Breakpoint chlorination and free-chlorine contact time: Implications for drinking water N-nitrosodimethylamine concentrations. *Water Res.* **2007**, *41*, 674–682.
24. Mitch, W. A.; Sedlak, D. L. Formation of *N*-Nitrosodimethylamine (NDMA) from Dimethylamine during Chlorination. *Environ. Sci. Technol.* **2002**, *36*, 588–595.
25. Park, S. H.; Wei, S.; Mizaikoff, B.; Taylor, A. E.; Favero, C.; Huang, C. H. Degradation of Amine-Based Water Treatment Polymers during Chloramination as *N*-Nitrosodimethylamine (NDMA) Precursors. *Environ. Sci. Technol.* **2009**, *43*, 1360–1366.
26. Mitch, W. A.; Sedlak, D. L. Characterization and Fate of *N*-Nitrosodimethylamine Precursors in Municipal Wastewater Treatment Plants. *Environ. Sci. Technol.* **2004**, *38*, 1445–1454.
27. Kemper, J. M.; Walse, S. S.; Mitch, W. A. Quaternary Amines as Nitrosamine Precursors: A Role for Consumer Products? *Environ. Sci. Technol.* **2010**, *44*, 1224–1231.
28. Mitch, W. A.; Gerecke, A. C.; Sedlak, D. L. A *N*-nitrosodimethylamine (NDMA) precursor analysis for chlorination of water and wastewater. *Water Res.* **2003**, *37*, 3733–3741.
29. Holman, A. Formation of *N*-Nitrosamines During Drinking Water Treatment. Chemistry Honors Dissertation, Curtin University, Perth, Western Australia, 2012.
30. Becker, N. S. C.; Bennett, D. M.; Bolto, B. A.; Dixon, D. R.; Eldridge, R. J.; Le, N. P.; Rye, C. S. Detection of polyelectrolytes at trace levels in water by fluorescent tagging. *React. Funct. Polym.* **2004**, *60*, 183–193.
31. Pehlivanoglu-Mantas, E.; Sedlak, D. L. Measurement of dissolved organic nitrogen forms in wastewater effluents: Concentrations, size distribution and NDMA formation potential. *Water Res.* **2008**, *42*, 3890–3898.

Chapter 9

The Role of Pre-Oxidation in Controlling NDMA Formation: A Review

Meric Selbes,¹ Malcolm Glenn,² and Tanju Karanfil*³

¹Hazen and Sawyer, Environmental Engineers and Scientists,
Fairfax, Virginia 22030, U.S.A.

²Alliance Consulting Engineers, Columbia, South Carolina 29202, U.S.A.

³Department of Environmental Engineering and Earth Sciences,
Coulombslemson University, Anderson, South Carolina 29625, U.S.A.

*E-mail: tkaranf@clemson.edu.

N-nitrosodimethylamine (NDMA), a probable human carcinogen, is a disinfection by-product (DBP) that has been detected in chloraminated drinking water systems. Options for NDMA control include the physical removal of either precursors or precursor deactivation prior to chloramination. This review summarizes some of the recent findings related to the control of NDMA formation with commonly used oxidants in drinking water treatment. Each oxidant (chlorine, chlorine dioxide, ozone) has the potential to reduce NDMA formation with varying degree of efficiencies depending on the precursors in source waters. In general, ozone and chlorine are effective oxidants for controlling NDMA precursors, likely due to their high reaction rate constants with amines. In some cases, the oxidants themselves have been shown to increase the NDMA formation. The selection of pre-oxidant type, dose and application location for NDMA control would site-specific. Utilities intend on using pre-oxidation as a strategy for NDMA control should also the impacts on the formation of regulated DBPs and other unintended consequences that can be associated with those oxidants.

Introduction

N-nitrosodimethylamine (NDMA), a probable human carcinogen, is a disinfection by-product (DBP) that has been detected in chloraminated drinking water systems. Due to their adverse health effects, methods to control the formation of nitrosamines during water treatment have gained increased attention during the past decade. These methods mainly involve either the removal of NDMA precursors or their transformation into less reactive forms. Since most of the nitrosamine precursors have been linked low molecular weight hydrophilic compounds (*1*), their removal from water is challenging. Pre-oxidation (e.g., using chlorine, ozone, or chlorine dioxide) prior to chloramination can be a viable approach for some water utilities to control the NDMA levels. However, the use of oxidants should be optimized for a given source water and water treatment process configuration since these oxidants are also associated with the formation of both regulated DBPs and NDMA (without chloramination). The objective of this chapter is to provide a literature review on the oxidant applications for controlling NDMA formation during drinking water treatment.

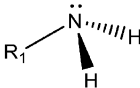
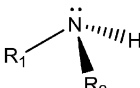
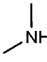
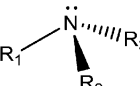
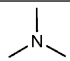
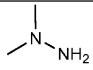
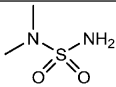
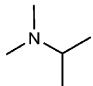
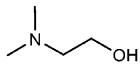
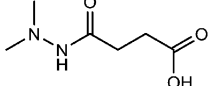
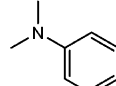
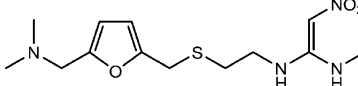
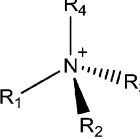
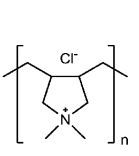
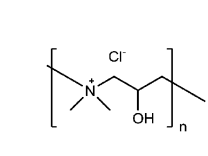
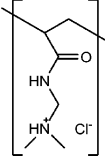
The Role of Oxidants/Disinfectants in NDMA Formation

Several pathways have been proposed for the formation of nitrosamines. In drinking water, formation of nitrosamines with chloramines is practically most important pathway. It has been shown that mono- and dichloramines can lead to formation nitrosamines from DMA, tertiary or quaternary amines with DMA moieties, natural organic matter, polyelectrolytes, ion-exchange resins, fungicides, pesticides, herbicides, pharmaceuticals, personal care products, and wastewater effluent impacted waters. In addition to these chloramines (*2–11*),. The molecular structures of precursors mentioned in this review are given in Table 1. Besides chloramine, some other oxidants/disinfectants may lead to NDMA formation (Figure 1).

Chlorine

The first pathway that has been suggested to form NDMA is through nitrosation of nitrogen-containing compounds. Nitrosation involves introducing a nitroso group (-NO) into an organic compound causing the formation of nitroso compounds. By *N*-nitrosation of nitrogen-containing organic compounds, nitrosamines are formed. Possible nitrosating agents include nitrous acid (HNO₂), nitrogen oxides (N₂O₃, N₂O₄), and some others (*4*). For example, the nitrosation reaction induced by nitrite is as follows: “Under acidic conditions, nitrite (NO₂⁻) is transformed to nitrous acid (HNO₂), which is not stable in aqueous solution but decomposes either to the nitrosyl cation (NO⁺) or to dinitrogen trioxide (N₂O₃). Both of which are capable of reacting with nitrogen-containing organic compounds to form nitrosamines (*4*).

Table 1. Some of the Structures of NDMA Precursors

Group	Structure
 <p>Primary Amines</p>	<p>Not Applicable</p>
 <p>Secondary Amines</p>	 <p>Dimethylamine (DMA)</p>
 <p>Tertiary Amines</p>	<div style="display: flex; justify-content: space-around;"> <div data-bbox="405 630 531 777">  <p>Trimethylamine (TMA)</p> </div> <div data-bbox="588 630 680 777">  <p>1,1-Dimethylhydrazine (UDMH)</p> </div> <div data-bbox="738 630 944 777">  <p>N,N-Dimethylsulfamide (DMS)</p> </div> </div> <div style="display: flex; justify-content: space-around; margin-top: 20px;"> <div data-bbox="405 821 531 977">  <p>N,N-Dimethylisopropylamine (DMiPA)</p> </div> <div data-bbox="554 821 692 977">  <p>2-Dimethylaminoethanol (DMAEtOH)</p> </div> <div data-bbox="738 821 944 977">  <p>Daminozid (DMNZD)</p> </div> </div> <div style="display: flex; justify-content: space-around; margin-top: 20px;"> <div data-bbox="405 1012 543 1168">  <p>N,N-Dimethylaniline (DMAN)</p> </div> <div data-bbox="588 1012 944 1168">  <p>Ranitidine (RNTD)</p> </div> </div>
 <p>Quaternary Amines</p>	<div style="display: flex; justify-content: space-around;"> <div data-bbox="405 1177 543 1407">  <p>Poly(diallyldimethylammonium chloride) (PolyDADMAC)</p> </div> <div data-bbox="588 1177 795 1407">  <p>Poly(dimethylamine-co-epichlorohydrin), quaternized (PolyAMINE)</p> </div> <div data-bbox="841 1177 944 1407">  <p>DMA-based polyacrylamide (PolyACRYL)</p> </div> </div>

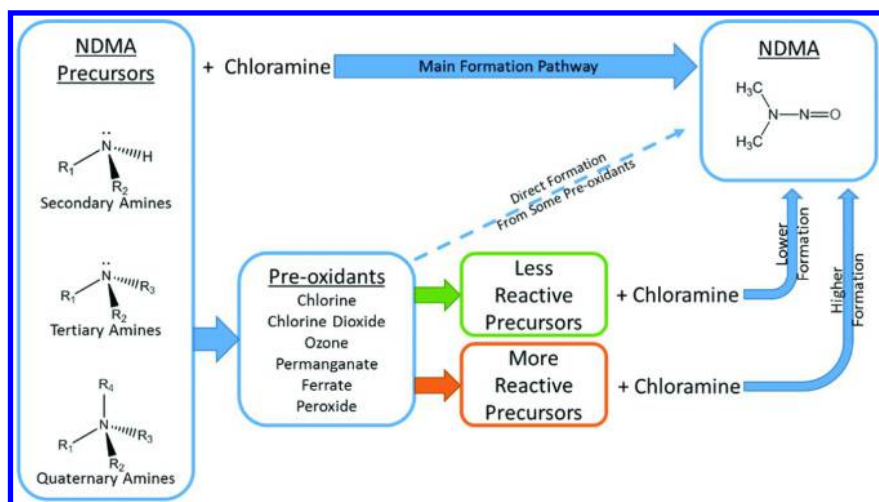


Figure 1. NDMA formation and the effect of pre-oxidation.

Choi and Valentine (12) proposed that NDMA is formed by nitrosation of dimethylamine (DMA) with nitrite that was catalyzed by free chlorine. Specifically, they attributed NDMA formation to the formation of a dinitrogen tetraoxide (N_2O_4) intermediate, which is the product of oxidation of nitrite by free chlorine. This intermediate is a very effective nitrosating agent with its formation more favorable at neutral pH, which is typical in water treatment facilities, in contrast to the formation of N_2O_3 , which occurs at low pH. Although the reaction is rapid, the yields are approximately two orders of magnitude lower than that of the chloramination pathway (9). Due to reliance on nitrite for NDMA formation, this pathway has been suggested for NDMA formation in chlorinated wastewater effluents and natural-bodied, recreational waters (13, 14).

Chlorine Dioxide

Andrzejewski and Nawrocki (15) have shown that chlorine dioxide reaction with DMA led to the formation of NDMA. The highest observed yield was 0.2% molar conversion under very high chlorine dioxide concentrations (i.e., 36 mg/L) at pH 8.0. Compared to chloramination or other oxidants, however, this much yield is expected to be negligible under drinking water treatment conditions.

Ozone

Ozonation of DMA forms NDMA but yields generally are <0.02% at neutral pH (16). The yield of reaction was somewhat higher than 0.02% yet still below 0.4% molar conversion with the increasing pH (16). In another study of NDMA

formation, Yang et al. (17) used a nitrosation pathway to generate the formation of NDMA from DMA at pH level of 3.4. They also observed, through an unknown pathway, the formation of NDMA during ozonation at a level of pH greater than 7.0. Subsequent studies of NDMA formation during ozonation showed that *1,1*-Dimethyl Hydrazine (UDMH), daminozide and semicarbazide, both with UDMH-like functional groups, formed NDMA at yields >50% (5, 18, 19). The ozonation of *N,N*-Dimethylsulfamide (DMS), a transformation product of the fungicide tolylfluanide, was observed to form NDMA at a 52% yield (18). Lastly, the ozonation of polyDADMAC, a polymer used in water treatment plants also formed NDMA (20). These results clearly indicate that the ozonation of polyDADMAC can release the DMA moiety while concurrently forming hydroxylamines. The simultaneous reaction of these two products could form UDMH, at which point the formed UDMHs would be converted to NDMA in the presence of ozone.

Permanganate

Andrzejewski and Nawrocki (21) have shown that potassium permanganate reaction with DMA led to the formation of NDMA. The highest observed yield was 0.04% molar conversion under very high permanganate concentrations (i.e., 700 mg/L) and alkali pH conditions (pH>8.35). Compared to the chloramination or other oxidants, this much lower yield is expected to be negligible under actual drinking water treatment conditions.

UV Irradiation

Ultraviolet (UV) irradiation of nitrite at <400 nm could form reactive nitrogen species (22, 23), and those reactive species can react with secondary amines present in waters. NDMA formation yields were reported less than 0.02% from selected secondary amines with UV-A at 300-400 nm wavelengths with the highest yields observed at alkali conditions (pH ≈10.0) (22). Similar findings have also been reported by Soltermann et al. (23). UV-C treatment at 254 nm wavelength (dose of 350-850 mJ/cm²) of chlorinated secondary amines in the presence of monochloramine increased nitrosamine concentrations at swimming pools (23). However, this NDMA formation mechanism is unlikely to be important for drinking waters due to the low prevalence of secondary amines. Furthermore, UV leads to breakage of N-N bond destroying the NDMA molecule (24). Additional discussion about NDMA's removal by UV can be found in the next section.

The Use of Pre-Oxidants for NDMA Control

The oxidants described below, which are commonly used in drinking water treatment, have been evaluated in different studies for transforming nitrosamine precursors.

Chlorine

The high reaction kinetics of both chlorine and amines (i.e., NDMA precursors) makes pre-chlorination an effective strategy for minimizing NDMA formation (25). However, the use of chlorine also leads to the formation of halogenated DBPs, of which the trihalomethanes (THMs) and haloacetic acids (HAAs) are regulated, which may limit the application of chlorine as a pre-oxidant.

The chlorination of wastewaters with ammonia can also cause the formation of chloramines, which can react with certain forms of organic nitrogen to produce NDMA. This phenomenon in turn causes the formation of NDMA in secondary wastewater effluents (2). Therefore, prior to the application of chlorine for controlling NDMA formation, the ammonia levels in the water should be analyzed because high levels of ammonia can hinder the inactivation of NDMA precursors. Lauer (26) observed this phenomenon while investigating the use of oxidants for controlling the discharge of NDMA precursors in wastewaters. Presence of ammonia higher than 0.5 mg/L in wastewater samples was sufficient to negate the chlorine at doses 5-10 mg/L. Only after the breakpoint chlorination, removal of NDMA precursors was observed which was achieved at 20 mg/L chlorine dose. However, the wastewater samples that contained ammonia levels lower than 0.5 mg/L, even 5 mg/L of chlorine dose achieved the removal of NDMA precursors by 25 to 50% in two minutes of contact time. Higher NDMA precursors removal (70-95%) with increasing chlorine doses and contact times (26). The distinct effect of ammonia, however, precluded the mention of studies in this review that concern unintended chloramination during the pre-chlorination process.

Charrois and Hrudrey (27) investigated two full-scale water treatment plants as well as some bench-scale experiments with samples collected from those treatment plants. Their results have showed that 2 mg/L free-chlorine contact of two hours followed by an additional 2 mg/L chloramine, resulted in lower NDMA levels (16 ± 3.5 ng/L) compared to no free-chlorine contact time (51 ± 8.3 ng/L). In these bench-scale experiments, they found that a higher dose of free chlorine (4 mg/L) applied for two hours followed by a 4 mg/L chloramine dose, resulted in even lower NDMA formation (3 ± 0.7 ng/L). In samples collected from surface water and the Iowa River (Total Organic Carbon [TOC] = 3.4 mg/L), Chen and Valentine (28) found that NDMA formation decreased with the application of free chlorine. The samples were exposed to 0.08 mM of free chlorine at pH 7.0, which reduced NDMA formation from ~ 32 ng/L to ~ 12 ng/L within 5 minutes of contact time and reached the lowest NDMA formation potential (FP) of ~ 6 ng/L after 120 minutes. Furthermore, the amount formed decreased with an increase pre-chlorination dosage for a fixed free chlorine contact time. One hour contact time with chlorine doses of 0.035, 0.05, 0.06, and 0.08 mM reduced NDMA FP to ~ 26 , ~ 18 , ~ 10 and ~ 6 ng/L, respectively, from the original NDMA FP of ~ 33 ng/L (with no chlorine exposure). In their studies, they determined that an increase in both the chlorine dose and contact time decreased the formation of NDMA during subsequent chloramination.

In another study, grab samples were collected upstream of any oxidant addition for 10 source waters (29). Following pre-chlorination, samples were

chloraminated for 72 hours under uniform formation conditions (UFC) and then analyzed for NDMA formation. In general their findings have shown that chlorine can reduce the NDMA formation by more than 50% within a concentration \times time (CT) of <70 mg \times min/L. For instance, pre-chlorination of one of the samples (pH=8.3, TOC=5.0 mg/L, Br=170 μ g/L, NH₄⁺=0.06 mg/L) reduced NDMA formation from 25 to 5 ng/L by a CT of 37 mg \times min/L (29). They also determined that the pre-oxidation with chlorine at a low exposure followed by chloramination increased NDMA formation for three wastewater-impacted source waters. In all three samples, the NDMA formation increased significantly at the lowest exposure, representing a 3 minute contact time with chlorine before ammonia addition, but declined at higher exposures (29). Because all three sample waters contained some level of nitrite, it was hypothesized that NDMA formation was perhaps due to the reaction of chlorine with nitrite that formed N₂O₄ (29), a nitrosating agent linked to the NDMA formation. It was also possible that the increase in NDMA at low exposures was because the chlorination converted NDMA precursors to more potent forms, an effect observed by Chen and Valentine (28). At higher exposures, however NDMA formation declined, likely because of the deactivation of these more potent NDMA precursors (29).

In separate study of samples at a water facility, Uzun et al. also reported a decrease in NDMA formation in chlorine treated waters (30). In the utilities they surveyed even small doses of chlorine (i.e., 0.5 mg/L) used for maintenance purposes were found to decrease NDMA FP by an average of 10%. Furthermore, the application of chlorine prior to the addition of ammonia in clearwells resulted in a removal rate of 10 to 65%. The minimum and maximum chlorination CT in these clearwells was 101 mg \times min/L and 504 mg \times min/L, respectively. However, no strong correlation was observed between the chlorine CT and NDMA FP reduction at the full-scale plants surveyed.

Several mechanistic studies have also been undertaken to elucidate the pre-oxidation of NDMA precursors. These studies can be classified based on the group of amines investigated: *(i) Secondary Amines:* The NDMA formation from the secondary amine, namely DMA, decreased from 1.6% to 1.1% within 5 minutes (CT of 15 mg \times min/L) of contact time with chlorine. This increased chlorine contact time (CT of 180 mg \times min/L) did not result in a further decrease in NDMA formation (19). Previous studies also indicated the high reactivity of DMA with chlorine (k_{app} at pH 7 \approx 104 M⁻¹ s⁻¹), which caused the formation of chlorinated-DMA (23, 25, 31). Therefore, formed chlorinated-DMAs could remain in the solution and still form NDMA during sequential chloramination. *(ii) Tertiary Amines:* Research performed by Shen and Andrews (32) examined the impact of pre-chlorination on NDMA formation from tertiary amines (amine-based pharmaceuticals). Here, eight pharmaceuticals (i.e. ranitidine, nizatidine, tetracycline, doxylamine, chlorphenamine, carbinoxamine, diltiazem, and sumatriptan) were examined under contact times of 0.5 to 120 minutes with chlorine ([Cl₂]₀ = 2.5 mg/L). Their results showed no change in the rate of NDMA formation from diltiazem upon pre-chlorination. Surprisingly, however, the chlorination of sumatriptan resulted in a three-fold increase of the initial yield. Except for those two precursors, the NDMA formation from other pharmaceuticals decreased by 10 to 90% with an increases in the pre-chlorination

contact time (32). In their investigation of the interactions between chlorine and tertiary amines, Selbes et al. (19) examined the pre-chlorination at different contact times (5 to 60 minutes) with chlorine ($[\text{Cl}_2]_0 = 3 \text{ mg/L}$) at pH 7.5 from a wide array of NDMA precursors. After chlorination, with the exception of compounds in both the carbonyl and sulfonyl groups, an overall decrease in the NDMA formation rate was observed, which was influenced by the selected tertiary amines. The NDMA yield of the former compounds decreased to approximately half of the initial yield during pre-chlorination within 5 to 15 minutes, resulting in a corresponding CT of 15 to 45 $\text{mg}\times\text{min/L}$ (19). (iii) *Quaternary Amines:* There are mixed findings for the pre-chlorination of quaternary amines, and the reasons for those differences remain unclear. Chlorination had no distinct effect on the NDMA yields from quaternary amines (polyDADMAC, polyamine and polyACRYL), because the positive charge on the nitrogen atoms of the polymers hindered the nucleophilic substitution (9, 19). A separate analysis however, did indicate that the pre-chlorination of polyDADMAC and polyAMINE did decrease NDMA formation within 10 minutes of contact time (33). The decrease was attributed to the structural changes of either the polymers or the DMAs, which made them less reactive to further chloramination.

Overall, the effectiveness of pre-oxidation with chlorine is highly dependent on the type of precursors, a finding supported by mechanistic studies. There are also precursors that exhibit no reactivity with chlorine. Indeed, chlorination has caused an increase in NDMA formation, which occurred i) in the presence of nitrite from chlorine-triggered nitrosation pathways, or ii) or in the presence of ammonia-forming chloramines that then directly created NDMA.

Chlorine Dioxide

Chlorine dioxide is sometimes used in lieu of chlorine in water treatment processes as it produces fewer chlorinated organic substances, does not form THMs, and significantly suppresses the formation of HAAs. A potential drawback, however, associated with the use of chlorine dioxide is that approximately 70% of the compound is reduced to chlorite (ClO_2^-), which is a regulated DBP in the United States. Chlorate (ClO_3^-) may also form, which while not currently regulated, is associated with adverse health effects at elevated concentrations (34).

Lee et al. (3) also used chlorine dioxide to investigate the effect of pre-oxidation on the NDMA FPs in natural waters from the Rhein, Neckar, and Pfalz rivers in central Europe and in Lake Greifensee, a small lake near Zurich, Switzerland. In experiments performed under typical drinking water treatment conditions an initial dose of 2.1 mg/L of chlorine dioxide at pH 7.0 were added to the samples. Subsequent results showed that the residual chlorine dioxide was quenched after 5 minutes. The samples were then chloraminated for NDMA FP analyses, which showed an NDMA FP removal rate ranging from 32 to 94% depending upon the water sample from a given river. In another study, grab samples were collected upstream of any oxidant addition for several source waters (29). Following pre-oxidation, samples were chloraminated for 72 hours under UFC conditions. After 72 hours, the chloramine residual was quenched, and the DBPs were analyzed. The results showed that a pre-oxidation with chlorine

dioxide exposure ($\text{mg}\times\text{min}/\text{L}$) resulted in a reduction in NDMA formation in some samples by an average of 50% (29). Pre-oxidation with chlorine dioxide reduced the NDMA formation to approximately 7-9 ng/L at the highest exposure. These results, however, were not concurrent with all source waters sampled in the study. Pre-oxidation with chlorine dioxide increased NDMA formation by an average of 50%. The water samples with an elevated level of NDMA were affected by wastewaters, polyDADMAC polymers, and anion exchange resin-related precursors, making it likely that pretreatment with chlorine dioxide converted the precursors in these source waters to more potent forms (29).

In another study, 12 water sources (9 surface water, 1 groundwater, and 2 wastewater effluents) were exposed to pre-oxidation with chlorine dioxide at a dose of 1.0 mg/L at pH 6.0 to 7.0 (35). After chlorine dioxide pretreatment, reductions in NDMA FP were observed in most of the samples (with a top range of ~33%). Although an average reduction of 58% was observed in the wastewaters under study, in other samples NDMA FP either remained relatively constant or increased (with a top range of ~140%).

In a recent study to determine the effect of pre-oxidation, Uzun et al. (36) conducted experiments using chlorine dioxide on NDMA FPs in pristine surface waters blended with wastewaters at different facilities. While they found that chlorine dioxide both increased and decreased in the levels of NDMA FP, chlorine dioxide oxidation was more effective in NDMA formation in wastewater impacted sources than non-impacted sources. Also, the percentage of the NDMA precursor removed using chlorine dioxide increased with an increase in the level of wastewater (36). They also observed a rapid oxidation of chlorine dioxide (<10 min. contact time), which resulted in a maximum level of NDMA FP removal in all waters in their study. Lauer (26) investigated the effect of pre-oxidation in five wastewater samples collected prior to disinfection and exposed them to 2.5, 5, and 10 mg/L at contact times of 2-60 minutes. Chlorine dioxide was observed to be the most efficient in removing NDMA precursors with the highest removal (~90%) at a dose of 10 mg/L. At a dose of 2.5 and 5 mg/L, however, the removal rate was much greater, ranging from 19% to 90% depending on the dose, contact time and background organic matter concentrations. These lower reductions at the lower doses was perhaps due to a competition for the chlorine dioxide between the background organic matter and the NDMA precursors (26).

There are also model compound studies in the literature that can provide insight regarding these mixed results regarding chlorine dioxide pre-oxidation in natural water samples. For example, in their 2007 study to determine the change rate of NDMA FP in eight model precursors (i.e., DMA, trimethylamine) to 0.5 or 1.0 mM of chlorine dioxide at pH 7.0, they observed no distinct difference in the DMA in the NDMA FP. However, pre-oxidation with chlorine dioxide of the other tertiary amines did reduce the presence of NDMA FP from 41 to 63% (3). In another comprehensive mechanistic study recently conducted by Selbes et al. (19), they examined the effectiveness of pre-oxidation with chlorine dioxide ($[\text{ClO}_2]_0 = 1 \text{ mg/L}$) at different contact times (5 to 30 minutes) and in a pH range of 7.5 for 15 NDMA precursors, including secondary amines, tertiary amines and quaternary amines. They observed no obvious reactivity of the DMA to the

chlorine dioxide. The exposure of chlorine dioxide to a high level of NDMA yielded (>5%) precursors, which in turn decreased the formation of NDMA formation. However, upon contact with chlorine dioxide, tertiary amines (e.g. methylene blue) with a low NDMA formation (<1%) increased the level of the NDMA FP. This increase was attributed to a release of the DMA moiety from the parent compound, which transformed the moiety into a more potent form. These findings suggest that the origin of the various deactivation efficiencies of precursors may be attributed to one single major product, namely DMA. Consequently, the application of chlorine dioxide as a pre-oxidant to control NDMA formation could be effective in source waters with high levels of NDMA yielding precursors (i.e., >5%). For source waters containing either DMA or lower NDMA yielding precursors than DMA as major precursors (i.e., <1%), however, the application would be redundant (19). These findings are supported by studies from both Selbes et al. (19) and Park et al. (33), who reported that the pre-oxidation of quaternary amines (polyDADMAC, polyAMINE, and polyACRYL) with chlorine dioxide did not affect the overall NDMA yields.

These findings indicate that pre-oxidation with chlorine dioxide can either increase or decrease NDMA formation. It is more likely that the chlorine dioxide treatment would be beneficial for utilities if the water does have a wastewater content. The use of chlorine dioxide may be detrimental, however, for those utilities with a low level of reactivity precursors in their source waters.

Ozone

Ozone is a strong oxidizing agent that can oxidize many organic and inorganic compounds in water. While ozone does not lead to the formation of halogenated DBPs, it can lead to the formation bromate (BrO_3^-), which is a regulated DBP in the United States.

Previous studies with ozone have provided some promising results to reduce NDMA formation, despite some observations reporting enhanced NDMA formation (3, 19, 27–29, 37, 38). The overall body of research here shows ozone an effective oxidant for reducing NDMA formation, likely because of the high reaction rate constants with amines, especially in their deprotonated forms (25). For example, ozone reduced NDMA formation by over 50% within a very short contact time (i.e., $\text{CT} \leq 0.5 \text{ mg} \times \text{min/L}$) (3, 28, 29), with only a few cases of ozonation actually causing the formation of NDMA (18, 39).

In their study to determine pre-oxidation in the Rhein, Neckar, and Pfingz rivers and in Lake Greifensee, Lee et al. also investigated the effect of pre-ozonation on the NDMA FPs in those waters (3). Oxidation treatments were performed under typical drinking water treatment conditions with 1 and 2 mg/L of ozone at pH 7.0. The NDMA FPs of the treated natural waters was then measured after a complete depletion of the ozone, with a removal rate ranging from 32 to 94% depending on the natural water. There was however, no distinct difference between two ozone doses. In another study to determine the effects of treated wastewaters, polyDADMAC polymers, and anion exchange resin on ten different natural systems, Shah et al. (29) observed that ozone similarly reduced NDMA formation by as much as 50% and at exposures as low as $0.4 \text{ mg} \times \text{min/L}$.

Zhao et al. (40) used ozone as an oxidant to control the formation of NDMA in two source waters, with the contact time set as the length of time required to achieve the desired dose ($CT = 10 \text{ mg}\times\text{min/L}$). In both instances, higher concentrations of NDMA were recorded compare to the untreated source waters used as the control. The DMA pathway reported by Andrzejewski et al. (16) was found to be cause of this NDMA formation during ozonation. In a similar study supporting these finds, Zhao et al. (40) also investigated ozonation followed by chlorination in two separate water bodies, and observed higher concentrations of NDMA over the ozone treatment alone.

These results suggested that the ozone oxidation of natural organic matter may release precursors into the source waters that can react with chlorine to form NDMA. Although Zhao (40) examined ozonation only and then ozonation followed by chlorination, the increasing trend involving the use of ozonation closely agrees with more recent analysis. In one German study detailing how elevated NDMA formation potentials might affect ozonation in areas of the country under intense agricultural cultivation, DMS, was detected in ground and surface waters at concentrations ranging from 100-1000 ng/L and 50-90 ng/L, respectively (5). Batch ozonation experiments in ultrapure buffered water, surface water, and tap water found that 52% of the DMS, created from the degradation of the tolylfluanide fungicide, was converted to NDMA (5). The researchers also identified the following precursors that exhibited high NDMA conversions during ozonation: *N,N*-dimethyl-*N'*-(4-methylphenyl)-sulfamide, tolylfluanid, daminozid. The authors also found that a 54% molar conversion rate of the NDMA yield for an initial concentration of DMS (5). Similarly, von Gunten et al. (18) examined how bromide, from DMS, might affect NDMA formation. Although the initial ozonation of DMS in samples of phosphate-buffered ultrapure water ($\text{pH} = 7.0$) yielded a low rate of NDMA conversions (<3%), the addition of a few $\mu\text{g/L}$ of bromide substantially enhanced the NDMA formation during the ozonation process. Notably, this addition of bromide to levels of 15 – 20 $\mu\text{g/L}$, which are typical for drinking waters, greatly enhanced the maximum NDMA yield to approximately 50%.

A similar study, but in Japan, was undertaken to determine the association of NDMA formation (2.2-10 ng/L) and ozonation in finished drinking waters from the Yodo River (37). Relatively high concentrations of NDMA were found after ozonation of water samples taken from wastewater treatment plants located upstream of the water intake points of the drinking water treatment plants in the Yodo River basin, and the NDMA formation was associated with the anti-yellowing agents used by the industries.

In the United States, ozone induced NDMA formation in drinking water treatment plants have not been observed so far. In 10 water samples, ozone reduced NDMA formation by over 50% within a very short contact time (i.e., $CT \leq 0.5 \text{ mg}\times\text{min/L}$) (29). Recently, Lauer (26) investigated the effect of pre-ozonation in five wastewater samples collected prior to disinfection and exposed them to 2.5, 5, and 10 mg/L at contact times of 2, 5, and 10 minutes. Ozone was highly effective at removing NDMA precursors, and reacted very quickly. A higher than 90% decrease in NDMA FP was observed with a 2.5 mg/L ozone dose and 2 minutes of contact time, with little to no further removal

observed after 2 minutes or higher doses of ozone. However, ozonation can lead to the formation of NDMA in some wastewater discharges (41, 42). In selected wastewaters the net direct formation of NDMA of 6-33 ng/L was observed after ozonation by Pisarenko et al. (41). Similar findings, reported by Gerrity et al. (42) indicated that ozonation may lead to the direct formation of both NDMA and some other nitrosamines (i.e., *N*-nitrosomorpholine). A recent survey also indicates that the de facto use of wastewater in drinking water treatments is increasing in the US (43). In the light of these studies, ozone triggered NDMA formation may well occur in US drinking water treatment plants impacted by wastewaters in the near-future.

A number of mechanistic studies connected ozonation to the significant removal of NDMA precursors at low CT values (<1 mg×min/L) (3, 19). Other studies, however, indicate the occurrence of NDMA formation during ozonation, specifically from model compounds with *N,N*-dimethylamino functions (including secondary, tertiary and quaternary amines) (19, 20, 33, 38, 39, 44).

This NDMA formation can occur through the liberation of the DMA moiety that reacts with ozone to form NDMA; and (ii) through direct a reaction of the precursor to form NDMA. In their investigation of the pre-oxidation at different contact times (1 to 10 minutes) with ozone ($[O_3]_0 = 3$ mg/L), Selbes et al. (19) found that NDMA forming compounds had the highest NDMA yields within 1-2 min, and that the overall NDMA formation decreased with an increase in contact time.

Ozone decomposes spontaneously in water though a complex mechanism that involves the generation of hydroxyl free radicals (45), which can also decompose NDMA (19, 46). In experiments both with and without hydroxyl radical scavengers, Lv et al. (46) identified the transformation products using mass spectrometry. Results indicated that hydroxyl radicals did indeed decompose NDMA into DMA and the following nitrogenous compounds: methylamine, nitromethane, and ammonia. Recently, Selbes et al. (19) has reported that while ozone may stimulate NDMA formation from some precursors, the simultaneous production of hydroxyl radicals would work against this effect.

The overall premise, based upon these findings is that ozone has been shown as an effective method for removing NDMA precursors. It may also, however, cause NDMA formation without subsequent chloramination. Hydroxyl radicals formed from the decomposition of ozone would decompose the formed NDMA, reducing the overall levels at longer contact times. Indeed, case studies in Germany and Japan have shown that ozonation may increase NDMA formation, which was attributed to anthropogenic contaminants. Such cases have yet to be reported in any US water treatment operation, however.

Other Oxidants/Disinfectants

Other oxidants/disinfectants, such as potassium permanganate (KMnO₄), hydrogen peroxide (H₂O₂), ferrate, and UV irradiation, are all viable disinfectant alternatives in drinking water treatment processes. A brief overview of these oxidants/disinfectants and certain treatment strategies are elucidated in this section.

Chen and Valentine (28) examined the influence of three pre-oxidation strategies (sun simulation, hydrogen peroxide and potassium permanganate) on the NDMA formation in the Iowa River to determine any correlation in specific UV absorbance (SUVA) caused by oxidation. They observed in sample concentrates (TOC = 3.4 mg/L, pH = 7.0, $[\text{NH}_2\text{Cl}]_0 = 0.05 \text{ mM}$), a decrease in NDMA formation for both oxidants. The application of 10 mg/L permanganate for a contact time of one hour reduced NDMA formation by approximately 50% compared to samples not subjected to pre-oxidation. Although a notable decrease, it was achieved with permanganate doses much greater than used in typical drinking water treatment strategies. Overall, the standard dosage of permanganate in drinking water treatment protocols neither contributed to NDMA formation nor did it destroy NDMA precursors.

Ferrate was also the subject of study regarding its use as a pre-oxidant (in the form of potassium ferrate (K_2FeO_4)) on natural waters and in synthetic buffered solutions containing NDMA precursors. Mechanistic studies with model precursors, specifically DMA and trimethylamine, in which ferrate (1.0 mM) at pH 7.0 was used to determine the NDMA FP of precursors (0.1 mM) both with and without pre-oxidation (47). The pre-oxidation with Fe(VI) for 10 seconds reduced the fast-reacting compounds by 89–99% (dimethyldithiocarbamate, dimethylaminobenzene, 3-(dimethylaminomethyl)indole, 4-dimethylaminoantipyrine), unlike the slow-reacting compounds (DMA, trimethylamine, dimethylethanolamine, dimethylformamide), which did not. There was however a high (95%) NDMA FP rate of removal for most precursors for all samples subjected to pre-oxidation for 30 minutes. In this same study, the effectiveness of ferrate on natural water samples from the Rhein, Neckar, and Pfalz rivers in Germany and Central Europe was also investigated. A high and a low dose (21 and 1.1 mg/L as Fe) were used in determining the effectiveness of ferrate in reducing NDMA precursors and formation. At the higher dose of 21 mg/L, the NDMA FPs of the natural waters was significantly reduced with an efficiency of 46 – 84%. However, there was no significant removal of NDMA FP (5 – 25%) for the dose of 1.1 mg/L. In another study, 12 water sources (9 surface waters, 1 groundwater, and 2 wastewater effluents) were exposed to pre-oxidation with ferrate at a dose of 20.0 mg/L as Fe at pH 6.0 to 7.0 (35). The findings of that study showed that that is was possible to remove nearly 80% of the NDMA precursors after the depletion of the ferrate. Although no change in NDMA formation was reported in three surface waters, in several samples the authors reported an increase in NDMA formation of 60%.

In their Iowa River study, Chen and Valentine (28) also tested the viability of using hydrogen peroxide as a pre-oxidant. Using a concentrate of 3.0 mg/L of hydrogen peroxide, they reduced NDMA formation by approximately 50% compared pre-oxidation levels. They also determined that an elevation in e peroxide concentration to 30.0 mg/L increased the removal of NDMA precursors to as high as 70%. For both doses of peroxide the minimum NDMA formation occurred 40 minutes after the introduction of hydrogen peroxide; no further increases were observed after that time, even after 120 minutes (28). The coupling of hydrogen peroxide with ozone was expected to increase the removal percentage of NDMA due to the reaction of hydroxyl radicals with either precursors. This

reaction would in turn either decrease precursor reactivity or destroy any formed NDMA during ozonation. Indeed, a recent study conducted by Pisarenko et al. (41), reported that the use of ozone/peroxide was 20% more effective in removing NDMA precursors than with ozone alone.

Factors Influencing Effectiveness of Pre-oxidants

As the background water chemistry is likely to affect the efficiency of the oxidants described in the previous section, the influential factors of pH, temperature, background organics and background inorganics are next described.

pH

Reactions between amines and oxidants are highly sensitive to pH changes (25), which in turn increases the overall NDMA formation from amine precursors. Indeed, most of the amines have high pK_a values (i.e., DMA's pK_a is 10.6), and it is well-known that chlorine reacts with deprotonated NDMA precursors. Therefore, the mid-point of pK_a 's of two reactants during chlorination will represent an optimum pH for the inactivation of NDMA precursors since both species may coexist at the highest concentrations (25). Similarly, chlorine dioxide and ozone also reacts more rapidly with deprotonated amines (25). Since these two oxidants lack pK_a 's, the reaction is only limited by the availability of deprotonated amines, possibly indicating the importance of the oxidation pH in NDMA deactivation. These mechanistic findings in relevance to NDMA precursors have been reported by Selbes et al. (19). Specially, by switching the pre-oxidation pH from 5.5 to 8.5 (for chlorine, chlorine dioxide, and ozone), they increased, by ten-fold, the level of NDMA precursor *N,N*-dimethylisopropylamine's removed within the same CT of an oxidant. Furthermore, a recent investigation of the pre-oxidation with chlorine dioxide showed the importance of pH in surface waters and wastewater impacted waters (36). In that study, an increase in the pre-oxidation pH from 6.0 to 7.8 increased the removal of the NDMA precursor removal by 20 to 40%. These findings indicate the importance of pH during pre-oxidation of NDMA precursors.

Temperature

It is well-know that the reactivity (i.e., reaction kinetics) of pre-oxidants is dependent on the temperature. A study conducted by Krasner et al. (48) showed that chlorine was more effective in destroying NDMA precursors at 25°C than at 5°C. This finding indicates that the efficiency of precursor removal by pre-oxidation may change throughout the year depending on the season. Therefore, utilities may need to develop different strategies control their NDMA formation especially during cold months.

Background Ions

As discussed previously, nitrite also reacts with chlorine to form NDMA without chloramination (14, 26, 29). The presence of ammonia can also cause the formation of chloramines which would decrease the efficiency of pre-oxidation result in the direct formation of NDMA (2, 26). The presence of background ammonia may also shift the chloramine speciation which would influence the overall NDMA formation (10). Bromide can also enhance the formation of NDMA during chloramination at concentrations higher than 400 µg/L (8, 29). Furthermore, ozone can also react with bromide and act as a catalyst for the formation of NDMA from DMS at low concentrations (15-20 µg/L) (5, 18).

Background Organics

Background organics can compete for chloramine species and decrease the NDMA formation from some NDMA precursors (10). Furthermore, it is expected that the presence of background organic matter would create competition with NDMA precursors for the pre-oxidants. Consequently, this competition would affect the overall efficiency and the kinetics of NDMA precursor inactivation. This impact can be clearly seen during the pre-oxidation of surface waters spiked with NDMA precursors in which the removal of NDMA precursors have been reported to be lower compared to lab grade water (3, 32). This hindrance was also observed during pre-oxidation with chlorine dioxide in waters (30) and wastewaters (26). However, there has been no systematic investigation to determine the effect of organic matter, on NDMA formation especially during pre-oxidation of NDMA precursors.

The Use of UV for NDMA Control

The use of UV treatment at doses less than 100 mJ/cm² has yielded a minimal effect on NDMA precursors in both surface waters and wastewaters, with a 10 to 20% decrease in NDMA formation at advanced oxidation doses (<2000 mJ/cm²) (26, 29). In another study, the effects of oxidation of treatment water by various simulated sunlight (250 W/m²) up to 60% removal of NDMA precursors was achieved within 2 hours (28). Both studies suggest the poor efficacy of UV treatment in mitigating NDMA precursors under typical drinking water disinfection conditions. While UV can also cause NDMA formation (22, 23), this has yet to occur in a full-scale water treatment operation.

Although UV treatment is seemingly ineffective for NDMA precursor control, it is most effective for destroying NDMA that are present. NDMA removal by sunlight has been shown to ranges from 12% to 65% within 1.5 hours and almost complete NDMA removal was observed after 3.0 hours (49). Moreover, low pressure UV produces light in a narrow band of 254 nm wavelength which is between the NDMA absorption bands, and medium pressure UV lamps produce wavelength in the range of 200 to 270 nm which also covers the NDMA adsorption bands. NDMA has an adsorption peak at 228-nm wavelength and strongly absorbs UV light from 185 to 275 nm. It also weakly absorbs from 330 to 400 nm (24).

Therefore, UV light between the absorption bands will lead to the breakage of N-N bond destroying the NDMA molecules (24). Due to the low (nanograms per liter) concentrations of NDMA desired in the distribution system, UV exposure must be operated at higher doses (i.e., 600-800 mJ/cm²) than typically used for disinfection (i.e., 100 mJ/cm²) (24). In a study, 90% reduction of NDMA was achieved at 1000 mJ/cm² of UV exposure, approximately 10 times higher than that required for virus removal. NDMA reduction using UV irradiation is technically feasible but expensive (50, 51). The principal by-products of UV photolysis of NDMA are DMA and nitrite (50, 52). The released DMA's could react with residual chlorine or chloramine and continue to form NDMA. However, the yield of this reaction is relatively low ($\leq 3.0\%$). Consequently, UV exposure (i.e., in clearwells) is an effective strategy for controlling the NDMA levels in distribution systems.

Conclusions

As a review of the studies in this chapter clearly show, the use of pre-oxidation prior to disinfection with chloramines is a promising NDMA control strategy for some utilities. However, each oxidant has its own associated regulated DBP formation and has a varying degree of efficiency in reducing NDMA formation. Key findings from the literature are summarized in Table 2.

Although an increase of the CT of chlorine prior to chloramination did decrease the amount of NDMA formation, utilities employing this method of precursor control must be cautious, as regulated carbonaceous-DBPs (i.e., THMs and HAAs) may result. In studies of several wastewater sources, pre-chlorination caused an increase in NDMA formation due to the nitrosation pathway facilitated by the presence of nitrite. Even though ozonation is very effective in destroying NDMA precursors at low CT values, ozonation still leads to an increase in NDMA via direct formation from specific precursors (i.e., amides). Although chlorine dioxide is a potential mechanism for controlling NDMA formation, it may increase the overall NDMA formation-like ozone depending on the precursors in the source water. Both chlorine dioxide and ozone may convert precursors into more potent forms (by liberating the DMA moiety). Thus, there is no single oxidant that is effective for controlling NDMA in all water types, but rather their effectiveness is highly dependent upon the characteristics of the existing precursors in source waters. Furthermore, each of those oxidants is associated with a regulated DBP formation (THMs, HAAs, chlorite, bromate), which results in a trade-off between the destruction of NDMA precursors and other DBPs formation. The other oxidants/disinfectants including permanganate, ferrate, peroxide and UV, did, however exhibit a negligible effect on NDMA precursors. Of these, UV was found quite effective in the destruction of formed NDMA's.

The selection of pre-oxidant type, dose and application location for NDMA control will be site-specific. Managers in water utilities that intend to use pre-oxidation as a strategy for NDMA control should also assess the effects on the formation of regulated DBPs as well as other unintended consequences inherent with the use of oxidants.

Table 2. Summary of Key Findings from the Literature

	<i>NDMA Formation</i>	<i>Pre-Oxidants/ Disinfectants Effect on NDMA Precursors</i>		<i>Reaction with NDMA</i>	<i>Other DBPs of Concern</i>
		<i>Source Waters</i>	<i>Model Compounds</i>		
Chlorine	Direct NDMA formation has been reported during chlorination in the presence of nitrosating agents (4) but unlikely to be significant compared to chloramination in drinking water treatment conditions.	<ul style="list-style-type: none"> · Chlorine can reduce the NDMA formation by more than 50% within a concentration×time (CT) of <70 mg×min/L (27, 29, 30). Even at low doses (0.5 mg/L) used for maintenance purposes 10% NDMA FP removal can be achieved (30). · May lead to increased NDMA formation in the presence of nitrite which may be a concern in wastewaters impacted sources (29). 	<ul style="list-style-type: none"> · High reactivity with DMA to form chlorinated DMAs (19, 23, 25, 31). · Effectiveness depends on the tertiary amines structure. May lead to increases, decreases or have no effect in NDMA formation (19, 32). · No change or some decreases in NDMA FP from quaternary amines (19). 	NA	THMs HAAs
Chlorine Dioxide	Direct NDMA formation has been reported (15) but unlikely to be significant compared to chloramination in drinking water treatment conditions.	<ul style="list-style-type: none"> · NDMA precursors can be removed in the range of 19-90% (3, 26, 36). · May lead to increased NDMA formation by an average of 50-140% (29, 35, 36). 	<ul style="list-style-type: none"> · No reactivity with DMA (3, 19). · Effectiveness depends on the tertiary amines structure. May lead to increases or decreases in NDMA formation (3, 19). · No reactivity with quaternary amines (19, 33). 	NA	Chlorite Chlorate

Continued on next page.

Table 2. (Continued). Summary of Key Findings from the Literature

	<i>NDMA Formation</i>	<i>Pre-Oxidants/ Disinfectants Effect on NDMA Precursors</i>		<i>Reaction with NDMA</i>	<i>Other DBPs of Concern</i>
		<i>Source Waters</i>	<i>Model Compounds</i>		
Ozone	Direct NDMA formation has been reported and it can be comparable to chloramination in drinking water treatment conditions (18, 19, 37, 39).	<ul style="list-style-type: none"> · Can reduce NDMA formation by 32-94% within a very short CT (≤ 2 mg\timesmin/L) in both drinking waters and wastewaters (3, 26, 28, 29). · Some NDMA formation has been observed upon ozonation in surface waters (37) and wastewater effluents (41, 42). 	<ul style="list-style-type: none"> · Ozonation can remove NDMA precursors at low CT values (< 1 mg\timesmin/L) (3, 19). · NDMA can be formed during ozonation of precursors with <i>N,N</i>-dimethylamino functions (including secondary, tertiary and quaternary amines) (19, 20, 38, 39, 44). 	Ozone does not react with NDMA; however, \bullet OH formed during ozonation can decompose NDMA (19, 46).	Bromate
Potassium Permanganate	Direct NDMA formation has been reported (21) but unlikely to be significant compared to chloramination in drinking water treatment conditions.	<ul style="list-style-type: none"> · Not effective at doses relevant to drinking water treatment (28). · Can remove ~50% of NDMA FP at high doses (10 mg/L) (28). 	NA	NA	NA

	<i>NDMA Formation</i>	<i>Pre-Oxidants/ Disinfectants Effect on NDMA Precursors</i>		<i>Reaction with NDMA</i>	<i>Other DBPs of Concern</i>
		<i>Source Waters</i>	<i>Model Compounds</i>		
Potassium Ferrate	NA	<ul style="list-style-type: none"> · Not effective at doses relevant to drinking water treatment (1 mg/L as Fe) (35). · Can remove 46-84% of NDMA FP at high doses (21 mg/L as Fe) (35, 47). 	<ul style="list-style-type: none"> · Effectiveness depends on the tertiary amines structure. May decrease NDMA formation or have no effect on the precursor (47). 	NA	NA
UV Irradiation	Direct NDMA formation has been reported (22, 23) but unlikely to be significant compared to chloramination in drinking water treatment conditions.	<ul style="list-style-type: none"> · Relatively ineffective over exposures relevant to disinfection (<100 mJ/cm²) (26, 29). · 10-30% reduction of NDMA formation for UV fluence relevant to advanced oxidation (>1000 mJ/cm²) (26, 29). 	NA	UV leads to breakage of N-N bond (24). Moreover, •OH formed with UV (if applicable) can decompose NDMA (19, 46).	NA

NA: Information not available.

Acknowledgments

This review and some of the work presented in this review was supported, in part, by a research grant from the National Science Foundation (CBET 106657). However, the manuscript has not been subjected to peer and policy review of the agency and therefore does not necessarily reflect its views.

References

1. Chen, Z.; Valentine, R. L. *Environ. Sci. Technol.* **2007**, *41*, 6059–6065.
2. Mitch, W. A.; Sedlak, D. L. *Environ. Sci. Technol.* **2002**, *36*, 588–595.
3. Lee, C.; Schmidt, C.; Yoon, J.; von Gunten, U. *Environ. Sci. Technol.* **2007**, *41*, 2056–2063.
4. Sacher, F.; Schmidt, C. K.; Lee, C.; Von Gunten, U. *Strategies for minimizing nitrosamine formation during disinfection*; Water Research Foundation Report: Denver, CO, 2008.
5. Schmidt, C. K.; Brauch, H. J. *Environ. Sci. Technol.* **2008**, *42*, 6340–6346.
6. Mitch, W. A.; Krasner, S. W.; Westerhoff, P.; Dotson, A. 2009. *Occurrence and formation of nitrogenous disinfection by-products*; Water Research Foundation Report: Denver, CO, 2009.
7. Shen, R.; Andrews, S. A. *Water Res.* **2011**, *45*, 944–952.
8. Le Roux, J.; Gallard, H.; Croué, J.-P.; Papot, S.; Deborde, M. *Environ. Sci. Technol.* **2012**, *46*, 11095–11103.
9. Krasner, S. W.; Mitch, W. A.; McCurry, D. L.; Hanigan, D.; Westerhoff, P. *Water Res.* **2013**, *47*, 4433–4450.
10. Selbes, M.; Kim, D.; Ates, N.; Karanfil, T. *Water Res.* **2013**, *47*, 945–953.
11. Liu, Y. D.; Selbes, M.; Zeng, C.; Zhong, R.; Karanfil, T. *Environ. Sci. Technol.* **2014**, *48*, 8653–8663.
12. Choi, J.; Valentine, R. L. *Environ. Sci. Technol.* **2003**, *37*, 4871–4876.
13. Walse, S. S.; Mitch, W. A. *Environ. Sci. Technol.* **2008**, *42*, 1032–1037.
14. Shah, A. D.; Mitch, W. A. *Environ. Sci. Technol.* **2012**, *46*, 119–131.
15. Andrzejewski, P.; Nawrocki, J. *Water Sci. Technol.* **2007**, *56*, 125–131.
16. Andrzejewski, P.; Kasprzyk-Hordern, B.; Nawrocki, J. *Water Res.* **2008**, *42*, 863–870.
17. Yang, L.; Chen, Z. L.; Shen, J. M.; Xu, Z. Z.; Liang, H.; Tian, J. Y.; Ben, Y.; Zhai, X.; Shi, W. X.; Li, G. B. *Environ. Sci. Technol.* **2009**, *43*, 5481–5487.
18. von Gunten, U.; Salhi, E.; Schmidt, C. K.; Arnold, W. A. *Environ. Sci. Technol.* **2010**, *44*, 5762–5768.
19. Selbes, M.; Kim, D.; Karanfil, T. *Water Res.* **2014**, *66C*, 169–179.
20. Padhye, L.; Luzinova, Y.; Cho, M.; Mizaikoff, B.; Kim, J.-H.; Huang, C.-H. *Environ. Sci. Technol.* **2011**, *45*, 4353–4359.
21. Andrzejewski, P.; Nawrocki, J. *Water Res.* **2009**, *43*, 1219–28.
22. Lee, C.; Yoon, J. *J. Photochem. Photobiol. A* **2007**, *189*, 128–134.
23. Soltermann, F.; Lee, M.; Canonica, S.; von Gunten, U. *Water Res.* **2013**, *47*, 79–90.

24. Sedlak, D.; Kavanaugh, M. *Removal and Destruction of NDMA and NDMA precursors during wastewater treatment*; Water Reuse Foundation Report: Alexandria, VA, 2006.
25. Lee, Y.; von Gunten, U. *Environ. Sci. Technol.* **2010**, *44*, 555–566.
26. Lauer, J. P. The use of oxidants for NDMA precursor deactivation in wastewater treatment. Master's Thesis, Clemson University, Clemson, South Carolina, 2014.
27. Charrois, J. W. A.; Hrudey, S. E. *Water Res.* **2007**, *41*, 674–682.
28. Chen, Z.; Valentine, R. L. *Environ. Sci. Technol.* **2008**, *42*, 5062–5067.
29. Shah, A. D.; Krasner, S. W.; Lee, C. F. T.; von Gunten, U.; Mitch, W. A. *Environ. Sci. Technol.* **2012**, *46*, 4809–4818.
30. Uzun, H.; Kim, D.; Ates, N.; Karanfil, T. In *Proceedings of AWWA Annual Conference and Exposition*, Dallas, TX, 2012.
31. Deborde, M.; von Gunten, U. *Water Res.* **2008**, *42*, 13–51.
32. Shen, R.; Andrews, S. A. *Water Res.* **2013**, *47*, 2446–2457.
33. Park, S. H.; Padhye, L. P.; Wang, P.; Cho, M.; Kim, J. H.; Huang, C. H. *J. Hazard. Mater.* **2015**, *282*, 133–140.
34. Alam, M.; Cantwell, R.; Hofmann, R.; Andrews, R.; Rand, J.; Gagnon, G.; VanderMarck, M.; Moffat, E.; Andrews, S. *J. Environ. Eng.* **2008**, *134*, 478–485.
35. Yang, X.; Guo, W.; Zhang, X.; Chen, F.; Ye, T.; Liu, W. *Water Res.* **2013**, *47*, 5856–5864.
36. Uzun, H.; Kim, D.; Karanfil, T. In *Proceedings of AWWA Water Quality and Technology Conference*, New Orleans, LA, 2014.
37. Kosaka, K.; Asami, M.; Konno, Y.; Oya, M.; Kunikane, S. *Environ. Sci. Technol.* **2009**, *43*, 5236–5241.
38. Oya, M.; Kosaka, K.; Asami, M.; Kunikane, S. *Chemosphere* **2008**, *73*, 1724–1730.
39. Asami, M.; Oya, M.; Kosaka, K. *Sci. Total Environ.* **2009**, *407*, 3540–3545.
40. Zhao, Y. Y.; Boyd, J. M.; Woodbeck, M.; Andrews, R. C.; Qin, F.; Hrudey, S. E.; Li, X. F. *Environ. Sci. Technol.* **2008**, *42*, 4857–4862.
41. Pisarenko, A. N.; Stanford, B. D.; Yan, D.; Gerrity, D.; Snyder, S. A. *Water Res.* **2012**, *46*, 316–326.
42. Gerrity, D.; Pisarenko, A. N.; Marti, E.; Trenholm, R. A.; Geringer, F.; Reungoat, J.; Dickenson, E. *Water Res.* **2014**, *72*, 251–261.
43. Rice, J.; Wutich, A.; Westerhoff, P. *Environ. Sci. Technol.* **2013**, *47*, 11099–11105.
44. Marti, E. J.; Pisarenko, A. N.; Peller, J. R.; Dickenson, E. R. V. *Water Res.* **2014**, *72*, 262–270.
45. Hoigné, J.; Bader, H. *Water Res.* **1983**, *17*, 173–183.
46. Lv, J.; Li, Y.; Song, Y. *Water Res.* **2013**, *47*, 4993–5002.
47. Lee, C.; Lee, Y.; Schmidt, C.; Yoon, J.; Von Gunten, U. *Water Res.* **2008**, *42*, 433–441.
48. Krasner, S. W.; Lee, C. F. T.; Liang, S.; Mitch, W.; von Gunten, U.; Westerhoff, P. In *Proceedings of the AWWA Annual Conference and Exposition*, Dallas, TX, 2012.

49. Soroushian, F.; Shen, Y.; Patel, M.; Wehner, M. In Proceedings of AWWA Annual Conference and Exposition, Washington, DC, 2001.
50. Mitch, W. A.; Sharp, J. O.; Trussell, R. R.; Valentine, R. L.; Alvarez-Cohen, L.; Sedlak, D. L. *Environ. Eng. Sci.* **2003**, *20*, 389–404.
51. *Guidelines for Canadian Drinking Water Quality: Guideline Technical Document — N-Nitrosodimethylamine*; Health Canada, Ottawa, ON, 2011.
52. Bolton, J. R.; Stefan, M. I. In Proceedings of AWWA Water Quality and Technology Conference, Salt Lake City, UT, 2000.

Chapter 10

pH Effect on Nitrosamine Precursor Removal by Activated Carbon Adsorption

**Chao Chen,^{*,1,2,3} David Hanigan,⁴ Xiaobin Liao,^{1,5} Jun Wang,¹
Xiaojian Zhang,¹ I. H. (Mel) Suffet,³ Stuart W. Krasner,⁶
and Paul Westerhoff⁴**

¹School of Environment, Tsinghua University, Beijing 100084, China

²State Key Joint Laboratory of Environment Simulation and Pollution Control (SKLESPC), Beijing 100084, China

³Department of Environmental Health Sciences, School of Public Health, University of California at Los Angeles, Los Angeles, California 90095, U.S.A.

⁴School of Sustainable Engineering and the Built Environment, Arizona State University, Tempe, Arizona 85287-3005, U.S.A.

⁵College of Civil Engineering, Huaqiao University, Xiamen 361021, China

⁶Metropolitan Water District of Southern California, 700 Moreno Avenue, La Verne, California 91750, U.S.A.

*E-mail: chen_water@tsinghua.edu.cn.

Powdered activated carbon (PAC) adsorbs certain nitrosamine (NA) precursors from water. We hypothesized that varying pH levels influence the extent of NA precursor removal. For two model NA precursors (ranitidine and chloropheniramine) and ambient NA precursors present in a treated wastewater (WW), removal increased on PAC at higher pH. However, the removal of NDMA formation potential (FP) from an aquaculture-impacted lake water by PAC declined at higher pH. The PAC adsorption results agreed with experimental findings from the Polarity Rapid Assessment Method (PRAM) for characterizing WW-derived NDMA precursors. The differences in NDMA precursor removal by PAC adsorption at varying pH between different waters was likely due to the different characteristics of NDMA precursors in the two water samples.

1. Nitrosamine Precursor Removal by Activated Carbon Adsorption

Several nitrosamines (NAs) are disinfection by-products, found in both wastewater (WW) and drinking water all over the world (1, 2). The present N-nitrosodimethylamine (NDMA) regulatory and notification levels in Ontario, Canada (9 ng/L), Massachusetts and California, U.S.A. (10 ng/L) present major challenges for drinking water treatment plants, especially for those with high NA formation potential (FP). A major source of NDMA precursors is from treated WW discharges (2). Some of these precursors can be attributed to the presence of pharmaceuticals and personal care products (PPCPs) (3).

Conventional coagulation, sedimentation, and filtration processes result in very limited removal of nitrosamine precursors (4). The basic strategies to control nitrosamine formation in water include precursor removal with powdered or granular activated carbon (PAC, GAC) (5, 6), destruction of precursors with pre-oxidation (6, 7), and/or optimization of the chloramination conditions (8).

AC adsorption is a practical process to remove non-polar or weakly polar organic contaminants of various molecular weights (MW), including taste- and odor-causing compounds, natural organic matter (NOM), endocrine disrupting chemicals (EDCs), PPCPs, pesticides, and precursors for halogenated disinfection by-products (DBPs). As PAC or GAC are considered for meeting multiple water quality objectives, it is important to understand factors influencing AC adsorption of nitrosamine precursors.

NA precursor removal by AC was recently studied due to its possible future regulation. Hanigan et al. demonstrated the potential of GAC and PAC to adsorb NDMA precursors from blends of river water and secondary effluent from a wastewater treatment plant (WWTP) (5). They suggested that “further research is needed to better understand NDMA precursor chemical properties”. Liao et al. reported that GAC was effective at removing several NA precursors (e.g., median of 88% for NDMA FP and 83% for N-nitrosodiethylamine [NDEA FP]) in a source water in China highly impacted by aquaculture (6). However, these investigations presented the removal efficacy or treatability of NA precursors by AC adsorption without discussion of the influence of key water quality factors.

Moreover, AC adsorption did not always result in satisfactory removal of NDMA FP under certain conditions. According to Krasner et al. (9) and Hanigan et al. (10), the addition of the amine-containing polymer polydiallyldimethylammonium chloride (polyDADMAC) contributed NDMA FP to the water that was recalcitrant to AC adsorption. Such an amine-containing polymer is of high charge density. Another unusual performance of AC adsorption occurred at one drinking water treatment plant (DWTP) in the U.S. where the water was lime softened at pH 11 and PAC was applied (9). The NDMA FP removal by AC was less than 20%. However, in subsequent sample events, NDMA FP removal was 42-58%. During the first sample event, the source water was not as wastewater-impacted as it was in subsequent events.

A previous study showed that the basic structure of NA precursors in secondary and tertiary effluent from a WWTP included a protonated amine functional group and a generally non-polar moiety (11). We hypothesized that

the potential for the amine functional group to be protonated could account for sensitivity to pH, whereas the non-polar moiety was responsible for strong adsorption by AC.

The efficiency of AC adsorption is affected by the interactions between the AC, the adsorbate, and the solvent. Thus, the influencing factors for NA precursor adsorption include AC surface characteristics, precursors properties, and the pH of the solvent (water). Therefore, we conducted experiments with different types of AC, different types of NA precursors, and at different pH levels in water.

Calgon WPH PAC (10) was used in this research in the laboratory at Arizona State University and the pulverized Calgon F400 GAC was used in the laboratory at Tsinghua University. The two ACs presented similar properties according to the tests reported in Table 1.

Jar tests were conducted for AC adsorption experiments. The jar test was conducted at 100 rpm. After the addition of certain amounts of PAC, the timer was started. After certain spans of adsorption time, the jar test was stopped. The PAC was removed from the solution by glass-fiber filtration. The residual concentration of known NDMA precursors or NDMA FP and other water quality indices of the water samples were measured.

Table 1. Properties of Activated Carbons Used in This Study

<i>Carbon name</i>	<i>Iodine number</i>	<i>Methylene blue number</i>	<i>BET (m²/g)</i>	<i>Pore volume (mL/g)</i>	<i>Micro-pore volume (mL/g)</i>	<i>Meso-pore volume (mL/g)</i>	<i>Macro-pore volume (mL/g)</i>
WPH	800		1185	0.840	0.412	0.329	0.099
F400	1071	225	1077	0.667	0.380	0.210	0.077

Note: Micropore is defined as having a diameter of 0 to 2 nm; mesopore and macropore from 2 to 50 nm and >50 nm, respectively. BET = Brunauer–Emmett–Teller theory specific surface area.

2. pH Effect on NDMA FP Removal by PAC Adsorption in Different Water Samples

Two water samples were used to investigate the effect of pH. One was a blended river/wastewater obtained by mixing secondary effluent of a WWTP (20% volume) and river water (80% volume), both from central Arizona, U.S.A. The other was taken from an aquaculture-impacted lake in the Yangtze River Delta, China. The water quality of these samples is presented in Table 2.

Table 2. Basic Water Quality of Water Samples

<i>Water Tested</i>	<i>DOC (mg/L)</i>	<i>UV (cm⁻¹)</i>	<i>DON (mg N/L)</i>	<i>NDMA FP (ng/L)</i>	<i>NDEA FP (ng/L)</i>
Blended (80/20) river/wastewater (Arizona)	3.7	0.073	0.69	195	ND
Aquaculture- impacted lake water (Yangtze River Delta)	4.8	0.106	0.33	198	106

Note: DOC = Dissolved organic carbon, DON = dissolved organic nitrogen, UV = ultraviolet absorbance at 254 nm. DON = TDN - NH₃-N - NO₃-N - NO₂-N, where TDN is total dissolved nitrogen. NDMA and NDEA FP were measured by the method described in Mitch et al. (12). ND = Not detected.

2.1. Tests with the Blended Wastewater

Tests were conducted at pH 8.2; which was a common drinking water pH level; at 9.5 and 11, which represent the range of pH levels used for lime softening (calcium and magnesium removal, respectively); and at an acidic pH of 3, albeit lower than that used in drinking water. PAC at 8 mg/L was evaluated as a representative dose. In addition, at some pH levels, one or two other PAC doses were evaluated (3 and 20 mg/L).

Figure 1a shows that PAC effectively removed wastewater-derived NDMA precursors under alkaline conditions. However, removal was greatly impaired under acidic conditions for the one PAC dose (8 mg/L) evaluated.

With a PAC dose of 8 mg/L, the removal of NDMA FP at pH levels of 3.0, 8.2, 9.5, and 11.2 was 29, 54, 58, and 52%, respectively. At pH 8.2 and 11.2, the removal increased with increasing PAC dose for the three doses evaluated. For example, at pH 11.2, the removal with PAC doses of 3, 8, and 20 mg/L was 25, 52, and 71%, respectively. Note, NDMA FP removal did not increase proportionately with increasing PAC dose. It is likely that only a certain portion of the precursors were adsorbable, so there was a limit to how much the NDMA FP could be lowered with PAC. Note, the negative removal value at pH 8.2 and PAC dose of 3 mg/L was probably due to variability in NDMA FP determination and NDMA analysis (allowed relative standard derivation for analysis was $\pm 20\%$ according to USEPA method 521 (13)).

The adsorption capacity under different doses was calculated to clarify the influence of pH, as shown in Figure 1b. The adsorption isotherm points of PAC, i.e., Q_e at near neutral (pH 8.2) and alkaline (pH 9.5 and 11.2) pH were similar, whereas at the acidic pH of 3, the adsorption decreased over 50%. The adsorption capacity at pH 3.0 with $C_e = 138$ ng/L was 7.1 ng NDMA FP/mg PAC. The capacity at pH 11 was 16.3 ng NDMA FP/mg PAC, according to the simulated Freundlich isotherm: $Q_e = 0.193 * C_e^{0.900}$.

The efficacy for removing bulk organic matter (i.e., DOC and UV₂₅₄) was typically less than that of the nitrosamine precursors (Figures 1c-d). Hanigan et al. (5) observed the same phenomenon, which suggests that the nitrosamine precursors were trace organic contaminants (e.g., anthropogenic chemicals) that were better adsorbed than the bulk NOM. More importantly, the influence of pH on bulk organic matter removal was opposite that of the nitrosamine precursors. Acidic conditions tended to favor the adsorption of bulk organic matter due to hydrogenation of acid functional groups on the NOM.

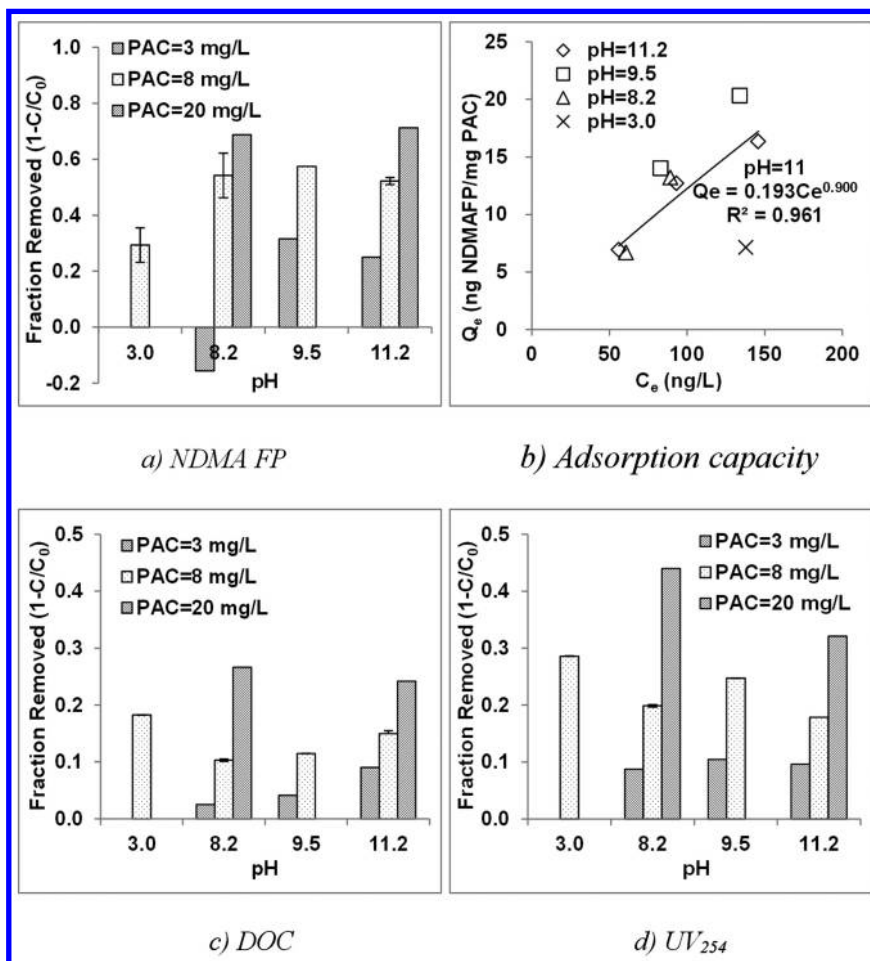


Figure 1. Removal of NDMA FP and bulk organic matter in blended river/wastewater with WPH PAC at varying pH levels and PAC doses (Note: Initial NDMA FP = 195 ng/L, adsorption time = 1 h, temperature = 11°C. Q_e is the adsorption capacity of NDMA FP with PAC. C_e is the equilibrium concentration in the water after adsorption. Triplicate tests were conducted for part of the dataset. The average value is shown with the relative percent difference as error bars.)

2.2. Tests with an Aquaculture-Impacted Lake Water

Figure 2 shows the removal of NDMA and NDEA precursors in an aquaculture-impacted lake water at acidic, neutral, and alkaline pH levels.

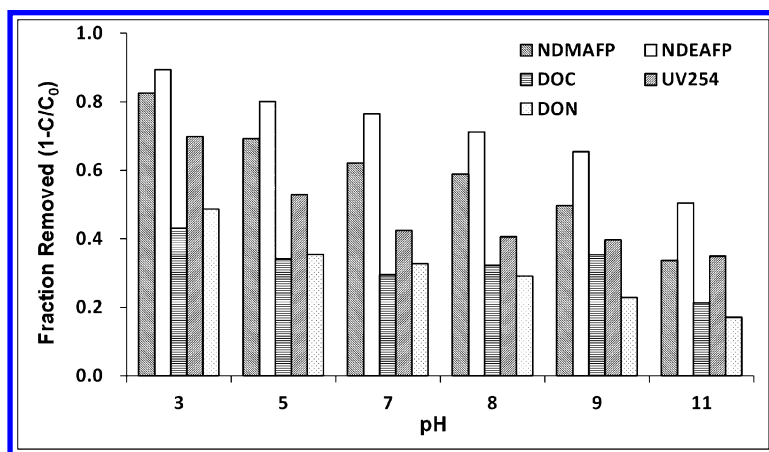


Figure 2. Removal of nitrosamine precursors and bulk organic matter in an aquaculture-impacted lake water with PAC at varying pH levels (Note: initial NDMA FP = 198 ng/L, initial NDEA FP = 106 ng/L; PAC dose = 20 mg/L, adsorption time = 24 h, temperature = 20°C. Pulverized Calgon F400 GAC was used in this test.)

At pH 3, PAC removed 83% of the NDMA precursors and 89% of the NDEA precursors. At pH 7 or 8, PAC removed ~60% of the NDMA precursors and ~75% of the NDEA precursors. At pH 11, PAC removed only 34% of the NDMA precursors and 51% of the NDEA precursors. Contrary to the trend shown in Section 2.1, nitrosamine precursor removal in this aquaculture-impacted lake water gradually decreased as pH increased. This indicates that the behavior of NA precursor with PAC adsorption can be quite site-specific.

Removal of bulk organic matter from the water samples was similar to that in Section 2.1. The DOC, UV₂₅₄, and DON removal gradually decreased as pH increased, which followed the same trend of the nitrosamine precursors in this lake water. In almost all cases, NA precursors were removed by PAC more effectively than the bulk organic matter. In general, the removal trend was as follows: NDEA FP > NDMA FP > UV₂₅₄ > DON ~ DOC.

The adsorption capacities of the NDMA FP in the two waters was very different. The capacity in the blended river/wastewater at pH 8 was 13.2 ng NDMA FP/mg PAC with $C_e = 89.4$ ng/L (Figure 1b) and the capacity for the aquaculture-impacted lake water NDMA precursors was 3.6 ng NDMA FP/mg PAC with the same C_e at the same pH (28% of the capacity for the blended river/wastewater precursors). The difference was likely due to the different characteristics of NDMA precursors in the two water samples.

3. pH Effect on Removal of Model NDMA Precursors with PAC Adsorption

The experiments above indicate that the removal of nitrosamine precursors in real waters with PAC adsorption is complex and site-specific. Therefore, two model NDMA precursors that are PPCPs, ranitidine and chlorpheniramine (3), were used to simplify the investigation of the fate of NA precursors during the PAC adsorption process.

Figure 3 shows the removal of the model NDMA precursors with PAC at varying pH levels and with different PAC doses (model compound concentrations = 0.01 mM each).

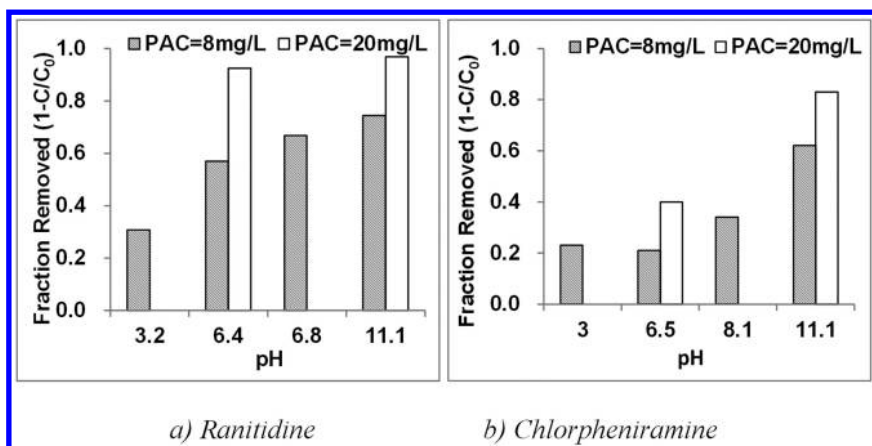


Figure 3. Removal of model NDMA precursors with WPH PAC at varying pH levels and with different doses (model compound concentrations = 0.01 mM each).

Ranitidine removal with PAC adsorption increased with increasing pH when 8 mg/L of PAC was used. The removal ranged from ~30 to ~70% for this dose. Alternatively, when 20 mg/L of PAC was used, pH (for the two values tested [6.4, 11.1]) had no impact. The removal was almost 100%, so the use of a high dose of PAC overshadowed the impact of pH. The behavior of chlorpheniramine followed the same trend (somewhat) as that of ranitidine for a PAC dose of 8 mg/L, but it removed 10-30% less than the ranitidine under the same conditions. In addition, the removal at pH 3 was the same as that at pH 6.5. For a PAC dose of 20 mg/L, there was substantially less removal at pH 6.5 than at pH 11.1.

The results with ranitidine and chlorpheniramine provide further evidence of the pH effect on PAC adsorption of the nitrosamine precursors, where increasing pH increased the removal of these model precursors. In a wastewater-impacted drinking water, there can be a wide range of anthropogenic chemicals, which can be impacted by pH to different extents.

4. pH Effect Study with Model NDMA Precursors via PRAM Approach

The polarity rapid assessment method (PRAM) uses solid-phase extraction (SPE) cartridges to isolate and fractionate organic matter with different polarities or charges (14). Reverse-phase (C₁₈) and strong cation exchange (SCX) SPE cartridges (Extract Clean SPE kit catalog #210100, Alltech Associates, Deerfield, IL, U.S.A.) have been used to elucidate NDMA precursors in wastewater (11) and were used in this study to investigate non-polar and ionic interactions of NDMA precursors with PAC.

Ranitidine or chlorpheniramine solutions at varying pH levels were fed into the C₁₈ or SCX cartridge and 40 mL of the effluent was collected. The removal of ranitidine by C₁₈ or SCX is shown in Figure 4, as well as the distribution of different species (protonated [RAN²⁺, RAN⁺] or de-protonated [RAN]) of ranitidine at varying pH levels. Those for chlorpheniramine (CA) are illustrated in Figure 5.

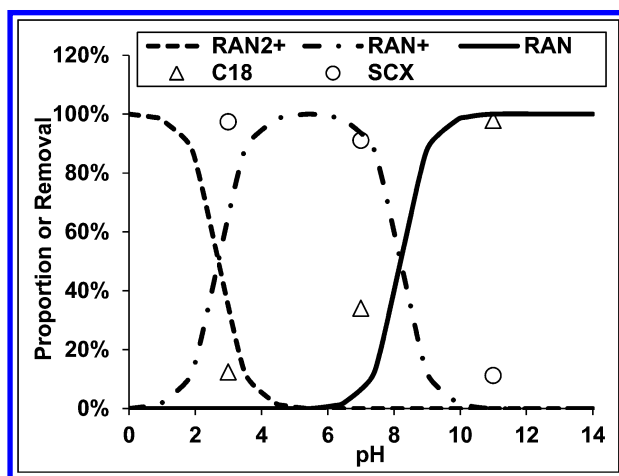


Figure 4. Chemaxon modeled speciation of ranitidine and its experimental removal by C₁₈ or SCX at varying pH levels. (Note: Duplicate tests were conducted. The average values are shown as points and the relative percent difference were less than 3%. Ranitidine concentration = 0.01 mM.)

It is clear that the adsorption capacity of C₁₈ for ranitidine or chlorpheniramine was quickly expended at pH 3, only ~20% removal or less was observed. Chlorpheniramine was better removed (~80%) than ranitidine (~30%) at pH 7. The capacity for each was almost 100% at pH 11: The C₁₈ cartridges retained nearly all of its adsorption capacity for the two chemicals, even after a 40-mL filtration.

At pH 11, both model NDMA precursors quickly broke through the SCX cartridge, with low adsorption affinity. The capacity of each was ~90-100% at pH 3 and 7: The SCX cartridges retained almost all of the chemicals at acidic or neutral pH levels, even after a 40-mL filtration.

In Figures 4 and 5, the removal of the two chemicals by C₁₈ matched well with the neutral species distribution of ranitidine or chlorpheniramine at varying pH levels. C₁₈ also adsorbed the monovalent cation species of chlorpheniramine (CA⁺). In addition, the removal of the two model compounds by SCX coincided with the presence of the two cationic species.

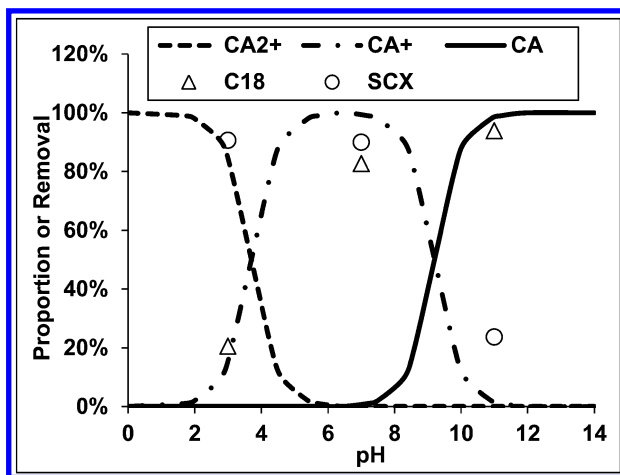


Figure 5. Chemaxon modeled speciation of chlorpheniramine and its experimental removal by C₁₈ or SCX at varying pH levels. (Note: Duplicate tests were conducted. The average values are shown as points and the relative percent difference were less than 3%. Chlorpheniramine concentrations = 0.01 mM.)

The two model NDMA precursors both have amine functional groups that are protonated at low pH. For example, the pK_a values of ranitidine are 2.7 and 8.2, respectively. When the pH was greater than 10, the molecule was deprotonated or neutral and did not sorb via ion exchange. When the pH was less than 6, the molecule was protonated and thus amenable to ion exchange.

The adsorption capacities of the two chemicals at pH 7 were different. Ranitidine was still recalcitrant to C₁₈ adsorption at pH 7, whereas chlorpheniramine was retained better by the C₁₈ cartridge. The difference could be attributed to the pK_a of the two chemicals, which are 9.2 (chlorpheniramine) and 8.2 (ranitidine).

In general, the neutral species were more easily adsorbed by the C₁₈ cartridge, but were recalcitrant to SCX. The positive charged species were sorbed to the SCX media, but were excluded from C₁₈ sorption.

5. Mechanism of pH Effect on NA Precursor Removal with PAC in Natural Waters

Figure 6 illustrates a scheme around our hypothesis that pH influences the removal of NA precursors on PAC. The NA precursors likely have at least one dialkylamine functional group, which is a potential target for oxidant attack and nitrosamine formation. In addition to the basic secondary amines, such as dimethylamine and diethylamine, other NA precursors have longer carbon chains and potentially contain functional groups such as carboxyl and hydroxyl. Therefore, we give a model structure formula for NDMA precursors with dimethylamine, followed by a carbon chain (R_m) containing carboxyl and hydroxyl groups, as shown in Figure 6.

Both van der Waals forces and electrostatic interaction influence the adsorption of organic contaminants on PAC. Van der Waals forces are favored for nonpolar moieties. The electrostatic interactions are stronger than van der Waals and, thus, will dominate for charged groups. The pH effect on NA precursor removal by PAC can be explained by their net effect.

The majority of the fractions of aquatic NOM has carboxyl and hydroxyl functional groups, bringing about the acidity of the NOM. These functional groups are negatively charged at neutral or alkaline conditions, but become protonated at lower pH levels (i.e., below the pK_a values common to carboxylic and hydroxyl groups). On the PAC side, high pH also makes the carboxyl and hydroxyl groups on the carbon surface deprotonate or become negatively charged, which excludes the organic matter. Other major fractions of NOM behave as net neutral molecules, and a very small amount of the NOM behave as basic molecules. The nonpolar adsorption by PAC will decline as pH increases, as shown in Figure 1a-1d (blended river/wastewater) and Figure 2 (aquaculture-impacted lake water).

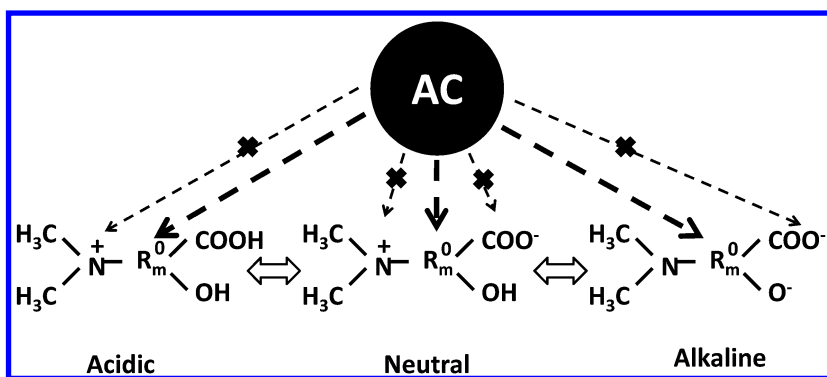


Figure 6. Possible mechanism of the pH effect on nitrosamine precursor removal by PAC adsorption. (Note: Bold dashed line indicates the interaction between PAC and a neutral moiety, light dashed line with a cross indicates the repulsion between PAC and a charged moiety.)

However, NA precursors present positive charges, due to the amine functional group, which is quite unique among the generally negative bulk organic matter. Thus, they have different behavior during PAC adsorption at different pH levels than with the bulk organic matter. Alkaline conditions will deprotonate the amine group and favor nonpolar adsorption on PAC. Alternatively, acidic or neutral conditions will increase the precursor's positive charge and weaken the PAC adsorption. This can occur if the amine functional group dominates, particularly in small molecules.

The hypothesis illustrated in Figure 6 neglects the net charge of PAC. The pulverized F400 GAC had a point of zero charge of pH 9.5, which means the net charge of this AC was negative at neutral and acidic pH levels. These negatively charged functional groups can sorb the positively charged NA precursors at neutral and acidic pH levels. This partially explains the removal of NA FP by WPH PAC in Figures 1 and 3, although the removal was quite limited.

However, the functional groups on PAC surfaces are limited. The majority of PAC adsorption sites are nonpolar, graphite or amorphous carbon. Thus, the charged (positive or negative) chemicals will be recalcitrant to the nonpolar carbon, as also demonstrated by the C₁₈ media, which does not contain ionized functional groups (Figure 4).

6. Conclusion

The following conclusions can be drawn according to the results of this investigation.

- (1) Experiments with different water samples and model NDMA precursors indicated that removal of NDMA precursors by PAC adsorption is pH dependent and site-specific. The removal of two model precursors (ranitidine and chloropheniramine) and the NDMA FP in a blended river/wastewater with PAC adsorption increased with higher pH. However, the NDMA FP in an aquaculture-impacted lake water had declining NDMA FP reduction with PAC adsorption with increasing pH.
- (2) PRAM indicated that the pH effect on PAC adsorption of NDMA precursors is potentially attributable to the protonization or charge of the precursors. Alkaline conditions deprotonate amine functional groups on model precursors and favor adsorption onto PAC, whereas acidic or neutral conditions result in a precursor with positive charge, which reduces the affinity for PAC.

Acknowledgments

The testing of the aquaculture-impacted lake water was supported by the National Natural Science Foundation of China (Grant No. 21477059 and 51290284) and Tsinghua University Initiative Scientific Research Program (Grant No. 20131089247). The testing of the blended river/wastewater was supported

by the Water Research Foundation, Denver, Colo., U.S.A. (project 4370, under the management of Djanette Khiari).

We highly appreciate Rita Chang from UCLA and Yueying Ouyang from Tsinghua University, who volunteered to be the laboratory interns and contributed much to the laboratory work of PRAM.

References

1. Krasner, S. W.; Westerhoff, P.; Chen, B.; Rittmann, B. E.; Amy, G. Occurrence of disinfection byproducts in United States wastewater treatment plant effluents. *Environ. Sci. Technol.* **2009**, *43* (21), 8320–8325.
2. Krasner, S. W.; Mitch, W. A.; McCurry, D. L.; Hanigan, D.; Westerhoff, P. Formation, precursors, control, and occurrence of nitrosamines in drinking water: A Review. *Wat. Res.* **2013**, *47* (13), 4433.
3. Shen, R.; Andrews, S. A. Demonstration of 20 pharmaceuticals and personal care products (PPCPs) as nitrosamine precursors during chloramine disinfection. *Wat. Res.* **2011**, *45* (2), 944–952.
4. Wang, C. K.; Zhang, X. J.; Wang, J.; Liu, S. M.; Chen, C.; Xie, Y. F. Effects of organic fractions on the formation and control of *N*-nitrosamine precursors during conventional drinking water treatment processes. *Sci. Total Environ.* **2013**, *449*, 295–301.
5. Hanigan, D.; Zhang, J.; Herckes, P.; Krasner, S.; Chen, C.; Westerhoff, P. Adsorption of *N*-nitrosodimethylamine precursors by powdered and granular activated carbon. *Environ. Sci. Technol.* **2012**, *46*, 12630–12639.
6. Liao, X.; Wang, C. K.; Wang, J.; Zhang, X. J.; Chen, C.; Krasner, S. W.; Suffet, I. H. Nitrosamine precursor and DOM control in a wastewater-impacted drinking water. *J. Am. Water Works Assoc.* **2014**, *106*, E307–E318.
7. Shah, A. D.; Krasner, S. W.; Lee, C. F. T.; von Gunten, U.; Mitch, W. A. Tradeoffs in disinfection byproduct formation associated with precursor pre-oxidation for control of *N*-nitrosodimethylamine formation. *Environ. Sci. Technol.* **2012**, *46*, 4809–4818.
8. Schreiber, I. M.; Mitch, W. A. Influence of the order of reagent addition on NDMA formation during chloramination. *Environ. Sci. Technol.* **2005**, *39*, 3811–3818.
9. Krasner, S. W.; Shirkhani, R.; Westerhoff, P.; Hanigan, D.; Mitch, W. A.; McCurry, D. L.; Chen, C.; Skadsen, J.; Von Gunten, U. *Controlling the formation of nitrosamines during water treatment*; Water Research Foundation Final Report; Water Research Foundation: Denver, CO, 2015.
10. Hanigan, D.; Zhang, J.; Herckes, P.; Zhu, E.; Krasner, S. W.; Westerhoff, P. Contribution and removal of watershed and cationic polymer *N*-nitrosodimethylamine precursors. *J. Am. Water Works Assoc.* **2015**, *107* (3), E152–E196.
11. Chen, C.; Leavey, S.; Krasner, S. W.; Suffet, I. H. Applying polarity rapid assessment method and ultrafiltration to characterize NDMA precursors in wastewater effluents. *Wat. Res.* **2014**, *57*, 115–126.

12. Mitch, W. A.; Gerecke, A. C.; Sedlak, D. L. A *N*-nitrosodimethylamine (NDMA) precursor analysis for chlorination of water and wastewater. *Wat. Res.* **2003**, *37*, 3733–3741.
13. USEPA. *Method 521: Determination of nitrosamines in drinking water by solid phase extraction and capillary column gas chromatography with large volume injection and chemical ionization tandem mass spectrometry (MS/MS)*; EPA/600/R-05/054; National Exposure Research Laboratory, Office of Research and Development, USEPA: Cincinnati, Ohio, 2004.
14. Rosario-Ortiz, F. L.; Snyder, S.; Suffet, I. H. Characterization of the polarity of natural organic matter under ambient conditions by the polarity rapid assessment method (PRAM). *Environ. Sci. Technol.* **2007**, *41*, 4895–4900.

Chapter 11

Formation of DBPs: State of the Science

Susan D. Richardson^{*,1} and Cristina Postigo²

¹Department of Chemistry and Biochemistry,
University of South Carolina, JM Palms Center,
631 Sumter Street, Columbia, South Carolina 29208

²Department of Environmental Chemistry,
Institute for Environmental Assessment and Water Research,
(IDAEA-CSIC), Carrer Jordi Girona 18-26, 08034 Barcelona, Spain

*E-mail: richardson.susan@sc.edu.

Drinking water disinfection by-products (DBPs) are primarily formed by the reaction of disinfectants with natural organic matter (NOM) and bromide or iodide. Precursors can also involve pollutants, such as pesticides, pharmaceuticals, antibacterial agents, estrogens, textile dyes, bisphenol A, parabens, surfactants, and algal toxins. DBPs are also formed in swimming pool water. Concerns arise due to adverse human health impacts, including bladder cancer, miscarriage, and birth defects. Emerging, unregulated DBPs include halonitromethanes, iodo-trihalomethanes, iodo-acids, haloamides, halofuranones, haloacetonitriles, nitrosamines, and halobenzoquinones. Many of these unregulated DBPs have been shown to be more genotoxic or cytotoxic than those currently regulated. This chapter discusses these issues, along with precursors and mechanisms for their formation.

Introduction

Drinking water disinfection by-products (DBPs) are an unintended consequence of using disinfectants to kill harmful pathogens in potable water. They are primarily formed by the reaction of disinfectants with natural organic matter (NOM) and bromide or iodide (*1*). But, they can also be formed from pollutants, such as pesticides, pharmaceuticals, antibacterial agents, estrogens, textile dyes, bisphenol A, parabens, surfactants, and algal toxins (Table 1) (*2, 3*). Popular disinfectants for drinking water include chlorine, chloramines, ozone, chlorine dioxide, and UV.

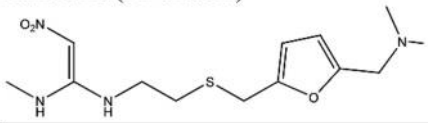
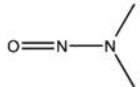
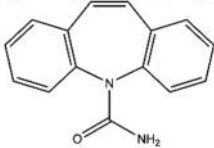
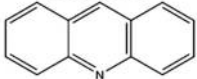
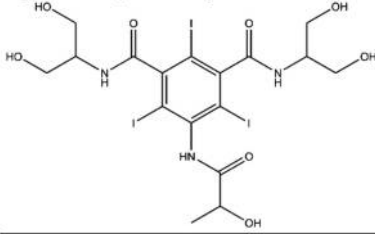
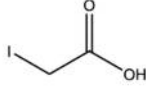
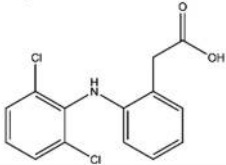
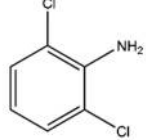
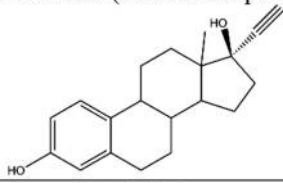
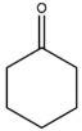
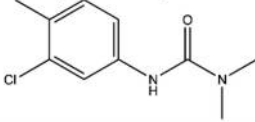
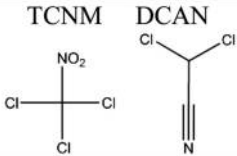
While 11 DBPs are regulated in the United States (*4*), more than 600 have been identified (*1*). While this seems like a great number, more than 50% of the halogenated material formed during chlorination is still unknown, and so is the toxicological risk that it poses to human health (*3, 5*).

Concerns exist due to adverse human health impacts, including bladder cancer, miscarriage, and birth defects, which have been seen in human epidemiologic studies (*1, 6–11*). It is not certain that regulations are adequately controlling for these human health effects, as none of the regulated DBPs cause the primary cancer observed (i.e., bladder cancer) in animals. Therefore, there is intense research in emerging, unregulated DBPs. These include halonitromethanes, iodo-trihalomethanes, iodo-acids, haloamides, halofuranones, haloacetonitriles, haloacetaldehydes, nitrosamines, and halobenzoquinones. Many of these unregulated DBPs have been shown to be more genotoxic or cytotoxic than those currently regulated (*1, 12–14*). For example, iodoacetic acid is the most genotoxic DBP identified to-date, and it is 2x more genotoxic than bromoacetic acid (*1*), which is regulated, but rarely detected in drinking water. Iodoacetic acid was also recently shown to be tumorigenic in mice (*15*).

Of the more than 600 DBPs that have been identified (Table 2), nitrogen-containing DBPs (N-DBPs) are becoming a new focus because they are generally more toxic than DBPs that do not contain nitrogen. For instance, many nitrosamines are known to be carcinogens (*1*). These compounds were on the U.S. Environmental Protection Agency's (EPA's) Unregulated Contaminant Monitoring Rule (*16*), and are currently being considered for regulation by the U.S. EPA.

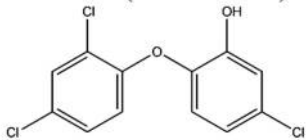
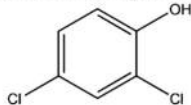
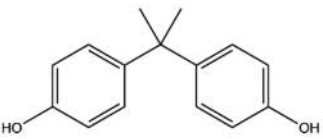
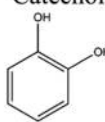
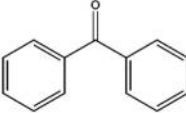
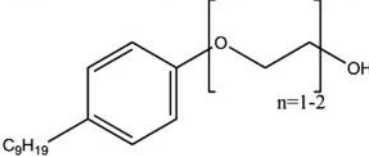
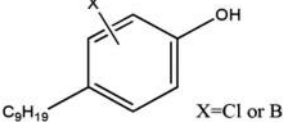
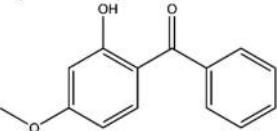
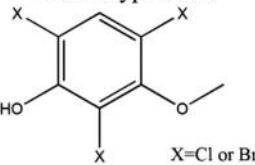
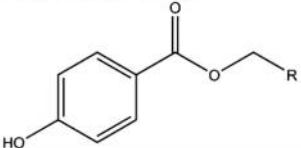
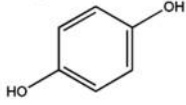
DBPs are also formed in disinfected swimming pool water (*17–21*). Swimming pool DBPs can be similar to those observed in drinking water, but they can also be quite different, due to the additional human precursors that can be present in pools (e.g., urine, sweat, hair, sunscreens, lotions, personal care products etc.) (*21, 22*). For example, a common DBP in chlorinated swimming pools is trichloramine, which is formed by the reaction of urea (from urine or sweat) and chlorine (*23*). Trichloramine is produced in the water, but is quickly transported to the air phase due to its high Henry's Law constant. It is suspected as the causal agent in the increased asthma that has been observed in epidemiologic studies of elite swimmers (*24, 25*). In addition to asthma, one study has also shown increased incidence of bladder cancer with heavy exposure from swimming pools (*26*), and there are also genotoxic effects that have been observed in swimmers (*27*).

Table 1. Examples of DBPs Generated by Water Pollutants

Water pollutants	Disinfectant	DBPs
Ranitidine (Ph-antacid) 	NH_2Cl	NDMA 
Carbamazepine (Ph-antiepileptic) 	ClO_2	Acridine 
Iopamidol (Ph-X-ray contrast media) 	NH_2Cl	Iodoacetic acid 
Diclofenac (Ph-anti-inflammatory) 	O_3	Dichloroaniline 
Ethinyl estradiol (Ph-contraceptive) 	O_3	Cyclohexanone 
Chlortoluron (Pesticide) 	Cl_2	TCNM DCAN 
Ph: pharmaceutical, NDMA: <i>N</i> -Nitrosodimethylamine, TCNM: trichloronitromethane, DCAN: dichloroacetonitrile		

Continued on next page.

Table 1. (Continued). Examples of DBPs Generated by Water Pollutants

Water pollutants	Disinfectant	DBPs
<p>Triclosan (Antimicrobial)</p> 	<p>$\text{Cl}_2/\text{NH}_2\text{Cl}$</p>	<p>2,4-Dichlorophenol</p> 
<p>Bisphenol A (Plasticizer)</p> 	<p>O_3</p>	<p>Catechol</p>  <p>Benzophenone</p> 
<p>Alkylphenol ethoxylates (surfactants)</p> 	<p>Cl_2</p>	<p>Halogenated nonylphenol</p> 
<p>2-Hydroxy-4-methoxybenzophenone (BP3) – (UV filter)</p> 	<p>Cl_2</p>	<p>Trihalogenated methoxyphenols</p> 
<p>Parabens (Preservatives)*</p> 	<p>O_3</p>	<p>Hydroquinone</p> 

*Methyl paraben, R = H; Ethylparaben, R = CH_3 ; Propylparaben, R = CH_3CH_2 ; and Butylparaben, R = $\text{CH}_3\text{CH}_2\text{CH}_2$.

Table 2. Examples of DBP Classes Identified (with N-DBPs Highlighted)

Halogenated DBPs	Non-halogenated DBPs
Halomethanes	Nitrosamines
Haloacids	Aldehydes
Haloaldehydes	Ketones
Haloketones	Carboxylic acids
Halonitriles	
Haloamides	
Halonitromethanes	
Halopyrroles	
Halofuranones (e.g., MX)	
Halobenzoquinones	
Halobenzene sulfonic acids	

In addition to cancer, adverse birth outcomes, and asthma, there are some newer concerns concerning severe skin rashes, and respiratory and digestive issues surrounding chloraminated drinking water. To-date, there has not been a controlled scientific study to investigate these newer adverse effects. Chloramination has become increasingly popular in the U.S., as drinking water utilities have struggled to meet the tightened DBP regulations (4). Chloramination is also popular in other countries, including the UK and Australia. Switching from chlorine to chloramines can result in ~90% reduction in the levels of regulated trihalomethanes (THMs) and haloacetic acids (HAAs), and it is also beneficial to utilities for maintaining disinfection in the distribution system.

The nature and quantity of DBPs formed depends on the type of disinfectant, dose, and the type of organic matter or other constituents present in the water (1, 28–31). Formation mechanisms for several DBPs and DBP classes have been investigated, including iodo-DBPs, halonitromethanes, nitrosamines, haloamides, halopyrroles, and halobenzoquinones (Figures 1-8). The state of the science for their formation follows.

Iodo-DBPs

Iodo-DBPs identified to-date are shown in Figure 1. They include iodo-THMs (dichloriodomethane, bromochloriodomethane, dibromiodomethane, chlorodiiodomethane, bromodiiodomethane, and iodoform); iodo-acids (iodoacetic acid, bromoiodoacetic acid, chloroiodoacetic acid, diiodoacetic acid, (*Z*)-3-bromo-3-iodopropenoic acid, (*E*)-3-bromo-3-iodopropenoic acid, and (*E*)-2-iodo-3-methylbutenedioic acid) (5, 32–35); iodo-amides (bromoiodoacetamide and chloroiodoacetamide) (1, 13, 36); and the recently reported iodoacetaldehyde (37, 38).

Iodo-THMs

Iodo-THMs were the first iodo-DBPs to be discovered, with a long history since the mid-1970s when dichloriodomethane was measured in chlorinated tap water and was referred to as the “5th trihalomethane” (39). Iodo-THMs have since been measured in drinking waters treated with chlorination or chloramination (5, 31, 40–44), with the highest levels observed in chloraminated water (up to 15 µg/L individually) (5). In fact, iodo-THMs can be formed at levels comparable to the regulated THMs (THM4). In the U.S. Nationwide Occurrence Study, one location showed iodo-THMs at 81% of the THM4 levels in a chloraminated drinking water (5, 44). A recent study also revealed that chlorine dioxide can form iodoform (45). In addition, point-of-use treatment with iodine can produce iodo-THMs (46). Of the three iodine treatments investigated (iodine tincture, iodine tablets, and the Lifestraw®), the highest levels were formed with iodine tincture treatments (46). Finally, new research has revealed that hydraulic fracturing (HF) wastewater can produce iodo-THMs when treated with chlorine or monochloramine (47). This is likely due to the high levels of iodide present in HF wastewater (47).

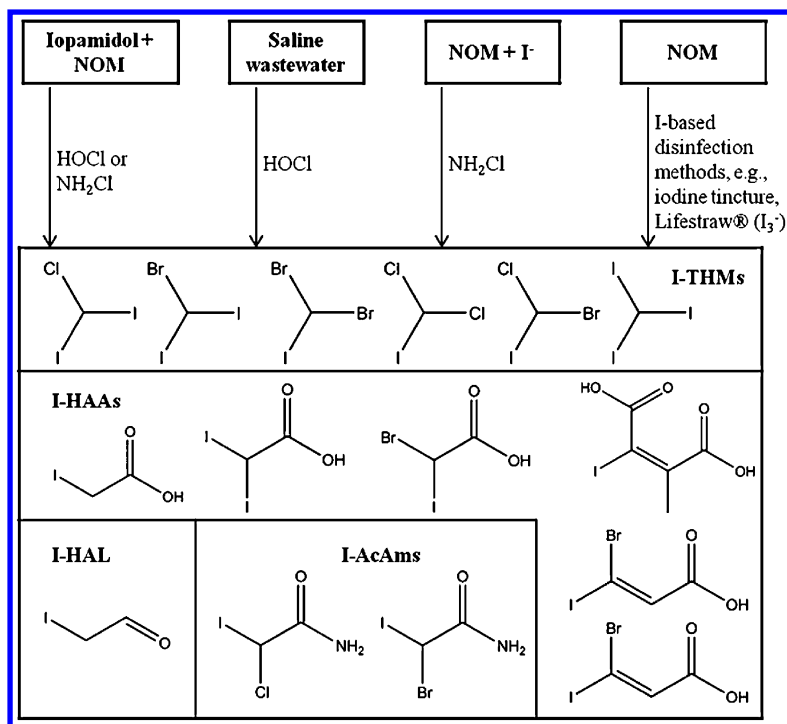


Figure 1. Formation mechanisms for emerging iodo-DBPs (NOM: natural organic matter, I-THMs: iodo-trihalomethanes, I-HAAs: iodo-acetic acids, I-HAL: iodoacetaldehyde, I-AcAms: iodo-acetamides) (34, 46, 48–51).

Iodo-acids

Iodo-acids, which are the most genotoxic of the iodo-DBPs (34, 35), were first identified as part of a U.S. Nationwide Occurrence Study (5, 35, 44). Levels up to 1.7 $\mu\text{g/L}$ were reported in a 23 city survey of chloraminated and chlorinated drinking water from the U.S. and Canada (34). Chlorine dioxide was also reported to form iodoacetic acid when reacted with source waters (45). Iodo-acids were also tentatively identified in simulated drinking waters treated with chlorine, monochloramine, and chlorine-chloramine (32). The authors used ultra-performance liquid chromatography (UPLC)/electrospray ionization (ESI)-tandem mass spectrometry (MS/MS) with precursor ion scanning for the m/z 127 ion of iodine to broadly detect iodo-DBPs formed in these reactions. This research revealed the presence of iodoacetic acid, chloroiodoacetic acid, (*E*)- and (*Z*)-iodobutenedioic acid, 4-iodobenzoic acid, 3-iodophthalic acid, 2,4-diiodobenzoic acid, 5,6-diiodosalicylic acid, and 5,6-diiodo-3-ethylsalicylic acid (32). In addition, iodoacetic acid and chloroacetic acid can form when chlorinated tap water is allowed to react with iodized table salt (containing potassium iodide) or with potassium iodide itself (33).

The rank order for genotoxicity is iodoacetic acid \gg diiodoacetic acid $>$ bromoiodoacetic acid $>$ (*E*)-2-iodo-3-methylbutenedioic acid $>$ (*E*)-3-bromo-3-iodopropenoic acid $>$ (*E*)-3-bromo-2-iodopropenoic acid. Iodoacetic acid is also teratogenic, producing developmental effects (neural tube closures) in mouse embryos, at levels (nM) similar to levels that induce DNA damage in mammalian cells (52, 53). As mentioned earlier, iodoacetic acid was also recently shown to be tumorigenic in mice (15).

Iodo-amides

Haloamides are formed primarily by chlorine or chloramine, and they were quantified for the first time in the U.S. Nationwide Occurrence Study (5, 44). Iodoacetamides—bromoiodoacetamide and chloroiodoacetamide—were subsequently identified in drinking water treated with chloramines or chlorine. Bromoiodoacetamide was initially found in chloraminated drinking water from several cities in the U.S. (13), and later, both bromoiodoacetamide and chloroiodoacetamide were found in chloraminated and chlorinated drinking water from three provinces in China (36). Haloacetamides can form by the hydrolysis of the corresponding haloacetonitriles (54, 55), and new research also shows that they can be formed by an independent pathway and that they are more favored with chloramination vs. chlorination (56).

Both of these iodoacetamides are highly cytotoxic and genotoxic in mammalian cells (13). As a class, haloamides are the most cytotoxic of all DBP classes measured to-date, and they are the second-most genotoxic DBP class, very close behind the halonitriles.

Iodo-DBP Formation Mechanisms

In all cases studied to-date, chloramination increases the formation of all of these iodo-DBPs. In practice, drinking water treatment plants can add pre-formed monochloramine (reaction of chlorine and ammonia), but they will generally add chlorine first and wait for a certain amount of time (free chlorine contact time) before the ammonia is added, so that a higher level of microbial inactivation is achieved. Most data shows increased formation of iodo-DBPs with lower free chlorine contact time (higher monochloramine contact time) (5, 29, 32, 34, 57, 58). This is consistent with a mechanism that Bichsel and von Gunten proposed for the formation of iodo-DBPs, based on controlled laboratory experiments of iodo-THMs, which involves competing mechanisms to form iodate and organic iodo-DBPs (59, 60). Reaction of aqueous chlorine with iodide initially forms hypoiodous acid (HOI), which can then react further with chlorine to form iodite and iodate (Figure 2). These reactions are much faster than the competing reactions to form organic iodo-DBPs (e.g., iodo-THMs and iodo-acids), such that chlorination favors the formation of iodate over organic iodo-DBPs. However, the reactions of monochloramine with HOI to form iodite and iodate are much slower than the corresponding reactions of chlorine with HOI, such that monochloramine favors the formation of organic iodo-DBPs over iodate.

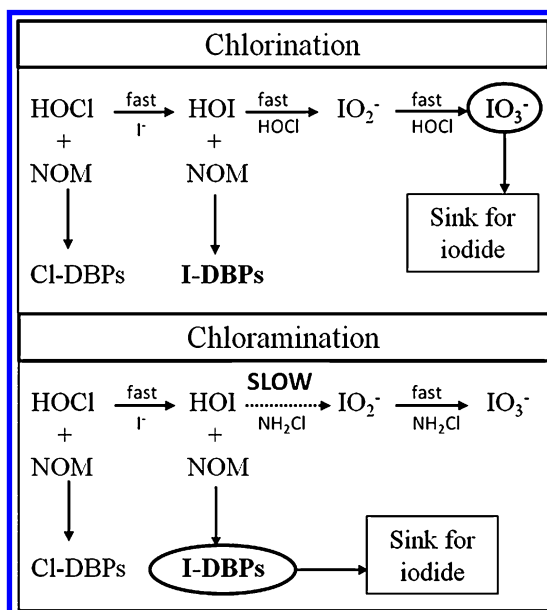


Figure 2. Mechanism of iodo-DBP formation with chlorine and chloramines (59, 60).

New research shows that ozone pretreatment at lower pH can be used to minimize iodo-DBP (and bromate) formation by selectively oxidizing iodide to iodate (61). Ozone could also be used to oxidize iodo-THMs that might already be present in the water.

Iodide salt is believed to be the major source of iodine in the formation of iodo-DBPs. But, new research has revealed that compounds used for medical imaging, i.e., iodinated X-ray contrast media (ICM) can also be a source of iodine (48, 49, 62). ICM are excreted within ~24 h after medical imaging, and they are stable during wastewater treatment, which has resulted in levels up to 100 µg/L in rivers and creeks (63) and up to 2.7 µg/L in drinking water reservoirs (49). These ICM compounds have a triiodobenzene core structure with 3 amide side chains, and research shows that chlorine or chloramine can react with ICM to form iodo-THMs and to a lesser extent, iodo-acids. NOM and pH substantially affect the formation, and OCl⁻ is believed to be the reacting species. In addition, new controlled laboratory studies indicate that iodo-THMs are favored at low chlorine doses, but are suppressed at higher doses (62).

To-date, iopamidol appears to be the most reactive, with much less formation of iodo-DBPs from other ICM investigated (e.g., iopromide, iohexol, iomeprol, diatrizoate, hiztodenz, and iodixanol) (48, 49, 62). New research using liquid chromatography (LC)-high resolution MS/MS and nuclear magnetic resonance (NMR) spectroscopy is revealing the initial points of reaction on the iopamidol structure, along with the initial high molecular weight DBPs formed (Figure 3) (48). The proposed reactions involve cleavage of one of the side chains, substitution of chlorine for iodine on the benzene ring, amide hydrolysis, cleavage of the other side chains, and oxidation of NH₂ to NO₂ (Figure 3). Structures for 19 high molecular weight DBPs were deduced in the reaction pathway.

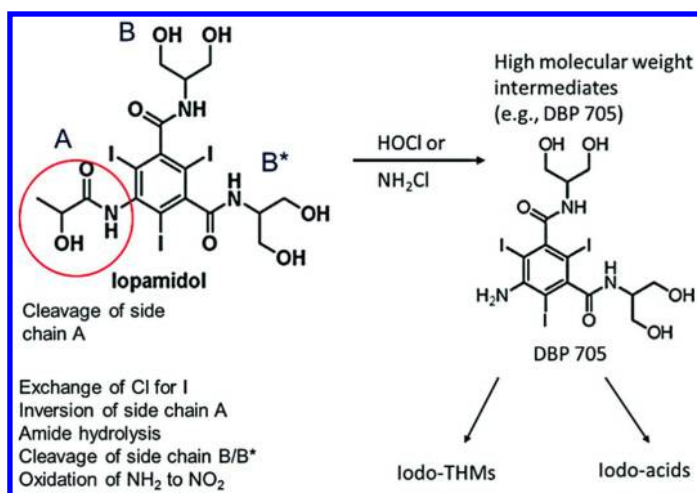


Figure 3. Proposed reaction of iopamidol with chlorine and monochloramine (48).

Nitrosamines

Nitrosamines were discovered to be DBPs in 2002 (64, 65) and have been of significant interest ever since because several, including *N*-nitrosodimethylamine (NDMA), are known carcinogens (1). NDMA was initially discovered in chlorinated drinking waters from Ontario, Canada (66), and was subsequently found in other locations (64, 65, 67). The detection of NDMA in drinking water is largely due to improved analytical techniques that allow its determination at low ng/L concentrations. Following the discovery of NDMA, other nitrosamines were identified as DBPs, including *N*-nitrosopiperidine, *N*-nitrosodiphenylamine, *N*-nitrosopyrrolidine, and *N*-nitrosomorpholine (68, 69). *N*-Nitrosodiphenylamine is thermally unstable and requires LC-MS/MS for its analysis (68). A recently developed total nitrosamine (TONO) assay indicates that the nitrosamines identified to-date only represent 5-10% of the total nitrosamines formed in drinking water and recreational waters (70, 71). The identity of these other nitrosamines is currently unknown. Interestingly, algal-derived organic matter was an insignificant precursor for EPA Method 521 nitrosamines during chloramination, but a potent precursor for other, uncharacterized *N*-nitrosamines, as measured using the TONO assay. In 2014, tobacco-specific nitrosamines—4-(methylnitrosamino)-1-(3-pyridyl)-1-butanone and 4-(methylnitrosamino)-1-(3-pyridyl)-1-butanol—were also discovered to be chloramination DBPs (72).

NDMA is regulated in California at 10 ng/L (73) and Ontario, Canada at 9 ng/L (74). A Canadian national drinking water guideline has also recently been established, which limits NDMA to 40 ng/L in drinking water (75), and the U.S. EPA is considering its regulation in the United States. NDMA was included in the U.S. EPA's second Unregulated Contaminants Monitoring Rule (UCMR-2), along with 5 other nitrosamines (*N*-nitrosodiethylamine, *N*-nitrosodibutylamine, *N*-nitrosodipropylamine, *N*-nitrosomethylethylamine, and *N*-nitrosopyrrolidine). National occurrence data are currently available (16). These new data revealed a maximum level of 530 ng/L for NDMA in chloraminated drinking water, which surpasses the previous maximum (180 ng/L) observed in Canadian chloraminated drinking water (68). In addition, NDMA and 4 other nitrosamines are also on the U.S. EPA's Contaminant Candidate List (CCL-3), a priority list of drinking water contaminants (76).

Nitrosamine Formation Mechanisms

NDMA is generally found at highest levels in chloraminated drinking water. Early research indicated that the nitrogen in monochloramine (NH_2Cl) was incorporated into the structure of the NDMA by-product (64); subsequent research revealed that dichloramine was actually the primary reactant (77). Dichloramine always coexists (at lower levels) with monochloramine under typical chloramination conditions. Nitrite can also serve as a nitrosamine precursor in chlorination reactions (78, 79). In these reactions, a dinitrogen tetraoxide (N_2O_4) intermediate is believed to form, which can nitrosate or nitrate amines.

Chlorination can also form NDMA when nitrogen precursors are present (e.g., natural ammonia in the source water or nitrogen-containing coagulants or ion-exchange resins used in the water treatment process) (80–83) (Figure 4). Consumer products, including shampoos, laundry detergents, dish washing liquids, and fabric softeners, can also be precursors in the formation of nitrosamines (84). Surprisingly, quaternary amine polymers appear to be more reactive than the monomers (84); this phenomenon was also observed in previous studies of diallyldimethylammonium chloride (DADMAC) polymers used as coagulants in drinking water treatment (83, 85, 86). These findings are important because nitrosamine formation is often attributed to lower order amine impurities, but these results clearly show that quaternary amine polymers can also form NDMA.

Amino acids and hydrophilic/low molecular weight dissolved organic nitrogen can also serve as nitrosamine precursors (87), as can amine-based pharmaceuticals (88). Diphenylamine was also shown to be a key precursor in the formation of *N*-nitrosodiphenylamine from chloramines (89, 90). The Lifestraw®, a point-of-use device that uses I₃-complexed resins with an activated carbon filter, can also produce NDMA, but levels rapidly decline to low levels (4 ng/L) after the first few flushes of water (46). Krasner et al. recently published an excellent review on the formation, precursors, control, and occurrence of nitrosamines in drinking water (91).

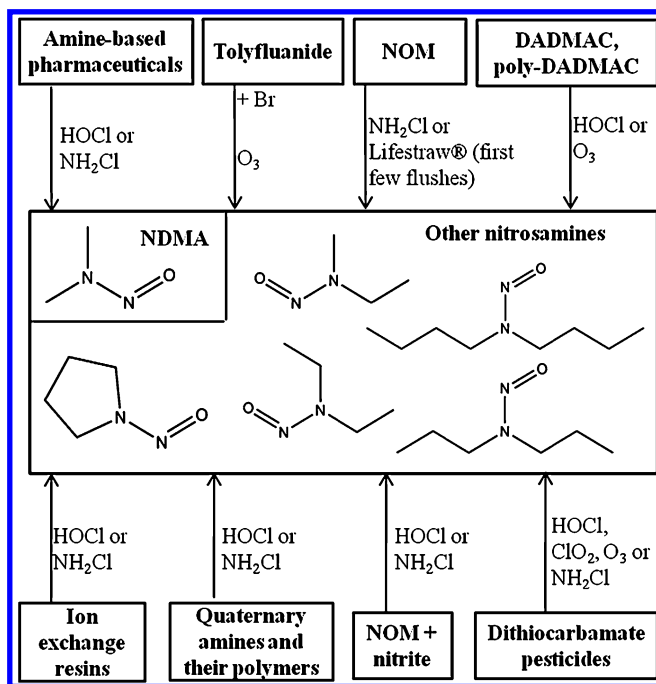


Figure 4. Formation mechanisms for NDMA and other nitrosamines (NOM: natural organic matter; DADMAC: diallyldimethylammonium chloride) (30, 82–84, 88, 92–95).

NDMA (and other nitrosamines) can dramatically increase in concentration in distribution systems (relative to finished water at the drinking water treatment plant). For example, an initial level of 67 ng/L in drinking water treatment plant effluent was shown to increase to 180 ng/L in the distribution system (68). As a result, measurements taken at water treatment plants may substantially underestimate the public's exposure to this carcinogen.

While generally attributed to the use of chloramines or chlorine, NDMA was recently identified in ozonated drinking water from Germany (92). A fungicide which contains a dimethylamine group—tolylfluanide—was discovered to be the precursor in its formation. Subsequent research also revealed that trace levels of bromide can catalyze its formation (96). Dithiocarbamate pesticides can also react with NH_2Cl , O_3 , Cl_2 , or ClO_2 to form NDMA (94). In these reactions, the dithiocarbamate forms an amine by hydrolysis/oxidation, which then forms NDMA (94).

Finally for the tobacco-specific nitrosamines just identified in 2014, tobacco alkaloids, including nicotine, nornicotine, and anabasine were determined to be precursors to their formation in chloraminated drinking water (72).

Haloamides

Haloamides are formed by both chlorine and chloramine, (5, 13, 44, 97, 98), but preferentially by monochloramine (56). The mechanism can involve the hydrolysis of the corresponding haloacetonitriles (54, 55), or reaction of monochloramine with organic nitrogen precursors (56) (Figure 5). Experiments involving ^{15}N -labeled monochloramine indicated initial rapid formation of both dichloroacetamide and dichloroacetonitrile, where the nitrogen originated from organic nitrogen precursors. However, slower formation occurs by pathways involving chloramine incorporation into organic precursors. In addition, experiments with asparagine as a model precursor also suggested that dichloroacetamide can be formed without a dichloroacetonitrile intermediate, and humic materials were found to be more potent precursors for dichloroacetamide formation, while wastewater effluents and algal substances were more potent precursors for dichloroacetonitrile formation (56). Therefore, there are independent mechanisms involved in the formation of haloacetamides, beyond the hydrolysis of the haloacetonitriles.

Several amino acids were also recently found to be precursors of haloamides, with aspartic acid, histidine, tyrosine, tryptophan, glutamine, asparagine, and phenylalanine reacting with chlorine to form dichloroacetamide (99).

Halonitromethanes

Nine chloro/bromo halonitromethanes have been identified to date (Figure 6). Chloropicrin (trichloronitromethane) is the most commonly measured example in this class, but it has not been a concern for toxicity in drinking water. Brominated nitromethanes, however, have shown significant toxicity (100) and have been found in drinking water up to 3 $\mu\text{g/L}$ individually

(5, 44, 100–102). Bromonitromethanes are more cytotoxic and genotoxic than most DBPs currently regulated (100). Dibromonitromethane is more than an order of magnitude more genotoxic to mammalian cells than MX (3-chloro-4-(dichloromethyl)-5-hydroxy-2(5*H*)-furanone, a carcinogenic DBP), and is more genotoxic than all of the regulated DBPs, except for monobromoacetic acid. Other brominated forms are also potent in this assay. Halonitromethanes are also mutagenic in the *Salmonella* bacterial cell assay (103), with mutagenic potencies greater than that of the regulated THMs (104). The halonitromethanes are also at least 10x more cytotoxic than the THMs, and the greater cytotoxic and mutagenic activities of the halonitromethanes was indicated to be likely due to the greater intrinsic reactivity conferred by the nitro group (104).

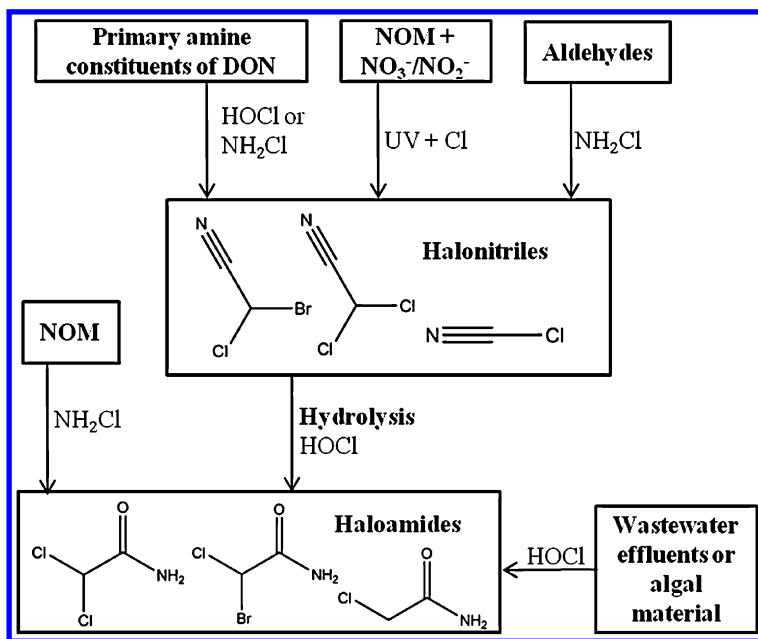


Figure 5. Formation mechanisms for haloamides (30).

Bromonitromethanes are substantially increased in formation with the use of pre-ozonation before post-chlorination or chloramination (5, 44). Laboratory-scale formation studies indicate that nitrite may also play a role in the formation of the nitro group in these DBPs (105). Research indicates that hydrophilic NOM is a more important precursor than hydrophobic or transphilic NOM (106).

Tribromonitromethane (bromopicrin) and other trihalonitromethanes (which include bromodichloro- and chlorodibromonitromethane) require particular analytical conditions for their analysis. These compounds are thermally unstable and decompose under commonly used injection port temperatures during gas chromatography (GC)-electron capture detection (ECD) or GC/mass spectrometry (MS) analysis (97).

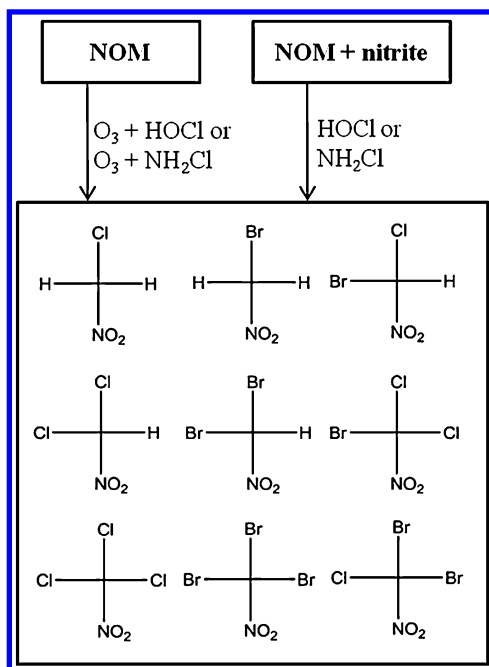


Figure 6. Formation mechanisms for halonitromethanes (30, 105).

Halopyrroles

A halogenated pyrrole —2,3,5-tribromopyrrole (Figure 7)— was first reported as a DBP in 2003 (107). It was found in finished drinking water from Israel that was treated with pre-chlorination followed by treatment with combined chlorine dioxide-chlorine or chlorine dioxide-chloramine. The source water contained exceptionally high bromide levels (approximately 2 ppm). This identification resulted from the first study of chlorine dioxide DBPs formed under high bromide/iodide conditions. Bromide levels in U.S. source waters generally range up to a maximum of approximately 0.5 ppm, and to-date, this tribromopyrrole has not been identified in drinking waters from the United States.

Tribromopyrrole is 8x more cytotoxic than dibromoacetic acid (a regulated DBP) and has about the same genotoxic potency as MX (107), which is also an animal carcinogen (109). Formation studies of different NOM precursors revealed that tribromopyrrole forms primarily from humic acid (vs. fulvic acid), and this isolated humic acid contained a greater contribution of nitrogen in its chemical structure than the isolated fulvic acid. It is interesting to note that a soil humic model proposed by Schulten and Schnitzer (110) includes a pyrrole group in its structure (110), but tribromopyrrole represented the first time a halopyrrole was reported as a DBP. In none of the samplings from this research

was tribromopyrrole found in pre-chlorinated waters (with chlorine treatment only). Thus, the combination of chlorine dioxide and chlorine (or chloramines) may be necessary for its formation. It is also possible that chloramination alone may also be important for its formation.

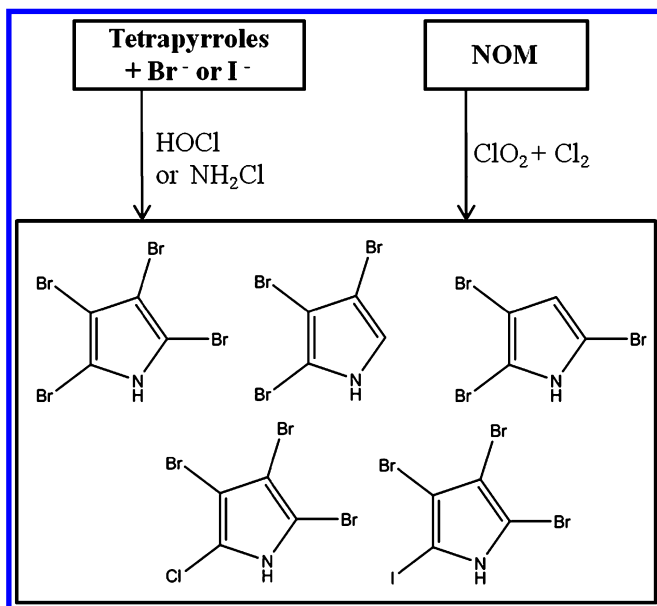


Figure 7. Formation mechanisms for halopyrroles (107, 108).

New research has revealed that halopyrroles can form as DBPs in chlorinated saline wastewater effluents (108). Tri- and tetra-halopyrroles were identified, including brominated, chlorinated, and iodinated analogues (Figure 7). In mechanistic experiments, chlorophyllin (which contains pyrrole units in its structure) was found to be an important precursor in their formation. The chlorinated saline wastewaters were also found to be developmentally toxic to marine polychaetes (108).

Halobenzoquinones

Halobenzoquinones (HBQs) are a new class of DBP recently identified (Figure 8). Four HBQs—2,6-dichlorobenzoquinone, 2,6-dibromobenzoquinone, 2,6-dichloro-3-methylbenzoquinone, and 2,3,6-trichlorobenzoquinone—were initially identified in drinking waters treated with chlorine, chloramines, chlorine-chloramines, ozone-chloramines, and chloramines-UV (111, 112). Levels ranged up to 275 ng/L. 2,6-Dichlorobenzoquinone, 2,3,6-trichloro-1,4-benzoquinone,

2,3-dibromo-5,6-dimethyl-1,4-benzoquinone, and 2,6-dibromo-1,4-benzoquinone were also formed in chlorinated swimming pools (113). And, subsequent work has also revealed the formation of hydroxylated HBQs with UV treatment (114). Quantitative structure-toxicity relationship (QSTR) analysis had predicted that haloquinones are highly toxic and may be formed during drinking water treatment. The chronic lowest observed adverse effect levels (LOAELs) of haloquinones are predicted to be in the low $\mu\text{g}/\text{kg}$ body weight per day range, which is 1000x lower than most regulated DBPs, except bromate.

Separate controlled laboratory studies using phenol as a precursor demonstrated that chlorination produced the highest levels of 2,6-dichlorobenzoquinone, while preozonation increased the formation of 2,6-dibromobenzoquinone in the presence of bromide. UV filters and other aromatic compounds found in lotions and sunscreens were also determined to be precursors of the HBQs found in swimming pools (113).

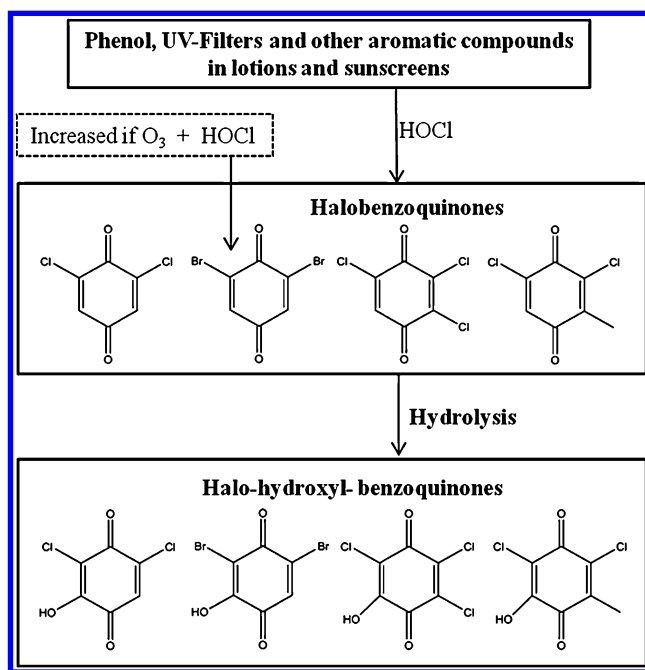


Figure 8. Formation mechanisms for halo-benzoquinones (112, 113, 115).

Conclusions

In conclusion, the nature and quantity of DBPs formed depends on the type of disinfectant, dose, and the type of organic matter or other constituents present in the water. Due to the significant occurrence and toxicity of many emerging

DBPs, it is important to understand their formation so that treatment methods can be developed to minimize them in drinking water. For example, formation of several of these DBPs is enhanced by chloramination, which is a popular disinfection alternative that many treatment plants have switched to in order to minimize regulated THMs and HAAs. However, due to the significant toxicity associated with several chloraminated DBPs, such as NDMA, iodoacetic acid, and haloamides, it may be wise to investigate other treatment technologies, such as granular activated carbon (GAC) or membranes, which could be used in combination with chlorine or chlorine dioxide to potentially minimize both emerging chloramination DBPs and regulated DBPs. However, research is needed to ensure that these treatment changes do not cause other unintended consequences, such as increased brominated DBP formation. In this regard, when exploring new treatment methods, it is wise to combine chemistry and toxicology.

While the U.S. EPA is considering regulation of NDMA and other nitrosamines, it is not known whether other emerging DBPs will be seriously considered for regulation. A major stumbling block for new regulations is the lack of *in vivo* toxicology data and national occurrence data. These are two key criteria that the U.S. EPA uses to determine whether or not to regulate new contaminants in drinking water. Because nitrosamines were contaminants of concern for many decades prior (before they were known to be DBPs), a wealth of *in vivo* toxicity data already existed for them, which allowed regulators to have the data necessary to place them on priority lists, such as the CCL-3 and the UCMR-2. Once contaminants are on these lists, EPA Methods can be created for them and national data can be collected (through the UCMR). However, in recent years, there is reduced emphasis on collecting *in vivo* data, due to the expense and effort involved, and it is unlikely that the U.S. EPA would regulate new DBPs without *in vivo* data. Thus, there is a tremendous need for *in vivo* data to determine whether compounds like iodoacetic acid and dibromonitromethane are carcinogens or teratogens.

Another limitation lies in the fact that we are still currently missing more than 50% of the DBPs with our current analytical techniques. LC-MS/MS is helping to reveal a few more DBP classes, such as halobenzoquinones and new bromo- and iodo-DBPs, and it can measure a broader spectrum of polar chemicals, where GC/MS is more limited. In addition, the use of halogen-specific total organic halogen (TOX), which allows chlorinated, brominated, and iodinated DBP species to be measured as total organic chlorine (TOCl), total organic bromine (TOBr), and total organic iodine (TOI), is helping to provide new information. As research continues, it will be important to determine whether TOBr and TOI correlate with adverse health impacts, and if they do, then possibly new cost-effective technologies can be developed to remove Br⁻ and I⁻ from source waters.

While many challenges still exist, there has been a renaissance of research in DBPs, with increased efforts in several countries throughout the world. Drinking water safety remains an important goal, and it is hopeful that the remaining health issues surrounding drinking water will be solved.

Acknowledgments

C.P. acknowledges support from the European Union Seventh Framework Programme (FP7/2007-2013) under grant agreement no. 274379 (Marie Curie IOF). This work has been financially supported by the Generalitat de Catalunya (Consolidated Research Groups “2014 SGR 418 - Water and Soil Quality Unit” and 2014 SGR 291 - ICRA). This work reflects only the author’s views. The EU is not liable for any use that may be made of the information contained therein.

References

1. Richardson, S. D.; Plewa, M. J.; Wagner, E. D.; Schoeny, R.; DeMarini, D. M. Occurrence, genotoxicity, and carcinogenicity of regulated and emerging disinfection by-products in drinking water: A review and roadmap for research. *Mutat. Res.* **2007**, *636*, 178–242.
2. Postigo, C.; Richardson, S. D. Transformation of pharmaceuticals during oxidation/disinfection processes in drinking water treatment. *J. Hazard. Mater.* **2014**, *279*, 461–475.
3. Richardson, S. D.; Postigo, C. Drinking water disinfection by-products. In *Emerging Organic Contaminants and Human Health - The Handbook of Environmental Chemistry*; Barcelo, D., Ed.; Springer-Verlag Berlin Heidelberg: Germany, 2012; Vol. 20, pp 93–138.
4. U.S. Environmental Protection Agency (U.S. EPA). *Drinking water contaminants*; <http://goo.gl/90OBMZ> (accessed November, 2014).
5. Krasner, S. W.; Weinberg, H. S.; Richardson, S. D.; Pastor, S. J.; Chinn, R.; Scilimenti, M. J.; Onstad, G. D.; Thruston, A. D., Jr. Occurrence of a new generation of disinfection byproducts. *Environ. Sci. Technol.* **2006**, *40*, 7175–7185.
6. Bove, F.; Shim, Y.; Zeitz, P. Drinking water contaminants and adverse pregnancy outcomes: A review. *Environ. Health Perspect.* **2002**, *110*, 61–74.
7. Cantor, K. P.; Villanueva, C. M.; Silverman, D. T.; Figueroa, J. D.; Real, F. X.; Garcia-Closas, M.; Malats, N.; Chanock, S.; Yeager, M.; Tardon, A.; Garcia-Closas, R.; Serra, C.; Carrato, A.; Castaño-Vinyals, G.; Samanic, C.; Rothman, N.; Kogevinas, M. Polymorphisms in GSTT1, GSTZ1, AND CYP2E1, disinfection by-products, and risk of bladder cancer in Spain. *Environ. Health Perspect.* **2010**, *118*, 1545–1550.
8. Nieuwenhuijsen, M. J.; Toledano, M. B.; Eaton, N. E.; Fawell, J.; Elliott, P. Chlorination disinfection byproducts in water and their association with adverse reproductive outcomes: A review. *Occup. Environ. Med.* **2000**, *57*, 73–85.
9. Savitz, D. A.; Singer, P. C.; Hartmann, K. E.; Herring, A. H.; Weinberg, H. S.; Makarushka, C.; Hoffman, C.; Chan, R.; Maclehose, R. *Drinking Water Disinfection By-Products and Pregnancy Outcome*; AWWA Research Foundation: Denver, CO, 2005; p 212.

10. Villanueva, C. M.; Cantor, K. P.; Cordier, S.; Jaakkola, J. J. K.; King, W. D.; Lynch, C. F.; Porru, S.; Kogevinas, M. Disinfection byproducts and bladder cancer: A pooled analysis. *Epidemiology* **2004**, *15*, 357–367.
11. Waller, K.; Swan, S. H.; DeLorenze, G.; Hopkins, B. Trihalomethanes in drinking water and spontaneous abortion. *Epidemiology* **1998**, *9*, 134–140.
12. Plewa, M. J.; Wagner, E. D. *Mammalian Cell Cytotoxicity and Genotoxicity of Disinfection By-Products*; Water Research Foundation: Denver, CO, 2009; pp 134.
13. Plewa, M. J.; Muellner, M. G.; Richardson, S. D.; Fasano, F.; Buettner, K. M.; Woo, Y. T.; McKague, A. B.; Wagner, E. D. Occurrence, synthesis, and mammalian cell cytotoxicity and genotoxicity of haloacetamides: An emerging class of nitrogenous drinking water disinfection byproducts. *Environ. Sci. Technol.* **2008**, *42*, 955–961.
14. Plewa, M. J.; Simmons, J. E.; Richardson, S. D.; Wagner, E. D. Mammalian cell cytotoxicity and genotoxicity of the haloacetic acids, a major class of drinking water disinfection by-products. *Environ. Mol. Mutagen.* **2010**, *51*, 871–878.
15. Wei, X.; Wang, S.; Zheng, W.; Wang, X.; Liu, X.; Jiang, S.; Pi, J.; Zheng, Y.; He, G.; Qu, W. Drinking water disinfection byproduct iodoacetic acid induces tumorigenic transformation of NIH3T3 cells. *Environ. Sci. Technol.* **2013**, *47*, 5913–5920.
16. U.S. Environmental Protection Agency (U.S. EPA). *Unregulated Contaminant Monitoring Rule 2 - UCMR 2*; <http://goo.gl/EQD8bI> (accessed November, 2014).
17. Li, J.; Blatchley, E. R., III. Volatile disinfection byproduct formation resulting from chlorination of organic - Nitrogen precursors in swimming pools. *Environ. Sci. Technol.* **2007**, *41*, 6732–6739.
18. Zwiener, C.; Richardson, S. D.; DeMarini, D. M.; Grummt, T.; Glauner, T.; Frimmel, F. H. Drowning in disinfection byproducts? Assessing swimming pool water. *Environ. Sci. Technol.* **2007**, *41*, 363–372.
19. Richardson, S. D.; DeMarini, D. M.; Kogevinas, M.; Fernandez, P.; Marco, E.; Lourencetti, C.; Ballesté, C.; Heederik, D.; Meliefste, K.; McKague, A. B.; Marcos, R.; Font-Ribera, L.; Grimalt, J. O.; Villanueva, C. M. What's in the pool? a comprehensive identification of disinfection by-products and assessment of mutagenicity of chlorinated and brominated swimming pool water. *Environ. Health Perspect.* **2010**, *118*, 1523–1530.
20. Weaver, W. A.; Li, J.; Wen, Y.; Johnston, J.; Blatchley, M. R.; Blatchley, III, E. R. Volatile disinfection by-product analysis from chlorinated indoor swimming pools. *Water Res.* **2009**, *43*, 3308–3318.
21. Chowdhury, S.; Al-hooshani, K.; Karanfil, T. Disinfection byproducts in swimming pool: Occurrences, implications and future needs. *Water Res.* **2014**, *53*, 68–109.
22. Kim, H.; Shim, J.; Lee, S. Formation of disinfection by-products in chlorinated swimming pool water. *Chemosphere* **2002**, *46*, 123–130.
23. Schmalz, C.; Frimmel, F. H.; Zwiener, C. Trichloramine in swimming pools - Formation and mass transfer. *Water Res.* **2011**, *45*, 2681–2690.

24. Bougault, V.; Boulet, L. P. Airway dysfunction in swimmers. *Brit. J. Sport. Med.* **2012**, *46*, 402–406.
25. Florentin, A.; Hautemaniere, A.; Hartemann, P. Health effects of disinfection by-products in chlorinated swimming pools. *Int. J. Hyg. Environ. Health.* **2011**, *214*, 461–469.
26. Villanueva, C. M.; Cantor, K. P.; Grimalt, J. O.; Malats, N.; Silverman, D.; Tardon, A.; Garcia-Closas, R.; Serra, C.; Carrato, A.; Castaño-Vinyals, G.; Marcos, R.; Rothman, N.; Real, F. X.; Dosemeci, M.; Kogevinas, M. Bladder cancer and exposure to water disinfection by-products through ingestion, bathing, showering and swimming in pools. *Am. J. Epidemiol.* **2007**, *165*, 148–156.
27. Kogevinas, M.; Villanueva, C. M.; Font-Ribera, L.; Liviac, D.; Bustamante, M.; Espinoza, F.; Nieuwenhuijsen, M. J.; Espinosa, A.; Fernandez, P.; DeMarini, D. M.; Grimalt, J. O.; Grummt, T.; Marcos, R. Genotoxic effects in swimmers exposed to disinfection by-products in indoor swimming pools. *Environ. Health Perspect.* **2010**, *118*, 1531–1537.
28. Liang, L.; Singer, P. C. Factors influencing the formation and relative distribution of haloacetic acids and trihalomethanes in drinking water. *Environ. Sci. Technol.* **2003**, *37*, 2920–2928.
29. Hua, G.; Reckhow, D. A. Comparison of disinfection byproduct formation from chlorine and alternative disinfectants. *Water Res.* **2007**, *41*, 1667–1678.
30. Shah, A. D.; Mitch, W. A. Halonitroalkanes, halonitriles, haloamides, and N-nitrosamines: A critical review of nitrogenous disinfection byproduct formation pathways. *Environ. Sci. Technol.* **2012**, *46*, 119–131.
31. Zhang, Z.; Echigo, S.; Minear, R. A.; Plewa, M. J. Characterization and comparison of disinfection by-products of four major disinfectants. In *Natural Organic Matter and Disinfection By-Products: Characterization and Control in Drinking Water*; Barrett, S. E., Krasner, S. W., Amy, G. L., Eds.; American Chemical Society: Washington, DC, 2000; pp 299–314.
32. Ding, G.; Zhang, X. A picture of polar iodinated disinfection byproducts in drinking water by (UPLC/ESI-tqMS). *Environ. Sci. Technol.* **2009**, *43*, 9287–9293.
33. Becalski, A.; Lau, B. P. Y.; Schrader, T. J.; Seaman, S. W.; Sun, W. F. Formation of iodoacetic acids during cooking: Interaction of iodized table salt with chlorinated drinking water. *Food Addit. Contam.* **2006**, *23*, 957–962.
34. Richardson, S. D.; Fasano, F.; Ellington, J. J.; Crumley, F. G.; Buettner, K. M.; Evans, J. J.; Blount, B. C.; Silva, L. K.; Waite, T. J.; Luther, G. W.; McKague, A. B.; Miltner, R. J.; Wagner, E. D.; Plewa, M. J. Occurrence and mammalian cell toxicity of iodinated disinfection byproducts in drinking water. *Environ. Sci. Technol.* **2008**, *42*, 8330–8338.
35. Plewa, M. J.; Wagner, E. D.; Richardson, S. D.; Thruston, Jr., A. D.; Woo, Y. T.; McKague, A. B. Chemical and biological characterization of newly discovered iodoacid drinking water disinfection byproducts. *Environ. Sci. Technol.* **2004**, *38*, 4713–4722.
36. Chu, W.; Gao, N.; Yin, D.; Krasner, S. W.; Templeton, M. R. Trace determination of 13 haloacetamides in drinking water using liquid

chromatography triple quadrupole mass spectrometry with atmospheric pressure chemical ionization. *J. Chromatogr. A* **2012**, *1235*, 178–181.

37. Jeong, C. H.; Postigo, C.; Richardson, S. D.; Simmons, J. E.; Kimura, S. Y.; Marinas, B. J.; Barcelo, D.; Wagner, E. D.; Plewa, M. The occurrence and comparative toxicity of haloacetaldehyde disinfection byproducts in drinking water. *Environ. Sci. Technol.* **2014** Submitted for publication.
38. Postigo, C.; Jeong, C. H.; Richardson, S. D.; Wagner, E. D.; Plewa, M.; Simmons, J. E.; Barcelo, D., Analysis, occurrence and toxicity of haloacetaldehydes in drinking waters: iodoacetaldehyde as an emerging disinfection byproduct. In *Occurrence, Formation, Health Effects, and Control of Disinfection By-Products*; Karanfil, T., Mitch, W., Westerhoff, P., Yuefeng, X., Eds.; ACS Symposium Series 1190; American Chemical Society: Washington, DC, 2014.
39. Brass, H. J.; Feige, M. A.; Halloran, T.; Mello, J. W.; Munch, D.; Thomas, R. F. The national organic monitoring survey: samplings and analysis for purgeable organic compounds. In *Drinking Water Quality Enhancement Through Source Protection*; Pojasek, R. B., Ed.; Ann Arbor Science: Ann Arbor, MI, 1977; pp 393–416.
40. Cancho, B.; Ventura, F.; Galceran, M.; Diaz, A.; Ricart, S. Determination, synthesis and survey of iodinated trihalomethanes in water treatment processes. *Water Res.* **2000**, *34*, 3380–3390.
41. Wei, X.; Chen, X.; Wang, X.; Zheng, W.; Zhang, D.; Tian, D.; Jiang, S.; Ong, C. N.; He, G.; Qu, W. Occurrence of regulated and emerging iodinated DBPs in the Shanghai drinking water. *PLoS One* **2013**, *8*, 1–7.
42. Criquet, J.; Allard, S.; Salhi, E.; Joll, C. A.; Heitz, A.; von Gunten, U. Iodate and iodo-trihalomethane formation during chlorination of iodide-containing waters: Role of bromide. *Environ. Sci. Technol.* **2012**, *46*, 7350–7357.
43. Krasner, S. W.; McGuire, M. J.; Jacangelo, J. G.; Patania, N. L.; Reagan, K. M.; Aieta, E. M. The occurrence of disinfection byproducts in United States drinking water. *J. Am. Water Works Assoc.* **1989**, *81*, 41–53.
44. Weinberg, H. S.; Krasner, S. W.; Richardson, S. D.; Thruston, A. D., Jr. *The Occurrence of Disinfection By-Products (DBPs) of Health Concern in Drinking Water: Results of a Nationwide DBP Occurrence Study*; National Exposure Research Laboratory, Office of Research and Development, U.S. Environmental Protection Agency: Athens, GA, 2002.
45. Ye, T.; Xu, B.; Lin, Y. L.; Hu, C. Y.; Lin, L.; Zhang, T. Y.; Gao, N. Y. Formation of iodinated disinfection by-products during oxidation of iodide-containing waters with chlorine dioxide. *Water Res.* **2013**, *47*, 3006–3014.
46. Smith, E. M.; Plewa, M. J.; Lindell, C. L.; Richardson, S. D.; Mitch, W. A. Comparison of byproduct formation in waters treated with chlorine and iodine: Relevance to point-of-use treatment. *Environ. Sci. Technol.* **2010**, *44*, 8446–8452.
47. Parker, K. M.; Zeng, T.; Harkness, J.; Vengosh, A.; Mitch, W. A. Enhanced formation of disinfection byproducts in shale gas wastewater-impacted drinking water supplies. *Environ. Sci. Technol.* **2014**, *48*, 11161–11169.

48. Wendel, F. M.; Lütke Eversloh, C.; Machek, E. J.; Duirk, S. E.; Plewa, M. J.; Richardson, S. D.; Ternes, T. A. Transformation of iopamidol during chlorination. *Environ. Sci. Technol.* **2014**, *48*, 12689–12697.
49. Duirk, S. E.; Lindell, C.; Cornelison, C. C.; Kormos, J.; Ternes, T. A.; Attene-Ramos, M.; Osiol, J.; Wagner, E. D.; Plewa, M. J.; Richardson, S. D. Formation of toxic iodinated disinfection by-products from compounds used in medical imaging. *Environ. Sci. Technol.* **2011**, *45*, 6845–6854.
50. Gong, T.; Zhang, X. Detection, identification and formation of new iodinated disinfection byproducts in chlorinated saline wastewater effluents. *Water Res.* **2015**, *68*, 77–86.
51. Zhang, T. Y.; Xu, B.; Hu, C. Y.; Lin, Y. L.; Lin, L.; Ye, T.; Tian, F. X. A comparison of iodinated trihalomethane formation from chlorine, chlorine dioxide and potassium permanganate oxidation processes. *Water Res.* **2015**, *68*, 394–403.
52. Hunter, I. E. S.; Rogers, E. H.; Schmid, J. E.; Richard, A. Comparative effects of haloacetic acids in whole embryo culture. *Teratology* **1996**, *54*, 57–64.
53. Hunter, E. S. I.; Tugman, J. A. Inhibitors of glycolytic metabolism affect neurulation-stage mouse conceptuses in vitro. *Teratology* **1995**, *52*, 317–323.
54. Glezer, V.; Harris, B.; Tal, N.; Iosefzon, B.; Lev, O. Hydrolysis of haloacetonitriles: Linear free energy relationship. Kinetics and products. *Water Res.* **1999**, *33*, 1938–1948.
55. Reckhow, D. A.; MacNeill, A. L.; Platt, T. L.; MacNeill, A. L.; McClellan, J. N. Formation and degradation of dichloroacetonitrile in drinking waters. *J. Water Supply: Res. Technol. –AQUA* **2001**, *50*, 1–13.
56. Huang, H.; Wu, Q. Y.; Hu, H. Y.; Mitch, W. A. Dichloroacetonitrile and dichloroacetamide can form independently during chlorination and chloramination of drinking waters, model organic matters, and wastewater effluents. *Environ. Sci. Technol.* **2012**, *46*, 10624–10631.
57. Jones, D. B.; Saglam, A.; Triger, A.; Song, H.; Karanfil, T. I-THM formation and speciation: Preformed monochloramine versus prechlorination followed by ammonia addition. *Environ. Sci. Technol.* **2011**, *45*, 10429–10437.
58. Jones, D. B.; Song, H.; Karanfil, T. The effects of selected preoxidation strategies on I-THM formation and speciation. *Water Res.* **2012**, *46*, 5491–5498.
59. Bichsel, Y.; von Gunten, U. Oxidation of iodide and hypiodous acid in the disinfection of natural waters. *Environ. Sci. Technol.* **1999**, *33*, 4040–4045.
60. Bichsel, Y.; von Gunten, U. Formation of iodo-trihalomethanes during disinfection and oxidation of iodide-containing waters. *Environ. Sci. Technol.* **2000**, *34*, 2784–2791.
61. Allard, S.; Nottle, C. E.; Chan, A.; Joll, C.; von Gunten, U. Ozonation of iodide-containing waters: Selective oxidation of iodide to iodate with simultaneous minimization of bromate and I-THMs. *Water Res.* **2013**, *47*, 1953–1960.
62. Ye, T.; Xu, B.; Wang, Z.; Zhang, T. Y.; Hu, C. Y.; Lin, L.; Xia, S. J.; Gao, N. Y. Comparison of iodinated trihalomethanes formation during aqueous chlor(am)ination of different iodinated X-ray contrast media compounds in the presence of natural organic matter. *Water Res.* **2014**, *66*, 390–398.

63. Ternes, T. A.; Hirsch, R. Occurrence and behavior of X-ray contrast media in sewage facilities and the aquatic environment. *Environ. Sci. Technol.* **2000**, *34*, 2741–2748.
64. Choi, J.; Valentine, R. L. Formation of N-nitrosodimethylamine (NDMA) from reaction of monochloramine: A new disinfection by-product. *Water Res.* **2002**, *36*, 817–824.
65. Mitch, W. A.; Sedlak, D. L. Formation of N-nitrosodimethylamine (NDMA) from dimethylamine during chlorination. *Environ. Sci. Technol.* **2002**, *36*, 588–595.
66. Jobb, D. B.; Hunsinger, R.; Meresz, O.; Taguchi, V. Y. A study of the occurrence and inhibition of formation of N-nitrosodimethylamine (NDMA) in the Ohsweken water supply. In *Proceedings of the Fifth National Conference on Drinking Water*; September 13–15, 1992, American Water Works Association (AWWA), Winnipeg, Canada, 1993; pp 241–252.
67. Boyd, J. M.; Hrudey, S. E.; Li, X. F.; Richardson, S. D. Solid-phase extraction and high-performance liquid chromatography mass spectrometry analysis of nitrosamines in treated drinking water and wastewater. *TrAC, Trends Anal. Chem.* **2011**, *30*, 1410–1421.
68. Charrois, J. W. A.; Arend, M. W.; Froese, K. L.; Hrudey, S. E. Detecting N-nitrosamines in drinking water at nanogram per liter levels using ammonia positive chemical ionization. *Environ. Sci. Technol.* **2004**, *38*, 4835–4841.
69. Zhao, Y. Y.; Boyd, J.; Hrudey, S. E.; Li, X. F. Characterization of new nitrosamines in drinking water using liquid chromatography tandem mass spectrometry. *Environ. Sci. Technol.* **2006**, *40*, 7636–7641.
70. Kulshrestha, P.; McKinstry, K. C.; Fernandez, B. O.; Feelisch, M.; Mitch, W. A. Application of an optimized total N-nitrosamine (TONO) assay to pools: Placing N-nitrosodimethylamine (NDMA) determinations into perspective. *Environ. Sci. Technol.* **2010**, *44*, 3369–3375.
71. Dai, N.; Mitch, W. A. Relative importance of N-nitrosodimethylamine compared to total N-nitrosamines in drinking waters. *Environ. Sci. Technol.* **2013**, *47*, 3648–3656.
72. Wu, M.; Qian, Y.; Boyd, J. M.; Leavey, S.; Hrudey, S. E.; Krasner, S. W.; Li, X. F. Identification of tobacco-specific nitrosamines as disinfection byproducts in chloraminated water. *Environ. Sci. Technol.* **2014**, *48*, 1828–1834.
73. California Department of Health - Drinking Water Program. *Drinking Water Notification Levels and Response Levels: An Overview*. <http://goo.gl/XvsT74> (accessed November, 2014).
74. Ontario Regulation 169/03. *Ontario Drinking Water Quality Standards. Safe Drinking Water Act, 2002*. <http://goo.gl/6OTlkl> (accessed November 2014).
75. Health Canada. *Guidelines for Canadian Drinking Water Quality: Guideline Technical Document - N-Nitrosodimethylamine (NDMA)*; Water, Air and Climate Change Bureau, Healthy Environments and Consumer Safety Branch, Health Canada, Ottawa, Ontario (Catalogue No H128-1/11-662E) 2011 <http://goo.gl/yAUstU> (accessed November, 2014).
76. U.S. Environmental Protection Agency (U.S. EPA) *Contaminant Candidate List 3 - CCL 3*. <http://goo.gl/6M90rO> (accessed November, 2014).

77. Schreiber, I. M.; Mitch, W. A. Nitrosamine formation pathway revisited: The importance of chloramine speciation and dissolved oxygen. *Environ. Sci. Technol.* **2006**, *40*, 6007–6014.
78. Choi, J.; Valentine, R. L. N-Nitrosodimethylamine formation by free-chlorine-enhanced nitrosation of dimethylamine. *Environ. Sci. Technol.* **2003**, *37*, 4871–4876.
79. Schreiber, I. M.; Mitch, W. A. Enhanced nitrogenous disinfection byproduct formation near the breakpoint: Implications for nitrification control. *Environ. Sci. Technol.* **2007**, *41*, 7039–7046.
80. Mitch, W. A.; Gerecke, A. C.; Sedlak, D. L. A N-Nitrosodimethylamine (NDMA) precursor analysis for chlorination of water and wastewater. *Water Res.* **2003**, *37*, 3733–3741.
81. Mitch, W. A.; Sharp, J. O.; Trussell, R. R.; Valentine, R. L.; Alvarez-Cohen, L.; Sedlak, D. L. N-nitrosodimethylamine (NDMA) as a drinking water contaminant: A review. *Environ. Eng. Sci.* **2003**, *20*, 389–404.
82. Kemper, J. M.; Westerhoff, P.; Dotson, A.; Mitch, W. A. Nitrosamine, dimethylnitramine, and chloropicrin formation during strong base anion-exchange treatment. *Environ. Sci. Technol.* **2009**, *43*, 466–472.
83. Wilczak, A.; Assadi-Rad, A.; Lai, H. H.; Hoover, L. L.; Smith, J. F.; Berger, R.; Rodigari, F.; Beland, J. W.; Lazzelle, L. J.; Kincannon, E. G.; Baker, H.; Heaney, C. T. Formation of NDMA in chloraminated water coagulated with DADMAC cationic polymer. *J. Am. Water Works Assoc.* **2003**, *95*, 94–106+112.
84. Kemper, J. M.; Walse, S. S.; Mitch, W. A. Quaternary amines as nitrosamine precursors: A role for consumer products? *Environ. Sci. Technol.* **2010**, *44*, 1224–1231.
85. Park, S. H.; Piyachaturawat, P.; Taylor, A. E.; Huang, C. H. Potential N-nitrosodimethylamine (NDMA) formation from amine-based water treatment polymers in the reactions with chlorine-based oxidants and nitrosifying agents. *Water Sci. Technol.* **2009**, *9*, 279–288.
86. Park, S. H.; Wei, S.; Mizaikoff, B.; Taylor, A. E.; Favero, C.; Huang, C. H. Degradation of amine-based water treatment polymers during chloramination as N-nitrosodimethylamine (NDMA) precursors. *Environ. Sci. Technol.* **2009**, *43*, 1360–1366.
87. Pehlivanoglu-Mantas, E.; Sedlak, D. L. Measurement of dissolved organic nitrogen forms in wastewater effluents: Concentrations, size distribution and NDMA formation potential. *Water Res.* **2008**, *42*, 3890–3898.
88. Shen, R.; Andrews, S. A. Demonstration of 20 pharmaceuticals and personal care products (PPCPs) as nitrosamine precursors during chloramine disinfection. *Water Res.* **2011**, *45*, 944–952.
89. Zhou, W.; Chen, C.; Lou, L.; Yang, Q.; Zhu, L. Formation potential of nine nitrosamines from corresponding secondary amines by chloramination. *Chemosphere* **2014**, *95*, 81–87.
90. Zhou, W. J.; Boyd, J. M.; Qin, F.; Hrudey, S. E.; Li, X. F. Formation of N-nitrosodiphenylamine and two new N-containing disinfection byproducts from chloramination of water containing diphenylamine. *Environ. Sci. Technol.* **2009**, *43*, 8443–8448.

91. Krasner, S. W.; Mitch, W. A.; McCurry, D. L.; Hanigan, D.; Westerhoff, P. Formation, precursors, control, and occurrence of nitrosamines in drinking water: A review. *Water Res.* **2013**, *47*, 4433–4450.
92. Schmidt, C. K.; Brauch, H. J. N,N-dimethylsulfamide as precursor for N-nitrosodimethylamine (NDMA) formation upon ozonation and its fate during drinking water treatment. *Environ. Sci. Technol.* **2008**, *42*, 6340–6346.
93. Padhye, L.; Luzinova, Y.; Cho, M.; Mizaiikoff, B.; Kim, J. H.; Huang, C. H. PolyDADMAC and dimethylamine as precursors of N -nitrosodimethylamine during ozonation: Reaction kinetics and mechanisms. *Environ. Sci. Technol.* **2011**, *45*, 4353–4359.
94. Padhye, L. P.; Kim, J. H.; Huang, C. H. Oxidation of dithiocarbamates to yield N-nitrosamines by water disinfection oxidants. *Water Res.* **2013**, *47*, 725–736.
95. Shen, R.; Andrews, S. A. In *Nitrosamine Formation from PPCPs in Three Water Types During Chloramine Disinfection*; Water Quality Technology Conference and Exposition, 2010; pp 1323–1329.
96. Von Gunten, U.; Salhi, E.; Schmidt, C. K.; Arnold, W. A. Kinetics and mechanisms of N-nitrosodimethylamine formation upon ozonation of N,N-dimethylsulfamide-containing waters: Bromide catalysis. *Environ. Sci. Technol.* **2010**, *44*, 5762–5768.
97. Chen, P. H.; Richardson, S. D.; Krasner, S. W.; Majetich, G.; Glish, G. L. Hydrogen abstraction and decomposition of bromopicrin and other trihalogenated disinfection byproducts by GC/MS. *Environ. Sci. Technol.* **2002**, *36*, 3362–3371.
98. Chu, W.; Gao, N.; Yin, D.; Krasner, S. W. Formation and speciation of nine haloacetamides, an emerging class of nitrogenous DBPs, during chlorination or chloramination. *J. Hazard. Mater.* **2013**, *260*, 806–812.
99. Chu, W. H.; Gao, N. Y.; Deng, Y.; Krasner, S. W. Precursors of dichloroacetamide, an emerging nitrogenous DBP formed during chlorination or chloramination. *Environ. Sci. Technol.* **2010**, *44*, 3908–3912.
100. Plewa, M. J.; Wagner, E. D.; Jazwierska, P.; Richardson, S. D.; Chen, P. H.; McKague, A. B. Halonitromethane drinking water disinfection byproducts: chemical characterization and mammalian cell cytotoxicity and genotoxicity. *Environ. Sci. Technol.* **2004**, *38*, 62–68.
101. Krasner, S. W.; Chinn, R.; Hwang, C. J.; Barrett, S. Analytical methods for brominated organic disinfection by-products. In *Proceedings of the 1990 American Water Works Association Water Quality Technology Conference*; American Water Works Association: Denver, CO, 1991.
102. Richardson, S. D.; Thruston, A. D., Jr.; Caughran, T. V.; Chen, P. H.; Collette, T. W.; Floyd, T. L.; Schenck, K. M.; Lykins, B. W.; Sun, G.-R.; Majetich, G. Identification of new ozone disinfection byproducts in drinking water. *Environ. Sci. Technol.* **1999**, *33*, 3368–3377.
103. Kundu, B.; Richardson, S. D.; Swartz, P. D.; Matthews, P. P.; Richard, A. M.; DeMarini, D. M. Mutagenicity in Salmonella of halonitromethanes: A recently recognized class of disinfection by-products in drinking water. *Mutat. Res.* **2004**, *562*, 39–65.

104. Kundu, B.; Richardson, S. D.; Granville, C. A.; Shaughnessy, D. T.; Hanley, N. M.; Swartz, P. D.; Richard, A. M.; DeMarini, D. M. Comparative mutagenicity of halomethanes and halonitromethanes in Salmonella TA100: Structure-activity analysis and mutation spectra. *Mutat. Res.* **2004**, *554*, 335–350.
105. Choi, J.; Richardson, S. D. Formation of halonitromethanes in drinking water. In *Proceedings of the International Workshop on Optimizing the Design and Interpretation of Epidemiologic Studies to Consider Alternative Disinfectants of Drinking Water*; U.S. EPA: Raleigh, NC, 2005.
106. Hu, J.; Song, H.; Addison, J. W.; Karanfil, T. Halonitromethane formation potentials in drinking waters. *Water Res.* **2010**, *44*, 105–114.
107. Richardson, S. D.; Thruston, Jr., A. D.; Rav-Acha, C.; Groisman, L.; Popilevsky, I.; Juraev, O.; Glezer, V.; McKague, A. B.; Plewa, M. J.; Wagner, E. D. Tribromopyrrole, brominated acids, and other disinfection byproducts produced by disinfection of drinking water rich in bromide. *Environ. Sci. Technol.* **2003**, *37*, 3782–3793.
108. Yang, M.; Zhang, X. Halopyrroles: A new group of highly toxic disinfection byproducts formed in chlorinated saline wastewater. *Environ. Sci. Technol.* **2014**, *48*, 11846–11852.
109. McDonald, T. A.; Komulainen, H. Carcinogenicity of the chlorination disinfection by-product MX. *J. Environ. Sci. Health - C* **2005**, *23*, 163–214.
110. Schulten, H. R.; Schnitzer, M. A state of the art structural concept for humic substances. *Naturwissenschaften* **1993**, *80*, 29–30.
111. Qin, F.; Zhao, Y. Y.; Zhao, Y.; Boyd, J. M.; Zhou, W.; Li, X. F. A toxic disinfection by-product, 2,6-dichloro-1,4-benzoquinone, identified in drinking water. *Angew. Chem., Int. Ed.* **2010**, *49*, 790–792.
112. Zhao, Y.; Anichina, J.; Lu, X.; Bull, R. J.; Krasner, S. W.; Hrudey, S. E.; Li, X. F. Occurrence and formation of chloro- and bromo-benzoquinones during drinking water disinfection. *Water Res.* **2012**, *46*, 4351–4360.
113. Wang, W.; Qian, Y.; Boyd, J. M.; Wu, M.; Hrudey, S. E.; Li, X. F. Halobenzoquinones in swimming pool waters and their formation from personal care products. *Environ. Sci. Technol.* **2013**, *47*, 3275–3282.
114. Qian, Y.; Wang, W.; Boyd, J. M.; Wu, M.; Hrudey, S. E.; Li, X. F. UV-induced transformation of four halobenzoquinones in drinking water. *Environ. Sci. Technol.* **2013**, *47*, 4426–4433.
115. Wang, W.; Qian, Y.; Li, J.; Moe, B.; Huang, R.; Zhang, H.; Hrudey, S. E.; Li, X. F. Analytical and toxicity characterization of halo-hydroxylbenzoquinones as stable halobenzoquinone disinfection byproducts in treated water. *Anal. Chem.* **2014**, *86*, 4982–4988.

Chapter 12

Carbonaceous and Nitrogenous Disinfection By-Product Formation Potentials of Amino Acids

Meric Selbes,¹ Junhong Shan,² S. Sule Kaplan Bekaroglu,³
and Tanju Karanfil*,⁴

¹Hazen and Sawyer, Environmental Engineers and Scientists,
Fairfax, Virginia 22030, USA

²Public Utilities Board, Singapore 608576, Singapore

³Water Institute, Suleyman Demirel University, Isparta 32260, Turkey

⁴Department of Environmental Engineering and Earth Sciences,
Clemson University, Anderson, South Carolina 29625, U.S.A.

*E-mail: tkaranf@clemson.edu.

Nine amino acids (AAs) were examined under different oxidation conditions to determine their formation potential for regulated carbonaceous DBPs (trihalomethanes (THMs) and haloacetic acids (HAAs)) and selected emerging nitrogenous DBPs (haloacetonitriles (HANs), halonitromethanes (HNMs) and nitrosamines). Aspartic acid and histidine exhibited very high dihalogenated-HANs and HAAs formation during chlorination, but their reactivity significantly decreased after ozonation. Glycine followed by lysine yielded the highest level of HNMs and THMs formation during ozonation-chlorination, but they did not have measurable yields for either classes of DBPs during chlorination. All other AAs showed very low carbonaceous and nitrogenous DBP yields. The nitrosamine yields of all nine AAs were very low or below the minimum reporting levels during chloramination, ozonation, and ozonation-chloramination. These results indicated that the presence of AAs in natural waters can result in some contributions to certain halogenated DBPs depending on the oxidation conditions. However, they do not appear to be an important contributor to nitrosamines formation.

Introduction

Recent research has shown that emerging nitrogenous disinfection by-products (N-DBPs) exhibit orders of magnitude higher cyto- and geno-toxicity than the regulated carbonaceous DBPs (C-DBPs) (1). Therefore, it should not be surprising to see N-DBP regulated in the near future. Recent research has shown that nitrogen-rich organic materials in natural waters play an important role in the formation of N-DBPs (2–4). However, the important precursors and the formation mechanisms of N-DBPs still remain largely unknown.

Amino acids (AAs) have been found in fresh waters in a wide range of concentrations from 5 to 2000 $\mu\text{g/L}$, in either free or combined peptides, nucleic acids, purines, pyrimidines, and proteins (5, 6). Thurman (7) reported that the total AAs, which were the sum of the free and combined AAs, accounted for 2.6% of the dissolved organic carbon (DOC) and 35% of the dissolved organic nitrogen (DON) in some lakes. Hagedorn and colleagues (8) observed in their studies of catchment runoff a 20% to greater than 75% of the DON of the total AAs observed. Elevated amino acid levels were also found in the presence of algae blooms, the degradation of which is a major cause of increased AA levels in natural waters (7, 9–11). In a recent survey of sixteen water treatment plants in the United States, the total AA concentrations, identified as glycine, glutamic acid, alanine, aspartic acid, leucine, proline and serine, constituted an average 15% of the DON in the source waters (2, 7, 12–14).

The presence of AAs in raw and treated waters requires substantial amounts of chlorine for treatment (15, 16). The relative chlorine reactivity of the AAs depends on the side chain groups attached to the α -carbon. Studies conducted for purposes of reacting AAs with chlorine clearly indicated the formation of various classes of DBPs including haloacetaldehydes, haloacetonitriles (HANs), cyanogen chloride, trihalomethanes (THMs) and haloacetic acids (HAAs) (15, 17, 18). A recent study showed that AAs with activated aromatic structures (e.g. tryptophan, tyrosine) were potent precursors of THMs and HAAs (17). Additionally, absent the reactive ring structure, aspartic acid and asparagines produced high levels of HAAs.

Investigations conducted on the reaction(s) of ozone with AAs determined that the side chains of AAs were responsible for the high ozone reactivity in polypeptide structures (19). Structures that possess side groups such as amino nitrogen or activated aromatic ring were identified as the most reactive AAs. This AA ozonation leads to the formation of aldehydes such as formaldehyde, acetaldehyde, glyoxal and glyoxal derivatives.

Unlike the carbonaceous DBPs (C-DBPs), very little is known regarding how N-DBPs form from amino acids, especially for halonitromethanes (HNMs) and N-nitrosamines. HNM constitutes one group of N-DBPs that exhibits high degrees of cyto- and geno-toxicity (1, 21). Drinking waters and wastewater effluents under chloramination conditions are a particularly relevant medium in which nitrosamine, especially *N*-nitrosodimethylamine (NDMA), can form (20). Nitrosamines, which have been classified as a probable human carcinogen by the United States Environmental Protection Agency, can pose important health risks even at ng/L concentrations. As a result, the Canada Ontario Ministry of

the Environmental and Energy established a maximum allowable concentration of 9 ng/L for NDMA, and the California Department of Health Service set an interim action level of 10 ng/L. Although nitrosamines are not currently regulated in the United States, NDMA and four other nitrosamines [*N*-nitrosodiethylamine (NDEA), *N*-nitroso-di-*n*-propylamine (NDPA), *N*-nitrosodiphenylamine (NDPhA), *N*-nitrosopyrrolidine (NPYR)] are on the USEPA's Contaminant Candidate List-3, and are monitored under the Unregulated Contaminant Monitoring Rule 2.

Recent studies on the formation potentials of HNMs in natural waters found that HNM yields increased with decreasing DOC/DON ratios (i.e., increasing organic nitrogen content per organic carbon in water) during ozonation followed by chlorination (3). The hydrophilic components of dissolved NOM, especially nitrogenous organic compounds, are important precursors of HNMs in the NOM pool (2, 3). Only a limited number of studies, however, have been conducted to elucidate trichloronitromethane (TCNM) formation by AAs during chlorination, using glycine (4, 22), tyrosine (4), tryptophan and aspartic acid (23). Similarly, very little is known about of the formation of NDMA caused by AAs, aside from that undertaken by Mitch et al. (4). Specifically, they observed nitrosamine formation (NDMA, NMEA and NDEA) in aspartic acid, proline and histidine after chloramination (24); and NDMA formation of <2ng/L in glycine after chloramination (4).

Produced during chlorination HANs consist of an acetate derivative group, known as a cyano (-CN) group, and up to three halogens replacing the hydrogen atoms. Dichloroacetonitrile (DCAN), the most prevalent of the HANs, was detected at 0.3-8.1 µg/L in 10 chlorinated drinking waters in southern Ontario (25), and at median and maximum concentrations of 1 and 12 µg/L, in 12 wastewater treatment plans in the US (26). In both studies, DCAN levels were 10% of the molar concentration for THMs. DCAN formation also occurred when amino acid moieties were used to during the chlorination of AAs, polypeptides, and hydrophobic substances (27). Moreover, aspartic acid (16, 23) and alanine (28) used in chlorination has caused the formation of HANs from AAs.

Since AAs constitute an important fraction of organic nitrogen pool in natural waters, and previous studies have mainly focused on the formation regulated C-DBPs (e.g., THM and/or HAA) from AAs mostly for chlorination, the objective of this study was to concurrently investigate formation potential of both regulated C-DBPs (THMs and HAAs) and selected N-DBPs (HANs, HNMs and nitrosamines) from AAs ozonation, chloramination and chlorination conditions. The results were also used to provide additional insight to the DBP formation mechanisms from AAs.

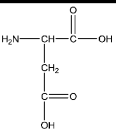
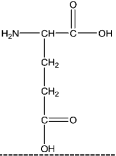
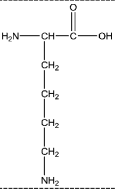
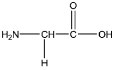
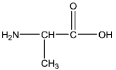
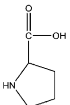
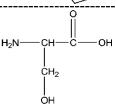
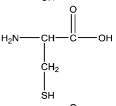
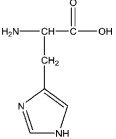
Materials and Methods

Amino Acids

Nine AAs (alanine, aspartic acid, cysteine, glutamic acid, glycine, lysine, histidine, proline and serine) were carefully selected based on charge property, polarity and hydrophobicity. They were classified into four groups depending upon

their acidity and polarity: acidic, basic, polar, and nonpolar. The physicochemical characteristics and structures of the selected AAs are listed in Table 1.

Table 1. AAs Selected for This Study

Type	Amino Acid	Structure	pK ₁	pK ₂	pK ₃	Designation*
Acidic	Aspartic Acid		2.0	10.0	4.04	W
	Glutamic Acid		2.2	9.7	4.39	W
Basic	Lysine		2.2	9.2	11.1	W
Non-Polar	Glycine		2.4	9.8	-	W
	Alanine		2.3	9.9	-	N
	Proline		2.0	10.6	-	W
Polar	Serine		2.1	9.2	-	W
	Cysteine		1.8	10.8	8.6	L
	Histidine		1.8	9.2	6.8	N

* Hydrophobic = L, Hydrophilic = W, Neutral = N

Amino acids were purchased from a certified vendor (Sigma-Aldrich) and a 500 mg/L stock solution of each AA was prepared in deionized distilled water. For the formation potential (FP) tests, 1 mg/L (and 10 mg/L in selected experiments) AA sample solutions were prepared with dilution from the main stock. These solutions were buffered at pH 6.0 or 8.0 using 4 mM sodium bicarbonate and adjusted with 1M HCl or NaOH. The AA concentrations (1 or 10 mg/L) in the diluted solutions were confirmed using a TOC analyzer (Shimadzu Corp., USA). Although these AA concentrations are higher than their typical occurrence levels in fresh waters, they were intentionally selected at these high levels to magnify and better examine the DBP formation; an approach that has been used in previous studies (4, 29).

Formation Potential Tests

The solutions of chlorine stock (500–2,000 mg/L) were prepared by diluting sodium hypochlorite (~5% available free chlorine). The preformed monochloramine stock solutions (1,000 mg/L) were generated by mixing the sodium hypochlorite and ammonium sulfate solutions at a Cl₂-to-N mass ratio of 4:1 at pH of 9. The ozone stock solutions (28–32 mg/L) were produced using an ozone generator (Griffin Technics, GTC-1B) fed with ultra-high-purity oxygen gas. These oxidants were used to determine the precursor levels of each class of DBPs under their favorable disinfection conditions. Chlorination and ozonation-chlorination were used in the FP tests to examine the formation of the following halogenated DBPs: THMs, HAAs, HANs and HNMs. Chloramination, ozonation and ozonation-chloramination were applied for the nitrosamine FP tests, which were conducted in the presence of an excess disinfectant. The formula developed by Krasner and co-workers (30) (Equation 1 and 2) was used to determine the chlorine dosage.

$$\text{Chlorine Dose (mg/L)} = 3 \times \text{DOC (mg-C/L)} + 10 \quad (1)$$

$$\text{Chloramine Dose (mg/L)} = 3 \times \text{DOC (mg-C/L)} \quad (2)$$

$$\text{Ozone Dose (mg/L)} = 10 \times \text{DOC (mg-C/L)} \quad (3)$$

Based on the Equation 1, typical chlorine doses were around 11–12 mg/L for 1 mg/L AA concentration. Ozonation was carried out by adding ozone stock solution to the samples approximately at 4 mg/L (Equation 3). Following ozone addition, the samples were mixed on a stir plate for 5 min. After 5 minutes, they were also exposed same doses of chlorine. Prior to chlorination presence of residual ozone confirmed and thus, ozone was not a limiting factor during ozonation period. Since 10 mg/L AA concentration was used for nitrosamine FP test conditions, initial chloramine dose was 10–15 mg/L. Although AAs have high oxidant demands (i.e., chlorine, ozone), the levels of oxidants were sufficient to maintain a residual concentration at the end of the reaction time.

Table 2. Analytical Methods and Minimum Reporting Levels

<i>Parameter</i>	<i>Unit</i>	<i>Measurement Method</i>	<i>Instrument</i>	<i>MRL or Accuracy^a</i>
DOC ^b	mg/L	SM 5310B	TOC-V _{CHS} & TNM-1, Shimadzu Corp., Japan	0.1
DN (=DON) ^c	mg/L	High Temperature Combustion	TOC-V _{CHS} & TNM-1, Shimadzu Corp., Japan	0.1
pH	-	SM 4500-H ⁺	420A, Orion Corp., USA	±0.01 ^d
THMs & HANs ^e	µg/L	US EPA Method 551.1	6890 GC-ECD, Agilent, USA	1.0
HAAs ^f	µg/L	SM 6251 B ^g	6890 GC- ECD, Agilent, USA	1.0
HNMs ^g	µg/L	US EPA Method 551.1	6850 GC-ECD, Agilent, USA	0.7
Nitrosamines ^h	ng/L	US EPA 521	Varian GC/MS/MS	3.0
FAC	mg/L	SM 4500-Cl F	NA	0.1

^a MRLs were determined in the lab in previous works (31). Accuracy as reported by the manufacturer. ^b Reagent grade potassium hydrogen phthalate was used to prepare external standards. ^c Reagent grade potassium nitrate was used to prepare external standards. Since there was no inorganic nitrogen present, measured DN values were equal to DON. ^d Accuracy (pH units). ^e THMs and HANs were extracted by liquid-liquid extraction with methyl-tert butyl ether (MtBE) and analyzed by GC-µECD. ^f HAAs were extracted by liquid-liquid extraction with MtBE, derivatized with diazomethane and analyzed by GC-µECD. ^g HNM were extracted by liquid-liquid extraction with MtBE and analyzed by GC-µECD. ^h Nitrosamines were extracted by solid phase extraction, eluted with dichloromethane and analyzed by GC-MS. DOC (Dissolved Organic Carbon), DN (Dissolved Nitrogen), DON (Dissolved Organic Nitrogen), THM (Trihalomethanes), HAN (Haloacetonitriles), HAA (Haloacetic acids), HNM (halonitromethanes), SM (Standard Methods), EPA (Environmental Protection Agency), GC (Gas Chromatography), MS (Mass Spectrometer), FAC (Free Available Chlorine), NA (Not Applicable).

Experiments for THM, HAA, HAN and HNM FP tests were conducted in 125-ml amber glass bottles without headspace at room temperature (~22°C) in the dark for one day. For the nitrosamines FP test, 1-L amber glass bottles were used due to higher sample volume required for extraction, and the reaction time was seven days.

Analytical Methods

The analytical methods used in the study and their respective minimum reporting levels (MRLs) are provided in Table 2. Either standard methods (SM) or USEPA methods were used in the DBP analyses with minor modifications. The detailed information about these methods can be found elsewhere (31). For DOC, DN and DBP analyses, samples were analyzed in duplicates. The error bars in all the graphs show the variability due to multiple analysis (n=2) under the same conditions.

Results and Discussion

The FP results have been discussed individually for each class of DBP, specifically for the experiments conducted at a pH of 8.0. An overall evaluation of the pH level (6.0 vs. 8.0) is provided at the end.

Nitrogenous-DBPs

Halonitromethanes (HNMs)

The formation of all HNM species from nine amino acids after chlorination was below MRL, which is in agreement with the reports in the literature. Merlet et al. (22) reported <0.01% mole/mole yield rate (<0.7 µg/mg-C) of TCNM from glycine after chlorination at pH 7.1. A recent report by Mitch et al. (4) also showed low yields of TCNM from glycine and tyrosine during chlorination FP tests (0.8 µg/L from 64 µM glycine (4.8mg/L)). No TCNM formation was found from chlorinated tryptophan and aspartic acid (23).

Ozonation followed by chlorination was more favorable than chlorination for HNM formation, as previously observed in natural waters (3, 26, 32–35). Furthermore, trihalogenated HNMs (i.e., TCNM) was the major species detected which is consistent with the literature (34). The ozonation of amines in aqueous solutions can lead to oxidation at both the amine and on the side chain of the molecule (19, 36). The higher TCNM formation caused by AAs during pre-ozonation may be due to the oxidation of the amine group by the strong oxidant ozone to form a nitro group (22, 37). The nitro compound will, then, be further substituted to form nitromethanes and react with chlorine. TCNM was the only HNM species formed in our study, with glycine showing remarkably high TCNM formation (223.4 µg/L), followed by lysine and proline (14.6 and 17.2 µg/L). We also detected a small amount of TCNM in glutamic acid (0.8 µg/L) and serine (0.9 µg/L), while for the remainder of the AAs examined, the HNM

concentrations were either below MRL or were not detected. A comparison of our AA results are plotted and normalized in Figure 1 based on their DOC ($\mu\text{g-TCNM}/\text{mg-DOC}$). The levels of TCNM during ozonation-chlorination were comparable with our previously reported findings (32).

These findings were used to provide additional insight to the formation mechanism of TCNM from glycine. The ozonation of glycine is known to form nitrate, formic acid and carbon dioxide as by-products (38). Under certain conditions, the formation of formic acid can be relatively high (>0.05 mM formed from 1.5 mM O_3 vs. 1.1 mM glycine, in the presence of 0.2 mM hydrogenocarbonate ions) (29), suggesting the possible rupture of the C-C bond and the subsequent formation of nitromethanes. It has been hypothesized that the rupture of the C-C bond may occur with the formation of a strongly reducing α -aminoradical in an unprotonated amino group; this rupture may occur when the electron abstraction from the amine nitrogen is then re-arranged with decarboxylation (39). It is also hypothesized that the reaction follows the oxidation of the carboxyl group from ozone to peroxide (37), followed by decarboxylation (29, 39), which in turn causes the oxidation of the amine group to the nitro group (22, 37). A halogenation reaction with chlorine, which causes TCNM formation, is the result.

The greater TCNM yield from lysine after ozonation-chlorination was attributed to the production of glycine and glycine-like intermediates formed during ozonation. The long chain structure of α -C of lysine makes the breakage of the C-C bond easier compared to other amino acids examined in this study.

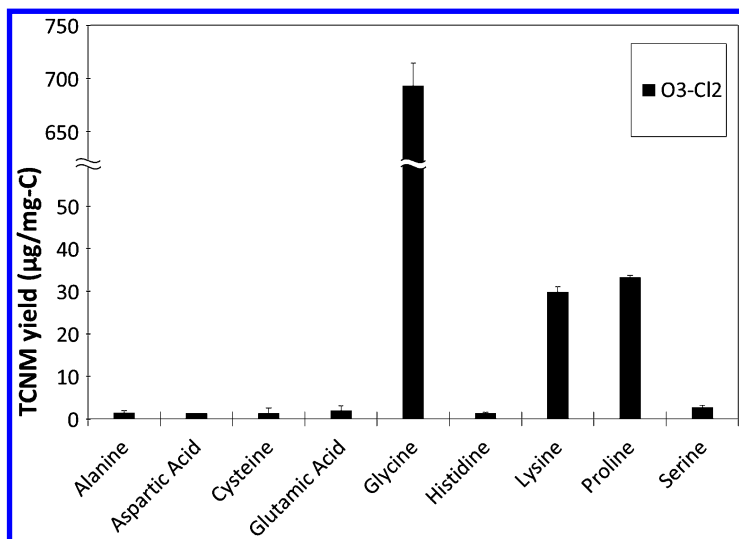


Figure 1. TCNM formation potential results from amino acids during ozonation-chlorination at pH 8.0 (DOC = 0.3 ~ 0.5 mg/L, DON = 0.04 ~ 0.30 mg/L). TCNM formation during chlorination were below MRL and thus, were not included in this figure.

Haloacetonitriles (HANs)

In this study, we also observed aspartic acid to form high levels of DCAN (549.2 $\mu\text{g}/\text{mg-C}$) during chlorination at a pH of 8.0, with histidine the second most reactive AA, forming 173.7 $\mu\text{g}/\text{mg-C}$ (seen Figure 2). The high level of DCAN FP of aspartic acid has been validated in two previous studies: that of Trehy et al. (16) in which they used 158 $\mu\text{g}/\text{mg-C}$ at pH of 6.4; and that of Bond et al. (23) in which they used 0.06 mol/mol 130 $\mu\text{g}/\text{mg-C}$ at pH of 7. Both studies concur with a study by Ram et al. in which the chlorination of AAs, polypeptides, and hydrophobic substances with amino acid moieties were used to create DCAN (27). Although Chu et al. (28) reported the formation of non-detectable HANs (DCAN and TCAN) in 0.1 mM of alanine after chlorination, in our study we observed a DCAN formation level of only 3.9 $\mu\text{g}/\text{mg-C}$ DCAN after chlorination. We hypothesize that the different experimental conditions, such as pH or oxidant dosage is perhaps the reason for this greater alanine yield. We also observed the formation of 6.1 $\mu\text{g}/\text{mg-C}$ chloroacetonitrile (CAN).

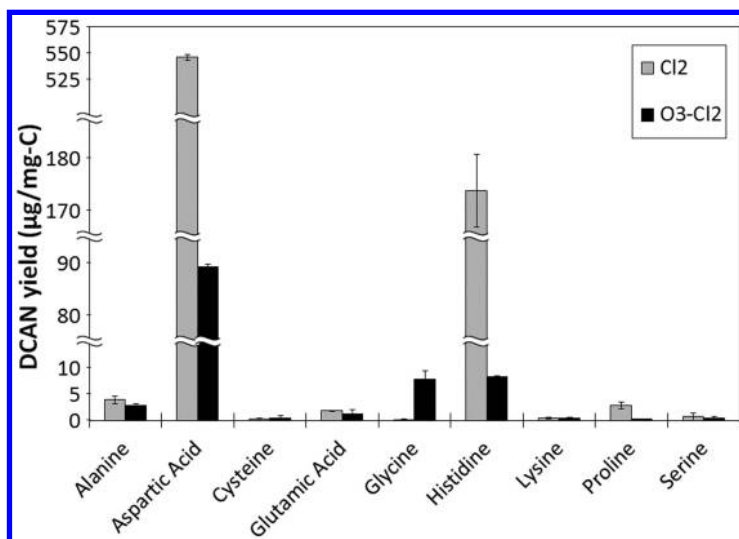


Figure 2. DCAN formation potential results from amino acids during chlorination and ozonation-chlorination at pH 8.0 (DOC = 0.3 ~ 0.5 mg/L, DON = 0.04 ~ 0.30 mg/L).

In their chlorination studies of free and combined amino acids, Hureiki et al. (15) also determined that the chlorination of AAs can cause nitrile formation. Specifically, after chlorination they observed a substantial formation of DCAN from histidine, but not for alanine, suggesting that the DCAN is not formed from the side chain of histidine. If the substitution reaction for chlorine to replace the side chain of the heterocyclic ring in histidine occurs, an intermediate with a similar structure to alanine should form. To produce the DCAN, a ring-opening reaction must occur during the chlorination of histidine. This reaction is possible

because the activated aromatic ring was the essential reactive site for tyrosine with its high chlorine demand and high TCM formation (15). For pre-ozonation, the oxidation with ozone likely results in the nitro compounds formation and thus, reduces the formation of nitriles. This oxidation can explain the dramatic decrease in the DCAN formation compared to chlorination (e.g. from 549.2 to 89.2 $\mu\text{g}/\text{mg-C}$ for aspartic acid and from 173.7 to 8.2 $\mu\text{g}/\text{mg-C}$ for histidine).

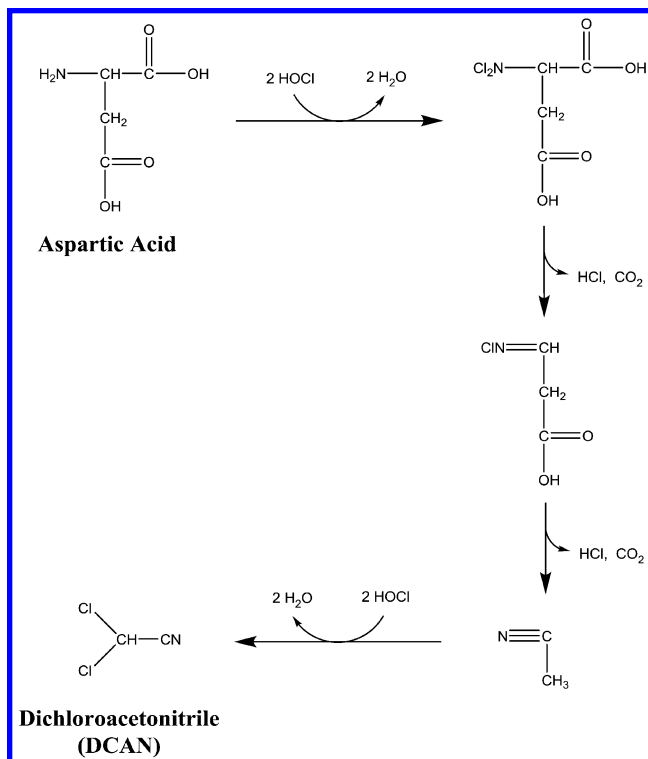


Figure 3. Proposed reaction mechanism of DCAN formation from aspartic acid during chlorination. (Figure Adopted from Hureiki et al. (15)).

Nitrosamines

Initial nitrosamines FP test for three selected AAs at 1.0 mg/L concentration did not produce measurable nitrosamines. To further confirm the results, it was decided to magnify the initial concentration of AAs during the experiments by increasing to 10.0 mg/L. Three different oxidation scenarios, monochloramination, ozonation and ozonation-chloramination were tested for all nine AAs. Ozonation was also examined independently because of the recently reported NDMA formation after ozonation in both the lab (40, 41) and in full scale ozonation plants (42, 43).

Despite this increase to 10 mg/L, NDMA and NDBA FP concentrations remained very low at levels of 5 ng/L NDBA from lysine after chloramination (Table 3). Mitch and co-workers reported non-detectable nitrosamine (NDMA, NMEA and NDEA) formation from aspartic acid, proline and histidine during chloramination (24); and NDMA formation of <2 ng/L from glycine and tyrosine during chloramination (4).

Table 3. Nitrosamine FPs of AAs Tested in This Study

<i>Amino Acids*</i>	<i>DOC (mg C/L)</i>	<i>DON (mg N/L)</i>	<i>Chloramine</i>	<i>Ozone- Chloramine</i>		<i>Ozone</i>
			<i>NDBA (ng/L)</i>	<i>NDBA (ng/L)</i>	<i>NPYR (ng/L)</i>	<i>NPYR (ng/L)</i>
Alanine	4.0	1.6	<MRL	<MRL	<MRL	<MRL
Aspartic Acid	3.6	1.1	<MRL	<MRL	<MRL	<MRL
Cysteine	3.0	1.2	<MRL	<MRL	<MRL	<MRL
Glutamic Acid	4.1	1.0	<MRL	<MRL	<MRL	<MRL
Glycine	3.2	1.9	<MRL	<MRL	<MRL	<MRL
Histidine	4.6	2.7	<MRL	<MRL	<MRL	<MRL
Lysine	4.9	1.9	5	9	<MRL	<MRL
Proline	5.2	1.2	<MRL	3	4	4
Serine	3.4	1.3	<MRL	3	<MRL	<MRL

* Initial concentration of amino acids were 10 mg/L. Other nitrosamines including NDMA, NDEA, NMEA, NMOR, NDPA, and NPYP were not detected.

Principally all amines with the exception of primary amines (i.e., amino acids) have the potential to form nitrosamines (44). During chloramination, only lysine was observed to form NDBA (5 ng/L). This may be due to reaction of butyl chains of two lysine's with chloramines. Since ozone is a stronger oxidant, it is likely to form intermediates that are more prone to reaction (45). Thus, during ozonation-chloramination NDBA yield from lysine increased to 9 ng/L. In addition, during ozonation-chloramination, NDBA formation of 3 ng/L from proline and serine was also observed. Proline also lead to formation of 4 ng/L NPYR during both ozonation and ozonation-chloramination conditions. Other nitrosamines were undetected. NPYR is formed from proline because of its structure; once ozonation causes the decarboxylation of proline followed by nitrosation, the nitrogen of the nitrosating agent is likely sourced from the oxidation of the nitrogen atom in the proline's ring. The direct formation of nitrosamines during ozonation has also occurred with other precursors (45). The authors observed very low nitrosamine yields of AAs during the FP tests (<0.01% molar conversion). Considering the occurrence concentrations of total AAs in

natural waters, it is unlikely that AAs will play a role in the formation of NDMA and other nitrosamines during chloramination, ozonation, and ozonation that is followed by chloramination.

Carbonaceous-DBPs

Trihalomethanes (THMs)

Trichloromethane (TCM) was the only THM species observed during both chlorination and ozonation-chlorination (Figure 4), with the selected AAs in this study forming TCMs within the range of <MRL-13.5 $\mu\text{g/L}$ after chlorination. These values are consistent with that previously reported by the authors (32). Ozonation can increase in TCM formation. Bond et al. (23) reported that 0.02 mol TCM formed from 1 mol aspartic acid after chlorination (i.e., 49.7 $\mu\text{g/mg-C}$), which is relatively comparable to the yield observed in this study, 18.8 $\mu\text{g/mg-C}$. Chu et al. (28) reported a yield rate of 0.23% (i.e., 5.7 $\mu\text{g/mg-C}$) for TCM formation from 0.1 mM alanine after chlorination, while no TCM formation from alanine was measurable during chlorination in this study. Hong et al. (17) studied chlorination of all 20 amino acids at pH 7 and found low THM formation (<4.9 $\mu\text{g/mg-C}$), except for tryptophan and tyrosine. The results of our study showed that pre-ozonation prior to chlorination had a drastic effect on TCM formation from glycine and lysine which was similar to HNMs. TCMs formation of glycine and lysine increased from <MRL to 83.4 and 33.9 $\mu\text{g/L}$, respectively. Other AA's TCM formations during ozonation-chlorination were comparable and were within the range of 6.7-11.8 $\mu\text{g/L}$.

Reaction sequences have been developed for the molecular ozone attack on amines (46), which suggests that amides and formylamine are caused by i) the breakdown of the carbon-nitrogen bond, ii) the formation of inorganic nitrogen and hydroxylamine, oxime or amine oxide, and iii) by the oxidation of the carbon.. All these reactions were shown to involve decarboxylation. Specifically, a study of glycine (29) determined that, for AAs, the intermediate created from the addition of ozone either released oxygen to create monohydroxylamine or caused carbon oxidation via a probable ozonide intermediate. Also the presence of oxamic and oxalic acids indicates that these reactions can occur without decarboxylation. Based on these findings reported in the literature, ozone should first launch an electrophilic attack on nitrogen and followed by two steps of oxidation on N with or without decarboxylation to form hydroxylamines (R-NHOH) and hypothetical hydronitrous acid, $\text{N}(\text{OH})_2\bullet$. Then oxime will be formed through dehydration and further oxidized to form aldehyde which has been previously reported in the literature (29). Since aldehyde could be generated by the hydrolysis of dihalogenated compound, the backward reaction could lead the formaldehyde to TCM with further halogenation during chlorination.

A significant amount of THM formation in lysine after ozonation-chlorination (Figure 4), prompted a comparison of the molar yields of DBP/amino acid of TCM and TCNM from glycine and lysine under ozonation-chlorination. The yields for glycine was 5.24% mole TCM and 10.20% mole TCNM per mole of glycine, respectively, and 4.15% mole TCM and only 1.29% of TCNM for lysine. These

results suggested that the mechanism for TCM formation from lysine may not follow the pathway proposed for TCNM. It is possible that intermediates other than glycine may form. In their study of the formation trends of THM and HNM Hu et al. (34) also observed a divergence in formation pathways. The findings of this study would explain these previously observed trends.

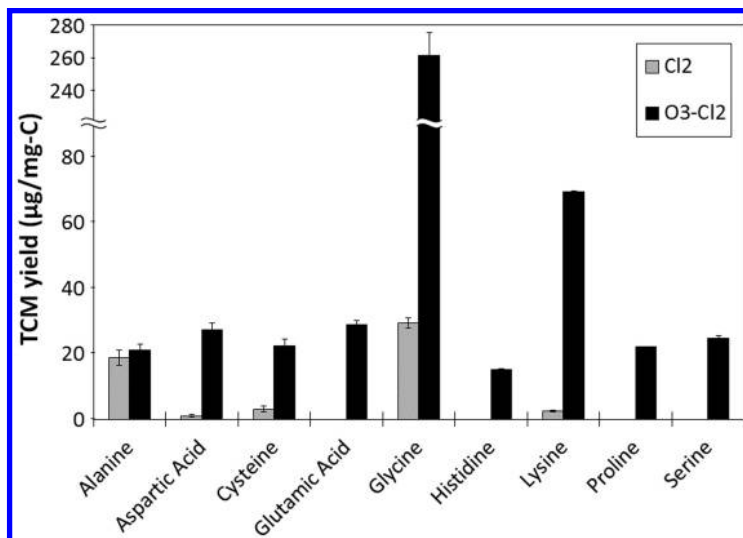


Figure 4. TCM formation potential results from amino acids during chlorination and ozonation-chlorination at pH 8.0 (DOC = 0.3 ~ 0.5 mg/L, DON = 0.04 ~ 0.30 mg/L).

Haloacetic Acids (HAAs)

The most reactive AA that caused DCAA formation was aspartic acid, which yielded a formation of 992.5 µg/mg-C during chlorination (Figure 5), followed by histidine, which yielded a formation of 336.3 µg/mg-C. These results were validated by the earlier study of Hong et al. (17), who also confirmed that of the 20 amino acids studied, aspartic acid and histidine caused the highest DCAA formation during chlorination at pH 7.0. Also since the DCAN produces DCAA after hydrolysis, these results were also consistent with HAN findings (15, 16, 47). Aspartic acid is also known to function as a reactive DCAA precursor, forming 0.26 mol/mol (693 µg/mg-C) after chlorination at pH 7.0 (23). Its reactivity is thought to result from the formation of a β-keto acid intermediate upon chlorination, a moiety known to have a high DCAA FP (15, 48). In terms of HAA speciation, aspartic acid and histidine (basic and hydrophilic AAs) formed very high concentrations of DCAA, whereas the formation of TCAA was significantly lower. This finding may be partially the result of the hydrophobicity of the

surrogate which was reported by Bond et al. (23). In that study, it was determined that the hydrophilic-acid or transphilic-acid surrogates (i.e., aspartic acid) formed predominantly DCAA during chlorination. In contrast, the hydrophobic-acid and hydrophobic-neutral surrogates (i.e., tryptophan and tyrosine) formed mainly TCAA.

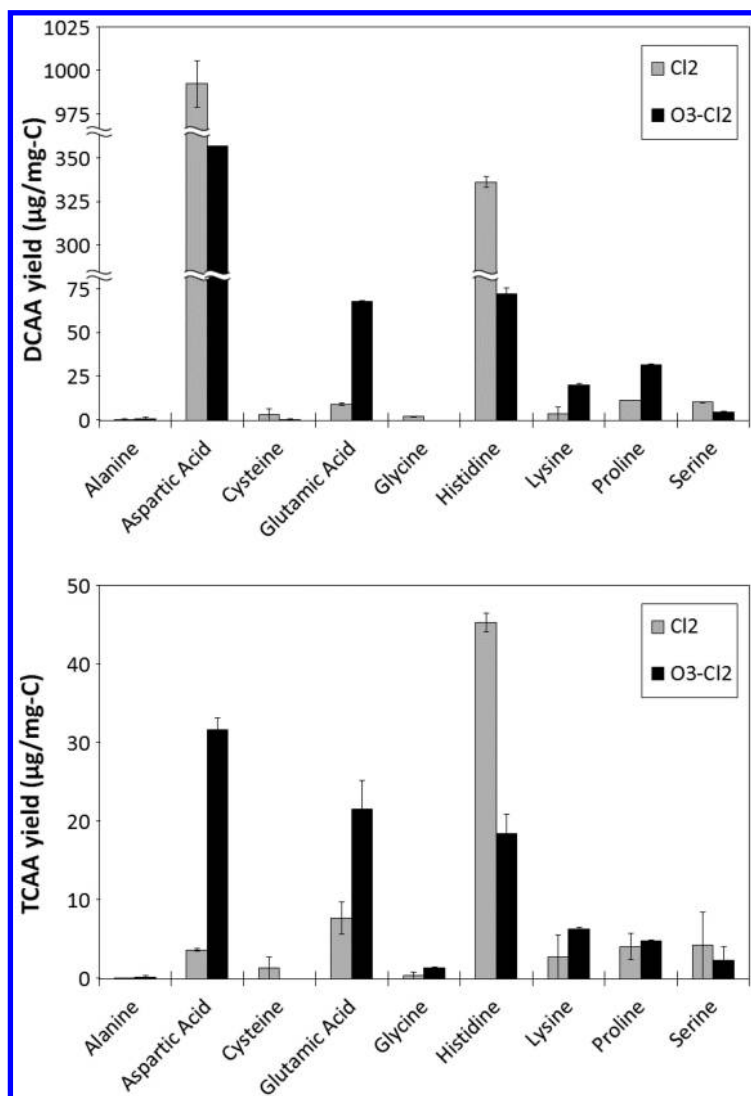


Figure 5. DCAA and TCAA formation potential results from amino acids during chlorination and ozonation-chlorination at pH 8.0 (DOC = 0.3 ~ 0.5 mg/L, DON = 0.04 ~ 0.30 mg/L).

Table 4. DBP FPs of AAs Tested in This Study at pH 6.0 and 8.0

<i>Amino Acid*</i>	<i>DOC (mg/L)</i>	<i>DON (mg/L)</i>	<i>TCNM (µg/L)</i>		<i>DCAN (µg/L)</i>		<i>TCM (µg/L)</i>		<i>DCAA (µg/L)</i>		<i>TCAA (µg/L)</i>	
			<i>pH 6.0</i>	<i>pH 8.0</i>	<i>pH 6.0</i>	<i>pH 8.0</i>	<i>pH 6.0</i>	<i>pH 8.0</i>	<i>pH 6.0</i>	<i>pH 8.0</i>	<i>pH 6.0</i>	<i>pH 8.0</i>
			Alanine	0.40	0.16	<MRL	<MRL	<MRL	1.6	<MRL	<MRL	<MRL
Aspartic Acid	0.36	0.11	<MRL	<MRL	211.3	197.7	<MRL	6.8	106.5	357.3	1.0	1.3
Cysteine	0.30	0.12	<MRL	<MRL	<MRL	<MRL	1.4	<MRL	<MRL	1.0	<MRL	<MRL
Glutamic Acid	0.41	0.10	<MRL	<MRL	<MRL	<MRL	<MRL	1.3	2.4	3.8	1.5	3.2
Glycine	0.32	0.19	<MRL	<MRL	<MRL	<MRL	<MRL	<MRL	<MRL	<MRL	<MRL	<MRL
Histidine	0.46	0.27	<MRL	<MRL	73.2	79.9	2.1	13.5	42.4	154.7	13.6	20.9
Lysine	0.49	0.19	<MRL	<MRL	<MRL	<MRL	2.5	<MRL	<MRL	1.9	<MRL	1.4
Proline	0.52	0.12	<MRL	<MRL	<MRL	1.5	<MRL	1.3	<MRL	5.9	<MRL	2.1
Serine	0.34	0.13	<MRL	<MRL	<MRL	<MRL	<MRL	<MRL	<MRL	3.5	<MRL	1.4

Continued on next page.

Chlorination

Table 4. (Continued). DBP FPs of AAs Tested in This Study at pH 6.0 and 8.0

<i>Amino Acid</i> [*]	<i>DOC</i> (mg/L)	<i>DON</i> (mg/L)	<i>TCNM</i> ($\mu\text{g/L}$)		<i>DCAN</i> ($\mu\text{g/L}$)		<i>TCM</i> ($\mu\text{g/L}$)		<i>DCAA</i> ($\mu\text{g/L}$)		<i>TCAA</i> ($\mu\text{g/L}$)			
			<i>pH 6.0</i>	<i>pH 8.0</i>	<i>pH 6.0</i>	<i>pH 8.0</i>	<i>pH 6.0</i>	<i>pH 8.0</i>	<i>pH 6.0</i>	<i>pH 8.0</i>	<i>pH 6.0</i>	<i>pH 8.0</i>		
			Ozonia- tion- Chlori- nation	Alanine	0.40	0.16	<MRL	<MRL	<MRL	1.1	<MRL	8.4	<MRL	<MRL
	Aspartic Acid	0.36	0.11	<MRL	<MRL	183.7	32.1	<MRL	9.8	41.6	128.4	6.0	11.4	
	Cysteine	0.30	0.12	<MRL	<MRL	<MRL	<MRL	<MRL	6.7	<MRL	<MRL	<MRL	<MRL	<MRL
	Glutamic Acid	0.41	0.10	<MRL	0.8	2.4	<MRL	1.5	11.8	7.4	27.8	1.9	8.8	
	Glycine	0.32	0.19	25.9	223.4	<MRL	2.5	7.4	83.4	<MRL	<MRL	<MRL	<MRL	<MRL
	Histidine	0.46	0.27	<MRL	<MRL	6.4	3.8	1.1	6.9	12.7	33.3	3.3	8.5	
	Lysine	0.49	0.19	12.0	14.6	1.5	<MRL	10.5	33.9	12.9	9.8	1.5	3.1	
	Proline	0.52	0.12	16.4	17.3	<MRL	<MRL	5.0	11.5	7.2	16.6	1.2	2.5	
	Serine	0.34	0.13	<MRL	0.9	<MRL	<MRL	2.0	8.4	1.3	1.5	1.1	<MRL	

* Initial concentration of AA's were 1mg/L. DOC and DON values are calculated based AA concentration and AA formulas. MRL: Minimum Reporting Limit.

Pre-ozonation dramatically decreased the DCAA formation from aspartic acid and histidine, from 992.5 $\mu\text{g}/\text{mg-C}$ and 336.3 $\mu\text{g}/\text{mg-C}$ to 356.8 $\mu\text{g}/\text{mg-C}$ and 72.3 $\mu\text{g}/\text{mg-C}$, respectively (Figure 5). These findings were consistent with DCAN findings that are explained in the next section. No obvious effect of pre-ozonation was observed on DCAA formation from either the AAs or TCAA formations under study.

The Effect of pH on the Formation of DBPs

The results show that the THMs and HAAs formation increased with increasing pH (Table 4). It has been previously reported in the drinking water literature that THM formation decreases with a decrease in pH, while this decrease in pH leads to an increase in HAAs formation (49). However, in this study, a decreasing trend was observed for both THMs and HAAs formation with the decrease in pH, which was consistent with the previous findings (32). Furthermore, the decrease in pH from 8.0 to 6.0 also decreased the yields of HNMs and HANs. The only exception was observed with the formation of DCAN from aspartic acid. It has been also reported that decreases in pH decreased formation of HNMs in natural waters (34, 50).

Also the protonated states of the AAs, which reduced their reactivity also decreased the DBP yields, indicating that alkali conditions facilitated the formation of DBPs for the selected AAs. The extent of this increase was compound-specific, however. Moreover, the distinct DBP yield differences observed in our study highlights the sensitivity of AAs to pH and also explains the differences observed in the literature. Overall, the results indicate that reducing pH from 8.0 to 6.0 would result in distinct decreases in the formation of THMs, HAAs, HANs, and HNMs because the AAs are highly sensitive to changes in pH.

Conclusions

The C-DBP and N-DBP formation potentials of AAs tested in this study were summarized in Table 4. Of the nine AAs analyzed, aspartic acid, glycine and histidine showed the highest reactivity, which contributed to the formation of N-DBPs and C-DBPs. Aspartic acid also exhibited the highest DCAN and DCAA formation during both chlorination and ozonation-chlorination. Under the same conditions, the highest HNM and THM formation was formed from glycine, although it did not yield HNM and THM during chlorination. HNM formation from glycine under ozonation-chlorination condition was remarkably higher than all AAs tested. Further, although a substantial amount of TCM, DCAA, TCAA and DCAN was formed with the introduction of histidine during chlorination, the reactivity was lower for chlorination after ozonation. All other AAs showed very low C-DBP and N-DBP yields, with nitrosamine yields from all nine AAs during chlorination either being very low or below the minimum reporting levels. Furthermore, the DBP yield of the selected AAs was higher at pH 8.0 than 6.0 with the only exception of DCAN formation from aspartic acid.

Aspartic acid and glycine are the most commonly detected AAs in natural waters. Although the total AA concentrations in natural waters were low, their elevated concentrations during seasonal events (e.g., algae blooms, die-off, run off) and the presence of aspartic acid and glycine type structures in the organic nitrogen molecules in natural waters caused a partial generation of certain C-DBPs and N-DBPs depending on the oxidation conditions. The results from this study indicate that AAs are an unlikely contributor to NDMA formation because of the very low yields generated during chloramination.

Acknowledgments

This work was partly supported by a research grant from the National Science Foundation (CBET 106657). However, the manuscript has not been subjected to the peer and policy review of the agency and therefore does not necessarily reflect its views.

References

1. Plewa, M. J.; Wagner, E.; Muellner, M.; Hsu, K.; Richardson, S. *ACS Symp. Ser.* **2008**, *995*, 36–50.
2. Dotson, A.; Westerhoff, P.; Krasner, S. W. *Water Sci. Technol.* **2009**, *60*, 135–143.
3. Hu, J.; Song, H.; Addison, J. W.; Karanfil, T. *Water Res.* **2010**, *44*, 105–114.
4. Mitch, W. A.; Krasner, S. W.; Westerhoff, P.; Dotson, A. *Occurrence and formation of nitrogenous disinfection by-products*; Water Research Foundation Report: Denver, CO, 2009.
5. Ram, N. M.; Morris, J. C. *Environ. Int.* **1980**, *4*, 397–405.
6. Rice, R. G.; Gomez-Taylor, M. *Environ. Health Perspect.* **1986**, *69*, 31–44.
7. Thurman, E. M. *Organic Geochemistry of Natural Waters*; Martinus Nijhoff/Dr W. Junk Publishers: Dordrecht, Netherlands, 1985.
8. Hagedorn, F.; Schleppi, P.; Waldner, P.; Fluhler, H. *Biogeochemistry* **2000**, *50*, 137–161.
9. Meon, B.; Kirchman, D. L. *Mar. Chem.* **2001**, *75*, 185–199.
10. Sellner, K. G.; Nealey, E. W. *Mar. Chem.* **1997**, *56*, 193–200.
11. Jørgensen, N. O. G. *Limnol. Oceanogr.* **1987**, *32*, 97–111.
12. Dotson, A.; Westerhoff, P. *J. Am. Water Works Assoc.* **2009**, *101*, 101–115.
13. Chinn, R.; Barrett, S. E. *ACS Symp. Ser.* **2000**, *761*, 96–108.
14. Münster, U. *Environ. Int.* **1999**, *25*, 209–224.
15. Hureiki, L.; Croue, J. P.; Legube, B. *Water Res.* **1994**, *28*, 2521–2531.
16. Trehy, M. L.; Yost, R. A.; Miles, C. J. *Environ. Sci. Technol.* **1986**, *20*, 1117–1122.
17. Hong, H. C.; Wong, M. H.; Liang, Y. *Arch. Environ. Contam. Toxicol.* **2009**, *56*, 638–645.
18. Na, C.; Olson, T. M. *Environ. Sci. Technol.* **2006**, *40*, 1469–1477.
19. Hureiki, L.; Croue, J. P.; Legube, B.; Dore, M. *Ozone Sci. Eng.* **1998**, *20*, 381–402.

20. Sacher, F.; Schmidt, C. K.; Lee, C.; Von Gunten, U. *Strategies for minimizing nitrosamine formation during disinfection*; Water Research Foundation Report: Denver, CO, 2008.
21. Richardson, S. D.; Plewa, M. J.; Wagner, E. D.; Schoeny, R.; DeMarini, D. M. *Mutat. Res., Rev. Mutat. Res.* **2007**, *636*, 178–242.
22. Merlet, N.; Thibaud, H.; Dore, M. *Sci. Total Environ.* **1985**, *47*, 223–228.
23. Bond, T.; Henriot, O.; Goslan, E. H.; Parsons, S. A.; Jefferson, B. *Environ. Sci. Technol.* **2009**, *43*, 5982–5989.
24. Mitch, W. A.; Sedlak, D. L. *Water Sci. Technol.: Water Supply* **2002**, *2*, 191–198.
25. Oliver, B. G. *Environ. Sci. Technol.* **1983**, *17*, 80–83.
26. Krasner, S. W.; Weinberg, H. S.; Richardson, S. D.; Pastor, S. J.; Chinn, R.; Scilimenti, M. J.; Onstad, G. D.; Thruston, A. D. *Environ. Sci. Technol.* **2006**, *40*, 7175–7185.
27. Ram, N. M. *Environ. Int.* **1985**, *11*, 441–451.
28. Chu, W. H.; Gao, N. Y.; Deng, Y.; Dong, B. Z. *Chemosphere* **2009**, *77*, 1346–1351.
29. Berger, P.; Leitner, N. K. V.; Dore, M.; Legube, B. *Water Res.* **1999**, *33*, 433–441.
30. Krasner, S. W.; Westerhoff, P.; Chen, B.; Rittmann, B. E.; Nam, S. N.; Amy, G. *Environ. Sci. Technol.* **2009**, *43*, 2911–2918.
31. Gan, X.; Kim, D.; Karanfil, T. *J. Am. Water Works Assoc.* **2013**, *105*, E195–E206.
32. Shan, J.; Hu, J.; Kaplan-Berkaroglu, S. S.; Song, H.; Karanfil, T. *Chemosphere* **2012**, *86*, 323–328.
33. Song, H.; Addison, J. W.; Hu, J.; Karanfil, T. *Chemosphere* **2010**, *79*, 174–179.
34. Hu, J.; Song, H.; Karanfil, T. *Environ. Sci. Technol.* **2010**, *44*, 794–799.
35. Hoigné, J.; Bader, H. *Water Res.* **1988**, *22*, 313–319.
36. Bailey, P. S.; Mitchard, D. A.; Khashab, A. I. Y. *J. Org. Chem.* **1968**, *33*, 2675–2680.
37. Le Lacheur, R. M.; Gaze, W. H. *Environ. Sci. Technol.* **1996**, *30*, 1072–1080.
38. Duguet, J. P.; Jaulin, L.; Aurelle, Y.; Roques, H.; LeÂgeron, J. P. *Ozone Sci. Eng.* **1980**, *2*, 105–122.
39. Moenig, J.; Chapman, R.; Asmus, K. D. *J. Phys. Chem.* **1985**, *89*, 3139–3144.
40. Andrzejewski, P.; Kasprzyk-Hordern, B.; Nawrocki, J. *Water Res.* **2008**, *42*, 863–870.
41. Yang, L.; Chen, Z. L.; Shen, J. M.; Xu, Z. Z.; Liang, H.; Tian, J. Y.; Ben, Y.; Zhai, X.; Shi, W. X.; Li, G. B. *Environ. Sci. Technol.* **2009**, *43*, 5481–5487.
42. Asami, M.; Oya, M.; Kosaka, K. *Sci. Total Environ.* **2009**, *407*, 3540–3545.
43. Planas, C.; Palacios, O.; Ventura, F.; Rivera, J.; Caixach, J. *Talanta* **2008**, *76*, 906–913.
44. Selbes, M.; Kim, D.; Ates, N.; Karanfil, T. *Water Res.* **2013**, *47*, 945–953.
45. Selbes, M.; Kim, D.; Karanfil, T. *Water Res.* **2014**, *66C*, 169–179.
46. Bailey, P. S. Ozonation of nucleophiles. In *Ozonation in Organic Chemistry*; Wasserman H. H., Eds.; Academic Press Inc.: New York, 1982.

47. Glezer, V.; Harris, B.; Tal, N.; Iosefzon, B.; Lev, O. *Water Res.* **1999**, *33*, 1938–1948.
48. Dickenson, E. R. V.; Summers, R. S.; Croué, J.-P.; Gallard, H. *Environ. Sci. Technol.* **2008**, *42*, 3226–3233.
49. Hua, G.; Reckhow, D. A. *J. Am. Water Works Assoc.* **2008**, *100*, 82–89.
50. Joo, S. H.; Mitch, W. A. *Environ. Sci. Technol.* **2007**, *41*, 1288–1296.

Chapter 13

Formation of Disinfection By-Products from Bacterial Disinfection

T. W. Ng,¹ B. Li,² A. T. Chow,² and P. K. Wong*,¹

¹The School of Life Science, The Chinese University of Hong Kong,
Hong Kong, China

²The Belle W. Baruch Institute of Coastal Ecology and Forest Science,
Clemson University, Clemson, South Carolina 29631, U.S.A.

*E-mail: pkwong@cuhk.edu.hk. Tel.: +852 3943 6383. Fax: +852 2603 5767.

Controlling the disinfection by-product (DBP) formation, while balancing the risk of bacterial contamination in finished water, requires an in depth understanding in both the chemistry of DBPs and the kinetic and mechanism of bacterial disinfection. Although numerous studies have examined different strategies on the reduction of DBP formation in finished waters, their main focuses are on natural organic matter (NOM) in source waters. Few studies evaluated the contributions of bacterial organic matter (BOM) on DBP formation. Breaking down of bacterial cells, releasing BOM into water, is an essential process in water disinfection. Prevalence of bacterial contamination in source waters and occurrences of biofilms in water treatment units and distribution systems are frequently reported. The contributions of organic matter from bacterial and microbial sources in drinking water treatment cannot be ignored. In this study, we compared the contributions of bacterial cells and humic acid (HA), under controlled laboratory environments, on the DBP formation from chlorination. We also evaluated the effects of HA, pH, and chlorine dosage on both disinfection efficiency and DBP formation. The results showed that bacterial cells are also potential DBP precursor. Presence of HA not only increased the DBP formation, but also decreased the disinfection efficiency of chlorination. pH and chlorine dosage also affect the disinfection efficiency and DBP formation of chlorination. High dosage of chlorine would increase both the

disinfection efficient and DBP formation, while low pH increase the disinfection efficient with a lower DBP formation. The results suggest that high disinfection efficiency with low DBP formation of chlorination can be achieved by optimization of operation conditions. Based on our knowledge, this pioneering work is the first study to investigate the relationship between bacteria and DBP contaminations in water treatment processes at the same time.

1. Introduction

Adding disinfectants in drinking water treatment is a common practice to protect us from infectious diseases. In spite of its advantage to inactivate waterborne pathogens, disinfectants, such as chlorine and chloramines react with constituents in waters to form a variety of disinfection by-products (DBPs), such as trihalomethanes (THMs), haloacetic acids (HAAs), chloral hydrate (CHD), haloacetonitriles (HANs), and N-nitrosodimethylamine (NDMA) (1, 2). Since THMs was first identified in finished drinking water in 1976 (3), more than 600 DBPs have been identified but which only account for 30% of total halogenated DBPs in chlorinated waters (4). Importantly, most of identified DBPs are cytotoxic and genotoxic (5–7) and are rapidly absorbed into our bodies through showering, hand washing, drinking, and even breathing (8–11). Consuming water bearing DBPs could cause bladder cancer, rectal cancer, adverse birth outcomes, and other adverse health related issues (12–14). Noticeably, both disinfection efficacy and DBP formation are increased with the dosage of disinfectants (15)(Figure 1). Therefore, it is a great challenge to balance the risk between microbial and DBP contaminations for safe drinking water.

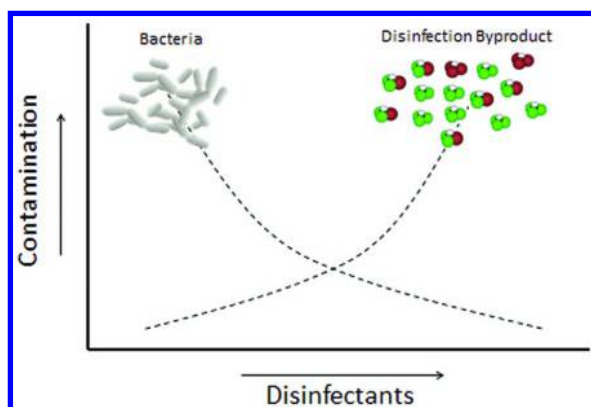


Figure 1. Disinfection / Disinfection by-product risk trade-offs. (modified from Lykins et al. (15))

Conventionally, natural organic matter (NOM) such as humic substance is considered as the major precursor of DBPs (16, 17). Bacterial organic matter (BOM) is rarely studied although the major function of disinfection is to inactivate bacterial pathogens. Bacterium can be an important source of organic matter and DBP precursors in potable water treatment systems because prevalence of bacterial contamination in source waters (18, 19) and biofilms in water treatment unit and distribution systems (20, 21) are frequently reported worldwide. Extracellular polymeric substance (EPS) and many biochemical compounds released from bacteria and microorganisms such as polysaccharides, protein, and nucleic acid are commonly found in water treatment systems (22). Many of these biomolecules have been considered reactive precursors in forming THMs and other DBPs during chlorination (23–25). Notably, the formation of DBPs is unavoidable in bacterial disinfection because bacterium is composed of a variety of organic compounds which can release into water after cell lysis. This BOM can react with excess disinfectants in water to form DBPs. Moreover, BOM is relatively enriched in nitrogen than other sources of NOM in natural waters (26, 27). Therefore, BOM could be an important precursor in forming nitrogenous DBPs (N-DBPs) such as HANs and NDMA, which could be more hazardous compared to currently regulated DBPs (i.e. THMs and HAAs) in finished drinking waters (6, 28, 29).

In this study, we hypothesize that BOM is a DBP precursor and it can react with chlorine to form a variety of DBP during bacterial disinfection. We conducted a series of controlled laboratory experiments to evaluate the effect of water pH, chlorine dosage, and concentrations of NOM on the disinfection efficiency and DBP formation. The objective of this study is to illustrate the relationship between bacteria and DBP contaminations in chlorination processes, as demonstrated in Figure 1. Results of the study could be useful for water engineers and microbiologists to define the end point of bacterial disinfection and provide referable information to balance the risk between microbial control and production of DBPs in finished waters.

2. Experimental

2.1. Chemicals

All the stock solutions and supplies including pipette tips and filter papers for disinfection experiment were autoclaved (at 121°C for 20 min) to avoid culture contamination. All glassware were soaked in 5% DECON for 24 h, washed with Milli-Q water (Millipore, USA), and placed in a furnace at 500°C for 5 h to eliminate organic contaminants. All the working solutions were conducted in the phosphate buffered saline (PBS) prepared by suspending 8.01 g of NaCl, 0.20 g of KCl, 1.78 g of Na₂HPO₄•2H₂O, 0.27 g of KH₂PO₄ into 1 L Milli-Q water. Suwannee River Humic Acid (HA) was purchased from International Humic Substances Society. A stock solution of 100 mg/L of HA was prepared in 0.01 M KCl. The stock solution was filtered through 0.45 μm membrane filter and kept in clean and glass-topped amber bottle in a refrigerator set at 4°C. The stock solution was diluted with Milli-Q water to 2 or 4 mg/L of HA for the disinfection

studies. The 2 or 4 mg/L of HA solution was equivalent to 0.92 or 1.84 mg/L of dissolved organic carbon (DOC), respectively, based on our measurements using Shimadzu TOC analyzer.

2.2. Bacterial Cultures

Seven bacteria commonly found in soil and water, including three gram positive strains (*Bacillus cereus*, *Bacillus subtilis*, and *Staphylococcus sciuri*) and four gram negative strains (*Acinetobacter junii*, *Aeromonas hydrophila*, *Escherichia coli*, and *Shigella sonnei*), were examined in this study. After a pre-incubation test to determine the time span of the stationary phase for each bacterial species, seven strains of bacteria were inoculated individually into nutrient broth (10% of the instructed dosage) and grown overnight (16 - 20 h) to reach the stationary phase. Aliquots of bacterial cultures were centrifuged at 11,600 x g for 5 min, and bacterial cells were collected and washed three times with saline solution (0.9% of NaCl) to remove the nutrient broth. The cell pellets were re-suspended in deionized water in Duran bottles to obtain a cell density in the range of 10⁴–10⁷ colony forming units per milliliter (cfu/mL) for the chlorination test. Total organic carbon of cell pellets were tested in SSM-5000A solid sample combustion unit connected to Shimadzu TOC analyzer. The relationships between total organic carbon and bacterial count of the seven bacterial strains are summarized in Table 1. To study the effects of pH, chlorine dosage, and NOM levels, *E. coli* was inoculated in a low level and a high level for each parameter as summarized in Table 2.

Table 1. Regressions between Bacterial Total Organic Carbon Bacterial Cell Count

<i>Bacterial species</i>	<i>Relationship</i>	<i>n</i>	<i>R</i> ²
<i>Acinetobacter junii</i>	$y = 4.9351x - 37.377$	15	0.9970
<i>Aeromonas Hydrophila</i>	$y = 5.0291x - 45.483$	15	0.9713
<i>Escherichia coli</i>	$y = 5.7935x - 52.225$	15	0.9954
<i>Shigella sonnei</i>	$y = 3.5049x - 31.618$	15	0.9493
<i>Bacillus cereus</i>	$y = 2.3581x - 8.448$	15	0.9775
<i>Bacillus substilis</i>	$y = 5.2644x - 50.018$	15	0.9856
<i>Staphylococcus sciuri</i>	$y = 2.2655x - 18.632$	15	0.9886

y = TOC (mg/L), x = bacterial cell density (cfu/mL).

Table 2. A Low Level and a High Level of pH, Chlorine Dosage, and NOM Were Tested in This Study

	<i>Low Level</i>	<i>High Level</i>
pH	5	8
Chlorine Dosage (mg/L)	0.5	1.5
Humic Acid (mg/L)	2	4

2.3. Chlorine Inactivation

Free chlorine (HOCl) stock solution (3,000 mg/L of Cl₂) was prepared by diluting ≥4% sodium hypochlorite (NaOCl) (Aldrich) and buffered to pH to 8.0 ± 0.2. For the effects of pH and chlorine dosage on DBP formation and disinfection efficiency, working solutions of 0.5 and 1.5 mg/L of HOCl were prepared by diluting stocking solutions with PBS solution. Their pH was adjusted to 5.0 or 8.0 ± 0.2 using 2 mM of sodium hydroxide or 1 mM of sulfuric acid. The HOCl concentration was tested daily with a HACH chlorine pocket colorimeter (Hach Co., Loveland, CO) in accordance with Standard Method 4500-Cl B.

Chlorination was conducted in 60-mL glass bottles. The bottles were all covered in order to prevent chlorine degradation from light. Bottles were placed in a shaker with a constant vibration frequency to prevent cell settling. For the effects of pH, chlorine dosage, and NOM levels, the final concentration of *E. coli* was adjusted to 1.5 × 10⁷ cfu/mL. Bacteria and/or HA spiked into the solution and mixed continuously at room temperature. An aliquot of 0.5 mL of treated mixture was sampled at 5, 20, 40, and 80 min during the reaction. The mixture was then quickly diluted with sterilized saline solution. Each 0.1 mL of original or diluted sample was then immediately placed on the sterilized and dry nutrient agar. Agar plates were incubated at 37°C for 24 h. The bacteria cell density at each time interval was computed by the colonies counted on the agar plates.

2.4. Fluorescence Spectroscopy

A fluorescence spectrometer (F-7000, Hitachi, Japan) was used to obtain the three-dimensional emission-excitation matrix (EEM) spectra of the samples with excitation wavelengths in the range of 200-500 nm in 5-nm intervals and with emission wavelengths in the range of 290-500 nm in 5-nm intervals. The emission and excitation slits were fixed at 5 nm and the scanning speed was 12,000 nm/min. The second-order Raleigh scattering in the EEM measurements was eliminated using a 290 nm emission cutoff filter. The instrument was corrected for excitation and emission according to the manufacturer's suggested protocols. Variations in fluorescence intensity were calibrated using both pure water and quinine sulfate solution after the measurements of every 5 samples. The fluorescence intensity values were standardized in quinine sulfate units (QSU) (30).

2.5. DBP Analysis

The DBPs analyzed including four THMs (chloroform (TCM), bromodichloromethane (BDCM), dibromochloromethane (DBCM) and bromoform (TBM)), four HANs (trichloroacetonitrile (TCAN), dichloroacetonitrile (DCAN), bromochloroacetonitrile (BCAN) and dibromoacetonitrile (DBAN)), dichloropropanone (DCP) and chloral hydrate (CHD). All DBP standards were purchased from Sigma Aldrich and prepared before experiments for calibration. All water samples were quenched with sodium thiosulfate ($\text{Na}_2\text{S}_2\text{O}_3$) and then treated with methyl-tertiary-butyl-ether (MTBE) (Fluka, Switzerland) and sodium sulfate (Na_2SO_4) for liquid/liquid extraction of DBPs from aqueous solution according to U.S. EPA Method 551.1 (31). Samples were kept in refrigerator at 4 °C and analyzed within 10 days. Gas chromatography and electron capture detection (GC-ECD) was used to quantify the DBP concentrations. GC column (A - 0.25 mm ID x 30 m fused silica capillary) was used and the temperature program was slightly modified as follows: held at 30°C for 7 min then increased to 100°C at 20°C/min and held for 3min, and then increased to 260°C at 30°C/min and held for 2 min. The injector and detector temperature were set at 250°C.

3. Results

3.1. DBP Formation During Bacteria Inactivation

The results of DBP formation from disinfecting seven strains of bacteria were summarized in Figure 2. Similar to other NOM, THM was the dominant species. The specific THM formation ranged from 6.1 to 37.6 $\mu\text{g-THM/mg-C}$ with an average of 22.4 $\mu\text{g-THM/mg-C}$. The specific HAN formation ranged 3.1 to 16.3 $\mu\text{g-HAN/mg-C}$ with an average of 6.1 $\mu\text{g-HAN/mg-C}$. The specific CHD formation ranged 0.6 to 1.8 $\mu\text{g-CHD/mg-C}$ with an average of 1.1 $\mu\text{g-CHD/mg-C}$. Results confirmed that DBPs could be formed directly from bacteria during water chlorination even no other NOM existed in water. Fluorescence EEM of water containing *E. coli* before and after the chlorination was shown in Figure 3. Before chlorination, only two peaks at $\text{Ex} = 280 \text{ nm} / \text{Em} = 340 \text{ nm}$ and $\text{Ex} = 220 \text{ nm} / \text{Em} = 340 \text{ nm}$, occurring in microbial-by-product and aromatic protein regions, respectively, were observed (Figure 3a). After a low dosage of chlorine treatment (i.e. 0.5 mg/L), the intensities of the two peaks were decreased and signals in fulvic acid-like region at $\text{Ex} = 230 \text{ nm} / \text{Em} = 420 \text{ nm}$ were observed (Figure 3b). After a high dosage of chlorine treatment (i.e. 1.5 mg/L), a peak at fulvic acid-like region was produced (Figure 3c). Results demonstrated a transition of BOM during water chlorination.

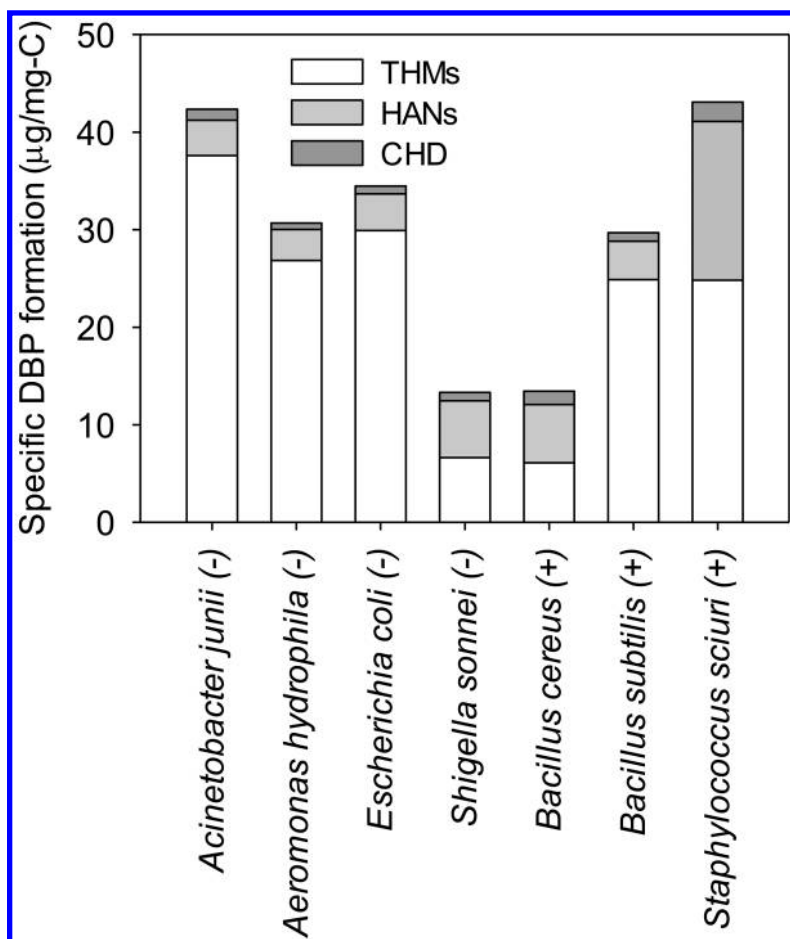


Figure 2. The specific DBP formation of halogenation of different bacteria. The sign in the parenthesis indicates the bacteria belong to Gram positive (+) or Gram negative (-).

3.2. Effects of NOM on Bacterial Inactivation and DBP Formation

To demonstrate the inhibition effect of NOM on disinfection processes, chlorination of *E. coli* solution with two concentrations of HA and two chlorine dosages were examined. The results were summarized in Figure 4. In all cases, bacterial inactivation was the most efficient when no HA existed in water. Existence of HA in water consumed chlorine, lowering the disinfection efficiency. Consider low chlorine dosage at 0.5 mg/L of Cl₂ at pH 8 as an example. The cell density slightly dropped from 7.5 to 6.5 log cfu/ml in first 5 min with the presence of 4 mg/L of HA in water and only achieved 2-log reduction after 80 minutes. Results were significantly lower than the 0 and 2 mg/L of HA treatments, which reached almost 4-log reduction after 80 min. Bacterial inactivation by

chlorination generally occurred in a relatively short time after chlorine was added. Significant decreases in cell density generally occurred in the first 5 min of the disinfection in water solutions with or without HA. No obvious change in cell density was observed in later reaction time.

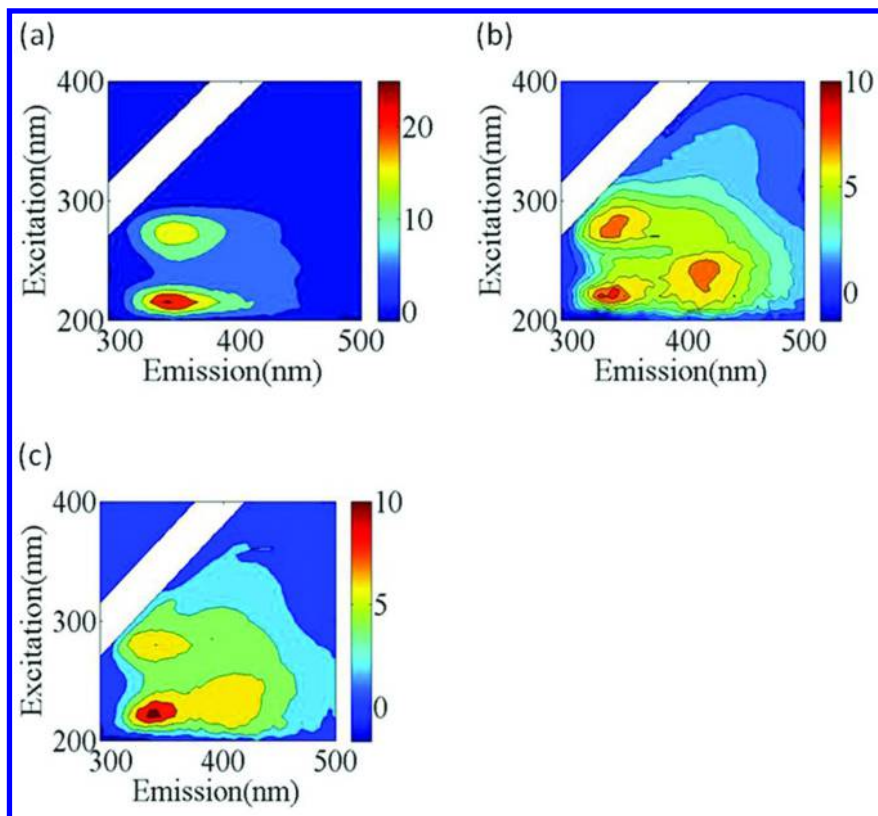


Figure 3. (a) Fluorescence EEM of water solution containing *E. coli*: (a) before disinfection treatment, (b) after 80-min treatment with 0.5 mg/L Cl_2 at pH 8, and (c) after 80-min treatment with 1.5 mg/L Cl_2 at pH 8. Quenching solution $\text{Na}_2\text{S}_2\text{O}_3$ was added after 80-min treatment before fluorescence measurement was taken.

Both HA and BOM can react with chlorine in forming DBPs. The formations of DBPs were generally increased with the chlorine dosage (Figures 5). For pure *E. coli* culture solution with 1.5×10^7 cfu/mL at pH 8, 1.1 and 5.7 $\mu\text{g/L}$ of THMs were produced at 0.5 and 1.5 mg/L of chlorine, respectively. For the pure NOM solutions with 2 and 4 mg/L of HA at pH 8, 5.0 – 5.2 $\mu\text{g/L}$ and 33.4 – 40.1 $\mu\text{g/L}$ of THMs were produced at 0.5 and 1.5 mg/L of chlorine, respectively. Other types of DBPs were also produced but their levels were in ng/L range. The water solutions containing both *E. coli* and HA generated less THMs than pure *E. coli* or pure HA water solutions at pH 8. Fluorescence EEM demonstrated that different

characteristics of BOM and HA. A strong humic acid-like peak was observed in Ex = 250 nm / Em 450 nm in pure HA solution (Figure 6a) but a strong microbial by-product-like peak was observed in Ex = 280 nm / Em = 250 nm when bacteria was added into the solution (Figure 6b).

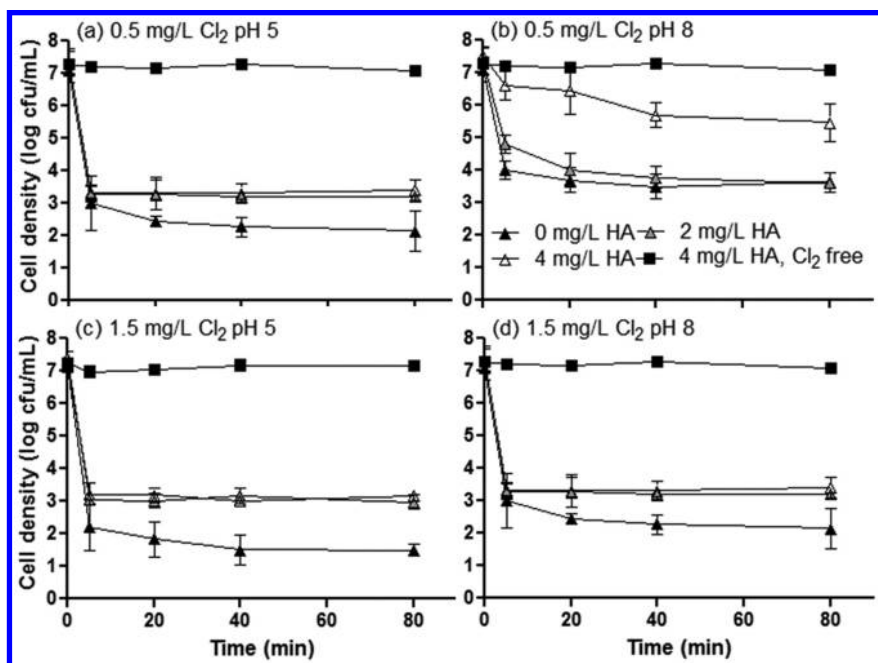


Figure 4. Effects of humic acid and pH on *E. coli* cell density in water solution during 80-min chlorination.

3.3. Effects of pH and Dosage on Bacterial Inactivation and DBP Formation

In general, acidic condition could enhance the effectiveness of bacterial inactivation. As shown in Figure 4, the cell viability of *E. coli* after 80 minutes was significantly lower at pH of 5 (1.5 to 3 log cfu/mL) than those at pH of 8 (2.0 to 5.5 log cfu/mL) in the same chlorine dosage. It is well known that THM formation is favored at alkaline pH (32). THM formations from pure bacterial cell culture were higher in pH 8 (1.7 to 5.7 μg -THM/L) than those in pH 5 (0.8-1.1 μg -THM/L). Similarly, THM formation of pure HA solution in pH 8 (5.0 to 40.1 μg /L) was higher than those in pH 5 (2.0 to 16.2 μg /L). Moreover, the yields of DBP were generally increased with chlorine dosage (32, 33). THM formation in 0.5 mg/L of Cl₂ was in the range of 0.8 to 5.3 μg /L and THM formation in 1.5 mg/L of Cl₂ ranged from 1.1 to 40.1 μg /L.

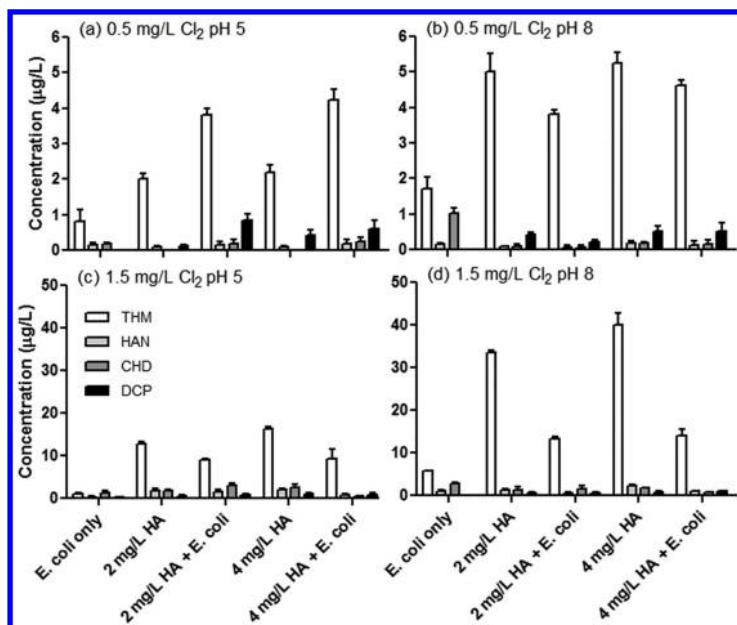


Figure 5. Effects of humic acid and pH on DBP formation in water solution after 80-min chlorination.

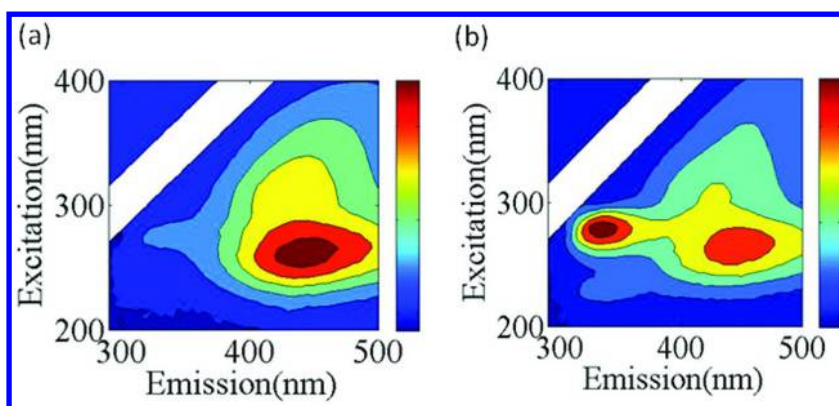


Figure 6. Fluorescence EEM of water solution after chlorination with initial 1.5 mg/L of Cl_2 at pH=8 for 80 min (a) 4 mg/L Humic acid only (b) 4 mg/L Humic acid + 10^7 cfu/mL *E. coli* K-12. Quenching solution $Na_2S_2O_3$ was added after 80-min treatment before fluorescence measurement was taken.

4. Discussions

4.1. Microbial Cells and Cellular Components as DBPs Precursor

Many studies had examined biological molecules such as amino acids, nucleic acids, carbohydrates on DBP formation and concluded that they are reactive DBP precursors (23–25, 34, 35). Generally specific THM formation of these biomolecules usually low than 10 $\mu\text{g-THM/mg-C}$ except few exceptions such as tryptophan and tyrosine which can be over 100 $\mu\text{g-THM/mg-C}$ (34, 35). Differences from other previous studies, we examined DBP formation directly disinfecting bacterial cells. Our results showed the specific THM formation from bacterial cells ranged from 6.1 to 37.6 $\mu\text{g/mg-C}$ and specific HAN formation from 3.6 to 16.3 $\mu\text{g/mg-C}$. These numbers are generally comparable to those monomers or standard chemicals studies as discussed above. The results confirmed that that these bacterial components can also be the DBP precursor as long as halogenating reagent exists. We have also demonstrated that there is a positive correlation between DBP formation and the log-reduction of *E. coli* by both chlorination and chloramination (33). The results further confirmed that the DOM released from the breakdown of bacteria can contribute to DBP formation.

In addition to the source waters, bacteria existed as biofilm are commonly observed within water delivery systems (36). Disinfectants could react with extracellular polymeric substance (EPS) released from biofilm in forming DBPs (37). Not only do the quantity and quality of EPS affect the yield of DBPs, but also they determine the speciation of DBP formation. For example, the surrogate protein of EPS favors the formation of HAA formation while the surrogate lipid favors THM formation. In addition, the bacterial phenotypes and the materials on which biofilm attached also have a great impact on the bacterial derived DBP formation. Our research group demonstrated that planktonic cells formed 7–11 times greater THMs per carbon than those from biofilm. Furthermore, biofilms on the polyvinyl chloride consumed comparable chlorine but produced more THMs than those on galvanized zinc surface (33). All these results indicated the important of BOM in the DBP formation in the drinking water supply.

There is no obvious difference on the bacteria type, such as Gram staining, size or source of the bacteria, on the DBP formation of chlorination. However, as mentioned, the quality of cell components (i.e. EPS) would have great impact on the DBP formation. Therefore, the DBP formation potential of bacteria maybe mainly affect by the quality of cell components instead of the thickness of cell wall. Therefore, no obvious trend is observed in this study.

4.2. Natural Organic Matter versus Bacterial Organic Matter

Our study demonstrated that the specific THM formation of bacterial cell ranged from 6.1 to 37.6 $\mu\text{g-THM/mg-C}$, which is relatively less reactive than the conventional DBP precursors such as humic and fulvic acids, which generally ranged from 40 to 140 $\mu\text{g-THM/mg-C}$ (38). The bacterial concentration in source water is generally around 10^4 – 10^5 cells/mL (39). Consider the specific THM Formation = 22.4 $\mu\text{g-THM/mg-C}$, specific HAN formation = 6.1 $\mu\text{g-HAN/mg-C}$, and specific CHD formation = 1.1 $\mu\text{g-CHD/mg-C}$ as shown in

the section 3.1, an estimated DBP formation contributed from bacterial cells in drinking water chlorination could range from 10-100 ng-THM/L, 3-30 ng-HAN/L, and 0.5-5 ng-CHD/L. According to the results of humic acid effect (Figure 5), if source water contains 2-4 mg/L of DOM such as HA, DBP formation should be in the range of 2-45 μg -THM/L, 0.1-2.2 μg -HAN/L, and 0-2.6 μg -CHD/L. This calculation demonstrated that the DBP formation from bacterial cells is considerably lower than that from the NOM. However, the DBP formation from BOM could be important in some special occasions such as wastewater treatments or water disinfection in medical facilities. In wastewater effluent, the bacterial cells concentration can be even up to 10^7 - 10^8 cells/mL (39) and the THM formation can be as high as 10-100 μg -THM/L, 3-30 μg -HAN/L, and 0.5-5 μg -CHD/L. Any level of chemical contaminants in hospital water supply could increase risk to the patients who are sensitive to any chemical agents. Notably, biological molecules such as amino acid and nucleic acid are N-rich. With a lower C/N ratio, BOM could have a higher reactivity in forming more toxic N-DBPs when comparing with other sources of NOM (34).

The addition of HA would inhibit the disinfection efficiency as HA competed for chlorine during the process, resulting in a lower effective chlorine concentration for bacterial inactivation in water solutions. Chlorine could react with either *E. coli* or HA to form DBPs. However, *E. coli* and HA do not exhibit an additive effect in DBP formation when they co-existed in the water solutions, although both of them are DBP precursors. In some cases, the existence of *E. coli* in HA solution even resulted a lower DBP formation than the HA solution alone (Figure 5). A simple competitive reaction model (i.e. *E. coli* and HA compete for free chlorine) may not explain the phenomenon when there was excess chlorine in water. This observation could also attribute to N-rich organic matter from bacterial cells. N-rich BOM could affect the residual chlorine in water throughout forming organic chlorine and breakpoint reaction, depending on the Cl-to-N ratio (40). In fact, studies had demonstrated that organic N could reduce THM formation during water chlorination (41). These experiments demonstrated “competition” relationships of HA and bacteria during water chlorination. HA reduces bacterial inactivation efficiency by consuming reactive chlorine whereas BOM from lysed cells changes the chlorine chemistry in water and reduces THM formation from HA. The combined effects showed less disinfection efficiency and less DBP formation than HA or *E. coli* existed alone in water. In natural source waters, other organic matters such as fulvic acid also exist but HA is generally larger in size than fulvic acid and it should have a greater shielding effect protecting bacteria from disinfection.

4.3. Alternative Disinfectants on Bacterial Inactivation and DBP Formation

As chlorination produces toxic and carcinogenic DBPs, scientists begin to find ways to decrease the DBP formation with maintaining high efficiency in disinfection processes. Use of other alternative disinfectants is one of the promising approaches to achieve the goal. For example, the disinfection by TiO_2/UV , a type of advance oxidation processes (AOPs), shows much lower DBP formation in term of type and quantity (42). However, the bacterial inactivation of

these AOPs is relatively less efficient than the conventional disinfection methods such as chlorination and chloramination (43). Our recent study comparatively investigated the DBP formation and disinfection efficiency of four disinfectants (chlorination, chloramination, photo-Fenton reaction and TiO₂/UV photocatalytic disinfection) under different pH (5 and 8) and different dosages (43). Among different disinfectants, chlorination had the fastest bacterial inactivation following with chloramination, whereas photo-Fenton, and TiO₂/UV treatments required a relatively longer contact times to achieve the same inactivation efficacy. Nevertheless, chlorination had the highest DBP formation, followed by chloramination, and the DBP formation from photo-Fenton reaction and TiO₂/UV photocatalytic disinfection were all below the detection limits (1 ng/L). Although DBP formation can be greatly reduced using AOPs (photo-Fenton reaction or TiO₂/UV photocatalytic disinfection), longer reaction time could significantly increase the operation costs. More important, the recovery and the impacts of nanoparticles are still uncertain.

5. Conclusions

The results of this study confirmed our hypothesis that BOM is a DBP precursor and it can react with chlorine to form a variety of DBP during bacterial disinfection. Since bacteria in source water are ubiquitous, their relative contribution to DBP formation in water disinfection has been overlooked. The DBP formation from inactivating bacterial cells is greatly affected by different factors, such as types and dosages of disinfectants, water pH, physiology and phenotypes of bacteria, etc. Results of this study also suggested that a lower DBP formation and better inactivation efficiency could be achieved in the acidic condition.

Acknowledgments

This work was funded by the Research Grant Council of Hong Kong SAR Government (CUHK 477610). P.K. Wong was also supported by the CAS/SAFEA International Partnership Program for Creative Research Teams, Chinese Academy of Sciences, China. This research is also based upon work supported by NIFA/USDA under the project number SC-1700489 and SCN-2013-02784, and Joint Fire Science Program 14-1-06-19. This manuscript is a technical contribution no. 6349 of the Clemson University Experimental Station.

References

1. Krasner, S. W. Chemistry of disinfection by-product formation. In *Formation and Control of Disinfection By-Products in Drinking Water*; Singer, P. C., ed.; American Water Works Association: Denver, 1999.; pp. 27-52.
2. Xie, Y. *Disinfection Byproducts in Drinking Water: Formation, Analysis, and Control*; Lewis Publishers: Boca Raton, 2004.

- Rook, J. J. Haloforms in drinking-water. *J. Am. Water Works Assoc.* **1976**, *68*, 168–172.
- Krasner, S. W.; Weinberg, H. S.; Richardson, S. D.; Pastor, S. J.; Chinn, R.; Scilimenti, M. J.; Onstad, G. D.; Thruston, A. D. Occurrence of a new generation of disinfection byproducts. *Environ. Sci. Technol.* **2006**, *40*, 7175–7185.
- Plewa, M. J.; Kargalioglu, Y.; Vanker, D.; Minear, R. A.; Wagner, E. D. Mammalian cell cytotoxicity and genotoxicity analysis of drinking water disinfection by-products. *Environ. Mol. Mutagen.* **2002**, *40*, 134–142.
- Plewa, M. J.; Wagner, E. D.; Jazwierska, P.; Richardson, S. D.; Chen, P. H.; McKague, A. B. Halonitromethane drinking water disinfection byproducts: Chemical characterization and mammalian cell cytotoxicity and genotoxicity. *Environ. Sci. Technol.* **2004**, *38*, 62–68.
- Cemeli, E.; Wanger, E. D.; Anderson, D.; Richardson, S. D.; Plewa, M. J. Modulation of the cytotoxicity and genotoxicity of the drinking water disinfection byproduct iodoacetic acid by suppressors of oxidative stress. *Environ. Sci. Technol.* **2006**, *40*, 1878–1883.
- Erdinger, L.; Kuhn, K. P.; Kirsch, F.; Feldhues, R.; Frobel, T.; Nohynek, B.; Gabrio, T. Pathways of trihalomethane uptake in swimming pools. *Int. J. Hyg. Environ. Health* **2004**, *207*, 571–575.
- Miles, A. M.; Singer, P. C.; Ashley, D. L.; Lynberg, M. C.; Mendola, P.; Langlois, P. H.; Nuckols, J. R. Comparison of trihalomethanes in tap water and blood. *Environ. Sci. Technol.* **2002**, *36*, 1692–1698.
- Xu, X.; Weisel, C. P. Dermal uptake of chloroform and halo ketones during bathing. *J. Expo. Anal. Environ. Epidemiol.* **2005**, *15*, 289–296.
- Zwiener, C.; Richardson, S. D.; De Marini, D. M.; Grummt, T.; Glauner, T.; Frimmel, F. H. Drowning in disinfection byproducts? Assessing swimming pool water. *Environ. Sci. Technol.* **2007**, *41*, 363–372.
- Bove, F.; Shim, Y.; Zeitz, P. Drinking water contaminants and adverse pregnancy outcomes: A review. *Environ. Health Persp.* **2002**, *110*, 61–74.
- Bull, R. J.; Krasner, S. W.; Daniel, P. A.; Bull, R. D. *Health Effects and Occurrence of Disinfection By-Products*; AWWA Research Foundation and American Water Works Association: Denver, CO, 2001.
- Hinckley, A. F.; Bachand, A. M.; Reif, J. S. Late pregnancy exposures to disinfection by-products and growth-related birth outcomes. *Environ. Health Perspect.* **2005**, *113*, 1808–1813.
- Lykins, B. W., Jr.; Goodrich, J. A.; Clark, R. M.; Harrison, J. Point-of-use treatment. Point-of-use/point-of-entry treatment of drinking water. *Water Supply* **1994**, *12* (1/2), SS4/1–SS4/5.
- Leenheer, J. A.; Croue, J. P. Characterizing aquatic dissolved organic matter. *Environ. Sci. Technol.* **2003**, *37*, 18a–26a.
- Zsolnay, A. 2003. Dissolved organic matter: artefacts, definitions, and functions. *Geoderma* **2003**, *113*, 187–209.
- Davis, K.; Anderson, M. A.; Yates, M. V. Distribution of indicator bacteria in Canyon Lake, California. *Water Res.* **2005**, *39*, 1277–1288.
- Ruecker, N. J.; Braithwaite, S. L.; Topp, E.; Edge, T.; Lapen, D. R.; Wilkes, G.; Robertson, W.; Medeiros, D.; Sensen, C. W.; Neumann, N.

- F. 2007. Tracking host sources of *Cryptosporidium* spp. in raw water for improved health risk assessment. *Appl. Environ. Microbiol.* **2007**, *73*, 3945–3957.
20. Lehtola, M. J.; Torvinen, E.; Kusnetsov, J.; Pitkanen, T.; Maunula, L.; von Bonsdorff, C. H.; Martikainen, P. J.; Wilks, S. A.; Keevil, C. W.; Miettinen, I. T. Survival of *Mycobacterium avium*, *Legionella pneumophila*, *Escherichia coli*, and caliciviruses in drinking water-associated biofilms grown under high-shear turbulent flow. *Appl. Environ. Microbiol.* **2007**, *73*, 2854–2859.
 21. September, S. M.; Els, F. A.; Venter, S. N.; Brozel, V. S. Prevalence of bacterial pathogens in biofilms of drinking water distribution systems. *J. Water Health* **2007**, *5*, 219–227.
 22. Doumeche, B.; Galas, L.; Vaudry, H.; Di Martino, P. Membrane foulants characterization in a drinking water production unit. *Food Bioprod. Process.* **2007**, *85* (C1), 42–48.
 23. Li, J.; Blatchley, E. R., III Volatile disinfection byproduct formation resulting from chlorination of organic-nitrogen precursors in swimming pools. *Environ. Sci. Technol.* **2007**, *41*, 6732–6739.
 24. Hong, H. C.; Mazumder, A.; Wong, M. H.; Liang, Y. Yield of trihalomethanes and haloacetic acids upon chlorinating algal cells, and its prediction via algal cellular biochemical composition. *Water Res.* **2008**, *42*, 4941–4948.
 25. Navalon, S.; Alvaro, S.; Garcia, H. Carbohydrates as trihalomethanes precursors. Influence of pH and the presence of Cl and Br on trihalomethane formation potential. *Water Res.* **2008**, *42*, 3990–4000.
 26. Stevenson, F. J.; Cole, M. A. *Cycles of Soil: Carbon, Nitrogen, Phosphorus, Sulfur, Micronutrients*, 2nd ed.; John Wiley & Sons, Inc.: New York, 1999.
 27. Tate, R. *Soil Microbiology*; John Wiley: New York, 2000.
 28. Moudgal, C. J.; Lipscomb, J. C.; Bruce, R. M. Potential health effects of drinking water disinfection byproducts using a quantitative structure toxicity relationship. *Toxicology* **2000**, *147*, 109–131.
 29. U.S. EPA. *N-Nitrosodimethylamine CASRN 62-75-9, Integrated Risk Information Service (IRIS) Substance File*; U.S. EPA: Washington, DC, 1997.
 30. Yamashita, Y.; Tanoue, E. Chemical characterization of protein-like fluorophores in DOM in relation to aromatic amino acids. *Marine Chem.* **2003**, *82*, 255–271.
 31. U.S. EPA. Method 551.1. *Determination of Chlorination Disinfection By-Products, Chlorinated Solvents, and Halogenated Pesticides/Herbicides in Drinking Water by Liquid–Liquid Extraction and Gas Chromatograph with Electron-Capture Detection (Revision 1.0)*; Munch, D. J., Hautman, D. P., Eds.; U.S. EPA: Cincinnati, 1995.
 32. Xie, Y. *Disinfection Byproducts in Drinking Water: Formation, Analysis, and Control*; Lewis Publishers: Boca Raton, 2003.
 33. Wang, J. J.; Liu, X.; Ng, T. W.; Xiao, J. W.; Chow, A. T.; Wong, P. K. Disinfection byproduct formation from chlorination of pure bacterial cells and pipeline biofilms. *Water Res.* **2013**, *47*, 2701–2709.

34. Wang, J. J.; Ng, T. W.; Zhang, Q.; Yang, X. B.; Dahlgren, R. A.; Chow, A. T.; Wong, P. K. Reactivity of C1 and C2 organohalogen formation – from plant litter to bacteria. *Biogeosciences* **2012**, *9*, 3721–3727.
35. Hong, H. C.; Wong, M. H.; Liang, Y. Amino acids as precursors of trihalomethane and haloacetic acid formation during chlorination. *Arch. Environ. Contam. Toxicol.* **2009**, *56*, 638–645.
36. Williams, M. M.; Domingo, J. W. S.; Meckes, M. C.; Kelty, C. A.; Rochon, H. S. Phylogenetic diversity of drinking water bacteria in a distribution system simulator. *J. Appl. Microbiol.* **2004**, *96*, 954–964.
37. Wang, Z.; Kim, J.; Seo, Y. Influence of bacterial extracellular polymeric substances on the formation of carbonaceous and nitrogenous disinfection byproducts. *Environ. Sci. Technol.* **2012**, *46*, 1136–11369.
38. Chow, A. T.; Gao, S.; Dahlgren, R. A. Physical and chemical fractionation of dissolved organic matter and trihalomethane precursors: A review. *J. Water Supply: Res. Technol. – AQUA* **2005**, *54*, 475–507.
39. Van Nevel, S.; De Roy, K.; Boon, N. Bacterial invasion potential in water is determined by nutrient availability and the indigenous community. *FEMS Microbiol. Ecol.* **2013**, *85*, 593–603.
40. Shang, C.; Gong, W. L.; Blatchley, E. R. Breakpoint chemistry and volatile byproduct formation resulting from chlorination of model organic-N compounds. *Environ. Sci. Technol.* **2000**, *34*, 1721–1728.
41. Yang, X.; Shang, C. Chlorination byproduct formation in the presence of humic acid, model nitrogen organic compounds, ammonia, and bromide. *Environ. Sci. Technol.* **2004**, *38*, 4995–5001.
42. Richardson, S. D.; Thruston, A. D., Jr; Collette, T. W. Identification of TiO₂/UV disinfection byproducts in drinking water. *Environ. Sci. Technol.* **1996**, *30*, 3327–3334.
43. Li, B. Comparisons of Bacterial Inactivation Efficiency and Disinfection Byproduct Formation from Four Different Disinfection Processes. Ph.D. Thesis, Clemson University, South Carolina, August 2014.

Chapter 14

Catalysis of DBP-Precursor Bromination by Halides and Hypochlorous Acid

John D. Sivey,* Mark A. Bickley, and Daniel A. Victor

Department of Chemistry and
Urban Environmental Biogeochemistry Laboratory,
Towson University, 8000 York Road, Towson, Maryland 21252, United States
*E-mail: jsivey@towson.edu.

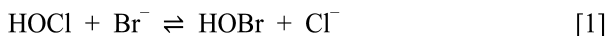
When bromide-containing waters are disinfected with free chlorine, bromide can be converted into free bromine (principally HOBr). Although often overlooked, chloride and bromide are capable of catalyzing bromination reactions of organic compounds by promoting the formation of BrCl and Br₂, respectively. Similarly, HOCl can catalyze bromination reactions by enhancing concentrations of BrOCl. As brominating agents, BrCl, Br₂, BrOCl (and the related species Br₂O) have been shown to be several orders of magnitude more inherently reactive than HOBr toward several non-ionizable aromatic compounds. Under conditions representative of chlorinated drinking water, BrCl and BrOCl can contribute more than HOBr to overall bromination rates of modestly nucleophilic aromatic compounds. This chapter reviews the literature regarding these reactive brominating agents and discusses their potential influence on bromination rates of disinfection by-product precursors.

Introduction

In 1902, for the first time in the United States, chlorine was added to drinking water (DW) to protect the public from water-borne diseases (1). Since then, countless lives have been saved by this potent microbicidal agent. Not until the 1970s, however, were the unintended consequences of DW chlorination discovered (2, 3). In addition to inactivating bacteria and viruses, chlorine can

also react with natural organic matter (4–7) to form potentially toxic disinfection by-products (DBPs) (8).

In water with low nitrogen levels, chlorine consists primarily of hypochlorous acid (HOCl, $pK_a = 7.58$ at 20 °C) (9) and ClO^- ; the sum of such species is termed *free chlorine*. In addition to reactions with organic DBP precursors, free chlorine can rapidly oxidize bromide (eq 1) (10).



HOCl-mediated oxidation of bromide (eq 1) has a large equilibrium constant (1.5×10^5 , 25 °C, $\mu = 0$) (11) and will proceed “to completion” in the presence of excess HOCl. The forward-reaction rate associated with eq 1 is proportional to $[HOCl]$ (k_{1+} = forward-reaction rate constant = $1.55 \times 10^3 \text{ M}^{-1} \text{ s}^{-1}$, 25 °C, $\mu = 1 \text{ M}$) (10) and is therefore anticipated to decrease with increasing pH.

As with HOCl, the presence of HOBr in DW is concurrently beneficial and problematic. Like its chlorinated analogue, HOBr is both a potent microbicide (1, 12–14) and a reactive electrophile capable of forming organobromine compounds in DW (1, 5, 15–22), wastewater (23, 24), and recreational waters (e.g., pools and spas) (25–27). Some of these organobromine compounds are DBPs whose concentrations are regulated in drinking water (28–31) due to their potential cytotoxic (32, 33) and genotoxic effects (34–36). Brominated DBPs are generally more toxic than their chlorinated analogs (34). Therefore, strategies for minimizing their formation are highly desirable. Such DBP-minimization strategies necessitate a comprehensive understanding of bromine chemistry.

The purpose of this chapter is to review recent discoveries in the literature pertaining to the chemistry of free bromine, particularly as it relates to the bromination of aromatic DBP precursors. We begin with a brief overview of bromide occurrence in natural and engineered aquatic systems and then discuss the chemistry of free bromine generated when bromide-containing source waters undergo disinfection (e.g., with free chlorine). The bulk of our discussion, however, is devoted to the often-overlooked ability of halides (chloride and bromide) and HOCl to catalyze bromination reactions. We conclude with an analysis of how these catalytic reactions can influence DBP precursor bromination under model DW treatment conditions.

Natural and Anthropogenic Sources of Bromide

Bromide is a ubiquitous constituent of natural waters (Table 1), with median concentrations ranging from low $\mu\text{g/L}$ in precipitation (37) to 65 mg/L in seawater (38). Bromide concentrations in groundwater range from low $\mu\text{g/L}$ to low mg/L (39, 40). Brackish-water or seawater intrusion can, however, increase bromide concentrations in aquifers near the coasts (41). Bromide levels measured in DW (39) and wastewater (23) influents (50–250 $\mu\text{g/L}$) align with the upper levels measured in fresh surface waters. Even higher levels have been reported for surface waters impacted by produced water from hydraulic fracturing operations (Table 1) (42–44).

Table 1. Bromide Concentrations in Natural Waters, Drinking Water, and Wastewaters

<i>Natural Waters</i>	<i>[Br⁻], (μg/L)</i>		<i>Ref</i>
	<i>median</i>	<i>maximum</i>	
Precipitation	~6	12	(37)
U.S. groundwater (potable waters only)	16	58	(40)
U.S. freshwater lakes	23	322	(39)
U.S. rivers	63	426	(39)
U.S. groundwater (includes non-potable waters)	62	2.7 x 10 ³	(39)
Seawater	6.5 x 10 ⁴	not reported	(38)
Surface water impacted by produced water from hydraulic fracturing	not reported	7.5 x 10 ⁴	(43)
<i>Drinking Water and Wastewater</i>	<i>Reported Ranges of [Br⁻], (μg/L)</i>		<i>Ref</i>
U.S. drinking water influent	50–200		
Municipal wastewater influent	100–250		(23)

Chemistry of Free Bromine

The oxidation state of bromine is +I in species such as HOBr ($pK_a = 8.70$ at 20 °C) (45) and BrO⁻; the sum of all Br(+I) species is referred to as *free bromine*. The direct application of free bromine as a disinfectant of DW is uncommon due to the increased costs, increased DBP formation, and difficulty in maintaining a disinfectant residual throughout the distribution system relative to free chlorine (1). Free bromine is, however, employed as a disinfectant in some recreational waters (e.g., spas) (1). In waters disinfected with ozone (O₃), free bromine can form via the incomplete oxidation of bromide (46–48). Bromide can also be oxidized into free bromine in solutions dosed with chloramines (49–51).

Conventional wisdom in the literature generally assumes HOBr is the predominant brominating agent in solutions of free bromine (52). Under this assumption, bromination rates can be described via eq 2:

$$\frac{d[\text{Org-Br}]}{dt} = k_{\text{HOBr}}[\text{HOBr}][\text{Org-H}] \quad [2]$$

where k_{HOBr} is a second-order rate constant ($\text{M}^{-1} \text{s}^{-1}$), [HOBr] is the concentration of HOBr (mol/L), [Org-H] is the concentration of the parental organic compound (mol/L), and [Org-Br] is the concentration of the brominated product (mol/L). When HOBr is present in large excess, k_{HOBr} can be calculated by eq 3:

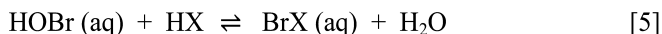
$$k_{\text{HOBr}} = \frac{k_{\text{obs}}}{[\text{HOBr}]} \quad [3]$$

where k_{obs} is a pseudo-first-order rate constant (s^{-1}). Apparent rate constants (k_{app}) are also commonly reported for bromination reactions:

$$k_{\text{app}} = \frac{k_{\text{obs}}}{[\text{Br(I)}]_{\text{tot}}} \quad [4]$$

where $[\text{Br(I)}]_{\text{tot}}$ denotes the total concentration of free bromine. Values of k_{app} typically vary as a function of pH (e.g., due to the weak-acid character of HOBr). That BrO^- possesses a net negative charge and requires expulsion of a weakly-labile leaving group (O^{2-}) suggests HOBr will be a more reactive brominating agent than BrO^- (53).

The kinetic models represented by eqs 3 and 4 do not account for the potential influence of bromination catalysts. A catalyst is “a substance that affects the rate of a reaction but emerges from the process unchanged (54).” Below, we describe the chemistry by which chloride, bromide, and HOCl can catalyze bromination reactions. Each of these reagents can promote the formation of reactive brominating agents via eq 5:



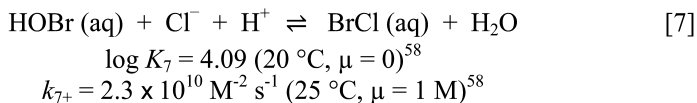
where $\text{HX} = \text{HCl}$, HBr , or HOCl . BrX ostensibly represents a more inherently reactive brominating agent relative to HOBr (55). BrX can participate in bromine substitution reactions with organic compounds via eq 6:



Because HX emerges from this series of reactions (eqs 5 and 6) unchanged, HX species can be viewed as catalysts of bromination. Although the examples herein focus on bromination of aromatic compounds, the chemistry described below conceivably also applies to other organic nucleophiles (e.g., alkenes, ketones, and amines) present in DW and wastewater.

Catalysis by Chloride

Although commonly overlooked, bromination rates of organic compounds can depend on the concentration of chloride ions (53, 55–57). For example, a recent investigation involving the herbicide dimethenamid (a substituted thiophene) revealed that rates of bromination in solutions of free bromine increased linearly with the concentration of added chloride (Figure 1) (53). The influence of chloride on rates of dimethenamid bromination (represented by the slopes in Figure 1) increased with decreasing pH. These findings are consistent with the participation of BrCl as a brominating agent, whose concentration is proportional to the concentration of chloride (eq 7):



Although an additional free bromine species (BrCl_2^-) can also form in the presence of chloride (58), the formal negative charge on BrCl_2^- is anticipated to render this species significantly less electrophilic compared to neutral free bromine species (e.g., BrCl and HOBr) (55).

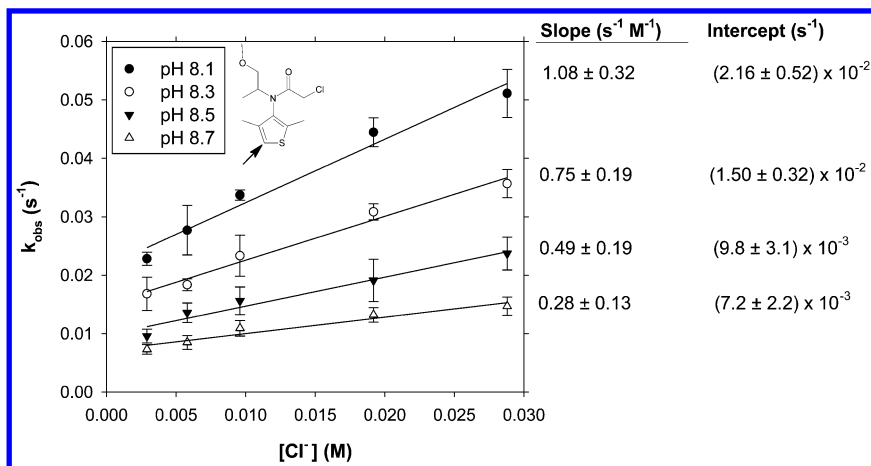
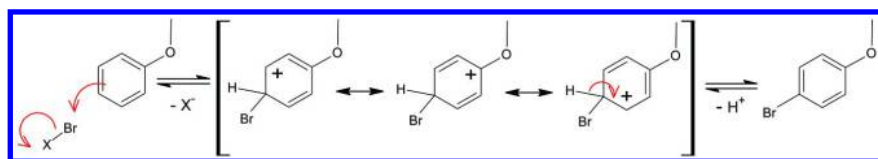


Figure 1. Pseudo-first-order rate constants of dimethenamid bromination as a function of chloride concentration. Arrow denotes site of bromination on dimethenamid. Error estimates denote 95% confidence intervals. Conditions: free chlorine dose = 0.43 mM = 30 mg/L as Cl_2 , $[\text{Br}^-]_0 = 0.10 \text{ mM} = 8.0 \text{ mg/L}$, $[\text{dimethenamid}]_0 = 9 \mu\text{M}$, $[\text{NaNO}_3] + [\text{NaCl}] = 0.1 \text{ M}$, $[\text{borate buffer}] = 10 \text{ mM}$, $T = 20.0 \text{ }^\circ\text{C}$. Adapted from reference (53). Copyright 2013, ACS.

The greater electronegativity of chlorine imparts a partial positive charge on bromine in BrCl . Consequently, BrCl is anticipated to function as a brominating agent. During the course of aromatic substitutions involving BrCl as the electrophile, chloride is released as a leaving group from BrCl (Scheme 1). Accordingly, chloride can be viewed as a catalyst of bromination reactions. Chloride catalysis via BrCl formation has also been quantified for bromination of *p*-xylene (56, 57) and anisole (55).



Scheme 1. Proposed Mechanism of Aromatic Compound Bromination by Free Bromine Species ($X = \text{Cl}, \text{Br}, \text{OCl}, \text{OBr}, \text{or OH}$) Using Anisole as a Model Compound. From Reference (55). Copyright 2015, ACS.

BrCl has an inherent reactivity 3.6×10^6 - and 1.4×10^7 -times greater than HOBr toward dimethenamid (53) and the *para* position of anisole, respectively (55). As such, the potency of chloride as a bromination catalyst can be substantial.

The median chloride concentration in raw DW is approximately 10 mg/L (59). Treatment processes (e.g., coagulation) can increase the chloride concentration of DW. For example, addition of FeCl₃ at 2 mM (~300 mg/L) as a coagulant concomitantly increases the chloride concentration by ~200 mg/L. This additional chloride is sufficient to increase bromination rates of anisole and dimethenamid by more than a factor of 11 (Figure 2).

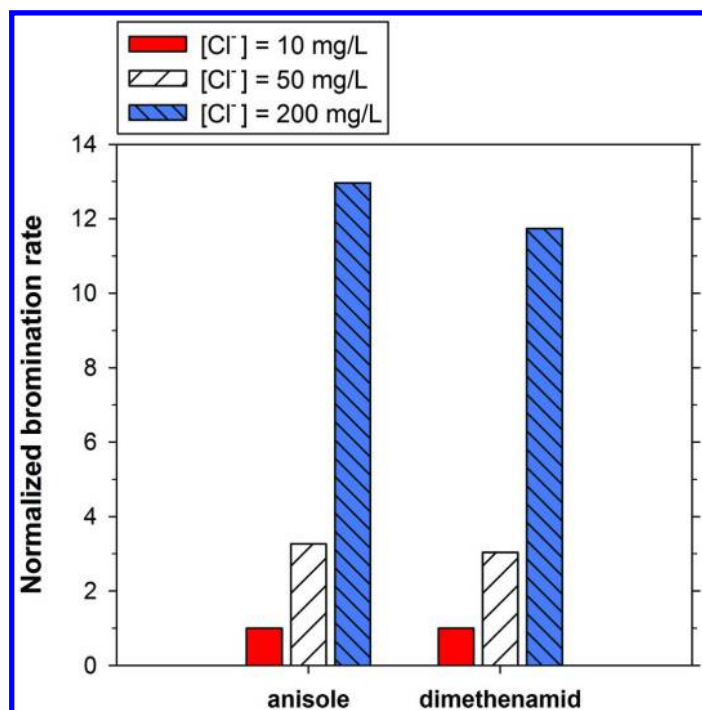
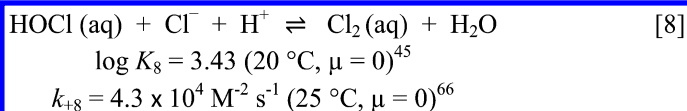


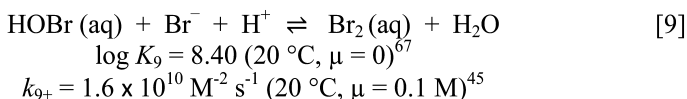
Figure 2. Catalysis of bromination of anisole (to give 4-bromoanisole (55)) and of dimethenamid (53) as a function of chloride concentration. Bromination rates are normalized to values calculated at $[Cl^-] = 10 \text{ mg/L}$. Conditions: $pH = 7.00$, free chlorine dose = 2.0 mg/L as Cl_2 , $[Br^-]_o = 0.10 \text{ mg/L}$, $T = 20.0 \text{ }^\circ\text{C}$.

In addition to catalyzing bromination reactions, chloride can similarly catalyze chlorination reactions of several organic compounds (including *p*-xylene (56, 57), the antimicrobial agent trimethoprim (60), polycyclic aromatic hydrocarbons (61), dimethenamid (62), phenolic compounds (63, 64), and aromatic ethers (65)) by promoting the formation of aqueous molecular chlorine (Cl_2).



Catalysis by Bromide

Unoxidized bromide can coexist in solutions of free bromine, including when (1) free chlorine is added substoichiometrically relative to bromide, (2) bromide is incompletely oxidized by ozone, or (3) free bromine is added directly to aqueous solutions containing bromide (e.g., in some pools and spas). Under these conditions, unoxidized bromide can enhance rates of organic compound bromination by promoting the formation of molecular bromine (eq 9):



When Br_2 serves as a brominating agent via transfer of Br(I) to an organic compound, bromide is released as a leaving group from Br_2 . As such, bromide can function as a catalyst of bromination reactions involving Br_2 .

Additional free bromine species (i.e., Br_2Cl^- and Br_3^-) can also form in the presence of excess bromide (58, 68). The formal negative charge on these species suggests that they will be significantly less reactive as brominating agents relative to neutral free bromine species (e.g., BrCl and HOBr) (55).

The ability of (unoxidized) bromide to increase bromination rates has been demonstrated for the sequential bromination of anisole to give mono- and dibrominated anisoles (55). Figure 3 demonstrates the catalytic effect of bromide on reactions of anisole with free bromine. Bromide catalysis of bromination has also been reported for other aromatic compounds, including *p*-xylene (56), phenols (69), and dimethenamid (53).

The ratio of second-order rate constants for Br_2 and HOBr (i.e., $k_{\text{Br}_2}/k_{\text{HOBr}}$) is a means of quantifying the catalytic efficacy of bromide during bromination reactions involving free bromine. For bromination of dimethenamid (53) and anisole (*para* position) (55) at 20 °C, $k_{\text{Br}_2}/k_{\text{HOBr}} = 6.6 \times 10^4$ and 3.2×10^5 , respectively. The greater catalytic potency of bromide toward bromination of anisole (relative to the more nucleophilic thiophene ring of dimethenamid) is consistent with the reactivity-selectivity principle, which predicts an increase in selectivity toward more reactive (brominating) agents as the reactivity of a substrate (here, an aromatic compound) decreases (70). The increased catalytic potency of bromide toward bromination of anisole relative to dimethenamid is also evident in Figure 4, which depicts normalized bromination rates as a function of the excess bromide concentration under conditions representative of DW treatment.

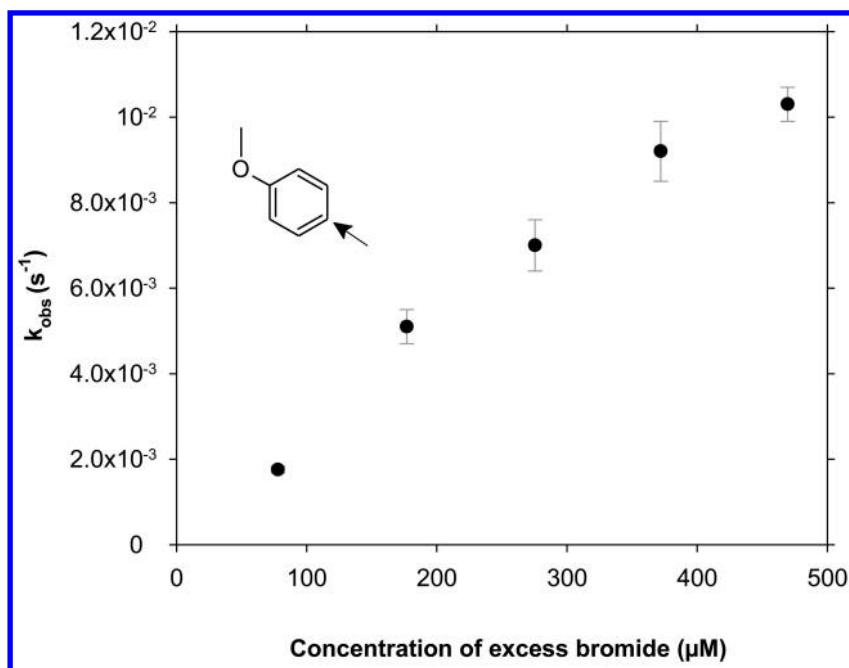
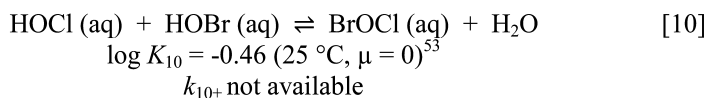


Figure 3. Effects of excess bromide (calculated as $[Br]_{xs} = [NaBr]_o - [free\ chlorine]_o$) on pseudo-first-order rate constants of para bromination of anisole in solutions of free bromine. Arrow denotes site of bromination. Error bars represent 95% confidence intervals. Conditions: $pH = 7.31$, $[bicarbonate\ buffer] = 20\ mM$, $[free\ chlorine]_o = 119\ \mu M$, $[Br]_o = 197\text{-}588\ \mu M$, $[anisole]_o = 10\ \mu M$, $[NaNO_3] = 98\ mM$, no added $NaCl$, $T = 20.0\ ^\circ C$. Adapted from reference (55). Copyright 2015, ACS.

Catalysis by Hypochlorous Acid

As with chloride and bromide, HOCl can also serve as a catalyst of bromination reactions. For example, bromination rates of dimethenamid in model laboratory reactors were previously shown to increase as the dose of free chlorine increased (53). The authors rationalized this finding by invoking BrOCl as a reactive brominating agent:



As with BrCl, the partial positive charge on the bromine atom of BrOCl and the greater leaving group ability of ClO⁻ (relative to BrO⁻) suggest this mixed halogen will function as a brominating agent (53). As HOCl is a product of aromatic bromination reactions involving BrOCl (53, 55), HOCl can be viewed as a bromination catalyst. Catalysis of bromination by HOCl has also been reported for reactions of anisole in solutions prepared by adding excess free chlorine to sodium bromide (Figure 5) (55).

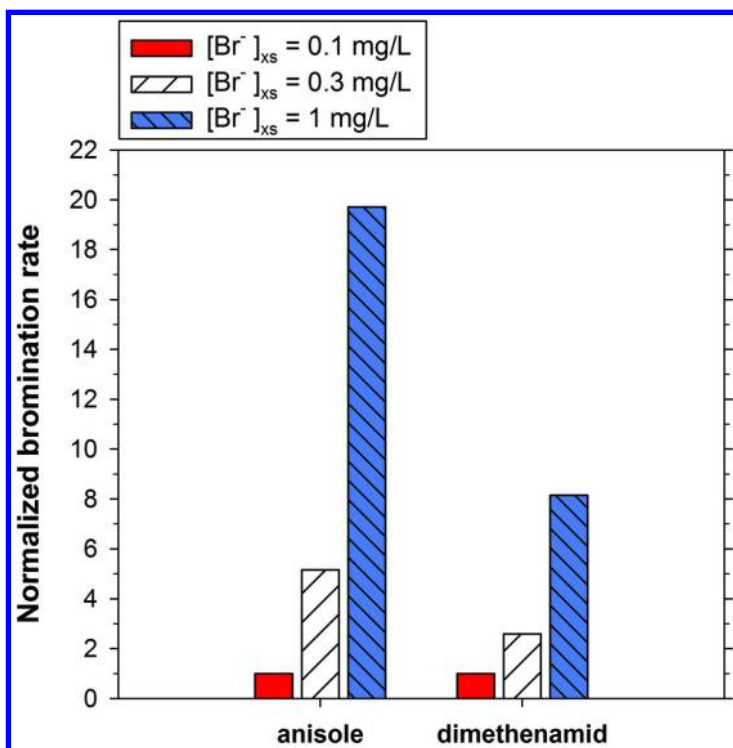


Figure 4. Catalysis of bromination of anisole (to give 4-bromoanisole (55)) and of dimethenamid (53) as a function of excess bromide concentration (calculated as $[Br^-]_{xs} = [NaBr]_o - [free\ chlorine]_o$). Bromination rates are normalized to values calculated at $[Br^-]_{xs} = 0.1 \text{ mg/L}$. Conditions: pH = 7.00, $[free\ chlorine]_o = 1.2 \mu\text{M}$, $[Cl^-] = 0.3 \text{ mM} = 11 \text{ mg/L}$, $T = 20.0 \text{ }^\circ\text{C}$.

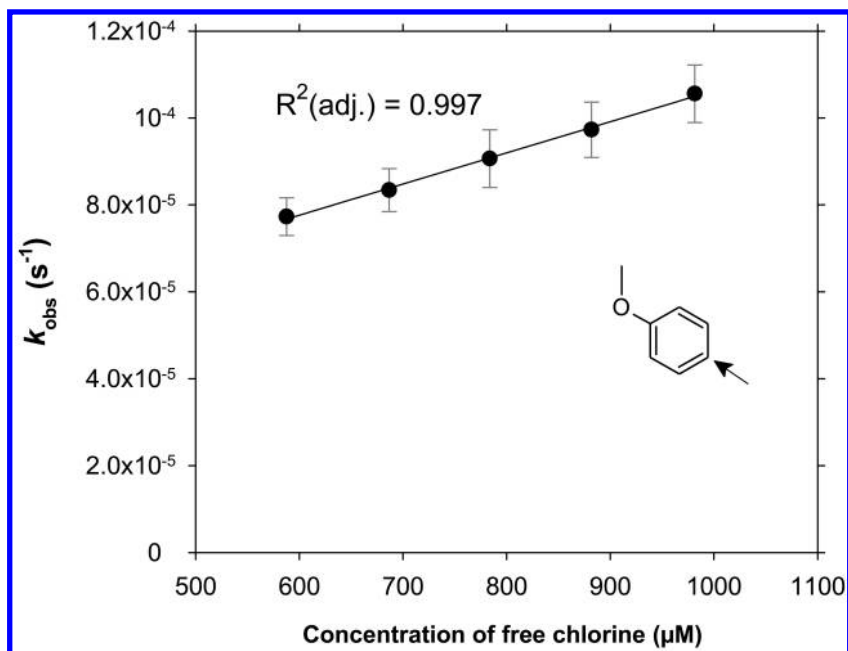


Figure 5. Influence of free chlorine concentration on pseudo-first-order rate constants of para bromination of anisole in solutions of free bromine. Arrow denotes site of bromination. Error estimates denote 95% confidence intervals. Conditions: pH 8.49, $[\text{Br}]_o = 230 \mu\text{M}$, $[\text{NaNO}_3] = 93 \mu\text{M}$, $[\text{Cl}^-] = 3.9 \text{ mM}$, $[\text{anisole}]_o = 19 \mu\text{M}$, and $T = 20.0 \text{ }^\circ\text{C}$. Adapted from reference (55). Copyright 2015, ACS.

The influence of free chlorine dose on bromination rates of anisole and dimethenamid are shown in Figure 6 for solution conditions typical of DW chlorination. A ten-fold increase in free chlorine dose (from 1 to 10 mg/L as Cl_2) results in a predicted 2.6- and 1.8-fold increase in bromination rates of anisole (*para* position) and dimethenamid, respectively.

In addition to promoting the formation of BrOCl , residual free chlorine may also increase observed rates of bromination in natural waters by facilitating re-oxidation of bromide (e.g., formed via reduction of free bromine by endogenous reductants) (71).

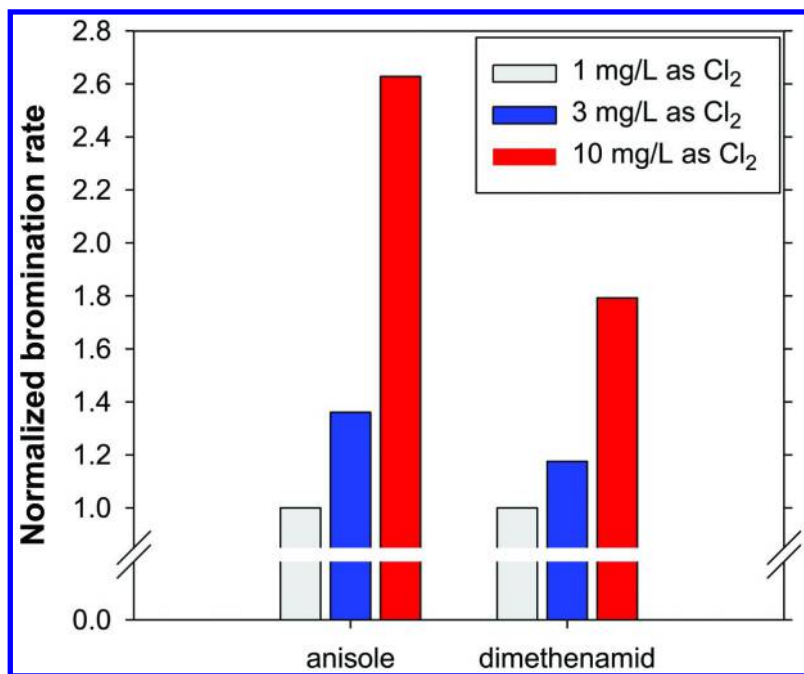
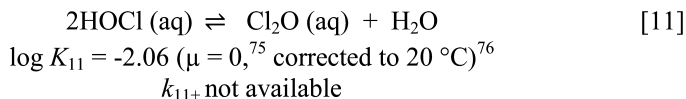


Figure 6. Catalysis of bromination of anisole (to give 4-bromoanisole (55)) and of dimethenamid (53) as a function of initial free chlorine concentration. Conditions: pH 7.00, $[Br]_o = 0.1 \text{ mg/L} = 1.25 \text{ }\mu\text{M}$, $[Cl] = 11 \text{ mg/L} = 0.3 \text{ mM}$, $T = 20.0 \text{ }^\circ\text{C}$.

In addition to catalyzing bromination reactions, HOCl can also enhance chlorination rates of organic compounds (including anisole (72), *p*-xylene (56), biphenyl (73), *trans*-2-butenic acid (74), dimethenamid (62), and aromatic ethers (65)) by promoting the formation of Cl₂O (eq 11).



Br₂O as a Putative Brominating Agent

Bromination reactions of organic compounds in solutions of free bromine are often assumed to be first-order in $[Br(I)]_{\text{tot}}$. This assumption was recently tested for bromination reactions of dimethenamid (53). Sivey et al. (53) discovered that bromination rates of dimethenamid had reaction orders in $[HOBr]$ ranging from near 1.0 to approximately 1.7 (Figure 7).

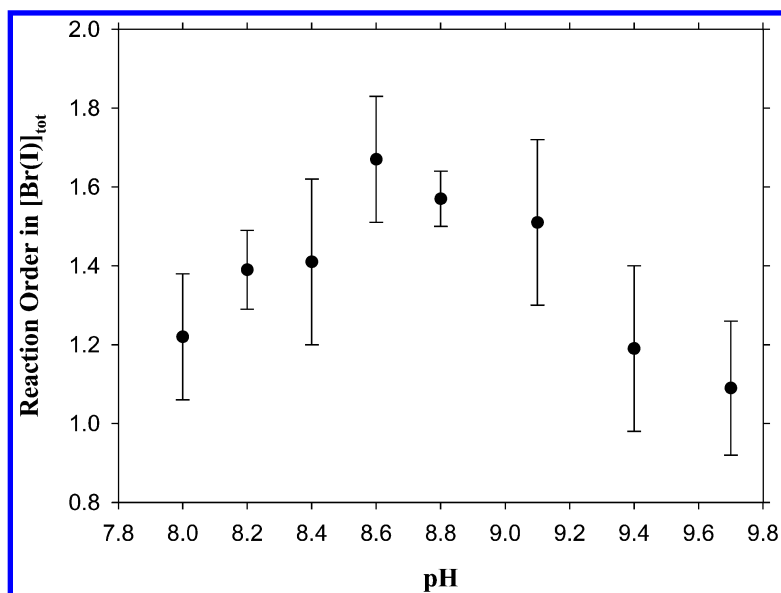
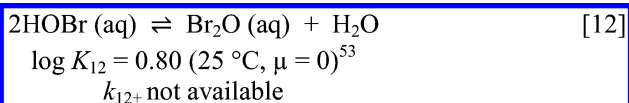


Figure 7. Reaction order in total free bromine concentration, $[\text{Br(I)}]_{\text{tot}}$, as a function of pH for reactions of dimethenamid with free bromine. Conditions: $[\text{dimethenamid}]_o = 8 \mu\text{M}$, $[\text{Br}^-]_o = (1.0 - 4.0) \times 10^{-4} \text{ M}$, initial free chlorine concentration = $430 \mu\text{M}$, $[\text{borate buffer}] = 10 \text{ mM}$, $T = 20.0 \text{ }^\circ\text{C}$. Adapted from reference (53). Copyright 2013, ACS.

Sivey et al. (53) suggested that the participation of Br_2O (eq 12) as a brominating agent could account for the measured reaction rates exhibiting a greater-than-first-order dependence on total free bromine.



Eq 12 indicates $[\text{Br}_2\text{O}]$ is proportional to $[\text{HOBr}]^2$. Unlike Br_2O , all other brominating agents discussed herein (HOBr , BrCl , Br_2 , and BrOCl) have concentrations that scale linearly with HOBr . Accordingly, Br_2O is the only examined free bromine species anticipated to produce reaction orders in $[\text{Br(I)}]_{\text{tot}}$ greater than 1.0. Br_2O is 7100- and 4100-times more inherently reactive than is HOBr in reactions with dimethenamid (53) and anisole (55), respectively.

A More Complete View of Free Bromine Speciation

Although HOBr and BrO^- are typically the most abundant constituents of free bromine (Figure 8), previous reports (53, 55–57) indicate the generally less-abundant free bromine species (BrCl , Br_2 , BrOCl , and Br_2O) are sufficiently reactive as to influence overall bromination rates of modestly nucleophilic aromatic compounds.

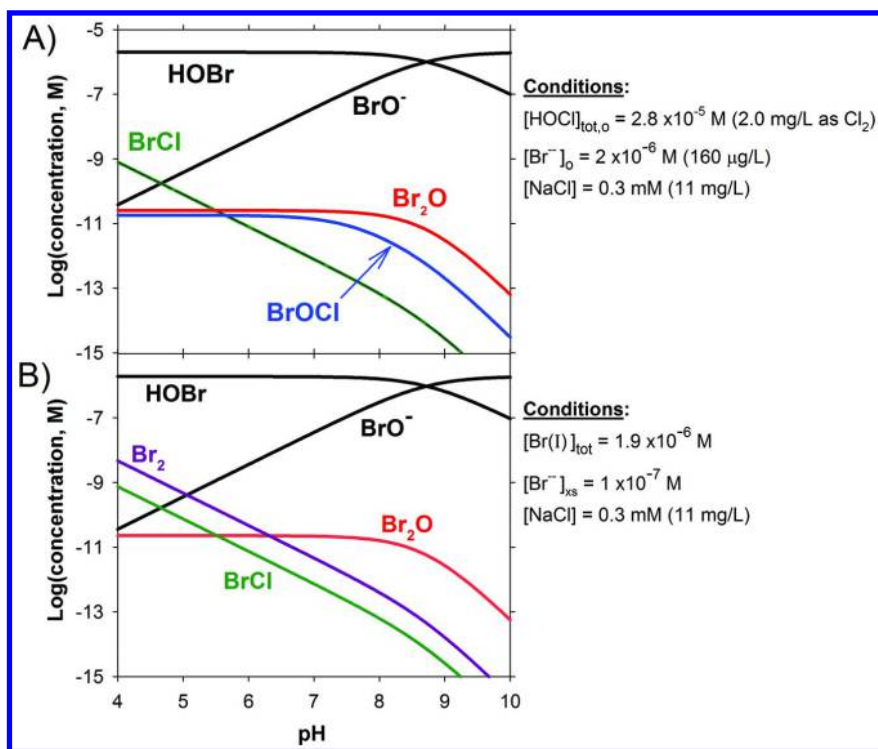


Figure 8. Speciation of free bromine for a model water containing bromide (160 µg/L) that undergoes disinfection by (A) free chlorine and (B) a sufficient amount of ozone to convert 95% of initial bromide into free bromine, Br(I) , and assuming higher oxidation products of bromine (e.g., bromate) are not formed. Data from reference (55) and sources cited therein.

The extent to which these often-overlooked brominating agents influence bromination rates under conditions representative of drinking water treatment can be calculated using second-order bromination rate constants reported for dimethenamid (53) and anisole (Figure 9) (55). As shown in Figure 9A, HOBr contributes <20% to the total bromination rate of anisole (to give 4-bromoanisole) at pH 7.0. The contribution of HOBr to the total bromination rate of dimethenamid at pH 7.0 is approximately 40% (Figure 9B). For both aromatic compounds, the influence of HOBr decreases with decreasing pH due to the increasing importance of BrCl . In solutions containing higher concentrations of bromide and/or chloride (e.g., wastewater (23) and DW impacted by seawater intrusion (77)) and in waters receiving larger doses of free chlorine, the importance of brominating agents other than HOBr is anticipated to increase.

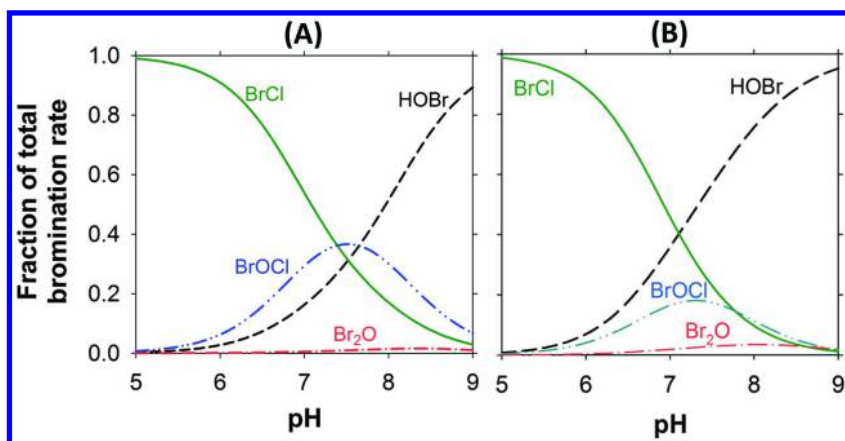


Figure 9. Contributions of brominating agents to overall bromination rate of (A) anisole (yielding 4-bromoanisole) (55) and (B) dimethenamid (adapted from reference (53), copyright 2013, ACS), both under typical drinking water chlorination conditions (free chlorine dose = 2 mg/L as Cl_2 , $[\text{Cl}^-] = 11 \text{ mg/L}$, $[\text{Br}]_o = 0.1 \text{ mg/L}$, $T = 20.0 \text{ }^\circ\text{C}$).

Overall, recent literature reports (53, 55, 56) suggest kinetic models that do not account for the less abundant free bromine species (BrCl , Br_2 , Br_2O , and BrOCl) are unable to satisfactorily explain the effects of solution chemistry conditions on measured bromination rates of modestly nucleophilic aromatic compounds. Accordingly, caution should be exerted when interpreting published rate constants (e.g., k_{app} and k_{HOBr}) that include (often untested) assumptions about the effects of halides and hypochlorous acid on rates of bromination. The extent to which catalysis by halides (via formation of BrCl and Br_2) and hypochlorous acid (via formation of BrOCl) influences formation rates of *regulated* DBPs merits future research. Such catalysis might be particularly influential, for example, during reactions involving the “slowly reacting fraction” of trihalomethane precursors (78).

References

1. Black & Veatch Corporation. *White's Handbook of Chlorination and Alternative Disinfectants*, 5th ed.; Wiley: Hoboken, NJ, 2010.
2. Rook, J. Formation of haloforms during the chlorination of natural water. *Water Treat. Exam.* **1974**, *23*, 234–243.
3. Rook, J. Haloforms in drinking water. *J. Amer. Water Works Assoc.* **1976**, *68*, 168–172.
4. Norwood, D.; Johnson, J.; Christman, R.; Hass, J.; Bobenrieth, M. Reactions of chlorine with selected aromatic models of aquatic humic acid. *Environ. Sci. Technol.* **1980**, *14*, 187–190.

5. Boyce, S. D.; Hornig, J. F. Reaction pathways of trihalomethane formation from the halogenation of dihydroxyaromatic model compounds for humic acid. *Environ. Sci. Technol.* **1983**, *17*, 202–211.
6. de Leer, E.; Damste, J.; Erkelens, C.; de Galan, L. Identification of intermediates leading to chloroform and C-4 diacids in the chlorination of humic acid. *Environ. Sci. Technol.* **1985**, *19*, 512–522.
7. de Leer, E.; Erkelens, C. Chloroform production from model compounds of aquatic humic material. The role of pentachlororesorcinol as an intermediate. *Sci. Total Environ.* **1985**, *47*, 211–216.
8. Sedlak, D.; von Gunten, U. The chlorine dilemma. *Science* **2011**, *331*, 42–43.
9. Morris, J. C. The acid ionization constant of HOCl from 5 to 35°. *J. Phys. Chem.* **1966**, *70*, 3798–3805.
10. Kumar, K.; Margerum, D. W. Kinetics and mechanism of general-acid-assisted oxidation of bromide by hypochlorite and hypochlorous acid. *Inorg. Chem.* **1987**, *26*, 2706–2711.
11. Bard, A.; Pearson, R.; Jordan, J. *Standard Potentials in Aqueous Solution*; Marcel Dekker: New York, 1985.
12. Hewitt, J. H. The bacterial quality of whirlpools: A study of water in commercially operated bromine disinfected spa pools. *Environ. Health* **1991**, *99*, 324–326.
13. Ao, X.; Li, X. J.; Li, H.; Liang, H. S. Observation on efficacy of bromine-containing disinfectant in on-the-spot disinfection of swimming pool water. *Chin. J. Disinfect.* **2007**, *6*, 024.
14. Das, T. K. Disinfection. In *Kirk-Othmer Encyclopedia of Chemical Technology*; Wiley: New York, 2002.
15. Ichihashi, K.; Teranishi, K.; Ichimura, A. Brominated-trihalomethane formation from phenolic derivatives as a model of humic materials by the reaction with hypochlorite and hypobromite ions. *Chem. Lett.* **1999**, *9*, 957–958.
16. Acero, J. L.; Piriou, P.; von Gunten, U. Kinetics and mechanisms of formation of bromophenols during drinking water chlorination: Assessment of taste and odor development. *Water Res.* **2005**, *39*, 2979–2993.
17. Crittenden, J. C.; Trussell, R. R.; Hand, D. W.; Howe, K. J.; Tchobanoglous, G. *Water Treatment Principles and Design*; Wiley: Hoboken, NJ, 2005.
18. Westerhoff, P.; Chao, P.; Mash, H. Reactivity of natural organic matter with aqueous chlorine and bromine. *Water Res.* **2004**, *38*, 1502–1513.
19. Zhai, H.; Zhang, X. Formation and decomposition of new and unknown polar brominated disinfection byproducts during chlorination. *Environ. Sci. Technol.* **2011**, *45*, 2194–2201.
20. Zhao, Y.; Anichina, J.; Lu, X.; Bull, R. J.; Krasner, S. W.; Hrudey, S. E.; Li, X.-F. Occurrence and formation of chloro- and bromo-benzoquinones during drinking water disinfection. *Water Res.* **2012**, *46*, 4351–4360.
21. Pan, Y.; Zhang, X. Four groups of new aromatic halogenated disinfection byproducts: Effect of bromide concentration on their formation and speciation in chlorinated drinking water. *Environ. Sci. Technol.* **2013**, *47*, 1265–1273.

22. Gonsior, M.; Schmitt-Kopplin, P.; Stavklint, H.; Richardson, S. D.; Hertkorn, N.; Bastviken, D. Changes in dissolved organic matter during the treatment processes of a drinking water plant in Sweden and formation of previously unknown disinfection byproducts. *Environ. Sci. Technol.* **2014**, *48*, 12714–12722.
23. Tchobanoglous, G.; Burton, F. L.; Stensel, H. D. *Wastewater Engineering: Treatment and Reuse*; McGraw-Hill: Boston, 2003.
24. Sun, Y.; Wu, Q.; Hu, H.; Tian, J. Effect of bromide on the formation of disinfection by-products during wastewater chlorination. *Water Res.* **2009**, *43*, 2391–2398.
25. Zwiener, C.; Richardson, S. D.; De Marini, D. M.; Grummt, T.; Glauner, T.; Frimmel, F. H. Drowning in disinfection byproducts? Assessing swimming pool water. *Environ. Sci. Technol.* **2007**, *41*, 363–372.
26. LaKind, J. S.; Richardson, S. D.; Blount, B. C. The good, the bad, and the volatile: Can we have both healthy pools and healthy people? *Environ. Sci. Technol.* **2010**, *44*, 3205–3210.
27. Xiao, F.; Zhang, X.; Zhai, H.; Lo, I. M. C.; Tipoe, G. L.; Yang, M.; Pan, Y.; Chen, G. New halogenated disinfection byproducts in swimming pool water and their permeability across skin. *Environ. Sci. Technol.* **2012**, *46*, 7112–7119.
28. Amy, G. L.; Chadik, P. A.; King, P. H.; Cooper, W. J. Chlorine utilization during trihalomethane formation in the presence of ammonia and bromide. *Environ. Sci. Technol.* **1984**, *18*, 781–786.
29. Hua, G.; Reckhow, D. A.; Kim, J. Effect of bromide and iodide ions on the formation and speciation of disinfection byproducts during chlorination. *Environ. Sci. Technol.* **2006**, *40*, 3050–3056.
30. Hu, J.; Song, H.; Karanfil, T. Comparative analysis of halonitromethane and trihalomethane formation and speciation in drinking water: The effects of disinfectants, pH, bromide, and nitrite. *Environ. Sci. Technol.* **2010**, *44*, 794–799.
31. Shan, J.; Hu, J.; Kaplan-Bekaroglu, S. S.; Song, H.; Karanfil, T. The effects of pH, bromide and nitrite on halonitromethane and trihalomethane formation from amino acids and amino sugars. *Chemosphere* **2012**, *86*, 323–328.
32. Plewa, M. J.; Simmons, J. E.; Richardson, S. D.; Wagner, E. D. Mammalian cell cytotoxicity and genotoxicity of the haloacetic acids, a major class of drinking water disinfection by-products. *Environ. Mol. Mutagen.* **2010**, *51*, 871–878.
33. Plewa, M. J.; Wagner, E. D.; Mitch, W. A. Comparative mammalian cell cytotoxicity of water concentrates from disinfected recreational pools. *Environ. Sci. Technol.* **2011**, *45*, 4159–4165.
34. Richardson, S. D.; Plewa, M. J.; Wagner, E. D.; Schoeny, R.; DeMarini, D. M. Occurrence, genotoxicity, and carcinogenicity of regulated and emerging disinfection by-products in drinking water: A review and roadmap for research. *Mutat. Res.* **2007**, *636*, 178–242.
35. Liviak, D.; Wagner, E. D.; Mitch, W. A.; Altonji, M. J.; Plewa, M. J. Genotoxicity of water concentrates from recreational pools after various disinfection methods. *Environ. Sci. Technol.* **2010**, *44*, 3527–3532.

36. Hansen, K. M. S.; Willach, S.; Antoniou, M. G.; Mosbak, H.; Albrechtsen, H.-J.; Andersen, H. R. Effect of pH on the formation of disinfection byproducts in swimming pool water - Is less THM better? *Water Res.* **2012**, *46*, 6399–6409.
37. Lundstrom, U.; Olin, A. Bromide concentration in Swedish precipitation, surface and ground waters. *Water Res.* **1986**, *20*, 751–756.
38. Stumm, W.; Morgan, J. *Aquatic Chemistry: Chemical Equilibria and Rates in Natural Waters*, 3rd ed.; John Wiley & Sons, Inc.: New York, 1996.
39. Westerhoff, P.; Siddiqui, M.; Debroux, J.; Zhai, W.; Ozekin, K.; Amy, G. Nation-wide bromide occurrence and bromate formation potential in drinking water supplies. In *Critical Issues in Water and Wastewater Treatment: Proceedings of the 1994 National Conference on Environmental Engineering*; Ryan, J. N., Edwards, M., Eds.; American Society of Civil Engineers: New York, 1994; pp 670–677.
40. Davis, S.; Fabryka-Martin, J.; Wolfsberg, L. Variations in bromide in potable ground water in the United States. *Groundwater* **2004**, *42*, 902–909.
41. Andreasen, D.; Fleck, W. Use of bromide:chloride ratios to differentiate potential sources of chloride in a shallow, unconfined aquifer affected by brackish-water intrusion. *Hydrogeol. J.* **1997**, *5*, 17–26.
42. Wilson, J. M.; Van Briesen, J. M. Source water changes and energy extraction activities in the Monongahela River, 2009–2012. *Environ. Sci. Technol.* **2013**, *47*, 12575–12582.
43. Hladik, M. L.; Focazio, M.; Engle, M. Discharges of produced waters from oil and gas extraction via wastewater treatment plants are sources of disinfection by-products to receiving streams. *Sci. Total Environ.* **2014**, *466-467*, 1085–1093.
44. Harkness, J. S.; Dwyer, G. S.; Warner, N. R.; Parker, K. M.; Mitch, W. A.; Vengosh, A. Iodide, bromide, and ammonium in hydraulic fracturing and oil and gas wastewaters: Environmental implications. *Environ. Sci. Technol.* **2015**, *49*, 1955–1963.
45. Eigen, M.; Kustin, K. The kinetics of halogen hydrolysis. *J. Am. Chem. Soc.* **1962**, *84*, 1355–1361.
46. Haag, W. R.; Hoigne, J. Ozonation of bromide-containing waters: kinetics of formation of hypobromous acid and bromate. *Environ. Sci. Technol.* **1983**, *17*, 261–267.
47. Pinkernell, U.; von Gunten, U. Bromate minimization during ozonation: Mechanistic considerations. *Environ. Sci. Technol.* **2001**, *35*, 2525–2531.
48. Bonacquisti, T. P. A drinking water utility's perspective on bromide, bromate, and ozonation. *Toxicology* **2006**, *221*, 145–148.
49. Trofe, T. W.; Inman, G. W.; Johnson, J. D. Kinetics of monochloramine decomposition in the presence of bromide. *Environ. Sci. Technol.* **1980**, *14*, 544–549.
50. Bousher, A.; Brimblecombe, P.; Midgley, D. Kinetics of reactions in solutions containing monochloramine and bromide. *Water Res.* **1989**, *23*, 1049–1058.
51. Gazda, M.; Dejarne, L. E.; Choudhury, T. K.; Cooks, R. G.; Margerum, D. W. Mass-spectrometric evidence for the formation of bromochloramine and

N-bromo-*N*-chloromethylamine in aqueous solution. *Environ. Sci. Technol.* **1993**, *27*, 557–561.

52. Heeb, M. B.; Criquet, J.; Zimmermann-Steffens, S.; von Gunten, U. Bromine production during oxidative water treatment of bromide-containing waters and its reactions with inorganic and organic compounds – A critical review. *Water Res.* **2014**, *48*, 15–42.
53. Sivey, J. D.; Arey, J. S.; Tentscher, P. R.; Roberts, A. L. Reactivity of BrCl, Br₂, BrOCl, Br₂O, and HOBr toward dimethenamid in solutions of bromide + aqueous free chlorine. *Environ. Sci. Technol.* **2013**, *47*, 1330–1338.
54. Fogler, H. *Elements of Chemical Reaction Engineering*, 4th ed.; Prentice Hall: Upper Saddle River, NJ, 2006.
55. Sivey, J. D.; Bickley, M. A.; Victor, D. A. Contributions of BrCl, Br₂, BrOCl, Br₂O, and HOBr to regiospecific bromination rates of anisole and bromoanisoles in aqueous solution. *Environ. Sci. Technol.* **2015**, *49*, 4937–4945.
56. Voudrias, E. A.; Reinhard, M. Reactivities of hypochlorous and hypobromous acid, chlorine monoxide, hypobromous acidium ion, chlorine, bromine, and bromine chloride in electrophilic aromatic substitution reactions with *p*-xylene in water. *Environ. Sci. Technol.* **1988**, *22*, 1049–1056.
57. Voudrias, E. A.; Reinhard, M. A kinetic model for the halogenation of *p*-xylene in aqueous HOCl solutions containing Cl⁻ and Br⁻. *Environ. Sci. Technol.* **1988**, *22*, 1056–1062.
58. Liu, Q.; Margerum, D. W. Equilibrium and kinetics of bromine chloride hydrolysis. *Environ. Sci. Technol.* **2001**, *35*, 1127–1133.
59. Davis, S. N.; DeWiest, R. J. M. *Hydrogeology*; Wiley: New York, 1966.
60. Dodd, M. C.; Huang, C.-H. Aqueous chlorination of the antibacterial agent trimethoprim: Reaction kinetics and pathways. *Water Res.* **2007**, *41*, 647–655.
61. Georgi, A.; Reichl, A.; Trommler, U.; Kopinke, F. Influence of sorption to dissolved humic substances on transformation reactions of hydrophobic organic compounds in water. I. Chlorination of PAHs. *Environ. Sci. Technol.* **2007**, *41*, 7003–7009.
62. Sivey, J. D.; McCullough, C. E.; Roberts, A. L. Chlorine monoxide (Cl₂O) and molecular chlorine (Cl₂) as active chlorinating agents in reaction of dimethenamid with aqueous free chlorine. *Environ. Sci. Technol.* **2010**, *44*, 3357–3362.
63. Deborde, M.; Rabouan, S.; Gallard, H.; Legube, B. Aqueous chlorination kinetics of some endocrine disruptors. *Environ. Sci. Technol.* **2004**, *38*, 5577–5583.
64. Curtis, M. P.; Hicks, A. J.; Neidigh, J. W. Kinetics of 3-chlorotyrosine formation and loss due to hypochlorous acid and chloramines. *Chem. Res. Toxicol.* **2011**, *24*, 418–428.
65. Sivey, J. D.; Roberts, A. L. Assessing the reactivity of free chlorine constituents Cl₂, Cl₂O, and HOCl toward aromatic ethers. *Environ. Sci. Technol.* **2012**, *46*, 2141–2147.

66. Wang, T. X.; Margerum, D. W. Kinetics of reversible chlorine hydrolysis: temperature dependence and general-acid/base-assisted mechanisms. *Inorg. Chem.* **1994**, *33*, 1050–1055.
67. Liebhafsky, H. A. The equilibrium constant of the bromine hydrolysis and its variation with temperature. *J. Am. Chem. Soc.* **1934**, *56*, 1500–1505.
68. Wang, T. X.; Kelley, M. D.; Cooper, J. N.; Beckwith, R. C.; Margerum, D. W. Equilibrium, kinetic, and UV-spectral characteristics of aqueous bromine chloride, bromine, and chlorine species. *Inorg. Chem.* **1994**, *33*, 5872–5878.
69. Tee, O.; Paventi, M.; Bennett, J. Kinetics and mechanism of the bromination of phenols and phenoxide ions in aqueous solution. Diffusion-controlled rates. *J. Am. Chem. Soc.* **1989**, *111*, 2233–2240.
70. Anslyn, E. V.; Dougherty, D. A. *Modern Physical Organic Chemistry*; University Science: Sausalito, CA, 2005.
71. Allard, S.; Fouche, L.; Dick, J.; Heitz, A.; von Gunten, U. Oxidation of manganese(II) during chlorination: Role of bromide. *Environ. Sci. Technol.* **2013**, *47*, 8716–8723.
72. Swain, C. G.; Crist, D. R. Mechanisms of chlorination by hypochlorous acid. The last of chlorinium ion, Cl⁺. *J. Am. Chem. Soc.* **1972**, *94*, 3195–3200.
73. Snider, E. H.; Alley, F. C. Kinetics of the chlorination of biphenyl under conditions of waste treatment processes. *Environ. Sci. Technol.* **1979**, *13*, 1244–1248.
74. Craw, D.; Israel, G. The kinetics of chlorohydrin formation. Part III. The reaction between hypochlorous acid and crotonic acid at constant pH. *J. Chem. Soc.* **1952**, 550–553.
75. Roth, W. A. Zur Thermochemie des Chlors und der unterchlorigen Säure. *Z. Phys. Chem., Abt. A* **1929**, *145*, 289–297.
76. Reinhard, M.; Redden, G. D.; Voudrias, E. A. The hydrolysis constant of chlorine monoxide and bromine chloride in water. In *Water Chlorination: Environmental Impact and Health Effects*; Jolley, R. L., Ed.; Ann Arbor Science: Ann Arbor, MI, 1990; pp 859–870.
77. Ged, E. C.; Boyer, T. H. Effect of seawater intrusion on formation of bromine-containing trihalomethanes and haloacetic acids during chlorination. *Desalination* **2014**, *345*, 85–93.
78. Gallard, H.; von Gunten, U. Chlorination of natural organic matter: kinetics of chlorination and of THM formation. *Water Res.* **2002**, *36*, 65–74.

Chapter 15

Prescribed Fire Alters Dissolved Organic Matter and Disinfection By-Product Precursors in Forested Watersheds - Part I. A Controlled Laboratory Study

Hamed Majidzadeh,^{1,2,3} Jun-Jian Wang,^{2,3} and Alex T. Chow^{*,2}

¹School of Forestry and Wildlife Science, Auburn University,
Auburn, Alabama 36849

²Baruch Institute of Coastal Ecology & Forest Science, Clemson University,
Georgetown, South Carolina 29442

³H.M. and J.W. contributed equally.

*E-mail: achow@clemson.edu.

Detritus material in forested watersheds is the major terrestrial source of dissolved organic matter (DOM) and disinfection by-product (DBP) precursors in source waters. Forest fire reduces the thickness of detritus layer and changes foliar litters into pyrogenic organic matter (PyOM) on the forest floor, resulting in different quantity and quality of DOM exported from forested watersheds. Many studies have examined DBP precursors exported from forested watersheds; however, DOM leaching from PyOM, or dissolved black carbon (BC), could have different reactivity in DBP formation compared to the DOM leaching from unburned detritus layer. Using controlled laboratory burning in this study, characteristics of foliar litters before and after burn were compared. Quality and quantity of water extractable organic matter (WEOM) from raw and burned foliar litters commonly found in the southeastern United States, including baldcypress (*Taxodium distichum*), boxelder (*Acer negundo*), longleaf pine (*Pinus palustris*), pop ash (*Fraxinus caroliniana*), sweetgum (*Liquidambar styraciflua*), and water tupelo (*Nyssa aquatica*) was compared, and evaluated for their disinfection by-product yield and specific DBP formation using a uniform formation condition test. Laboratory analysis

using pyrolysis gas chromatography mass spectrometry showed that foliar litters after burn contain significantly less lignins, nitrogenous compounds, and polysaccharides because of loss of organic matter. However, both the formula numbers and relative abundance of PAHs increased, which can be a potential health concern. Water extractable organic carbon (WEOC) and total nitrogen (WETN) decreased after burn and in particular raw material had less humic acid and fulvic acid-like compounds. PyOM aromaticity may be either enhanced or lowered by prescribed fire and highly depending upon the plant species. The specific formation of chloroform (a prevalent DBP species) decreased by 12%-60% for all plant species after burn. However, dissolved BC was more reactive in the formation of nitrogenous disinfection by-products (N-DBPs), and the specific haloacetonitriles formation increased after burn for all species.

Introduction

Forests are critically important to the supply of clean drinking water in the United States. National forests and grasslands, which represent 30% of the forest area in the U.S., provide drinking water for over 60 million people (1). The number of people served by all forests and grasslands in the U.S. are far greater than this number. Hot temperatures and longer dry periods due to climate change will increase the likelihood of larger and more severe wildfires (2). Forest fire rapidly modifies the chemical composition of the detritus layer on the forest floor, converting lignin and polysaccharide rich and relatively degradable carbon pools to polycyclic aromatic and charcoal rich and recalcitrant black carbon (BC) (3). Dissolved organic matter (DOM) leaching from pyrogenic organic matter (PyOM), or dissolved BC, could have different treatability and reactivity in disinfection by-product (DBP) formation compared to the DOM leaching from unburned detritus layer. In contrast to wildfire, prescribed fire is low-intensity burning of accumulated detritus materials to reduce the fuel amount on forest floor to prevent catastrophic wildfires (4). It is often conducted when soil is moderately moist to reduce the intensity, and it brings benefits to decrease the invasive species and release different nutrients from plant materials (5). While forested ecosystems have been identified as persistent sinks for atmospheric carbon (6), prescribed burns can affect forest's capacity to sequester carbon and carbon quality and quantity in soil organic matter pools (7, 8). For example, forest fire converts plant biomass into forms of BC such as polycyclic aromatic hydrocarbons (PAHs) that are resistant to microbial attack and persist in the soil for thousands of years (9). These new compounds are the products of incomplete combustion of biomass, which usually had lower H/C and O/C ratios (10). Hockaday, et al. (2007) (11) found that export of BC from soils via dissolution and biological transformation could constitute an important C loss mechanism. In fact, charred plant materials

can cause accelerated breakdown of simple carbohydrates (12) and enhance the loss of forest humus (13). As detritus in forest floor is one major source of terrestrial DOM (14), export of these newly formed and modified compounds is of great concern because they may alter the water quality by changing DOM quantity and quality.

The well-documented toxicological properties of DBPs suggested that exposure to DBPs in disinfected water may increase the risk of cancers such as bladder and colorectal cancers (15, 16). As DOM is an important precursor reacting with disinfectants during water treatment to yield carbonaceous (e.g., trihalomethanes; THMs) and nitrogenous disinfection by-products (N-DBPs) (e.g., haloacetonitriles; HANs) (17–19) increasing studies are focusing on the sources of DOM and the associated chlorine reactivity (20, 21). Litters have been identified as a significant watershed source of DOM contributing to the downstream water supply and DBP precursors (14, 22–24). Different plant species can have a diverse amount and composition of organic compounds such as polysaccharides, lignin, tannin, and aliphatic biopolymers (25). Thus, variation in plant species can affect the DOM composition and may affect the budget and speciation of DBPs in water treatment process. Burning of diverse plant materials would affect the quality and quantity of DOM and the subsequent DBP formation as well, which, however, has not been well studied.

In order to understand the effects of low intensity prescribed forest fire on the productions of DOM and DBP precursors in forested watersheds, we conducted a controlled laboratory study (Part I) and a controlled field study (Part II) independently. In this chapter we present Part I, the laboratory study where we compared characteristics of water extractable organic matter (WEOM) from raw and laboratory-controlled burned foliar litters of six plant species commonly found in the southeastern United States, including baldcypress (*Taxodium distichum*), boxelder (*Acer negundo*), longleaf pine (*Pinus palustris*), pop ash (*Fraxinus caroliniana*), sweetgum (*Liquidambar styraciflua*), and water tupelo (*Nyssa aquatica*), and evaluated their DBP formation using a uniform formation condition test. Results of this study would illustrate the productions of DOM and DBP precursors among different tree species under prescribed fire practices. Results of this controlled experiment would also be used to compare to the real prescribed fire practices (Part II), as described in the other chapter of Part II.

Material and Methods

Litter Collection and Black Carbon Preparation

Fresh litter samples in Congaree National Park (SC, U.S.A.) were collected using five 0.5 m × 0.5 m litterfall traps with 1 mm mesh fiberglass screen bottoms during the winter of 2010. The Congaree River drains a large portion of upstate South Carolina, and thus, can flood rapidly during heavy rain events (26). The Congaree National Park has 10 flooding events per year on average, with mean annual precipitation of 1220 mm (27). The foliar litter of six common tree species in Congaree National Park, including baldcypress (*Taxodium distichum*),

sweetgum (*Liquidambar styraciflua*), water tupelo (*Nyssa aquatica*), pop ash (*Fraxinus caroliniana*), longleaf pine (*Pinus palustris*), and boxelder (*Acer negundo*) were separated from the mixed litterfall. After collection, all litter samples were oven-dried at 50 °C for 48 hr. To simulate the burning, 10.00 g of dried litter material was placed in a pre-heated furnace at 340 °C for 4 minutes and then cooled down gradually in the muffle furnace for three hours. Samples that had flame were not put out manually during the whole process. The temperature of 340 °C has been reported to be average soil temperature in Ichauway Reserve during a prescribed fire on 1994 (28). After cooling, samples were weighed again to determine the weight lost. The burning for each plant species was conducted in triplicate. To reduce the heterogeneity of the sample, all unburned and burned litter materials were grounded and all passed through a 2-mm copper screen (20).

Chemical Characteristics of Original and Burned Litters

Pyrolysis gas chromatography mass spectrometry (Py-GC/MS) was used to analyze the most common three litters (longleaf pine, pop ash, and sweetgum) before and after burn following the same method described in Song et al. (2010) (29). Py-GC/MS results are presented as the relative abundance of specific compound by dividing the peak area of the identified compound with the total area of all compounds. The major identified compounds were categorized into seven groups: aromatics, lignin, lipid, PAHs, phenolics, polysaccharide, and nitrogen. The detail compounds under each group were listed in Table A1.

Characterization of DOM from Litter

Water extractable organic matter (WEOM) was obtained by mixing one gram of unburned or burned litter with 200 mL Milli-Q water shaking at room temperature for 2 hr at 210 rpm. Each water extract was filtered through pre-washed 0.45 μm polyethersulfone membrane Supor-450 (Pall Corporation), and the filtrate was refrigerated at 4 °C through completion of analysis. Dissolved organic carbon (DOC) and dissolved total nitrogen (DTN) were measured by Shimadzu TOC-V CHS analyzer. The extractability of litter material was defined as the mass of extractable organic carbon per gram original (unburned) or burned litter. The post-burn water extractable organic carbon (WEOC) yield from original litter ($\text{mg-C/g-original-litter}$) was calculated as the extractability of burned litter multiplied by the mass remaining of burned material compared to original material.

The UV-VIS absorption (UVA) spectroscopy between 200 and 700 nm was conducted using Shimadzu UV-1800 in room temperature (25 ± 1 °C) in 1 cm quartz cell. Specific ultraviolet absorbance at 254 nm (SUVA) was determined by normalizing UVA with DOC concentration and was reported in units of liter per milligram carbon per meter ($\text{L mg}^{-1} \text{m}^{-1}$) (30). The E2:E3 ratio has been calculated as the absorbance at 250 nm divided by the absorbance at 365 nm (31). SUVA and E2:E3 ratios are considered as surrogates for aromatic carbon and molecular weight of DOM, respectively.

Fluorescence emission and excitation matrices (EEMs) were obtained using a Shimadzu RF5301 with 5 nm slit in excitation and 5 nm slit in emission. EEMs were corrected and analyzed by a numerical method, the fluorescence regional integration based on Simpson's Rule (FRI-SR) as described in Zhou et al. (2013) (32). The fluorescence regional integration (FRI) is a quantitative technique that integrates the volume beneath an EEM. Five regions in EEMs were operationally defined using consistent excitation (ex) and emission (em) wavelength boundaries based on fluorescence of model compounds, and DOM fractions: I: Aromatic Protein I (ex: 220 nm-250 nm, em: 280 nm-330 nm), II: Aromatic Protein II (ex: 220 nm-250 nm, em: 330 nm-380 nm), III: Fulvic acid-like (ex: 220 nm-250 nm, em: 380 nm-550 nm), IV: Soluble microbial by-product-like (250 nm < ex < 400 nm, em: 280 nm-380 nm), and V: Humic acid-like (250 nm < ex < 400 nm, em: 380 nm-550 nm). Volume integrated under the EEM within region I is normalized to the projected excitation-emission area and resulted in a normalized percent fluorescence response ($P_{1,n}$) (32, 33).

Disinfection By-Products Formation

The uniform formation condition (34) was the chlorination procedure used in this study and three replicates were analyzed for each litter extract. Briefly, the uniform formation condition is the condition that yields 1 ± 0.4 mg L⁻¹ free chlorine residual at pH 8 ± 0.2 after 24 hr of incubation in the dark at 20 °C after chlorination with freshly prepared NaOCl/H₃BO₃ dosing solution. Chlorine demand was calculated as the difference between chlorine dose and residual chlorine concentration after 24 h. Chlorinated samples were analyzed using headspace GC-ECD (35). Four trihalomethanes (chloroform, dichlorobromomethane, dibromochloromethane, and bromoform) and four haloacetonitriles (trichloroacetonitrile, dichloroacetonitrile, bromochloroacetonitrile, and dibromoacetonitrile) were quantified with the minimum reporting levels at approximately 0.5 µg/L. Specific DBP formation, defined as DBP concentration normalized to the initial DOC concentration, was used to evaluate the reactivity of DOC in forming DBPs and was expressed in molar units, as mmol/mol-C (20).

Statistical Analyses

All statistical analyses conducted in "R" version 2.15.0 (Copyright (C) 2012 The R Foundation for Statistical Computing). Relationships were considered to be significant at $P < 0.05$. Pearson's correlation was used to examine correlation between different parameters.

Results and Discussion

Chemical Characteristics of Litter Materials

In the spectra from Py-GCMS, both intensity and number of peaks decreased in burned litter compared to original litter, which is mainly due to the loss

of most organic matter during burning. The lignins, nitrogenous compounds, and polysaccharides all decreased for all three plant species, which can be explained by the degradation and volatilization at high temperatures (8). It has been reported that distillation of volatiles and loss of organic carbon start at temperatures between 100 and 200 °C (36, 37). Between 130 and 190 °C lignin and hemicelluloses begin to degrade, and at temperatures above 250 °C, polyaromatic structure start to form, whereas above 300 °C PAHs can be detected as well in plant char derived from cellulose, pectin, lignin and chlorogenic acid (38–40). This data matches our results considering significant decrease in lignin and polysaccharide as depicted in Figure 1. Some new peaks were observed in burned litters as well. The results indicate increases in both the abundance of PAH types (7 types of PAHs before burn to 15 types after burn) and relative abundance of PAHs (2.2% before burn and 7.7% after burn). This result is in agreement with the well-documented PAH formation in burning process (41). The percentage of aromatic compounds also increased from 15.2% to 32.3%, suggesting the formation of new aromatic structure in the organic matter. Production of these carcinogenic PAHs (42) from forest fires and prescribed burns is of great health concern to firefighters, forest workers and nearby rural communities including several Native American tribes (43, 44). The characteristics and mutagenic activities of biomass-derived PAHs from forest fires have been described, principally on the particulate matter emission to the atmosphere (45, 46).

Effect of Prescribed Fire on Carbon and Nitrogen Quantity

Comparing litters of different plant species before burning, sweetgum litter was the largest producer of water extractable organic carbon (WEOC), generating 84.62 mg-DOC per gram of litter (mg-DOC/g-original-litter), followed by longleaf pine, tupelo, baldcypress and pop ash (53.49 to 31.66 mg-DOC/g-original-litter) (Table 1). After burning, the DOC leached from burned litter decreased by 83% on average and ranged from 20.72 (longleaf pine) to 1.78 mg-DOC/g-original-litter (pop ash) (Table 1). Higher WEOC leaching from original litters was expected because they contained a greater portion of readily soluble and degradable organic C, and the burning processes caused a substantial loss of organic matter (47, 48). Thermal treatments such as prescribed fire remove preferentially external oxygen groups yielding materials with comparatively reduced solubility and colloidal properties (49, 50).

Water extractable total nitrogen (WETN) was also higher before burn, ranging from 0.36 (longleaf pine) to 1.65 mg-N/g-original-litter (boxelder) (average = 0.69 mg-N/g-original-litter), while after burn WETN ranged 0.05 (ash) to 0.87 mg-N/g-original-litter (boxelder) (average = 0.25 mg-N/g-original-litter). WETN after burn decreased mainly due to volatilizing of nitrogen. At 200 °C nitrogen starts to volatilize and above 500 °C half of the nitrogen in organic matter is lost to the atmosphere (8). The carbon to nitrogen ratio (C/N) was also calculated before and after burn. As expected, the C/N decreases after burn for all the species except for longleaf pine although both C and N quantity was decreased for this species. A positive relation between litter's weight lost after burn and initial litter C/N was observed ($r^2 = 0.69$, $p = 0.04$).

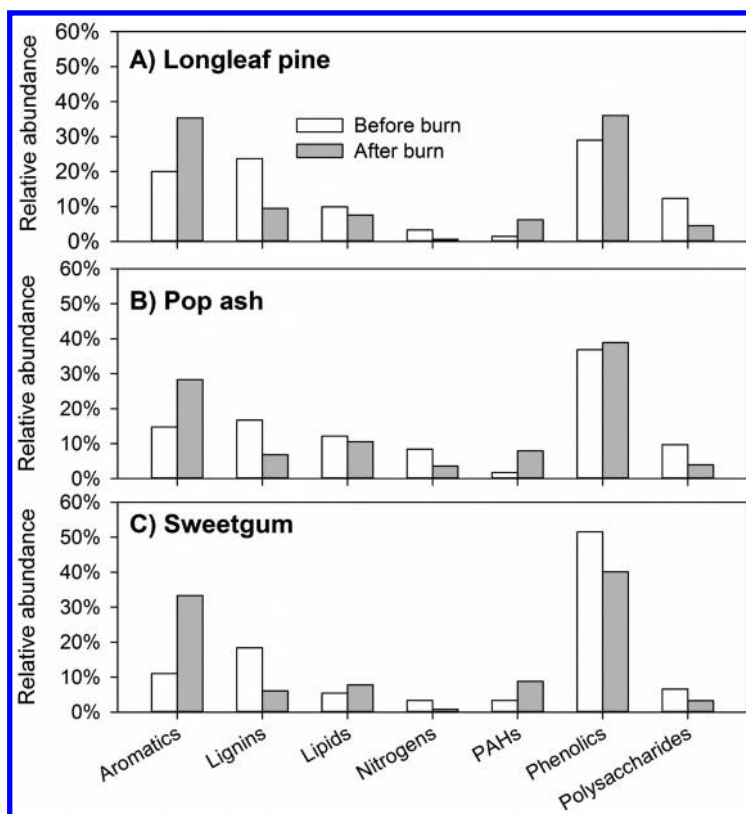


Figure 1. Chemical composition of original (white bars) and burned (gray bars) litters as determined from pyrolysis gas chromatography mass spectrometry (Py-GC/MS).

Effect of Fire on Carbon Quality

UV-VIS Spectrometry

SUVA, an indicator of the degree of aromaticity, increased significantly after burn for baldcypress, boxelder, longleaf pine, pop ash, and sweetgum except for water tupelo (Table 2). E2/E3 decrease for baldcypress, longleaf pine, pop ash, and sweet gum, but not for water tupelo and boxelder. Vergnoux et al. (2011) (44) reported that after burn WEOM exhibited both a higher aromaticity due to the increase of the hydrophilic aromaticity and lower humification and less high weighted compounds by the contribution of transphilic and hydrophobic compounds. However, our results revealed that the WEOM aromaticity of litter materials may be either enhanced or lowered by prescribed fire highly depending on the plant species. There were strong correlations between DOC and UVA both before and after burn. However, different SUVA suggested that their slopes were different before and after burn (Table 2), indicating a chemical change in

DOM occurred. While there is no correlation between DOC and SUVA ($r^2 = 0.06$, $p = 0.6$) before burn, a strong correlation can be seen after burn ($r^2 = 0.79$, $p = 0.01$) (Table 3 & Table 4). DOC from different litters appears to have more complex composition before burn in comparison to after burn, which reveals the homogenization of biomass substrate in black carbon, which is in accordance with a previous study (44) A stronger correlation between DOC and UVA after burn might be the result of homogenization as well (Table 3 & Table 4).

Table 1. Weight of Litters and Chemical Characteristics of Water Extracts of Litters before and after Burns (Means of Triplicates Are Present). One Gram of Raw Litter or Burned Litter Was Mixed with 200 mL Milli-Q Water and Shaken at Room Temperature for 2 Hours at 210 rpm.

<i>Sample</i>	<i>Weight loss</i>	<i>Pre-burn WEOC^a</i>	<i>Post-burn WEOC</i>	<i>Pre-burn WETN^a</i>	<i>Post-burn WETN</i>	<i>Pre-burn C/N</i>	<i>Post-burn C/N</i>
Bald-cypress	70.3%	35.8	6.7	0.72	0.35	57.7	21.6
Boxelder	68.6%	47.1	16.0	1.65	0.87	33.4	21.6
Longleaf pine	48.1%	62.2	20.7	0.36	0.07	200.3	348.8
Pop ash	65.8%	31.7	1.8	0.61	0.05	60.6	39.1
Sweet-gum	54.7%	84.6	3.8	0.48	0.04	206.1	103.4
Water tupelo	64.3%	53.5	3.4	0.34	0.11	183.7	34.6

^a WEOC and WETN are both in mg /g-original-litter.

Fluorescence Spectrometry

A substantial loss of organic matter was observed in region I of the EEM (Aromatic protein I). The percent fluorescence response in region I ($P_{I,n}$) ranged from 29% to 43% before burn, and decreased by 45%-87% after burn for all species (Table 2 & Figure 2). No significant changes in region II response was observed after burn except for longleaf pine. Region III and V percentages, which are related to fulvic acid-like and humic acid-like DOM, both have increased dramatically after burn (Table 2 & Figure 2). Sum of regions III and V showed an increase of 31%-76% after burn.

The more recalcitrant and aromatic structures formed by fires are derived from the alteration of carbohydrates, lipids, alkylated macromolecules, and peptides (51, 52). Consequently, some of these newly formed structures, initially non-humified, can become extractable like the humic- and fulvic- like fractions (46, 53). The FRI data reveals the difference in DOM composition before and after burning which is in accordance with our SUVA and E2:E3 data. While before burn region I exhibited high fluorescence response after burn region III and V had the highest responses except for longleaf pine.

Table 2. Optical Properties of Water Extracts of Litters before and after Burns. Fluorescence Regional Integration (FRI) Percentage Distribution of the Water Samples, SUVA, and E2/E3 Ratio.

<i>Species</i>	<i>UV-Vis properties</i>		<i>Percent fluorescence response (%)</i>				
	<i>SUVA (L/mg/m)</i>	<i>E2/E3</i>	<i>I</i>	<i>II</i>	<i>III</i>	<i>IV</i>	<i>V</i>
	Before burn						
Baldcypress	1.32	6.19	30.52	29.49	12.53	18.39	9.07
Boxelder	1.14	4.05	29.31	31.13	15.75	15.66	8.16
Longleaf pine	1.01	9.24	43.08	29.21	7.11	16.65	3.94
Pop ash	1.55	4.92	39.16	28.29	11.86	15.20	5.49
Sweetgum	1.93	5.28	38.19	33.10	9.11	15.36	4.24
Water tupelo	2.56	4.89	37.05	29.95	13.55	12.37	7.09
	After burn						
Baldcypress	2.09	5.42	12.00	30.84	29.11	14.56	13.49
Boxelder	2.07	5.56	10.83	32.16	29.8	14.63	12.58
Longleaf pine	1.21	8.66	23.27	43.48	11.73	17.14	4.39
Pop ash	2.50	4.31	4.92	26.48	36.50	11.88	20.22
Sweetgum	2.32	5.27	7.41	26.17	37.44	11.87	17.11
Water tupelo	2.27	5.73	6.14	26.77	36.85	12.32	17.92

Table 3. Pearson's Correlation Coefficients (r) between Measured Parameters of Litters before Burn. Significant Correlations (p < 0.05) Are Highlighted in Bold.

	<i>WEOC</i>	<i>TN</i>	<i>C/N</i>	<i>UVA</i>	<i>SUVA</i>	<i>E2/E3</i>	<i>I</i>	<i>II</i>	<i>III</i>	<i>IV</i>	<i>V</i>	<i>Specific THM formation</i>
TN	-0.3											
C/N	0.81	-0.74										
UVA	0.79	-0.45	0.75									
SUVA	0.25	-0.47	0.44	0.78								
E2/E3	0.21	-0.51	0.48	-0.2	-0.44							
I	0.39	-0.77	0.72	0.28	0.13	0.6						
II	0.79	0.2	0.34	0.7	0.24	-0.31	-0.21					
III	-0.55	0.7	-0.7	-0.21	0.17	-0.81	-0.82	-0.02				
IV	-0.21	0.21	-0.37	-0.6	-0.80	0.44	-0.26	-0.12	-0.25			
V	-0.63	0.56	-0.71	-0.38	-0.02	-0.48	-0.91	-0.14	0.83	0.17		
Specific THM formation	0.80	-0.35	0.59	0.81	0.41	-0.03	0.1	0.80	-0.38	-0.03	-0.3	
Specific HAN formation	-0.35	0.18	-0.42	-0.67	-0.76	0.45	-0.3	-0.27	-0.16	0.98	0.31	-0.14

Table 4. Pearson's Correlation Coefficients (r) between Measured Parameters of Litters after Burn. Significant Correlations (p < 0.05) Are Highlighted in Bold.

	<i>WEOC</i>	<i>TN</i>	<i>C/N</i>	<i>UVA</i>	<i>SUVA</i>	<i>E2/E3</i>	<i>I</i>	<i>II</i>	<i>III</i>	<i>IV</i>	<i>V</i>	<i>Specific THM formation</i>
TN	0.41											
C/N	0.67	-0.39										
UVA	0.91	0.75	0.31									
SUVA	-0.89	-0.01	-0.87	-0.63								
E2/E3	0.81	-0.12	0.90	0.53	-0.97							
I	0.88	0.03	0.85	0.64	-0.99	0.93						
II	0.92	0.08	0.84	0.68	-0.98	0.92	0.98					
III	-0.89	-0.04	-0.84	-0.64	0.98	-0.91	-0.99	-1.00				
IV	0.92	0.28	0.68	0.77	-0.94	0.84	0.96	0.96	-0.96			
V	-0.93	-0.17	-0.79	-0.74	0.98	-0.92	-0.99	-0.97	0.97	-0.97		
Specific THM formation	-0.27	0.15	-0.36	-0.09	0.23	-0.15	-0.24	-0.36	0.36	-0.23	0.16	
Specific HAN formation	-0.73	-0.48	-0.32	-0.72	0.72	-0.67	-0.71	-0.69	0.68	-0.82	0.78	-0.28

In other words, raw litter extracts have much less humic acid and fulvic acid-like compounds in comparison to black carbon extracts. Longleaf pine had the lowest increase both in region III and V after burn and also the lowest decrease in region I. It also had the lowest weight loss and DOC decrease, suggesting that longleaf shows significantly fewer changes both in carbon quality and quantity after burn in comparison to other studied species. It is in accordance with its classification as a “fire-resistant” species. Resistance against fire is mainly due to its moist and dense needles (54).

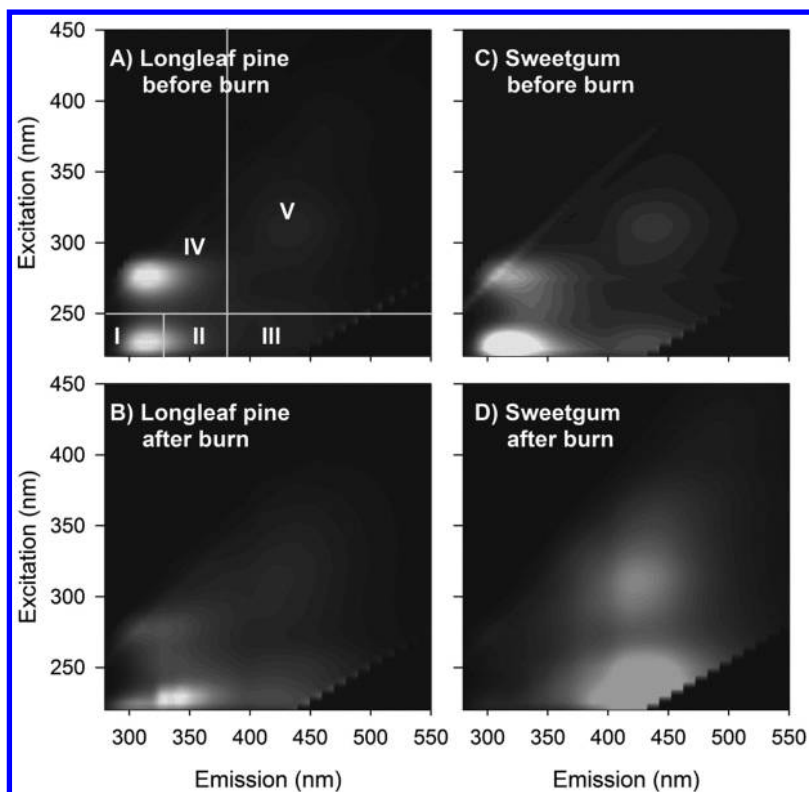


Figure 2. Fluorescence emission-excitation matrix of longleaf pine and sweetgum water extracts before and after burn.

Effect of Prescribed Burning on Formation of Disinfection By-Products

DOC has been implicated as a primary contributor to the formation of THMs (19), while dissolved organic nitrogen has been identified as a precursor to both THMs and N-DBPs (e.g., HANs) during drinking water purification (55). However, little is known about how BC (burned litters) contributes to DBP formation. As shown in our results, chloroform was the major DBP species after

chlorination for all plant species (Figure 3). For the original litters before burn, the specific chloroform formation followed the order: sweetgum (8.34 ± 1.11 mmol/mol-C) > baldcypress (4.67 ± 0.18 mmol/mol-C) = water tupelo (4.45 ± 0.21 mmol/mol-C) > longleaf pine (3.61 ± 0.17 mmol/mol-C) > boxelder (2.99 ± 0.06 mmol/mol-C) > pop ash (2.59 ± 0.03 mmol/mol-C). The dichlorobromomethane was the other detectable THM species, with similar specific formation (0.008-0.011 mmol/mol-C) among all original unburned litters. For the HAN, dichloroacetonitrile and trichloroacetonitrile were the only two detectable species. The specific dichloroacetonitrile formation followed: boxelder (0.214 ± 0.003 mmol/mol-C) > pop ash (0.137 ± 0.001 mmol/mol-C) > baldcypress (0.127 ± 0.008 mmol/mol-C) > longleaf pine (0.092 ± 0.011 mmol/mol-C) > sweetgum (0.083 ± 0.006 mmol/mol-C) > water tupelo (0.066 ± 0.004 mmol/mol-C). The specific trichloroacetonitrile formation was much lower than dichloroacetonitrile, which was highest for boxelder (0.007 ± 0.000 mmol/mol-C) and did not show difference among other plant species (0.003-0.005 mmol/mol-C).

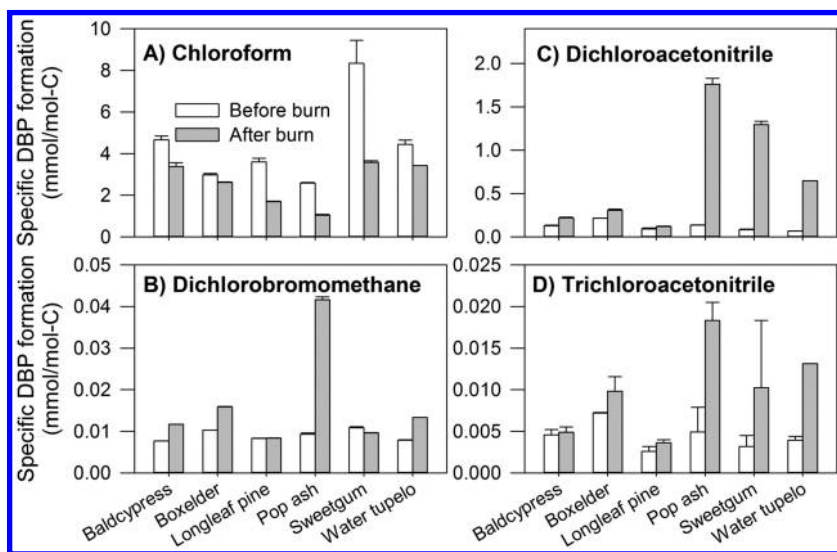


Figure 3. Chlorine reactivity of dissolved organic carbon extracted from litter materials as indicated by the specific DBP formation.

After burning, both the specific THM formation and specific HAN formation were significantly altered, which is in agreement with the results of field studies of prescribed fire (Part II) and wildfire. The specific chloroform formation decreased by 12%-60% for all plant species (56). However, the specific dichlorobromomethane formation increased for baldcypress (52%), boxelder (55%), pop ash (347%), and water tupelo (69%). Different from chloroform, the specific haloacetonitriles formation increased for all species. While the specific dichloroacetonitrile formation increased by 30%-1457%, the specific trichloroacetonitrile formation increased by 7%-73%. There was no correlation between the percent decrease of specific THM formation and the percent decrease

of specific HAN formation, suggesting that the fire's effects on the THM precursor and HAN precursor were independent. However, correlation between specific HAN formation and percent fluorescence response of region IV was significant for both before and after burn (Table 3). This may provide a fast easy method for prediction of specific HAN formation both before and after burn.

Multiplying the specific DBP formation with the WEOC, we can estimate the DBP precursor yield ($\mu\text{g}/\text{g}$ -original-litter) from the litter material (Figure 4). Before burn, the litter materials can potentially produce THMs ranging from 82.3 ± 1.0 μg -THMs/g-original-litter (pop ash) to 706.4 ± 93.7 μg -THMs/g-original-litter (sweetgum). After burn, the THM yield decreased by 70%-98% for all species (Figure 4a). For HANs, these litter materials had the HAN yield ranging from 3.72 ± 0.24 μg -HANs/g-original-litter (water tupelo) to 10.40 ± 0.14 μg -HANs/g-original-litter (boxelder). As the specific HAN formation has increased after burn, there was a much less decrease in HAN yield compared to THM yield after burn. The HAN yield dropped by 29%-69%, for all species (Figure 4b).

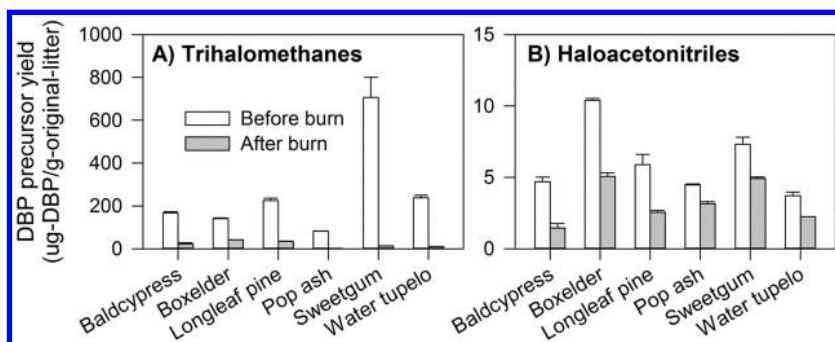


Figure 4. The disinfection by-product yields as in trihalomethane (A) and haloacetoneitriles (B) before and after burn at 340 °C. The yield calculations were based on the original unburned biomass.

The results demonstrated the effects of low intensity burning (i.e. 340 °C) on changes in quantity and quality of DBP precursors on the forest floor. Because fire can largely consume organic matter in detritus layer, WEOM (i.e. WEOC and WETN) decreased after burn. Such consumption of litter materials is likely an overriding effect to reduce the DBP precursors, which resulted in the overall reduction in DBP yield from litter materials (Figure 4). Chlorine reactivity of the burned litter in forming HANs is much higher than that of original litter. As the HANs have been documented to be much more toxic than the common carbonaceous DBPs such as THMs and haloacetic acids, attention should be placed on the nitrogenous DBPs in water treatment of fire-affected DOM.

The study revealed the effect of vegetation cover on the potential DBP export. We found that among the major plant species within the watershed, the sweetgum has a much larger content of DBP precursor because its litter has high WEOM that is also very reactive in forming DBPs (ranking 1st for THM

yield and the 2nd for HAN yield; Figure 4). In contrast, the pop ash is a species with much less contribution to the watershed export of DBP precursor, with only 12% THM formation and 61% HAN formation relative to the sweetgum. The response of DBP precursors in litter materials is highly dependent upon plant species as shown in Figure 4. Therefore, the knowledge acquired in one watershed about the fire effect on the DBP export may not be directly applicable to estimate the DBP export in another watershed that has quite different dominant plant species. The controlled lab study here is designed for elucidating the effects of simulated burning on the DBP precursor in litter materials without any interference from other environmental factors such as mixes of vegetations, fuel moistures, decomposition stages, etc. To evaluate a real situation on DBP precursor production from a burnt forest, our research team conducted a controlled burning experiment and natural exposure of WEOM in a natural forest at Hobcaw Bonary, Georgetown SC. Results and findings of the controlled field study, as the Part II of this prescribed fire study, are discussed in the following chapter.

Acknowledgments

Jun-Jian Wang received financial support from the China Scholarship Council (CSC[2011]3010). Portions of this study were also supported by NIFA/USDA under project number SC1700489 and 2014-67019-21615, Joint Fire Science Program 14-1-06-19, and NSF Rapid Grant 1264579 as presented in technical contribution number 6359 of the Clemson University Experiment Station.

Appendix

Table A1. The Categorization of Pyrogenic Products from Results of Pyrolysis Gas Chromatography Mass Spectrometry: Ar = aromatics; Lg = lignins; Lp = lipids; Ps = polysaccharides; N = nitrogens; PAHs = polycyclic aromatic hydrocarbons; Ph = phenolics.

#	Compound	Type	#	Compound	Type
1	Phenol, 2-methoxy-	Lg	77	Heptadecane	Lp
2	Phenol, 2-methoxy-4-methyl-	Lg	78	1-Eicosene	Lp
3	Phenol, 4-methoxy-3-methyl-	Lg	79	1-Nonene	Lp
4	1,2-Benzenediol, 3-methoxy-	Lg	80	Tridecane	Lp
5	Phenol, 4-ethyl-2-methoxy-	Lg	81	Heptadecane	Lp
6	4-Hydroxy-3-methoxystyrene	Lg	82	Toluene	Ar
7	Phenol, 3-methoxy-5-methyl-	Lg	83	Ethylbenzene	Ar
8	Phenol, 2,6-dimethoxy-	Lg	84	P-Xylene	Ar
9	Phenol, 2-methoxy-4-(1-propenyl)-	Lg	85	P-Xylene	Ar

Continued on next page.

Table A1. (Continued). The Categorization of Pyrogenic Products from Results of Pyrolysis Gas Chromatography Mass Spectrometry: Ar = aromatics; Lg = lignins; Lp = lipids; Ps = polysaccharides; N = nitrogens; PAHs = polycyclic aromatic hydrocarbons; Ph = phenolics.

#	Compound	Type	#	Compound	Type
10	3,4-Dimethoxyphenol	Lg	86	Benzene, Popyle-	Ar
11	Vanillin	Lg	87	4-Ethyltoluene	Ar
12	Eugenol	Lg	88	1,2,4-Trimethylbenzene	Ar
13	Phenol,2-methoxy-4-(1E)-1-propenyl-	Lg	89	2-Ethyltoluene	Ar
14	4-methoxy-3-hydroxyacetophenone	Lg	90	2-Methylstyrene	Ar
15	3-methoxy-2,4,6-trimethylphenol	Lg	91	Benzene,1-methyl-2-(1-methylethyl)-	Ar
16	2-Propanone,1-(4-hydroxy-3-methoxyphenyl)-	Lg	92	Benzene, 2-propynyl	Ar
17	Phenol,2,6-dimethoxy-4-(2-propenyl)-	Lg	93	Benzene,1-methyl-4-(1-methylethenyl)-	Ar
18	3,5-Dimethoxy-4-hydroxybenzaldehyde	Lg	94	Benzene, 1-butynyl-	Ar
19	Phenol,2,6-dimethoxy-4-(2-propenyl)-	Lg	95	Benzene,(1-methylene-2-propenyl)	Ar
20	4-Ethyl-2-methoxyphenol	Lg	96	Resorcinol	Ar
21	1,2,4-Trimethoxybenzene	Lg	97	1-ethyl-2,4,5-trimethylbenzene	Ar
22	Phenol, 3,5-dimethoxy-	Lg	98	Benzene, 1,3,5-trimethyl-2-(1,2-propadienyl)-	Ar
23	Vanillyl ethyl ether	Lg	99	Benzene, (1-ethynyl-2-methyl-1-propenyl)-	Ar
24	2,5-Dimethylfuran	Ps	100	Mesitylene	Ar
25	2(5H)-Furanone	Ps	101	Benzene	Ar
26	Furfural	Ps	102	Benzene, 1-propynyl-	Ar
27	Cyclopentene,1-(1-methylethyl)-	Ps	103	Cinnamaldehyde	Ar
28	2-Cyclopenten-1-one,2-methyl-	Ps	104	Mesitaldehyde	Ar
29	Furfuryl alcohol	Ps	105	1-Indanone	Ar
30	2-Furancarboxaldehyde,5-methyl-	Ps	106	Benzene, octyl-	Ar

Continued on next page.

Table A1. (Continued). The Categorization of Pyrogenic Products from Results of Pyrolysis Gas Chromatography Mass Spectrometry: Ar = aromatics; Lg = lignins; Lp = lipids; Ps = polysaccharides; N = nitrogens; PAHs = polycyclic aromatic hydrocarbons; Ph = phenolics.

#	Compound	Type	#	Compound	Type
31	2(5H)-Furanone,3-methyl-	Ps	107	Phenol	Ph
32	Furan, 2,4-dimethyl-	Ps	108	2,5-Dimethylphenol	Ph
33	2(3H)-Furanone,5-methyl-	Ps	109	Phenol,3,5-dimethyl-	Ph
34	2,5-Dimethyl furane	Ps	110	Phenol,2-ethyl-5-methyl-	Ph
35	Furan, 2-ethenyl-	Ps	111	Phenol,4-ethyl-3-methyl-	Ph
36	2H-Pyran-2-one, 4-ethenyltetrahydro-	Ps	112	Hydroquinone	Ph
37	2H-Pyran-2-one	Ps	113	1,2-Benzenediol,4- methyl-	Ph
38	2-Cyclopenten-1-one,2-methyl-	Ps	114	1,2-Benzenediol,4-ethyl-	Ph
39	2-Acetylfuran	Ps	115	Phenol,4-(2-propen-1- yl)-	Ph
40	2(3H)-Furanone	Ps	116	1,4-Benzene- diol,dimethyl-	Ph
41	2H-Pyran-2-one, 5,6-dihydro-3,5,5-trimethyl-	Ps	117	1,2-Benzenediol,4-ethyl-	Ph
42	Furfuryl alcohol	Ps	118	Pyrogallol	Ph
43	3-Methyl-2-cyclopenten-1-one	Ps	119	Methylparaben	Ph
44	2-Cyclopenten-1-one,2,3- dimethyl-	Ps	120	1,4-Benzenediol,2,3,5,6- tetramethyl-	Ph
45	2-Cyclopentenone	Ps	121	1,2-Benzenediol,4- methyl-	Ph
46	Pyridine	N	122	1,3-Benzenediol,4-ethyl-	Ph
47	Benzonitrile	N	123	Pyrogallol	Ph
48	Oxazole,2-ethyl-4,5-dihydro-	N	124	1,4-Benzenediol,2,3,5- trimethyl-	Ph
49	1H-Pyrrole, 1-methyl-	N	125	m-Tolualdehyde	Ph
50	N-Methyl pyrrole	N	126	3-Ethylphenol	Ph
51	Pyrrole	N	127	Phenol,2-methyl-	Ph
52	2-Oxocyclohexanepropiononi- trile	N	128	Phenol,4-methyl-	Ph
54	3-Pyrazolidinone, 1,4-dimethyl-	N	129	2,3-Dimethylphenol	Ph

Continued on next page.

Table A1. (Continued). The Categorization of Pyrogenic Products from Results of Pyrolysis Gas Chromatography Mass Spectrometry: Ar = aromatics; Lg = lignins; Lp = lipids; Ps = polysaccharides; N = nitrogens; PAHs = polycyclic aromatic hydrocarbons; Ph = phenolics.

#	Compound	Type	#	Compound	Type
55	Perillartine	N	130	2,3-Dimethylphenol	Ph
56	3-Methylpyrazole	N	131	3,5-Dimethylphenol	Ph
57	Benzyl cyanide	N	132	2,5-Dimethylphenol	Ph
58	3-Methylindole	N	133	3-Ethylphenol	Ph
59	Benzeethanamine,4-ethyl-2,5-dimethoxy-a-methyl-	N	134	Pyrocatechol	Ph
60	Pyridine, 3-methyl-	N	135	1,2-Benzenediol,3-methyl-	Ph
61	3-Methylpyrrole	N	136	4-Methylcatechol	Ph
62	Pyrazine, 2,3 dimethyl-5-(1-Propenyl)-	N	137	4-Ethylresorcinol	Ph
63	Benzeethanamine, 2,5-dimethoxy-	N	138	1,4-Benzenediol,2,3,5-trimethyl-	Ph
64	Pyrazine, tetraethyl-	N	139	Naphthalene	PAHs
65	6-Hydroxy-1,2,3,4-tetrahydroisoquinoline-1-carboxylic acid	N	140	2-Methylnaphthalene	PAHs
66	1H-Indole, 4-(3-methyl-2-butenyl)-	N	141	2-Methylnaphthalene	PAHs
67	Undecane	Lp	142	Naphthalene,1,2-dimethyl-	PAHs
68	Tetradecane	Lp	143	2,6-Dimethylnaphthalene	PAHs
69	Nonadecane	Lp	144	Naphthalene,1,6,7-trimethyl-	PAHs
70	1-Hexacosene	Lp	145	Naphthalene,1,6,7-trimethyl-	PAHs
71	Heptadecane	Lp	146	1-Methylnaphthalene	PAHs
72	1-Eicosene	Lp	147	Biphenyl	PAHs
73	1-Hexacosene	Lp	148	Naphthalene, 1-ethyl-	PAHs
74	3-Eicosyne	Lp	149	2-Naphthol	PAHs
75	1-Docosene	Lp	150	Dibenzofuran	PAHs
76	1-Nonadecene	Lp	151	Carbaryl	PAHs
			152	Fluorene	PAHs

References

1. *USDA Guidance for implementation of federal wildland fire management policy*; U.S. Department of Agriculture and US Department of the Interior: Washington, DC, 2009.
2. Williams, A. P.; Allen, C. D.; Millar, C. I.; Swetnam, T. W.; Michaelsen, J.; Still, C. J.; Leavitt, S. W. Forest responses to increasing aridity and warmth in the southwestern United States. *Proc. Natl. Acad. Sci. U.S.A.* **2010**, *107*, 21289–21294.
3. Vila-Escale, M.; Vegas-Vilarrubia, T.; Prat, N. Release of polycyclic aromatic compounds into a Mediterranean creek (Catalonia, NE Spain) after a forest fire. *Water Res.* **2007**, *41*, 2171–2179.
4. Certini, G. Effects of fire on properties of forest soils: A review. *Oecologia* **2005**, *143*, 1–10.
5. Battle, J.; Golladay, S. W. Prescribed fire's impact on water quality of depressional wetlands in southwestern Georgia. *Am. Midl. Nat.* **2003**, *150*, 15–25.
6. Richter, D. D.; Markewitz, D.; Trumbore, S. E.; Wells, C. G. Rapid accumulation and turnover of soil carbon in a re-establishing forest. *Nature* **1999**, *400*, 56–58.
7. Gonzalez-Perez, J. A.; Gonzalez-Vila, F. J.; Almendros, G.; Knicker, H. The effect of fire on soil organic matter - a review. *Environ Int.* **2004**, *30*, 855–870.
8. Knicker, H. How does fire affect the nature and stability of soil organic nitrogen and carbon? A review. *Biogeochemistry* **2007**, *85*, 91–118.
9. Harden, J. W.; Trumbore, S. E.; Stocks, B. J.; Hirsch, A.; Gower, S. T.; O'Neill, K. P.; Kasischke, E. S. The role of fire in the boreal carbon budget. *Global Change Biol.* **2000**, *6*, 174–184.
10. Hammes, K.; Schmidt, M. W. I.; Smernik, R. J.; Currie, L. A.; Ball, W. P.; Nguyen, T. H.; Louchouart, P.; Houel, S.; Gustafsson, O.; Elmquist, M.; Cornelissen, G.; Skjemstad, J. O.; Masiello, C. A.; Song, J.; Peng, P.; Mitra, S.; Dunn, J. C.; Hatcher, P. G.; Hockaday, W. C.; Smith, D. M.; Hartkopf-Froeder, C.; Boehmer, A.; Luer, B.; Huebert, B. J.; Amelung, W.; Brodowski, S.; Huang, L.; Zhang, W.; Gschwend, P. M.; Flores-Cervantes, D. X.; Largeau, C.; Rouzaud, J. N.; Rumpel, C.; Guggenberger, G.; Kaiser, K.; Rodionov, A.; Gonzalez-Vila, F. J.; Gonzalez-Perez, J. A.; de la Rosa, J. M.; Manning, D. A. C.; Lopez-Capel, E.; Ding, L. Comparison of quantification methods to measure fire-derived (black/elemental) carbon in soils and sediments using reference materials from soil, water, sediment and the atmosphere. *Global Biogeochem. Cycles* **2007**, *21*, 1–18.
11. Hockaday, W. C.; Grannas, A. M.; Kim, S.; Hatcher, P. G. The transformation and mobility of charcoal in a fire-impacted watershed. *Geochim. Cosmochim. Acta* **2007**, *71*, 3432–3445.
12. Hamer, U.; Marschner, B.; Brodowski, S.; Amelung, W. Interactive priming of black carbon and glucose mineralisation. *Org. Geochem.* **2004**, *35*, 823–830.

13. Wardle, D. A.; Nilsson, M. C.; Zackrisson, O. Fire-derived charcoal causes loss of forest humus. *Science* **2008**, *320*, 629–629.
14. Chow, A. T.; Lee, S. T.; O’Geen, A. T.; Orozco, T.; Beaudette, D.; Wong, P. K.; Hernes, P. J.; Tate, K. W.; Dahlgren, R. A. Litter contributions to dissolved organic matter and disinfection byproduct precursors in California oak woodland watersheds. *J. Environ. Qual.* **2009**, *38*, 2334–2343.
15. Richardson, S. D.; Plewa, M. J.; Wagner, E. D.; Schoeny, R.; DeMarini, D. M. Occurrence, genotoxicity, and carcinogenicity of regulated and emerging disinfection by-products in drinking water: A review and roadmap for research. *Mutat. Res. Rev. Mutat. Res.* **2007**, *636*, 178–242.
16. Wang, J. J.; Chow, A. T.; Sweeney, J. M.; Mazet, J. A. Trihalomethanes in marine mammal aquaria: Occurrences, sources, and health risks. *Water Res.* **2014**, *59*, 219–228.
17. Sedlak, D. L.; von Gunten, U. The chlorine dilemma. *Science* **2011**, *331*, 42–43.
18. Shah, A. D.; Mitch, W. A. Halonitroalkanes, halonitriles, haloamides, and *N*-nitrosamines: A critical review of nitrogenous disinfection byproduct formation pathways. *Environ. Sci. Technol.* **2012**, *46*, 119–131.
19. Karanfil, T.; Krasner, S. W.; Westerhoff, P.; Xie, Y. F. *Disinfection By-Products in Drinking Water: Occurrence, Formation, Health Effects, and Control*; Oxford University Press: New York, 2008; Vol. 995.
20. Chow, A. T.; O’Geen, A. T.; Dahlgren, R. A.; Diaz, F. J.; Wong, K. H.; Wong, P. K. Reactivity of litter leachates from California oak woodlands in the formation of disinfection by-products. *J. Environ. Qual.* **2011**, *40*, 1607–1616.
21. Wang, J. J.; Ng, T. W.; Zhang, Q.; Yang, X. B.; Dahlgren, R. A.; Chow, A. T.; Wong, P. K. Technical note: Reactivity of C1 and C2 organohalogen formation – from plant litter to bacteria. *Biogeosciences* **2012**, *9*, 3721–3727.
22. Beggs, K. M. H.; Summers, R. S. Character and Chlorine Reactivity of dissolved organic matter from a mountain pine beetle impacted watershed. *Environ. Sci. Technol.* **2011**, *45*, 5717–5724.
23. Pellerin, B. A.; Hernes, P. J.; Saraceno, J.; Spencer, R. G. M.; Bergamaschi, B. A. Microbial degradation of plant leachate alters lignin phenols and trihalomethane precursors. *J. Environ. Qual.* **2010**, *39*, 946–954.
24. Reckhow, D. A.; Rees, P. L. S.; Bryan, D. Watershed sources of disinfection byproduct precursors. *Water Supply* **2004**, *4*, 61–69.
25. Hernes, P. J.; Hedges, J. I. Tannin signatures of barks, needles, leaves, cones, and wood at the molecular level. *Geochim. Cosmochim. Acta* **2004**, *68*, 1293–1307.
26. Friebel, B. A. *Home range and habitat use of feral hogs (Sus scrofa) in Congaree National Park*. Clemson University, 2007.
27. Wohl, E.; Polvi, L. E.; Cadol, D. Wood distribution along streams draining old-growth floodplain forests in Congaree National Park, South Carolina, USA. *Geomorphology* **2011**, *126*, 108–120.

28. Battle, J.; Golladay, S. W. Prescribed fire's impact on water quality of depressional wetlands in southwestern Georgia. *Am. Midl. Nat.* **2003**, *150*, 15–25.
29. Song, J. Z.; Peng, P. A. Characterisation of black carbon materials by pyrolysis-gas chromatography-mass spectrometry. *J. Anal. Appl. Pyrol.* **2010**, *87*, 129–137.
30. Chow, A. T.; Dahlgren, R. A.; Zhang, Q.; Wong, P. K. Relationships between specific ultraviolet absorbance and trihalomethane precursors of different carbon sources. *J. Water Supply: Res. Technol. –AQUA* **2008**, *57*, 471–480.
31. Dalrymple, R. M.; Carfagno, A. K.; Sharpless, C. M. Correlations between dissolved organic matter optical properties and quantum yields of singlet oxygen and hydrogen peroxide. *Environ. Sci. Technol.* **2010**, *44*, 5824–5829.
32. Zhou, J.; Wang, J. J.; Baudon, A.; Chow, A. T. Improved fluorescence excitation-emission matrix regional integration to quantify spectra for fluorescent dissolved organic matter. *J. Environ. Qual.* **2013**, *42*, 925–930.
33. Chen, W.; Westerhoff, P.; Leenheer, J. A.; Booksh, K. Fluorescence excitation - emission matrix regional integration to quantify spectra for dissolved organic matter. *Environ. Sci. Technol.* **2003**, *37*, 5701–5710.
34. Summers, R. S.; Hooper, S. M.; Shukairy, H. M.; Solarik, G.; Owen, D. Assessing the DBP yield: Uniform formation conditions. *J. Am. Water Works Ass.* **1996**, *88*, 80–93.
35. Cho, D.-H.; Kong, S.-H.; Oh, S.-G. Analysis of trihalomethanes in drinking water using headspace-SPME technique with gas chromatography. *Water Res.* **2003**, *37*, 402–408.
36. Kang, B. T.; Sajjapongse, A. Effect of Heating on Properties of Some Soils from Southern Nigeria and Growth of Rice. *Plant Soil* **1980**, *55*, 85–95.
37. Giovannini, G.; Lucchesi, S. Modifications induced in soil physico-chemical parameters by experimental fires at different intensities. *Soil Sci.* **1997**, *162*, 479–486.
38. Sharma, R. K.; Wooten, J. B.; Baliga, V. L.; Lin, X. H.; Chan, W. G.; Hajaligol, M. R. Characterization of chars from pyrolysis of lignin. *Fuel* **2004**, *83*, 1469–1482.
39. Sharma, R. K.; Hajaligol, M. R. Effect of pyrolysis conditions on the formation of polycyclic aromatic hydrocarbons (PAHs) from polyphenolic compounds. *J. Anal. Appl. Pyrol.* **2003**, *66*, 123–144.
40. Oanh, N. T. K.; Ly, B. T.; Tipayarom, D.; Manandhar, B. R.; Prapat, P.; Simpson, C. D.; Liu, L. J. S. Characterization of particulate matter emission from open burning of rice straw. *Atmos. Environ.* **2011**, *45*, 493–502.
41. Kim, E. J.; Oh, J. E.; Chang, Y. S. Effects of forest fire on the level and distribution of PCDD/Fs and PAHs in soil. *Sci. Total Environ.* **2003**, *311*, 177–189.
42. Smith, H. G.; Sheridan, G. J.; Lane, P. N. J.; Nyman, P.; Haydon, S. Wildfire effects on water quality in forest catchments: A review with implications for water supply. *J. Hydrol.* **2011**, *396*, 170–192.

43. Robinson, M. S.; Anthony, T. R.; Littau, S. R.; Herckes, P.; Nelson, X.; Poplin, G. S.; Burgess, J. L. Occupational PAH exposures during prescribed pile burns. *Ann. Occup. Hyg.* **2008**, *52*, 497–508.
44. Naeher, L. P.; Brauer, M.; Lipsett, M.; Zelikoff, J. T.; Simpson, C. D.; Koenig, J. Q.; Smith, K. R. Woodsmoke health effects: A review. *Inhal. Toxicol.* **2007**, *19*, 67–106.
45. Schmidl, C.; Bauer, H.; Dattler, A.; Hitzenberger, R.; Weissenboeck, G.; Marr, I. L.; Puxbaum, H. Chemical characterisation of particle emissions from burning leaves. *Atmos. Environ.* **2008**, *42*, 9070–9079.
46. Oanh, N. T. K.; Ly, B. T.; Tipayarom, D.; Manandhar, B. R.; Prapat, P.; Simpson, C. D.; Liu, L. J. S. Characterization of particulate matter emission from open burning of rice straw. *Atmos. Environ.* **2011**, *45*, 493–502.
47. Vergnoux, A.; Di Rocco, R.; Domeizel, M.; Guiliano, M.; Doumenq, P.; Theraulaz, F. Effects of forest fires on water extractable organic matter and humic substances from Mediterranean soils: UV-vis and fluorescence spectroscopy approaches. *Geoderma* **2011**, *160*, 434–443.
48. Hongve, D. Production of dissolved organic carbon in forested catchments. *J. Hydrol.* **1999**, *224*, 91–99.
49. Almendros, G.; Gonzalezvila, F. J.; Martin, F. Fire-induced transformation of soil organic-matter from an oak forest - an experimental approach to the effects of fire on humic substances. *Soil Sci.* **1990**, *149*, 158–168.
50. Almendros, G.; Gonzalezvila, F. J.; Martin, F.; Frund, R.; Ludemann, H. D. Solid-state NMR-studies of fire-induced changes in the structure of humic substances. *Sci. Total. Environ.* **1992**, *118*, 63–74.
51. Baldock, J. A.; Smernik, R. J. Chemical composition and bioavailability of thermally, altered *Pinus resinosa* (Red Pine) wood. *Org. Geochem.* **2002**, *33*, 1093–1109.
52. Almendros, G.; Knicker, H.; Gonzalez-Vila, F. J. Rearrangement of carbon and nitrogen forms in peat after progressive thermal oxidation as determined by solid-state C-13 and N-15-NMR spectroscopy. *Org. Geochem.* **2003**, *34*, 1559–1568.
53. Vergnoux, A.; Dupuy, N.; Guiliano, M.; Vennetier, M.; Theraulaz, F.; Doumenq, P. Fire impact on forest soils evaluated using near-infrared spectroscopy and multivariate calibration. *Talanta* **2009**, *80*, 39–47.
54. Outcalt, K. W. The longleaf pine ecosystem of the South. *Native Plants J.* **2000**, *1*, 42–53.
55. Westerhoff, P.; Mash, H. Dissolved organic nitrogen in drinking water supplies: a review. *J. Water Supply: Res. Technol. – AQUA* **2002**, *51*, 415–448.
56. Wang, J. J.; Dahlgren, R. A.; Ersan, M. S.; Karanfil, T.; Chow, A. T. Wildfire alters terrestrial precursors of disinfection byproducts in drinking water. *Environ. Sci. Technol.* **2015** Submitted for publication.

Chapter 16

Prescribed Fire Alters Dissolved Organic Matter and Disinfection By-Product Precursor in Forested Watersheds – Part II. A Controlled Field Study

Kuo-Pei Tsai,¹ Mary-Frances Rogers,¹ Alex T. Chow,^{*,1}
and Francisco Diaz²

¹Baruch Institute of Coastal Ecology and Forest Science,
Clemson University, Georgetown, South Carolina 29442, United States

²Department of Soil Science and Geology, University of La Laguna,
Canary Islands, Spain

*E-mail: achow@clemson.edu.

Forest detritus material is one of the major terrestrial sources of dissolved organic matter (DOM) in source waters. There is a health concern on DOM because it reacts with disinfectants to form a variety of potentially carcinogenic disinfection by-products (DBPs) during drinking water treatments. Prescribed fire is a common forest management practice in Southeastern US to reduce the risks of wildfire and beetle infestation. However, this forest management practice alters the composition and quantity of detritus materials on forest floor, changing the DOM and DBP precursors exports from those forested watersheds. In this book chapter, we discussed a prescribed fire study conducted in three 20m x 20m experimental plots in Hobcaw Barony, Georgetown, South Carolina. Litter and duff mixtures of field samples before and after prescribed fire were collected for water extraction experiments in the laboratory. In addition, water extracts were further exposed to sunlight for 15 days in order to understand the biogeochemical processes on the degradability of DOM and DBP precursors. The concentrations of water extractable organic carbon (WEOC) and water extractable total nitrogen (WETN) from unburned detritus (60.3 g-WEOC/m²

and 1.9 g-WETN/m²) were significantly greater than those from burned detritus (11.4 g-WEOC/m² and 0.5 g-WETN/m²). Importantly, the yield of DBP was significantly reduced from 3651 mg-THM/m² to 484 mg-THM/m² after fire. There was no change in specific DBP formation in both burn and unburned samples after sunlight exposure although significant decreases in ultraviolet absorbance and fluorescence intensity were observed. This field study showed that prescribed fire could significantly decrease the production of dissolved organic carbon (DOC) and dissolved total nitrogen (DTN) per unit area in forest floor and potentially decrease the DBP formation in water supply.

Introduction

It is well known that natural organic matter (NOM) is the major precursor of disinfection by-products (DBPs) during the chlorination process in water treatment systems (1, 2). It is estimated that NOM constitutes 50-90% of dissolved organic carbon (DOC) in freshwater systems (3). Reducing the import of DOC into natural waters used as drinking water sources can potentially minimize the formation of DBP during the chlorination process. Water in forested watersheds is a critical source of drinking water. Approximately 180 million people in over 68,000 communities in the United States rely on forested lands to capture and filter their drinking water (4). Large scale of natural disturbance in forest could substantially influence water characteristics and consequently impact the treatability downstream.

Several studies have reported negative effects of wildfire on the water quality of forested watersheds (5-7). Prescribed fire treatment is usually implemented as a low-cost-effective tool to reduce hazardous fuels in the forest and risks of unwanted wildfires as well as recycling nutrients back to the soil. Richter and colleagues in their watershed scale study (8) indicated that periodic prescribed fire within the Francis Marion National Forest in South Carolina is not likely to have appreciable effects on the quality of stream rivers. Also, Arkle and Pilliod (9) found that prescribed fire had no effects on stream habitats in Payette National Forest, Idaho. Caldwell and colleagues (10) reported that carbon-nitrogen ratios did not differ between streams affected by prescribed fire treatment and reference streams within a grassland system on the Valles Caldera National Preserve, New Mexico. It is noted that nutrients were measured quantitatively in those researches to assess the effects of prescribed fire on the aquatic systems; however, little is known regarding the effects of prescribed fire on the quantity and quality of DOM exported from forest fuels.

Dead and down woody materials, litter, grasses, herbaceous plant materials, and short shrubs are not only forest fuels but are also parts of terrestrial sources of DOM in forested watersheds. According to Chow and colleagues (11), the DOC extracted from California oak woodland litter is an important precursor in

forming DBPs and the reactivity of litter and leaf leachate is dependent on types and decomposition stages of vegetation. When prescribed fire occurs, those forest litter materials could be chemically oxidized and transformed and consequently alter the quantity and quality of DOM exported from the forested watersheds.

In order to study effects of prescribed fire on water quality of forested watersheds, it is important to understand the characteristics of DOC leaching from burned litter and duff materials. Moreover, DOM in natural water may undergo various chemical, physical, and biological reactions during water conveyance in streams before entering water treatment facilities. Photochemical reactions of DOM such as solar irradiation may cause oxidative degradation of DOM and result in smaller and more labile organic carbon moieties (12, 13). In fact, exposure of DOM to natural sunlight could alter the characteristics of carbon exported from foliar litters and consequently affect DBP formation in water disinfection processes (14, 15). The objectives of this field study were to understand the influence of prescribed fire on DOM and DBP precursor productions using detritus mixture burned in the field instead of using single vegetation species burned in a temperature controlled oven, as in Part I of the study. In addition, the leachates extracted from burned and unburned detritus were further incubated under dark and light conditions for 15 days in order to determine the influences of biogeochemical processes on the characteristics of DOM and DBP precursors.

Materials and Methods

Prescribed Burn in a Managed Forest

The controlled field study was conducted at Hobcaw Barony, a 71-km² wildlife refuges near Georgetown, South Carolina. The field site represents a typical coastal plain forest with loblolly pine (*Pinus taeda* L.) and longleaf pine (*Pinus palustris* P.). Within a mixed hardwood-pine stand that was scheduled to undergo a growing season prescribed fire, three adjacent 20×20m experimental plots (latitude 33°21'14 dpm, longitude 79°12'19") were established for the study. A field investigation on vegetation and fuel was conducted a month prior to the prescribed burn. Down woody materials were evaluated using Brown's Planar Intersect Method (16, 17) to obtain average litter and duff depths for each plot. Nine measurements were conducted in each plot. In addition, prior to the execution of the growing season prescribed fire, a representative sample containing detritus material from each 20m x 20m plot was collected in 17"x9" quadrants with care as to avoid as much mineral soil collection as possible. Samples were placed into labeled brown paper bags that were oven-dried and stored for later analysis. On May 29, 2014, a prescribed fire classified as a periodic growing season burn was conducted using a drip torch and a backing fire technique. Characteristics of the prescribed fire were visually observed and recorded according to the National Park Service Fire Monitoring Handbook (18). The fire was naturally extinguished after approximately 3 hours.

Characterization of DOM and DBP Precursors

An hour prior to ignition and immediately after fire extinction, destructive surface detritus materials samples including the mixture of litter and decomposed duff without mineral soil were randomly collected from each plot (one composite sample from 3 subsamples per plot). Sealed plastic bags were used to transport the samples to the lab where they were weighted and placed into a drying oven at 50°C. After 72h samples were re-weighted and moisture content calculated.

Dried unburned and burned forest detritus were grounded and sieved through a 2 mm screen and fraction < 2 mm was used for analysis. To simulate rainwater flush on forest detritus and to collect the leachate extracted, 20 g of sieved material was mixed with 200 ml Milli-Q water in a 250 ml Erlenmeyer flask and placed on an orbital shaker operated at 250 rpm for 2h. Milli-Q water was used because it generally extracts a greater amount of DOC comparing with other water solutions containing salt (18), and also minimize any contamination of carbon source. Extracts were filtered using 0.45 μm polyethersulfone membrane filters (Supor-450, Pall Gelman Science) previously flushed three times with Milli-Q water. Ultraviolet absorbance at 254 nm (UVA_{254}), fluorescence, water extractable organic carbon (WEOC) and water extractable total nitrogen (WETN) were measured in the filtered extracts. The ultraviolet absorbance scanning from 200 to 700 nm was measured using a Shimadzu UV-1800 in room temperature. WEOC and WETN were measured using a Shimadzu TOC-VCSH/CSN analyzer. Specific ultraviolet absorbance at 254 nm (SUVA_{254}) was defined as carbon normalized UVA_{254} ($\text{SUVA}_{254} = \text{UVA}_{254}/\text{WEOC}$). Fluorescence scans were conducted using a Shimadzu spectrofluorescence RF5301 with a 5-nm slit in excitation and a 5-nm slit in emission. In excitation-emission matrix (EEM) fluorescence spectroscopy, the matrixes were delineated and operationally defined into five regions using consistent excitation (ex) and emission (em) wavelength boundaries based on fluorescence of freshwaters (19): Region I, aromatic protein I (ex: 200-250 nm; em: 280-330 nm); Region II, aromatic protein II (ex: 200-250 nm; em: 330-380 nm); Region III, fulvic acid-like (ex: 200-250 nm; em: 380-550 nm); Region IV, soluble microbial by-product-like (250 nm < ex < 400 nm; em: 280-380 nm); and Region V, humic acid-like (250 nm < ex < 400 nm; em: 380-550 nm).

The analysis of DBPs formation was based on uniform formation condition (UFC) with sodium hypochlorite solution (Sigma-Aldrich) as a chlorination reagent as described in Part I. UFC was selected because its reaction condition is more closely related to conventional water treatment practice and the DBP formation in the UFC test is similar to those in finished water. DBPs including four trihalomethanes (THMs) (trichloromethane, dichlorobromomethane, dibromochloromethane, tribromomethane), four haloacetonitriles (HANs) (trichloro-acetonitrile, dichloro-acetonitrile, bromochloro-acetonitrile, dibromo-acetonitrile), and chloral hydrate (CHD) were measured according to USEPA method 551.1 using a gas chromatograph with a ^{63}Ni electron capture detector (Agilent 7890). The specific DBPs formation (i.e. specific THM formation, specific HAN formation, and specific CHD formation) were calculated by normalizing THM, HAN, and CHD concentrations with WEOC concentration

of water extracts. The measurement of specific DBP formation represents the reactivity of carbon in forming DBP during chlorination.

Potential changes in organic matter chemical composition due to fire effects were assessed using a pyrolyzer (CDS5500) connected to a GC–MS system Agilent 7890 equipped with a fused silica capillary column HP5MS (30 m×250 μm×0.25 μm inner diameter). Approximately 2 mg of unburned and burned samples were placed in tiny platinum capsules and pyrolysis was set to 700°C. Pyrolysis products were identified according to GC retention times, mass spectra with reference to the Wiley/NIST libraries and published mass spectra of pyrolysis products (20). Major identified compounds were classified as: aromatic (Ar), lignin (Lg), lipid (Lp), polycyclid aromatic hydrocarbon (PAH), phenolic (Ph), polysaccharide (Ps), and nitrogen compounds (N). Individual identified organic compounds are included in the list shown in Part I of this Chapter.

Dark and Light Incubations

To simulate effects of biogeochemical processes on DOM and DBP precursors during water conveyance from watershed to treatment facilities, 120 ml of diluted water extracts from burned and unburned samples were placed into 200 ml custom-made quartz tubes and exposed to sunlight. For each sample were used 2 quartz tubes, wrapping one with aluminum foil for a dark incubation and using the other one for sunlight incubation. All quartz tubes were placed in a wide-open area in the Baruch Institute (about 1 km from the burned experimental plots), for 15 days (October 7th to October 22^{ed}, 2014). According to the National Estuarine Research Reserve System sampling station from North Inlet Winyah Bay, SC (21), daily maximum photosynthetically active radiation (PAR) values ranged from 1200 to 1600 mmol/m²/15 min (except for 400 mmol/m²/15 min on October 12th) and temperature ranged from 12 to 30 °C during the entire experiment. After 15 days incubation, samples were characterized for DOC, DTN, UVA, fluorescence EEM, and DBP formation as described above.

Statistical Analysis

A paired t-test was used to determine differences in characteristics between water extracts from unburned and burned samples. The level of significance was set to $P < 0.05$. All data were analyzed using SPSS.

Results and Discussion

Controlled Field Burns

A field investigation on vegetation and fuel was conducted a month prior to the prescribed burn. The depth of litter and duff layers prior to fire in the experimental plots was 3.6 ± 2.3 cm and 1.1 ± 0.2 cm, respectively. Fuel moisture content was $11.6 \pm 5.7\%$ and top soil moisture content was $20.4 \pm 13.1\%$. At the start of the prescribed fire, cloud cover was 30% and the wind speed was 8 km/h out of the north as reported on the National Weather Service's website (22).

Precipitation was zero and the air temperature was 30°C with 63.5% of relative humidity as obtained from the HOBO U30-Wi-Fi station at the Baruch Institute (latitude 33°21'39", longitude 79°13'31"). Approximately, the average flame height ranged from 30 to 60 cm, and flame length and depth ranged from 15 to 30 cm. The area after the prescribed burn had a mosaic burn pattern and was categorized at light burn severity (23) with the percent burned area of the three plots visually determined as $35 \pm 5\%$. Mass of detritus before burn was $3.5 \pm 0.7 \text{ kg/m}^2$, being reduced to $1.1 \pm 0.4 \text{ kg/m}^2$ after fire. Images of detritus material prior to, during, and following the prescribed fire are shown in Figure 1.

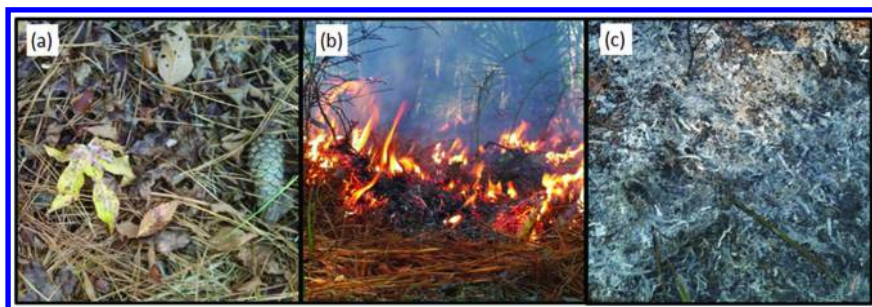


Figure 1. Images prior to (a), during (b), and following (c) the prescribed fire in Hobcaw Barony, SC.

Chemical Composition of Detritus Materials

Py-GCMS spectra from unburned and burned detritus materials are shown in Figure 2. A total of 53 and 46 peaks were identified in the unburned and burned sample respectively. Relative intensity of peaks usually decreased in burned detritus compared to original unburned detritus pointing to the loss of a high percentage of organic matter during burning. In addition, some of peaks such as trimethoxybenzene (38.8 min) and dimethoxyacetophenone (43.6 min) were missing in the burned samples (Figure 2). Meanwhile, an increase of peak intensity for compounds such as naphthalene (27.0 min) and biphenyl (36.0 min) were observed in burned samples, although those peaks were very small (Figure 2). Overall, Lg and Lp were decreased from 55 to 41% and 2 to < 1% respectively, whereas Ar, Ph, and PAH increased from 12 to 18%, 24 to 30%, and from 0.6 to 3%, respectively after fire. No obvious changes in N compounds and Ps were observed, staying at about 3 and 4% respectively. Importantly, the changes in relatively abundance of these fractions matched well with the controlled laboratory burns (Part I), suggesting mixed and individual species may not affect the results.

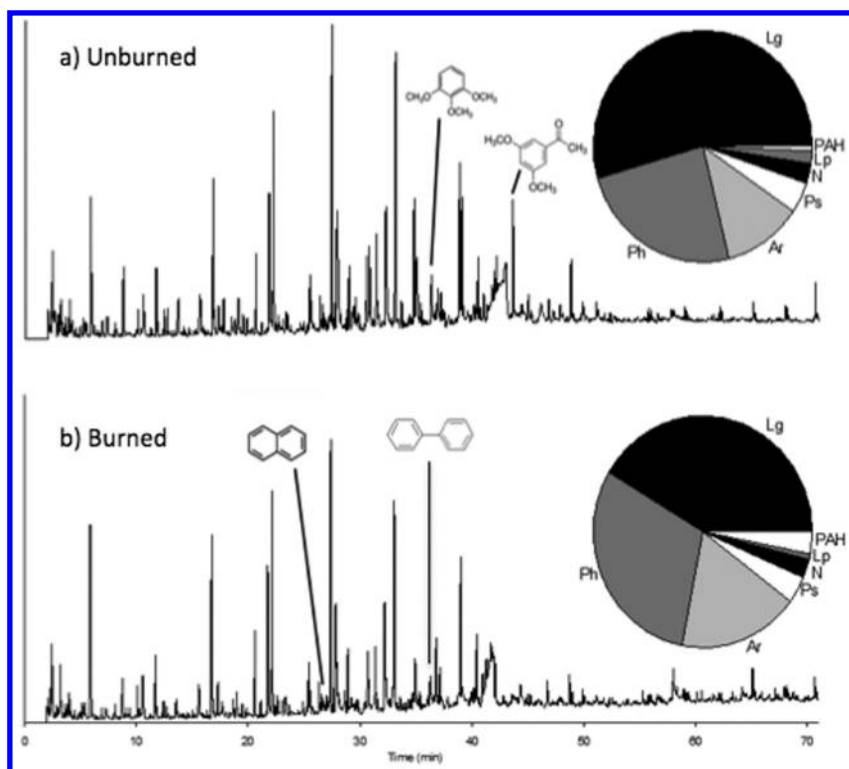


Figure 2. Py-GCMS Total Ion Chromatograms and relative abundance (pie charts; percentage) of different types of pyrogenic products from unburned and burned forest detritus material; aromatics (Ar); lignins (Lg); lipids (Lp); polysaccharides (Ps); nitrogens (N); polycyclic aromatic hydrocarbons (PAH); phenolics (Ph).

Yields of DOM and DBP Precursors

Results showed a significant reduction ($p = 0.01$) in WEOC after fire, decreasing from 1,703 to 925 mg/L. On a dried mass basis, WEOC was decreased from 17 to 9.3 mg-WEOC/g-detritus. In contrast, there was no significant changes in WETN, C:N ratio, and SUVA between unburned and burned extracts (Table 1).

Table 1. WEOC, WETN and DBPs Formation of Forest Detritus Samples before and after Burn; Average \pm Standard Deviation; n = 3

	<i>Before burn</i>	<i>After burn</i>	<i>P value</i>
Water Extractable Organic Matter (1:10 litter to water extraction)			
WEOC (mg/L)	1,703 \pm 271	925 \pm 373	0.01
WETN (mg/L)	55 \pm 15	43 \pm 17	0.29
C:N (mol: mol)	38 \pm 17	25 \pm 0	0.15
SUVA	2.03 \pm 0.16	1.98 \pm 0.47	0.44
Disinfection By-Product Formation			
THM (mmol/mol)	6.05 \pm 1.15	4.11 \pm 1.57	0.16
HAN (mmol/mol)	0.14 \pm 0.05	0.22 \pm 0.07	0.11
CHD (mmol/mol)	0.30 \pm 0.05	0.29 \pm 0.03	0.42

Fluorescence EEM of extracts of unburned and burned detritus materials with the same dilution factor are shown in Figure 3. The fluorescence intensities of the burned extracts were generally lower than that of unburned extracts, especially in fulvic acid-like (region III) and aromatic protein-like regions (regions I and II). However, the relative abundance of the five regions were no different when integrating with the fluorescence regional integration (FRI) method (data shown in Figure 5). Although changes in fluorescence regions were observed in Part I, the area after the prescribed burn had a mosaic burn pattern with the percent burned area of the three plots visually determined as $35 \pm 5\%$. In fact, significant portions of detritus materials, especially the lower layer of the detritus materials, were partially burned in this low intensity fire. DOM from this material may have influences on the overall characteristics of DOM in extracts.

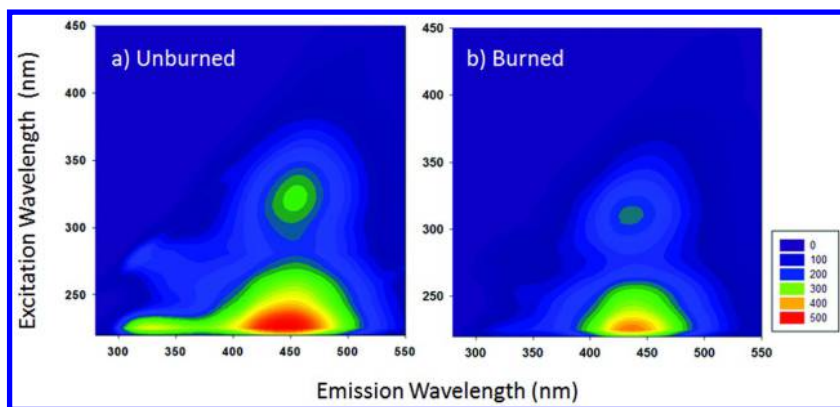


Figure 3. Fluorescence EEM of water extracts from (a) unburned and (b) burned detritus materials.

In terms of DBP formation, a lower reactivity in forming THM but a higher reactivity in forming HANs were observed after fire although those differences were statistically no significant. The reactivity of CHD was similar before and after burn. Therefore all the analyses showed that low intensity prescribed fire only reduced the quantity of WEOC but the chemistry, in terms of C:N ratio, optical properties including both UV/VIS and fluorescence measurements, and DBP formation, was no changed.

Biogeochemical Processes on DOM and DBP Precursors

Incubation experiment showed that quantity and quality of DOM in detritus leachate could be altered through biogeochemical process during water conveyance. Regardless of the fire effects, WEOC and WETN after both dark and sunlight incubations were lower than in the original samples (Figure 4), suggesting DOM in these extracts was highly degradable. These results were concomitant with the results showing that WEOC and WETN in burned detritus leachate were lower than in unburned detritus leachate (Figures 4a and 4b). Consider burned samples as an example, there were 76 and 59% decreases in WEOC and WETN respectively, in dark incubation, suggesting microbial processes possibly consumed these degradable organic matters. For the sunlight treatment, decreases of WEOC and WETN were even higher (78 and 72% respectively).

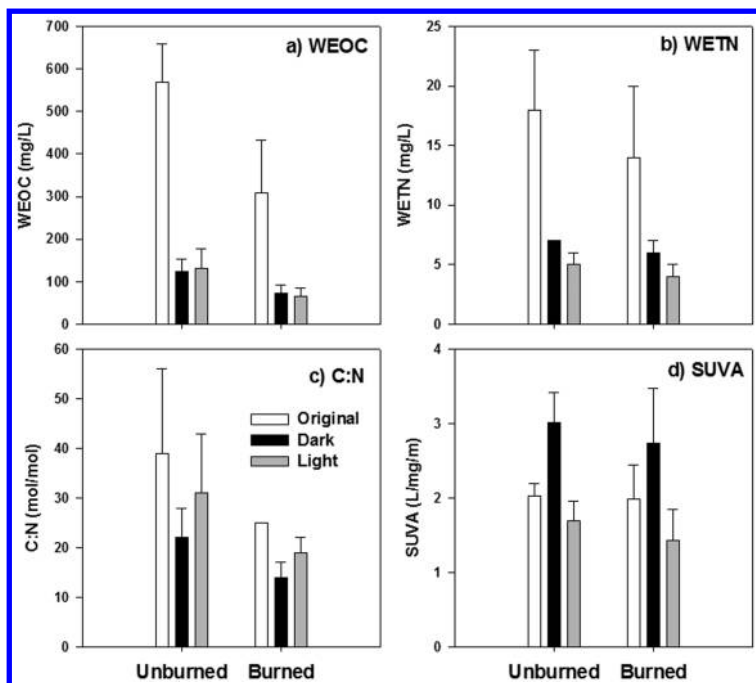


Figure 4. WEOC (a), WETN (b), C:N ratio (c), and SUVA (d) of the leachate extracted from unburned and burned detritus under 15-days dark and sunlight incubation; average \pm standard deviation; $n = 3$.

The C:N ratios of unburned and burned extracts after 15-days dark incubation were significantly lower than the values of original samples and sunlight incubation (Figure 4c), with an average of 22 and 14, respectively. On the other hands, the SUVA of dark incubation were highest among other treatments (Figure 4d). The SUVA values of unburn and burned extracts increased to 3.01 and 2.73 L/mg/m, respectively. Results might suggest microbial processes dominated in dark incubation and consumed degradable organic carbon, causing an increase in the proportion of relatively recalcitrant aromatic carbon in water. Lower C:N ratios and SUVA were observed after sunlight incubation when comparing to original samples (Figures 4c and 4d). In addition, an obvious decrease of humic acid-like fraction (Region V) in both unburned and burned extracts was observed after 15-day sunlight exposure (Figure 5). It has been demonstrated that sunlight could cause photobleaching of DOM is an important role in DOM characteristics in nature waters (24, 25).

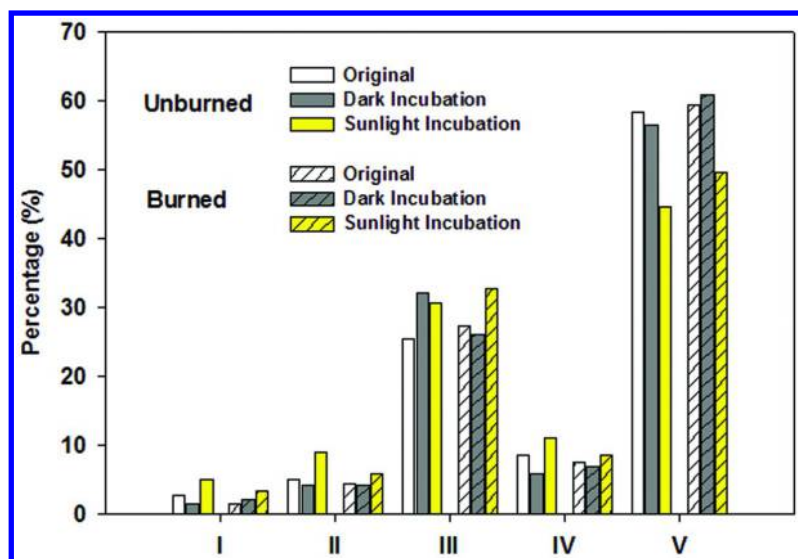


Figure 5. Percentage distributions of the five EEM regions of water extracts before and after prescribed fire and sunlight treatments. The five regions are: I (aromatic protein-like), II (aromatic protein-like II), III (Fulvic acid-like), IV (Microbial by-product-like), and V (Humic Acid-like).

Regardless of unburned and burned detritus leachate, results showed no significant changes on the THM formation after 15-day incubation (Figure 6a). $SUVA_{254}$ has been used as a measurement of DOC propensity to form THM and is generally proportional to specific THM formation (26, 27). However, this

study found that although sunlight exposure significantly decreased $SUVA_{254}$ values, the reactivity of DOC in forming THM was not significantly changed. Results also showed no significant changes on HAN formation after incubation, which suggested that the reactivity of DOC to form HAN was not sensitive to biogeochemical processes in such short time frame (Figure 6b). In contrast, an increase of CHD formation occurred after sunlight exposure as shown in Figure 6c, which is consistent with the previous studies (15).

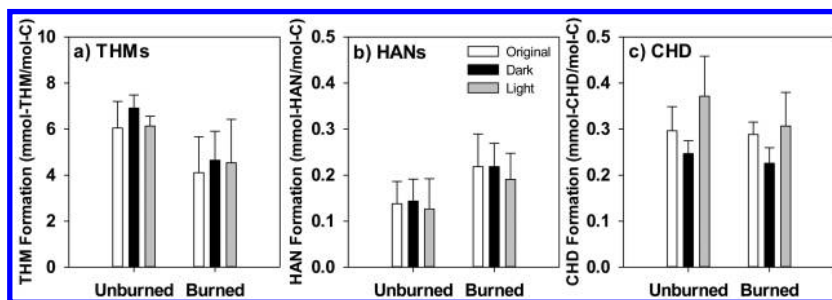


Figure 6. Specific formation potential of THMs (a), HANs (b), and CHD (c) of the leachate extracted from unburned and burned detritus under 15-days dark and sunlight incubation; average \pm standard deviation; $n = 3$.

Implications

Quantities of forest detritus, WEOC, WETN, and DBPs expressed per unit area in unburned and burned forest floor were summarized in Table 2. Prescribed fire consumed and oxidized detritus materials, reducing significantly ($p = 0.009$) the biomass per unit area ($\sim 65\%$ reduction). In addition, WEOC and WETN productions per unit biomass also reduced. Unburned detritus yielded 17 ± 2 g-WEOC/kg-detritus and 0.6 ± 0.2 g-WETN/kg-detritus, whereas burned detritus produced 9 ± 4 g-WEOC/kg-detritus and 0.4 ± 0.1 g-WETN/kg-detritus. Therefore there was a 81 and 74% reductions on WEOC and WETN per unit area, also resulting in a significant decrease in DBP yield per unit area. As summarized in Table 1, THM, HAN, and CHD yields were decreased in 87, 71, and 81%, respectively.

Table 2. Yields of Detritus, WEOC, WETN, and DBPs before and after Prescribed Burn in the Experimental Plots

	<i>Before burn</i>	<i>After burn</i>	<i>Reduction (%)</i>	<i>P value</i>
Detritus (kg/m ²)	3.5 ± 0.7	1.1 ± 0.4	65	0.009
WEOC (g/m ²)	60.3 ± 20.8	11.4 ± 8.5	81	0.01
WETN (g/m ²)	1.9 ± 0.6	0.5 ± 0.4	74	0.06
THM (mg/m ²)	3651 ± 682	484 ± 385	87	0.001
HAN (mg/m ²)	79 ± 6	23 ± 12	71	0.01
CHD (mg/m ²)	238 ± 56	46 ± 36	81	0.01

Both the controlled laboratory in Part I and controlled field studies in Part II (this chapter) demonstrated that prescribed forest fire could reduce DOM and DBP precursors in the detritus layers of forested watersheds in the southeastern US. Although our controlled laboratory study suggested DOM from burned materials could have a higher reactivity in forming N-DBPs during chlorination, significant loss in biomass and a reduction of extractability still result an overall reduction of DBP yield per unit area in a forested watershed. The results suggest that prescribed fire could be an effective watershed management controlling DBP precursors in source water.

Acknowledgments

Portions of this study were also supported by NIFA/USDA under project number SC1700489 and SCN-2013-02784, Joint Fire Science Program 14-1-06-19, and NSF Rapid grant 1264579 as presented in technical contribution number 6358 of the Clemson University Experiment Station.

References

1. Beggs, K. M. H.; Summers, R. S. Character and Chlorine Reactivity of Dissolved Organic Matter from a Mountain Pine Beetle Impacted Watershed. *Environ. Sci. Technol.* **2011**, *45*, 5717–5724.
2. Gopal, K.; Tripathy, S. S.; Bersillon, J. L.; Dubey, S. P. Chlorination byproducts, their toxicodynamics and removal from drinking water. *J. Hazard. Mater.* **2007**, *140*, 1–6.
3. Uyguner-Demirel, C. S.; Bekbolet, M. Significance of analytical parameters for the understanding of natural organic matter in relation to photocatalytic oxidation. *Chemosphere* **2011**, *84*, 1009–1031.
4. United States Department of Agriculture. *Some Facts About Water*; <http://www.fs.fed.us/managing-land/national-forests-grasslands/water-facts> (accessed Dec 14, 2014).

5. Brass, J. A.; Ambrosia, V. G.; Riggan, P. J.; Sebesta, P. D. Consequences of fire on aquatic nitrate and phosphate dynamics in Yellowstone National Park. In *Ecological Implications of Fire in Greater Yellowstone*; Greenlee, J. M., Ed.; International Association of Wildland Fire: Fairfield, WA, 1996; pp 53–57.
6. Riggan, P. J.; Lockwood, R. N.; Jacks, P. M.; Colver, C. G.; Weirich, F.; DeBano, L. F.; Brass, J. A. Effects of fire severity on nitrate mobilization in watersheds subject to chronic atmospheric deposition. *Environ. Sci. Technol.* **1994**, *28*, 369–375.
7. Emelko, M. B.; Silins, U.; Bladon, K. D.; Stone, M. Implications of land disturbance on drinking water treatability in a changing climate: Demonstrating the need for “source water supply and protection” strategies. *Water Res.* **2011**, *45*, 461–472.
8. Richter, D. D.; Ralston, C. W.; Harms, W. R. Prescribed fire: effects on water and forest nutrient cycling. *Science* **1982**, *215*, 661–663.
9. Arkle, R. S.; Pilliod, D. S. Prescribed fires as ecological surrogates for wildfires: A stream and riparian perspective. *For. Ecol. Manage.* **2010**, 893–903.
10. Caldwell, C. A.; Jacobi, G. Z.; Anderson, M. C.; Parmenter, R. R.; McGann, J.; Gould, W. R.; DuBey, R.; Jacobi, M. D. Prescribed-fire effects on an aquatic community of a southwest montane grassland system. *N. Am. J. Fish Manage.* **2013**, *33*, 1049–1062.
11. Chow, A. T.; Lee, S. T.; O’Geen, A. T.; Orozco, T.; Beaudette, D.; Wong, P. K.; Hernes, P. J.; Tate, K. W.; Dahlgren, R. A. Litter contributions to dissolved organic matter and disinfection byproduct precursors in California oak woodland watersheds. *J. Environ. Qual.* **2009**, *38*, 2334–2343.
12. Sharpless, C. M.; Blough, N. V. The importance of charge-transfer interactions in determining chromophoric dissolved organic matter (CDOM) optical and photochemical properties. *Environ. Sci.: Processes Impacts* **2014**, *16*, 654–671.
13. Méndez-Díaz, J. D.; Shimabuku, K. K.; Ma, J.; Enumah, Z. O.; Pignatello, J. J.; Mitch, W. A.; Dodd, M. C. Sunlight-Driven Photochemical Halogenation of Dissolved Organic Matter in Seawater: A Natural Abiotic Source of Organobromine and Organoiodine. *Environ. Sci. Technol.* **2014**, *48*, 7418–7427.
14. Chow, A. T.; Dahlgren, R. A.; Xhang, Q.; Wong, P. K. Relationships between specific ultraviolet absorbance and trihalomethane precursors of different carbon sources. *J. Water Supply: Res. Technol.-AQUA* **2008**, *57*, 471–480.
15. Chow, A. T.; Diaz, F. J.; Wong, K. H.; O’Geen, A. T.; Dahlgren, R. A.; Wong, P. K. Photochemical and bacterial transformations of disinfection byproduct precursors in water. *J. Environ. Qual.* **2013**, *42*, 1589–1595.
16. Brown, J. K. *Handbook for inventorying downed woody material*; Gen. Tech. Rep. INT-16; U.S. Department of Agriculture, Forest Service, Intermountain Forest and Range Experiment Station: Ogden, UT, 1974; pp 1–24.
17. USDI National Park Service. *Fire Monitoring Handbook*; Fire Management Program Center, National Interagency Fire Center: Boise, ID. 2003, 274.

18. Chow, A. T.; Tanji, K. K.; Gao, S. Production of dissolved organic carbon (DOC) and trihalomethane (THM) precursor from peat soils. *Water Res.* **2003**, *37*, 4475–4485.
19. Zhou, J.; Wang, J. J.; Baudon, A.; Chow, A. T. Improved fluorescence excitation-emission matrix regional integration to quantify spectra for fluorescent dissolved organic matter. *J. Environ. Qual.* **2013**, *49*, 925–930.
20. Song, J. Z.; Peng, P. A. Characterisation of black carbon materials by pyrolysis-gas chromatography-mass spectrometry. *J. Anal. Appl. Pyrolysis* **2010**, *87*, 129–137.
21. *National Estuarine Research Reserve System Home Page*; <http://cdmo.baruch.sc.edu/get/export.cfm> (accessed Dec 14, 2014).
22. *National Weather Service Home Page*; <http://www.weather.gov> (accessed Dec 14, 2014).
23. Keeley, J. E. Fire intensity, fire severity and burn severity: a brief review and suggested usage. *Int. J. Wildland Fire* **2009**, *18*, 116–126.
24. Brinkmann, T.; Sartorius, D.; Frimmel, F. H. Photobleaching of humic rich dissolved organic matter. *Aquat. Sci.* **2003**, *65*, 415–424.
25. Larson, J. H.; Frost, P. C.; Lodge, D. M.; Lamberti, G. A. Photodegradation of dissolved organic matter in forested streams of the northern Great Lakes region. *J. N. Am. Benthol. Soc.* **2007**, *26*, 416–425.
26. Chow, A. T.; Gao, S.; Dahlgren, R. A. Physical and chemical fraction of dissolved organic matter and trihalomethane precursors: a review. *J. Water Supply: Res. Technol.-AQUA* **2005**, *54*, 475–507.
27. Xie, Y. *Disinfection Byproducts in Drinking Water: Formation, Analysis and Control*; Lewis Publishers: Boca Raton, FL. 2004.

Chapter 17

Control of Halogenated N-DBP Precursors Using Traditional and Advanced Drinking Water Treatment Processes: A Pilot-Scale Study in China's Lake Taihu

Wenhai Chu,* Naiyun Gao, Yang Deng, and Xin Li

State Key Laboratory of Pollution Control and Resources Reuse,
College of Environmental Science and Engineering, Tongji University,
Shanghai, 200092, China

*E-mail: feedwater@126.com; 1world1water@tongji.edu.cn.

Tel: +86 21 65982691. Fax: +86 21 65986313.

Haloacetamides (HAcAms), an emerging class of nitrogen-based disinfection by-products (N-DBPs), have been frequently identified in drinking waters. However, there is a limited understanding on the performance of different treatment technologies in the control of HAcAms. The objective of this study was to evaluate the potential of traditional and advanced treatment technologies, including three pre-treatment processes (i.e., powdered activated carbon [PAC] adsorption, KMnO_4 oxidation, and biological contact oxidation [BCO]), two combined conventional treatment methods (i.e. coagulation - inclined plate sedimentation [IPS]-filtration, and coagulation-dissolved air flotation [DAF]-filtration), and an advanced processes (i.e. integrated ozone and biological activated carbon [O_3 -BAC] treatment), for removing the precursors of HAcAms while minimizing the formation of other typical N-DBPs in water. Among the three pre-treatment processes, PAC adsorption could effectively remove the precursors of chloroform (CF) (42.7%), dichloroacetonitrile (DCAN) (28.6%), dichloroacetamide (DCAcAm) (27.2%) and trichloronitromethane (TCNM) (35.7%), advantageous over KMnO_4 oxidation and/or BCO process. In contrast, the removal efficiency of dissolved organic carbon (DOC) by the BCO

process (76.5%) was superior to that by PAC adsorption (69.9%) and KMnO_4 oxidation (61.4%). However, BCO increased the dissolved organic nitrogen (DON) concentration, thereby leading to the formation of more N-DBPs during the subsequent chlorination. Soluble microbial products including numerous DON compounds produced as a result of the BCO treatment were observed to play an essential role in the DCaAm formation. Between the conventional processes, the removal of algae, DON, DOC and UV_{254} by the coagulation-DAF-filtration was better than the coagulation-IPS-filtration. On the average, the former achieved the removal of 53% DOC, 53% DON and 31% UV_{254} , while the latter only removed 47% DOC, 31% DON and 27% UV_{254} . Additionally, the coagulation-IPS-filtration removed less low molecular weight organic molecules than the coagulation-DAF-filtration process. Consequently, the concentrations of CF, DCaAm and DCAN formed from the coagulation-DAF-filtration treated water reached 13, 1.5 and 4.7 $\mu\text{g/L}$ during chlorination, respectively, which were lower than those from chlorination of the coagulation-IPS-filtration treated water (17 $\mu\text{g/L}$ CF, 2.9 $\mu\text{g/L}$ DCaAm and 6.3 $\mu\text{g/L}$ DCAN). Among the advanced treatment processes, O_3 -BAC significantly improved the removal of turbidity, DOC, UV_{254} , $\text{NH}_4^+\text{-N}$, and DON by 98–99%, 58–72%, 31–53%, 16–93% and 35–74%, respectively, and enhanced the removal efficiency of the DBP precursors. However, this option was almost ineffective in removing TCNM and DCaAm precursors. Ozonation alone could not substantially reduce the DCaAm formation, and increased the TCNM formation potential (FP). However, it chemically altered the molecular structures of the precursors and increased the biodegradability of N-containing organic compounds. Consequently, the subsequent BAC filtration dramatically reduced the formation of the both TCNM and DCaAm, thus highlighting a synergistic effect of O_3 and BAC. Additionally, O_3 -BAC was effective at controlling the formation of total organic halogen, which is recognized as an indicator of the formation of unidentified DBPs. Of note, more N-DBP precursors entered into the post-BAC water without pre-ozonation, leading to the formation of more N-DBPs during chlorination, compared with a control group with the pre-ozonation was continuously operated. Moreover, higher DBP FP was observed in the effluent of the BAC filter without pre-ozonation than the FP in the influent of the BAC filter. Therefore, while the intermittent operation of pre-ozonation may have cost and other operational benefits (bromate control), these may be outweighed against the increased N-DBP formation and potential N-DBP associated health risks.

1. Introduction

Water resource shortages and growing water demands have spurred utilities to exploit the source waters impacted by wastewater effluents and/or algal blooming. Such source waters are typically characterized by a higher level of dissolved organic nitrogen (DON). During chlorination or chloramination, the N-containing organic matters in water can react with the disinfectant to form halogenated nitrogenous disinfection by-products (N-DBPs), such as haloacetamides (HAcAms), halonitromethanes (HNMs) and haloacetonitriles (HANs) (1), which represent an emerging concern due to their cytotoxicity and genotoxicity (2–4). In particular, HAcAms, an emerging class of halogenated N-DBPs that have been found in tap waters (5), exhibited much higher genotoxicity and cytotoxicity than many carbonaceous DBPs (C-DBPs) (e.g., trihalomethanes [THMs] and haloacetic acids [HAAs]) (6).

N-DBPs are generally present in drinking water at lower concentrations than THMs and HAAs. One of the main reasons is that dissolved organic nitrogen DON, believed to be the main precursor of N-DBPs, is typically less than dissolved organic carbon (DOC), the important precursor of C-DBPs, in source water (e.g., THMs and HAAs) (7–12). However, algal blooms fed by industrial wastewater effluent and fertilizer runoff can cause a dramatic increase in DON in source waters (8, 13) and N-DBPs during chlorination. Therefore, special attention needs to be paid to the control of N-DBPs in the algal-rich source waters.

An effective strategy to control the formation of DBPs is to remove their precursors prior to chlorination. Generally, HAcAm and some other DBP precursors are characterized by low molecular weight (MW), low hydrophobicity, and poor removal efficiencies in a conventional DWTP using coagulation-sedimentation-filtration (14, 15), especially in polluted source waters characterized with high concentrations of algae [including both prokaryotic microalgae (blue-green algae) and other eukaryotic algae], $\text{NH}_4\text{-N}$ and organic matter content (16). Recently, certain pre-treatment processes (e.g., powdered activated carbon [PAC] adsorption, KMnO_4 oxidation, and biological contact oxidation [BCO]), conventional processes (coagulation-inclined plate sedimentation [IPS]-filtration, and coagulation-dissolved air flotation [DAF]-filtration), and an advanced processes (e.g., integrated ozone and biological activated carbon [$\text{O}_3\text{-BAC}$] treatment), are increasingly applied to improve the removal of algae, $\text{NH}_4\text{-N}$ and organic matters in China. However, the information regarding the performance of these treatment processes on the control of N-DBPs is highly limited.

The objective of this chapter was to evaluate the formation of halogenated N-DBPs and the removal of their precursors in algae-rich waters during the following water treatments, including three pre-treatment processes (i.e., PAC adsorption, KMnO_4 oxidation, and BCO treatment), two conventional processes (i.e., coagulation-IPS-filtration, and coagulation-DAF-filtration), and an advanced processes (i.e., $\text{O}_3\text{-BAC}$ treatment). Results are of importance for optimization of the treatment design and improvement of water treatment efficiencies in the treatment facilities with DON-rich waters.

2. Pilot-Plant Process Flow

The water samples used was collected from Lake Taihu, the third largest freshwater lake in China. Lake Taihu is a major potable water source of many cities and towns in Eastern China including Shanghai, Suzhou, and Wuxi. In recent years, the combined effects of nutrient enrichment and industrial pollution frequently degrade the water quality of Lake Taihu, and cause a fouling smell in the finished water from conventional treatment facilities. This pushes local WTPs to employ pre-treatment processes and O₃-BAC advanced process for further improvement of water quality. To test the additional treatments, a pilot plant (1 m³/h) was established in a conventional drinking water treatment plant (DWTP) near Lake Taihu. A flowchart of the pilot plant process is shown in Figure 1.

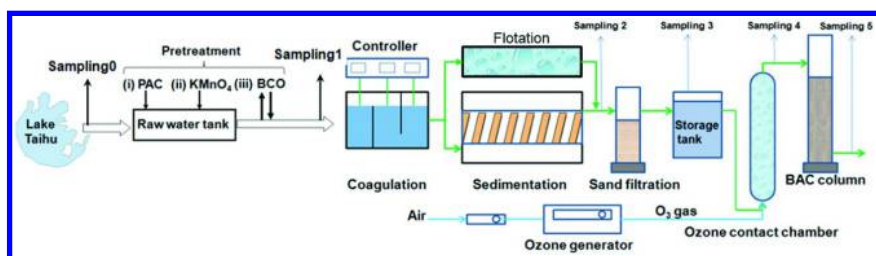


Figure 1. Flowchart of the pilotscale treatment process.

2.1. Pretreatment

(i) PAC adsorption: 20 mg/L PAC was dosed to a raw water tank from a hydrated PAC tank by a metering pump. The PAC was mixed in the raw water tank, and was continuously transported to a coagulation tank (three-stage flocculation plant). (ii) KMnO₄ oxidation: 1.0 mg/L KMnO₄ was added to the raw water tank. The dosages of PAC and KMnO₄ were selected based on our previous results of jar tests and economic considerations. (iii) BCO: The BCO reactor was composed of three flow-through columns (3.0 m length, 0.38 m diameter, 0.15 m elevation difference and 2 h residence time), as shown in Figure 2. In these columns, the filler vinylon silk was fixed firmly on plastic rings, and distributed evenly in the water, providing the sites for biological films. The raw water and air were pumped into the column bottom (gas-water ratio = 1:2), and the treated water overflowed from the top of column. Before the BCO treatment, one month was required to allow formation of the biomembrane by seeding Lake Taihu raw water. After biofilm colonization, plentiful brown biological films were found in the filler, and the removal rates of NH₄⁺-N-N and DOC in the BCO reactors ranged within 75–85% and 30–40%, respectively. The influent to the BCO reactor was from the raw water tank and the effluent of the BCO reactor was transported to the ensuing coagulation tank (three-stage flocculation plant) continuously (17).

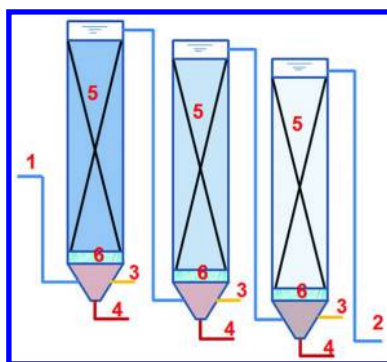


Figure 2. The pilot plant of BCO process (1- Influent pipe; 2- Effluent pipe; Air inflow pipe; 4- Discharge pipe; 5- Filler; 6- Water and air distributing device).

2.2. Conventional Process (Coagulation-IPS-Filtration versus Coagulation-DAF-Filtration)

The coagulation process was performed in a three-stage flocculation plant (1.2 m length, 0.4 m width, and 0.5 m height). The average velocity gradient (G) values in the first, second and third stages were set as 45, 24 and 11 s^{-1} , respectively, to match the operational practice requirements of the local WTP. The IPS process was carried out in an inclined sedimentation tank (1.5 m length, 0.7 m width, and 1.4 m height). The DAF system consisted of a DAF tank with 0.7 m diameter and 1.0 m height, a dissolved air vessel and an air compressor. A scum board was installed on the top of DAF tank to remove supernatant solids. Air was introduced into the dissolved air vessel by an air compressor intermittently. The operating pressure was 0.24–0.34 MPa. Part of the DAF effluent was recycled continuously back to the inlet of the DAF tank at a recycle ratio of 10–15%. Filtration was achieved by a filter column with a diameter of 0.3 m. The filter medium was quartz sand with a grain diameter of 0.7–1.0 mm. The depth of the filter material was 0.9 m and the filtration rate was 7 m/h. The details of the pilot scale conventional treatment was described in detail elsewhere (18).

2.3. Advanced Treatment Process (O_3 -BAC)

Ozonation was carried out in an ozone contact chamber (4.5 m height, and 0.4 m diameter) operated in a concurrent flow mode. Ozone was generated from air using an ozone generator (HMY-F, Huangming, China) and continuously introduced into the water in the form of small bubbles through a porous titanium plate. Dissolved ozone dosage was 1.5–2.0 mg/L, and the contact time was 30 min. Subsequent to ozonation, the water was fed into a granular activated carbon (GAC) filter (4.0 m height, and 0.3 m diameter) to perform the BAC treatment tests. The empty bed contact time and filtration rate of the BAC column

were maintained at 15 min and 7.0 m/h, respectively. The bed depth, effective size, uniformity coefficient, iodine value, methylene blue value, and density of the filled GAC were 1.6 m, 0.55–0.75 mm, <1.9, 1000 mg/g, 266 mg/g and 450 g/L, respectively. Results from the BAC treatment tests with and without pre-ozonation were compared (19).

2.4. Disinfection Process

In most cases, disinfection was carried out by adding 5 mg/L of chlorine (as Cl₂) to the intake of a clean water tank using a metering pump. The clean water tank was mixed intensively by mechanical agitation. The disinfectant residuals were quenched with ascorbic acid, and glacial acetic acid was injected to achieve pH 5.0 ± 0.2 for the subsequent N-DBPs analysis (17–19). The DBP formation potential (FP) test was conducted with 48 h of sample collection and involved chlorination for a further 24 h using free chlorine, as described in detail in previous papers (14).

3. Pretreatment Processes

3.1. Water Parameters

There were not any significant difference ($p=0.42, 0.27, 0.55$, corresponding to BCO, PAC adsorption, KMnO₄ oxidation, respectively) on the removal of turbidity among the three pre-treatment processes coupled with subsequent conventional treatment process. The removal effect of turbidity in the filtered water by the three different pretreatment processes (<0.5 NTU) was all better than that by conventional treatment process alone (approx 0.8 NTU). Moreover, the algae removal by the three different pretreatment processes was also all significantly better than the conventional treatment process alone; the PAC adsorption, KMnO₄ oxidation and BCO processes increased the average algal removal efficiency of the subsequent conventional treatment process from 90% to 97.5%, 98.2% and 99.6%, respectively. These findings confirmed that the three pretreatment process flows were operated as designed and expected. Additionally, compared with the PAC adsorption (<10%) and KMnO₄ oxidation (<20%), the BCO pretreatment process achieved a dramatically higher overall removal rate of NH₄⁺-N (> 60%).

From Table 1, PAC adsorption and KMnO₄ oxidation enhanced the average DON removal rate of the conventional water treatment process from 34.0% to 45.6% and 42.6% (Table 1). However, the BCO pretreatment process increased the DON concentration of the raw water by 5.1%, likely because the BCO process produced numerous metabolic by-products in the form of nitrogenous organic matters. It is known that a range of soluble microbial products (SMPs) are produced by microorganisms in the BCO process and can be found in BCO effluent (20). SMP is a pool of complex organic matters including many DON compounds such as proteins, nucleic acids and amino acids (21–23).

Table 1. DON Removal in Different Treatment Trains

<i>Treatment trains</i>	<i>DON (mg/L)</i>				<i>DON accumulative removal rate (%)</i>				<i>SUVA (L/(mg·m))</i>			
	<i>a</i>	<i>b</i>	<i>c</i>	<i>d</i>	<i>a</i>	<i>b</i>	<i>c</i>	<i>d</i>	<i>a</i>	<i>b</i>	<i>c</i>	<i>d</i>
A	0.53	-	0.41	0.35	0.0	-	22.6	34.0	2.46	-	2.23	2.09
B	0.57	0.49	0.37	0.31	0.0	14.0	35.1	45.6	2.45	1.75	1.45	1.59
C	0.61	0.52	0.39	0.35	0.0	14.8	36.1	42.6	2.48	1.94	1.98	1.66
D	0.59	0.62	0.53	0.51	0.0	-5.1	10.2	13.6	2.29	1.96	1.82	1.68

Sampling point: a: Original Lake Taihu raw water; b: After pretreatment; c: After coagulation-sedimentation; d: After filtration. Treatment trains: A: Conventional water treatment process only; B: PAC adsorption + conventional water treatment process; C: KMnO₄ oxidation + conventional water treatment process; D: BCO + conventional water treatment process.

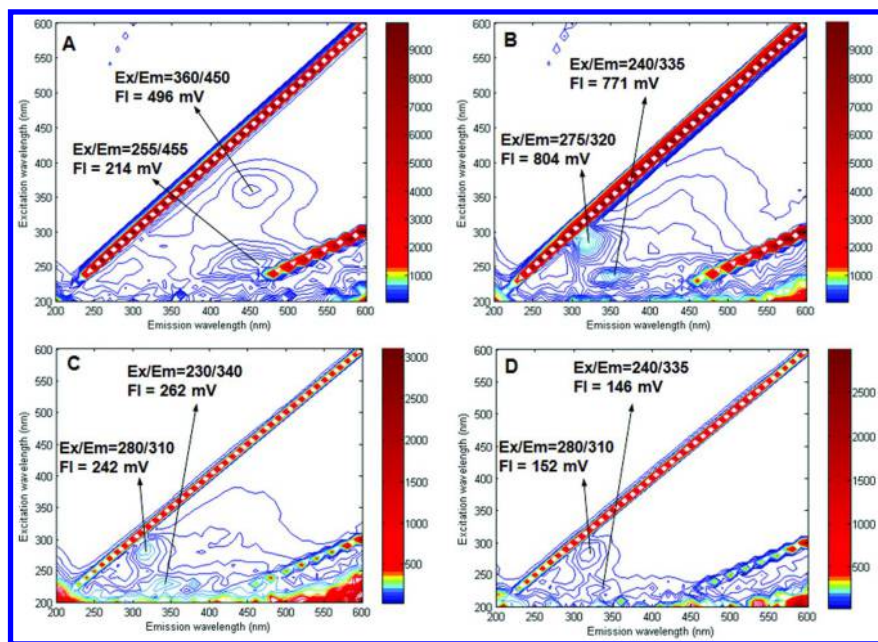


Figure 3. Fluorescence EEM spectra of Lake Taihu water. (TLW DOC = 4.2 mg/L, pH = 7.0, T = 23 °C) A: Original raw water; B: After BCO pretreatment; C: After coagulation-sedimentation; D: After filtration.

EEM spectra were used to characterize the Lake Taihu water natural organic matters (NOM), as shown in Figure 3. According to the fluorescence regional integration (FRI) method developed by Chen and colleagues (21), the EEM spectra were operationally summarized into five regions: five regions in the EEM spectra based on the fluorescence of model compounds: aromatic proteins (regions I and II, $\lambda_{\text{ex}} < 250$ nm, $\lambda_{\text{em}} < 380$ nm), fulvic acid-like (region III, $\lambda_{\text{ex}} < 250$ nm, $\lambda_{\text{em}} > 380$ nm), SMP-like, including tyrosine-, tryptophan-, and protein-like components (region IV, $\lambda_{\text{ex}} > 250$ nm, $\lambda_{\text{em}} < 380$ nm), and humic acid-like (region V, $\lambda_{\text{ex}} > 250$ nm, $\lambda_{\text{em}} > 380$ nm) regions.

As shown in Figure 3A, NOM in raw water had its intensest peak (496 mV) and second highest peak (214 mV) in the humic region. However, when the raw water was pretreated by the BCO process, the NOM showed the intensest peak (804 mV) at Ex/Em of 275/320 nm, which fell within the SMP-like region ($\lambda_{\text{ex}} > 250$ nm, $\lambda_{\text{em}} < 380$ nm), and the second-highest peak (771 mV) at Ex/Em of 240/335 nm within the aromatic protein region ($\lambda_{\text{ex}} < 250$ nm, $\lambda_{\text{em}} < 380$ nm) (Figure 3B). This confirmed previous speculation that SMP containing numerous DON compounds possibly weakens the DON removal performance of the BCO process. Moreover, SMPs cannot be removed completely by conventional treatment processes (coagulation-sedimentation-filtration) as shown in Figure 3(C) and (D).

3.2. DBPs

CF and DCAN were the most abundant species in most of the water samples (i.e. there were relatively few brominated analogues) (24). In addition, TCAN and TCACAm concentrations in most of the water samples were below our detection limits. Therefore, the study mainly focused on the chlorinated DBPs (CF, DCAN, DCACAm, and TCNM). The concentrations of CF, DCAN, DCACAm and TCNM measured after different pretreatment processes (PAC adsorption, KMnO_4 oxidation and BCO) and subsequent conventional treatment processes are summarized in Figure 4.

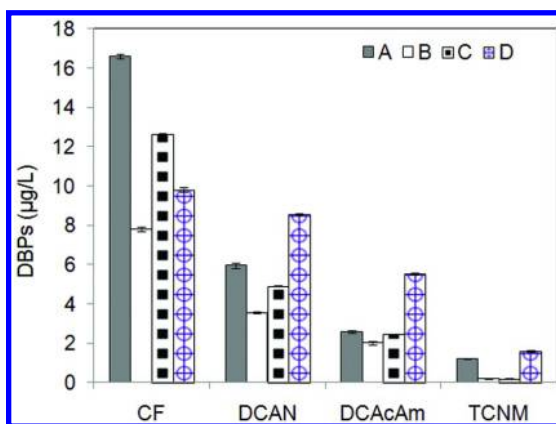


Figure 4. The concentrations of CF, DCAN, DCACAm and TCNM in chlorinated water. A: Conventional water treatment process only; B: PAC adsorption + conventional water treatment process; C: KMnO_4 oxidation + conventional water treatment process; D: BCO + conventional water treatment process. The error bars represent the standard deviation of replicate measurements ($n = 3$).

As shown in Figure 4, CF in water treated by conventional treatment processes only reached its maximum value of $16.7 \mu\text{g/L}$, which was substantially greater than that obtained by different pretreatment and subsequent conventional treatment processes. This finding indicated that the pretreatment processes could reduce the formation of CF effectively. It is worthwhile to note that mean N-DBP concentrations (DCAN: $8.6 \mu\text{g/L}$, DCACAm: $5.6 \mu\text{g/L}$, TCNM: $1.6 \mu\text{g/L}$) in chlorinated water treated by BCO process were significantly greater than from those of the water treated by conventional treatment processes alone (DCAN: $6.0 \mu\text{g/L}$, DCACAm: $2.6 \mu\text{g/L}$, TCNM: $1.2 \mu\text{g/L}$), and pretreated by PAC adsorption (DCAN: $3.6 \mu\text{g/L}$, DCACAm: $2.0 \mu\text{g/L}$, TCNM: $0.2 \mu\text{g/L}$) or by KMnO_4 oxidation (DCAN: $4.9 \mu\text{g/L}$, DCACAm: $2.5 \mu\text{g/L}$, TCNM: $0.2 \mu\text{g/L}$). Additionally, less CF and N-DBPs (DCAN, DCACAm and TCNM) were formed in chlorinated water post-PAC. There are two possible reasons for

this finding: (i) PAC adsorption can remove these DBP precursors effectively. (ii) PAC can enhance the performance of subsequent conventional treatment process (coagulation-sedimentation-filtration) on removing C-DBP and N-DBP precursors. In order to evaluate the impact of these pretreatment processes, the DBP FPs in different stages of the water treatment process were investigated.

3.3. DBP FPs

The FPs of CF, DCAN, DCACAm and TCNM in different stages of the water treatment trains were investigated (Figure 5). From Figure 5 (A), the mean FP removal rate of CF (65.7%) by conventional water treatment processes alone was higher than that of DCAN (50.2%), DCACAm (24.7%) and TCNM (57.0%), implying that the precursors of DCAN, DCACAm and TCNM were more recalcitrant than CF precursors by conventional water treatment processes alone, especially for DCACAm precursors.

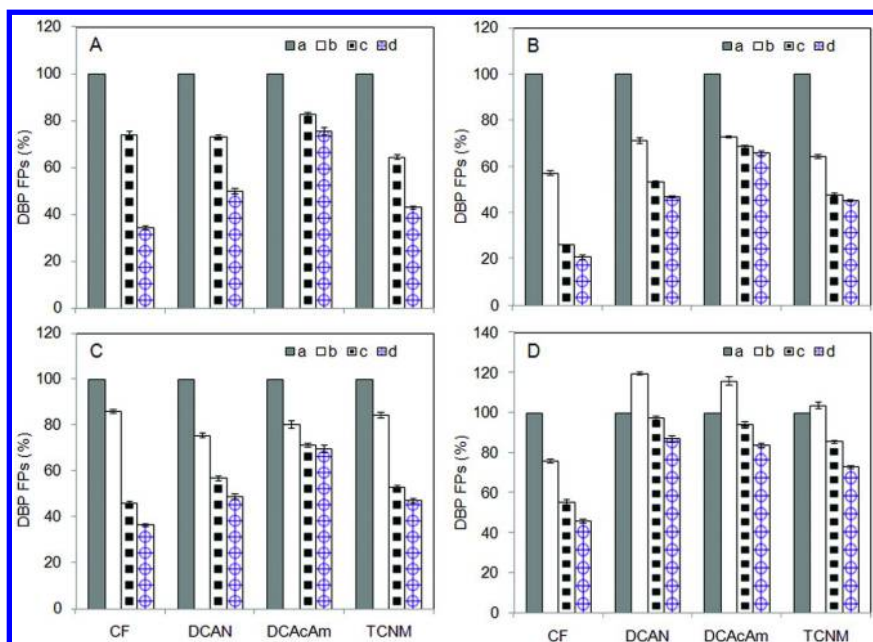


Figure 5. The FPs of CF, DCAN, DCACAm and TCNM in different stages of the water treatment process (DBP FPs of original raw water were defined as 100%). A: Conventional water treatment process only; B: PAC adsorption + conventional water treatment process; C: $KMnO_4$ oxidation + conventional water treatment process; D: BCO + conventional water treatment process. a: Original raw water; b After BCO pretreatment; c: After coagulation-sedimentation; d: After filtration. The error bars represent the standard deviation of replicate measurements ($n = 3$).

From Figure 5 (B) and (C), it can be seen that PAC adsorption can effectively remove the precursors of CF (42.7%), DCAN (28.6%), DCACAm (27.2%) and TCNM (35.7%), which were greater than the mean removal rate of the precursors of CF (14.0%), DCAN (24.5%), DCACAm (19.8%) and TCNM (15.6%) pre-treated by KMnO_4 oxidation. As shown in Table 1, the SUVA of raw water declined to below 2 L/mg·m after PAC adsorption and/or KMnO_4 oxidation. At $\text{SUVA} < 2$ L/mg·m, the organic matter was mostly comprised of non-humics and was of low hydrophobicity (25), indicating that humics and hydrophobic organic matter were absorbed by PAC or oxidized by KMnO_4 . This suggests that these humics and hydrophobic organic matters, which probably were a significant part of the THM precursors (26).

From Figure 5 (D), the mean FPs of N-DBPs (DCAN: 120%; DCACAm: 116%; TCNM: 104%) of pre-treated water by the BCO process were noticeably higher than that (100%) of the raw water before the BCO process. As discussed above, numerous metabolic by-products produced by the BCO process raised the DON level, believed to be the main N-DBP precursor, which probably caused the observed increase of N-DBP FPs. Figure 6 displays good linear relationships between the DON concentration and the three N-DBPs (DCAN: $R^2 = 0.82$; TCNM: $R^2 = 0.69$; DCACAm: $R^2 = 0.83$) in the DBP FP tests of BCO pretreatment and conventional treatment processes. This suggests that DON plays an important role in the formation of DCAN, DCACAm and TCNM, and the presence of DON in source waters may act as a reasonable surrogate indicator of N-DBP FPs. In addition, from Figure 6 (B), a linear relationship was observed between SMP peak intensity and DCACAm ($R^2 = 0.94$), implying that the SMP produced in the BCO process may be an important class of HAcAm precursors and caused the higher concentrations and FPs of DCACAm.

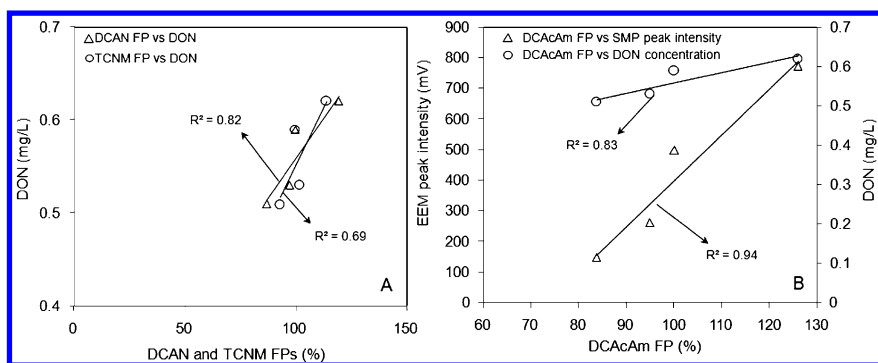


Figure 6. The relationships between N-DBP FPs and DON concentration, and DCACAm FP and fluorescence EEM SMP peak intensity in a typical run in November 2008 (DBP FPs of original raw water were defined as 100%).

4. Conventional Treatment (Coagulation-IPS-Filtration versus Coagulation-DAF-Filtration)

4.1. Precursors

Two conventional processes (coagulation-IPS-filtration vs coagulation-DAF-filtration) were compared, without regard to pre-treatment and advanced treatment processes. There were no observable differences on the removal of turbidity by the two conventional treatment processes. The turbidity and DOC of the filtered water through the IPS or DAF were both less than 1.0 NTU and 2.5 mg/L, respectively, indicating that the two process flows were operated as designed. Additionally, we found the UV_{254} and DOC in the filtered water post-IPS were higher than that post-DAF (Table 2), and the average removal efficiencies of UV_{254} (27%) and DOC (47%) in the filtered water post-IPS were lower than post-DAF (UV_{254} : 31%; DOC: 53%). This phenomenon was probably linked to the SUVA of the water (25). At $SUVA < 2$, the organic matter in the raw water was mostly comprised of non-humics, and had low hydrophobicity and low MW, resulting in a poor DOC removal. When $SUVA$ in the raw water was close to 2, the similar organic matter characteristics (low hydrophobicity and low molecular weight) in the raw water likely caused a poor DOC removal by the coagulation-IPS-filtration (26).

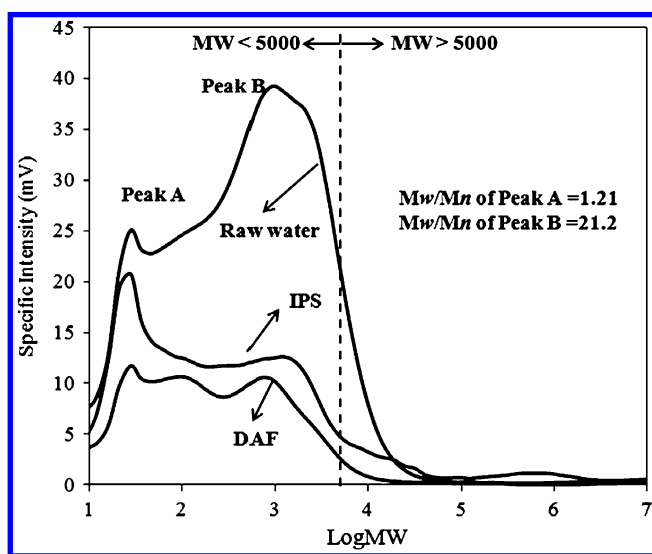


Figure 7. MW distribution of raw water and filtered water after the two different coagulation processes (IPS and DAF).

Table 2. DOC, DON and UV₂₅₄ in the Raw Water

<i>Data (d)</i>	<i>DOC (mg L⁻¹)</i>			<i>UV (cm⁻¹)</i>			<i>SUVA (L/(mg·m))</i>	<i>DON (mg L⁻¹)</i>	<i>DON/DOC mg/mg</i>
	<i>Raw water</i>	<i>IPS</i>	<i>DAF</i>	<i>Raw water</i>	<i>IPS</i>	<i>DAF</i>	<i>Raw water</i>	<i>Raw water</i>	<i>Raw water</i>
1 st	6.07	2.48	2.24	0.155	0.112	0.109	2.55	0.69	8.7
3 rd	3.25	1.85	1.64	0.062	0.045	0.043	1.91	0.67	4.9
6 th	5.29	3.26	2.85	0.097	0.073	0.068	1.83	0.79	6.7
13 rd	4.69	2.45	2.23	0.101	0.079	0.072	2.15	0.83	5.7
17 th	5.23	2.48	2.39	0.105	0.078	0.072	2.01	0.55	9.5
22 nd	5.38	2.46	2.37	0.118	0.077	0.075	2.19	0.62	8.7
28 th	4.82	3.07	2.53	0.085	0.065	0.061	1.76	0.73	6.6

The algae removal by the DAF was prominently better than IPS. This is probably because most of the algae are low-density and suspended in the upper water column and DAF is more effective than IPS in removing such suspended material. In addition, the higher removal efficiencies of DON was achieved in filtered water post-DAF probably because the dissolved nitrogenous organic compounds with low hydrophobicity and low MW were removed less well by the IPS process. The average removal efficiencies of DON by the two processes (IPS and DAF) were 31% and 53%, respectively.

Table 3. Guidelines on the Nature of NOM and Expected DOC Removals at Different SUVA Values

<i>SUVA</i> ($L\ mg^{-1}m^{-1}$)	<i>Composition</i>	<i>DOC removal by coagulation-sedimentation-filtration</i>
≥ 4	Mostly aquatic humics, High hydrophobicity High molecular weight (MW)	Good DOC removal
2-4	Mixture of Aquatic Humics and other NOM, Mixture of hydrophobic and hydrophilic Mixture of MWs	DOC removals should be fair to Good
< 2	Mostly Non-humics Low hydrophobicity Low MW	Poor DOC removal

As shown in Figure 7, the MW distribution of raw water revealed that organic matters in the raw water mainly consisted of low MW (MW < 5000 Da), which was in accordance with the reduction from SUVA in Table 3 (25). In addition, the polydispersity (Mw/Mn) value close to 1 means that the constituents in organic matters mostly made up of organic substances with identical or at least similar origin and/or properties (27). From Figure 7, Mw/Mn values of Peak A and Peak B are 1.2 and 21, respectively, implying coagulation-IPS-filtration performed less well at removing the low MW organics (Peak A: $1 < \text{LogMW} < 2$) with similar origin and/or properties.

4.2. C-DBPs

The CF concentrations measured after chlorination following the two algae removal processes (IPS and DAF) are presented in Figure 8. CF in chlorinated water post-IPS and post-DAF reached their maximum values of 17 and 13 $\mu\text{g/L}$, respectively. More CF was formed after IPS than after DAF, thereby suggesting

that DAF removed THM precursors more effectively than IPS. As shown in Table 2, less DOC, the most important precursor indicator of C-DBPs (e.g. CF), was removed by coagulation–IPS–filtration than by coagulation–DAF–filtration. In addition, algae also represented an important THM precursor (8, 28, 29). Less THM was formed during chlorination of post-DAF samples than post-IPS may be another reason for the improved CF precursors removal of the DAF over IPS.

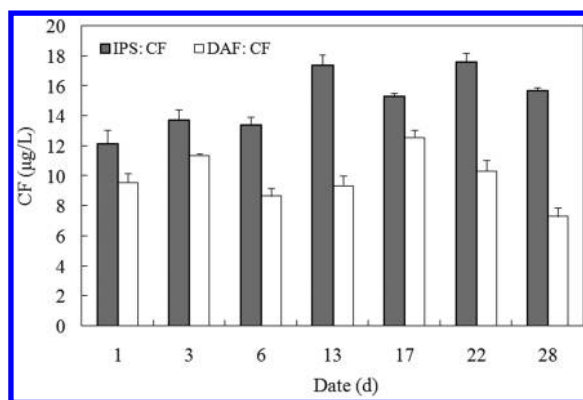


Figure 8. Chloroform concentration in chlorinated water after the two different coagulation processes (IPS and DAF). Error bars represent the standard deviation of replicate measurements ($n = 3$).

4.3. N-DBPs

The N-DBP concentrations in the water after chlorination following the two different processes (IPS and DAF) are summarized in Figure 9. DCACAm, DCAN and TCNM ranged within 1.5–2.9, 3.5–6.3 and 0.5–1.0 µg/L, respectively, in the water treated by coagulation–IPS–filtration–chlorination. Additionally, in the water treated by coagulation–DAF–filtration–chlorination, DCACAm, DCAN and TCNM varied within 0.6–1.5, 2.7–4.7 and 0.4–0.9 µg/L, respectively. Because the better removal in the entire MW range was achieved by the coagulation–IPS–filtration process, fewer precursors remained to form further DCACAm and DCAN. The TCNM concentrations after the two processes were similar, probably because the TCNM formation was influenced by DIN (30) instead of DON.

In addition, the average concentrations of DCACAm (2.3 µg/L) and DCAN (5.0 µg/L) in the water treated by coagulation–IPS–filtration–chlorination were higher than the average levels reported in a US N-DBP occurrence study (5). A low DOC/DON usually indicates that microorganism (e.g. algae, bacteria) products are a major fraction of the NOM (autochthonous) (8, 31, 32). In a survey of US plants that were impacted by algae and/or treated wastewater (33), the average DOC/DON ratio (13 mg/mg) of the surveyed waters confirmed that these sources were

influenced by elevated levels of DON compared to a previous US study (34), where the average DOC/DON ratio in a broader array of surface waters was 18 mg/mg. In the studied raw water (Table 2), DOC/DON was 4.9 to 9.5 mg/mg, with an average value of 7.3 mg/mg, indicating the Lake Taihu raw water was relatively organic nitrogen rich, which possibly caused relative higher DCACAm and DCAN yields. We also found a linear relationship ($R^2 = 0.83$) between DCACAm and DCAN. This is probably because DCACAm is a main hydrolysis product of DCAN, and the two N-DBPs share similar precursors and/or mechanisms of formation (7, 35).

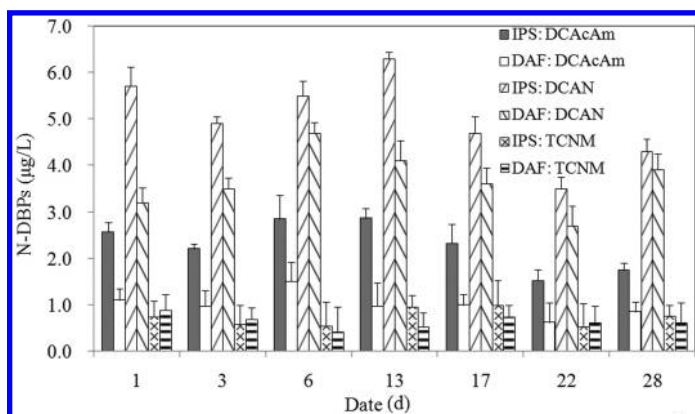


Figure 9. N-DBP concentrations in chlorinated water after the two different coagulation processes (IPS and DAF). Error bars represent the standard deviation of replicate measurements ($n = 3$).

5. Advanced Treatment (O₃-BAC)

5.1. Precursors

The advanced treatment process (O₃-BAC) were studied after the conventional processes, without regard to pre-treatment and advanced treatment processes. As shown in Figure 10, the mean removal rates of turbidity, DOC, and UV₂₅₄ reached 98.4%, 56.7%, and 30.9% after the conventional process (coagulation-sedimentation-filtration) and increased to 99.3%, 72.2%, and 52.6% after the O₃-BAC process, respectively. The final levels of turbidity, DOC, and UV₂₅₄ in the effluent after the combined process decreased to below 0.4 NTU, 2.0 mg/L, and 0.05 cm⁻¹, confirming that the combined process flows were operated as designed and expected.

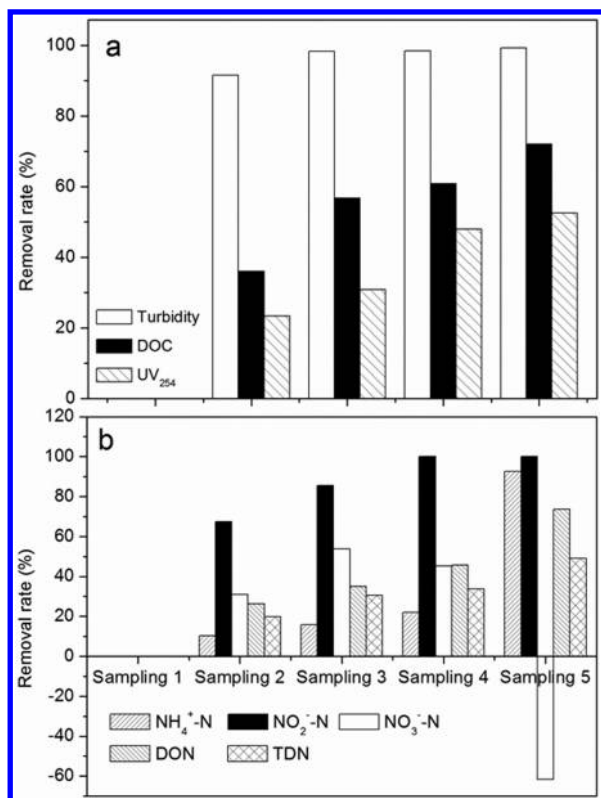


Figure 10. Removal rates of water quality parameters (Figure 10a: turbidity, DOC, and UV₂₅₄; Figure 10b: DON and DIN) in different stages of the water treatment process. (From Figure 1, Sampling 1, 2, 3, 4 and 5 represented the water samples collected from the raw water; after coagulation-sedimentation, filtration, O₃ and BAC processes, respectively.)

The conventional treatment process achieved a poor removal of NH₄⁺-N relative to turbidity, DOC and UV₂₅₄. However, the O₃-BAC process significantly improved the removal of NH₄⁺-N from 15.7% to 92.6%, which was in agreement with other studies (36–39). The BAC process removed 70% of NH₄⁺-N. After the conventional process (coagulation-sedimentation-filtration), the average removal rates of NO₂⁻-N and NO₃⁻-N reached 85.6% and 53.7%, and further increased to 100% and decreased to 45% in the ozonated water, respectively. This is probably because part of NO₂⁻-N was oxidized to NO₃⁻-N by the ozone. In addition, the removal rate of NO₃⁻-N decreased by 61.6% in the effluent of the BAC process, likely due to biological nitrification in the BAC bed. Although more NO₃⁻-N was formed in the BAC effluent, the measured concentrations of NO₃⁻-N were always lower than 2.0 mg/L that is far below the maximum contaminant level (10 mg/L) of Chinese National Standards of Drinking Water Quality and the USEPA National Primary Drinking Water Regulations for NO₃⁻-N.

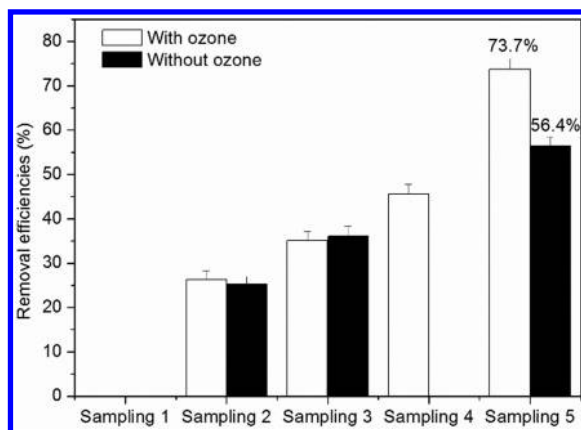


Figure 11. Removal of DON by the BAC process with and without pre-ozonation. (The removal rates were calculated based on the DON concentrations of raw waters; The error bars represent the standard deviation of replicate measurements ($n = 3$).)

The average removal rate of DON by the conventional process reached only 35.1%, while the post combined O₃-BAC process increased its removal efficiency to 73.7%. In addition, we compared the difference in the DON removal by BAC with and without pre-ozonation (Figure 11). It was found that only 21.3% of DON was removed by the BAC process without pre-ozonation, which was lower than that achieved with pre-ozonation (28.1%). This is likely because ozonation degrades large molecules of DON compounds into smaller ones and hence increases the biodegradability of DON.

5.2. DBPs

From Figure 12, the removal rates of the FPs for CF and DCAN both gradually increased throughout the treatment train. The coagulation-sedimentation-filtration process removed 52.7% and 49.9% of the precursors for CF and DCAN, respectively, and O₃-BAC combined process further enhanced the precursor removal efficiency of CF and DCAN to 85.0% and 80.4%, separately. The effect of O₃-BAC is in agreement with the previous observations that ozonation and BAC substantially reduce the formation of CF and appear not to be significantly affected by source water quality (36–38). Additionally, the conventional process (coagulation-sedimentation-filtration) and advanced treatment process (O₃-BAC) both had higher removal rates for the FPs of CF and DCAN than of TCNM and DCaAm. A plausible reason is that dissolved humic material, including a major fraction of the total organic matter in freshwaters (40), is the major precursor of CF and DCAN but makes little contribution to the formation of TCNM and DCaAm (7, 41). Also, hydrophilic organic matters with low-MW trend to form more TCNM and DCaAm, and it is more difficult to remove these substances than humic material with high-MW (16, 42).

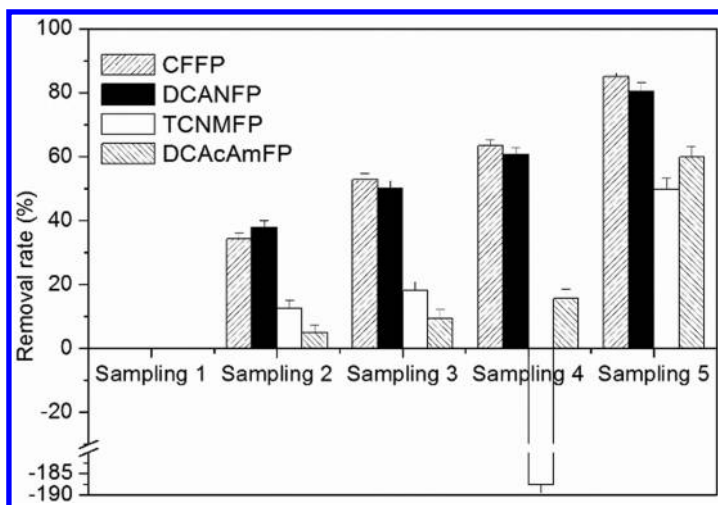


Figure 12. Removal rates of the FPs of CF, DCAN, TCNM and DCACAm in different stages of the water treatment process. (Sampling 1, 2, 3, 4 and 5 represented the water samples collected from raw water; after coagulation-sedimentation, filtration, O₃ and BAC processes, respectively, as shown in Figure 1, The removal rates were calculated based on the DBP FPs of raw waters; The error bars represent the standard deviation of replicate measurements (n = 3).)

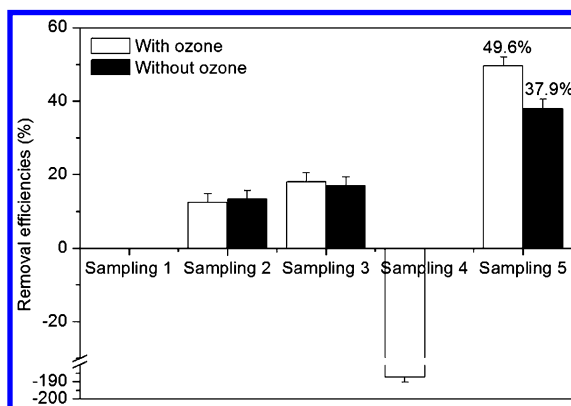


Figure 13. Removal of TCNMFP by the BAC process with and without pre-ozonation. (The error bars represent the standard deviation of replicate measurements (n = 3).)

From Figure 13, it would be noted that the conventional process could not effectively remove the precursors of TCNM, and the mean removal rates of TCNMFP decreased from 18% in filtrated water to -187.5% in ozonated water, but increased to 49.6% after the subsequent BAC process. After ozonation, 46% of DON was reduced relative to the raw water (Figure 10), but TCNMFP increased from 2.7 to 7.4 ug/L. This was probably because the ozone-induced oxidation increased the content of highly reactive specific organic compounds with high HNMFP (43), even though the overall DON was reduced. The performance of the BAC process in terms of controlling TCNM formation either with or without pre-ozonation was also examined (Figure 13). The TCNMFP removal efficiency accomplished by BAC without ozonation pre-treatment was only 38%, less than 50% achieved by the combined O₃-BAC. Thus, although ozone increased the TCNMFP, it enhanced the biodegradability of the organics responsible for HNMFP to facilitate their removal in the following BAC treatment.

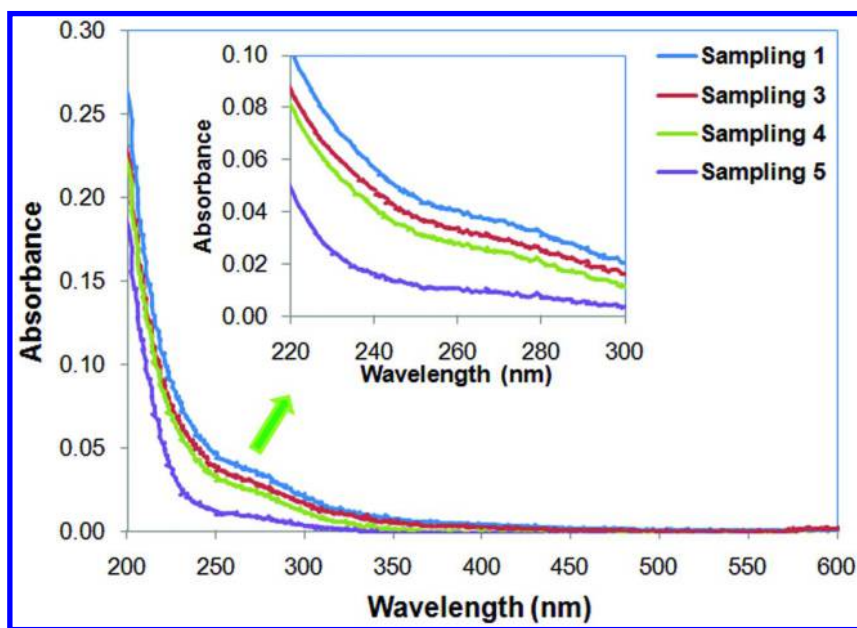


Figure 14. UV/vis optical spectrums of water samples in different stages of the water treatment process. (From Figure 1, Sampling 1, 3, 4 and 5 represent the raw water; after coagulation-sedimentation-filtration, after O₃ and after the BAC processes, respectively.)

Figure 12 also provided the important information in the removal of DCaAcAm. The subsequent BAC process significantly improved the removal of the precursors of DCaAcAm (60% removal). UV/Vis (Figure 14) and EEM (Figure 15) spectra were used to characterize the NOM. As seen in Figure 14, at any particular wavelength within the range of 220–300 nm, the UV absorbance of the

effluent from the BAC column was significantly lower than that of raw, filtered, and ozonated waters, indicating that BAC is an effective process to remove a range of organic compounds over a broad characteristic UV absorbance range.

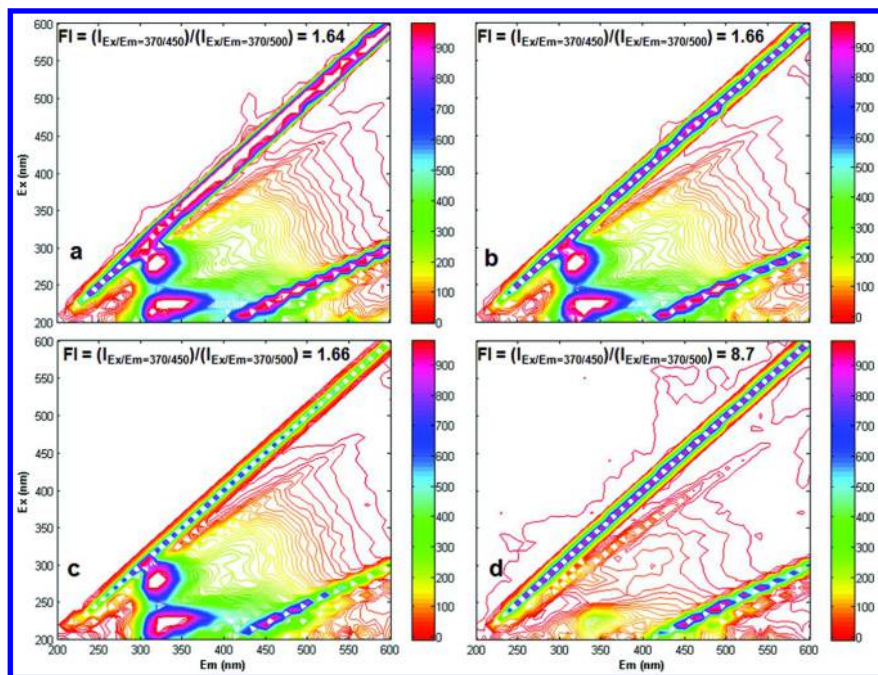


Figure 15. Representative fluorescence EEM spectra of DOM in raw water:

The fluorescence index (FI) can be calculated as the ratio of fluorescence intensities at emission 450 and 500 nm, at excitation 370 in the EEM data. Higher and lower FI values reflect organic contents of an autochthonous (microbial) origin and an allochthonous (terrestrial) origin, respectively (16, 44). From Figure 15, the FI value after BAC significantly increased from 1.7 to 8.7, probably because the allochthonous organics were metabolized to autochthonous organics as a result of microbial activities in BAC. According to the FRI method developed by Chen et al. (21), the NOM of the raw water (Figure 15a), filtered water (Figure 15b) and ozonated water (Figure 15c) all had two intense peaks in the SMPs ($\lambda_{ex} > 250$ nm, $\lambda_{em} < 380$ nm) and aromatic proteins (APs)-like regions ($\lambda_{ex} < 250$ nm, $\lambda_{em} < 380$ nm), and the fluorescence intensities of two peaks in the raw (SMP: 988.6 mV and AP: 988.2 mV), filtered (SMP: 985.0 mV and AP: 983.7 mV) and ozonated water (SMP: 982.5 mV and AP: 981.8 mV) were similar. Thus, the conventional treatment process and ozonation were ineffective at removing the SMP-like and AP-like substances.

The NOM in the BAC effluent showed an AP-like peak at relatively low fluorescence intensities (239.5 mV), and the SMP peak disappeared. Previous studies (14, 17) reported that SMP-like and AP-like substances, containing

elevated organic nitrogen, were the most important precursors of DCaAm. The results for the removal of DCaAmFP (Figure 12) and the variation in SMP-like and AP-like peak intensities in EEM spectra (Figure 13) suggest that the BAC process is able to reduce the precursors of DCaAm.

It should be noted that the FI and FRI methods both provide only a qualitative and/or semi-quantitative analysis of the data, but they cannot separate the complex measured signal into its individual underlying fluorescent phenomena with specific excitation. In order to further understand the characteristics of DBP precursors with the EEM spectra, and ascertain the performance of conventional and advanced treatment processes on removal of the DOMs with different characteristics, an improved EEM analysis model will be adopted in the future experiments. For example, parallel factor analysis is a valuable tool for characterizing and quantifying changes in DOM fluorescence, and enabling the tracing of different fractions in the natural environment (45).

5.3. Total Organic Halogen (TOX)

Korshin et al. (46) reported that a decrease in UV absorbance at 272 nm caused by the chlorination of DOM correlates linearly with the amount of TOX formed, under a wide range of water quality conditions and reaction times. In the present study, therefore, the decrease of UV₂₇₂ (DUV₂₇₂) before and after the DBPFP test was assessed and the removal efficiencies (DUV₂₇₂) in different stages of the treatment process were used to suggest the removal of TOXFP. Removal efficiencies of TOX (DUV₂₇₂) by the conventional process (coagulation–sedimentation–filtration), ozonation, and BAC filtration were 44%, 45% and 72%, respectively, suggesting that the BAC process had a potential to control halogenated DBPs, including unidentified DBPs.

5.4. Effect of Terminating Pre-Ozonation

Two O₃-BAC processes were operated in parallel (Figure 16) and initially achieved the same removal of DOC and DON and the same concentrations of C- and N-DBPs upon subsequent chlorination. Thereafter, ozone dosing was terminated in the second day after backwashing for one of the two O₃-BAC processes, which is represented as ‘T-O₃-BAC’ in the study. And the other O₃-BAC process was operated still with continuous ozonation before BAC filtration, which is represented as ‘C-O₃-BAC’. The performance of C-O₃-BAC and T-O₃-BAC was compared in terms of water quality in the effluents of sand filtration and BAC filtration in the second, third and fourth day after BAC backwashing. The removal rate of each parameter by C-O₃-BAC or T-O₃-BAC process is presented by equation (1).

$$\text{Removal}(\%) = \frac{c_A - c_B}{c_A} \times 100\% \quad (1)$$

c_A — Concentration detected after sand filtration

c_B — Concentration detected after BAC filtration

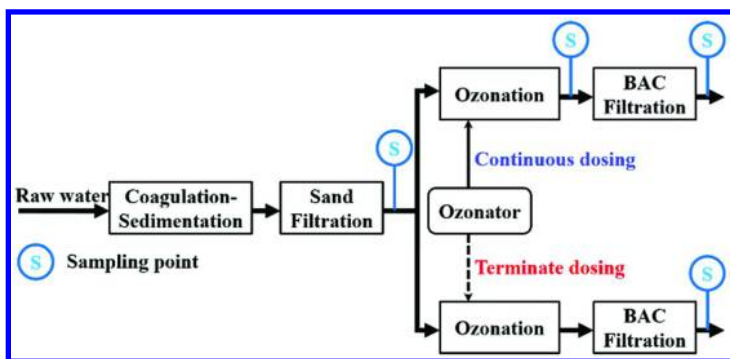


Figure 16. The parallel O_3 -BAC pilot plant process flows.

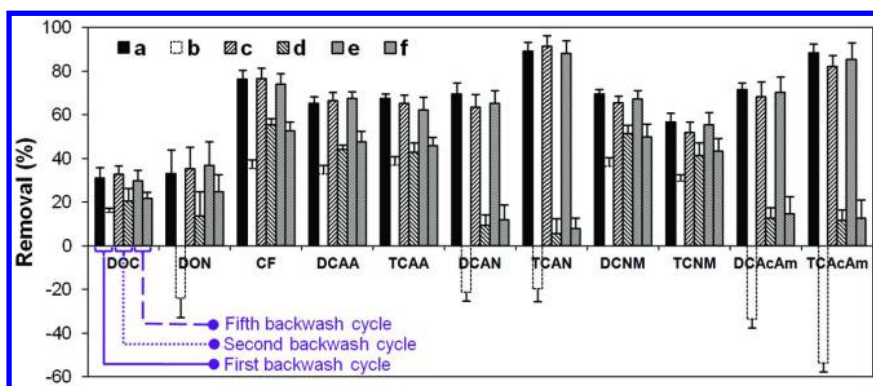


Figure 17. The removal of DOC, DON, C-DBPs and N-DBPs. (a and b Show the removal by the C- O_3 -BAC and T- O_3 -BAC in first backwash cycle after terminating ozone dosing, respectively; c and d show the removal by the C- O_3 -BAC and T- O_3 -BAC in the second backwash cycle after terminating ozone dosing, respectively; e and f show the removal by the C- O_3 -BAC and T- O_3 -BAC in the fifth backwash cycle after terminating ozone dosing, respectively. The removal is the average value of the samples collected three times on the second, third and fourth day after BAC backwashing. The error bars represent the standard deviation of three removal values.)

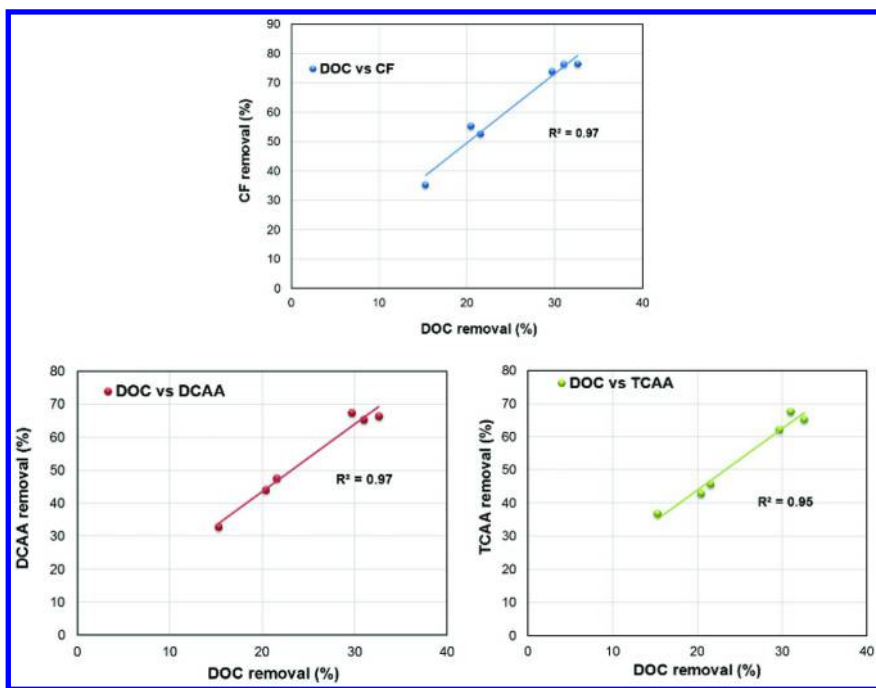


Figure 18. The relationship between DOC removal and C-DBP (CF, DCAA, and TCAA) formation potential (FP) removal by the BAC process.

As shown in Figure 17, the formation yields of C-DBPs upon chlorination of the sand filter effluent, C-O₃-BAC filter and T-O₃-BAC filter were measured. The reduction in C-DBP formation yields by the C-O₃-BAC and T-O₃-BAC filtration relative to sand filtration was calculated by equation (1). C-O₃-BAC achieved better reduction of C-DBPs (CF, DCAA and TCAA) than T-O₃-BAC ($p < 0.05$). The reduction in the C-DBP formation yields closely mirrored the reduction in DOC concentrations, as expected, since DOC is a known C-DBP precursor indicator measurement (47, 48). The linear correlation between DOC removal and C-DBP removal was observed in both the C-O₃-BAC and T-O₃-BAC waters (Figure 18).

The formation yields of N-DBPs upon chlorination of the sand filter effluent, C-O₃-BAC filter and T-O₃-BAC filter were measured, as shown in Figure 17. The reduction in N-DBP formation yields by the C-O₃-BAC and T-O₃-BAC was calculated by Eq. (1). C-O₃-BAC filtration achieved a stable removal of DCAN (63.4–69.7%), TCAN (88.1–89.2%), DCNM (65.5–69.5%), TCNM (51.7–56.9%), DCAcAm (68.2–71.6%) and TCAcAm (82.1–88.5%) from the first to fifth backwash cycles (p values of all selected N-DBPs were higher than 0.05). Some N-DBP concentrations increased in the T-O₃-BAC filter after the initial backwash cycle, which were 21.3%, 19.6%, 33.5% and 53.7% higher than

that in the chlorinated effluent of the sand filter for DCAN, TCAN, DCaAm and TCaAm (Figure 17), respectively. The increased N-DBP concentrations suggest that new N-DBP precursors were produced into the water in the T-O₃-BAC case. Also, the concentrations of DCNM and TCNM were only reduced by 36.3% and 29.5% compared to the chlorinated effluent water of the sand filter, respectively.

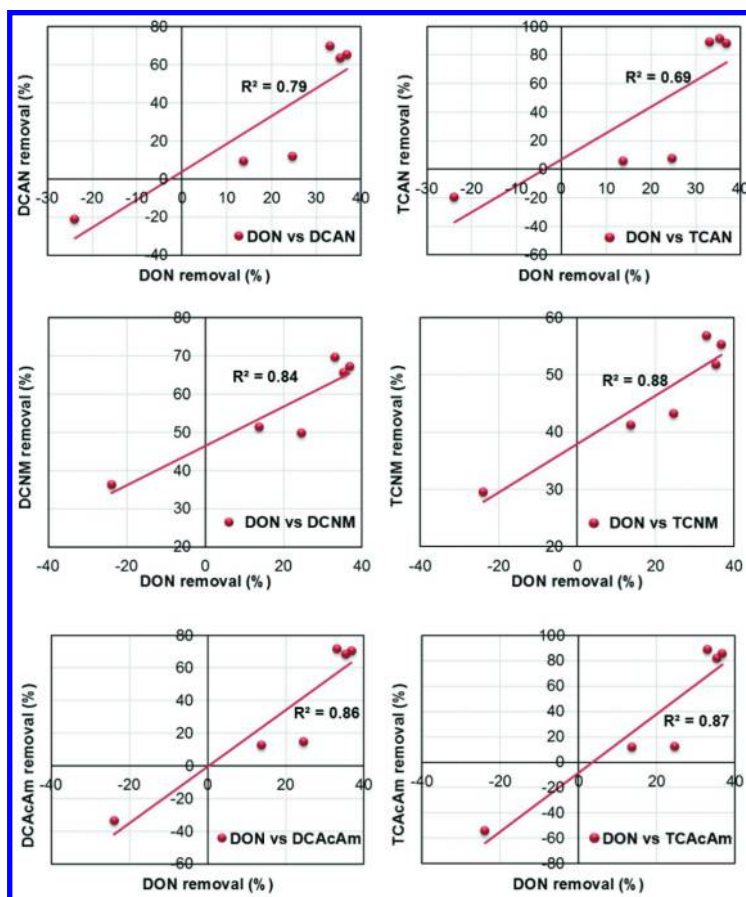


Figure 19. The relationship between DON removal and N-DBP (HANs [DCAN and TCAN], HNMs [DCNM and TCNM], and HAcAms [DCaAm and TCaAm]) formation potential (FP) removal by the two BAC processes.

As shown in Figure 17, C-O₃-BAC presented a stable removal of DOC (29.7%-32.6%) and DON (33.0%-36.7%) from the first to fifth backwash cycles (*p* values of DON and DOC was both higher than 0.05). T-O₃-BAC resulted in lower DOC and DON removal than C-O₃-BAC. Of note, T-O₃-BAC process significantly increased the DON concentration of the sand-filtered water by 23.9% (from 0.46 to 0.57 mg/L) in the first backwash cycle. After that, the T-O₃-BAC partially recovered the ability to remove DON from the second to fifth backwash

cycles. The increase in N-DBP formation yields also mirrored the increase in DON concentrations. As in the case of the relationship between DOC and C-DBP concentrations, the linear correlation between DON and N-DBP concentrations existed in both the C-O₃-BAC and T-O₃-BAC waters (Figure 19). However, the degree of linear correlation between DON and N-DBP concentrations ($R^2 < 0.90$, in Figure 19) was poorer than that between DOC and C-DBPs ($R^2 > 0.95$, in Figure 19), suggesting that not only the DON concentration but also the characteristics of the DON (e.g., SMPs) in the post-BAC water influences the N-DBP yield (14).

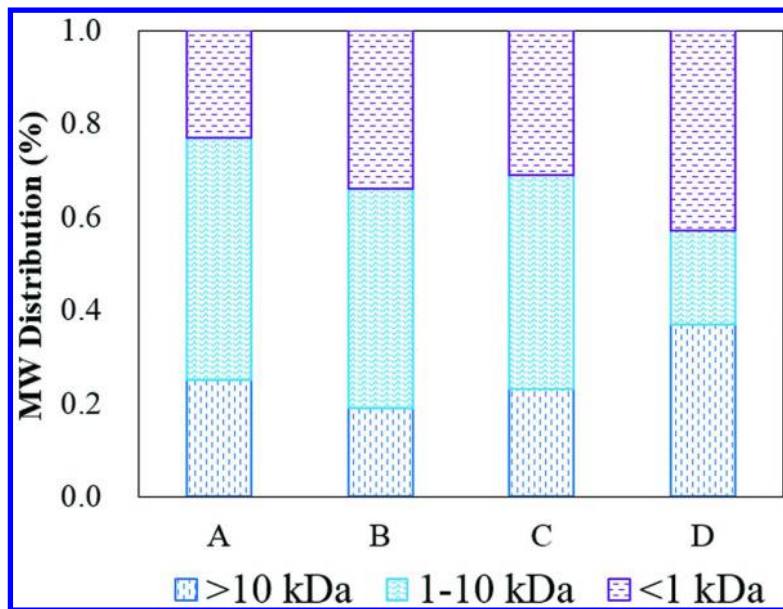


Figure 20. MW distribution of DOM treated by sand filtration, ozonation, and BAC filtration in the first backwash cycle. (SF: treated by sand filtration; O₃: treated by ozonation; C-O₃-BAC: treated by C-O₃-BAC; T-O₃-BAC: treated by T-O₃-BAC.)

It is well known that ozonation preferentially transforms higher molecular weight compounds into smaller molecules (Figure 20) and thereby increases the biodegradable organic matters (49) that are readily removed by a subsequent BAC process (19, 42) When ozone dosing was suddenly terminated, part of the microorganisms in the BAC might subsequently shift from exogenous respiration to endogenous respiration due to the reduction in biodegradable organic matters (39). Consequently, this resulted in the release of numerous soluble microbial products (SMPs) (50). It is known that a range of SMPs are produced by microorganisms in the BAC process and can be detected in BAC effluent (20, 51, 52). SMPs comprise a wide range of high and low molecular weight compounds including many DON compounds such as proteins, polysaccharide and amino acids (21, 53, 54), which can be divided into growth-related utilization associated

products (UAPs) and non-growth-related biomass associated products (BAPs). The formation of UAPs and BAPs is directly related to the cell growth rate and the cell endogenous respiration of the microorganisms, respectively (51). As shown in Figure 20, we investigated the MW distribution of the DOM in effluents of sand filtration, C-O₃-BAC filtration and T-O₃-BAC filtration, and found that C-O₃-BAC filtration slightly altered the MW distribution of DOM due to the ozonation oxidation. However, T-O₃-BAC filtration substantially increased the percentage of high-MW (>10 kDa) and low-MW (< 1 kDa) compared to C-O₃-BAC filtration ($p < 0.05$), which was in accordance with the deduction that SMPs were released in T-O₃-BAC filtration, considering that most of the SMPs consisted of the low-MW (<1 kDa, e.g., amino acids) and high-MW (>10 kDa, e.g., proteins, polysaccharide) compounds (52, 55).

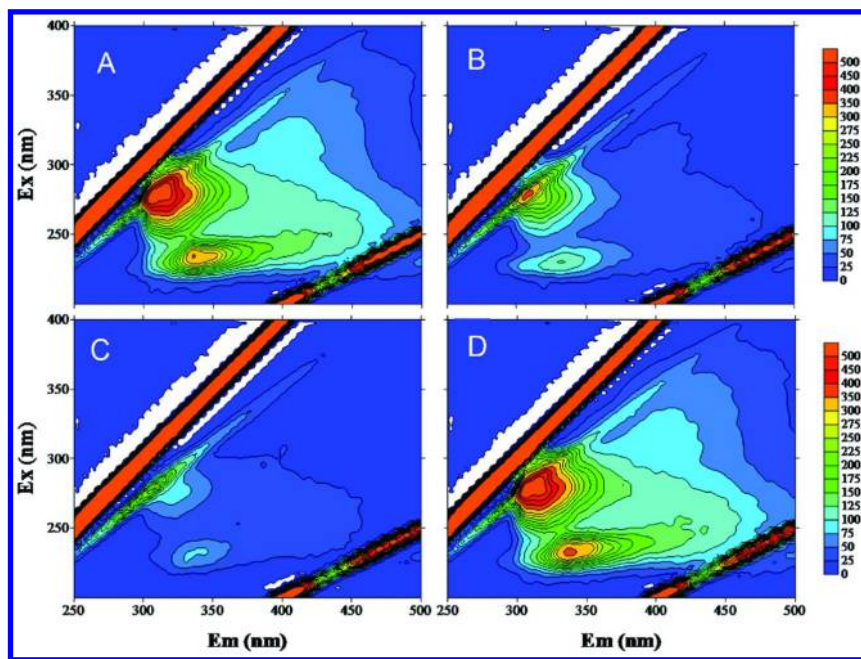


Figure 21. Fluorescence EEM spectra of Lake Taihu water treated by sand filtration, ozonation, and BAC filtration in the first backwash cycle. (SF: treated by sand filtration; O₃: treated by ozonation; C-O₃-BAC: treated by C-O₃-BAC; T-O₃-BAC: treated by T-O₃-BAC.)

EEM spectra were used to characterize the DOM in effluents of sand filtration, C-O₃-BAC filtration and T-O₃-BAC filtration, as shown in Figure 21. As shown, DOM in the sand-filtered water (Figure 21 A), ozonated water (Figure 21B), and BAC-filtered water (Figure 21C and D) all had two intense peaks in the SMP region ($\lambda_{\text{ex}} > 250 \text{ nm}$, $\lambda_{\text{em}} < 380 \text{ nm}$) and aromatic protein (AP)-like region ($\lambda_{\text{ex}} < 250 \text{ nm}$, $\lambda_{\text{em}} < 380 \text{ nm}$), and the fluorescence intensities of the two peaks (SMP and AP) in sand-filtered water was reduced by C-O₃-BAC filtration from 553

and 362 a.u. to 246 and 77 a.u.. Previous studies (14) reported that SMP-like and AP-like substances, containing elevated organic nitrogen, were the important precursors of N-DBPs (HANs and HAcAms). The results for the removal of HAN and HAcAm formation yields (Figure 17) and the variation in SMP-like and AP-like peak intensities in EEM spectra (Figure 21 A, B and C) suggest that the C-O₃-BAC process is able to reduce the precursors of these N-DBPs, which supports earlier evidence of this (19). However, from Figure 21D, it was noted that the fluorescence intensities of SMP and AP peaks in the effluent of T-O₃-BAC filtration actually increased to 649 and 357 mV, which mirrored the increase of HAN and HAcAm concentrations.

5. Conclusion

The application of pretreatment processes in water treatment can improve the removal of algae, NH₄⁺-N and organic matter, and reduce the formation of C-DBPs and certain N-DBPs. However, the BCO pretreatment process could also increase DON and result in an increase of the concentrations and FPs of some N-DBPs. KMnO₄ can enhance the performance of conventional water treatment processes in removing DBP precursors, although it removes less precursors than PAC adsorption. Hydrophilic SMP produced from the BCO process plays a key role in DCACAm formation. An additional benefit of improving the removal of hydrophilic nitrogenous organics by pretreatment is the reduced formation of certain NDBPs such as HAcAms.

The transition from coagulation–IPS-filtration to coagulation–DAF-filtration has the potential of removing DBP precursor indicators (e.g. DOC, DON and algae) and reducing the formation of C-DBPs and certain halogenated N-DBPs. Coagulation–DAF-filtration process removed, on the average, 53%, 53% and 31% of DOC, DON and UV254, which were better than 47%, 31% and 27% of that in coagulation–IPS-filtration process. Moreover, less low MW organics were removed by coagulation–IPS-filtration than coagulation–DAF-filtration. This study showed that some N-DBPs (DCACAm and DCAN) clearly exhibited higher formation in high-DON and algae-rich waters. Therefore, an additional benefit of improving DON and algae control is the reduction in the formation of certain N-DBPs. Additionally, the effect of DON may be a more important factor than DOC in the future study on risk assessment and concentration prediction of these N-DBPs in the water with high DON loadings.

The O₃-BAC integrated process is a very promising technology to control the formation of certain halogenated C-DBPs (THMs) and N-DBPs (HANs, HNMs and HAcAms). Ozonation increased the FPs of TCNM substantially, but also enhanced the biodegradability of TCNM precursors and further improved the removal of TCNM precursors by BAC filtration. Ozonation was inefficient in removing the precursors of DCACAm, however, the BAC process greatly improved the removal of DCACAm precursors including SMP-like and AP-like substances. The O₃-BAC combined process should therefore be considered as an option to address regulated and emerging DBPs. However, in some cases, ozone was intermittently dosed (versus continuously) before BAC filtration in DWTPs

in order to save costs by water treatment facilities, control the bromate formation or in emergency situations. This study has showed that a sudden termination of ozonation cannot effectively remove N-DBP (HAN and HAcAm) precursors even after only the first backwash cycle, and then leads to substantial formation of HANs and HAcAms during subsequent chlorination. Moreover, after the first backwash cycle, BAC filtration alone performed poorly for all measured C-DBPs and N-DBPs compared to C-O₃-BAC.

Acknowledgments

The authors gratefully acknowledge the National Natural Science Foundation of China (51108327, 51378366), and the National Major Science and Technology Project of China (2012ZX07403-001,004). The authors also thank their colleagues for their support on the sampling surveys and DBPs analysis.

Abbreviations

Bromochloroacetonitrile –BCAN; Biological contact oxidation –BCO; Carbonaceous disinfection by-products –C-DBPs; Chloroform –CF; Dibromoacetonitrile –DBAN; Disinfection by-products –DBPs; Dichloroacetamide –DCAcAm; Dichloroacetonitrile –DCAN; Dissolved inorganic nitrogen –DIN; Dissolved organic carbon –DOC; Dissolved organic nitrogen –DON; Drinking water treatment plant –DWTP; Excitation-emission matrix –EEM; Gas chromatograph/mass spectrometry –GC/MS; Fluorescence regional integration –FRI; Haloacetic acids –HAAs; Haloacetamides –HAcAms; Haloacetonitriles –HANs; Halonitromethanes –HNMs; Nitrogenous disinfection by-products –N-DBPs; N-nitrosodimethylamine –NDMA; Natural organic matter –NOM; Powdered activated carbon –PAC; Soluble microbial product –SMP; Specific ultraviolet absorption –SUVA; Trichloroacetamide –TCAcAm; Trichloroacetonitrile –TCAN; Trichloronitromethane –TCNM; Trihalomethanes –THMs; Total dissolved nitrogen –TDN; Total organic halogen –TOX.

References

1. Richardson, S. D.; Plewa, M. J.; Wagner, E. D.; Schoeny, R.; DeMarini, D. M. Occurrence, genotoxicity, and carcinogenicity of regulated and emerging disinfection by-products in drinking water: A review and roadmap for research. *Mutation Res.* **2007**, *636* (1-3), 178–242.
2. Plewa, M. J.; Wagner, E. D.; Jazwierska, P.; Richardson, S. D.; Chen, P. H.; McKague, A. B. Halonitromethane drinking water disinfection byproducts: chemical characterization and mammalian cell cytotoxicity and genotoxicity. *Environ. Sci. Technol.* **2004**, *38*, 62–68.
3. Muellner, M. G.; Wagner, E. D.; McCalla, K.; Richardson, S. D.; Woo, Y. T.; Plewa, M. J. Haloacetonitriles vs. regulated haloacetic acids: Are nitrogen-containing DBPs more toxic? *Environ. Sci. Technol.* **2007**, *41*, 645–651.

- Richardson, S. D.; Ternes, T. A. Water analysis: Emerging contaminants and current issues. *Anal. Chem.* **2014**, *86*, 2813–2848.
- Krasner, S. W.; Weinberg, H. S.; Richardson, S. D.; Pastor, S. J.; Chinn, R.; Scilimenti, M. J.; Onstad, G. D.; Thruston, A. D. Occurrence of a new generation of disinfection byproducts. *Environ. Sci. Technol.* **2006**, *40*, 7175–7185.
- Plewa, M. J.; Wagner, E. D.; Muellner, M. G.; Hsu, K. M.; Richardson, S. D. Comparative mammalian cell toxicity of N-DBPs and C-DBPs. In *Occurrence, Formation, Health Effects and Control of Disinfection by-Products in Drinking Water*; Karanfil, T., Krasner, S. W., Xie, Y., Eds.; ACS Symposium Series 995; American Chemical Society: Washington, DC, 2008; pp 36–50.
- Reckhow, D. A.; Platt, T. L.; MacNeill, A. L.; McClellan, J. N. Formation and degradation of dichloroacetonitrile in drinking waters. *J. Water Supply: Res. Technol. AQUA.* **2001**, *50* (1), 1–13.
- Westerhoff, P.; Mash, H. Dissolved organic nitrogen in drinking water supplies: a review. *J. Water Supply: Res. Technol. –AQUA* **2002**, *51*, 415–448.
- Joo, S. H.; Mitch, W. A. Nitrile, aldehyde, and halonitroalkane formation during chlorination/chloramination of primary amines. *Environ. Sci. Technol.* **2007**, *41*, 1288–1296.
- Chu, W. H.; Gao, N. Y.; Deng, Y. Stability of newfound nitrogenous disinfection byproducts haloacetamides in drinking water. *Chin. J. Org. Chem.* **2009**, *29*, 1569–1574.
- Chen, B. Y.; Westerhoff, P. Predicting disinfection by-product formation potential in water. *Water Res.* **2010**, *44*, 3755–3762.
- Chiang, P. C.; Chang, E. E.; Chuang, C. C.; Liang, C. H.; Huang, C. P. Evaluating and elucidating the formation of nitrogen-contained disinfection by-products during pre-ozonation and chlorination. *Chemosphere* **2010**, *80*, 327–333.
- Shah, A. D.; Mitch, W. A. Halonitroalkanes, halonitriles, haloamides, and N-nitrosamines: A critical review of nitrogenous disinfection byproduct formation pathways. *Environ. Sci. Technol.* **2012**, *46*, 119–131.
- Chu, W. H.; Gao, N. Y.; Deng, Y.; Krasner, S. W. Precursors of dichloroacetamide, an emerging nitrogenous DBP formed during chlorination or chloramination. *Environ. Sci. Technol.* **2010**, *44*, 3908–3912.
- Hou, Y. K.; Chu, W. H.; Ma, M. Carbonaceous and nitrogenous disinfection by-products formation in the surface and ground water treatment plants using Yellow River as water source. *J. Environ. Sci.* **2012**, *24*, 1204–1209.
- Chu, W. H.; Gao, N. Y.; Yang, D.; Templeton, M. R.; Yin, D. Q. Formation of nitrogenous disinfection by-products from pre-chloramination. *Chemosphere* **2011a**, *85*, 1187–1191.
- Chu, W. H.; Gao, N. Y.; Yang, D.; Templeton, M. R.; Yin, D. Q. Impacts of drinking water pretreatments on the formation of nitrogenous disinfection by-products. *Bioresour. Technol.* **2011b**, *102*, 11161–11166.

18. Chu, W. H.; Gao, N. Y.; Templeton, M. R.; Yin, D. Q. Comparison of inclined plate sedimentation and dissolved air flotation for the minimisation of subsequent nitrogenous disinfection by-product formation. *Chemosphere* **2011c**, *83*, 647–651.
19. Chu, W. H.; Gao, N. Y.; Yin, D. Q.; Deng, Y.; Templeton, M. R. Ozone-biological activated carbon integrated treatment for removal of precursors of halogenated nitrogenous disinfection by-products. *Chemosphere* **2012**, *86*, 1087–1091.
20. Barker, D. J.; Stuckey, D. C. A review of soluble microbial products (SMP) in wastewater treatment systems. *Water Res.* **1999**, *33*, 3063–3082.
21. Chen, W.; Westerhoff, P.; Leenheer, J. A.; Booksh, K. Fluorescence excitation–emission matrix regional integration to quantify spectra for dissolved organic matter. *Environ. Sci. Technol.* **2003**, *37*, 5701–5710.
22. Jiang, T. Characterization and modelling of soluble microbial products in membrane bioreactors. Ph.D. Thesis, Ghent University, Belgium, 2007.
23. Zhou, W. L.; Wu, B. T.; She, Q. H.; Chi, L.; Zhang, Z. J. Investigation of soluble microbial products in a full-scale UASB reactor running at low organic loading rate. *Bioresour. Technol.* **2009**, *100*, 3471–3476.
24. Chu, W. H.; Gao, N. Y.; Yin, D. Q.; Krasner, S. W. Formation and speciation of nine haloacetamides, an emerging class of nitrogenous DBPs, during chlorination or chloramination. *J. Hazard. Mater.* **2013**, *260*, 806–812.
25. Edzward, J. K.; Tobiasson, J. E. Enhanced coagulation: US requirements and a broader view. *Water Sci. Technol.* **1999**, *40*, 63–70.
26. Roe, J.; Baker, A.; Bridgeman, J. Relating organic matter character to trihalomethanes formation potential: a data mining approach. *Water Sci. Technol.: Water Supply* **2008**, *8*, 717–723.
27. Nam, S. N.; Krasner, S. W.; Amy, G. L. Differentiating effluent organic matter (EfOM) from natural organic matter (NOM): Impact of EfOM on drinking water sources. In *6th International Symposium on Advanced Environmental Monitoring*; Kim, Y. J., Platt, U., Eds.; Heidelberg, Germany, 2006; pp 259–270.
28. Hoehn, R. C.; Dietrich, A. M.; Farmer, W. S.; Orr, M. P.; Lee, R. G.; Aieta, E. M.; Wood, D. W.; Gordon, G. Household odors associated with the use of chlorine dioxide. *J. Am. Water Works Assoc.* **1990**, *82* (4), 166–172.
29. Huang, J.; Graham, N.; Templeton, M. R.; Zhang, Y.; Collins, C.; Nieuwenhuijsen, M. A comparison of the role of two blue-green algae in THM and HAA formation. *Water Res.* **2009**, *43*, 3009–3018.
30. Thibaud, H.; De Laat, J.; Merlet, N.; Dore, M. Chloropicrin formation in aqueous solution: effect of nitrites on precursors formation during the oxidation of organic compounds. *Water Res.* **1987**, *21*, 813–821.
31. Aiken, G.; Cotsaris, E. Soil and hydrology – their effect on NOM. *J. Am. Water Works Assoc.* **1995**, *87* (1), 36–45.
32. Lee, W. Occurrence, Molecular weight and treatability of dissolved organic nitrogen. Ph.D. Dissertation, Arizona State University, Tempe, AZ, 2005.
33. Mitch, W. A.; Krasner, S. W.; Westerhoff, P.; Dotson, A. *Occurrence and formation of nitrogenous disinfection by-products*; American Water Works Association Research Foundation: Denver, Colorado, 2009.

34. Lee, W. P.; Westerhoff, P.; Esparza-Soto, M. Occurrence and removal of dissolved organic nitrogen in US water treatment plants. *J. Am. Water Works Assoc.* **2006**, *98* (10), 102–110.
35. Pressman, J. G.; Richardson, S. D.; Speth, T. F.; Miltner, R. J.; Narotsky, M. G.; Hunter, E. S.; Rice, G. E.; Teuschler, L. E.; McDonald, A.; Parvez, S.; Krasner, S. K.; Weinberg, H. S.; McKague, A. B.; Parrett, C. J.; Bodin, N.; Chinn, R.; Lee, C. F. T.; Simmons, J. E. Concentration, chlorination and chemical analysis of drinking water disinfection byproduct mixtures health effects research: US EPA's four lab study. *Environ. Sci. Technol.* **2010**, *44*, 7184–7192.
36. Karnik, B. S.; Davies, S. H.; Baumann, M. J.; Masten, S. J. The effects of combined ozonation and filtration on disinfection by-product formation. *Water Res.* **2005**, *39*, 2839–2850.
37. Chiang, P. C.; Chang, E. E.; Chang, P. C.; Huang, C. P. Effects of pre-ozonation on the removal of THM precursors by coagulation. *Sci. Total. Environ.* **2009**, *407*, 5735–5742.
38. Yan, M. Q.; Wang, D. S.; Ma, X. N.; Ni, J. R.; Zhang, H. S. THMs precursor removal by an integrated process of ozonation and biological granular activated carbon for typical Northern China water. *Sep. Purif. Technol.* **2010**, *72*, 263–268.
39. Yapsakli, K.; Mertoglu, B.; Cecen, F. Identification of nitrifiers and nitrification performance in drinking water biological activated carbon (BAC) filtration. *Process Biochem.* **2010**, *45*, 1543–1549.
40. Lee, S. K.; Freitag, D.; Steinberg, C.; Kettrup, A.; Kim, Y. H. Effects of dissolved humic materials on acute toxicity of some organic chemicals to aquatic organisms. *Water Res.* **1993**, *27*, 199–204.
41. Rook, J. J. Formation of haloforms during chlorination of natural waters. *Water Treat. Exam.* **1974**, *23*, 234–239.
42. Xu, B.; Gao, N. Y.; Sun, X. F.; Xia, S. J.; Simonnot, M. O.; Causserand, C.; Rui, M.; Wu, H. H. Characteristics of organic material in Huangpu River and treatability with the O₃-BAC process. *Sep. Purif. Technol.* **2007**, *57*, 348–355.
43. Hu, J.; Jesse, H. S.; Addison, W.; Karanfil, T. Halonitromethane formation potentials in drinking waters. *Water Res.* **2010**, *44*, 105–114.
44. McKnight, D. M.; Boyer, E. W.; Westerhoff, P. K.; Doran, P. T.; Kulbe, T.; Andersen, D. T. Spectrofluorometric characterization of dissolved organic matter for indication of precursor organic material and aromaticity. *Limnol. Oceanogr.* **2001**, *46*, 38–48.
45. Jørgensen, L.; Stedmon, C. A.; Kragh, T.; Markager, S.; Middelboe, M.; Søndergaard, M. Global trends in the fluorescence characteristics and distribution of marine dissolved organic matter. *Mar. Chem.* **2011**, *126*, 139–148.
46. Korshin, G. V.; Li, C. W.; Benjamin, M. M. The decrease of UV absorbance as an indicator of TOX formation. *Water Res.* **1997**, *31*, 946–949.
47. Chellam, S.; Krasner, S. W. Disinfection byproduct relationships and speciation in chlorinated nanofiltered waters. *Environ. Sci. Technol.* **2001**, *35*, 3988–3999.

48. Xue, C. H.; Wang, Q.; Chu, W. H.; Templeton, M. R. The impact of changes in source water quality on trihalomethane and haloacetonitrile formation in chlorinated drinking water. *Chemosphere* **2014**, *117*, 251–255.
49. Santos, D. C.; Silva, L.; Albuquerque, A.; Simões, A.; Gomes, A. C. Biodegradability enhancement and detoxification of cork processing wastewater molecular size fractions by ozone. *Bioresour. Technol.* **2013**, *147*, 143–151.
50. Schiener, P.; Nachaiyasit, S.; Stuckey, D. C. Production of soluble microbial products (SMPs) in an anaerobic baffled reactor: compositin, biodegradability and the effect of process parameters. *Environ. Technol.* **1998**, *19*, 391–400.
51. Carlson, K. H.; Amy, G. L. The importance of soluble microbial products (SMPs) in biological drinking water treatment. *Water Res.* **2000**, *34*, 1386–1396.
52. Kunacheva, C.; Stuckey, D. C. Analytical methods for soluble microbial products (SMP) and extracellular polymers (ECP) in wastewater treatment systems: A review. *Water Res.* **2014**, *61*, 1–18.
53. Rittmann, B. E.; Bae, W.; Namkung, E.; Lu, C. J. A critical evaluation of soluble microbial products in biological processes. *Water Sci. Technol.* **1987**, *19*, 517–528.
54. Potvin, C. M.; Zhou, H. D. Interference by the activated sludge matrix on the analysis of soluble microbial products in wastewater. *Chemosphere* **2011**, *85*, 1139–1145.
55. Boero, V. J.; Bowers, A. R.; Eckenfelder, W. W., Jr Molecular weight distribution of soluble microbial products in biological systems. *Water Sci. Technol.* **1996**, *34*, 241–248.

Chapter 18

Variability of Non-Regulated Disinfection By-Products in Distribution Systems: Impact of the Storage Tank

Christelle Legay,¹ Patrick Levallois,²
Rocio Aranda-Rodriguez,³ Luda Dabeka,³ Joan Hnatiw,³
and Manuel J. Rodriguez*,¹

¹Centre de Recherche en Aménagement et Développement, Université Laval,
Pavillon Félix-Antoine-Savard, 2325 rue des Bibliothèques,
Québec City, QC G1V 0A6, Canada

²Direction de la Santé Environnementale et de la Toxicologie,
Institut National de Santé Publique du Québec, 945 avenue Wolfe,
Québec City, QC G1V 5B3, Canada

³Exposure and Biomonitoring Division, Environmental Health Science
Bureau, Health Canada, EHC, Tunney's Pasture 0800C, bktOttawa, ON
K1A 0K9, Canada

*E-mail: manuel.rodriguez@crad.ulaval.ca.

In this chapter, the spatial variability of non-regulated disinfection by-products (DBPs) in drinking water – haloacetonitriles (HANs), haloacetaldehydes (HAs), haloketones (HKs), chloropicrin (CP) and cyanogen chloride (CNCl) – was investigated in four distribution systems in the Québec City area. Attention was directed to the impact, on DBP levels, of water that is re-chlorinated in distribution system storage tanks. The results show that when there was a storage tank as part of the distribution system, flow through this led to an increase in targeted DBP levels except for CNCl for which levels were systematically lowest at sites located after the storage tank. However, for most DBP families, the variability within the storage tank was different from month to month. Moreover, the impact on DBP levels of water flowing through the storage tank differed between the four systems under study.

This study highlights that, as for regulated DBPs (trihalomethanes-THMs and haloacetic acids-HAAs), the selection of the sampling locations for non-regulated DBP monitoring represents a considerable challenge.

Introduction

Disinfection by-products (DBPs) in drinking water are known to vary within distribution systems. Several factors may influence DBP variability, such as raw water source characteristics, the treatment applied and some distribution system characteristics (1–3). The variability of DBP levels within systems makes it difficult to monitor these compounds.

Past studies have investigated the spatial variability of DBPs, but focused mainly on two prevalent families (trihalomethanes-THMs and haloacetic acids-HAAs) presently regulated in most industrialized countries. However, other non-regulated DBP families occurring at low levels in drinking water are considered as potentially of greater health concern than THMs and HAAs (4). These include, among others, haloacetonitriles (HANs), haloacetaldehydes (HAs), haloketones (HKs), and halonitromethanes (HNMs). A number of studies have focused specifically on the spatial variability of these DBPs within distribution systems where water is disinfected with chlorine (5–10). In Williams et al. (5) and Shin et al. (6), the spatial variability of DBPs within several systems was investigated through comparisons with the levels measured in finished water at the water treatment plant (WTP) and at only one site located in the system (in the middle or at the extremity according to the study). In Golfinopoulos et al. (7), finished water and a large number (eight) of sites were characterized within one distribution system. However, the variation of DBP levels between these sites was not really investigated. Koudjonou et al. (8) investigated the spatial variability of DBP levels within systems by sampling the finished water and water from three sites spatially distributed within each system, yet only one HA species was investigated in this study. Guilherme and Rodriguez (9) considered three sampling sites located in systems under study to investigate the spatial variability of three DBP families. However, the presence of DBPs in finished water was not measured. Moreover, it is important to note that in the above studies, the impact on DBP levels of water flowing through a distribution system storage tank (defined in this paper as the residence time added by the storage tank) was not investigated. Mercier-Shanks et al. (10) focused on the spatial variability of DBPs by sampling various sites spatially dispersed in one distribution system (which is also studied in this chapter), including two sites located after a storage tank with re-chlorination. In this study (10), the impact of water flowing through the storage tank was only briefly discussed, only one system was investigated and DBP families under study were limited (HANs, HKs and one HNM species).

In this chapter, the spatial variability within systems of non-regulated DBPs (HANs, HAs, HKs, one HNM species and cyanogen chloride) was investigated for four distribution systems where water was disinfected with chlorine. The focus was on the impact, on these DBPs, of water flowing through distribution

system storage tanks (where re-chlorination was applied). The variation of this impact according to season was also investigated. Moreover, the evolution within distribution systems of the relationship between the levels of regulated (THMs) and non-regulated DBPs was estimated. To conclude, strategies were discussed to control and survey these non-regulated DBPs within distribution systems for monitoring or exposure assessment studies.

Material and Methods

Case under Study

This study was carried out in four distribution systems located in the greater Québec City area (Province of Quebec, Canada) supplying approximately 350,000 inhabitants. The main characteristics of these systems are presented in Table 1. These systems are supplied by surface water and all apply chlorine as their primary or secondary disinfectant. However, the type of surface water source (e.g., lake, river), type and efficiency of treatment applied before secondary disinfection (e.g., presence of ozonation or not), and distribution system characteristics (e.g., size, hydraulic regime, pipe characteristics) differ between the systems. Each distribution system includes at least one storage tank with a re-chlorination point. However, the re-chlorination strategy applied (injection location, dose) and water residence time in the storage tank vary between the systems (Table 1).

The region under study is subject to important climatic variations during the year, with mean daily temperatures of ambient air ranging from -16.8°C to $+24.2^{\circ}\text{C}$ (11), and different lengths of seasons (i.e., long winters and relatively short summers). These climatic variations can result in great temporal variations in raw water quality.

Water Sampling

Bimonthly sampling campaigns were conducted between August 2006 and December 2007 (for logistical issues, data from the February 2007 campaign were not available). During these campaigns, four water samples were taken in each distribution system: at the finished water outlet the WTP and at three sites located within the distribution system. In order to investigate the impact of water flowing through the storage tank (that includes a re-chlorination step) at least one of these sites was not supplied by the storage tank and at least one was supplied by the storage tank.

The DBP measurements included the analysis of HAs, HANs, HKs, chloropicrin (HNM species and noted CP), cyanogen chloride (CNCl) and THMs (Table 2). Free residual chlorine (FRC) concentration, temperature (T), pH, turbidity and ultraviolet absorbance at 254 nm (UV254) were also measured for each sample.

Table 1. Description of the Four Distribution Systems under Study

<i>Systems</i>	<i>Water source</i>	<i>Main treatment process</i>	<i>Storage tank characteristics</i>		
			<i>Capacity (m³)</i>	<i>Estimated water residence time</i>	<i>Location of re-chlorination</i>
A	St. Lawrence River ^b	Pre-chlorination; PCT ^a ; Post-ozonation; Post-chlorination	4,550	~ 1 day	Outlet
B	St. Lawrence River ^b	Pre-chlorination; PCT ^a ; Post-chlorination	2,275	~ 1.5 days	Outlet
C	Chaudière River	Flocculation; Sedimentation; Inter-chlorination; Filtration; Post-ozonation; Post-chlorination	8,500	~ 4 days	Outlet
D ^c	St. Charles Lake	PCT ^a ; Post-ozonation; Post-chlorination	130,000	~ 3 to 5 days	Entrance and outlet

^a Complete physical-chemical treatment including sieving, coagulation-flocculation, sedimentation and filtration; ^b The location of the raw water intake is different for systems A and B; ^c This system was studied previously by Mercier-Shanks et al. (10)

In each sampling location (public building, private residence or stores), samples were taken at the faucet of the restroom (except for the finished water samples taken at the WTP). Cold tap water was allowed to flow for approximately five minutes to obtain water from the distribution system and not stagnant water from the building pipes. Duplicate samples were collected in 60 mL glass vials containing 1 mL of buffer solution (pH 4.1). In the field, 0.2 mL ascorbic acid solution (0.114 M), used as quenching agent, were added to each bottle just before the sampling. The samples were stored at 4°C until the time of analysis. FRC and T were measured in situ at the same time as the DBP sample collection. 250 mL plastic bottles were used to collect and transport samples for laboratory analysis of the other parameters.

Analytical Procedure

As presented in Table 2, seven HA species (the sum represents HA7), four HAN species (the sum represents HAN4), two HK species (the sum represents HK2), CP, CNCl and four THM species (the sum represents THM4) were analyzed. The analysis of HANs, HAs, HKs, CP, CNCl and THMs was conducted in the Health Canada laboratory and described previously (12–14). Briefly, liquid-liquid extraction was performed with MTBE containing internal standards. The extracts were analyzed using a Varian 3800 gas chromatograph equipped with dual electron capture detectors. Two chromatographic columns were used: a DB-5 column (30 m x 0.32 mm id; film thickness 1 μm) as the primary column, and a DB-1 column (30 m x 0.32 mm id; film thickness 1 μm) for confirmation (15). The method detection limit (MDL) associated with each individual DBP under study is presented in Table 2. Measurements below the MDL were considered as equal to zero.

Measurements of FRC were conducted using the DPD titrimetric method (Standard method 4500-Cl-F) with a DR-890 colorimeter from Hach. Water pH was measured with a Denver instrument AP15 pH/mV/FET meter. Turbidity was analyzed with a Hach 2100N Turbimeter. UV254 results were obtained by UV/visible spectrometry at 254 nm (Hach DR5000) with 5 cm optical path quartz cells.

Data Analysis

In order to investigate the spatial variability of non-regulated DBP levels in the systems under study and, specifically, the impact of water flowing through the storage tank with re-chlorination, sampling sites were divided into three categories according to their location in each system. The first category included the finished water, for which samples were taken at the WTP (noted as “FW” in the tables and figures). The second category included the sampling sites located within the distribution system and directly supplied by the WTP, thus not supplied by a storage tank (noted as “Sup/WTP” in the tables and figures). The third category included only the sites supplied by a storage tank within the distribution system (noted as “Sup/S.tank” in the tables and figures). Depending on the system, the second and third categories might include one or two sampling sites.

Table 2. DBPs under Study

<i>DBPs</i>	<i>Abbreviations</i>	<i>MDL ($\mu\text{g/L}$)</i>
HA7 (sum of the 7 HAs)		
Dichloroacetaldehyde	DCA	0.07
Trichloroacetaldehyde	TCA	0.06
Bromochloroacetaldehyde	BCA	0.05
Dibromoacetaldehyde	DBA	0.05
Bromodichloroacetaldehyde	BDCA	0.04
Chlorodibromoacetaldehyde	CDBA	0.06
Tribromoacetaldehyde	TBA	0.10
HAN4 (sum of the 4 HANs)		
Trichloroacetonitrile	TCAN	0.04
Dichloroacetonitrile	DCAN	0.05
Bromochloroacetonitrile	BCAN	0.06
Dibromoacetonitrile	DBAN	0.05
HK2 (sum of the 2 HKs)		
1,1-dichloro-2-propanone	DCP	0.07
1,1,1-trichloro-2-propanone	TCP	0.06
Chloropicrin	CP	0.04
Cyanogen chloride	CNCl	0.07
THM4 (sum of the 4 THMs)		
Chloroform	TCM	0.41
Bromodichloromethane	BDCM	0.10
Dibromochloromethane	DBCM	0.08
Bromoform	TBM	0.09

MDL represents the method detection limit.

As previously mentioned, this chapter focused mainly on the impact of water flowing through a storage tank with re-chlorination on non-regulated DBPs. THMs were considered in order to determine the evolution within systems of the relationship between regulated and non-regulated DBPs. With this aim in mind, correlation analyses (Spearman rank correlation coefficients- r_s) were conducted (using SPSS Version 22.0) between THM and non-regulated DBP levels and for each category of sampling sites previously described (i.e., FW, Sup/WTP and Sup/S.Tank).

Results and Discussion

DBP Occurrence in the Area under Study

The finished water quality data (at the WTP) for the four distribution systems during the study period are presented in Table 3.

DBP levels measured in each distribution system during the period under study are presented in Table 4. Irrespective of the system under study, the most abundant DBP family among those analyzed was HAs. As previously observed by Koudjonou et al. (8), statistically significant higher HA levels (significance level $p < 0.05$) were found in the three systems using ozonation in the treatment train (i.e., systems A, C and D). Among HAs, TCA (also known as chloral hydrate) was found to be the main species and represented, on average, 58% of HA7. TCA levels up to 24.65 $\mu\text{g/L}$ were found in the distribution systems under study. DCA and BDCA were also important HA species with a mean contribution to HA7 of 26% and 11%, respectively. BCA and CDBA were detected at very low levels (with maximum values of 0.44 $\mu\text{g/L}$ and 0.66 $\mu\text{g/L}$, respectively), while TBA and BDA were not detected in these systems.

Table 3. Average Characteristics of Finished Water at the WTP for the Four Systems during the Study Period

<i>Systems</i>	<i>T</i> (°C)	<i>FRC</i> (mg/L)	<i>pH</i>	<i>Turbidity</i> (NTU)	<i>UV₂₅₄</i> (cm^{-1})
A	13.1(9.4)	1.02(0.18)	7.39(0.24)	0.10(0.03)	0.024(0.006)
B	13.0(9.3)	1.05(0.23)	7.25(0.12)	0.14(0.07)	0.033(0.005)
C	11.6(9.3)	1.37(0.50)	7.53(0.26)	0.24(0.12)	0.028(0.007)
D	13.4(8.3)	1.36(0.12)	7.65(0.13)	0.32(0.11)	0.027(0.007)

Standard deviation values are shown into parenthesis. For each system and parameter $n=8$ except for UV_{254} which $n=7$.

HKs were the second major DBP family detected among those evaluated (Table 4) with HK2 levels ranging from 0.07 to 16.10 $\mu\text{g/L}$. TCP represented 60% to 100% of HK2 with levels varying between 0.07 and 15.02 $\mu\text{g/L}$. DCP was measured at lower levels with a maximum value of 3.41 $\mu\text{g/L}$. The same order of magnitude for HK levels was observed in the past for system D (10).

Table 4. Mean DBP Levels (µg/L) Found in the Four Systems during the Study Period

<i>Systems</i>	<i>FW</i>	<i>HA7 Sup/ WTP</i>	<i>Sup/ S.Tank</i>	<i>FW</i>	<i>HAN4 Sup/ WTP</i>	<i>Sup/ S.Tank</i>	<i>FW</i>	<i>HK2 Sup/ WTP</i>	<i>Sup/ S.Tank</i>
A	6.18	9.23	15.09	1.88	2.61	3.44	3.53	4.85	6.77
B	2.61	4.12	6.97	1.15	1.80	3.25	2.13	2.71	3.52
C	8.68	12.0	13.31	1.40	1.96	2.27	7.17	8.40	8.52
D	2.17	7.81	11.59	0.38	1.43	1.86	1.10	3.19	3.98

<i>Systems</i>	<i>FW</i>	<i>CP Sup/ WTP</i>	<i>Sup/ S.Tank</i>	<i>FW</i>	<i>CNCl Sup/ WTP</i>	<i>Sup/ S.Tank</i>
A	0.13	0.20	0.50	1.62	1.38	0.26
B	0.08	0.09	0.12	0.57	0.79	0.35
C	0.29	0.44	0.53	1.79	0.64	0.24
D	0.04	0.21	0.36	0.75	0.14	0.05

FW represents the finished water at the WTP. Sup/WTP represents the average of the sampling sites directly supplied by the WTP. Sup/S.Tank represents the average of the sampling sites supplied by the storage tank. For each system and parameter n=32.

HANs were detected in more than 99% of samples although they occurred at lower levels than HAs and HKs. Measured HAN4 levels (above MDL) ranged, during the period under study, from 0.07 (system D) to 5.58 $\mu\text{g/L}$ (system A). HAN levels were in the same order of magnitude relative to those previously measured in system D (10). DCAN was the main HAN species with a mean contribution to HAN4 of 92%. With a maximum value of 5.38 $\mu\text{g/L}$, DCAN levels measured in the study area were well below the World Health Organization provisional guideline value of 20 $\mu\text{g/L}$ for this compound (16). The rest of HAN4 was composed mainly of BCAN with levels not exceeding 0.83 $\mu\text{g/L}$. In fact, TCAN and DBAN were rarely detected.

CNCl and CP are detected in more than 93% of samples, but at very low levels. CP levels (above MDL) varied, in the four distribution systems investigated during the period under study, between 0.04 and 1.43 $\mu\text{g/L}$. Relatively similar levels were found in the past for system D (10). For CNCl, levels ranging from 0.07 to 3.84 $\mu\text{g/L}$ were measured during the study period.

Spatial Variability of Non-Regulated DBP Levels within Distribution Systems

The mean DBP levels found for each category of sampling sites in each distribution system are presented in Table 4. As observed in this table, the mean HA7 level tended to increase between the WTP and sites not supplied by the storage tank (i.e., directly supplied by the WTP) with an increasing factor ranging from 1.4 to 3.6 according to the system. However, this increase was only statistically significant ($p < 0.05$) for system D. Previous studies also observed an increase of TCA (the main HA species) levels with long water residence times (5, 8). Water flowing through the storage tank (including re-chlorination) also involved an increase of HA7 levels compared to levels measured at the WTP (not statistically significant at $p < 0.05$ for system C) from 1.5 to 5.3 times according to the system. This increase was due mainly to the water residence time in pipes during water transit until the storage tank, the water residence time within the storage tank (extension of DBP formation reactions) and the chlorine addition at the outlet of the latter (and the entrance for system D). Differences in the mean HA7 level between sites not supplied by the storage tank and sites supplied by the storage tank were only statistically significant for systems A and B. For these two systems, the mean FRC concentrations measured at sites supplied by the storage tank were lower than those observed for systems C and D (Table 5). It is important to note that the information about chlorine dose at the storage tank was not available for the majority of the systems under study.

As observed for HA7, the mean HK2 levels also varied within the systems (Table 4). In systems A, B and C, the mean HK2 level measured at sites not supplied by the storage tank was from 1.2 to 1.4 times higher (only statistically significant at level $p < 0.05$ for system A) than the mean level measured at the WTP. In the case of system D, the mean HK2 level measured at sites not supplied by the storage tank was 2.9 times higher than the level measured at the WTP (statistically significant at level $p < 0.05$). Water flowing through the storage tank also impacted HK2 with a mean level after the storage tank being 1.2 to 3.6 times higher (not

statistically significant at level $\rho < 0.05$ for system C) than the level measured at the WTP. The system A was the only system for which the HK2 mean level measured after the storage tank was significantly (level $\rho < 0.05$) different from the level measured at sites not supplied by the storage tank. Figure 2 demonstrates that the pattern of spatial variability of HK2 is not representative of the pattern observed for each individual HK species. In fact, as observed in previous studies (5–7, 10), the mean DCP level tended to decrease after water flowing through the storage tank (only statistically significant at level $\rho < 0.05$ for systems B and C). These results were probably due to the decomposition of DCP after the consumption of the majority of HK precursors into other compounds (10, 17). The mean TCP level increased between the WTP and sites not supplied by the storage tank (only statistically significant at level $\rho < 0.05$ for systems A and D) and also between WTP and sites located after the storage tank (not statistically significant at level $\rho < 0.05$ for system C) (Figure 2).

Table 5. Spatial Distribution of FRC Concentrations in the Four Systems during the Study Period

<i>Systems</i>	<i>FW</i>	<i>Sup/WTP</i>	<i>Sup/S.Tank</i>
A	1.02(0.80-1.32)	0.52(0.08-0.87)	0.20(0.04-0.42)
B	1.05(0.74-1.28)	0.71(0.27-1.47)	0.56(0.05-1.66)
C	1.37(0.61-1.92)	0.73(0.28-1.34)	0.73(0.00-1.74)
D	1.36(1.13-1.46)	0.73(0.22-1.21)	0.91(0.36-1.38)

FW represents the finished water at the WTP. Sup/WTP represents the average of the sampling sites directly supplied by the WTP. Sup/S.Tank represents the average of the sampling sites supplied by the storage tank. The range of FRC values measured in each system during the study period is shown into parenthesis.

The mean HAN4 level tended to increase within systems at sites not supplied by the storage tank (Table 4) with levels being 1.4 and 3.8 times higher than the level measured at the WTP. However, this increase was only statistically significant ($\rho < 0.05$) for system D. The increase of HAN levels related to the water residence time was observed previously in system D (10) and in other studies (5, 6). The water flowing through the storage tank resulted in a mean HAN4 level of, depending on the system, 1.6 to 4.9 times higher than the level measured at the WTP (not statistically significant at level $\rho < 0.05$ for system

C). Mercier-Shanks et al. (10) highlighted an increase of HAN4 levels in water flowing through the storage tank, but found a decrease of TCAN levels during summer for system D. Differences in the mean HAN4 levels measured at sites not supplied by the storage tank and those located after the storage tank were only statistically significant ($p < 0.05$) for system B. The absence of ozonation at WTP in system B could partially explain the higher mean HAN4 level compared to the other systems (18).

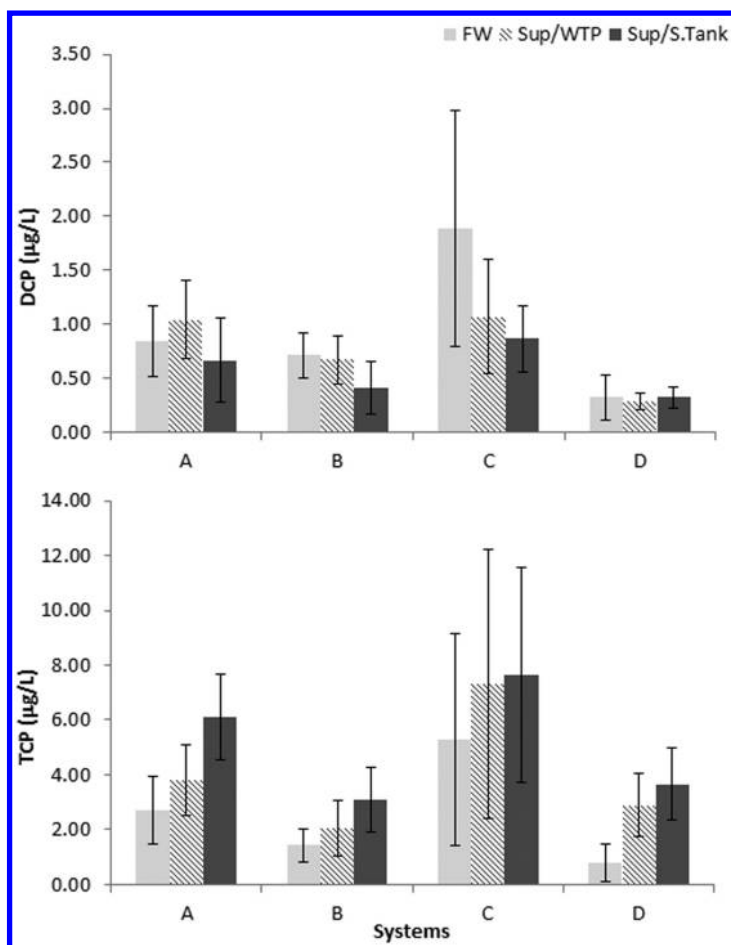


Figure 1. Spatial distribution of individual HK levels in the four systems under study. Error bars represent standard deviation values. FW represents the finished water at the WTP. Sup/WTP represents the average of the sampling sites directly supplied by the WTP. Sup/S.Tank represents the average of the sampling sites supplied by the storage tank.

As observed in previous studies (5, 6, 10), the mean CP level increased with the water residence time (Table 4). The spatial variability was only statistically significant ($p < 0.05$) for systems A and D. Again, the absence of ozonation in system B might partially explain the low formation and spatial variations of CP within this system (19). For systems A and D, the impact of water flowing through the storage tank on CP levels was relatively high with an increase of the mean level (compared to the measured level at the WTP) of 9.0 and 3.8 times, respectively. It is important to remember that CP was measured at very low levels in the systems under study.

Contrary to the other DBP families, the mean level of CNCI decreased within systems (Table 4) due to its decomposition (20). For system B, the mean CNCI level appeared to increase at sites not supplied by the storage tank (not statistically significant at level $p < 0.05$) and to decrease (statistically significant at level $p < 0.05$) at site supplied by the storage tank. In the other systems, a decrease of the mean CNCI level was observed at sites not supplied by the storage tank (not statistically significant at level $p < 0.05$ for system A). This increase was relatively important for systems C and D. Irrespective of the system, the mean CNCI level was lowest (statistically significant at level $p < 0.05$) after the storage tank.

Temporal Variability of the Impact of Water Flowing through the Storage Tank

As previously discussed, DBP levels varied within the distribution systems under study and their fate was affected by the presence of a storage tank (with a re-chlorination step). The influence of the sampling period (i.e., months) on the impact of water flowing through the storage tank was investigated more specifically in this section. It is important to remember that the data from the February campaign were not available.

Regardless of the sampling month, the HA7 levels measured after the storage tank were higher than the levels measured at the WTP (Figure 2) except for August 2006 in system C where one of the two sites located after the storage tank had levels below this measured at WTP. However, this increase of HA7 levels in water that has flowed through the storage tank also varied throughout the year and was generally higher in summer and fall (in terms of change in level between WTP and after the storage tank and not in terms of impact factor). These results could partially be associated with the increase of reaction kinetics in warmer waters (21, 22) and the seasonal variation of the nature and quantity of organic precursors (21). In the case of system C (Figure 2), the HA7 level measured at one of the two sites located after the storage tank was lower than what was measured at the WTP during August 2006. It was also lower than the levels measured at the site not supplied by the storage tank during October and December 2006, and August 2007. This decrease of HA7 levels was most likely associated, in part, with the absence of FRC at this site (FRC concentration was below 0.05 mg/L for five of the eight campaigns) might be due to a long residence time after the storage tank for water. In fact, Koudjonou et al. (8) highlighted the potential transformation of TCA to chloroform in warm waters associated with long residence times.

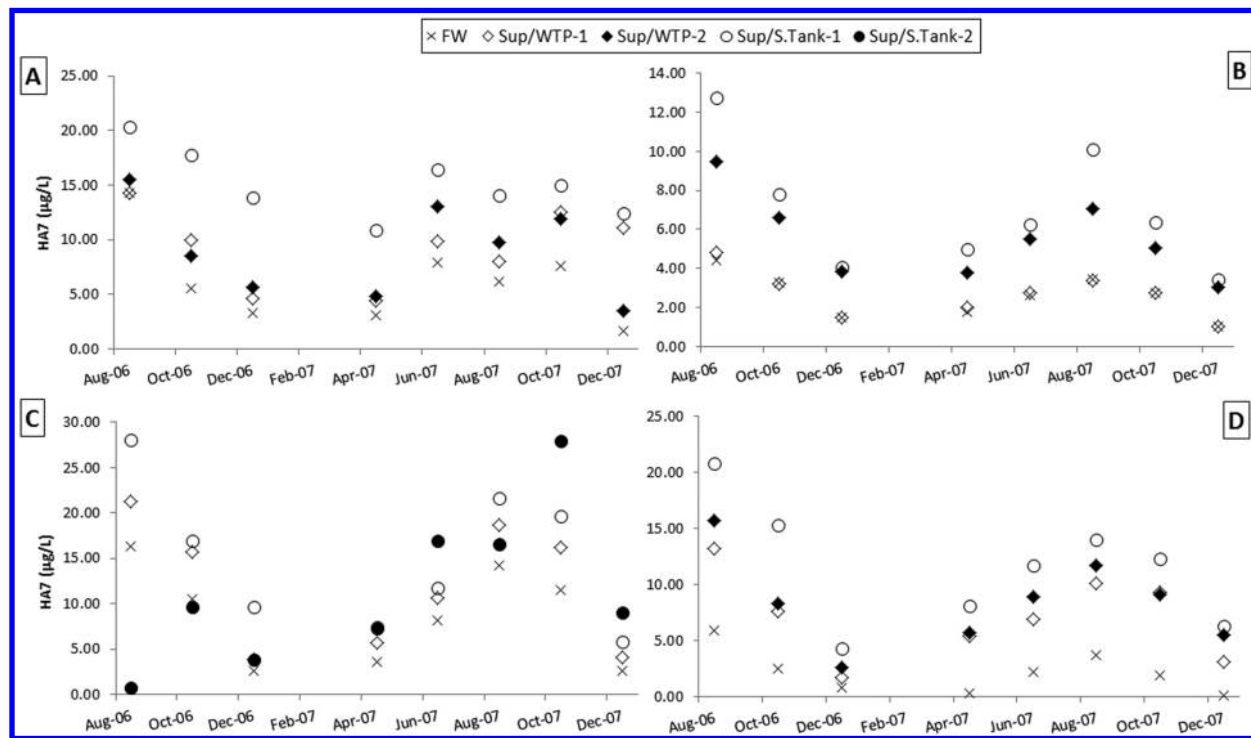


Figure 2. Temporal variations of spatial distribution of HA7 levels for systems A, B, C and D. Sup/WTP-1 and Sup/WTP-2 represent the individual sampling sites directly supplied by the WTP. Sup/S.Tank-1 and Sup/S.Tank-2 represent those supplied by the storage tank.

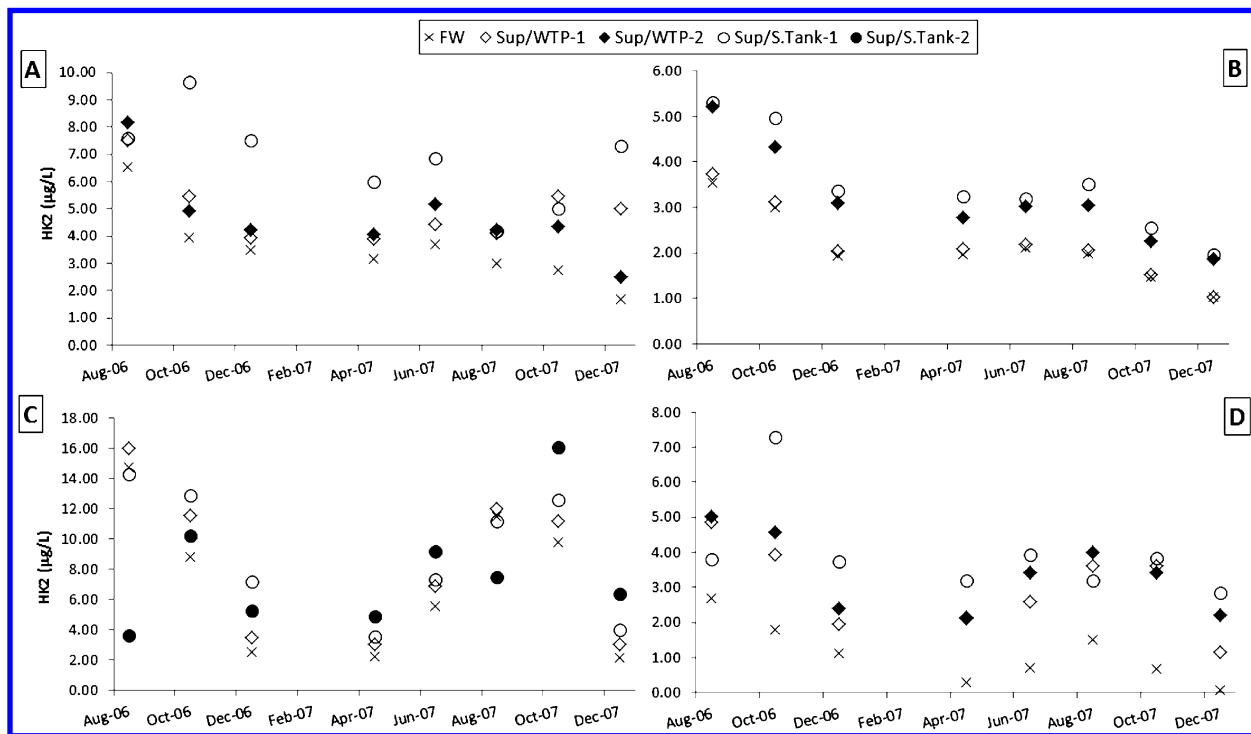


Figure 3. Temporal variations of spatial distribution of HK2 levels for systems A, B, C and D. Sup/WTP-1 and Sup/WTP-2 represent the individual sampling sites directly supplied by the WTP. Sup/S.Tank-1 and Sup/S.Tank-2 represent those supplied by the storage tank.

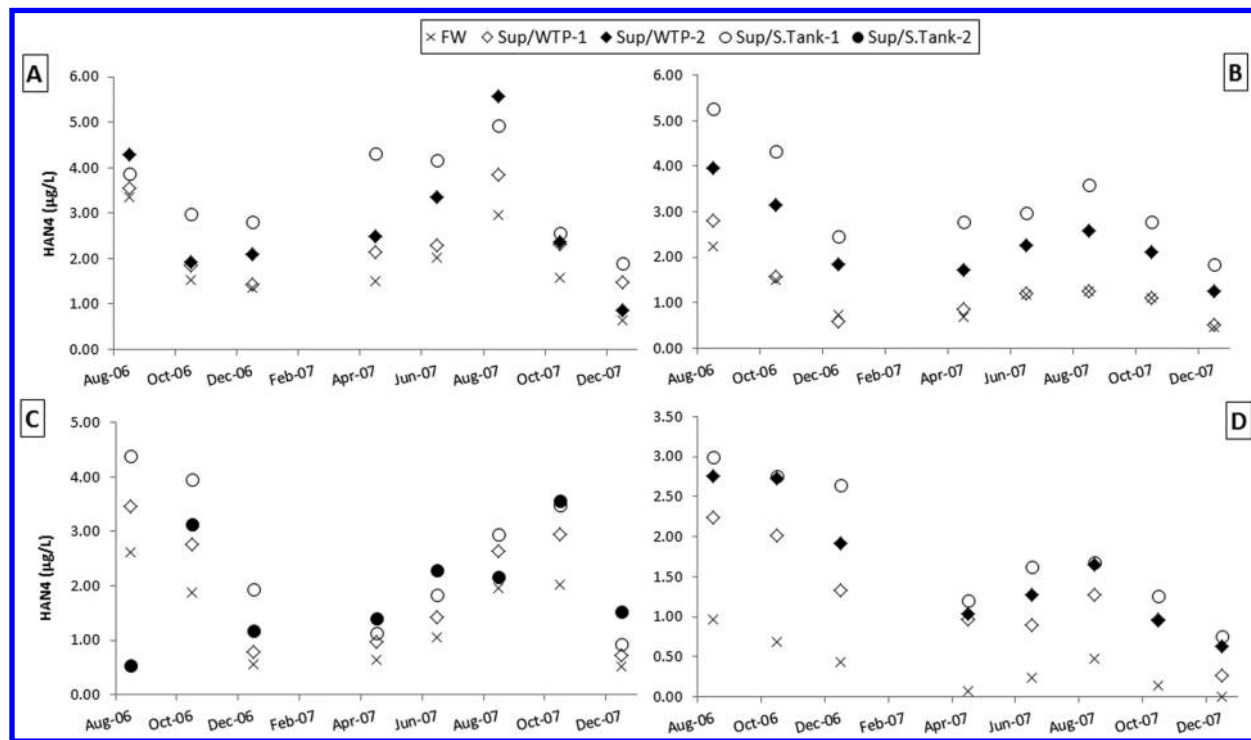


Figure 4. Temporal variations of spatial distribution of HAN4 levels for systems A, B, C and D. Sup/WTP-1 and Sup/WTP-2 represent the individual sampling sites directly supplied by the WTP. Sup/S.Tank-1 and Sup/S.Tank-2 represent those supplied by the storage tank.

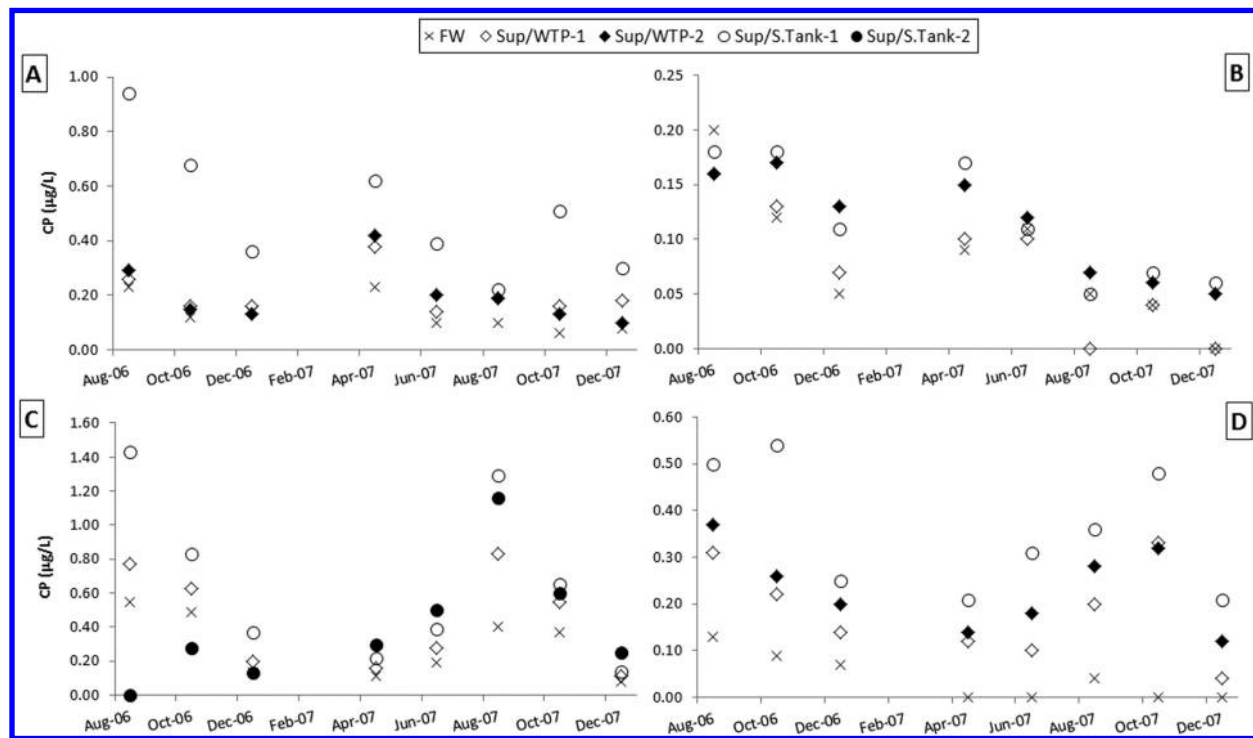


Figure 5. Temporal variations of spatial distribution of CP levels for systems A, B, C and D. Sup/WTP-1 and Sup/WTP-2 represent the individual sampling sites directly supplied by the WTP. Sup/S.Tank-1 and Sup/S.Tank-2 represent those supplied by the storage tank.

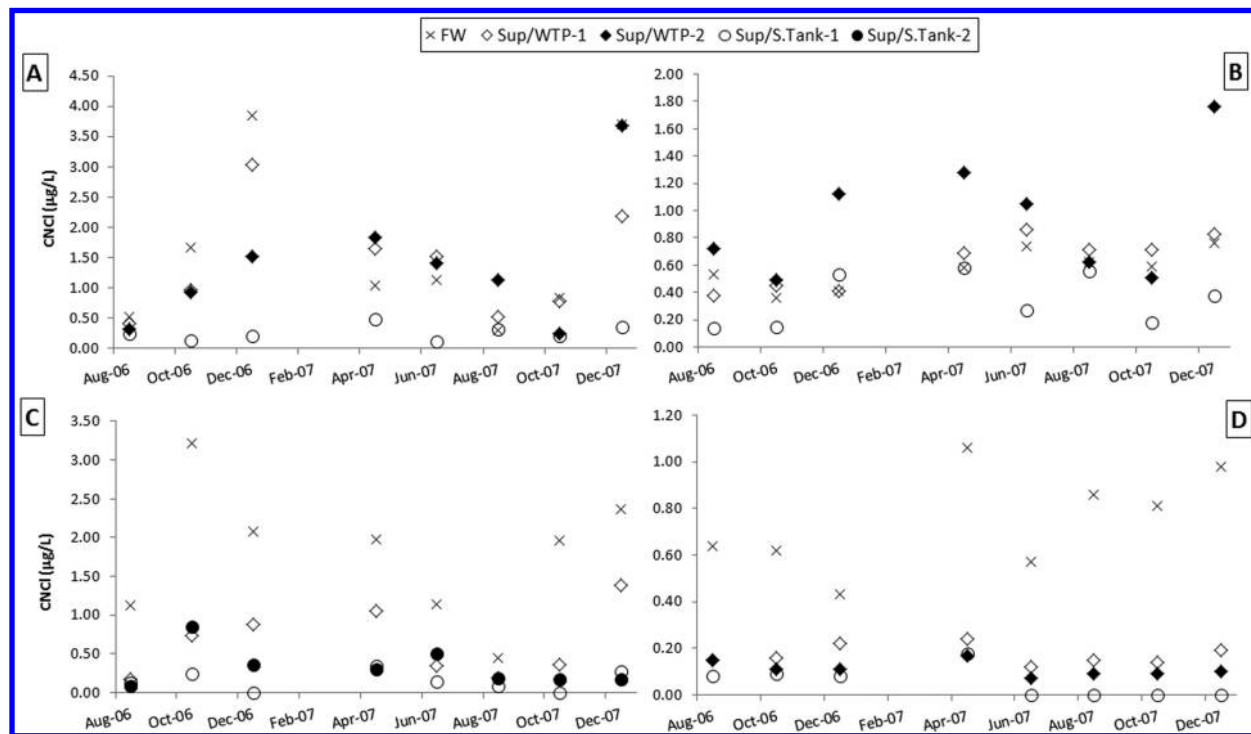


Figure 6. Temporal variations of spatial distribution of CNCl levels for systems A, B, C and D. Sup/WTP-1 and Sup/WTP-2 represent the individual sampling sites directly supplied by the WTP. Sup/S.Tank-1 and Sup/S.Tank-2 represent those supplied by the storage tank.

The temporal variations of the impact of water flowing through the storage tank on the HK2 level are illustrated in Figure 3. For systems A, C and D, the increase of the HK2 level between the WTP and sites located after the storage tank was lower in August, in terms of level and impact factor than the other months, even with a decrease of the HK2 level for one of the two sites of system C (for which the FRC concentration was generally very low). Moreover, for systems A, C (in this case, for the second site located after the storage tank) and D, the HK2 levels measured at a the sampling point after the storage tank were similar to or below those measured at some sites not supplied by the storage tank during several periods of the year. These results might be due mainly to the degradation of TCP (presents at higher levels than DCP in the study area) at longer water residence times (associated with flow through the storage tank) in water warm conditions (10, 17). In the case of system B, water flowing through the storage tank resulted systematically in an increase of HK2 level compared to levels measured at the WTP.

Increases in HAN4 levels associated with water flowing through the storage tank were observed during all sampling campaigns except in August 2006 for system C (Figure 4). For this system, a decrease was observed at one of the two sites located after the storage tank. HAN4 levels close to or below those measured at some sites not supplied by the storage tank were observed after the storage tank for systems A, C and D during August months. Mercier-Shanks et al. (10) did not report a decrease of DCAN and BCAN (representing the main HAN species detected in the systems under study) after the storage tank. However, the likelihood of dihaloacetonitriles being degraded with increased time and at higher pH was reported previously (2, 23). For system B, the levels measured at sites located after the storage tank were systematically the highest (Figure 4).

The impact of water flowing through the storage tank on CP levels also varied between sampling campaigns in the distribution systems investigated (Figure 5). CP levels measured after the storage tank were higher than those measured at the WTP except in systems B and C (in the latter, for only one of two sites located after the storage tank) during summer. In general, it is relatively difficult to define a temporal pattern of variability for the impact of water flowing through the storage tank on CP.

Regardless of the sampling campaign, CNCl levels measured after water flowing through the storage tank were lower than those measured at the WTP (Figure 6).

Relationship between Regulated and Non-Regulated DBPs within Systems

Correlations between THMs and non-regulated DBPs obtained for each category of sampling sites (FW, Sup/WTP and Sup/S.Tank) are presented in Table 6. Results show that in the finished water at the WTP, THM4 were very highly correlated (positively) with HAN4. THM4 were also strongly correlated with HA7 and HK2 and more moderately with CP. For sites directly supplied by the WTP, the correlations between these non-regulated DBPs and THM4 were relatively similar (Table 6). In the case of sites supplied by the storage tank, results show that the correlations between THM4 and, HA7, HAN4, HK2 and CP

were lower than those observed for finished water and for sites directly supplied by the WTP. This decrease in correlations was especially pronounced for HAN4 and HK2. Whatever the location within the system, THM4 and CNCl were not correlated (not statistically significant at level $\rho < 0.05$).

Previous studies have produced both comparable and contrasting correlations between THM4 and non-regulated DBPs (10, 24–26). However, in these studies the spatial variability of correlations associated with the presence of a storage tank was not investigated.

Table 6. Spearman Rank Correlation Coefficients (r_s) between THM4 and Non-Regulated DBP Levels within Systems

<i>Location</i>	<i>HA7</i>	<i>HAN4</i>	<i>HK2</i>	<i>CP</i>	<i>CNCl</i>
FW	0.81**	0.98**	0.83**	0.67**	-0.12
Sup/WTP	0.79**	0.91**	0.83**	0.57**	-0.05
Sup/S.Tank	0.70**	0.62**	0.53**	0.51**	-0.19

FW represents the finished water at the WTP. Sup/WTP represents the sampling sites directly supplied by the WTP. Sup/S.Tank represents the sampling sites supplied by the storage tank. Spearman rank correlation coefficients were calculated with DBP data obtained for the four systems and for the entire period under study. ** Correlation statistically significant at level $\rho < 0.01$.

Control and Monitoring of Non-Regulated DBP Levels

This study highlights that non-regulated DBPs varied significantly within the investigated systems. Except for CNCl, higher levels were generally measured at sites located after the storage tank where chlorine was added. However, the impact of water flowing through the storage tank, with a re-chlorination step, on the level of the investigated DBP differed during the year and between systems. This might be explained by the fact that several factors influence the formation and degradation of DBPs after water flowing through a storage tank. One possible factor is the water quality supplying the storage tank which, in turn, depends on the quality of treated water from the WTP (e.g., pH, amount and nature of natural organic matter, residual chlorine) and on the distribution conditions (e.g., water residence time, age and materials of pipes, presence of biofilm). The hydraulic characteristics of the storage tank (on which the water residence time is dependent) and the re-chlorination factors – chlorine dose and the injection location in the storage tank (at the entrance or/and at the outlet) – also affect DBP formation and degradation within and downstream of the storage tank. Storage tank management strategies may include optimization to minimize DBP levels within the distribution system. For this, further investigations focusing more specifically on the study of storage tank impact on DBPs should be conducted in order to compare water quality between the storage tank entrance and points

located immediately before and after re-chlorination at different periods of the year and with variable hydraulic regimes. Since storage tank characteristics and management differ from one distribution system to another, generalizing (for all systems) the impact of water flowing through a storage tank, where re-chlorination is done, on DBPs is not recommended.

As observed for regulated DBPs (e.g., THMs and HAAs), the high spatial variability of non-regulated DBP levels in distribution systems results in difficulties in selecting sampling locations for regulatory monitoring, managing issues and exposure assessment purposes. Except for CNCl, sites located after the storage tank may be selected for future regulatory monitoring of the DBPs studied in this chapter. Moreover, results suggest that sites where FRC concentration is very low (particularly in summer) do not necessarily represent the best locations for these regulatory survey purposes. In the case of exposure assessment studies, results presented in this chapter demonstrate that one sampling site for a system is probably not sufficient to estimate the public's exposure to these DBPs. This is exacerbated by the fact that DBP levels vary, according to the season and system, between sites supplied by the same water infrastructure (i.e., directly by the WTP or by the storage tank). Results also showed that THM levels could be used as a potential indicator of some non-regulated DBPs. However, the efficiency of THMs as indicator for other DBPs tended to decrease after water flowing through the storage tank where re-chlorination was applied.

Acknowledgments

The authors extend their gratitude to the Drinking Water Research Chair of Université Laval (Quebec City, Canada) and its partners (NSERC, Cities of Québec, Lévis and Saint-Jérôme, Avensys Solutions, SNC-Lavalin, Association pour la protection de l'environnement du lac Saint-Charles et des Marais du Nord (APEL)). The authors are also grateful to Sabrina Simard, Sylvie Leduc, Sonia Poulin and Annick Dion-Fortier for their laboratory technical support and to all those who participated in the collection of samples.

References

1. Rodriguez, M. J.; Serodes, J.; Levallois, P. Behavior of trihalomethanes and haloacetic acids in a drinking water distribution system. *Water Res.* **2004**, *38*, 4367–4382.
2. Hua, G. H.; Reckhow, D. A. DBP formation during chlorination and chloramination: Effect of reaction time, pH, dosage, and temperature. *J. – Am. Water Works Assoc.* **2008**, *100*, 82–95.
3. Krasner, S. W. The formation and control of emerging disinfection by-products of health concern. *Philos. Trans. R. Soc., A* **2009**, *367*, 4077–95.
4. Richardson, S. D.; Plewa, M. J.; Wagner, E. D.; Schoeny, R.; DeMarini, D. M. Occurrence, genotoxicity, and carcinogenicity of regulated and emerging

- disinfection by-products in drinking water: A review and roadmap for research. *Mutat. Res.* **2007**, *636*, 178–242.
- Williams, D. T.; LeBel, G. L.; Benoit, F. M. Disinfection by-products in Canadian drinking water. *Chemosphere* **1997**, *34*, 299–316.
 - Shin, D.; Chung, Y.; Choi, Y.; Kim, J.; Park, Y.; Kum, H. Assessment of disinfection by-products in drinking water in Korea. *J. Exposure Anal. Environ. Epidemiol.* **1999**, *9*, 192–199.
 - Golfinopoulos, S. K.; Nikolaou, A. D.; Lekkas, T. D. The occurrence of disinfection by-products in the drinking water of Athens, Greece. *Environ. Sci. Pollut. Res.* **2003**, *10*, 368–372.
 - Koudjonou, B.; LeBel, G. L.; Dabeka, L. Formation of halogenated acetaldehydes, and occurrence in Canadian drinking water. *Chemosphere* **2008**, *72*, 875–881.
 - Guilherme, S.; Rodriguez, M. J. Occurrence of regulated and non-regulated disinfection by-products in small drinking water systems. *Chemosphere* **2014**, *117*, 425–432.
 - Mercier-Shanks, C.; Sérodes, J.-B.; Rodriguez, M. J. Spatio-temporal variability of non-regulated disinfection by-products within a drinking water distribution network. *Water Res.* **2013**, *47*, 3231–3243.
 - Environnement Canada. *Normales et moyennes climatiques au Canada 1971-2000*. Service météorologique du Canada; http://climate.weather.gc.ca/climate_normals/index_f.html (date accessed: 11 December 2013)
 - LeBel, G. L.; Williams, D. T. Assessment of a method, optimized for cyanogen chloride, for the analysis of Method 551 target DBP compounds. In *Proc. – Water Qual. Technol. Conf. Expo.*, Boston, MA, 1996.
 - LeBel, G. L.; Benoit, F. M. Chloral hydrate in Canadian drinking water. In *Proc. – Water Qual. Technol. Conf. Expo.*, Salt Lake City, UT, 2000.
 - Koudjonou, B. K.; Lebel, G. L. Halogenated acetaldehydes: Analysis, stability and fate in drinking water. *Chemosphere* **2006**, *64*, 795–802.
 - Aranda-Rodriguez, R.; Koudjonou, B.; Jay, B.; Lebel, G. L.; Benoit, F. M. Disinfection by-products (DBPs) in drinking water from eight systems using chlorine dioxide. *Water Qual. Res. J. Can.* **2008**, *43*, 11–22.
 - World Health Organization (WHO). *Guidelines for drinking-water quality*, 4th ed.; World Health Organization: Geneva, Switzerland, 2011.
 - Nikolaou, A. D.; Lekkas, T. D.; Kostopoulou, M. N.; Golfinopoulos, S. K. Investigation of the behaviour of halo ketones in water samples. *Chemosphere* **2001**, *44*, 907–912.
 - Hua, G.; Reckhow, D. A. Effect of pre-ozonation on the formation and speciation of DBPs. *Water Res.* **2013**, *47*, 4322–30.
 - Hu, J.; Song, H.; Karanfil, T. Comparative analysis of halonitromethane and trihalomethane formation and speciation in drinking water: the effects of disinfectants, pH, bromide, and nitrite. *Environ. Sci. Technol.* **2010**, *44*, 794–799.
 - Na, C. Z.; Olson, T. M. Stability of cyanogen chloride in the presence of free chlorine and monochloramine. *Environ. Sci. Technol.* **2004**, *38*, 6037–6043.

21. Singer, P. Control of disinfection by-products in drinking water. *J Environ. Eng.* **1994**, *120*, 727–744.
22. Hong, H.; Xiong, Y.; Ruan, M.; Liao, F.; Lin, H.; Liang, Y. Factors affecting THMs, HAAs and HNMs formation of Jin Lan Reservoir water exposed to chlorine and monochloramine. *Sci. Total Environ.* **2013**, *444*, 196–204.
23. Reckhow, D. A.; Platt, T. L.; MacNeill, A. L.; McClellan, J. N. Formation and degradation of dichloroacetonitrile in drinking waters. *J. Water Supply: Res. Technol.-AQUA* **2001**, *50*, 1–13.
24. Villanueva, C. M.; Castano-Vinyals, G.; Moreno, V.; Carrasco-Turigas, G.; Aragonés, N.; Boldo, E.; Ardanaz, E.; Toledo, E.; Altzibar, J. M.; Zaldúa, I.; Azpiroz, L.; Goni, F.; Tardon, A.; Molina, A. J.; Martín, V.; Lopez-Rojo, C.; Jimenez-Moleon, J. J.; Capelo, R.; Gomez-Acebo, I.; Peiro, R.; Ripoll, M.; Gracia-Lavedan, E.; Nieuwenhuysen, M. J.; Rantakokko, P.; Goslan, E. H.; Pollan, M.; Kogevinas, M. Concentrations and correlations of disinfection by-products in municipal drinking water from an exposure assessment perspective. *Environ. Res.* **2012**, *114*, 1–1.1.
25. Gan, W.; Guo, W.; Mo, J.; He, Y.; Liu, Y.; Liu, W.; Liang, Y.; Yang, X. The occurrence of disinfection by-products in municipal drinking water in China's Pearl River Delta and a multipathway cancer risk assessment. *Sci. Total Environ.* **2013**, *447*, 108–115.
26. Wei, J. R.; Ye, B. X.; Wang, W. Y.; Yang, L. S.; Tao, J.; Hang, Z. Y. Spatial and temporal evaluations of disinfection by-products in drinking water distribution systems in Beijing, China. *Sci. Total Environ.* **2010**, *408*, 4600–4606.

Chapter 19

Chloral Hydrate Control by Point-of-Use and Household Appliances

Baiyang Chen,* Xiaoqi Guo, Zhong Tang, and Wenbiao Jin

Harbin Institute of Technology Shenzhen Graduate School,
Shenzhen Key Laboratory of Water Resource Utilization and Environmental
Pollution Control, Shenzhen, China, 518055

*E-mail: poplar_chen@hotmail.com. Phone: 86-134-80727605.

Unlike other pollutants occurring in raw water, disinfection by-product (DBP) is usually produced at the end point of the drinking water treatment plant (DWTP) and, once formed, it cannot be readily removed by engineering processes. As a result, treatments of existing DBP by point-of-use and/or household appliances have become the last line of defense in alleviating the impact of DBP for general family. In this study, we evaluated the effectiveness of several residential options, including reverse osmosis (RO) and granular activated carbon (GAC) cartridges, microwave oven, boiler, and ultrasonic cleaner, on the removal of chloral hydrate (CH) under various operating (e.g., power, stirring speed) and environmental (e.g., pH, initial concentration) conditions. The results indicate that heating by either boiler or microwave oven can reduce CH from tap water significantly (>90%) under automatic switch-off conditions. The degree of removal by heating was always greater in tap water than in ultrapure water, implying that certain compounds or residual chlorine in tap may have accelerated the CH transformation process, while CH removal in ultrapure water is mainly controlled by thermal hydrolysis. In contrast, volatilization by stirring or sonication exhibited little capacity (<5%) to remove CH. RO cartridge eliminated >90% of CH regardless of operating pressure, initial CH concentration, pH, and type of water, proving it as a robust tool in dealing with drinking water issues. Cartridges with GAC showed some potentials (45~90%) for CH removal, which were much greater

than cartridges made by PP cotton and carbon block filter (<5%); however, the adsorption ability of GAC can be highly compromised by rapid flowrate and limited retention time, which suggests that GAC adsorption is not the major contributor to CH removal in a commercial water purifier. Overall, the data have proven the effectiveness of many POU and household appliances on CH removal, and may help consumers to relieve DBP concerns in case of emergency.

Introduction

Chloral hydrate (CH) is the third most prevalent disinfection by-product (DBP) detected in water, after trihalomethane (THM) and haloacetic acid (HAA). Its occurrence has been widely reported around the world at levels up to 100 $\mu\text{g/L}$, but mostly below 10 $\mu\text{g/L}$ (1–3). Due to its potential toxicity related to DNA damage (4), carcinogenicity (5) and a series of health risks (6), CH has been regulated by the Chinese government (GB5749-2006) and is proposed to be regulated in Austria (7) and the World Health Organization guideline (8). The maximum contaminant level (MCL) is set as 10 $\mu\text{g/L}$ in China and by the WHO, and proposed to be 20 $\mu\text{g/L}$ in Austria. While accidents involving CH are not frequently reported, around 10% of finished waters from US drinking water treatment plants (DWTPs) have CH levels greater than 10 $\mu\text{g/L}$ under the Information Collection Rule (9), suggesting that CH may pose a risk in some regions and thus deserves more attention in future DBP studies.

In early studies, the control methods to remove CH from drinking water mostly focused on the removal of DBP precursors (8, 10–12), but not existing DBPs (i.e., preformed DBPs) (13). Although some post-formation methods have been evaluated, such as γ -irradiation (14), solar photolysis (15, 16), synthetic goethite and magnetite (17), and electrochemical reduction (18), they are somewhat difficult to apply in distribution systems or at the point of use (POU). Only a few studies have examined the effectiveness of household devices, such as boiling pot, on CH controls (19, 20); however, the boiling time in those experiments often took more than 1 minute to achieve the desired result, which is perhaps impractical because most commercial boilers are now equipped with an automatic switch-off function, meaning that the boiling effect may last for only seconds under normal operating conditions.

Of all drinking water DBP control strategies, treating DBP after its formation by POU and household facilities has never been the favorite option. Rather, removing DBP precursors from raw water before disinfection (12) and/or altering disinfectant agents and operating conditions (8) has often been applied in practice to meet the regulatory limit. The preference of pre-formation measures is likely related to the cost and efficiency advantages of DWTP facilities. However, the ability of POU and residential appliances to control DBP should not be ignored or deemed unimportant, as it may help consumers reduce the risk of DBPs themselves. Moreover, in epidemiology studies, such information may

help determine the actual intake levels of people with different drinking habits, and accordingly enable better understanding of the causes of DBP exposure and toxicity.

In light of the abovementioned need and knowledge gap, this study aims to evaluate the effectiveness of several POU and household appliances in removing CH under a series of operational and environmental conditions. The POU systems include a water purifier system composed of a series of cartridges: polypropylene (PP) cotton, granular activated carbon (GAC), carbon block filter (usually identified as CTO), and reverse osmosis (RO) in sequence. The household appliances include a boiler, a microwave oven, a mixer, and an ultrasonic cleaner. Some factors that may affect the CH removal efficiency were examined, including the initial concentration of CH, types of water (ultrapure vs. tap vs. lake), pH, stirring speed, power, capping conditions, etc. The roles of mechanisms on CH removal, such as volatilization and hydrolysis, were discussed to provide a fundamental understanding of these treatment processes.

Materials and Methods

Samples and Chemicals

The CH used in this study was purchased as powder (AR grade, >99% in purity) instead of dissolved in solvent to avoid potential interference of the solvent (21). Besides CH, the methyl-tert-butyl ether (MTBE) used for CH extraction and phosphorous buffer used for pH control were purchased from Aladdin Inc. at analytical grade (>99.9% in purity). Prior to experiments, stock CH solution was prepared by ultrapure water at a concentration of 2g/L and stored in a freezer at 4°C temperature if not used immediately. In all tests, control experiments were conducted.

The water samples were obtained from the city of Shenzhen, China, including lake water taken from Xili Lake, a drinking water source of the city; tap water from the laboratory; and ultrapure water produced on site by a Millipore water generator (Direct-Q3) with UV sterilizer. The lake and tap samples were filtered through a 0.45 µm glass fiber filter (Xingya, Co., Ltd) before use, and some water qualities are listed in Table 1. The selection of raw water for tests was intended to examine the potential influences of NOM and ions on CH treatability, although in practice it is impossible to have CH in raw water. Similarly, a comparison of ultrapure water and tap water may help better understand the CH treatment differences between ideal and real conditions.

Analytical Methods

CH was detected by a GC equipped with a ECD detector (GC-9720, Fuli, China) according to a modified EPA method 551.1, with the method detection limit (MDL) of 0.35 µg/L. Briefly, CH extraction was carried out for a 25ml sample by applying 5g of NaCl and 3ml of MTBE, shaking for 1 minute on a lab-dancer (IKA, Germany), and then letting it stand for 20 minutes. The GC column was initially set to be 60 °C for 3 minutes and then ramped up to 150°C

with a 20°C/min rate, and maintained the temperature for 1 minute; the flowrate of carrier gas (99.999% nitrogen in purity) was 2ml/min, and the temperature of ECD detector was set at 280°C. Residual chlorine was analyzed by the DPD method using a spectrophotometer (Hach 3900, USA) according to EPA 330.5. Chloride was analyzed by an ion chromatography instrument (IC2010, Tosoh Inc., Japan) with a MDL of 1 µg/L. Conductivity was recorded using an electrode (SX-650, San-Xin Instrumentation, Inc., China), and pH was analyzed using an electrode meter (pH100, Extech Instruments Corporation, USA). Dissolved organic carbon (DOC) was assessed by a TOC analyzer (TOC-L_{CPH}, Shimadzu, Japan) according to the EPA 415.3 method.

Table 1. Characteristics of Waters in This Study

	<i>COND (µs)</i>	<i>TDS (mg/L)</i>	<i>TOC (mg/L)</i>
Ultrapure Water	0.056	<0.26	<0.1
Tap Water	82	58.0	1.230
Lake Water	94.5	65.7	1.627

Apparatus

A series of domestic appliances were used in this study for CH removal assessment. In general, they are commercially available, domestic devices that can be readily purchased from most shopping malls in China. The boiler (BQ-150GA, Shenyi electronics, Inc., China) has an automatic switch-off function commonly used by owners, and it takes around 4 minutes and 10 seconds to reach 100°C from ambient temperature. The selected stirring speeds (1500 and 3000 RPM) of the mixer (CJ78-1, Jintan automatics, Inc. China) simulates a blending process of water and flour, but it is not a grinding machine. Although similar types of electronics are available in the market, such as a juicer and an automatic soybean milk machine, they are often operated under capped conditions and less likely to volatilize organic pollutants, and hence not selected in this study. The POU water purifier system (50GPD, Hercon Inc., China) consists of four major treatment units installed in sequence: PP cotton, GAC, CTO, and RO. For evaluation purpose, only one cartridge was used at a time and the other three cartridges were taken out to distinguish the efficiencies of each type of cartridge. Experiments using a microwave oven (P70OF20CL, Galanz Inc., China, with a frequency of 2450 MHz and adjustable power) and ultrasonic cleaner (KQ2200, Kunshan Ultrasonic Instrument Co., Ltd, 40 kHz, with various power inputs of 30W/50W/150W) were conducted in both capped and uncapped conditions. These two appliances are not designed to treat water, but if necessary, they may be employed to deal with polluted waters. To ensure the quality result, all tests were conducted in duplicate.

Results and Discussion

CH Treatment by Reverse Osmosis

RO is known to be a powerful tool for eliminating many types of pollutants, mainly because of the size difference between its membrane and target compounds. A recently study evaluated the rejection efficiency of RO on CH, and found that the removal degree of CH can reach almost 100%, regardless water temperature (23 - 35°C) (13). The tests were conducted at an operating pressure of 0.35 MPa, with the initial CH concentration at 50 µg/L. The spiked CH was initially dissolved in methanol solvent (13). Because the membrane and operating conditions are different from a household RO unit, we have done the following experiments to supplement above knowledge.

Firstly, considering the importance of pressure, we compared the transmembrane fluxes and CH removal potentials for a range of operating pressures (Table 2). With the increase of pressure, water recovery rate increased and wasted retentate decreased, while the removal efficiency (>90%) of CH appeared independent of the operating pressure (Figure 1a). So, by balancing the concerns of energy and efficiency, we selected 0.6 MPa in the subsequent tests. From a practical point of view, the tap pressure in a family house is normally less than 0.5 MPa and therefore cannot provide enough pressure to generate a sufficient amount of water within a limited time; however, a commercial, residential RO system is usually accompanied by a small-scale booster pump to provide extra pressure, so consumers often do not need to worry about the pressure issue unless the membrane becomes severely fouled.

Table 2. Effect of Operating Pressure on RO Flowrate

<i>Pressure(M- Pa)</i>	<i>Permeate rate (ml/s)</i>	<i>Retentate rate(ml/s)</i>	<i>Recove- ry (%)</i>	<i>Overall flowrate (ml/s)</i>
0.4	2	20	9%	22
0.6	3	9	25%	12
0.8	4	4	50%	8

The acid-dissociation constant (pK_a) of CH is predicted to be 9.51 by ChemAxon (13), meaning that CH will exist in ionic form at a pH value greater than 9.51, and consequently, it may exhibit different treatability by the RO process. However, this study exhibited no differences among waters at pH of 10.0 (Figure 1b), indicating that RO treatment of CH is mainly reliant upon the pressure-driven ability of the membrane rather than interactions of charged solute and membrane. However, since this test was conducted on ultrapure waters fortified with CH, the potential formation of precipitative solid by metals (e.g., calcium and magnesium) in real water at high pH condition may not be well reflected.

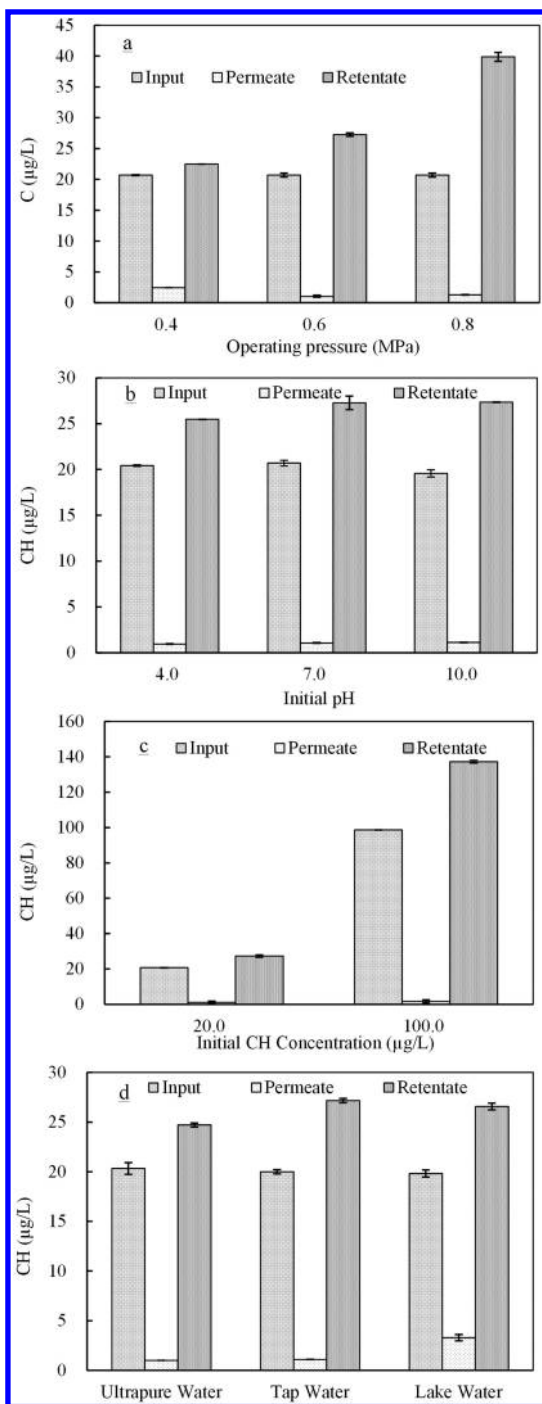


Figure 1. Effects of a) operating pressure, b) pH, c) initial concentration, and d) water type on CH removal by a domestic RO cartridge (working condition: 0.6 MPa, $C_0=20 \mu\text{g/L}$, $\text{pH}=7$, ultrapure water).

The influence of initial concentration had not been evaluated before, despite the fact that CH may exist in a wide range of concentration in DWTPs. In this study we compared the effect of two initial concentrations on CH removal. The results showed that there were no noticeable CH concentration differences in permeates, indicating that RO efficiency is independent of initial CH concentration (Figure 1c).

The presence of interfering compounds in tap and lake water, however, may impose an adverse effect on CH removal. Figure 1d shows that CH removal was lowered to 83% in lake water and such efficiency is less than those in ultrapure (95%) and tap water (94%), suggesting that a competing phenomenon from natural organic matter (NOM) may occur in raw water and treatment of NOM, e.g., coagulation, is necessary in practice for RO to achieve better performance.

CH Treatment by Adsorptive Materials

CH has a medium level of octanol-water partition coefficient ($K_{ow}=0.99$) so that it exhibits some levels of hydrophobicity in water. As a result, adsorption of CH by adsorptive materials, especially GAC, had been proven feasible by several early studies. However, the effectiveness of GAC on CH appeared inconsistent in the literature: some achieved complete removal of CH (22), and others observed varying levels of removal as a function of materials (23).

In this study, we evaluated three types of adsorption materials, i.e., GAC, PP cotton, and CTO, on CH removal (Figure 2). The results indicate that PP cotton and CTO have little capacity for CH control for a range of flowrates, suggesting that both materials have no size-excluding or adsorptive effects on CH. The major purpose of their uses in a commercial water purifier is probably to resist particles in the water. CTO is named after carbon for taste and odor, and the materials consist of activated carbon and polymers; however, the adsorptive capacity of activated carbon concentered in polymer seems to be minimal in practice and it is therefore useless for DBP control. In contrast, GAC demonstrated a considerable level of treatment ability (44~94%) for CH, with the efficiency increasing with the decrease of flowrate of water (Figure 2a). The study of extremely low flowrate (20ml/min, corresponding to a retention time of 16 minute) agreed well with an earlier study that applied GAC in a gravity filter (23), indicating that the GAC material is capable of removing most CH if sufficient contact time is allowed. However in reality, for the purpose of treating an adequate amount of water, the capability of GAC can be highly compromised.

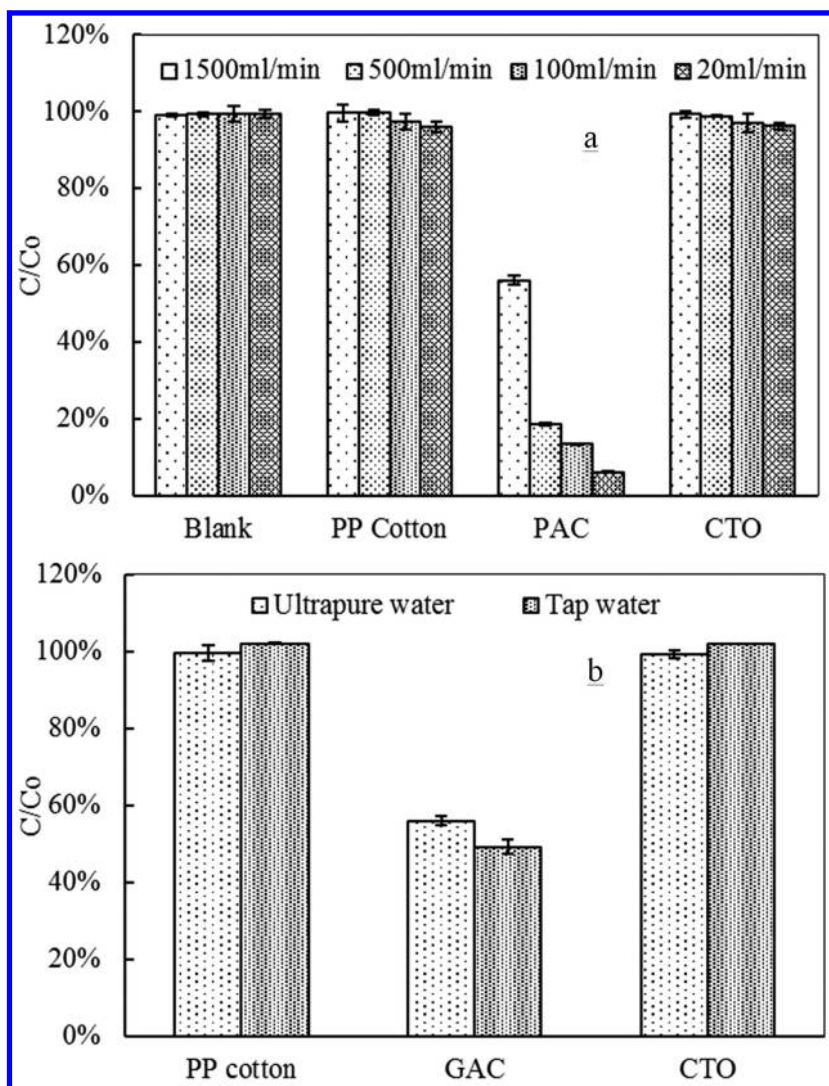


Figure 2. The effects of flowrate (a), adsorption material, and water type (b) on CH removal by domestic adsorptive cartridges (normal conditions: 1.5L/min, $C_o=20 \mu\text{g/L}$, $\text{pH}=7$).

Figure 2b shows the CH removal efficiency by virgin adsorbents at different waters. The treatment levels were independent of the type of water. With a combination of GAC and RO, the water purifier reduced an influent of $20 \mu\text{g/L}$ CH to an effluent of $\sim 1 \mu\text{g/L}$ (Figure 3), which is far below the regulatory MCL (i.e., $10 \mu\text{g/L}$), and therefore safeguards the water quality well with considerable confidence. Overall, the use of commercial water purifiers equipped with an RO unit is highly recommended in reducing the risks of CH from drinking water.

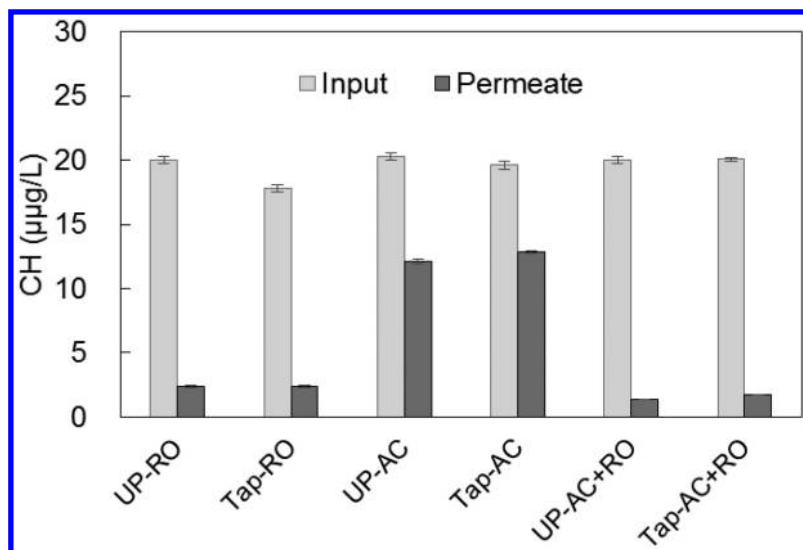


Figure 3. Removal of CH by RO and GAC alone or in combination.

CH Treatment by Boiler and Microwave Oven

Boiling water with pot or kettle has been a traditional way in many countries to inactivate pathogens or to make coffee and tea for daily life. Its roles and mechanisms in DBP removal, however, are not yet well-known although it has been proven robust in eliminating many types of DBPs (19, 20). For example, the results of Wu et al. reported non-detectable CH level after 1-min boiling of many types of waters originating from distilled water and tap water and in the presence of hydrophobic acid and bromide (19), indicating a complete removal of CH by the boiling process. Additionally, the results of Krasner et al. confirmed such efficiency in real samples, either chlorinated or chloraminated, with >97% of CH removals. These studies, however, did not consider the automatic switch-off function of boilers commonly used by the public. Since a boiler stops heating immediately, which often takes seconds, a more practical evaluation of the heating process (i.e., <1 min) appears necessary. In order to avoid the interference of concurrent formation of DBPs (19) during the transformation process of CH, this test evaluated the boiling effect on CH removal from both ultrapure and tap water.

Figure 4 shows the effectiveness of a boiler on the CH removals for two types of water. Notably, the efficiency of CH removal in tap water (with residual chlorine of 0.15 ppm) is significantly higher than that in ultrapure water (no

chlorine residual). Such phenomena were also observed in the microwave oven heating process (Figure 5a). Along with an increasing ratio of tap water to ultrapure water, the CH removal increased from 21% to 99%. In contrast, because the addition of sodium chloride (at 1000ppm) added no benefit to CH removal, the salinity of water is invalidated as an important factor in CH removal during the heating process (Figure 5a). Early literature suggested that residual chlorine and chloramine may facilitate the degradation of halogenated aldehydes (24) in water; and the presence of bromide can facilitate removal of CH (19), more in-depth study appears necessary to clarify this issue. In this context, we evaluated the effectiveness of free chlorine on CH degradation at ambient room temperature (Figure 6). Enhanced degradation of CH was observed with the increase of residual chlorine concentration. Combined with the information reported from a recent study that free chlorine can be more rapidly consumed in hot water than in cold water (25), we postulate that CH is likely subject to expedited degradation by chlorine under elevated temperatures.

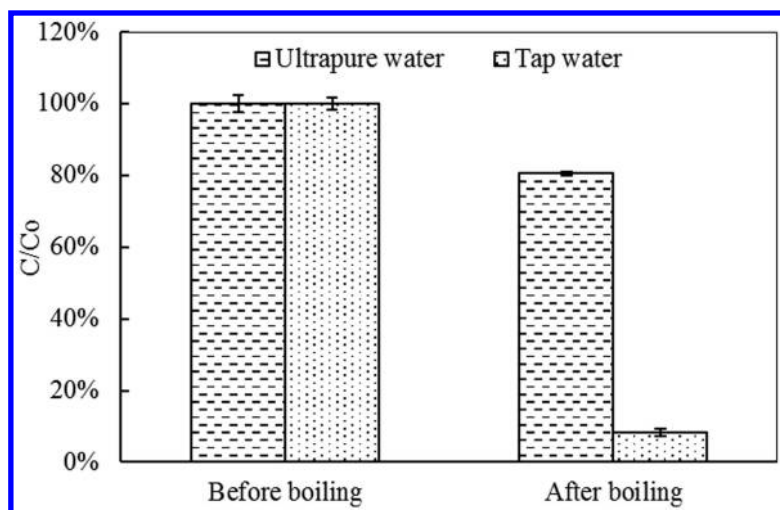


Figure 4. Removal of CH by boiling of spiked waters ($C_0=20 \mu\text{g/L}$, half-full volume in kettle, 4'10" duration, and automatic switch-off).

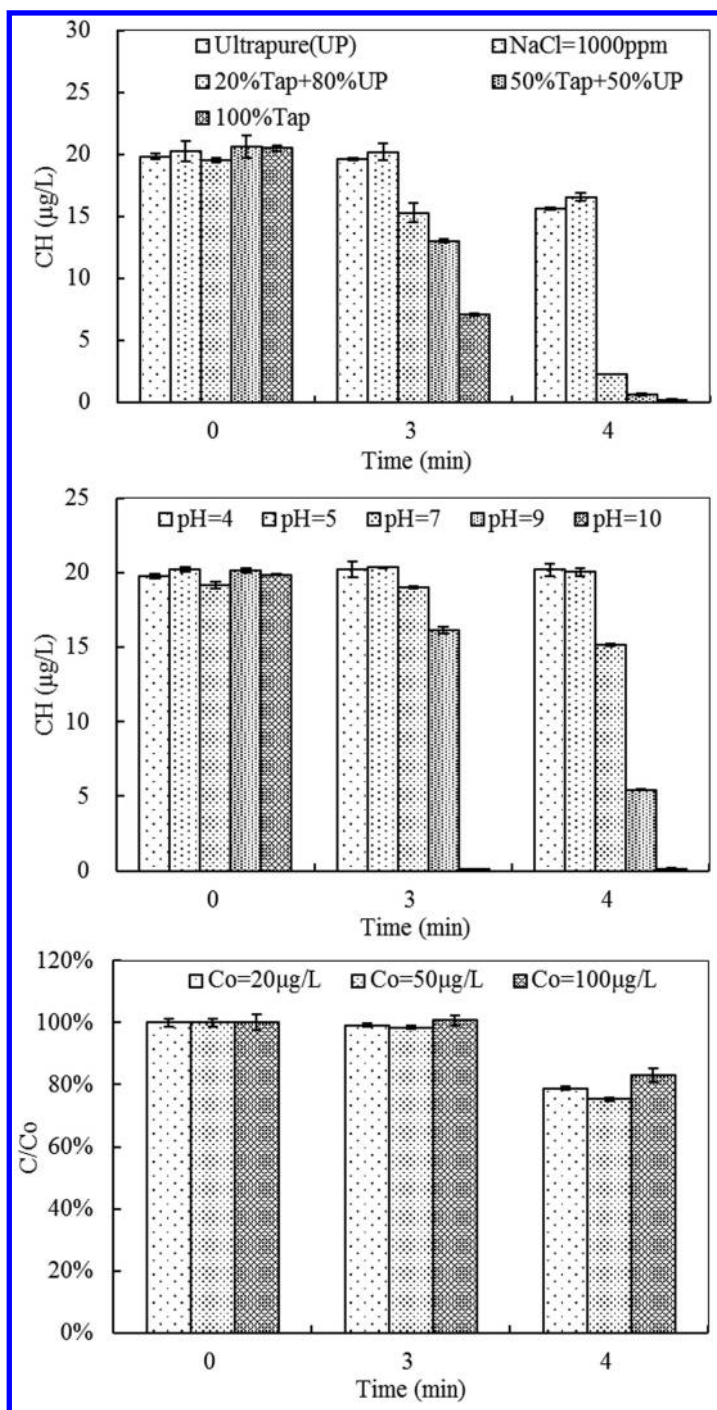


Figure 5. The effects of water type (a), pH (b), and initial concentration (c) on CH treatment by a domestic microwave oven ($C_0=20 \mu\text{g/L}$, headspace open).

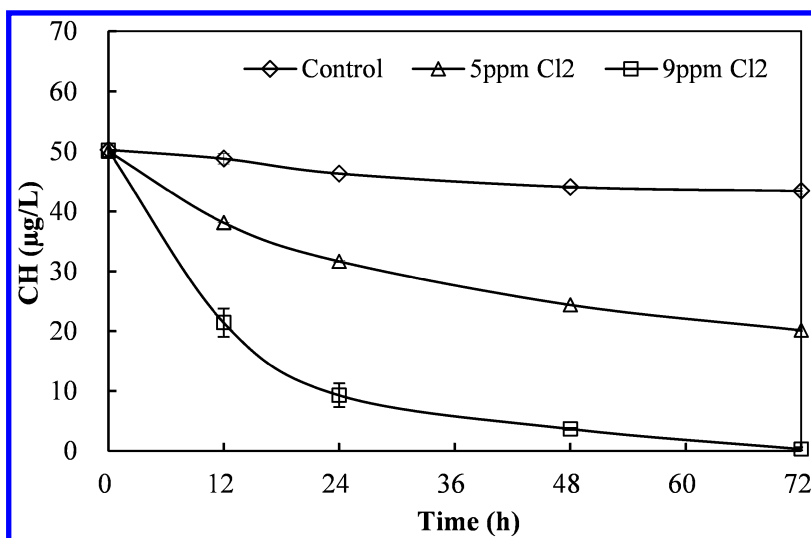


Figure 6. Effect of residual chlorine on CH degradation.

In addition to water type, CH removal during a heating process is highly related to the water pH but unrelated to initial concentration (Figure 5b and Figure 5c). The mechanism of pH effect is perhaps attributable to the base-catalyzed hydrolysis (26). As for volatilization, a comparison of capped and uncapped tests showed no preference in head-space open condition (Figure 7), indicating that the noticeable CH removal (~20%) is perhaps unrelated to volatilization of CH but a result of thermo-assisted hydrolysis. Or, because chloral hydrate has a boiling point of 98°C, it is likely that it was evaporated when the water temperature exceeds that point.

CH Treatment by Stirring and Ultrasonication

According to a US EPA modeling program called EPIsuite (version 4.11), CH (CAS No. 302-17-0, 165.4 g/mol) has a Henry's law constant (HLC) of 5.71E-009 atm·m³/mole, while its dehydrated form trichloroacetaldehyde (TCA, CAS No. 75-87-6, 147.4g/mol) has a HLC of 2.97E-006 atm·m³/mole. The difference in HLC indicates that CH is a non-volatile compound whereas TCA is a semi-volatile organic compound that may be eliminated by gas bubbling or air-stripping processes. In this study, we have found little removal of CH under a variety of stirring conditions (Figure 8a), which were designed to facilitate the volatilization effect. Similarly, while vortex was observed in the experiments, the concentrations of CH remained unchanged after the processes.

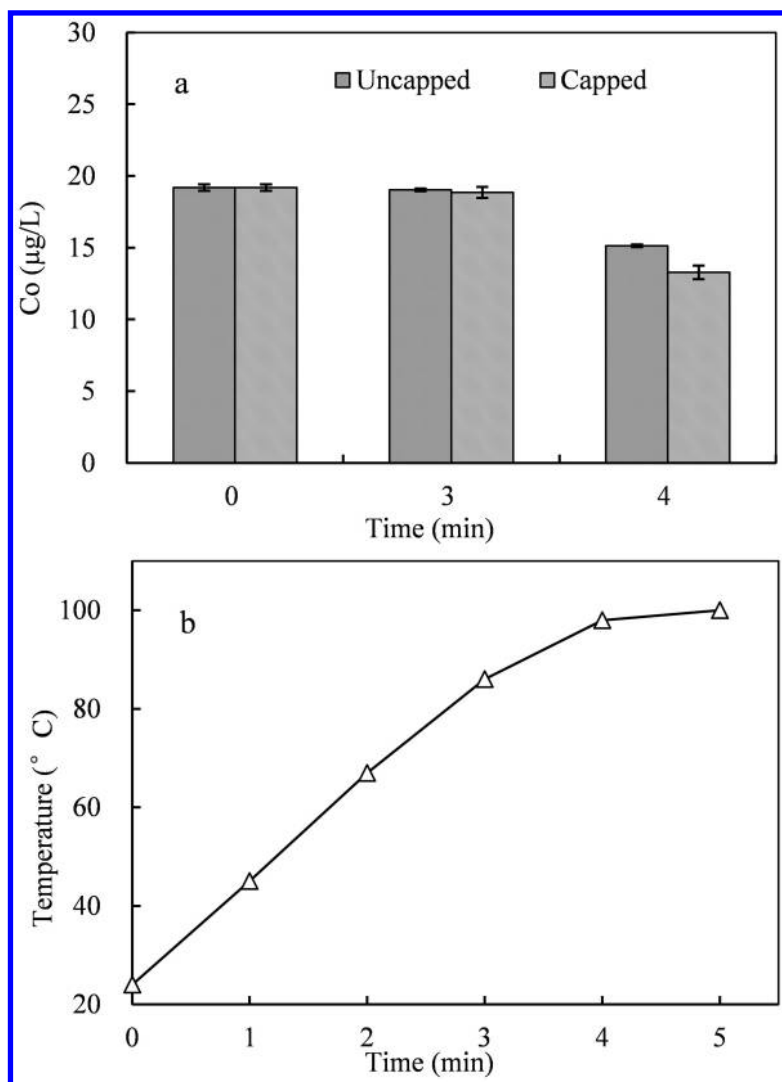


Figure 7. CH (a) and temperature (b) changes during microwave heating process.

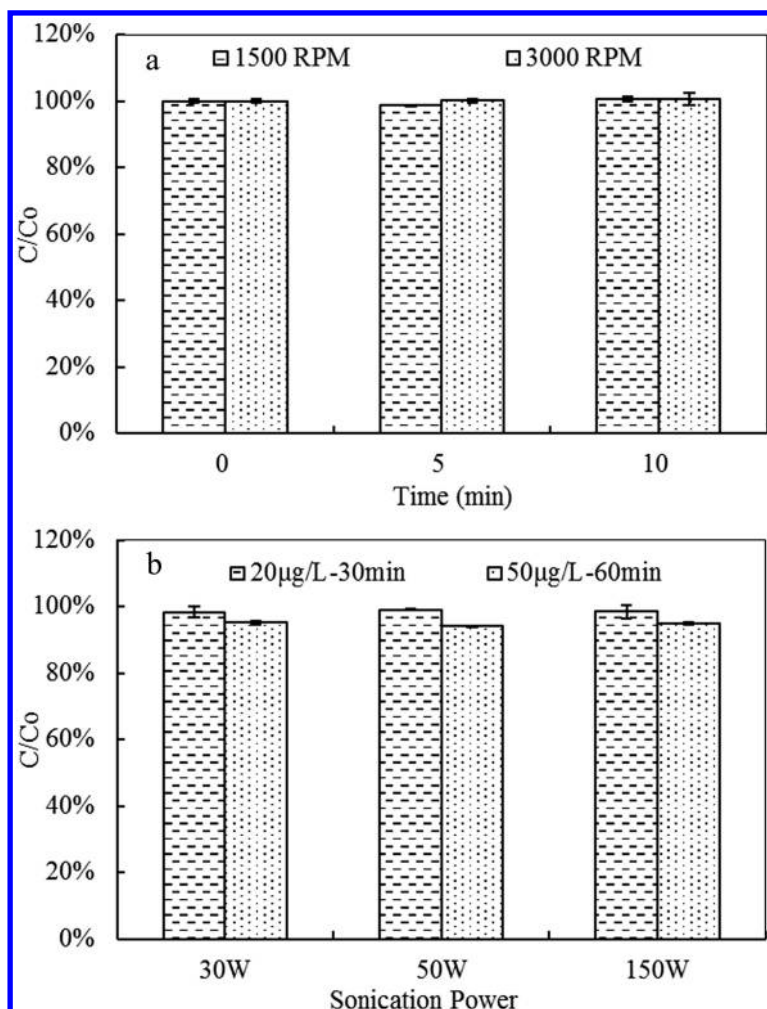


Figure 8. Effects of stirring speed (a, $C_0=10$ mg/L, half-full volume [125ml] in conical flask, uncapped) and ultrasonication (b, $C_0=20$ µg/L, 40kHz, 100ml water, uncapped) on CH removal from water:

Sonolysis has been found to remove volatile DBP compounds, such as trihalomethanes, successfully (27–29); and its application on CH was evaluated about four decades ago (30). These studies indicated that the performance of ultrasound technology is influenced by multiple factors including ultrasonic frequency, intensity, pH, initial concentration, and the presence of oxygen, catalysts or inhibitors -- mainly due to the formation of free radicals. However,

although the ultrasonic devices used in this experiment have comparable power inputs ($0.2\text{--}0.4\text{ w/cm}^2$) with those in the literature ($0.1\text{--}1.4\text{ w/cm}^2$) (30) and similar ultrasound frequency (40 kHz) as early study (29 kHz) (30), our tests showed almost no effectiveness on CH removal (Figure 8b). The exact reason for this is unclear, but may be attributable to the low initial CH concentration, lack of oxygen and catalysts, or inadequacy of conversion from electricity to ultrasonic power. What is certain is that ultrasound waves are incapable of either breaking the chemical bonds of CH directly or stripping CH away from water indirectly under the conditions of this study. Further study may evaluate more systematically the treatability and cost-effectiveness of sonolysis in the control of CH and other DBPs.

Conclusions

1. RO process can eliminate CH in a wide range of operating pressures, initial concentrations, pH, and water types, and serves as a convenient and robust tool for controlling CH at home.
2. Adsorption of CH by GAC exhibited some capacity (44~94%) for CH control, but in practice such capacity can be highly compromised by the short contact time. In contrast, adsorption of CH by PP cotton and CTO exhibited no effect on CH control.
3. Heating water to the boiling point by either boiler or microwave oven is very efficient in controlling CH, especially for CH in tap water (>90%), but not as high for CH in ultrapure waters (~20%). The underlying mechanism is perhaps attributable to the presence of residual chlorine, but not the salinity of the water. The reduction of CH in ultrapure water may be due to the thermal hydrolysis effect.
4. CH is a non-volatile compound and, as a result, stirring or ultrasonication technology are unable to lower its concentration to any great extent (<5%).

Overall, RO treatment and heating are two efficient and convenient POU methods for CH control by the public in daily life.

Acknowledgments

The study is financially supported by the National Natural Science Foundation of China (51278144), the Shenzhen Science & Technology R&D Funding (JCYJ20120613150442560), and the Funding for Returned Oversea Chinese from Shenzhen (KQCX20130627094615414). Thanks to the editors for organizing this book, and to reviewers for providing valuable comments and advice.

References

1. Gan, W. H.; Guo, W. H.; Mo, J. M.; He, Y. S.; Liu, Y. J.; Liu, W.; Liang, Y. M.; Yang, X. The occurrence of disinfection by-products in municipal drinking water in China's Pearl River Delta and a multipathway cancer risk assessment. *Sci. Total Environ.* **2013**, *447*, 108–115.
2. Krasner, S. W.; Weinberg, H. S.; Richardson, S. D.; Pastor, S. J.; Chinn, R.; Scilimenti, M. J.; Onstad, G. D.; Thruston, A. D., Jr. Occurrence of a new generation of disinfection byproducts. *Environ. Sci. Technol.* **2006**, *40*, 7175–7185.
3. Koudjonou, B.; LeBel, G. L.; Dabeka, L. Formation of halogenated acetaldehydes, and occurrence in Canadian drinking water. *Chemosphere* **2008**, *72*, 875–881.
4. Zhang, L.; Xu, L.; Zeng, Q.; Zhang, S. H.; Xie, H.; Liu, A. L.; Lu, W. Q. Comparison of DNA damage in human-derived hepatoma line (HepG2) exposed to the fifteen drinking water disinfection byproducts using the single cell gel electrophoresis assay. *Mutat. Res.* **2012**, *741*, 89–94.
5. Daniel, F. B.; Deangelo, A. B.; Stober, J. A.; Olson, G. R.; Page, N. P. Hepatocarcinogenicity of Chloral Hydrate, 2-Chloroacetaldehyde, and Dichloroacetic Acid in The Male B6c3f1 Mouse. *Fundam. Appl. Toxicol.* **1992**, *19*, 159–168.
6. Benson, R. *Toxicological Review of Chloral Hydrate (EPA/635/R-00/006) in Support of Summary Information on the Integrated Risk Information System (IRIS)*; U.S. Environmental Protection Agency: Washington DC, August 2000.
7. Simpson, K. L.; Hayes, K. P. Drinking water disinfection by-products: an Australian perspective. *Water Res.* **1998**, *32*, 1522–1528.
8. Barrott, L. Chloral hydrate: Formation and removal by drinking water treatment. *J. Water Supply: Res. Technol. –AQUA* **2004**, *53*, 381–390.
9. Wang, X.; Yang, H.; Xie, Y. Lessons of USA Disinfection Byproduct Database to Chinese Drinking Water Standard - Chloral Hydrate Concentration and Compliance Analysis (in Chinese). *Water Wastewater Eng.* **2014**, 13–19.
10. Singer, P. C. Control of Disinfection By-Products in Drinking-Water. *J. Environ. Eng. -ASCE* **1994**, *120*, 727–744.
11. Dąbrowska, A.; Nawrocki, J. Controversies about the occurrence of chloral hydrate in drinking water. *Water Res.* **2009**, *43*, 2201–2208.
12. Bond, T.; Goslan, E. H.; Parsons, S. A.; Jefferson, B. Treatment of disinfection by-product precursors. *Environ. Technol.* **2011**, *32*, 1–25.
13. Doederer, K.; Farre, M. J.; Pidou, M.; Weinberg, H. S.; Gernjak, W. Rejection of disinfection by-products by RO and NF membranes: Influence of solute properties and operational parameters. *J. Membrane Sci.* **2014**, *467*, 195–205.
14. Woods, R. J.; Akhtar, S. Radiation-Induced Dechlorination of Chloral Hydrate and 1,1,1-Trichloro-2,2-Bis(P-Chlorophenyl) Ethane (Ddt). *J. Agric. Food. Chem.* **1974**, *22*, 1132–1133.

15. Chen, B.; Lee, W.; Westerhoff, P. K.; Krasner, S. W.; Herckes, P. Solar photolysis kinetics of disinfection byproducts. *Water Res.* **2010**, *44*, 3401–3409.
16. Lekkas, T. D.; Nikolaou, A. D. Degradation of disinfection byproducts in drinking water. *Environ. Eng. Sci.* **2004**, *21*, 493–506.
17. Chun, C. L.; Hozalski, R. M.; Arnold, W. A. Degradation of drinking water disinfection byproducts by synthetic goethite and magnetite. *Environ. Sci. Technol.* **2005**, *39*, 8525–8532.
18. Radjenovic, J.; Farre, M. J.; Mu, Y.; Gernjak, W.; Keller, J. Reductive electrochemical remediation of emerging and regulated disinfection byproducts. *Water Res.* **2012**, *46*, 1705–1714.
19. Wu, W. W.; Benjamin, M. M.; Korshin, G. V. Effects of thermal treatment on halogenated disinfection by-products in drinking water. *Water Res.* **2001**, *35*, 3545–3550.
20. Krasner, S. W.; Wright, J. M. The effect of boiling water on disinfection by-product exposure. *Water Res.* **2005**, *39*, 855–864.
21. Koudjonou, B. K.; LeBel, G. L. Halogenated acetaldehydes: analysis, stability and fate in drinking water. *Chemosphere* **2006**, *64*, 795–802.
22. Lykins, B. W., Jr; Goodrich, J. A.; Koffskey, W. E.; Griese, M. H.; Water, E.; Utility, S. *Controlling disinfection by-products with alternative disinfectants*; USEPA: Cincinnati, OH, June 1991.
23. Canada, H. *Guidance on Chloral Hydrate in Drinking Water (H128-1/08-551E)*; Water, Air and Climate Change Bureau Healthy Environments and Consumer Safety Branch, Health Canada: Ottawa, Ontario, 2008.
24. Xie, Y. *Disinfection byproducts in drinking water: Formation, analysis, and control*; CRC Press: Boca Raton, FL, 2003.
25. Liu, B.; Reckhow, D. A. Disparity in disinfection byproducts concentration between hot and cold tap water. *Water Res.* **2015**, *70*, 196–204.
26. Chen, B. Hydrolytic Stabilities of Halogenated Disinfection Byproducts: Review and Rate Constant Quantitative Structure–Property Relationship Analysis. *Environ. Eng. Sci.* **2011**, *28*, 385–394.
27. Guo, Z.; Gu, C.; Zheng, Z.; Feng, R.; Jiang, F.; Gao, G.; Zheng, Y. Sonodegradation of halomethane mixtures in chlorinated drinking water. *Ultrason. Sonochem.* **2006**, *13*, 487–492.
28. Shemer, H.; Narkis, N. Trihalomethanes aqueous solutions sono-oxidation. *Water Res.* **2005**, *39*, 2704–2710.
29. Kim, I.-K.; Huang, C.-P. Sonochemical process for the removal of DBPs and precursor in water. *J. Environ. Eng. Manage.* **2007**, *17*, 39.
30. Sakai, Y.; Sadaoka, Y.; Takamaru, Y. Decomposition of chloral hydrate in aqueous solution by the action of ultrasound. *J. Phys. Chem.* **1977**, *81*, 509–511.

Chapter 20

Disinfection By-Products in Swimming Pool Water: Formation, Modeling, and Control

Hao L. Tang,¹ Ricky J. Ristau II,² and Yuefeng F. Xie^{*,2}

¹Department of Water Engineering and Science, College of Civil Engineering, Hunan University, Changsha, Hunan 410082, China

²Environmental Engineering Programs, The Pennsylvania State University, 777 West Harrisburg Pike, Middletown, Pennsylvania 17057, U.S.A.

*E-mail: yxx4@psu.edu.

Disinfection is practiced to minimize the occurrence and growth of microbial pathogens and thus ensure the hygienic safety of swimming pool water. However, potentially hazardous disinfection by-products (DBPs) are formed from the reaction between disinfectants and DBP precursors. This chapter discusses the formation of these DBPs in swimming pool water and modeling approaches for quantification of their levels given estimates of anthropogenic contaminant input in swimming pools. Promising DBP control technologies are also discussed. Overview of the three key aspects related to swimming pool water help readers to better understand the profile of DBPs and their control in swimming pool water.

Introduction

Swimming, as a physical activity for people of all ages, promotes fitness and has many advantages over land-based activities. It is generally considered as a health-enhancing and relatively injury-free activity; it can be a good aerobic exercise, which contributes to flexibility and muscle strength, and can have positive social aspects. Swimming pools can be found in different kinds and sizes in public areas, hotels and spas, or at private residential homes. In the U.S., more than 368 million pool visits occur each year. In Germany, around 250-300 million pool visits occur each year, averaging 3 visits per capita. In the UK, one-third of the children and around 36% of adults (>15 years of age) visit swimming pools at

least once a week, and 55% of children (5-9 years of age) use pools at least once a month. In the U.S., there are approximately 250,000 public pools and 10,000,000 residential pools. The highest numbers of existing in-ground and above-ground pools in Europe are found in France (773,000) and Germany (625,000), followed by UK with 155,000, and Italy with 94,000 (1).

However, after water leaves a public water system and enters a pool, its quality is no longer regulated as drinking water in the U.S. and many other countries, and in the U.S. the Safe Drinking Water Act makes no stipulation that the tap water meets additional requirements for use in pools or spas. Instead, pools are managed at the local level, usually by state or local public health departments, and sometimes by pool managers or lifeguards. As the pools are filled with swimmers, they contain hundreds to thousands of low levels of chemicals originating from natural and anthropogenic inputs, which complicate the water chemistry. The undesirable substances (e.g., skin, hair, bodily excretions such as sweat, urine, and saliva; pathogens; and personal care products such as lotions and sunscreens) introduced by swimmers also complicate the toxicity and expose swimmers to potential biological and chemical health risks (2, 3).

To conserve the positive aspects of aquatic activities, it is necessary to disinfect swimming pool water to prevent outbreaks of infectious illnesses (4, 5). To date, chlorination is still the most common measure for inactivation of microbial pathogens. Chlorine is added to swimming pools as chlorine gas, calcium/sodium hypochlorite, or through electrolytic generation of sodium hypochlorite. Regardless of the method of application, once the chlorine is in the water it forms hypochlorous acid which dissociates into hydrogen and hypochlorite ions. The sum of the concentrations of hypochlorous acid, hypochlorite ion and aqueous chlorine is referred as free chlorine residual. Chlorine's popularity is not only due to lower cost, but also to its higher oxidizing potential, which provides a minimum level of chlorine residual to inhibit microbial recontamination. Other disinfectants may be used, but less is known about their ability to inactivate pathogens (6). For effective disinfection, adequate disinfectant levels are required. In Canada, regulations in Quebec require free chlorine in swimming pools to be between 0.8 and 2.0 mg/L, while the required minimum level for British Columbia varies with pH: 0.5 mg/L for pH 7.4-7.8, and 1.0 mg/L for pH of greater than 7.8 (7). In the U.S., a survey of twenty-three indoor pools showed that the median chlorine residual was 3 mg/L (8). In practice, chlorine residuals of 2-4 mg/L are generally recommended for chlorinated pools (9). However, the reaction of chlorine and chloramines with organic and inorganic precursors, such as natural organic matter (NOM), anthropogenic inputs, bromide, etc, may cause the formation of undesirable disinfection by-products (DBPs). The types and concentrations of DBPs depend on several factors, including the type and amount of disinfectant used, characteristics of the swimming pool and pool water and users' hygiene (1). These DBPs can be inhaled or ingested by swimmers during swimming, bathing and showering, or absorbed dermally (10), resulting in negative effects on human health (11, 12). DBPs were observed to produce cancer in animal models and to have other toxic consequences, such as reproductive and developmental effects; in particular, users of chlorinated pools may have an elevated risk for bladder

cancer (13) and an increased frequency of micronuclei in peripheral blood cells (a marker of DNA damage) (14). These published epidemiology studies provide evidences that disinfected pool water might be genotoxic and carcinogenic to humans. Given the popularity of swimming that comes with the increased risk of exposure to pathogenic microorganisms, disinfectants and DBPs, we are only in the early stages of understanding swimming pool chemistry, human exposures, and potential health risks (6). Regulations must also ensure that efforts to reduce DBPs do not result in water that is impaired due to microbial contamination: This is the microbe-DBP balancing act of minimizing risks while maximizing beneficial effects.

Research has specifically focused on two classes of DBPs from chlorine-based disinfection: trihalomethanes (THMs) and haloacetic acids (HAAs) (15–19). THMs, including chloroform, bromodichloromethane, dibromochloromethane, and bromoform, are the best known and most intensively investigated class of DBPs and they are regulated in chlorinated drinking water in the U.S. with a maximum contaminant level at 80 $\mu\text{g/L}$. Reports on THMs in swimming pools first appeared in 1980s, and they showed a tendency of wide variations in the reported data. Fantuzzi et al. (20) found the THM levels ranged from 18 to 71 $\mu\text{g/L}$ in five indoor swimming pools in Italy. Chu and Nieuwenhuijsen (21) found the THM levels averaged at 133 $\mu\text{g/L}$ in 44 indoor swimming pools in the UK. HAAs, commonly referred as HAA6 including monochloroacetic acid (MCAA), monobromoacetic acid (MBAA), dichloroacetic acid (DCAA), trichloroacetic acid (TCAA), bromochloroacetic acid (BCAA), and dibromoacetic acid (DBAA), are also regulated for drinking water in the U.S., with a maximum contaminant level at 60 $\mu\text{g/L}$. There is limited information on HAA levels in swimming pools. Tang (22) reported the HAA level stabilized at approximately 1650 $\mu\text{g/L}$ in an indoor swimming pool in the U.S.. Simard et al. (23) analyzed 15 indoor and 39 outdoor municipal public pools in Canada and found the HAAs were higher in outdoor pools (808 vs 413 $\mu\text{g/L}$). Wang et al. (24) analyzed 5 outdoor pools in the U.S. and 9 indoor pools in China and found that the HAA levels in the pools in the U.S. averaged at 1440 $\mu\text{g/L}$ while in China the levels averaged at 117 $\mu\text{g/L}$ due to lower chlorine residuals.

Some nitrogen-containing DBPs that were previously reported in drinking water (25) are also identified in swimming pool water (26), due to the presence of nitrogen sources, such as urine or sweat. Haloacetonitriles (HANs) were the most significant toxic compounds detected by Hansen et al. (27), though they were found at much lower concentrations compared to THMs and HAAs. However, it is not known how much the HANs contribute to the overall mixture toxicity. The pH plays an important role on DBP classes. For decreasing pH, THM concentrations are observed to decrease, while HAN concentrations increased. Therefore caution is warranted if the pH level in swimming pool water is lowered for THM control, since the the concentration of more toxic HANs appear to increase. Besides HANs, many other DBPs, including dichloromethylamine (CH_3NCl_2), cyanogen chloride (CNCl), trichloronitromethane (TCNM), chloral hydrate (CH), halo ketones (HKs), N-nitrosodimethylamine (NDMA), chloramines and cyanogen bromide (CNBr) have also been reported in swimming pools (28, 29), though at much lower concentrations compared to the predominant

THM and HAA species. To date, their complete chemical and toxicological characterizations are not available.

In this chapter, we examine three key aspects related to swimming pool water.

Formation

DBP precursors lead to the formation of DBPs upon chlorination. Research on DBP precursors in swimming pool water is of keen interest by scientists (30, 31). One option to ensure the safety of public drinking water systems is to improve the quality of source water through pollution prevention and precursor removal. However, a source reduction approach is challenging for swimming pools, because the swimmers themselves are the largest source of organic/inorganic precursors for DBP formation. The incidental anthropogenic contaminant release as a result of human excreta such as urine and sweat, either accidentally or on purpose, is difficult to quantify (32, 33). And its impact on DBP formation in swimming pools is unclear. In this section, we discussed our research on investigating the formation of DBPs and the contributions from various precursors in a sample swimming pool.

Modeling

Models for DBP levels in swimming pool water are needed, aiming at identifying the significance of diverse operational and water quality parameters controlling the formation of DBPs or at investigating the kinetics for their formation. It may consist of empirical and mechanistic relationships of water quality and operational parameters with the prevailing levels of DBPs at various stages of a same single pool. In this section, we discussed our research on developing predictive models for DBPs based on data obtained from field and laboratory-scaled studies.

Control

Swimming pool water treatment in general includes flocculation, sand filtration, and subsequent disinfection with chlorine. The continuous chlorination and input of anthropogenic releases by bathers in combination with recirculation of the pool water may lead to an accumulation of DBPs in the water. Better technologies are needed to solve this issue. In this section, we discussed our research on potential technologies on DBP control from swimming pool water.

By giving an overview of our research efforts on the three topics in this chapter, readers can better understand the profile of DBPs and their precursors in swimming pool water.

Materials and Methods

Reagents

All chemicals and standard solutions, unless noted otherwise, were analytical grade purchased from Sigma-Aldrich.

Analysis of Dissolved Organic Carbon (DOC), Ammonia Nitrogen (NH₃-N), UV Absorbance at 254 nm (UV₂₅₄), and Chlorine

DOC was measured with a total organic carbon (TOC) analyzer (O.I. Analytical Model 1010, Maryland, USA). NH₃-N was measured using an ammonia-selective electrode method according to Standard Method 4500-NH₃ (34). UV₂₅₄ was measured using an Agilent 8453 UV-Visible Spectrophotometer (Agilent technologies, California, USA) with a 10 mm quartz cuvette. Free chlorine and total chlorine were measured immediately using the *N,N*-diethyl-*p*-phenylenediamine (DPD) method with a DR/890 portable colorimeter (Hach Company, Colorado, USA).

Analysis of THMs and HANs

Table 1 shows a list of investigated compounds. Residual chlorine in THM and HAN samples was quenched by adding 5 mg sodium sulfite to 40 mL borosilicate glass vials before they were filled head-space-free with the samples. The samples were stored at 4°C until analysis by a gas chromatograph (GC) (HP 6890 Series GC system, Hewlett Packard) with mass spectrometer (5973 Mass selective detector, Hewlett Packard). A DB-1 capillary column (30 m × 0.32 mm i.d., 1.0 μm film thickness) was used. The temperature ramping program was as follows: Initial at 35°C for 22 minutes, ramp to 145°C at 10°C/min and hold for 2 minutes. This method was also used for the detection of chloral hydrate (CH), trichloronitromethane (TCNM), dichloropropanone (DCP), and trichloropropanone (TCP). For more information refer to EPA 551.1 method.

Analysis of HAAs

For the analysis of HAAs, a modified version of the EPA 552.3 method was used. Sulfuric acid, sodium sulfate, surrogate standard (2-bromobutanoic acid) and methyl-*tert*-butyl ether (MtBE) was added to the samples which then were hand shaken for two minutes to extract HAAs. The MtBE phase was transferred to a test tube and acidified methanol was added. The samples were placed in a water bath at 50°C for 2 h to methylate the HAAs and then back-extracted with sodium sulfate solution to remove excess methanol. The MtBE phase was transferred to a GC vial and analyzed by a GC (HP 6890 Series GC system, Hewlett Packard) equipped with a DB-1701 capillary column (30 m × 0.25 mm i.d., 0.25 μm film thickness). The temperature ramping program was as follows: Initial at 35°C for 10 minutes, ramp to 75°C at 5°C/min, hold for 16 minutes, ramp to 200°C at 25°C/min and hold for 5 minutes.

DBP Formation Potential (DBPFP) test

A DBPFP test was started by applying an initial chlorine dose to the phosphate buffered samples, which had been pre-diluted to accommodate 3-day free chlorine demands (35). The incubation process took 3 days at 25°C in the dark. The DPD method was used to measure the free chlorine and total chlorine. Samples were

then quenched to eliminate chlorine residuals and analyzed for DBPs based on the above protocols. It is noted that five kinds of anthropogenic contaminants, i.e. sweat, saliva, skin wash, hair wash, and urine, were also sampled for the DBPFP tests. The anthropogenic inputs were obtained from a 26-yr-old college male, with sampling protocols approved by the Pennsylvania State University Institutional Review Board and a written informed consent obtained from the participant.

Table 1. List of Investigated Disinfection By-Products

	<i>Compound</i>	<i>Abbreviation</i>	<i>Chemical formula</i>
THMs	Chloroform	TCM	CHCl ₃
	Bromodichloromethane	BDCM	CHBrCl ₂
	Dibromochloromethane	DBCM	CHBr ₂ Cl
	Bromoform	TBM	CHBr ₃
HAAs	Chloroacetic acid	MCAA	CH ₂ ClCOOH
	Bromoacetic acid	MBAA	CH ₂ BrCOOH
	Dichloroacetic acid	DCAA	CHCl ₂ COOH
	Trichloroacetic acid	TCAA	CCl ₃ COOH
	Bromochloroacetic acid	BCAA	CHBrClCOOH
	Dibromoacetic acid	DBAA	CHBr ₂ COOH
HANs	Dichloroacetonitrile	DCAN	CHCl ₂ CN
	Trichloroacetonitrile	TCAN	CCl ₃ CN
	Bromochloroacetonitrile	BCAN	CHBrClCN
	Dibromoacetonitrile	DBAN	CHBr ₂ CN
Others	Dichloropropanone	DCP	CHCl ₂ COCH ₃
	Trichloropropanone	TCP	CCl ₃ COCH ₃
	Trichloronitromethane	TCNM	CCl ₃ NO ₂
	Chloral hydrate	CH	C ₂ H ₃ Cl ₃ O ₂

Formation

The Swimming Pool under Investigation

The DBP formation in a swimming pool was investigated. The pool, with a volume of 440 m³, was located in Capitol Union Building at The Pennsylvania State University, Middletown, Pennsylvania, USA. The pool was completely drained, and refilled with fresh water in the second week of June in 2009. Since then, the pool water was periodically sampled and analyzed for DBPs during a

1.5-yr investigation period. During the operation of the swimming pool, water was filtered and chlorinated through recirculation of the pool water. Some water was lost during back-washing of the filters and by evaporation, therefore fresh water was added to maintain a constant water level at a rate of approximately 1.8 m³ weekly. Some DBPs might be adsorbed to suspended solids in the pool and removed with the filtration; however, for this study that process and the loss of water through evaporation were neglected, since they account for a negligible fraction of the pool water. The pool was open year-around to students, faculty and staff of the university, members, and guests, i.e. walk-ins of the local community. Table 2 shows the year-around user statistics of the swimming pool. These data show that the pool accepted 1441 users per month or 48 users per day on average. As the typical pool hours were from 9 am to 9 pm in work days except national holidays, the pool accepted an average of 4 users per hour.

Table 2. Year-around User Statistics of the Swimming Pool

	<i>Members</i>	<i>Students</i>	<i>Faculty/Staff</i>	<i>Guests*</i>	<i>Total visits per month</i>
January	398	255	91	1579	2323
February	353	291	81	1006	1732
March	422	312	70	366	1536
April	346	275	65	665	1351
May	360	140	83	432	1015
June	307	141	78	388	1114
July	315	105	122	892	1434
August	290	164	111	224	789
September	396	231	80	651	1358
October	356	243	133	1148	1879
November	326	169	98	1326	1955
December	325	135	60	896	1416

* Guests include the pool users of swim lessons, swim teams, water fitness classes, and walk-ins of local community.

DBP Levels in the Swimming Pool

Figure 1 shows the profiles of THM and HAA concentrations in the swimming pool following the water change over a 1.5-yr period. After the pool water was completely drained and refilled with fresh water, the THM and HAA concentrations were 81 and 87 µg/L, respectively. These two numbers were similar to those of finished water (80 µg/L for THMs and 60 µg/L for HAAs)

from a typical surface water treatment plant. As the water age increased and more swimmers were admitted, the THM levels were relatively stable, being averaged at 62 $\mu\text{g/L}$ with a standard deviation of 35 $\mu\text{g/L}$. However, the HAA concentrations substantially increased. Two months following water change, 940 $\mu\text{g/L}$ HAAs were observed in the pool. During the 6th and 8th months following water change, the HAA level appeared to reach a plateau and fluctuated around 1600 $\mu\text{g/L}$. From the 8th to 12th month, the HAA level consistently declined to 780 $\mu\text{g/L}$, and after the 12th month, the HAA concentration steadily increased again to the 1600 $\mu\text{g/L}$ level when the 1.5-yr investigation period was close to the end. It is noticeable that the decline in HAA concentrations from January to June could be attributed to the decrease of the number of pool users during the same period, as the monthly number of pool users decreased from 2223 in January to 1114 in June. Figure 2 also shows that a positive correlation between the measured HAA levels in the pool and the numbers of pool users, and the R^2 value was 0.70.

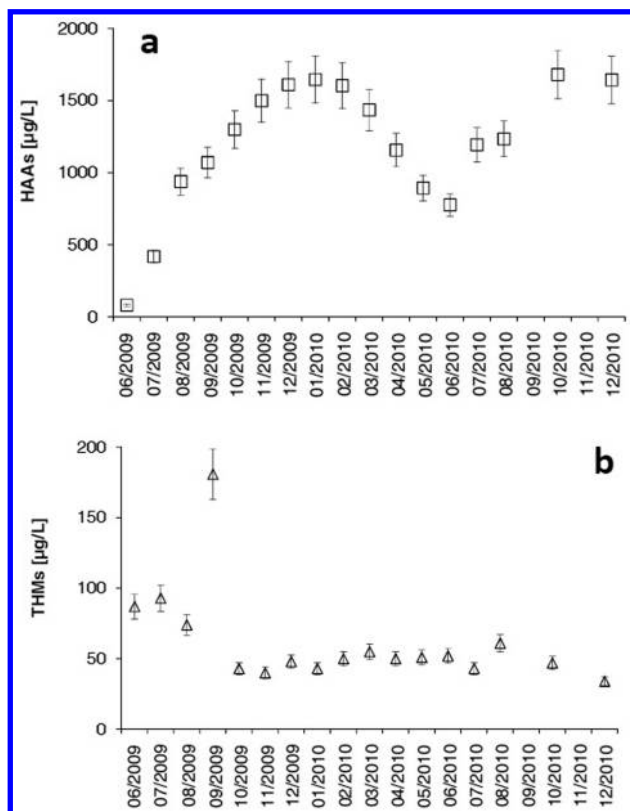


Figure 1. THM and HAA levels in an indoor swimming pool after water change.

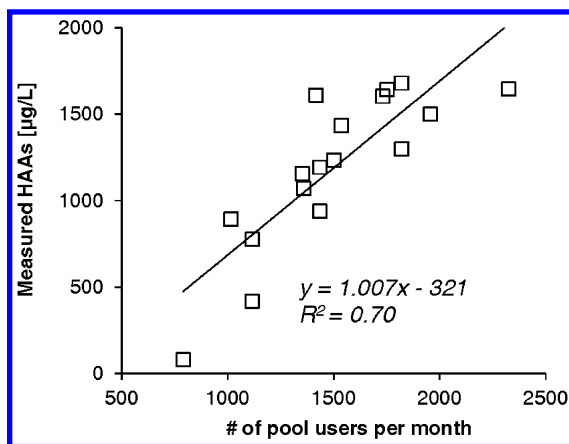


Figure 2. Correlation between the measured HAAs and the numbers of pool users.

The predominant species of HAAs, THMs, HANs, and HKs in the swimming pool water were DCAA and TCAA, TCM, DCAN, and TCP, respectively. Table 3 shows their concentrations in the pool water during the 1.5-yr investigation period since water change. DCAA was found to be in a higher concentration than TCAA. Because DCAA and TCAA are believed to be produced as a result of different mechanistic pathways (36), the ratio of DCAA/TCAA implies that the formation of DCAA is favoured in the swimming pool water, possibly due to the presence of more precursors for DCAA in pool water. HANs and HKs in swimming pools were investigated by fewer studies than those of THMs and HAAs. Lee et al. (37) reported DCAN in the chlorinated pools as $3.9 \pm 3.3 \mu\text{g/L}$, while TCAN was not reported. In this research, the DCAN in the swimming pool water was $1.3 \pm 0.7 \mu\text{g/L}$. The HAN concentrations were much lower than THM and HAA concentrations, possibly due to their decomposition to form HAAs at pH conditions higher than 7.0 (27). As the DBP formation is also attributable to precursors for DBPs, the profiles of individual species need to be reviewed to explore the contribution from their precursors.

DBP Precursors in the Swimming Pool

The widely accepted precursors for DBP formation in drinking water is the natural organic matter (NOM). However, this phenomenon is not completely applicable to swimming pools. Researchers have associated anthropogenic inputs, i.e. sweat and urine, by swimmers with main sources of DBP precursors (38–41). It was estimated that a swimmer introduces 25–80 mL of urine and 200–1000 mL of sweat into swimming pool water each swim session (42, 43). As anthropogenic contaminants are continuously brought in by swimmers and pools are continuously exposed to disinfectant, the disinfection process resembles

a DBPFP test, which maintains a sufficient free chlorine residual and a long reaction time to convert precursors to DBPs. To further explore their impact on DBP formation in swimming pools, five kinds of anthropogenic contaminants, i.e. sweat, saliva, skin wash, hair wash, and urine, were analyzed for DBPFPs

Table 3. Concentrations of Individual Species and the Ratio of DCAA/TCAA

<i>Month No.</i>	<i>DCAA</i>	<i>TCAA</i>	<i>TCM</i>	<i>DCAN</i>	<i>TCP</i>	<i>DCAA/TCAA*</i>
1	51	18	87	0.0	0.0	2.8
2	276	65	93	0.8	2.3	4.2
3	636	186	74	1.6	2.1	3.4
4	750	201	181	0.9	1.5	3.7
5	975	290	43	2.3	2.0	3.4
6	1100	326	40	2.7	2.5	3.4
7	1095	366	48	1.6	2.5	3.0
8	1119	381	43	1.8	1.8	2.9
9	1074	489	50	1.5	1.5	2.2
10	942	444	55	1.0	1.3	2.1
11	715	400	50	2.2	1.1	1.8
12	493	362	51	1.4	1.9	1.4
13	504	249	52	0.8	1.6	2.0
14	849	321	43	0.6	1.2	2.6
15	861	345	61	0.4	1.6	2.5
17	1167	480	47	1.6	2.1	2.4
19	1116	504	34	1.3	2.9	2.2

* Data in this ratio column are unitless. Data in the DCAA, TCAA, TCM, DCAN, and TCP columns are concentrations represented. in $\mu\text{g/L}$.

Table 4 shows the DBPFPs of the anthropogenic input samples. All the anthropogenic contaminants were found to contribute to the DBP formation, which was consistent with the results reported by Kim et al. (39). The HAA yields of chlorinated sweat, saliva, skin wash, hair wash, and urine samples were 300, 390, 380, 160, and 160 $\mu\text{g/mg C}$, respectively, while the THM yields of the corresponding samples were 67, 130, 96, 50, and 74 $\mu\text{g/mg C}$, respectively. The relative abundance of HAAs and THMs was presented by the ratio of HAA/THM. These anthropogenic contaminants contributed to more HAAs than THMs, with the HAA/THM ratio in the range of 2.1 and 4.5. It is noted that urine had the

lowest HAA/THM ratio of the 5 contaminants. For the 3-day Cl₂ demand per DOC, Kanan and Karanfil (8) reported 2-8 mg/L Cl₂ demand for 1 mg DOC of filling water NOM and 17-25 mg/L Cl₂ demand for 1 mg DOC of body fluid analogue. A slight higher number, 21-40 mg/L Cl₂ demand for 1 mg DOC of real anthropogenic contaminants, was found in this research. Table 4 also presents the yields of HAAs and THMs by normalizing HAAFP and THMFP based on DOC, to compare different anthropogenic contaminants regardless of their dilution ratios. Sweat was observed to have an HAA yield of 300 µg/mg C. Urine and hair were observed to have relatively low HAA yields (160 µg/mg C) compared to three other anthropogenic contaminants. The THM yields of sweat and urine were 67 and 74 µg/mg C, respectively. These DBP yield data will be used in the later modeling section.

Table 4. DBPFPs and DBP Yields of Anthropogenic Input Samples

	<i>Sweat</i> ¹	<i>Saliva</i> ¹	<i>Skin wash</i> ¹	<i>Hair wash</i> ¹	<i>Urine</i> ²
3-day Cl ₂ demand [mg Cl ₂ /L]	170	170	210	230	410
THMFP [µg/L]	430	1010	870	560	740
HAAFP [µg/L]	1930	3050	3420	1750	1560
3-day Cl ₂ demand per DOC [mg Cl ₂ /mg C]	27	22	23	21	41
THM yield [µg/mg C]	67	130	96	50	74
HAA yield [µg/mg C]	300	390	380	160	160
HAA/THM	4.5	3.0	3.9	3.1	2.1

¹ A dilution ratio of 1:25 was applied to accommodate free Cl₂ demand in DBPFP test. ² A dilution ratio of 1:33 was applied to accommodate free Cl₂ demand in DBPFP test. Data presented are average values of duplicate sets.

Interpretation of DBP Profile in Swimming Pools

Swimming pool water is found to have high DBP levels, especially in forms of HAAs. THMs, however, did not show an increase trend with water age but were relatively constant in the pool water. We have summarized four factors that lead to this specific DBP profile in swimming pools:

Firstly, the long water retention time in swimming pools is special. As the pool water is continuously exposed to disinfectants, all DBP precursors have a potential to be driven to DBPs. This tends to result in high DBP levels.

Secondly, continuous introduction of anthropogenic contaminants leads to high DBP levels. With an R^2 of 0.70, a positive correlation between the HAA levels and the numbers of pool users exists (Figure 2).

Thirdly, discrepancies in the chemical loss rates could lead to the high HAA but low THM profile. Benoit and Jackson (44) observed stable THM levels in 25 whirlpool spas affected by heat, aeration, and agitation. Although these factors, i.e. the degree of water agitation by pool users, were difficult to measure, the THM loss rate appeared to be faster than the HAA loss rate because of much higher Henry's law constants for THMs. The loss rate includes the effects of evaporation, adsorption, degradation, and other incurred processes.

Finally, the anthropogenic inputs of swimming pools consist of more HAA precursors than THM precursors, as data of this research presents (Table 4). It is obvious that reduction of anthropogenic contaminants will lead to reduction of DBPs. This research demonstrated the actual effect of anthropogenic contaminants on the level of DBPs.

Modeling

Model Development

In recent years, a particular interest has been grown on the development of models to estimate the formation and fate of DBPs. Several predictive models have been reported (45). These models used different types of explanatory variables for variety of applications in drinking water industry. The DBP profile in a swimming pool system can be conceptualized based on mass balance and decay kinetics (46, 47). For chlorination of pool water, a comprehensive model for DBPs should consider variation of DBP precursors, i.e. sweat and urine from anthropogenic inputs. Efforts should be focused on the gaps between specific models and their actual applications.

The concentration data used to model DBP formation in swimming pool water were obtained from the study by Tang (22) where samples were collected from an indoor pool once a month over a 1.5-yr period. The DBP model was developed based on four assumptions: (1) All DBP precursors from anthropogenic inputs have been converted to DBPs under the chlorination scenarios of swimming pools; (2) There is no water change during the entire modeling period and the amount of make-up water is negligible, because a 1.8 m³ weekly make-up water versus the pool volume of 440 m³ makes the influence of dilution within the range of variability for DBP analysis. (3) The DBP loss due to evaporation, degradation, dilution, and adsorption follows first-order kinetics (48); and (4) The DBP loss rates maintain constant since water temperature of the pool is stable. Equation 1 shows the mass balance of DBPs in swimming pools. It can be reformed to represent the computational algorithm on the basis of the contribution from daily anthropogenic inputs to DBPs (Equation 2 and 3).

Equation 1.

$$DBP \text{ Accumulation} = DBP \text{ In} + DBP \text{ Production} - DBP \text{ Out}$$

Equation 2.

$$DBP_i = DBP_{new,i} + DBP_{i-1} \times e^{-k}$$

Where

DBP_i = Accumulated DBP at Day i , $\mu\text{g DBP/L}$;

$DBP_{new,i}$ = New DBP In due to the anthropogenic input at Day i , $\mu\text{g DBP/L}$;

DBP_{i-1} = Accumulated DBP at the day before Day i , $\mu\text{g DBP/L}$;

$DBP_{i-1} \times e^{-k}$ = Remaining DBP after 1-day first-order decrease, $\mu\text{g DBP/L}$;

k = DBP loss coefficient, day^{-1} .

Equation 3.

$$DBP_{new,i} = [N_i(Y_S C_S + Y_U C_U)]/V$$

Where

N_i = Number of pool users at Day i , *persons*;

Y_S = DBP yield for sweat, $\mu\text{g DBP/mg C}$;

C_S = Sweat carbon released per person, mg C/person ;

Y_U = DBP yield for urine, $\mu\text{g DBP/mg C}$;

C_U = Urine carbon released per person, mg C/person ;

V = Volume of the swimming pool, *Liter*.

It is noted that C_S , C_U , and k were difficult to measure and show variances from one swimming pool to another. They need to be calibrated by computer-based regression programs. Shuffled complex evolution (SCE), a global optimization method developed by Duan et al. (49), was used to calibrate these difficult-to-measure parameters of the swimming pool. The calibration process used 48 (approximately 70%) of data sets (12 months \times 4 classes of DBPs) based on statistical requirements. The C_S , C_U , and k were assigned an initial value, respectively, to start the calibration. If the values were perfect, there would be an approximate prediction but not necessarily an exact match. To take care of small discrepancies, small adjustments were made to these parameters until the predicted data matches the measured ones. The SCE algorithm ensured that the root mean squared value between the predicted data and the measured ones was the lowest. The remaining 30% of data sets were used for validation. The coefficient of determination (R^2) was used to verify the regressions between the predicted DBP data the measured ones in the pool water.

Model Performance

The obtained parameters of the DBP model for the swimming pool after calibration were as follows:

C_S , Sweat carbon released per person = 1000 mg C/person;

C_U , Urine carbon released per person = 480 mg C/person;

k_{HAA} , HAA loss coefficient = 0.035 day⁻¹;

k_{THM} , THM loss coefficient = 0.23 day⁻¹;

Figure 3 presents the calibration and validation results of comparing the predicted and measured data without distinguishing different DBP classes. The 45° line the figure depicted the predicted DBP data that were precisely equal to the measured ones. As shown in Figure 3a, with an R^2 of 0.97, the predicted data showed a good fit to the measured ones. The validation process used the remaining 30% of data sets, and was still able to show a good fit to the measured data, with an R^2 of 0.96 (Figure 3b). Therefore, the model calibration led to sound results for the coefficients of the swimming pool system.

Figure 4 presents the predicted profiles of HAAs and THMs in comparison to the actual ones. The patterns were developed as a result of a combined effect of DBP formation and loss rates as described in the previous section. The predicted HAA curve captured the rising trends and descending trends very well. The predicted THM pattern also gave a quantitatively correct range. Because of the high loss rates, THM variations with water age were not as significant as those of HAAs. An extraordinary THM observation of 181 µg/L at the 104th day could be attributed to a peak hourly loading of swimmers during the sampling.

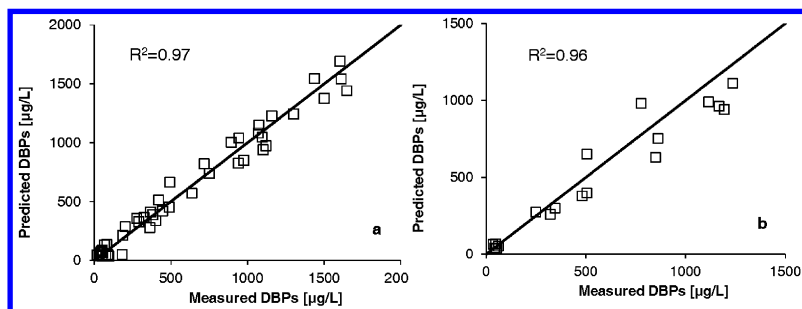


Figure 3. Calibration and validation results. (a) calibration based on 70% data; (b) validation based on 30% data.

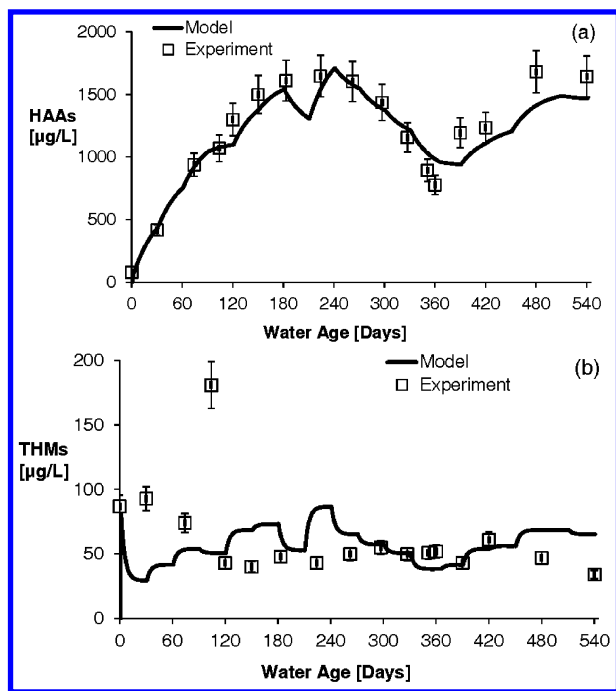


Figure 4. Predicted DBP profiles as a function of water age. (a) HAAs; (b) THMs.

Model Implications

Computer-based modeling is a useful tool for a number of tasks performed by water and wastewater professionals. Because of the high R^2 values of both calibration and validation, the DBP model developed based on mass balance and first-order kinetics is competent to predict DBPs in swimming pools. The model basically attributes the formation of DBPs to the continuous introduction of anthropogenic contaminants or the number of pool users.

Anthropogenic inputs represent the major cause of high DBP levels in swimming pool water. The model suggests 1000 mg carbon from sweat per person and 480 mg carbon from urine per person were released to the pool every day. According to Judd and Black (46), body fluids had a carbon content of approximately 6000 mg/L. The model implies that each pool user released approximately 170 mL sweat and 80 mL urine to the pool. These values were in the range reported by Gunkel and Jessen (42) and Erdinger et al. (43), who estimated that a swimmer introduces in water 25-80 mL/h of urine and 200-1000 mL/h of sweat. The model also presents an approach to estimate the DBP loss coefficients. It is believed that water agitation affects the DBP levels in swimming pool water. However, the degree of water agitation is difficult to measure. According to the model, the HAA loss coefficient was 0.035 per day while the THM loss coefficient was 0.23 per day in the investigated pool. Lower coefficient implies longer half life and thus higher concentration.

Control

Control Factors

DBPs in drinking water are typically controlled by limiting both the amount of disinfectants and the amount of NOM. In swimming pool water, the DBP formation may be limited by three factors: disinfectant residual, the amount of organic material in the water, and the recirculation of the pool water (50).

The amount of chlorine entering the pool water can be easily controlled, as the chlorine, in forms of granular powder or tablets, can be added by hand or by a mechanical dosing system. Proper dosing ensures chlorine residual kept at a minimum and still effectively eradicate pathogenic microorganisms, in the meanwhile keeps DBP concentrations at low levels. This is the microbe-DBP balancing act of minimizing risks while maximizing beneficial effects.

The amount of organic material can be controlled by reducing the input of DBP precursors (NOM and anthropogenic input). The anthropogenic input can be reduced considerably by the behavior of swimmers before and during swimming. For example, showering and using toilet facilities, washing off sunscreen lotions, and applying water-tight diapers can reduce the anthropogenic load and help to reduce DBP formation. Keuten et al. (51) found that the duration of shower has the largest influence on the removal of contaminants and most of contaminants can be removed within a 60-second shower. Although a showering protocol is an important first step to inform pool users about their personal influence on the pool water quality, showering protocols alone might not be enough. The aquatic staff also needs to be aware of the necessity of pre-swim showering. And finally, supportive policies (e.g., maintaining clean, well-stock bathroom facilities that not only encourage showering but also toileting) should be established, implemented, and enforced.

The recirculation of the pool water leads to an accumulation of DBPs in the water. From the technological point of view, the treatment efficiency to reduce DBP precursors and already-formed DBPs can be improved by more efficient filtration and oxidation. This includes tight membrane (e.g. nano or reverse osmosis membrane) filtration, carbon filtration, biological filtration, and advanced oxidation (52). Removal of the low-molecular-weight fraction would be advised because it contains a large part of the toxicity according to Zwiener et al. (1). Their toxicity data also suggest keeping bromide and iodide concentrations in pool water low and not using bromine because brominated and iodinated DBPs have been found to be even more toxic than chlorinated DBPs. It is also beneficial to increase air circulation in indoor pool settings to reduce the levels of volatile DBPs.

Filtration

Typical swimming pool water treatment includes sand filtration and disinfection with chlorine. Hansen et al. (27) reported a few swimming pools in Denmark use drum filters based on a weaved microsieve (cutoff 10 or 20 μm) which removes the particles from the pool water fast by washing the filter. Although most swimming pools remove particles through a filtration unit, the

filtration units are not designed to remove organic matter. Control of DBPs and their organic precursors using adsorbent, i.e. GAC, could be an effective approach.

Two types of GAC were investigated in bench-scale filters: virgin GAC supplied by Waterlink (USA) and biologically activated carbon (BAC) collected at a local drinking water treatment facility. The schematic setup of the GAC filters is depicted in Figure 5. Swimming pool water was directly added to the filter columns loaded with 40 mL of GAC and the flow rates were adjusted to 2 mL/min to have an empty bed contact time (EBCT) of 20 minutes.

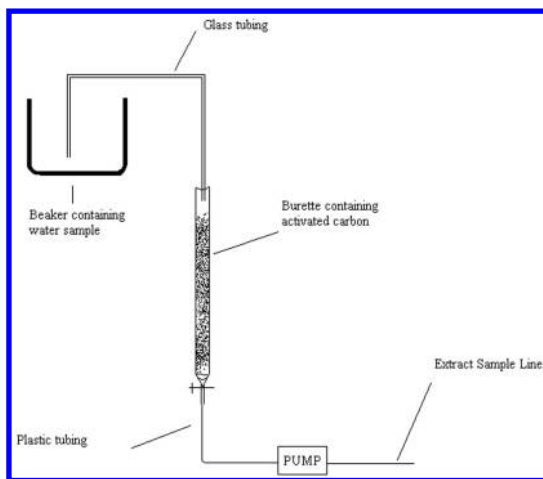


Figure 5. Schematic setup of bench-scale GAC filters.

The bench-scale GAC filter was operated for 400 hours. Results showed that TCAA was completely removed during the beginning of the experiment and the effluent concentration of DCAA steadily increased. Before the GAC column reached saturation, biological degradation of DCAA was observed after 128 hours of operation. This is shown in Figure 6 at the highest peak of the curve. At this point, the total HAA was 566 $\mu\text{g/L}$, and there was 48% reduction in total HAAs, a 9% reduction in DCAA and 99% reduction in TCAA. The results imply that GAC was effective in removing TCAA while the adsorption capacity for DCAA was relatively low.

The bench-scale BAC filter was initially operated for 2 hours filtering deionized water. Then it started filtering swimming pool water for 480 hours at the same settings with the GAC filter. Since BAC has almost no adsorption capacity, it became saturated almost immediately for TCAA (Figure 7). There was approximately 90% removal of DCAA throughout the entire experiment. Opposite to what was observed in the bench-scale GAC filter, this occurred because the bacteria capable of degrading DCAA were already established on the BAC. The TCAA degrading bacteria, however, took approximately 30 hours to

be established, and then the TCAA concentration in the effluent rapidly decreased throughout the experiment. In the end of the experiment, approximately 70% of TCAA was removed.

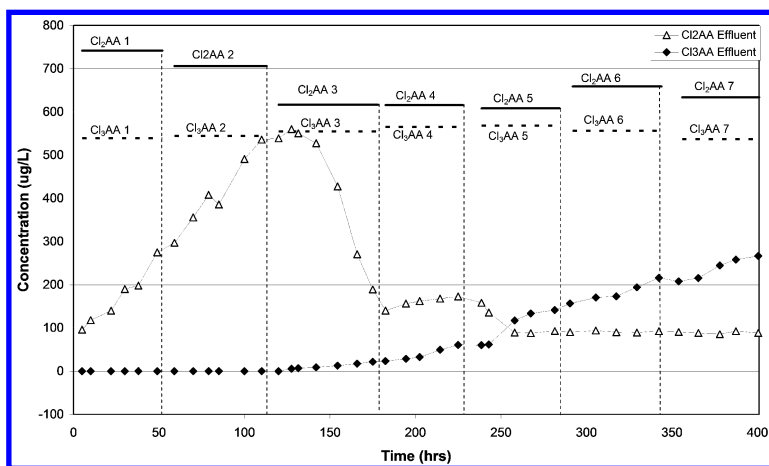


Figure 6. HAA removal from swimming pool water by a bench-scale GAC filter.

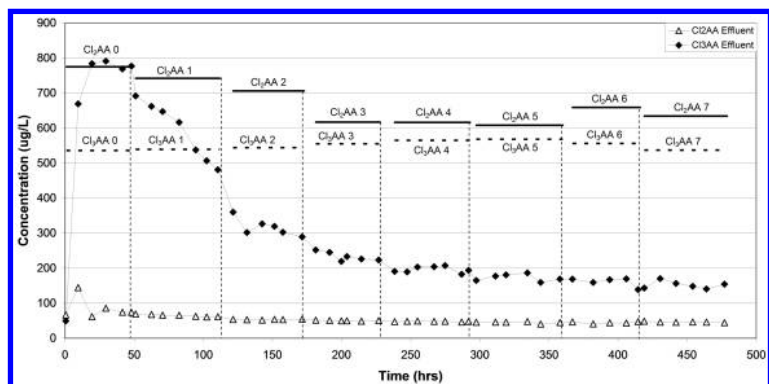


Figure 7. HAA removal from swimming pool water by a bench-scale BAC filter.

These experiments show that GAC is able to adsorb TCAA and BAC can remove DCAA efficiently at the beginning. Once TCAA degrading bacteria become established, BAC can efficiently remove HAAs from swimming pool water and outperforms GAC. The study also implies that, given enough time, bacteria capable of degrading HAAs will develop on the surface of GAC, converting it to BAC and reducing the need to replace the GAC. A disadvantage associated with both studies is that the filter effluent had zero chlorine residual. This may lead to problems when used on an actual swimming pool, because the

pool water needs to be continuously chlorinated to keep a residual typically in a range of 2-4 mg/L. Elevated costs for the use of additional chlorine could be expected.

Besides adsorption and biodegradation during the filtration process for DBP control in swimming pool water, other filtration technologies, i.e. membrane, zero-valent iron, etc, are also being investigated by scientists. Cost-effective HAA removal technologies for swimming pool water represent a promising direction of future research.

Conclusions

In this chapter, three key aspects related to swimming pool water were investigated:

Formation

We measured DBP formation in a swimming pool over a 1.5-yr period since water change. We found the HAA levels could go very high in the swimming pool, while THM levels remained relatively constant. By exploring the DBPFPs from anthropogenic contaminants, we found the anthropogenic inputs to swimming pools contributed to high HAAs and significantly impacted certain DBP species in the water.

Modeling

The DBP profile in swimming pools can be modeled and predicted. The DBP model was developed using the DBP data of the investigated swimming pool and a computer-based derivatization method based on mass balance and first-order kinetics. The predictive DBP model was competent to provide quantitatively acceptable DBP data. The model attributes the formation of DBPs to the continuous introduction of anthropogenic contaminants and the number of pool users, which helps the interpretation of the special DBP profile in swimming pool water.

Control

Of the three limiting factors to DBP formation in swimming pools, reducing the input of anthropogenic contaminants is critical. With the purpose of reducing DBP precursors and already-formed DBPs, filtration technologies using GAC and BAC were investigated by bench-scale experiments. GAC adsorption and BAC biodegradation were both found to be effective options on certain HAA species removal.

Future research efforts should be focused on three aspects: (1) monitoring and assessment of other emerging/remerging DBPs in swimming pools; (2) the potential health impact of swimming pool exposure to high level HAAs; and (3) cost-effective HAA removal technologies for swimming pools.

References

1. Zwiener, C.; Richardson, S. D.; De Marini, D. M.; Grummt, T.; Glauner, T.; Frimmel, F. H. Drowning in disinfection byproducts? Assessing swimming pool water. *Environ. Sci. Technol.* **2007**, *41*, 363–372.
2. Florentin, A.; Hautemaniere, A.; Hartemann, P. Health effects of disinfection by-products in chlorinated swimming pools. *Int. J. Hyg. Environ. Health* **2011**, *214*, 461–469.
3. De Laat, J.; Feng, W.; Freyfer, D. A.; Dossier-Berne, F. Concentration levels of urea in swimming pool water and reactivity of chlorine with urea. *Water Res.* **2011**, *45*, 1139–1146.
4. Friedman, M. S.; Roels, T.; Koehler, J. E.; Feldman, L.; Bibb, W. F.; Blake, P. Escherichia coli O157:H7 outbreak associated with an improperly chlorinated swimming pool. *Clin. Infect. Dis.* **1999**, *29*, 298–303.
5. Leoni, E.; Legnani, P.; Mucci, M. T.; Pirani, R. Prevalence of mycobacteria in a swimming pool environment. *J. Appl. Microbiol.* **1999**, *87*, 683–688.
6. LaKind, J. S.; Richardson, S. D.; Blount, B. C. The good, the bad, and the volatile: can we have both healthy pools and healthy people? *Environ. Sci. Technol.* **2010**, *44*, 3205–3210.
7. Dyck, R.; Sadiq, R.; Rodriguez, M. J.; Simard, S.; Tardif, R. Trihalomethane exposures in indoor swimming pools: a level III fugacity model. *Water Res.* **2011**, *45*, 5084–5098.
8. Kanan, A.; Karanfil, T. Formation of disinfection by-products in swimming pool water: The contribution from filling water natural organic matter and swimmer body fluids. *Water Res.* **2011**, *45*, 926–932.
9. Weaver, W. A.; Li, J.; Wen, Y.; Johnston, J.; Blatchley, M. R.; Blatchley, E. R., III Volatile disinfection by-product analysis from chlorinated indoor swimming pools. *Water Res.* **2009**, *43*, 3308–3318.
10. Xu, X.; Weisel, C. P. Dermal uptake of chloroform and halo ketones during bathing. *J. Exposure Anal. Environ. Epidemiol.* **2005**, *15*, 289–296.
11. Villaneuva, C. M.; Cantor, K. P.; Grimalt, J. O.; Malats, N.; Silverman, D.; Tardon, A.; Garcia-Closas, R.; Serra, C.; Carrato, A.; Castano-Vinyals, G.; Marcos, R.; Rothman, N.; Real, F. X.; Dosemeci, M.; Kogevinas, M. Bladder cancer and exposure to water disinfection by-products through ingestion, bathing, showering, and swimming in pools. *Am. J. Epidemiol.* **2007**, *165*, 148–156.
12. Richardson, S. D.; DeMarini, D. M.; Kogevinas, M. M.; Fernandez, P.; Marco, E.; Lourencetii, C.; Balleste, C.; Heederik, D.; Meliefste, K.; McKague, A. B.; Marcos, R.; Font-Ribera, L.; Grimalt, J. O.; Villanueva, C. M. What's in the pool? A comprehensive identification of disinfection by-products and assessment of mutagenicity of chlorinated and brominated swimming pool water. *Environ. Health Perspect.* **2010**, *118*, 1523–1530.
13. Cantor, K. P.; Villanueva, C. M.; Silverman, D. T.; Figueroa, J. D.; Real, F. X.; Garcia-Closas, M.; Malats, N.; Chanock, S.; Yeager, M.; Tardon, A.; Garcia-Closas, R.; Serra, C.; Carrato, A.; Castano-Vinyals, G.; Samanic, C.; Rothman, N.; Kogevinas, M. Polymorphisms M. Polymorphisms in GSTT1,

- GSTZ1, and CYP2E1, disinfection by-products, and risk of bladder cancer in Spain. *Environ. Health Perspect.* **2010**, *118*, 1545–1550.
14. Kogevinas, M.; Villanueva, C. M.; Font-Ribera, L.; Liviac, D.; Bustamante, M.; Espinoza, F.; Nieuwenhuijsen, M. J.; Espinosa, A.; Fernandez, P.; DeMarini, D. M.; Grimalt, J. O.; Grummt, T.; Marcos, R. Genotoxic effects in swimmers exposed to disinfection by-products in swimming pools. *Environ. Health Perspect.* **2010**, *118*, 1531–1537.
 15. Bessonneau, V.; Derbez, M.; Clement, M.; Thomas, O. Determinants of chlorination by-products in indoor swimming pools. *Int. J. Hyg. Environ. Health* **2011**, *215*, 76–85.
 16. Cardador, M. J.; Gallego, M. Haloacetic acids in swimming pools: swimmer and worker exposure. *Environ. Sci. Technol.* **2011**, *45*, 5783–5790.
 17. Catto, C.; Sabrina, S.; Ginette, C. T.; Manuel, R.; Robert, T. Occurrence and spatial and temporal variations of disinfection by-products in the water and air of two indoor swimming pools. *Int. J. Environ. Res. Publ. Health* **2012**, *9*, 2562–2586.
 18. Parinet, J.; Tabaries, S.; Coulomb, B.; Vassalo, L.; Boudenne, J. Exposure levels to brominated compounds in seawater swimming pools treated with chlorine. *Water Res.* **2012**, *46*, 828–836.
 19. Yeh, R. Y. L.; Farre, M. J.; Stalter, D.; Tang, J. Y. M.; Molendijk, J.; Escher, B. I. Bioanalytical and chemical evaluation of disinfection by-products in swimming pool water. *Water Res.* **2014**, *59*, 172–184.
 20. Fantuzzi, G.; Righi, E.; Predieri, G.; Ceppelli, G.; Gobba, F.; Aggazzotti, G. Occupational exposure to trihalomethanes in indoor swimming pools. *Sci. Total Environ.* **2001**, *264*, 257–265.
 21. Chu, H.; Nieuwenhuijsen, M. J. Distribution and determinants of trihalomethane concentrations in indoor swimming pools. *Occup. Environ. Med.* **2002**, *59*, 243–247.
 22. Tang, H. Disinfection byproduct precursors from wastewater organics: Formation potential and influence of biological treatment processes. Ph.D. Thesis, the Pennsylvania State University, University Park, PA, 2011.
 23. Simard, S.; Tardif, R.; Rodriguez, M. J. Variability of chlorination by-product occurrence in water of indoor and outdoor swimming pools. *Water Res.* **2013**, *47*, 1763–1772.
 24. Wang, X.; Leal, M I G.; Zhang, X.; Yang, H.; Xie, Y. Haloacetic acids in swimming pool and spa water in the United States and China. *Front. Environ. Sci. Eng.* **2014**, *8*, 820–824.
 25. Dotson, A.; Westerhoff, P.; Krasner, S. W. Nitrogen enriched dissolved organic matter (DOM) isolates and their affinity to form emerging disinfection by-products. *Water Sci. Technol.* **2009**, *60*, 135–143.
 26. Walse, S. S.; Mitch, W. A. Nitrosamine carcinogens also swim in chlorinated pools. *Environ. Sci. Technol.* **2008**, *42*, 1032–1037.
 27. Hansen, K.; Willach, S.; Mosbak, H.; Andersen, H. R. Particles in swimming pool filters – Does pH determine the DBP formation? *Chemosphere* **2012**, *87*, 241–247.
 28. Schmalz, C.; Frimmel, F. H.; Zwiener, C. Trichloramine in swimming pools – Formation and mass transfer. *Water Res.* **2011**, *45*, 2681–2690.

29. Chowdhury, S.; Alhooshani, K.; Karanfil, T. Disinfection byproducts in swimming pool: occurrences, implications and future needs. *Water Res.* **2014**, *53*, 68–109.
30. Bond, T.; Goslan, E. H.; Parsons, S. A.; Jefferson, B. A critical review of trihalomethane and haloacetic acid formation from natural organic matter surrogates. *Environmental Technology Reviews* **2012**, *1*, 93–113.
31. Farre, M. J.; Day, S.; Neale, P. A.; Stalter, D.; Tang, J. Y. M.; Escher, B. I. Bioanalytical and chemical assessment of the disinfection by-product formation potential: Role of organic matter. *Water Res.* **2013**, *47*, 5409–5421.
32. Weng, S.; Blatchley, E. R., III Disinfection by-product dynamics in a chlorinated, indoor swimming pool under conditions of heavy use: National swimming competition. *Water Res.* **2011**, *45*, 5241–5248.
33. Keuten, M. G. A.; Peters, M. C. F. M.; Daanen, H. A. M.; de Kreuk, M. K.; Rietveld, L. C.; van Dijk, J. C. Quantification of continual anthropogenic pollutants released in swimming pools. *Water Res.* **2014**, *53*, 259–270.
34. APHA. *Standard Method for the Examination of Water and Wastewater*, 20th ed.; American Water Works Association: 1998.
35. Tang, H. L.; Chen, Y.-C.; Xie, Y. F. Quantification of disinfection by-product formation potential in wastewater. Proceedings of IWA Micropol & Ecohazard, July 11–13, 2011, Sydney, Australia.
36. Reckhow, D. A.; Singer, P. C.; Malcolm, R. L. Chlorination of humic materials – by-product formation and chemical interpretations. *Environ. Sci. Technol.* **1990**, *24*, 1655–1664.
37. Lee, J.; Jun, M. J.; Lee, M. H.; Eom, S. W.; Zoh, K. D. Production of various disinfection byproducts in indoor swimming pool waters treated with different disinfection methods. *Int. J. Hyg. Environ. Health* **2010**, *213*, 465–474.
38. Judd, S.; Jeffrey, J. A. Trihalomethane formation during swimming pool water disinfection using hypobromous and hypochlorous acids. *Water Res.* **1995**, *29*, 1203–1206.
39. Kim, H.; Shim, J.; Lee, S. Formation of disinfection by-products in chlorinated swimming pool water. *Chemosphere* **2002**, *46*, 123–130.
40. Judd, S. J.; Bullock, G. The fate of chlorine and organic materials in swimming pools. *Chemosphere* **2003**, *51*, 869–879.
41. Li, J.; Blatchley, E. R., III Volatile disinfection byproduct formation resulting from chlorination of organic-nitrogen precursors in swimming pools. *Environ. Sci. Technol.* **2007**, *41*, 6732–6739.
42. Gunkel, K.; Jessen, H. J. The problem of urea in bathing water. *Z. Gesamte Hyg.* **1988**, *34*, 248–250.
43. Erdinger, L.; Kirsch, F.; Sonntag, H. G. Potassium as an indicator of anthropogenic contamination of swimming pool water. *Zbl. Hyg. Umweltmed.* **1997**, *200*, 297–308.
44. Benoit, F. M.; Jackson, R. Trihalomethane formation in whirlpool spas. *Water Res.* **1987**, *21*, 353–357.

45. Sadiq, R.; Rodriguez, M. J. Disinfection by-products (DBPs) in drinking water and predictive models for their occurrence: a review. *Sci. Total Environ.* **2004**, *321*, 21–46.
46. Judd, S. J.; Black, S. Disinfection byproduct formation in swimming pool waters: A simple mass balance. *Water Res.* **2000**, *34*, 1611–1619.
47. Sohn, J.; Gary, A.; Cho, J.; Lee, Y.; Yoon, Y. Disinfectant decay and disinfection by-products formation model development: chlorination and ozonation by-products. *Water Res.* **2004**, *38*, 2461–2478.
48. Aggazzotti, G.; Fantuzzi, G.; Righi, E.; Predieri, G. Environmental and biological monitoring of chloroform in indoor swimming pools. *J. Chromatogr. A* **1995**, *710*, 181–190.
49. Duan, Q. Y.; Gupta, V. K.; Sorooshian, S. Shuffled complex evolution approach for effective and efficient global minimization. *J. Optimiz. Theory App.* **1993**, *76*, 501–521.
50. Glauner, T.; Waldmann, P.; Frimmel, F. H.; Zwiener, C. Swimming pool water – fractionation and genotoxicological characterization of organic constituents. *Water Res.* **2005**, *39*, 4494–4502.
51. Keuten, M. G. A.; Schets, F. M.; Schijven, J. F.; Verberk, J. Q. J. C.; van Dijk, J. C. Definition and quantification of initial anthropogenic pollutant release in swimming pools. *Water Res.* **2012**, *46*, 3682–3692.
52. Glauner, T.; Kunz, F.; Zwiener, C.; Frimmel, F. Elimination of swimming pool water disinfection by-products with advanced oxidation processes (AOPs). *Acta Hydrochim. Hydrobiol.* **2005**, *33*, 585–594.

Chapter 21

Occurrence and Formation of Disinfection By-Products in Indoor U.S. Swimming Pools

Amer Kanan,¹ Meric Selbes,² and Tanju Karanfil^{*3}

¹Department of Environmental and Earth Sciences, Al-Quds University, Jerusalem, Palestine

²Hazen and Sawyer, Environmental Engineers and Scientists, Fairfax, Virginia 22030, U.S.A.

³Department of Environmental Engineering and Earth Sciences, Clemson University, Anderson, South Carolina 29625, U.S.A.

*E-mail: tkaranf@clemson.edu.

Chlorination is commonly used to prevent the spreading of waterborne infectious diseases in swimming pools. This required disinfection practice also results in the formation of undesirable disinfection by-products (DBPs) from the reactions of chlorine with the organic matter (released by swimmers or present in the pool filling water) and inorganics (i.e., bromide). The main objective of this research was to improve our understanding of the occurrence and formation of different classes of DBPs (trihalomethanes [THMs], haloacetic acids [HAAs], halonitromethanes [HNMs], haloacetonitriles [HANs], and nitrosamines) in indoor swimming pools operational conditions in the U.S.. The results showed that the DBPs in the investigated 23 swimming pools were far higher than the drinking water regulation values in the U.S. Average THMs, HAAs, HANs, HNMs, and *N*-nitrosodimethylamine concentrations were 80 µg/L, 1541 µg/L, 19 µg/L, 5.4 µg/L, and 27 ng/L, respectively. An increase in organic matter released by the swimmers and bromide (from the filling water or electrochemical generation of chlorine) levels in the water increased the overall formation of DBPs. Increases in free available chlorine, pH, and water temperature were shown to

enhance the formation of THMs and HAAs. These favorable conditions lead to rapid formation (i.e. 3-6 hours) of THMs and HAAs under swimming pool conditions.

Introduction

The average swimmer releases several grams of body fluids (BFs) and excretions during an average swim (1-3). The disinfection of this organic and inorganic matter from swimming pool water is essential for deactivating the pathogenic microorganisms that can thrive on the released organic matter. Swimming pool water is continuously circulated, filtered, and disinfected to maintain clear and biologically safe (4). Chlorine is commonly used in swimming pools and is added continuously to maintain free available chlorine (FAC) to prevent microbial growth (5). While deactivating microorganisms, the reaction of chlorine with the organic (e.g., hair, sweat, dead cells, saliva, cosmetics, dust and urine) and inorganic (e.g., urea, nitrates, nitrites and free ammonia) matter can form a wide array of DBPs including trihalomethanes (THMs), haloacetic acids (HAAs), haloacetonitriles (HANs), haloacids, halodiacids, iodo-THMs, haloaldehydes, halonitriles, halo ketones (HKs), halonitromethanes (HNMs), haloamides, haloalcohols, nitrosamines, combined available chlorine, and 3-chloro-4-(dichloromethyl)-5-hydroxy-2(5H)-furanone (MX) and MX homologues, etc. (6-11). Furthermore, bromide is introduced to when the pool is being filled and/or as impurities when chlorine is generated electrochemically from sodium chloride. Chlorine oxidizes bromide to HOBr that can react with organic matter to produce brominated DBPs. Although there are currently no federal DBP regulations in swimming pool waters in the U.S., some countries are including THMs within the swimming pool regulations (12, 13).

The overall formation of DBPs is correlated to the amount of precursors such as organic matter. It is also well known that temperature, pH, and chlorine dose influence the formation of DBPs. Therefore, the formation of DBPs in pool waters would be affected by the operation of the swimming pools. The pool operational requirements and regulations in the U.S. are variable among different states and enforced separately by each state department of health and environment. Generally in the U.S., FAC should be maintained in the range of 1 to 5 mg/L in the pool water to prevent microbial growth (5, 8, 14). The pH of swimming pool water is continuously adjusted mainly to assure an acceptable level of disinfection efficiency, comfortable water for swimmers, and elimination of the damage to the swimming pool structures. Typically, the pH of the pool water is maintained between 7.2 and 7.8 range (15). Swimming pool water temperature is maintained constant usually within the range of 26 to 40°C depending on pool type and usage. Finally, the turnover period for the water in swimming pools typically ranges from 4 to 8 hours (3, 5, 16). From a DBP formation perspective, the reaction period corresponds to the time available for chlorine to react with precursors and form DBPs before they are removed through the pool treatment processes. It is well-known that DBPs including THMs and HAAs have fast formation kinetics

at the levels of chlorine dose in drinking waters (17, 18). It is postulated that DBPs will form very rapidly in swimming pools due to much higher free chlorine residual concentrations than in drinking waters.

Although intensive work has been devoted to investigate the formation of regulated THMs and HAAs in drinking waters, there is relatively little known about the formation and occurrence of DBPs in swimming pools. Moreover, the effects of swimming pool operational parameters on the formation and speciation of DBPs in swimming pools have not been systematically investigated. Understanding the effect of operational parameters is essential for developing approaches to control the formation of DBPs in pools and reduce exposure of swimmers and swimming pool attendants to DBPs. Furthermore, to date there is no information regarding the DBP formation kinetics under swimming pool conditions.

The objectives of this study were to (i) investigate the occurrence of regulated DBPs (THMs and HAAs), as well as emerging DBPs including HNMs, HANs, and nitrosamines in 23 indoor swimming pools, (ii) examine the effects of different swimming pool operational parameters such as FAC in pool water, pH, organic carbon, temperature, bromide concentration on the formation and speciation of THMs and HAAs and (iii) determine how fast THMs and HAAs are produced under swimming pool conditions.

Materials and Methods

Samples Collection

Indoor swimming pools ($n=23$) located in South Carolina, Georgia and North Carolina were sampled to investigate the occurrence of five classes of DBPs. Furthermore, three of the swimming pools were monitored over a nine-month period. Grab samples were collected from 30 cm below the water surface of the pool. FAC, pH, and temperature of the swimming pool were obtained from the facilities. A 125-mL amber bottle was used to collect total organic carbon (TOC) and total nitrogen (TN) samples without any preservatives. A 125-mL amber glass was used for the halogenated DBPs analysis (THMs, HAAs, HNMs, HANs), and ammonium chloride was used to quench the free chlorine in these samples. For nitrosamine analysis, a 1L sample was collected in an amber glass bottle and quenched by sodium thiosulfate. All samples were transferred immediately to the lab using an ice box for DBPs analyses, which was conducted either on the same day of sampling or stored at 4°C for the following day.

Synthetic Swimming Pool Waters

Two synthetic pool waters were prepared using two different filling waters and a body fluids analog (BFA) recipe developed by Goeres and co-workers (19) to simulate the body fluids that are introduced in swimming pool water by swimmers (9). The filling waters were collected from Myrtle Beach (MB) and

Startex-Jackson-Wellford-Duncan (SJWD) drinking water treatment plants in South Carolina prior to the final addition of the disinfectant. These two filling waters served as two different background matrices for the synthetic swimming pool waters. The selected waters had distinct differences in their aromaticity of the organic components determined by their specific ultraviolet absorbances at 254 nm wavelength (SUVA₂₅₄). The MB water had a high aromaticity with a SUVA₂₅₄ value of 4-6 mg/L-m, whereas the SJWD had a lower level of aromatic organics with a SUVA₂₅₄ of 2-3 mg/L-m. Both waters were diluted to 1 mg/L TOC to provide the same amount of background organic carbon in the synthetic solution. For every experiment 1 mg/L TOC was from the fill water and the remaining TOC was provided by the BFA. Here and after the two synthetic pool waters will be referred to as BFA-MB and BFA-SJWD.

DBP FP and Kinetics Tests

THM and HAA formation potential (FP) tests were conducted in the presence of an excess disinfectant. Chlorine stock solutions (500–2,000 mg/L) were prepared by diluting sodium hypochlorite (~5% available free chlorine). The chlorination FP tests were performed in 125 mL amber bottles filled headspace free with the sample and capped with Teflon-lined PTFE caps. After mixing for five minutes with magnetic stir bars, the bottles were stored headspace free in a water bath for 5 days at 26 or 40°C. For the kinetic experiments an initial dose of 100 mg/L chlorine was used. Each solution was chlorinated, and DBPs were determined at different reaction times during 5 days (e.g., 0.5, 1, 3, 5, 7, 10, 15, 24, 48, 72, 96, 120 hours).

Analytical Methods

Analytical methods used in the study and their respective minimum reporting levels (MRLs) are provided in Table 1. Either standard methods (SM) or USEPA methods were used for DBP analyses with minor modifications. The detailed information about these methods can be found elsewhere (20–23). For TOC, TN and DBP analyses, samples were analyzed in duplicates. Error bars in all the graphs show the variability due to multiple analysis (n=2) under the same conditions.

Table 1. Analytical Methods and Minimum Reporting Levels

<i>Parameter</i>	<i>Unit</i>	<i>Measurement Method</i>	<i>Instrument</i>	<i>MRL or Accuracy^a</i>
TOC ^b	mg/L	SM 5310B	TOC-V _{CHS} & TNM-1, Shimadzu Corp., Japan	0.1
TN ^c	mg/L	High Temperature Combustion	TOC-V _{CHS} & TNM-1, Shimadzu Corp., Japan	0.1
UV Absorbance ^d	cm ⁻¹	SM 5910	DU 640, Beckman Inst. Inc., USA	±0.005 ^d
Bromide	µg/L	US EPA Method 300	ED 40, Dionex Corp., USA	10
pH	-	SM 4500-H ⁺	420A, Orion Corp., USA	±0.01 ^e
THMs & HANs ^f	µg/L	US EPA Method 551.1	6890 GC-ECD, Agilent, USA	1.0
HAAs ^g	µg/L	SM 6251 B ^g	6890 GC- ECD, Agilent, USA	1.0
HNMs ^h	µg/L	US EPA Method 551.1	6850 GC-ECD, Agilent, USA	0.7
Nitrosamines ⁱ	ng/L	US EPA 521	Varian GC/MS/MS	3.0
FAC	mg/L	SM 4500-Cl F	NA	0.1

^a MRLs were determined in the lab in previous works (24). Accuracy as reported by the manufacturer. ^b Reagent grade potassium hydrogen phthalate was used to prepare external standards. ^c Reagent grade potassium nitrate was used to prepare external standards. ^d At wavelengths of 254 nm using a 1- or 5-cm cell. Photo-metric accuracy (absorbance units). ^e Accuracy (pH units). ^f THMs and HANs were extracted by liquid-liquid extraction with methyl-tert butyl ether (MtBE) and analyzed by GC-µECD. ^g HAAs were extracted by liquid-liquid extraction with MtBE, derivatized with diazomethane and analyzed by GC-µECD. ^h HNM were extracted by liquid-liquid extraction with MtBE and analyzed by GC-µECD. ⁱ Nitrosamines were extracted by solid phase extraction, eluted with dichloromethane and analyzed by GC-MS. THM (Trihalomethanes), HAN (Haloacetonitriles), HAA (Haloacetic acids), HNM (halonitromethanes), SM (Standard Methods), EPA (Environmental Protection Agency), GC (Gas Chromatography), MS (Mass Spectrometer), FAC (Free Available Chlorine), NA (Not Applicable).

Results and Discussion

Water Characteristics of the Selected Indoor Swimming Pools (n=23)

All of the indoor swimming pools selected in this study used chlorine as disinfectant. Some of the sampled pools used calcium hypochlorite directly, whereas others generated chlorine in situ electrochemically using sodium chloride. Most of the pools were operated at an approximate temperature of 26°C and some at 34°C. Except for a single pool that used groundwater from a local well, all the pools used the local water distribution system for both fill and make-up water. Of the 23 pools under study, sand-filter filtration was used to treat water, and micro-filter filtration used for the other two. The water samples characteristics of all pools under study are shown in Table 2. The FAC in the pools was between <0.1 and 4.0 mg/L, and the pH, TOC and TN ranged between 7.2 to 7.8, 3 to 23.6 mg/L, and 0.8 to 12.3 mg/L, respectively. The TOC was higher than TN except for four of the swimming pools in this study.

Occurrence of DBPs in Indoor Swimming Pools (n=23)

The occurrence ranges of the five classes of DBPs in the selected twenty three indoor pools are shown in Figure 1. The concentration of each DBP class, along with their speciation for each swimming pool is summarized in Table 3 and Table 4. In general, carbonaceous DBPs concentrations were higher than nitrogenous DBPs. In this survey, the HAAs were the highest measured class of DBPs, followed by the THMs>HANs>HNMs>nitrosamines. The median, maximum, and minimum HAAs were 960, 9005, and 172 µg/L, respectively. Trichloroacetic acid (TCAA) and dichloroacetic acid (DCAA) were the dominant species among the measured HAAs. Bromochloroacetic acid (BCAA) and bromodichloroacetic acid (BDCAA) were also detected in all samples although at much lower levels compared to DCAA and TCAA. In some of the samples dibromoacetic acid (DBAA) and bromoacetic acid (BAA) were detected at concentrations <6 and <25 µg/L, respectively. These exceptionally (compared to drinking water samples) high values of HAAs are attributed to (i) nonvolatile and soluble nature of these compounds resulting in accumulate in the pool waters provided that pool water dilution is not common in U.S., and (ii) human body fluids that have been shown to have a high formation potential of HAAs (7, 9).

The median, maximum, and minimum THMs measured in the pools were 63, 213 and 26 µg/L, respectively, with chloroform the major THM determined in all pools. Although the brominated THM species were at low levels in most cases, there were relatively high in pools that use sodium chloride to generate chlorine electrochemically and in the pool that was filled with groundwater. In 43% of the pools, the total THMs was equal to or higher than 80 µg/L (MCL in U.S. drinking water), while in all the pools, the measured THM was greater than 20 µg/L (the maximum allowed in some European countries for swimming pools).

Table 2. Water Characteristics of the Selected Indoor Swimming Pools

<i>Swimming Pool Code</i>	<i>Temperature (°C)</i>	<i>pH</i>	<i>FAC (mg-/L)</i>	<i>Disinfectant</i>	<i>Filter Type</i>	<i>TOC (mg C/L)</i>	<i>TN (mg N/L)</i>
S1	27	7.5	3.0	Cl ₂	Sand	4.3	1.4
S2C	18	7.4	3.0	Cl ₂	Sand	4.1	1.8
S2W	31	7.4	3.0	Cl ₂	Sand	11.3	4.7
S3S	29	7.4	1.4	Cl ₂	Microfilter	10.3	4.5
S3D	28	7.3	3.1	Cl ₂	Microfilter	5.5	2.8
S4C	27	7.4	4.0	Cl ₂ *	Sand	7.1	9.1
S4W	30	7.4	3.0	Cl ₂ *	Sand	6.5	3.2
S5	27	7.4	2.0	Cl ₂	Sand	3.0	1.2
S6L	29	7.6	2.0	Cl ₂ *	Sand	7.9	4.8
S6T	34	7.4	3.0	Cl ₂ *	Sand	7.7	2.5
S7	27	7.2	1.0	Cl ₂	Sand	7.8	4.3
S10	31	7.4	3.0	Cl ₂	Sand	8.4	5.2
S11L	28	7.2	2.0	Cl ₂	Sand	5.2	3.4
S11D	30	7.2	3.0	Cl ₂	Sand	5.3	3.6
S12L	27	7.5	2.7	Cl ₂	Sand	3.7	10.2
S12I	30	7.5	2.4	Cl ₂	Sand	4.3	7.4
S13	29	7.6	1.0	Cl ₂	Sand	3.9	1.2
S14	27	7.8	3.0	Cl ₂	Sand	13.8	12.3
S15L	27	7.7	2.8	Cl ₂ *	Sand	3.8	0.8
S15T	32	7.8	1.2	Cl ₂ *	Sand	7.5	1.2
S16	27	7.2	<0.1	Cl ₂	Sand	7.5	2.2
S17L	28	7.6	3.5	Cl ₂ *	Sand	7.3	4.1
S17T	33	7.4	3.5	Cl ₂ *	Sand	23.6	4.4
Median	28	7.4	3.0			7.1	3.6
Maximum	34	7.8	4.0			23.6	12.3
Minimum	18	7.2	<0.0			3.0	0.8

* Electrochemically generated chlorine. FAC (free available chlorine), TOC (total organic carbon), TN (total nitrogen).

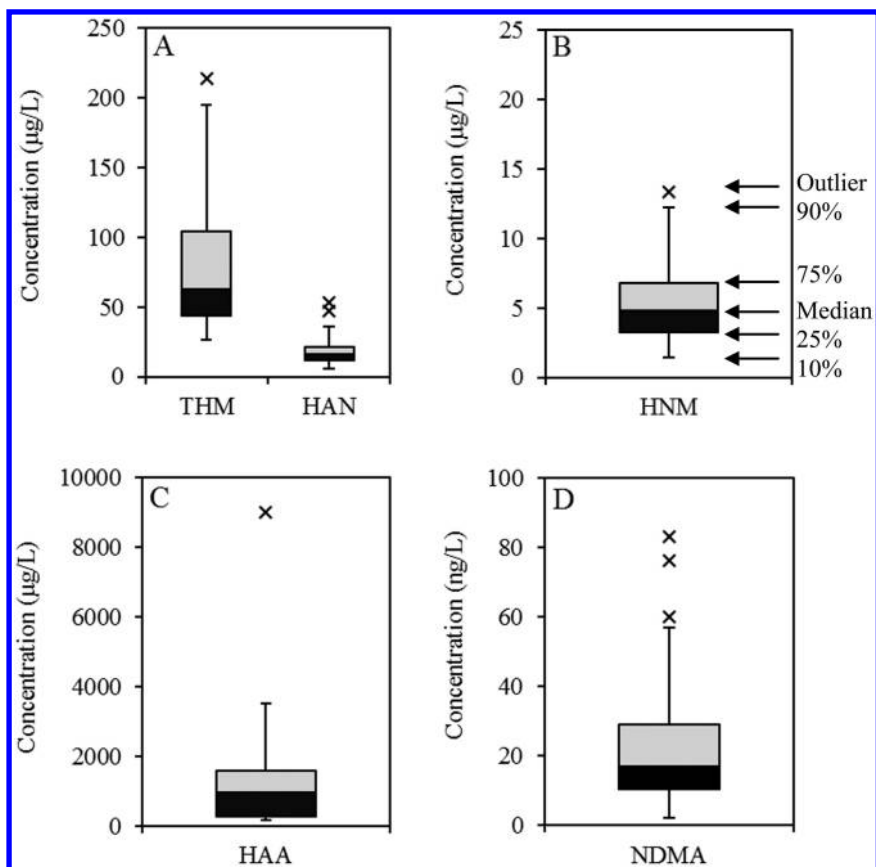


Figure 1. Box and Whisker plots of the occurrence of (A) THMs & HANs, (B) HNMs, (C) HAAs, and (D) NDMA in indoor swimming pools ($n=23$).

The median, maximum and minimum HANs were 16, 53, and 5 $\mu\text{g/L}$, respectively. The major haloacetonitrile quantified was dichloroacetonitrile (DCAN) among the six measured HANs. In few pools, brominated acetonitriles were detected at low levels (1-3 $\mu\text{g/L}$) except in the pool which was filled with groundwater. In general, it was observed that the pool waters with high levels of HAAs had high levels of HANs. Furthermore, when brominated

HAA species were high, the brominated HANs species also increased. Since HANs hydrolyze to HAAs, it is expected to have a positive correlation between these two classes of DBPs (25). Among the nine HNM species, only three HNM species [trichloronitromethane (TCNM), bromonitromethane (BNM), and bromochloronitromethane (BCNM)] were detected in the collected swimming pool samples. Total HNMs were between 1.4 and 13.3 $\mu\text{g/L}$.

Among the nitrosamines analyzable using the current method (22), NDMA was the only species detected in the selected 23 indoor swimming pool water samples, with NDMA concentrations ranging between 2 and 83 ng/L with a median of 17 ng/L . These levels of NDMA are somewhat higher than the drinking water levels, which was consistent with the literature (6), and also indicating that some NDMA precursors are released with body fluids and excretions. Nitrosamines are mainly formed during chloramination of amines (26). Although swimming pools are mostly chlorinated, the ammonia coming from urea would inevitably lead to the formation of chloramines in the pools. Therefore, it is not surprising to see some NDMA formation in swimming pools. Furthermore, there was no correlation between NDMA and the other classes of DBPs, which clearly indicates that their precursors differ from carbonaceous DBPs precursors, a finding consistent with the literature (27, 28). Although the nitrogenous DBPs (HANs, HNMs, NDMA) were detected at lower levels than carbonaceous DBPs, they were still significant regarding their cyto- and geno-toxicity (29).

DBPs Measured in the Selected Indoor Pools (n=3) for 9-Months

Three indoor swimming pools were further monitored for a 9-month sampling period. The operational conditions, water quality and DBPs occurrences in these pools are summarized in Table 5. The average FAC fell within the range of 3 mg/L , which is well within the state guidelines in place regarding adequate pool chlorination. Although the TN varied over a narrower range, between 2.0 and 5.0 mg/L in the three pools under study, the temperature and pH remained relatively constant and the TOC fell within a wide range of 5.3 to 25.4 mg/L .

During the nine-month monitoring period for these three pools, a narrow variation in the DBPs occurrence was observed in each (Table 5). The THM concentrations in all of them ranged from 29 to 259 $\mu\text{g/L}$ with an average of 108 $\mu\text{g/L}$. The highest THMs measured were in the warmest pool (S17T), which also had the highest TOC measurements. Of the THM levels measured in the three pools, chloroform was the most predominant (data not shown). The authors also found higher levels of measured BDCM in pools S17L and S17T because sodium chloride was used in both to generate chlorine electrochemically. The range of the BDCM in these three pools was 0 to 29 $\mu\text{g/L}$. The HAAs in all three pools was also higher than the THMs, which fell within a range between 667 to 11695 $\mu\text{g/L}$, with an average of 2820 $\mu\text{g/L}$ DCAA. The TCAA were the dominant species, and BDCAA was the major brominated HAA species. The maximum amount of BDCAA was 151 $\mu\text{g/L}$ and the minimum was 9 $\mu\text{g/L}$ with an average of 57 $\mu\text{g/L}$. The levels of all of the dibrominated species were much lower (<20 $\mu\text{g/L}$), however.

Table 3. Carbonaceous-DBPs Occurrence in Indoor Swimming Pools Water (n=23)

<i>Swimming Pool Code</i>	<i>Trihalomethanes (µg/L)</i>					<i>Halooacetic Acids (µg/L)</i>							
	<i>TCM</i>	<i>BDCM</i>	<i>DBCM</i>	<i>TBM</i>	<i>Total</i>	<i>BAA</i>	<i>DCAA</i>	<i>BCAA</i>	<i>TCAA</i>	<i>DBAA</i>	<i>BDCAA</i>	<i>DBCAA</i>	<i>Total</i>
S1	41	1	<MRL	ND	42	<MRL	100	1	87	<MRL	8	1	198
S2C	49	1	<MRL	ND	51	<MRL	314	3	224	<MRL	13	1	555
S2W	119	3	<MRL	ND	122	1	896	14	718	<MRL	36	<MRL	1665
S3S	77	2	<MRL	ND	80	<MRL	712	5	1537	<MRL	21	<MRL	2276
S3D	62	1	<MRL	ND	63	<MRL	937	7	776	<MRL	16	1	1738
S4C	37	1	<MRL	ND	38	<MRL	688	10	789	1	27	3	1518
S4W	49	3	<MRL	ND	53	1	81	4	241	<MRL	60	5	392
S5	26	1	<MRL	ND	28	<MRL	82	3	141	<MRL	22	2	251
S6L	72	3	<MRL	ND	76	1	928	30	552	2	48	3	1563
S6T	72	12	4	1	90	1	1033	36	351	4	36	7	1468
S7	113	1	<MRL	ND	114	<MRL	1139	5	418	<MRL	22	<MRL	1585
S10	89	2	<MRL	ND	91	<MRL	1297	4	416	<MRL	13	<MRL	1731
S11L	29	2	<MRL	ND	31	<MRL	123	2	76	<MRL	15	<MRL	216
S11D	111	2	<MRL	ND	113	<MRL	360	3	149	<MRL	11	<MRL	523
S12L	25	1	<MRL	ND	26	<MRL	162	1	95	<MRL	8	3	269
S12I	32	1	<MRL	ND	34	<MRL	242	2	216	<MRL	22	2	484
S13	74	28	10	1	114	1	73	13	100	2	55	15	260

<i>Swimming Pool Code</i>	<i>Trihalomethanes (µg/L)</i>					<i>Haloacetic Acids (µg/L)</i>							
	<i>TCM</i>	<i>BDCM</i>	<i>DBCM</i>	<i>TBM</i>	<i>Total</i>	<i>BAA</i>	<i>DCAA</i>	<i>BCAA</i>	<i>TCAA</i>	<i>DBAA</i>	<i>BDCAA</i>	<i>DBCBA</i>	<i>Total</i>
S14	47	3	<MRL	ND	50	<MRL	52	2	92	<MRL	25	2	172
S15L	38	6	1	ND	45	2	115	21	102	5	47	14	306
S15T	121	5	1	ND	127	2	690	31	183	6	45	2	960
S16	61	2	<MRL	ND	63	<MRL	549	5	568	<MRL	20	1	1143
S17L	82	11	2	ND	95	5	504	106	288	25	110	32	1070
S17T	207	6	<MRL	ND	213	4	6787	176	1925	16	93	4	9005
Median					63								960
Maximum					213								9005
Minimum					26								172

TCM (Trichloromethane), BDCM (bromodichloromethane), DBCM (dibromochloromethane), TBM (tribromomethane), CAA (chloroacetic acid), BAA (bromoacetic acid), DCAA (dichloroacetic acid), BCAA (bromochloroacetic acid), TCAA (trichloroacetic acid), DBAA (dibromoacetic acid), DBCAA (dibromoacetic acid), TBAA (tribromoacetic acid), MRL (Minimum Reporting Level), ND (Not Detected).

Table 4. Nitrogenous-DBPs occurrence in indoor swimming pools water (n=23).

<i>Swimming Pool Code</i>	<i>Haloacetonitriles (µg/L)</i>							<i>Halonitromethanes (µg/L)</i>				<i>Nitrosamines (ng/L)</i>
	<i>CAN</i>	<i>TCAN</i>	<i>DCAN</i>	<i>BAN</i>	<i>BCAN</i>	<i>DBAN</i>	<i>Total</i>	<i>TCNM</i>	<i>BNM</i>	<i>BCNM</i>	<i>Total</i>	<i>NDMA</i>
S1	1	ND	8	ND	ND	ND	9	<MRL	<MRL	2.4	2.9	30
S2C	ND	ND	4	ND	ND	ND	5	0.8	<MRL	7.5	8.3	9
S2W	1	ND	22	ND	1	ND	25	<MRL	<MRL	1.3	1.9	83
S3S	1	ND	27	ND	1	ND	30	0.7	<MRL	6.3	7.0	28
S3D	1	ND	7	ND	ND	ND	8	0.9	<MRL	3.9	4.8	14
S4C	1	ND	15	ND	1	ND	16	<MRL	<MRL	2.5	3.0	16
S4W	1	ND	21	ND	2	ND	24	<MRL	<MRL	1.1	1.7	18
S5	1	ND	14	ND	1	ND	15	<MRL	<MRL	3.2	3.7	28
S6L	1	ND	12	ND	1	ND	15	0.8	<MRL	2.6	3.6	9
S6T	1	ND	13	ND	4	2	21	<MRL	2.2	3.8	6.5	60
S7	1	ND	14	ND	ND	ND	15	2	<MRL	3.4	5.4	9
S10	2	ND	16	ND	ND	1	18	2.3	<MRL	11	13.3	3
S11L	1	ND	11	ND	ND	ND	13	<MRL	<MRL	3.6	4.1	12
S11D	1	ND	7	ND	ND	1	9	0.9	<MRL	4.6	5.5	17
S12L	1	ND	15	ND	ND	ND	16	1	<MRL	4.3	5.4	2
S12I	1	ND	17	ND	ND	ND	18	1.1	<MRL	5.5	6.6	6
S13	1	ND	27	1	13	5	47	<MRL	2.0	4.7	7.3	13

<i>Swimming Pool Code</i>	<i>Haloacetonitriles (µg/L)</i>							<i>Halonitromethanes (µg/L)</i>				<i>Nitrosamines (ng/L)</i>
	<i>CAN</i>	<i>TCAN</i>	<i>DCAN</i>	<i>BAN</i>	<i>BCAN</i>	<i>DBAN</i>	<i>Total</i>	<i>TCNM</i>	<i>BNM</i>	<i>BCNM</i>	<i>Total</i>	<i>NDMA</i>
S14	1	ND	13	ND	1	ND	15	0.9	<MRL	3.7	4.7	18
S15L	1	ND	7	ND	2	1	11	<MRL	0.7	1.5	2.7	15
S15T	1	ND	4	ND	ND	ND	6	<MRL	<MRL	0.8	1.4	76
S16	1	ND	15	ND	ND	ND	16	0.8	<MRL	2.6	3.4	53
S17L	1	ND	16	1	3	1	22	0.7	1.6	5.8	8.1	17
S17T	3	1	47	ND	2	ND	53	1.4	1	6.8	9.2	42
Median							16				4.8	17
Maximum							53				13.3	83
Minimum							5				1.4	2

CAN (chloroacetonitrile), TCAN (trichloroacetonitrile), DCAN (dichloroacetonitrile), BAN (bromoacetonitrile), BCAN (bromochloroacetonitrile), DBAN (dibromoacetonitrile), TCNM (trichloronitromethane), BNM (bromonitromethane), BCNM (bromochloronitromethane), NDMA (*N*-nitrosodimethylamine), MRL (Minimum Reporting Level), ND (Not Detected).

Table 5. Characteristics of the Three Selected Indoor Swimming Pools Waters Monitored for 9-Months

<i>Swimming Pool/ Sampling date</i>	<i>TOC mg/L</i>	<i>TN mg/L</i>	<i>FAC mg/L</i>	<i>Temp. °C</i>	<i>pH</i>	<i>THMs µg/L</i>	<i>HAAs µg/L</i>	
S16	22/05/2009	5.6	2.1	2.6	28	7.8	60	2039
	24/05/2009	5.6	2.1	3.9	28	7.3	52	1648
	30/05/2009	6.2	2.1	4.6	28	6.7	53	1725
	02/06/2009	6.4	2.1	3.2	28	7.0	56	1691
	06/06/2009	6.3	2.1	0.7	26	7.0	48	1708
	09/06/2009	6.6	2.1	2.1	27	7.6	40	1674
	18/10/2009	5.3	2.0	2.3	28	7.5	81	1804
	25/10/2009	5.5	2.0	0.6	27	7.5	38	1673
	22/12/2009	NM	NM	NM	NM	NM	NM	NM
	10/01/2010	6.9	2.4	1.6	27	7.7	29	1479
	17/01/2010	7.3	2.4	2.9	27	7.6	54	1005
	17/02/2010	7.5	2.2	0.1	27	7.2	63	1143

<i>Swimming Pool/ Sampling date</i>	<i>TOC mg/L</i>	<i>TN mg/L</i>	<i>FAC mg/L</i>	<i>Temp. °C</i>	<i>pH</i>	<i>THMs µg/L</i>	<i>HAAs µg/L</i>	
S17L	22/05/2009	6.8	3.4	3	28	7.6	92	NM
	24/05/2009	6.1	3.4	3.5	28	7.6	91	1437
	30/05/2009	6.5	3.5	3	28	7.6	83	1392
	02/06/2009	7.0	3.5	1.5	28	7.6	77	1377
	06/06/2009	7.4	3.6	4	28	7.6	77	1434
	09/06/2009	7.2	3.6	3	28	7.6	84	1470
	18/10/2009	6.6	4.3	3.5	27	7.2	79	1174
	25/10/2009	6.6	4.2	3	28	7.2	79	1196
	22/12/2009	5.8	4.2	3	27	7.6	64	955
	10/01/2010	6.3	4.3	4.5	26	7.5	72	793
	17/01/2010	6.4	4.4	3.5	29	7.6	91	667
17/02/2010	7.3	4.1	3	27	7.6	95	1070	

Continued on next page.

Table 5. (Continued). Characteristics of the Three Selected Indoor Swimming Pools Waters Monitored for 9-Months

<i>Swimming Pool/ Sampling date</i>		<i>TOC mg/L</i>	<i>TN mg/L</i>	<i>FAC mg/L</i>	<i>Temp. °C</i>	<i>pH</i>	<i>THMs µg/L</i>	<i>HAAs µg/L</i>
S17T	22/05/2009	14.5	2.1	3	33	7.6	163	NM
	24/05/2009	14.8	2.2	2	33	7.6	161	2244
	30/05/2009	15.5	2.3	4	33	7.6	199	2397
	02/06/2009	16.5	2.1	3	33	7.6	192	2427
	06/06/2009	16.9	2.3	4	33	7.6	137	2869
	09/06/2009	16.9	2.2	2	33	7.6	160	2884
	18/10/2009	21.7	3.1	3.5	34	7.8	259	9691
	25/10/2009	20.9	3.2	6	33	7.2	249	9348
	22/12/2009	22.3	4.7	3.5	34	7.6	176	11695
	10/01/2010	25.2	5.0	3	34	7.6	182	7392
	17/01/2010	25.4	5.0	3.5	32	7.4	188	6291
17/02/2010	23.6	4.4	3	33	7.5	213	9005	

FAC (free available chlorine), TOC (total organic carbon), TN (total nitrogen), THM (Trihalomethanes), HAA (Haloacetic acids), NM (Not measured).

The Effects of Swimming Pool Operational Conditions on DBPs

The swimming pool operational parameters that affect both the THM and HAA formation is presented in Figure 2. An overall comparison of the results between the filling background waters (MB and SJWD) showed that formation of THMs and HAAs was approximately 10% higher in BFA-MB than in BFA-SJWD water. Although both synthetic pool waters had the same TOC concentration (1 mg/L from the filling water and 5 mg TOC from BFA), there was a slightly higher rate of THM and HAA formation in the MB than in the SJWD water, which was due to the aromatic nature of the MB source water. Specifically, the MB water exhibited a somewhat higher SUVA₂₅₄ (~2.0 L/mg-m) compared to the SJWD water (~1.7 L/mg-m), indicating it's slightly higher aromatic character over SJWD. An analysis of each parameter, except the filling waters is provided below.

Effect of FAC

FAC levels 1, 3, and 5 mg/L were tested in this study. It was determined that an increase in FAC concentrations resulted in a slight increase in THM formation: 5% for BFA-MB and 14% for BFA-SJWD (Figure 2). There was, however, a distinct increase in HAA formation observed, which was caused when the chlorine dose was increased from 1 mg/L to 5 mg/L. Specifically, the HAA formation increased 25% and 27%, respectively for the BFA-MB and BFA-SJWD (Figure 2).

This dependence was attributed to the reaction(s) of chlorine with albumin in BFA. An increase in dosage in turn increased the rate of albumin decomposition (hydrolysis), which in turn generated more HAA precursors (free amino acids). The lesser effect of the chlorine concentrations on the THM than HAA was due to the effect of the chlorine dose on the formation of different DBPs. After satisfying the demand, a linear relationship has been previously established between the demand for chlorine demand and THM formation (30), and a weak correlation between the chlorine levels and chloroform formation (31). Consistent with these observations, the results indicate that once the chlorine demand was satisfied, there was no effect of the chlorine dose on the THM formation.

Effect of Temperature

To examine the effect of temperature on DBP formation, the two synthetic swimming pool waters were also chlorinated at 40°C, the highest possible temperature allowable in therapeutic swimming pools, hot tubs, and whirlpool spas. Although this increase in temperature from 26°C to 40°C nearly doubled the formation of THMs in synthetic pool waters, there was only a 60% increase in HAA formation (Figure 2). These results clearly indicate that exposure to DBPs in hot tubs or any other type of elevated temperature indoor swimming pools will

be higher. The increase in DBP formation with temperature can be explained by reaction of un-reacted DBPs precursors with chlorine and increase in the reactivity of chlorine with precursors (35, 36).

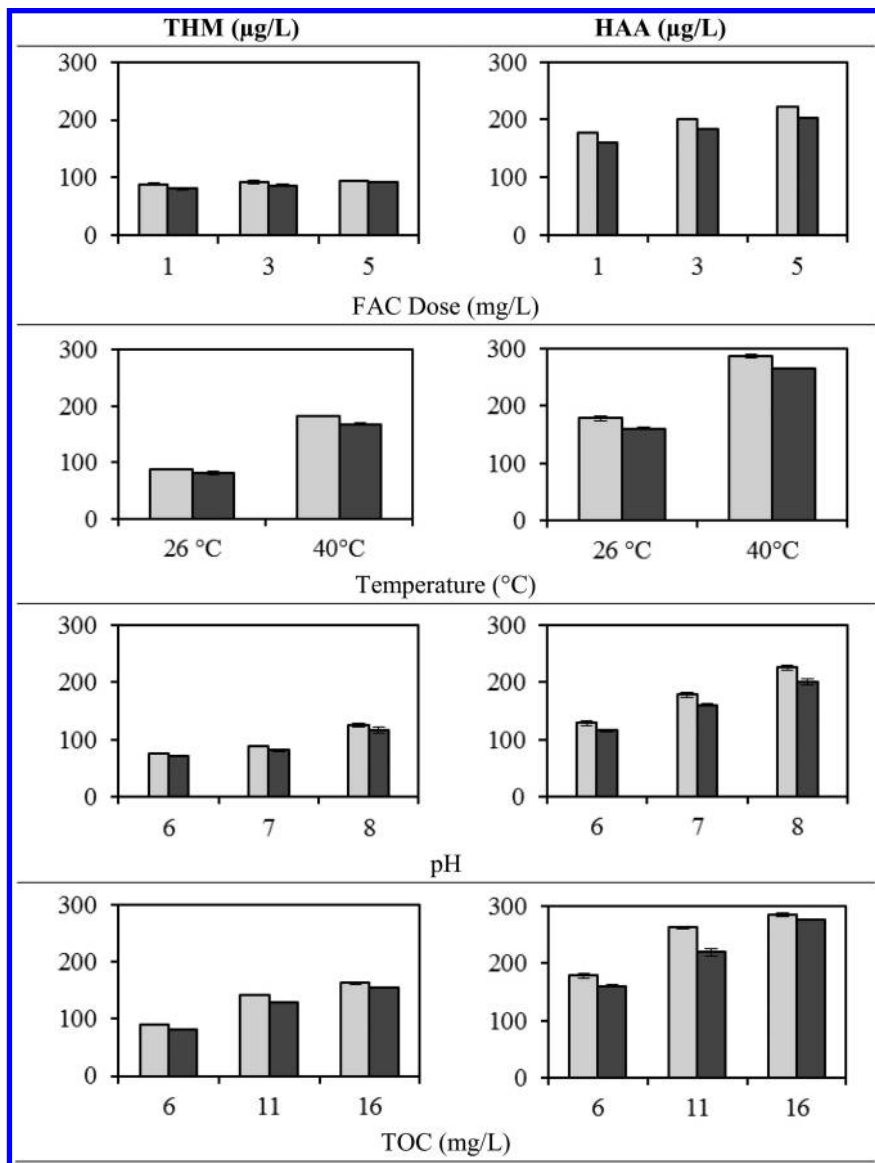


Figure 2. The effect of operational parameters on DBPs formation in swimming pools waters. □ BFA-MB, ■ BFA-SJWD

Effect of pH

The results show that the formation of THMs and HAAs increased with an increase in pH (Figure 2). It is also known that THM formation increases with an increase in pH, while the trend is the opposite for HAA formation (32). However, in this study, an increase in pH resulted in both an increase in both THM and HAA formation. The opposite behavior that was observed for pH dependence of HAAs in synthetic swimming water solution was once again attributed to the hydrolysis of albumin, one of the main components of the BFA, and its reactivity with chlorine. The observed pH trends for HAAs also indicated that the filling water NOM was not a major contributor to HAA formation in synthetic pool waters because in drinking waters, the HAA concentration decreased with an increase in pH, as mentioned above. Finally, the results clearly indicate that the reduction of pH from 8.0 to 6.0 would result in a decrease in both THM and HAA formation by 40-60%. This decrease in pH would also result in a corresponding decrease in the disinfection efficiency of chlorine, particularly below the pK_a of chlorine where HOCl is a more effective disinfectant agent than OCl^- (33, 34).

Effect of Bather Load

Although TOC cannot be controlled directly by the facility, there is a correlation to the number of bathers and their BFs in a swimming pool. Thus, pool managers can control the TOC level by controlling the number of bathers using the pool at a given time. As predicted, the formation of both THMs and HAAs increased with an increase in the concentration of BFAs. This dependence on TOC concentration confirms a substantial correlation between the DBPs formation in swimming pools with the population of swimmers (the main TOC source).

Effect of Bromide

Bromide was spiked at three levels in addition to the ambient fill waters concentration. The change in THMs and HAAs speciation with the increasing bromide concentrations is shown in Figure 3. This increase in bromide concentrations yielded a corresponding increase in both THM and HAA concentration, which was expected since the brominated species increased while the chlorinated species decreased. However, bromide caused a greater increase in THM than HAA formation. The overall mass of THM concentration increased by 65-72%, 106-116%, and 162-167% in synthetic pool waters at 100, 300, and 600 $\mu\text{g/L}$ bromide concentrations, respectively compared to the ambient fill waters THM formation. However, during these same experiments the increase in HAA concentration was only within a fairly limited range of 22 and 39%. Bromine incorporation factor (BIF) “n” is the molar amount of bromine in the

halogenated compound (THM or HAA) divided by the molar total of that halogen (37). That is to say when $n = 0$ only chlorinated compounds form whereas when $n > 0$ brominated species begin to appear. Subsequent BIF analysis determined that the presence of bromide increased the formation of brominated THM over HAA formation (data not shown).

Specifically, the incorporation factor a synthetic swimming water sample for a bromide level of 600 $\mu\text{g/L}$ was 1.3 for THMs but only 0.8 for HAAs. This difference in bromide incorporation is also consistent with higher bromine incorporation of THMs than HAAs in sample testing (38). These results clearly demonstrate that the use of water with low bromide levels to either fill swimming pools and as make up water is critical to reduce DBP formation, especially THMs. Thus, bromide impurities should be minimized, if possible, when generating chlorine from sodium chloride. Furthermore, the use of seawater or saline water as either make-up or filling water should be avoided to reduce the DBPs formation in swimming pools.

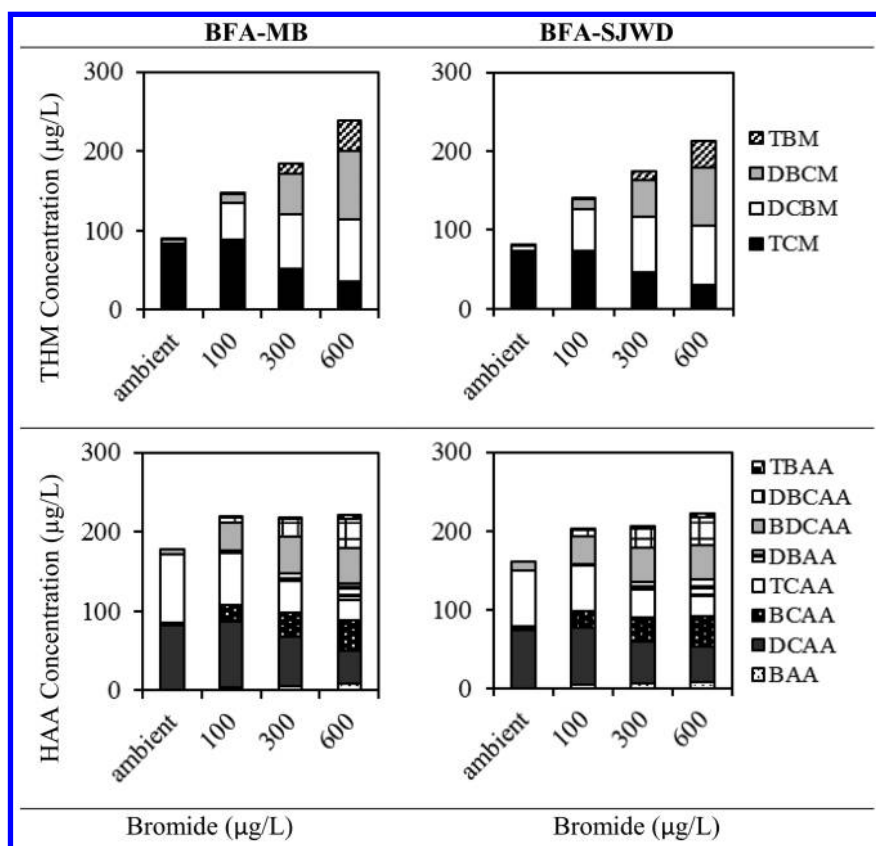


Figure 3. The effect of bromide on the formation and speciation of THMs and HAAs during chlorination of BFA-MB and BFA-SJWD synthetic pool water.

DBPs Formation as Function of Time

DBP formation as function of time are presented in Figure 4 for three synthetic pool waters: (i) a pool water at 6 mg-C/L (5 mg-C/L from BFA and 1 mg-C/L from MB as the background filling water), (ii) 5 mg-C/L BFA, and (iii) 1 mg-C/L BFA. The last two samples were used to investigate the formation kinetics from BFAs alone and the formation kinetics at two Cl₂/TOC ratios. Results indicate that THM formation (within a range of 53% to 68%) occurred during the first five hours of a five-day formation cycle in the absence and the presence of bromide for synthetic pool water (BFA-MB) and BFA (Figure 4).

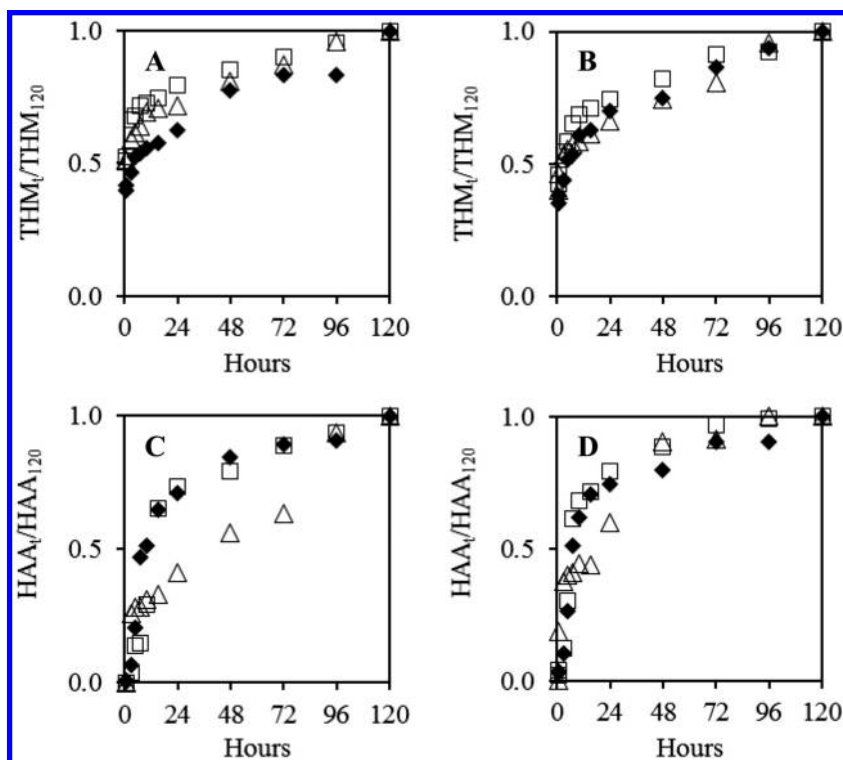


Figure 4. THM formation fraction during five days (A) without bromide and (B) with bromide (200 µg/L), HAA formation fraction during five days (C) without bromide and (D) with bromide (200 µg/L). THM_{*i*} (THM formed at time *t*), THM₁₂₀ (THM formed at 120 hours), HAA_{*i*} (HAA formed at time *t*), HAA₁₂₀ (HAA formed at 120 hours). ◆ BFA-MB (5+1 mg-C/L), □ BFA (5 mg-C/L), △ BFA (1 mg-C/L)

This is a faster rate of THMs production at early contact times compared to previous studies using several chlorination scenarios, which produced only 15-30% of THMs after at least five hours after treatment (17, 18). Although the fast

formation of THMs observed in this study indicates that a significant portion of THMs formed in the pool prior to treatment, only 15% to 30% of the five-day HAA formation occurred during the first 5 hours under the same experimental conditions (Figure 4). This rate was lower as compared to the formation rate of THMs. The slower rate of HAA formation indicates that there is more opportunity to remove their precursors through swimming pool water treatment processes during pool water turnover.

Two BFA solutions at 1 and 5 mg TOC/L showed similar THM formation patterns indicating very little effect of the Cl_2/TOC ratio (100 vs. 20) on the THM formation rate (Figure 4). Thus, the formation rates observed in this study are representative of THM formation in swimming pools. There was, however, some difference between the trends of the BFA solutions at 1 and 5 mg-C/L, indicating that the decrease in Cl_2/TOC ratio from 100 to 20 increased the HAA formation rate. This difference was attributed to the changes in the formation rates of di-halogenated HAAs vs. tri-halogenated HAAs (data not shown). Since there is always a high FAC concentration in the pool water, the HAA formation rates in swimming pools are likely to be rapid for HAAs. This is especially true for swimming pools in the U.S. where the dilution of pool water with the filling water is not regularly practiced and the pool water is not replaced for long time. Therefore, chlorine demand of filling water is exhausted at the very early period of operation after filling the pool. Afterwards, the BF components serve as the primary catalyst for THM and HAA formation.

The presence of NOM (i.e., BFA-MB synthetic pool water) (BFA = 5 mg-C/L) reduced the formation rate of THMs by ~20% during the first 24 hours as compared to the absence of NOM. This behavior is due to the higher reactivity of NOM compared to BFA with chlorine to form THM but which occurs at a slower rate, as compared to BFA. Concurrently, the presence of NOM (i.e., BFA-MB) did not affect the formation rate of HAAs, indicating that while the filling water NOM can affect the THM formation, the formation rate of HAAs remains constant.

There were small differences in the formation rates under ambient bromide levels for both THMs and HAAs. In the presence of bromide, the difference in the formation rates of both DBPs diminished. Since halogenation reactions are faster with bromide than chloride (39–41), higher formation rates observed in this study is attributed to the formation of brominated DBP species from NOM at high bromide levels.

The overall formation rate of THMs was higher than that of HAAs in swimming pools Figure 5. THMs were formed almost instantaneously when chlorine reacted with BFs, whereas HAA formation occurred at a slower rate. Practically, these results indicate that within the typical turnover time of swimming pools most HAA precursors can be removed by the treatment system whereas THM precursors cannot. Thus, precursors control (i.e., the release of human BFs) will be critical in reducing the formation of THMs in swimming pools. The precursor control requires improving the practices and behavior of swimmers, and implementing more strict hygienic conditions by swimming pools utilities. Better hygienic conditions include showering immediately before swimming and not releasing urine intentionally during swimming.

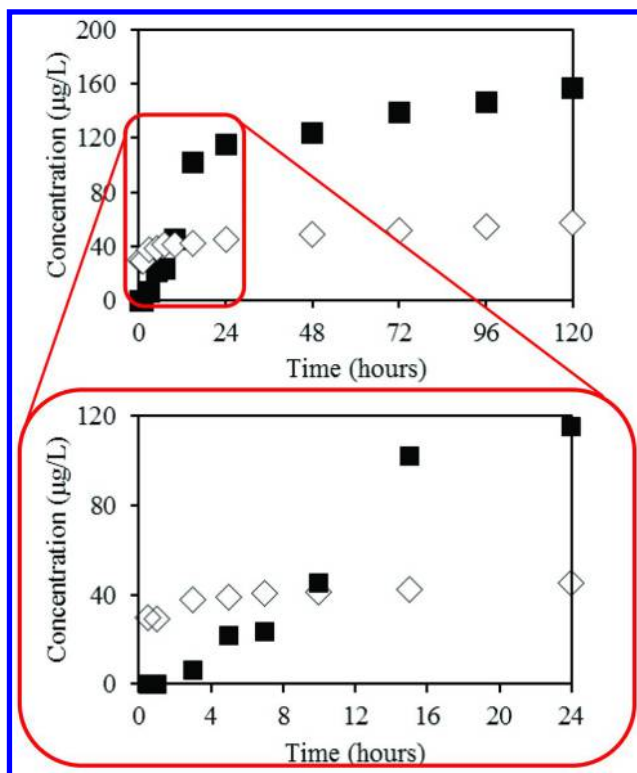


Figure 5. \diamond THMs and \blacksquare HAAs formation during 5-day reaction from BFA.

Conclusions

The DBPs in the 23 swimming pools that were the subject of this study were far higher than the drinking water regulation values in the U.S., with THM levels ranging between 26 and 213 $\mu\text{g/L}$ with an average of 80 $\mu\text{g/L}$. The HAAs ranged between 173 and 9005 $\mu\text{g/L}$ with an average of 1541 $\mu\text{g/L}$. HNMs ranged between 1.4 and 13.3 $\mu\text{g/L}$ with an average of 5.4 $\mu\text{g/L}$. HANs ranged between 5 and 53 $\mu\text{g/L}$ with an average of 19 $\mu\text{g/L}$. The NDMA ranged between 2 and 83 ng/L with an average of 26.5 ng/L . The electrochemically generation of chlorine increased the brominated species of halogenated DBPs (THMs, HAAs, HNMs, HANs). Furthermore, during the sampling period for nine months, the water quality (TOC, TN, pH, FAC) and DBPs concentrations (THMs, HAAs) in the swimming pools remained relatively constant. However, some fluctuation was observed likely due to time of the year and the specific pool events/activities on the time of sampling.

The formation and speciation of THMs and HAAs were also investigated under various disinfection and operation conditions typically used in U.S. swimming pools. Although the increases in free available chlorine, pH, TOC, water temperature, and bromide levels in the water increased overall DBP formation, these factors affected the different classes of DBPs at different

magnitudes. Higher levels of free available chlorine increased the HAA levels more than the THMs. The temperature effect was greater on the formation of THMs than for HAAs whereas contact time increased HAAs more than THMs. The authors also determined that under swimming pool related conditions, DPB formation was quite rapid, with an appreciable percentage of the increase occurring in the first 3-6 hours, which is the typical turnover time for the pool water. Moreover, THM formation was faster than HAA formation, with 53 to 68% of five-day THMs formed within the first 3-6 hours and 15 to 30% of five-day HAAs formed during the first six hours. Although it is possible to reduce DBP formation by the controlling operational parameters (pH, free available chlorine, bather load, the number of swimmers in a pool in a 24 hour period- or dilution), these fast formation rates imply that DBP control strategies in swimming pools should mainly focus on control the DBP precursors at the source (i.e., swimmers).

References

1. Batjer, K.; Cetinkaya, M.; Duszeln, J. V.; Gabel, B.; Lahl, U.; Stachel, B. *Chemosphere* **1980**, *9*, 311–316.
2. Thacker, N. P.; Nitnaware, V. *Bull. Environ. Contam. Toxicol.* **2003**, *71*, 633–640.
3. Zwiener, C.; Richardson, S. D.; De Marini, D. M.; Grummt, T.; Glauner, T.; Frimmel, F. H. *Environ. Sci. Technol.* **2007**, *41*, 363–372.
4. Surveillance for waterborne disease and outbreaks associated with recreational water use and other aquatic facility-associated health events - United States, 2005-2006; Center for Disease Control and Prevention: Atlanta, GA, 2008.
5. *Guidelines for Safe Recreational Water Environments, volume 2: swimming pools and similar environments*; World Health Organization, 2006.
6. Walse, S.; Mitch, W. *Environ. Sci. Technol.* **2008**, *42*, 1032–1037.
7. Kanan, A. Occurrence and Formation of Disinfection Byproducts in Indoor Swimming Pools Water. Ph.D. Thesis, Clemson University, Clemson, SC, 2010.
8. Richardson, S. D.; DeMarini, D. M.; Kogevinas, M. *Environ. Health Perspect.* **2010**, *118*, 1523–1530.
9. Kanan, A.; Karanfil, T. *Water Res.* **2011**, *45*, 926–932.
10. Chowdhury, S.; Al-Hooshani, K.; Karanfil, T. *Water Res.* **2014**, *53*, 68–109.
11. Teo, T. L.; Coleman, H. M.; Khan, S. *J. Environ. Int.* **2015**, *76*, 16–31.
12. Borgmann-Strahsen, R. *Int. Biodeterior. Biodegrad.* **2003**, *51*, 291–297.
13. Barbot, E.; Moulin, P. *J. Membrane Sci.* **2008**, *314*, 50–57.
14. Weisel, C. P.; Richardson, S. D.; Nemery, B.; Aggazzotti, G.; Baraldi, E.; Blatchley, E. R.; Blount, B. C.; Carlsen, K. H.; Eggleston, P. A.; Frimmel, F. H.; Goodman, M.; Gordon, G.; Grinshpun, S. A.; Heederik, D.; Kogevinas, M.; LaKind, J. S.; Nieuwenhuijsen, M. J.; Piper, F. C.; Sattar, S. A. *Environ. Health Perspect.* **2009**, *117*, 500–507.
15. *Certified Pool-Spa Operator Handbook*; National Swimming Pool Foundation: Colorado Springs, CO, 2006.

16. R. 61-51 *Public Swimming Pools - Bureau of Water*; South Carolina Department of Health and Environmental Control: Columbia, SC, 2007.
17. Gallard, H.; Gunten, U. *Water Res.* **2002**, *36*, 65–74.
18. Nikolaou, A. D.; Lekkas, T. D.; Golfinopoulos, S. K. *Chem. Eng. J.* **2004**, *100*, 139–148.
19. Goeres, D. M.; Palys, T.; Sandel, B. B.; Geiger, J. *Water Res.* **2004**, *38*, 3103–3109.
20. *Method 300.0 - Determination of Inorganic Anions by Ion Chromatography*; U.S. Environmental Protection Agency: Washington, DC, 1993.
21. *Method 551.1 - Determination of Chlorination Disinfection Byproducts, Chlorinated Solvents, and Halogenated Pesticides/Herbicides in Drinking Water by Liquid–Liquid Extraction and Gas Chromatography With Electron-Capture Detection*, revision 1.0.; U.S. Environmental Protection Agency: Washington, DC, 1995.
22. *Method 521 - Determination of Nitrosamines in Drinking Water by Solid Phase Extraction and Capillary Column Gas Chromatography with Large Volume Injection and Chemical Ionization Tandem Mass Spectrometry (MS/MS)*, version 1.0.; U.S. Environmental Protection Agency: Washington, DC, 2004.
23. *Standard Methods for the Examination of Water and Wastewater*, 21st ed.; APHA, AWWA, and WEF, 2005.
24. Hu, J. *Exploring formation and distribution of halonitromethanes in drinking waters*, Ph.D. Thesis, Clemson University, Clemson, SC, 2009.
25. Glezer, V.; Harris, B.; Tal, N.; Iosefzon, B.; Lev, O. *Water Res.* **1999**, *33*, 1938–1948.
26. Selbes, M.; Kim, D.; Ates, N.; Karanfil, T. *Water Res.* **2013**, *47*, 945–953.
27. Uzun, H.; Kim, D.; Ates, N.; Karanfil, T. In *Proceedings of AWWA Annual Conference and Exposition*; Dallas, TX, 2012.
28. Uzun, H.; Kim, D.; Karanfil, T. *Water Res.* **2015**, *69*, 162–172.
29. Plewa, M. J.; Wagner, E.; Muellner, M.; Hsu, K.; Richardson, S. *ACS Symp. Ser.* **2008**, *995*, 36–50.
30. Boccelli, D. L.; Tryby, M. E.; Uber, J. G.; Summers, R. S. *Water Res.* **2003**, *37*, 2654–2666.
31. Garcia-Villanova, R. J.; Garcia, C.; Cesar; Gomez, J. A.; Garcia, M. P.; Ardanuy, R. *Water Res.* **1997**, *31*, 1405–1413.
32. Hua, G.; Reckhow, D. A. *J. Am. Water Works Assoc.* **2008**, *100*, 82–89.
33. Edzwald, J. K. *Water Quality and Treatment: A Handbook of Community Water Supplies*, 4th ed.; McGraw-Hill: New York, 1990.
34. White, G. C. *Handbook of Chlorination and Alternative Disinfectants*, 4th ed.; Wiley: New York, 1999.
35. Weisel, C. P.; Chen, W. J. *Risk Anal.* **1994**, *14*, 101–106.
36. Al-Omari, A.; Fayyad, M.; Qader, A. *Environ. Model. Asses.* **2004**, *9*, 245–52.
37. Gould, J. P.; Fitchorn, L. E.; Urheim, E. Formation of brominated trihalomethanes: Extent and kinetics. In *Water Chlorination: Environmental Impact and Health Effects, Chemistry and Water Treatment*; Jolley, R. L., Ed.; Ann Arbor Science, Ann Arbor, Michigan, 1983; Vol. 4.

38. Kitis, M.; Karanfil, T.; Wigton, A.; Kilduff, J. E. *Water Res.* **2002**, *36*, 3834–3848.
39. Westerhoff, P.; Chao, P.; Mash, H. *Water Res.* **2004**, *38*, 1502–1513.
40. Adin, A.; Katzhendler, J.; Alkaslassy, D.; Rav-Acha, C. *Water Res.* **1991**, *25*, 797–805.
41. Cowman, G. A.; Singer, P. C. *Environ. Sci. Technol.* **1996**, *30*, 16–24.

Chapter 22

Ion Mobility Spectrometry To Monitor Trichloramine in Indoor Pool Air

C. Zwiener* and C. Schmalz

Environmental Analytical Chemistry, University of Tuebingen,
Hoelderlinstrasse 12, 72074 Tuebingen, Germany

*E-mail: Christian.zwiener@uni-tuebingen.de.

Trichloramine (TCA) is a volatile, irritant disinfection by-product formed by reactions of nitrogenous compounds with chlorine. TCA analysis was performed by a hand-held ion mobility spectrometer (IMS) with direct intake of gas samples from indoor air environments. Ionization with a ^{63}Ni beta emitter produced chloride ions with a characteristic ion mobility which are completely separated from bromide and other ions by IMS. The limit of quantification for TCA is 0.1 mg/m^3 , sufficient for the TCA guideline value of 0.2 mg/m^3 and therefore to use IMS for monitoring in indoor pool air. The contribution of further interfering chlorinated disinfection by-products (DBPs) to the chloride signal from TCA has been estimated to be less than 15 %. The mobility, the short measurement times of about 20 s and the stability of the calibration curve of the instrument qualify IMS to determine the spatial and temporal variability of TCA in indoor pool air. This was demonstrated for the increase of TCA concentrations dependent on the number and activity of swimmers. An immediate increase of TCA was detected after a school class entered the pool, which can be explained by the sudden increase of the mass transfer coefficient of TCA from water to air. A further example shows the acquisition of a spatial profile and the increase of TCA from the inlet to the outlet region of a non-swimmer area.

Introduction

Swimming is a healthy sport activity which can provide benefits for people of all ages and physical abilities. Sufficient hygienic and chemical water quality is a prerequisite to keep the positive aspects of aquatic activities. To guarantee the hygienic safety of swimming pool water (SPW) disinfection, mostly with chlorine, is used according to the recommendations from the World Health Organization (WHO) and to further national standards for swimming pools in order to inactivate pathogens (1). The chlorine concentrations used are a compromise between sufficient disinfection and minimized formation of disinfection by-products. Chlorine levels applied in Germany are in the range of 0.3 and 0.6 mg/L according to the German Industrial Norm DIN 19643. In other countries up to 3 mg/L chlorine are typically used for pool water disinfection (United States of America, Australia and other European countries). Public pools in Germany rely primarily on the treatment scheme, operation, and surveillance described in DIN 19643. Despite minor differences in threshold values, applied chemical concentrations, and the requirement for an initial flocculation step, DIN 19643 can serve as a good example of pool water treatment that is similar to that in much of Western Europe, North America, and Australia (2).

Disinfection By-Products

During operation the swimming water is continuously loaded by compounds which are introduced by bathers and permanently cycled through the treatment. The constituents of the bather load are from body fluids, skin, hair, and cosmetics. Further compounds from natural organic matter are introduced to the pool from filling water. Since there is no efficient elimination of the organic bather load, during the continuous recirculation and dosing of reactive chlorine, disinfection by-products are formed by reactions between organic and inorganic water constituents and chlorine (2). Most prevalent DBPs are trihalomethanes (THMs) and halogenated acetic acids (HAAs) (3). From nitrogen containing precursors a variety of nitrogenous DBPs has been found like halogenated acetonitriles (HAcNs), nitrosamines (e.g. NDMA), and chloramines (2–6). Some DBPs are carcinogenic, fetotoxic and/or irritant to airways (7). More than 100 DBPs have been identified in swimming pool waters, many of them were brominated and nitrogen-containing DBPs. The mutagenicity of pool water has been found to be in the same range of drinking water (1,200 revertants/L-equivalents in strain TA100–S9 mix) (3). An increased risk for bladder cancer has been associated with swimming pool attendance, however with inconclusive evidence (8). Epidemiological studies showed an association of the attendance of chlorinated swimming pools and adverse health effects of respiratory functions and on the risk of developing asthma (9–11). So far no specific DBPs have been identified, but trichloramine and other volatile DBPs are suspected of contributing to these effects.

Trichloramine in Swimming Pools

Trichloramine (TCA, NCl_3) is a volatile, instable disinfection by-product of pungent odor, which causes the typical indoor pool smell. TCA is the most volatile of all chloramines and irritates eyes and upper airways. The irritant potency of TCA is in the same order as chlorine or formaldehyde (12). An inhalation study for TCA with rats showed acute toxicity with a LC_{50} of 550 mg/m^3 (13). A first proof of the effects of TCA on humans is from an *in vitro* exposure study with human alveolar epithelial lung cells from the cell line A-549 (14). Decreasing cell viability and an increase in pre-inflammatory biomarkers (cytokines IL-6 and IL-8) have been found at TCA concentrations above 10 mg/m^3 .

Therefore exposure of swimmers and pool personnel to TCA should be minimized. The National Research and Safety Institute for occupational accidents prevention in France (INRS) and the WHO recommended a reference value of 0.5 mg/m^3 for TCA in air (1). The reference value has been derived from studies, where symptoms of irritation of eyes, nose and throat have been reported by swimming instructors and lifeguards in indoor pools at TCA levels from 0.5 mg/m^3 (5, 15). Recent monitoring studies from Switzerland and Germany showed, that the occurrence of TCA in indoor pools are typically in the range of 0.1 and 0.5 mg/m^3 (16, 17) with maximum levels at worst case of more than 18 mg/m^3 (18). Under consideration of a precautionary principle, the median TCA levels in indoor pools and further results from a study in which the lowest observed no-effect levels for TCA were found at 0.35 mg/m^3 Parrat et al. proposed an occupational exposure limit of 0.3 mg/m^3 (17).

Measurement methods for TCA in air are mostly based on reactive air sampling and have to cope with the instability of TCA. The most applied method uses reduction of TCA to chloride on glass fiber filters impregnated with As_2O_3 and subsequent quantification of chloride by ion chromatography (5). Another reactive method uses an impinger system and the colorimetric chlorine test reagent *N,N*-diethyl-*p*-phenylenediamine (DPD) with potassium iodide (19, 20). Both methods are not specific and prone to interferences from other halogenated DBPs and oxidizing air constituents, which can be reduced to chloride or are able to oxidize the DPD reagent. Another disadvantage is the rather long sampling time of several hours necessary to obtain sufficiently low detection limits. An alternative approach for direct TCA measurements in air would be ion mobility spectrometry.

Ion Mobility Spectrometry

Ion mobility spectrometry (IMS) is an analytical technique for the separation and detection of gas phase ions at atmospheric pressure and emerged in the late 1960s (21, 22). IMS is widely applied to detect pollutants, explosives or illicit drugs by military forces (23), airport and workplace security and it gained increasing interest as orthogonal separation principle for mass spectrometry (24, 25). The advantages of IMS are its flexibility, speed and low detection limits paired with its ease of maintenance, the relatively low investment costs and the availability of handheld devices. More than 10,000 IMS based detectors

are therefore used in security checkpoints and more than 50,000 handheld IMS analyzers are in use for chemical-weapons monitoring by armed forces. Further application areas for robust and easy-to-use handheld IMS are for example in the areas of first response and logistics used by police, rescue forces, fire fighters, or customs and recently in food safety monitoring, clinical diagnostics, forensics (26) and environmental monitoring (27). In this work we used IMS to monitor the volatile and instable disinfection by-product TCA in the air of indoor swimming pools.

The principle of operation includes soft ionization with ^{63}Ni , UV light or corona discharge to form reactant ion species from the carrier gas, which is generally air, formation of analyte ions and ion clusters (atmospheric pressure chemical ionization), electrical injection to a drift region and detection. Ions are accelerated in an electrostatic field in the drift region against a counter-flow drift gas and travel at characteristic speeds that are related to the mass, charge, size and shape of the ions or ion clusters.

The general set-up of an IMS device is shown in Figure 1. The heart of the IMS is the drift tube which includes an ionization chamber separated by the shutter grit (21). The tube is built from a stack of metal guard rings which are separated by thin isolators and attached to a voltage divider so that a smooth increase of voltages can be applied over the whole string. A steady flow of drift gas (nitrogen or air) at ambient pressure serves as collision and reactant gas and prevents the tube from contamination.

Gaseous samples can be introduced directly into the ionization chamber where an ionization source, e.g. a beta emitter (^{63}Ni) produces reactant ions. Analytes are ionized by proton-transfer and charge exchange reactions in a kind of atmospheric chemical ionization mechanism. The type of ionization source and drift gas is critical for ionization mechanisms and efficiencies, which was demonstrated for monosubstituted toluenes and anilines for three ionization types (^{63}Ni beta emitter, corona discharge and photoionization (28)). Corona discharge sources often combine mixed ionization mechanisms and therefore lead to more complicated response behavior than beta emitters. Photoionization can be used for direct ionization without reactant ions and therefore lead to much simpler response behavior and often large ranges of quantitative responses (27).

Ionized analytes are then transferred to the drift tube via an electronic shutter grid which is periodically triggered. In the drift tube ions experience acceleration by the electrical field and a number of collisions with the drift gas. This results in a rather constant drift velocity v_d which is proportional to the mobility of an ion K and the electric field strength E (Equation 1). Analyte ions with different ion mobilities K due to differences in size, mass and charge experience a separation. Since the ion mobilities K depend on environmental conditions, generally normalized mobilities K_0 are given, where T is the absolute temperature of the drift gas, T_0 the standard temperature (273 K), P the atmospheric pressure during the measurement and P_0 the standard pressure (760 mm Hg) (Equation 2).

$$K = \frac{v_d}{E} \quad (\text{Eq. 1})$$

$$K_0 = K \cdot \left(\frac{T_0}{T} \right) \cdot \left(\frac{P}{P_0} \right) \quad (\text{Eq. 2})$$

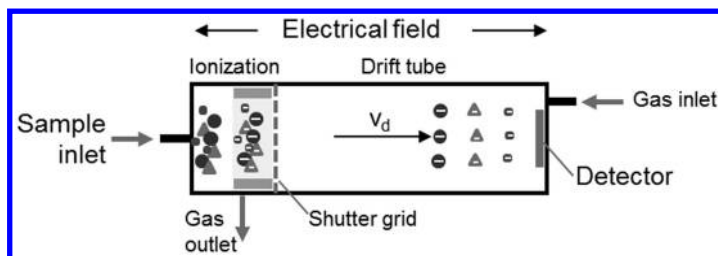


Figure 1. Ion mobility spectrometry (IMS) set-up.

Methods

Trichloramine Gas Generation

TCA gas standards were produced continuously in a gas generation unit as described by Schmalz et al. (14). Shortly, ammonia chloride and sodium hypochlorite were continuously dosed to a phosphate buffer solution (pH 3) in a reaction bottle. Nitrogen gas with a flow rate of 100 mL/min was used to strip out the formed TCA. The gas stream was cleaned in impingers with amidosulfonic acid solutions and water. The TCA gas stream was splitted into two fractions. The concentrated gas stream was trapped in cooled *iso*-octane and the other part was diluted with synthetic air. The continuous TCA gas generation was controlled by UV-absorption of the *iso*-octane solutions every 30 minutes. The diluted gas stream with a flow rate of up to 7 L/min was adjusted to produce concentrations in the range of 0.1 and 0.8 mg/m³. The concentration of the diluted gas stream was determined by the impinger and reactive adsorption method as described below (TCA analysis). The air humidity was varied by an impinger with water and controlled with a hygrometer.

Further DBP Gas Standards

The pure substances of trihalomethanes and dichloroacetonitrile were purchased from Sigma-Aldrich. Aqueous stock solutions of mono- and dichloramine were synthesized according to literature (29) and dichloromethylamine according to Cimetiere and De Laat (30). The stock solutions were analyzed by photometry, for NH₂Cl at $\lambda = 254$ nm ($\epsilon = 388$ L mol⁻¹cm⁻¹), for NHCl₂ at $\lambda = 282$ nm ($\epsilon = 221$ L mol⁻¹cm⁻¹) and for CH₃NCl₂ at $\lambda = 302$ nm ($\epsilon = 330$ L mol⁻¹cm⁻¹).

For qualitative and semi quantitative IMS analysis defined amounts (0.5 to 10 μL) of pure THMs were vaporized and diluted in gas-tight bottles and Tedlar bags filled with nitrogen. Final concentrations in the Tedlar bags were between 0.1 mg/m^3 and 1.0 g/m^3 .

For quantitative analyses diluted aqueous solutions of THMs, dichloroacetonitrile and synthesized chloramines between 0.01 and 10 mg/L were prepared (DBP solutions). A total volume of 2.5 L of these DBP solutions was filled in three stripping vessels (2 L, 0.25 L, 0.25 L) in series. The stripping gas flow was 64 mL/min and the dilution gas flow was 1932 mL/min at a temperature of $23 \pm 1^\circ\text{C}$. The system equilibrium was checked with varied volumes of DBP solutions. Hence the concentration of the DBP gas stream could be calculated using the Henry constant, the initial aqueous concentrations and the adjusted gas flows.

Trichloramine Analysis

Photometric Method

The photometric analyses of *iso*-octane solutions containing the absorbed TCA were performed by a Cary 50 spectrophotometer (Varian, Germany). The concentration of TCA was analyzed at three wavelengths ($\lambda = 343 \text{ nm}$, $\epsilon = 185 \text{ Lmol}^{-1}\text{cm}^{-1}$; $\lambda = 260 \text{ nm}$, $\epsilon = 399 \text{ Lmol}^{-1}\text{cm}^{-1}$; $\lambda = 225 \text{ nm}$, $\epsilon = 5,470 \text{ L mol}^{-1}\text{cm}^{-1}$).

Reactive Adsorption Method

Reduction of TCA to chloride on impregnated glass fiber filters was performed according to literature (5, 16).

Glass fiber filters ($d = 50 \text{ mm}$, QM-A, Whatman Schleicher Schuell, Germany) were impregnated with 0.9 mL of a solution of 40 g/L glycerol, 107 g/L Na_2CO_3 und 8 g/L As_2O_3 . The flow rate through two impregnated filters in series was 1 L/min (pump: Gilian 5000, Sensidyne, USA). The sampling time was 3 hours. After sampling the filters were eluted with water and the chloride concentrations were determined by ion chromatography after ion exchange with OnGuard II Na-Cartridges (Dionex, Idstein).

Impinger Method

The reaction of TCA with the reagent *N,N*-diethyl-phenylenediamine (DPD) and potassium iodide (KI) was carried out in solution in an impinge (19, 20). DPD and KI (Chlorine test, Merck, Germany) were dissolved in 50 mL water and filled into two impingers. The air flow rate through the two impingers in series was 1 L/min . Sampling time was 90 minutes. The red color of the oxidized DPD was photometrically determined directly after sampling at a wavelength of 510 nm.

IMS measurements were performed by a hand-held GDA2 spectrometer (Airsense, Germany) equipped with a 100 MBeq ^{63}Ni -ionisation source. The drift tube had a length of 6.3 cm and was operated at a temperature between 40 and 45°C and at a voltage between 1.7 and 1.9 kV. The gas inlet was equipped with a silicone membrane and the total gas flow rate through the system was regulated by internal pumps at 470 mL/min. One complete IMS-spectrum was acquired per second, recorded by the software Winmuster GDA Version 1.2.6.0 and stored on a SD card. Generally a stable signal was obtained after about 10 to 20 seconds and the average signal height of at least 40 spectra were used for quantitative analysis. For field measurements the GDA2 was supplied by a Li-Ion accumulator. The negative IMS spectra were analyzed for chloride and bromide ions at a normalized drift time (K_0) of 2.7 $\text{cm}^2/(\text{Vs})$ and 2.5 $\text{cm}^2/(\text{Vs})$.

Investigation of Indoor Pool Air

Indoor air measurements were performed in an indoor pool with a swimmer pool ($V = 980 \text{ m}^3$), a non-swimmer pool ($V = 240 \text{ m}^3$) and a baby pool ($V = 4.7 \text{ m}^3$). The total air volume of the hall is 4890 m^3 . The baby pool is completely separated. Analyses with the reactive adsorption method (As_2O_3 filter) and the DPD/KI method were done at sampling heights of 20 cm above the water surface and at a distance of 20 cm from the edge of the pool. The analyses with the IMS were done at different sampling locations and heights at the windows, at fresh air inlets and outlets and above the surface of the water in the swimming pool hall and in the engineering rooms and offices.

Results

Trichloramine (TCA) analysis was performed by a hand-held ion mobility spectrometer (IMS) with direct intake of gas samples from indoor air environments, gas generation units or from Tedlar bags for spiked gas standards. A silicone membrane at the IMS inlet protects the IMS analyzer and keeps it at a constant humidity. A typical measurement cycle consists of the continuous intake of gaseous sample by a built-in pump and the signal readout after constant signal intensity was obtained. Single IMS measurements can be performed within 20 seconds and the results are stored on a storage device or can be directly viewed, if the instrument is calibrated for the analytes. The mobility of the hand-held instrument and the short response time allow quite flexible applications and measurements of high spatial and temporal resolution in indoor pool settings. In contrast to that, the conventional filter method for TCA determination requires typically three hours of sampling time, further laboratory work for filter extraction, sample clean-up and ion chromatographic determination of the formed chloride. Generally, the filter method allows only the determination of

averaged concentrations over time periods of several hours, which doesn't allow monitoring of the dynamic behavior of TCA concentrations in dependence of bather activity or of the sampling location in an indoor pool hall.

IMS Signals of Volatile DBPs

The IMS spectra of different halogenated DBPs after ionization by a ^{63}Ni source generally show two signals, if the compounds contain bromine and chlorine, and one signal if only chlorinated DBPs have been measured (Figure 2). Further signals can be assigned to reactant ions from ionized gas and water species. This result shows that from different DBPs primarily only chloride and bromide ions are produced by electron capture in a dissociative electron attachment mechanism and therefore only chloride and bromide ions are separated in the drift tube of the IMS. This process is already known from electron capture detectors (ECD) and described for halo- and nitro-substituted benzenes (22). For example halogenated benzenes and alkyl halides only yielded halide ions by a simple dissociative electron capture, whereas nitrobenzene exhibited an associative electron capture resulting in negatively charged molecular ions. Halogenated nitrobenzenes showed both mechanisms associative and dissociative electron capture.

The normalized ion mobilities for chlorinated compounds are at $K_0 = 2.7 \text{ cm}^2/(\text{Vs})$ (chloride ion) and for brominated compounds at $K_0 = 2.5 \text{ cm}^2/(\text{Vs})$ (bromide ion, Figure 2). For bromodichloromethane both signals could be detected. Bromoform has only one signal for bromide. Other ions in the mobility spectrum are from reactant gas ions which are formed from air (oxygen) and water (signals 3 and 4 in Figure 2). The implications of the generalized signal response of the IMS to different halogenated compounds are that the IMS signal is not specific for individual DBPs but provides the possibility to measure all chlorinated DBPs and all brominated DBPs in a kind of sum parameter. The contribution of single DBPs to the sum parameter strongly depends on their response factor and individual concentration in the gas sample.

IMS Response and Calibration

Response factors and limits of quantitation (LOQ) have been determined by IMS individually for some selected DBPs to check for their contribution to the sum signal based on chloride and bromide. For the selection of DBPs the major chlorinated compounds like three chloramines and three chlorinated THMs have been considered, as well as some trace compounds like dichloroacetonitrile and dichloromethylamine, which are regularly occurring in swimming pool water (31). From recent monitoring programs there is information available on typical indoor pool air concentrations of TCA, which are in the range of 0.1 and 0.5 mg/m^3 (17, 18). Chloroform concentrations are typically in the same range between 0.1 and 0.5 mg/m^3 (32, 33). Further typical air concentrations have been estimated from published data for indoor pool air or were calculated from data of aqueous concentrations and the corresponding Henry's law coefficients. The most prominent volatile DBPs are chloroform and TCA. The air concentrations

of other brominated and chlorinated THMs and DBPs are by a factor of about ten to one hundred lower.

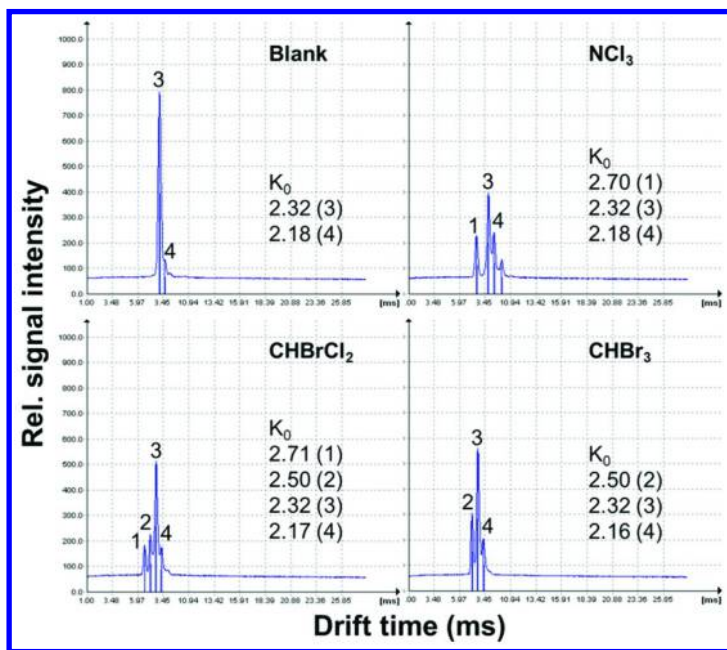


Figure 2. IMS spectra (signal intensity vs. drift time) of a blank and volatile DBPs (TCA, bromodichloromethane and bromoform). Signals are from chloride (1) and bromide (2) with normalized ion mobilities of $K_0 = 2.7 \text{ cm}^2/(\text{Vs})$ and $K_0 = 2.5 \text{ cm}^2/(\text{Vs})$, respectively.

The response factors for the selected DBPs range over four orders of magnitude between 3896 (arbitrary signal units m^3/mg) for dichloroacetonitrile and 0.5 (arbitrary signal units m^3/mg) for chloroform (Table 1). The response factors are mostly dependent on the ionization efficiency during dissociative electron capture, since the detected ion is in any case chloride for chlorinated DBPs. Therefore differences in electron capture cross sections and bond energies of the individual compounds account for the overall response. Interestingly all chloramines, where the halogen is bound to a nitrogen atom, show a rather high response. However, the highest value was found for dichloroacetonitrile with a response factor of almost 4000 (arbitrary signal units m^3/mg). Due to a more than 400fold less response, chloroform contributes to only much less than 1 % of the chloride signal of TCA in typical indoor swimming pool environments and can therefore be neglected. The two other THMs (bromodichloromethane, dibromochloromethane) and dichloroaceto-nitrile also contribute to less than 1 % to the chloride signal. Also the contribution of chlorine can be neglected due to the low partitioning of hypochlorous acid to the gas phase and therefore the resulting low concentrations in the air (31). Only the contribution of dichloromethylamine is estimated to be in the range of 10 %.

Table 1. Response Factors, Limits of Quantitation (LOQ) and Typical Air Concentrations for Halogenated DBPs in Indoor Swimming Pools Measured As Chloride and Bromide in Negative Ion Mobility Spectra

<i>Ion mobility K₀ (cm²/(Vs))</i>	<i>DBP</i>	<i>Response factor (m³/mg)</i>	<i>LOQ (mg/m³)</i>	<i>Typical air concentration (mg/m³)</i>
2.7 (Cl ⁻)	NCl ₃	221	0.1	0.1 - 0.5
2.7	CHCl ₃	0.5	24	0.1 - 0.5
2.7	CHBrCl ₂	33	0.4	< 0.02
2.7	CHBr ₂ Cl	21	1.0	< 0.02
2.7	NH ₂ Cl	300	0.1	< 0.004
2.7	NHCl ₂	180	0.1	< 0.006
2.7	CH ₃ NCl ₂	906	0.01	0.01-0.07
2.7	CHCl ₂ CN	3896	0.003	< 0.0002
2.5 (Br ⁻)	CHBrCl ₂	46	0.4	< 0.02
2.5	CHBr ₂ Cl	247	0.1	< 0.02
2.5	CHBr ₃	-	0.2	< 0.02

In a realistic estimate we come to the conclusion that in indoor swimming pool environments the major contribution to the IMS signal of chlorinated compounds is from TCA (more than 85 %) with a minor contribution of dichloromethylamine (about 10 %). Therefore IMS measurements are capable to detect TCA - the DBP of most concern - together with a further nitrogenous reaction product. For other environments and air compositions the contribution of interferences has to be reconsidered separately.

The limit of quantification (LOQ) for the IMS measurement of TCA in air was determined to be 0.1 mg/m³. The LOQ is therefore sufficient for indoor pool air monitoring where exposure limits and reference values between 0.3 and 0.5 mg/m³ have to be considered. LOQs of other DBPs are in most cases higher than the typical air concentrations with the exception of dichloromethylamine.

IMS measurements of TCA in the negative ionization mode between 0.1 and 0.7 mg/m³ show linear and quite robust calibration functions. This is demonstrated in Figure 3 for calibrations on three days (e.g. on Nov. 8, 9 and 14) for dry air and humid air with 65 % relative humidity (at 25 °C). Humidity of the gas sample can affect IMS measurements by formation of water-analyte clusters in the IMS tube which causes analyte discrimination due to different migration times of the analyte-water clusters compared to the naked analyte ions. The results show that humidity doesn't significantly affect IMS calibration. This may be a result of the silicone membrane in the instrument inlet, which should guarantee a constant humidity in the IMS instrument independent of the humidity of the gas sample.

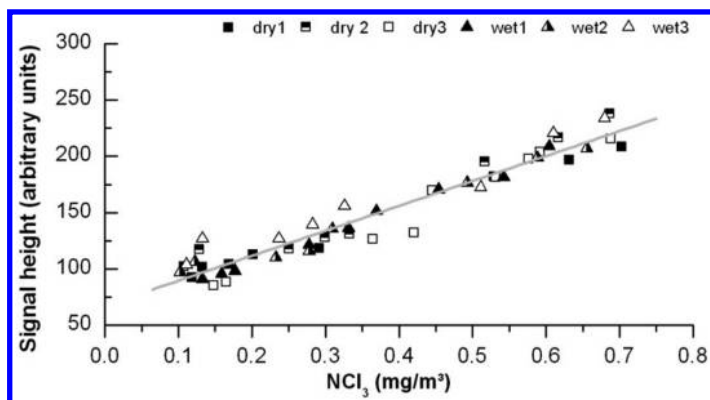


Figure 3. Calibration of trichloramine for IMS signals based on chloride ($K_0 = 2.7 \text{ cm}^2/(Vs)$) for 3 different days within a week in dry and humid air (65 % relative humidity at 25 °C).

Table 2. Figures of Merit for the Linear IMS Calibration Measured at Three Days for Dry and Humid Air (65 % Relative Humidity at 25 °C)

<i>Day/Humidity (%)</i>	<i>Slope</i>	<i>Standard error of slope</i>	<i>Intercept</i>
1/0	200	8.6	70
2/0	235	22.1	69
3/0	259	20.2	42
1/65	246	8.8	56
2/65	209	15.0	71
3/65	211	20.2	84

The slopes of the IMS calibration for 3 different days with dry and humid air show no significant differences, if the two means of the slopes from dry air (mean: 231.3; STD 29.7; $n = 3$) and from humid air (mean: 222.0; STD 20.8; $n = 3$) are subjected to a t-test (Table 2). The interday statistical error is higher than that between dry and humid gas samples and is also caused by systematic errors of the production of TCA gas standards. TCA is a rather instable compound which has to be produced and diluted online to suitable concentration levels for calibration, which is a rather tedious task. The relative standard errors of the slopes of single calibration functions are within 4.3 % and 9.4 %, which is a quite acceptable range for this type of measurement.

Temporal Dynamics of Trichloramine Concentrations in Indoor Pool Air

The quick response time of IMS measurements and the mobility of the instrument allowed us to use it for the investigation of the temporal dynamics of TCA concentrations at various locations of an indoor pool setting with a large swimmer hall, which is connected to a non-swimmer pool with low ceiling, and a separated, confined baby pool area (children area). The measurements were done for defined time intervals of typically 10 to 15 min.

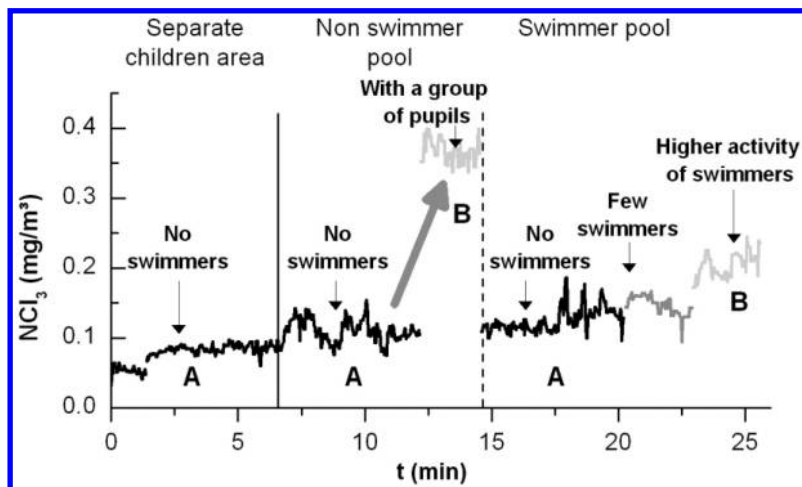


Figure 4. Temporal dynamics of trichloramine in different compartments of an indoor pool air in dependence of the number of bathers and their activity. Temporal separated measurement intervals are presented in grey and black. Measurement was done at about 20 cm above water surface.

Selected results for the concentrations of TCA in air in dependence of the number and activity of swimmers are shown in Figure 4. The first samples before a group of swimmers came in the pool (region A in Figure 4) showed generally very low TCA concentrations (0.06 mg/m^3 in the baby pool, 0.11 mg/m^3 in the non-swimmer and 0.12 mg/m^3 in the swimmer area), since no or almost no kids or swimmers used the pools. This is considered as background levels, which established overnight. Then a school class with about 45 children attended the non-swimmer area, many pupils jumped into the water or were splashing around. This caused a sudden increase of the TCA concentration to about 0.36 mg/m^3 in this area (region B in Figure 4), which can be explained by a sudden increase of the mass transfer coefficient for TCA from water to air due to the agitation of the pupils' activity. It has been shown that the mass transfer coefficient can be increased from $1.8 \times 10^{-3} \text{ g/(h m}^2)$ in a quiescent pool to $7.0 \times 10^{-3} \text{ g/(h m}^2)$ by swimming activity and even to $12.6 \times 10^{-3} \text{ g/(h m}^2)$ by increased splashing activity or by sparging the water in a whirlpool (34). Since the mass transfer is a limiting factor for an empty pool with smooth water surface, TCA can be built up in the water overnight and then contribute to a sudden increase of TCA concentration in

the air. This example shows that the TCA concentration in indoor pools can be highly dynamic. For the swimmer pool there is observed also an increase of TCA concentration with increasing swimmer activity, but it is less pronounced due to much less swimmers per surface area of the water and due to much higher air space of the swimming pool hall (10 m) compared to the low ceiling of the non-swimmer area (about 3.50 m height of the room).

These examples clearly show the necessity to monitor the temporal variability of TCA concentrations for a more accurate estimation of the exposure of bathers and personnel in a swimming pool.

Concentration Profiles of TCA in an Indoor Pool

The fast response time of IMS measurements allowed also to measure concentration profiles of TCA in an indoor pool at different sampling locations. The assumption was made, that the concentration regime didn't change during the short time period of less than 10 min for the complete measurement of the profile. The results are again from the non-swimmer area with low ceiling and suboptimal ventilation. The air of the ventilation system is guided on a space diagonal from the left lower corner to the right upper corner in this non-swimmer area (Figure 5). All measurements were taken at a height of 20 cm above water level. TCA concentrations show an increasing trend from 0.13 mg/m³ in the inflow region of air to about 0.26 mg/m³ in the outflow region. This result is clearly a sign of insufficient ventilation of this area. The air takes TCA up on its way through the non-swimmer compartment which doubles the TCA concentration. This example reveals that it is necessary to monitor TCA concentrations at various sampling locations within one indoor area to get a more complete picture on TCA exposure of bathers and personnel.

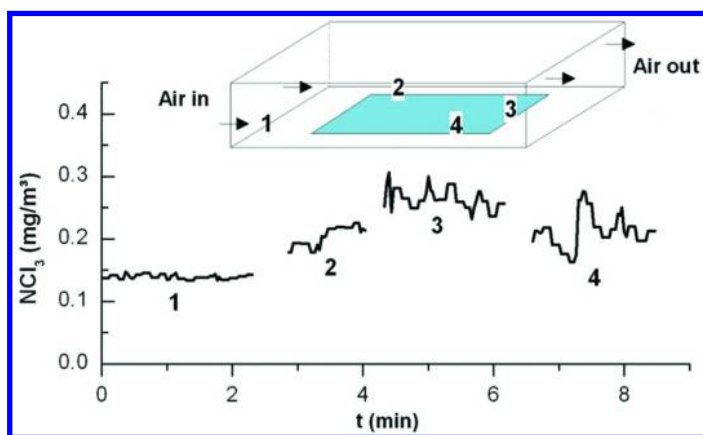


Figure 5. Trichloramine concentration profiles in an indoor non-swimmer pool area with low ceiling and insufficient air ventilation (measured at 20 cm above water surface; numbers indicate sampling locations).

Conclusions

Ion mobility spectrometry (IMS) revealed as a valuable tool to measure trichloramine (TCA) concentrations in indoor swimming pool environments. Since during the ionization in IMS chloramines and other chlorinated DBPs can contribute to the chloride signal, interfering compounds and their contribution to the chloride signal have to be considered and found to be less than 15 % in typical indoor pool air. The short response time of about 20 s, the mobility and stability of the IMS calibration enable to monitor the highly dynamic behavior in time and space of TCA and therefore to determine more accurately the exposure of swimmers and pool personnel.

Acknowledgments

This work was supported by the German Federal Ministry of Education and Research (BMBF 02WT1090) in the joint project “Health-Related Optimization of Swimming Pool Water Treatment”. We further thank J. Chrapan and V. Kuemmel for their contribution to the generation of TCA gas standards and IMS calibration.

References

1. WHO. *Guidelines for Safe Recreational Water Environments, Volume 2: Swimming pools and similar environments*; World Health Organization: Geneva, CH, 2006.
2. Zwiener, C.; Richardson, S. D.; De Marini, D. M.; Grummt, T.; Glauner, T.; Frimmel, F. H. Drowning in Disinfection Byproducts? Assessing Swimming Pool Water. *Environ. Sci. Technol.* **2007**, *41*, 363–372.
3. Richardson, S. D.; DeMarini, D. M.; Kogevinas, M.; Fernandez, P.; Marco, E.; Lourencetti, C.; Balleste, C.; Heederik, D.; Meliefste, K.; McKague, A. B.; Marcos, R.; Font-Ribera, L.; Grimalt, J. O.; Villanueva, C. M. What’s in the Pool? A Comprehensive Identification of Disinfection By-products and Assessment of Mutagenicity of Chlorinated and Brominated Swimming Pool Water. *Environ. Health Perspect.* **2010**, *118*, 1523–1530.
4. Walse, S. S.; Mitch, W. A. Nitrosamine carcinogens also swim in chlorinated pools. *Environ. Sci. Technol.* **2008**, *42*, 1032–1037.
5. Hery, M.; Hecht, G.; Gerber, J. M.; Gender, J. C.; Hubert, G.; Rebuffaud, J. Exposure to Chloramines in the Atmosphere of Indoor Swimming Pools. *Ann. Occup. Hyg.* **1995**, *39*, 427–439.
6. Kim, H.; Shim, J.; Lee, S. Formation of disinfection by-products in chlorinated swimming pool water. *Chemosphere* **2002**, *46*, 123–130.
7. Villanueva, C. M.; Font-Ribera, L. Health impact of disinfection by-products in swimming pools. *Ann. Ist. Super Sanità* **2012**, *48*, 387–396.
8. Villanueva, C. M.; Cantor, K. P.; Grimalt, J. O.; Malats, N.; Silverman, D.; Tardon, A.; Garcia-Closas, R.; Serra, C.; Carrato, A.; Castano-Vinyals, G.; Marcos, R.; Rothman, N.; Real, F. X.; Dosemeci, M.; Kogevinas, M. Bladder Cancer and Exposure to Water Disinfection By-Products through Ingestion,

Bathing, Showering, and Swimming in Pools. *Am. J. Epidemiol.* **2007**, *165*, 148–156.

9. Nickmilder, M.; Bernard, A. Ecological association between childhood asthma and availability of indoor chlorinated swimming pools in Europe. *Occup. Environ. Med.* **2007**, *64*, 37–46.
10. Bernard, A.; Carbone, S.; de Burbure, C.; Michel, O.; Nickmilder, M. Chlorinated Pool Attendance, Atopy, and the Risk of Asthma during Childhood. *Environ. Health Perspect.* **2006**, *114*, 1567–1573.
11. Lévesque, B.; Duchesne, J.-F.; Gingras, S.; Lavoie, R.; Prud'Homme, D.; Bernard, E.; Boulet, L.-P.; Ernst, P. The determinants of prevalence of health complaints among young competitive swimmers. *Int. Arch. Occup. Environ. Health* **2006**, *80*, 32–39.
12. Gagnaire, F.; Azim, S.; Bonnet, P.; Hecht, G.; Hery, M. Comparison of the sensory irritation response in mice to chlorine and nitrogen trichloride. *J. Appl. Toxicol.* **1994**, *14*, 405–409.
13. Barbee, S. J.; Thackara, J. W.; Rinehart, W. E. Acute inhalation toxicology of nitrogen trichloride. *Am. Ind. Hyg. Assoc. J.* **1983**, *19* (44), 145–146.
14. Schmalz, C.; Wunderlich, H. G.; Heinze, R.; Frimmel, F. H.; Zwiener, C. Application of an optimized system for the well-defined exposure of human lung cells to trichloramine and indoor pool air. *J. Water Health* **2011**, *9*, 586–596.
15. Massin, N.; Bohadana, A. B.; Wild, P.; Héry, M.; Toamain, J. P.; Hubert, G. Respiratory symptoms and bronchial responsiveness in lifeguards exposed to nitrogen trichloride in indoor swimming pools. *Occup. Environ. Med.* **1998**, *55*, 258–263.
16. Schmoll, B.; Kellner, R.; Breuer, D.; Buxtrup, M.; Engel, C.; Fliedner, G.; Franke, U.; Friedrich, C.; Geilenkirchen, A.; van Gelder, R.; Neumann, H.-D.; Radtke, R.; Richter, D.; Salvadori, U.; Spreckelsen, F.; Stöcker, S.; Thullner, I.; Weber, B.; Wegscheider, W.; Wimmer, B.; Zirbs, R. Trichloramin in der Schwimmhallenluft. *Archiv Badewes.* **2009**, *10*, 591–611.
17. Parrat, J.; Donze, G.; Iseli, C.; Perret, D.; Tomicic, C.; Schenk, O. Assessment of Occupational and Public Exposure to Trichloramine in Swiss Indoor Swimming Pools: A Proposal for an Occupational Exposure Limit. *Ann. Occup. Hyg.* **2012**, *56*, 264–277.
18. Stottmeister, E.; Voigt, K. Trichloramine prevention remains better than cure. *Recreation* **2006**, *3*, 30–33.
19. Weng, S. C.; Weaver, W. A.; Zare Afifi, M.; Blatchley, T. N.; Cramer, J. S.; Chen, J.; Blatchley, E. R. Dynamics of gas-phase trichloramine (NCl₃) in chlorinated, indoor swimming pool facilities. *Indoor Air* **2011**, *21*, 391–399.
20. Predieri, G.; Giacobazzi, P. Determination of nitrogen trichloride (NCl₃) levels in the air of indoor chlorinated swimming pools: an impinger method proposal. *Intern. J. Environ. Anal. Chem.* **2012**, *92*, 645–654.
21. Hill, H. H.; Siems, W. F.; St. Louis, R. H. Ion mobility spectrometry. *Anal. Chem.* **1990**, *62*, 1201A–1209A.
22. Karasek, F. W. Plasma Chromatography. *Anal. Chem.* **1974**, *46*, 710A–720A.

23. Eiceman, G. A.; Stone, J. A. Peer Reviewed: Ion Mobility Spectrometers in National Defense. *Anal. Chem.* **2004**, *76*, 390A–397A.
24. Cottingham, K. Product Review: Ion mobility spectrometry rediscovered. *Anal. Chem.* **2003**, *75*, 435A–439A.
25. Liuni, P.; Romanov, V.; Binette, M.-J.; Zaknoun, H.; Tam, M.; Pilon, P.; Hendrikse, J.; Wilson, D. J. Unambiguous Characterization of Analytical Markers in Complex, Seized Opiate Samples Using an Enhanced Ion Mobility Trace Detector-Mass Spectrometer. *Anal. Chem.* **2014**, *86*, 10772–10779.
26. Armenta, S.; Alcalá, M.; Blanco, M. A review of recent, unconventional applications of ion mobility spectrometry (IMS). *Anal. Chim. Acta* **2011**, *703*, 114–123.
27. Márquez-Sillero, I.; Aguilera-Herrador, E.; Cárdenas, S.; Valcárcel, M. Ion-mobility spectrometry for environmental analysis. *Trends Anal. Chem.* **2011**, *30*, 677–690.
28. Borsdorf, H.; Neitsch, K.; Eiceman, G. A.; Stone, J. A. A comparison of the ion chemistry for mono-substituted toluenes and anilines by three methods of atmospheric pressure ionization with ion mobility spectrometry. *Talanta* **2009**, *78*, 1464–1475.
29. Li, J.; Blatchley, E. R., III. UV Photodegradation of Inorganic Chloramines. *Environ. Sci. Technol.* **2009**, *43*, 60–65.
30. Cimetiere, N.; De Laat, J. Henry's law constant of N,N-dichloromethylamine: Application to the contamination of the atmosphere of indoor swimming pools. *Chemosphere* **2009**, *77*, 465–470.
31. Weaver, W. A.; Li, J.; Wen, Y.; Johnston, J.; Blatchley, M. R.; Blatchley, E. R., III Volatile disinfection by-product analysis from chlorinated indoor swimming pools. *Water Res.* **2009**, *43*, 3308–3318.
32. Aggazzotti, G.; Fantuzzi, G.; Righi, E.; Predieri, G. Environmental and biological monitoring of chloroform in indoor swimming pools. *J. Chromatogr. A* **1995**, *710*, 181–190.
33. Lévesque, B.; Ayotte, P.; Tardif, R.; Charest-Tardif, G.; Dewailly, E.; Prud'Homme, D.; Gingras, G.; Allaire, S. Evaluation of the Health Risk Associated with Exposure to Chloroform in Indoor Swimming Pools. *J. Toxicol. Environ. Health, Part A* **2000**, *61*, 225–243.
34. Schmalz, C.; Frimmel, F. H.; Zwiener, C. Trichloramine in swimming pools – Formation and mass transfer. *Water Res.* **2011**, *45*, 2681–2690.

Subject Index

A

- Advanced treatment (O₃-BAC)
 - DBPs, 324
 - DOC removal and C-DBP FP removal, 330*f*
 - DON removal and N-DBP, HNMs, and HAcAms FP removal, 331*f*
 - effect of terminating pre-ozonation, 328
 - fluorescence EEM spectra of treated Lake Taihu water, 333*f*
 - MW distribution, 332*f*
 - parallel O₃-BAC pilot plant process flows, 329*f*
 - precursors, 322
 - removal of DOC, DON, C-DBPs and N-DBPs, 329*f*
 - removal of DON by BAC process, 324*f*
 - removal of TCNMF by the BAC process, 325*f*
 - removal rates of FPs, 325*f*
 - removal rates of water quality parameters, 323*f*
 - representative fluorescence EEM spectra of DOM in raw water, 327*f*
 - total organic halogen (TOX), 328
 - UV/vis optical spectrums of water samples, 326*f*
- Amino acids, 215
 - analytical methods and minimum reporting levels, 220*t*
 - carbonaceous-DBPs
 - DBP FPs of AAs tested, 229*t*
 - DCAA and TCAA formation potential results, 228*f*
 - haloacetic acids (HAAs), 227
 - trihalomethanes (THMs), 226
 - formation of DBPs, effect of pH, 231
 - materials and methods
 - amino acids, 217
 - analytical methods, 221
 - formation potential tests, 219
 - selected amino acids, 218*t*
 - nitrogenous-DBPs
 - DCAN formation potential results, 223*f*
 - haloacetonitriles (HANs), 223
 - halonitromethanes (HNMs), 221
 - nitrosamine FPs of AAs tested, 225*t*
 - nitrosamines, 224
 - TCNM formation potential results, 222*f*

C

- Chloral hydrate control
 - CH degradation, effect of residual chlorine, 374*f*
 - CH removal
 - boiling of spiked waters, 372*f*
 - domestic adsorptive cartridges, 370*f*
 - domestic RO cartridge, 368*f*
 - effects of stirring speed and ultrasonication, 376*f*
 - RO and GAC alone or in combination, 371*f*
 - CH treatment
 - adsorptive materials, 369
 - boiler and microwave oven, 371
 - domestic microwave oven, 373*f*
 - reverse osmosis, 367
 - stirring and ultrasonication, 374
 - effect of operating pressure on RO flowrate, 367*t*
 - materials and methods
 - analytical methods, 365
 - apparatus, 366
 - characteristics of waters, 366*t*
 - samples and chemicals, 365
 - microwave heating process, CH and temperature changes, 375*f*
 - point-of-use and household appliances, 363
- Comparative haloacetaldehyde toxicity, 35
- Control of halogenated N-DBP precursors. *See* Advanced treatment (O₃-BAC)
 - advanced treatment (O₃-BAC)
 - advanced treatment process (O₃-BAC), 311
 - coagulation-IPS-filtration versus coagulation-DAF-filtration, 311
 - conventional process, 311
 - conventional treatment (coagulation-IPS-filtration versus coagulation-DAF-filtration)
 - DBP FPs, 316
 - DBPs, 315
 - disinfection process, 312
 - pilot-plant process flow, pretreatment, 310
 - pilot-scale treatment process, flowchart, 310*f*
 - pretreatment processes
 - DON removal in different treatment trains, 313*t*

- fluorescence EEM spectra of Lake Taihu water, 314*f*
 water parameters, 312
 using traditional and advanced drinking water treatment processes, 307
- Controlling NDMA formation, role of pre-oxidation, 151
 NDMA formation, role of oxidants/disinfectants
 chlorine, 152
 chlorine dioxide, 154
 ozone, 154
 permanganate, 155
 UV irradiation, 155
 NDMA formation and effect of pre-oxidation, 154*f*
 NDMA precursors, structures, 153*t*
- Conventional treatment (coagulation-IPS-filtration versus coagulation-DAF-filtration)
 C-DBPs, 320
 coagulation processes
 chloroform concentration in chlorinated water, 321*f*
 N-DBP concentrations in chlorinated water, 322*f*
 different SUVA values, 320*t*
 DOC, DON and UV₂₅₄ in raw water, 319*t*
 N-DBPs, 321
 precursors, 318
- D**
- DBP formation models, 64
 DBP-precursor bromination, catalysis aromatic compound bromination, proposed mechanism, 255*s*
 Br₂O as putative brominating agent, 261
 bromination of anisole and dimethenamid, catalysis as a function of chloride concentration, 256*f*
 as a function of excess bromide concentration, 259*f*
 as a function of initial free chlorine concentration, 261*f*
 catalysis by bromide, 257
 catalysis by chloride, 254
 catalysis by hypochlorous acid, 258
 different sources, bromide concentrations, 253*t*
 dimethenamid bromination, pseudo-first-order rate constants, 255*f*
 excess bromide, effects on pseudo-first-order rate constants, 258*f*
 free bromine, chemistry, 253
 free bromine speciation, more complete view, 262
 free chlorine concentration, influence on pseudo-first-order rate constants, 260*f*
 model water containing bromide, speciation of free bromine, 263*f*
 natural and anthropogenic sources of bromide, 252
 overall bromination rate, contributions of brominating agents, 264*f*
 reaction order in total free bromine concentration, 262*f*
- Disinfection by-products (DBPs), 3
 Disinfection by-products in swimming pool water control, 384
 bench-scale GAC filters, schematic setup, 397*f*
 factors, 396
 filtration, 396
 formation, 384
 anthropogenic input samples, DBPFs and DBP yields, 391*t*
 concentrations of individual species and ratio of DCAA/TCAA, 390*t*
 DBP levels in swimming pool, 387
 DBP precursors in swimming pool, 389
 indoor swimming pool, THM and HAA levels, 388*f*
 interpretation of DBP profile in swimming pools, 391
 measured HAAs and numbers of pool users, correlation, 389*f*
 swimming pool under investigation, 386
 year-around user statistics of swimming pool, 387*t*
- HAA removal from swimming pool water
 bench-scale BAC filter, 398*f*
 bench-scale GAC filter, 398*f*
 list of investigated disinfection by-products, 386*t*
 materials and methods
 ammonia nitrogen (NH₃-N), analysis, 385
 chlorine, analysis, 385

DBP formation potential (DBPFP)
test, 385
dissolved organic carbon (DOC),
analysis, 385
HAAs, analysis, 385
reagents, 384
THMs and HANs, analysis, 385
UV absorbance, analysis, 385
modeling, 384
calibration and validation results, 394*f*
model development, 392
model implications, 395
model performance, 394
predicted DBP profiles as function of
water age, 395*f*
Dissolved organic matter and disinfection
by-product precursors, forest fire effect,
271
before and after prescribed burn, yields
of detritus, WEOC, WETN, and
DBPs, 304*t*
before and after prescribed fire and
sunlight treatments, EEM regions of
water extracts, 302*f*
DOM and DBP precursors,
biogeochemical processes, 301
forested watersheds, 293
implications, 303
materials and methods
dark and light incubations, 297
disinfection by-products formation,
275
DOM and DBP precursors,
characterization, 296
DOM from litter, characterization,
274
litter collection and black carbon
preparation, 273
original and burned litters, chemical
characteristics, 274
prescribed burn in managed forest,
295
statistical analyses, 275
pyrogenic products, categorization, 285*t*
results and discussion
carbon and nitrogen quantity, effect of
prescribed fire, 276
controlled field burns, 297
detritus materials, chemical
composition, 298
forest detritus samples before and
after burn, 300*t*
litter materials, chemical
characteristics, 275
yields of DOM and DBP precursors,
299

unburned, and burned detritus material,
fluorescence EEM of water extracts,
300*f*
unburned and burned detritus, leachate
extracted, 301*f*
specific formation potential, 303*f*

E

Effect of fire on carbon quality
fluorescence emission-excitation matrix,
282*f*
fluorescence spectrometry, 278
litters before and after burns
optical properties, 279*t*
weight and chemical characteristics,
278*t*
Pearson's correlation coefficients
litters after burn, 281*t*
litters before burn, 280*t*
UV-VIS spectrometry, 277

F

Factors influencing effectiveness of
pre-oxidants
background ions, 165
background organics, 165
pH, 164
temperature, 164
Formation of DBPs, 189
DBP classes identified, examples, 193*t*
DBPs generated by water pollutants,
examples, 191*t*
haloamides, 200
formation mechanisms, 201*f*
halobenzoquinones, 203
formation mechanisms, 204*f*
halonitromethanes, 200
formation mechanisms, 202*f*
halopyrroles, 202
formation mechanisms, 203*f*
iodo-DBPs, 193
iodo-acids, 195
iodo-amides, 195
iodo-DBP formation mechanisms, 196
iodo-THMs, 194
mechanism of iodo-DBP formation
with chlorine and chloramines, 196*f*
proposed reaction of iopamidol with
chlorine and monochloramine, 197*f*
NDMA and other nitrosamines,
formation mechanisms, 199*f*

Formation of disinfection by-products, effect of prescribed burning, 282
 before and after burn, disinfection by-product yields, 284f
 dissolved organic carbon extracted from litter, chlorine reactivity, 283f

Formation of disinfection by-products from bacterial disinfection, 235
 alternative disinfectants, 246
 bacterial inactivation and DBP formation, effects of pH and dosage, 243
 DBP formation during bacteria inactivation, 240
 effects of humic acid and pH on *E. coli* cell density, 243f
 effects of NOM on bacterial inactivation and DBP formation, 241
 experimental
 bacterial cultures, 238
 chemicals, 237
 chlorine inactivation, 239
 DBP analysis, 240
 fluorescence spectroscopy, 239
 fluorescence EEM of water solution after chlorination, 244f
 fluorescence EEM of water solution containing *E. coli*, 242f
 microbial cells and cellular components as DBPs precursor, 245
 natural organic matter versus bacterial organic matter, 245
 specific DBP formation of halogenation of different bacteria, 241f

H

Haloacetaldehydes, 25
 determination in water, 27
 analyte detection, 31
 analytical methodologies, 29t
 derivatization reaction of PFBHA, 30s
 sample collection, 28
 sample extraction, 28
 occurrence in water, 31
 disinfected water, 32t

Halogenated DBPs, 45
 experimental methods
 chemicals and seawater, 48
 developmental toxicity bioassay with *P. dumerilii*, 50
 tap water samples with/without boiling, pretreatment, 48
 TOX measurement, 49

(UPLC)/ESI-tqMS analyses, 49
 water sampling and characterization, 47
 results and discussion
 concentrations, effect of boiling, 55f
 ESI-tqMS PIS spectra of *m/z* 35, 54f
 ESI-tqMS PIS spectra of *m/z* 79, 53f
 polar brominated and chlorinated DBPs, decomposition, 51
 real tap water, detoxification by boiling, 56
 TOX during boiling, reduction, 51

I

Indoor U.S. swimming pools, disinfection by-products, 405
 analytical methods and minimum reporting levels, 409t
 carbonaceous-DBPs occurrence, 414t
 DBPs formation as function of time, 425
 effects of swimming pool operational conditions on DBPs, 422f
 effect of bather load, 423
 effect of bromide, 423
 effect of FAC, 421
 effect of pH, 423
 effect of temperature, 421
 formation and speciation of THMs and HAAs, effect of bromide, 424f
 materials and methods
 analytical methods, 408
 DBP FP and kinetics tests, 408
 samples collection, 407
 synthetic swimming pool waters, 407
 nitrogenous-DBPs occurrence, 416t
 occurrence, 410
 box and whisker plots, 412f
 selected pools
 DBPs measured, 413
 monitored for 9-months, characteristics, 418t
 water characteristics, 410, 411t

M

Modeling NDMA formation kinetics during chloramination, 79
 model description
 chloramine decomposition kinetics and associated rate constants, 84t
 chloramines, decomposition reactions in water, 83

- monochloramine degradation, 84
 - NDMA formation model, 82
 - NDMA formation from model compounds, 87
 - optimized rate constant k_{app} , 90*t*
 - NDMA formation from model precursor compound data, 88*f*
 - NDMA formation in NOM, 85
 - rate constant and monochloramine decomposition rate constants, 86*t*
 - NDMA formation of amine precursors in river water, 92*f*
 - NDMA formation of pharmaceutical compounds, 90
 - optimized rate constant k_{app} , 91*t*
 - NDMA formation pathways, 81*f*
 - Monitor trichloramine in indoor pool air blank and volatile DBPs, IMS spectra, 439*f*
 - calibration of trichloramine for IMS signals, 441*f*
 - disinfection by-products, 432
 - further DBP gas standards, 435
 - halogenated dbps in indoor swimming pools, response factors, limits of quantitation and typical air concentrations, 440*t*
 - ion mobility spectrometry, 431, 433
 - ion mobility spectrometry (IMS), set-up, 435*f*
 - linear IMS calibration measured, 441*t* results, 437
 - IMS response and calibration, 438
 - volatile DBPs, IMS signals, 438
 - TCA, concentration profiles, 443
 - trichloramine analysis
 - impinger method, 436
 - investigation of indoor pool air, 437
 - ion mobility spectrometry, 437
 - photometric method, 436
 - reactive adsorption method, 436
 - trichloramine concentrations, temporal dynamics, 442
 - trichloramine gas generation, 435
 - trichloramine in swimming pools, 433
- N**
- Natural organic matter (NOM),
 - bromination and chlorination background, 63
 - bromide concentration, effects on proportionality coefficients, 72*f*
 - changes of differential absorbance, modelling kinetics, 66
 - correlations between concentration tribromoacetic acid (TBAA) and differential absorbance, 70*f*, 71*f*
 - trichloroacetic acid (TCAA) and differential absorbance, 70*f*, 71*f*
 - correlations between proportionality coefficients, 73*f*
 - DBP formation in chlorinated water, kinetics, 66
 - differential absorbance of chlorinated LK water, kinetic profiles, 67*f*
 - experimental, 65
 - modelling DBPs formation and speciation via differential absorbance, 68
 - NDMA control, use of UV, 165
 - NDMA formation in chloraminated systems
 - operational parameters, influence, 142
 - chloramination practice, 143
 - coagulation and coagulation aids, 144
 - Nitrosamine
 - formation mechanisms, 198
 - precursors and wastewater indicators
 - Nitrosamine precursor removal, 173
 - activated carbon adsorption, 174
 - activated carbons, properties, 175*t*
 - Chemaxon modeled speciation of chlorpheniramine, 181*f*
 - NA precursor removal with PAC in natural waters, pH effect mechanism, 182
 - pH effect, model NDMA precursors removal
 - PAC adsorption, 179
 - PRAM approach, 180
 - pH effect, NDMA FP removal, 175
 - removal of NDMA FP and bulk organic matter, 177*f*
 - tests with aquaculture-impacted lake water, 178
 - tests with blended wastewater, 176
 - water samples, basic water quality, 176*t*
 - N*-Nitrosodimethylamine (NDMA),
 - national occurrence, 135
 - coagulant aids, NDMA formation potentials, 145*t*
 - methods
 - data analysis, 139
 - sample sites, 136
 - sampling and NDMA analysis, 138
 - raw water chemistry, 146

results and discussion, occurrence data, overview, 140

P

Precursors and wastewater indicators

analytical methods

hydraulic flow modeling, 123

nitrosamine precursors, 122

nitrosamines, 122

PPCPs, 122

sucralose, 123

map of Sacramento –San Joaquin Delta, 120*f*

NDMA precursors

Sacramento river, 127*f*

San Joaquin river, 127*f*

percentage of river flow,

wastewater-impacted, 128

Sacramento and San Joaquin rivers,

impact of WWTP effluents, 126

sampling locations, 121*t*

Stockton WWTP

N-nitrosamine FP, impact of tertiary treatment, 124*f*

N-nitrosamines and their precursors, 123

study overview, 121

study sites

Sacramento Regional WWTP, 122

Stockton WWTP, 121

wastewater indicators, relationship to

NDMA FP, 129*f*

wastewater indicators and estimated

wastewater effluent, 125

wastewater indicators and NDMA FP,

concentrations, 128*t*

WWTP effluent, estimated percentage

R

Resolve adverse health effects of DBPs, 3

action of DBP forcing agents, molecular mechanisms, 6

CHO cell chronic cytotoxicity analyses

carbon based DBPs, 8*f*

N-DBPs, 9*f*

CHO cell cytotoxicity and genotoxicity

and abbreviations, 11*t*

CHO cell genotoxicity analyses, 10*f*

DBP exposure, toxicity, biomarkers,

and adverse health outcomes,

epidemiological studies, 15

drinking water toxicity, forcing agents, 6

human biomarkers, identification, 7

MonoHAA-induced transcriptome

profile pathways, 14*t*

nationwide drinking water in vitro

toxicity survey, 5

new pathway, 5, 17*f*

selected waters, DBP exposure, 15

T

Toxicity, 34

assays

Chinese hamster ovary cells, 35

CHO cell chronic cytotoxicity, 35

single cell gel electrophoresis, 35

mammalian cell cytotoxicity and

genotoxicity, 36*t*

index values, 37*t*

Trihalomethane formation models, 97

application to bromide intrusion, 110

log (Base 10), goodness of fit statistics,

108*t*

log₁₀(THM4) measured *versus*

log₁₀(THM4) predicted, 104*f*, 112*f*

methods, 99

model 21 and model 9, predictive

accuracy, 109*t*

predictive capability, 102

summary, 100*t*

U

Use of pre-oxidants for NDMA control, 155

chlorine, 156

chlorine dioxide, 158

other oxidants/disinfectants

hydrogen peroxide, 163

potassium ferrate, 163

potassium permanganate, 163

UV irradiation, 162

ozone, 160

secondary amines, 157

tertiary amines, 157

V

Variability of non-regulated disinfection by-products in distribution systems, 341

DBPs under study, 346*t*

- four distribution systems
 - description, 344*t*
 - finished water at WTP, average characteristics, 347*t*
 - FRC concentrations, spatial distribution, 350*t*
 - individual HK levels, spatial distribution, 351*f*
 - material and methods
 - analytical procedure, 345
 - case under study, 343
 - data analysis, 345
 - water sampling, 343
 - mean DBP levels ($\mu\text{g/L}$) found in four systems during study period, 348*t*
 - results and discussion
 - DBP occurrence in area under study, 347
 - impact of water flowing through storage tank, temporal variability, 352
 - non-regulated DBP levels, control and monitoring, 359
 - non-regulated DBP levels within distribution systems, spatial variability, 349
 - regulated and non-regulated DBPs within systems, relationship, 358
 - spatial distribution, temporal variations
 - CNCI levels, 357*f*
 - CP levels, 356*f*
 - HA7 levels, 353*f*
 - HAN4 levels, 355*f*
 - HK2 levels, 354*f*
 - Spearman rank correlation coefficients, 359*t*
- W**
- WWTP effluent, estimated percentage hydraulic flow modeling, 130*f*
 - wastewater indicators, 131*f*